

# Chlorophyll fluorescence measurements and plant stress responses, volume II

**Edited by**

Hazem M. Kalaji, Marcin Rapacz, Marian Brestic and Vasilij Goltsev

**Published in**

Frontiers in Plant Science



## FRONTIERS EBOOK COPYRIGHT STATEMENT

The copyright in the text of individual articles in this ebook is the property of their respective authors or their respective institutions or funders. The copyright in graphics and images within each article may be subject to copyright of other parties. In both cases this is subject to a license granted to Frontiers.

The compilation of articles constituting this ebook is the property of Frontiers.

Each article within this ebook, and the ebook itself, are published under the most recent version of the Creative Commons CC-BY licence. The version current at the date of publication of this ebook is CC-BY 4.0. If the CC-BY licence is updated, the licence granted by Frontiers is automatically updated to the new version.

When exercising any right under the CC-BY licence, Frontiers must be attributed as the original publisher of the article or ebook, as applicable.

Authors have the responsibility of ensuring that any graphics or other materials which are the property of others may be included in the CC-BY licence, but this should be checked before relying on the CC-BY licence to reproduce those materials. Any copyright notices relating to those materials must be complied with.

Copyright and source acknowledgement notices may not be removed and must be displayed in any copy, derivative work or partial copy which includes the elements in question.

All copyright, and all rights therein, are protected by national and international copyright laws. The above represents a summary only. For further information please read Frontiers' Conditions for Website Use and Copyright Statement, and the applicable CC-BY licence.

ISSN 1664-8714  
ISBN 978-2-8325-2413-8  
DOI 10.3389/978-2-8325-2413-8

## About Frontiers

Frontiers is more than just an open access publisher of scholarly articles: it is a pioneering approach to the world of academia, radically improving the way scholarly research is managed. The grand vision of Frontiers is a world where all people have an equal opportunity to seek, share and generate knowledge. Frontiers provides immediate and permanent online open access to all its publications, but this alone is not enough to realize our grand goals.

## Frontiers journal series

The Frontiers journal series is a multi-tier and interdisciplinary set of open-access, online journals, promising a paradigm shift from the current review, selection and dissemination processes in academic publishing. All Frontiers journals are driven by researchers for researchers; therefore, they constitute a service to the scholarly community. At the same time, the *Frontiers journal series* operates on a revolutionary invention, the tiered publishing system, initially addressing specific communities of scholars, and gradually climbing up to broader public understanding, thus serving the interests of the lay society, too.

## Dedication to quality

Each Frontiers article is a landmark of the highest quality, thanks to genuinely collaborative interactions between authors and review editors, who include some of the world's best academicians. Research must be certified by peers before entering a stream of knowledge that may eventually reach the public - and shape society; therefore, Frontiers only applies the most rigorous and unbiased reviews. Frontiers revolutionizes research publishing by freely delivering the most outstanding research, evaluated with no bias from both the academic and social point of view. By applying the most advanced information technologies, Frontiers is catapulting scholarly publishing into a new generation.

## What are Frontiers Research Topics?

Frontiers Research Topics are very popular trademarks of the *Frontiers journals series*: they are collections of at least ten articles, all centered on a particular subject. With their unique mix of varied contributions from Original Research to Review Articles, Frontiers Research Topics unify the most influential researchers, the latest key findings and historical advances in a hot research area.

Find out more on how to host your own Frontiers Research Topic or contribute to one as an author by contacting the Frontiers editorial office: [frontiersin.org/about/contact](https://frontiersin.org/about/contact)



# Chlorophyll fluorescence measurements and plant stress responses, volume II

## Topic editors

Hazem M. Kalaji — Warsaw University of Life Sciences - SGGW, Poland

Marcin Rapacz — University of Agriculture in Krakow, Poland

Marian Brestic — Slovak University of Agriculture, Slovakia

Vasilij Goltsev — Sofia University, Bulgaria

## Citation

Kalaji, H. M., Rapacz, M., Brestic, M., Goltsev, V., eds. (2023). *Chlorophyll fluorescence measurements and plant stress responses, volume II*.

Lausanne: Frontiers Media SA. doi: 10.3389/978-2-8325-2413-8

# Table of contents

- 05 **Differential Response of the Photosynthetic Machinery to Fluctuating Light in Mature and Young Leaves of *Dendrobium officinale***  
Ying-Jie Yang, Qi Shi, Hu Sun, Ren-Qiang Mei and Wei Huang
- 15 **Photosynthetic Induction Under Fluctuating Light Is Affected by Leaf Nitrogen Content in Tomato**  
Hu Sun, Yu-Qi Zhang, Shi-Bao Zhang and Wei Huang
- 26 **Cold Stress Resistance of Tomato (*Solanum lycopersicum*) Seedlings Is Enhanced by Light Supplementation From Underneath the Canopy**  
Tao Lu, Yangfan Song, Hongjun Yu, Qiang Li, Jingcheng Xu, Yong Qin, Guanhua Zhang, Yuhong Liu and Weijie Jiang
- 40 **Integrated Analyses of Transcriptome and Chlorophyll Fluorescence Characteristics Reveal the Mechanism Underlying Saline–Alkali Stress Tolerance in *Kosteletzkya pentacarpos***  
Jian Zhou, Anguo Qi, Baoquan Wang, Xiaojing Zhang, Qidi Dong and Jinxiu Liu
- 54 **NaCl Pretreatment Enhances the Low Temperature Tolerance of Tomato Through Photosynthetic Acclimation**  
Xiaolong Yang, Fengyu Zou, Yumeng Zhang, Jiali Shi, Mingfang Qi, Yufeng Liu and Tianlai Li
- 68 **The Transcription Factor MYB37 Positively Regulates Photosynthetic Inhibition and Oxidative Damage in Arabidopsis Leaves Under Salt Stress**  
Yuanyuan Li, Bei Tian, Yue Wang, Jiechen Wang, Hongbo Zhang, Lu Wang, Guangyu Sun, Yongtao Yu and Huihui Zhang
- 81 **Chloroplastic photoprotective strategies differ between bundle sheath and mesophyll cells in maize (*Zea mays* L.) Under drought**  
Wen-Juan Liu, Hao Liu, Yang-Er Chen, Yan Yin, Zhong-Wei Zhang, Jun Song, Li-Juan Chang, Fu-Li Zhang, Dong Wang, Xiao-Hang Dai, Chao Wei, Mei Xiong, Shu Yuan and Jun Zhao
- 98 **Dissecting photosynthetic electron transport and photosystems performance in Jerusalem artichoke (*Helianthus tuberosus* L.) under salt stress**  
Kun Yan, Huimin Mei, Xiaoyan Dong, Shiwei Zhou, Jinxin Cui and Yanhong Sun
- 108 **Exogenous melatonin strongly affects dynamic photosynthesis and enhances water-water cycle in tobacco**  
Hu Sun, Xiao-Qian Wang, Zhi-Lan Zeng, Ying-Jie Yang and Wei Huang

- 121 **PEG-induced physiological drought for screening winter wheat genotypes sensitivity – integrated biochemical and chlorophyll a fluorescence analysis**  
Vesna Peršić, Anita Ament, Jasenka Antunović Dunić, Georg Drezner and Vera Cesar
- 143 **Insights into melatonin-induced photosynthetic electron transport under low-temperature stress in cucumber**  
Pei Wu, Yadong Ma, Golam Jalal Ahammed, Baoyu Hao, Jingyi Chen, Wenliang Wan, Yanhui Zhao, Huimei Cui, Wei Xu, Jinxia Cui and Huiying Liu
- 160 **Photosynthetic performance and nutrient uptake under salt stress: Differential responses of wheat plants to contrasting phosphorus forms and rates**  
Aicha Loudari, Asmae Mayane, Youssef Zeroual, Gilles Colinet and Abdallah Oukarroum
- 176 **Environmental stress - what can we learn from chlorophyll a fluorescence analysis in woody plants? A review**  
Tatiana Swoczyna, Hazem M. Kalaji, Filippo Bussotti, Jacek Mojski and Martina Pollastrini



# Differential Response of the Photosynthetic Machinery to Fluctuating Light in Mature and Young Leaves of *Dendrobium officinale*

Ying-Jie Yang<sup>1</sup>, Qi Shi<sup>1,2</sup>, Hu Sun<sup>1,2</sup>, Ren-Qiang Mei<sup>1\*</sup> and Wei Huang<sup>1,3\*</sup>

<sup>1</sup> Kunming Institute of Botany, Chinese Academy of Sciences, Kunming, China, <sup>2</sup> University of Chinese Academy of Sciences, Beijing, China, <sup>3</sup> Bio-Innovation Center of DR PLANT, Kunming Institute of Botany, Chinese Academy of Sciences, Kunming, China

## OPEN ACCESS

### Edited by:

Marian Brestic,  
Slovak University of Agriculture,  
Slovakia

### Reviewed by:

Lorenzo Ferroni,  
University of Ferrara, Italy  
Sajad Hussain,  
Sichuan Agricultural University, China  
Piotr Andrzej Dąbrowski,  
Warsaw University of Life Sciences,  
Poland

### \*Correspondence:

Ren-Qiang Mei  
meirenqiang@mail.kib.ac.cn  
Wei Huang  
huangwei@mail.kib.ac.cn

### Specialty section:

This article was submitted to  
Plant Abiotic Stress,  
a section of the journal  
Frontiers in Plant Science

**Received:** 06 December 2021

**Accepted:** 27 December 2021

**Published:** 03 February 2022

### Citation:

Yang Y-J, Shi Q, Sun H, Mei R-Q and Huang W (2022) Differential Response of the Photosynthetic Machinery to Fluctuating Light in Mature and Young Leaves of *Dendrobium officinale*. *Front. Plant Sci.* 12:829783. doi: 10.3389/fpls.2021.829783

A key component of photosynthetic electron transport chain, photosystem I (PSI), is susceptible to the fluctuating light (FL) in angiosperms. Cyclic electron flow (CEF) around PSI and water-water cycle (WWC) are both used by the epiphytic orchid *Dendrobium officinale* to protect PSI under FL. This study examined whether the ontogenetic stage of leaf has an impact on the photoprotective mechanisms dealing with FL. Thus, chlorophyll fluorescence and P700 signals under FL were measured in *D. officinale* young and mature leaves. Upon transition from dark to actinic light, a rapid re-oxidation of P700 was observed in mature leaves but disappeared in young leaves, indicating that WWC existed in mature leaves but was lacking in young leaves. After shifting from low to high light, PSI over-reduction was clearly missing in mature leaves. By comparison, young leaves showed a transient PSI over-reduction within the first 30 s, which was accompanied with highly activation of CEF. Therefore, the effect of FL on PSI redox state depends on the leaf ontogenetic stage. In mature leaves, WWC is employed to avoid PSI over-reduction. In young leaves, CEF around PSI is enhanced to compensate for the lack of WWC and thus to prevent an uncontrolled PSI over-reduction induced by FL.

**Keywords:** photosynthesis, photosystem I, photoprotection, cyclic electron flow, water-water cycle

## INTRODUCTION

A typical light condition for plants in nature is the fluctuations of light intensity owing to cloud, wind, and shading from upper leaves and plants (Percy, 1990). When light intensity transiently shifts from low to high, photosystem II (PSII) electron flow rapidly increases but CO<sub>2</sub> assimilation rate increased slowly (Gerotto et al., 2016; Acevedo-Siaca et al., 2020; De Souza et al., 2020; Grieco et al., 2020; Kimura et al., 2020; Yamori et al., 2020), leading to the imbalance between light and dark reactions (Yamori et al., 2016; Slaterry et al., 2018). Within the first seconds after light intensity suddenly increase, electrons transported



from PSII to photosystem I (PSI) cannot be immediately transported to  $\text{NADP}^+$  because the consumption of nicotinamide adenine dinucleotide phosphate (NADPH) is restricted, resulting in the accumulation of reducing power in PSI as demonstrated by PSI over-reduction (Yamamoto et al., 2016; Wada et al., 2018). Therefore, fluctuating light (FL) can give rise to a risk of PSI photoinhibition in photosynthetic organisms (Suorsa et al., 2012; Kono et al., 2014; Yamamoto and Shikanai, 2019; Storti et al., 2020). As PSI is the key component of photosynthetic electron flow, PSI photoinhibition suppresses  $\text{CO}_2$  fixation and photoprotection (Sejima et al., 2014; Brestic et al., 2015, 2016; Zivcak et al., 2015, 2019; Chovancek et al., 2019, 2021; Shimakawa and Miyake, 2019). In addition, the rate of PSI repair is much slower than that of PSII (Zhang and Scheller, 2004; Zivcak et al., 2015; Lima-Melo et al., 2019). Therefore, plants should protect PSI from damage when exposed to natural FL conditions (Tikkanen et al., 2012; Allahverdiyeva et al., 2015; Ferroni et al., 2020).

The photoprotective mechanisms coping with the FL in photosynthetic organisms is related to the evolutionary process (Ilík et al., 2017). In non-angiosperms,  $\text{O}_2$  photo-reduction catalyzed by flavodiiron proteins is the main regulatory mechanism coping with FL, which is supplemented by cyclic electron flow (CEF) (Gerotto et al., 2016; Jokel et al., 2018; Storti et al., 2019, 2020). Interestingly, the genes of flavodiiron proteins are completely lost in angiosperms (Yamamoto et al., 2016; Ilík et al., 2017). However, CEF pathways, such as proton gradient regulation 5 (*pgr5*) and chloroplast NADH dehydrogenase-like (NDH) pathways, are retained in the most angiosperms to sustain photosynthesis (Takahashi et al., 2009; Johnson, 2011; Yamori et al., 2011; Nishikawa et al., 2012; Yamori and Shikanai, 2016; Shikanai and Yamamoto, 2017; Rantala et al., 2020). *Arabidopsis thaliana* and rice (*Oryza sativa*) mutants lacking *pgr5* and NDH display stronger PSI over-reduction under high light and thus are susceptible to PSI photoinhibition in the FL (Suorsa et al., 2012; Kono et al., 2014; Yamori et al., 2016; Tikkanen et al., 2017; Yamamoto and Shikanai, 2019). In particular, *pgr5* seedlings died when grown under FL owing to an uncontrolled PSI photoinhibition (Suorsa et al., 2012). After light intensity abruptly increases, CEF is highly stimulated in model C3 plants *Arabidopsis* and tobacco (*Tabacum nicotiana*) (Kono et al., 2014; Yang et al., 2019a). Such activation of CEF favors the proton gradient ( $\Delta\text{pH}$ ) formation, which is essential for the PSI photoprotection by slowing down plastoquinone oxidation at the cytochrome b6f (Cyt b6f) and enhancing the electron downstream of PSI (Armbruster et al., 2017). However, the activation of CEF cannot immediately consume the excess electrons in PSI and has some delay in alleviating PSI over-reduction. In addition, a pseudo-CEF in angiosperms, called water-water cycle (WWC), can rapidly consume the excess electrons in PSI and thus protects PSI from damage under FL more efficiently than CEF in angiosperms (Alric and Johnson, 2017; Huang et al., 2019b; Yang et al., 2019b, 2020; Sun et al., 2020). During WWC, electrons transported from  $\text{H}_2\text{O}$  to PSI are consumed by photo-reduction of  $\text{O}_2$ . The resulting reactive oxygen species (ROS) are scavenged by superoxide dismutase and ascorbate peroxidase (Asada, 1999). This process not only

consumes excess reducing power in PSI but also enhance  $\Delta\text{pH}$  formation (Asada, 2000; Rizhsky et al., 2003; Hirotsu et al., 2004; Roberty et al., 2014). Moreover, PSI redox state is always affected by electron flow from PSII. Once PSII activity is downregulated, FL-induced PSI over-reduction can be alleviated (Tikkanen et al., 2014; Suorsa et al., 2016; Terashima et al., 2021). Therefore, the strategies employed to cope with FL vary among angiosperms.

In addition to species difference, the response of PSI to FL can be affected by leaf ontogenetic stage. In field-grown *Cerasus cerasoides* plants, mature leaves displayed more severe PSI over-reduction than young leaves after light increased, leading to stronger FL-induced PSI photoinhibition in mature leaves (Yang et al., 2019c). By comparison, in the crassulacean acid metabolism (CAM) plant *Bryophyllum pinnatum*, FL induced more severe PSI over-reduction and PSI photoinhibition in young leaves than mature leaves (Yang et al., 2019b). These contrasting reports indicated that young and mature leaves might display different responses of PSI to FL. Furthermore, the regulatory mechanisms related to PSI photoprotection significantly differed between young and mature leaves in *C. cerasoides* and *B. pinnatum*. In C3 plant *C. cerasoides* young leaves, the downregulation of PSII activity and enhancement of CEF finely protected PSI under FL (Yang et al., 2019c). In CAM plant *B. pinnatum*, WWC was operational in mature leaves but was negligible in young leaves (Yang et al., 2019b). In the facultative CAM plant *Dendrobium officinale*, WWC was functional in PSI photoprotection under FL in mature leaves (Yang et al., 2020, 2021b; Huang et al., 2021; Sun et al., 2021). CAM plants usually experience drought stress under natural habitats. When  $\text{CO}_2$  assimilation is restricted under drought stress (Zhou et al., 2007; Zhu et al., 2009; Zivcak et al., 2014; Dąbrowski et al., 2019), WWC is a potential protective valve for excess energy (Zivcak et al., 2013; Yi et al., 2014). Therefore, WWC might be a common strategy employed by obligatory and facultative CAM plants to cope with the drought stress and FL. However, it is unclear whether the response of PSI to FL and the related strategies for photosynthetic regulation are also affected by the leaf ontogenetic stage in *D. officinale*. Specifically, we hypothesize that the relative importance of CEF and WWC is dependent on leaf age in *D. officinale*.

*Dendrobium officinale* is a perennial herb that belongs to the *Dendrobium* of Orchidaceae. It is a traditional and extremely precious Chinese herb with high medicinal value. Recently, *D. officinale* has been widely cultivated to meet the market requirement. However, little is known about the characteristics of photosynthetic physiology. In this study, we measured the chlorophyll fluorescence and P700 signals in young and mature leaves of *D. officinale*. This study aimed to: (1) examine whether the response of PSI to FL differs between young and mature leaves, and (2) assess whether the mechanisms of photosynthetic regulation under FL is influenced by the leaf ontogenetic stage. Our results indicated that, when exposed to FL, PSI over-reduction was observed in young leaves but disappeared in mature leaves. The WWC activity contributed to the rapid consumption of excess reducing power in mature leaves. In contrast, CEF was enhanced in young leaves to compensate for the lack of WWC activity and to adjust PSI redox state under FL.

## MATERIALS AND METHODS

### Plant Materials and Growth Conditions

Tissue-cultured seedlings of *D. officinale* Kimura et Migo plants came from the Kunming Institute of Botany, Chinese Academy of Sciences and were cultivated in this place. All plants were grown in a greenhouse with moderate relative air humidity (60–70%) and 40% of full sunlight. Light condition is controlled using non-woven shade net, and the maximum light intensity at daytime is approximately  $800 \mu\text{mol photons m}^{-2} \text{s}^{-1}$ . To avoid water or nutrition stresses, plants were watered every day and fertilized by compound fertilizer. Young (flushed within 20 days) and mature (flushed 2 months ago) leaves were used for photosynthetic measurements that were conducted in late July 2021.

### Chlorophyll Content Measurement *in vivo*

The relative content of chlorophyll per unit leaf area was measured using a two-wavelength-type, handy chlorophyll meter (SPAD-502 Plus; Minolta, Tokyo, Japan).

### Redox Changes of P700 After Transition From Dark to Actinic Light

The redox change of P700 after transition from dark to actinic light was measured using a Dual-PAM 100 measuring system (Heinz Walz, Effeltrich, Germany). After dark adaptation for at least 60 min to inactivate the Calvin–Benson cycle, intact leaves were illuminated at  $1,809 \mu\text{mol photons m}^{-2} \text{s}^{-1}$  under atmospheric air condition at approximately  $25^\circ\text{C}$  (Ilík et al., 2017).

### Photosystem I and II Measurements

In the morning (9–11 a.m.), PSI and PSII parameters were measured on intact uncut leaves at approximately  $25^\circ\text{C}$  using a Dual-PAM 100 measuring system (Heinz Walz, Effeltrich, Germany) (Schreiber and Klughammer, 2008). The initial PSI and PSII parameters were measured after dark-adaptation for 30 min. A 635-nm light-emitting diode array was used as actinic light for illumination. After photosynthetic induction at  $923 \mu\text{mol photons m}^{-2} \text{s}^{-1}$  for 15 min, leaves were illuminated at a low light of  $59 \mu\text{mol photons m}^{-2} \text{s}^{-1}$  for 5 min. Afterward, leaves were exposed to FL alternating between 1,809 and  $59 \mu\text{mol photons m}^{-2} \text{s}^{-1}$ . During two cycles of low/high light, PSI and PSII parameters were measured. PSI parameters were calculated as follows: the quantum yield of PSI photochemistry,  $Y(I) = (P'_m - P) / P_m$ ; the oxidation ratio of P700,  $Y(ND) = P / P_m$ ; and the extent of PSI over-reduction,  $Y(NA) = (P_m - P'_m) / P_m$ . The PSII parameters were calculated as follows: the quantum yield of PSII photochemistry,  $Y(II) = (F'_m - F_s) / F'_m$ ; the quantum yield of non-regulatory energy dissipation in PSII,  $Y(NO) = F_s / F_m$ ; and the quantum yield of non-photochemical quenching in PSII,  $Y(NPQ) = 1 - Y(II) - Y(NO)$ .

The photosynthetic electron transport rates (ETRs) through PSI and PSII were calculated as follows: electron transport rate through PSI ( $ETR_I$ ) =  $PAR \times Y(I) \times 0.84 \times 0.5$ ; electron transport rate through PSII ( $ETR_{II}$ ) =  $PPFD \times Y(II) \times 0.84 \times 0.5$ . PPFD is the photosynthetically active radiation; 0.84, the light absorption of incident irradiance; 0.5, the fraction of absorbed light reaching PSI or PSII. The apparent rate of CEF was estimated by subtracting  $ETR_{II}$  from  $ETR_I$  (Zivcak et al., 2013; Hepworth et al., 2021). These ETR calculations based on assumptions that the light absorption and the fraction of absorbed light reaching PSI or PSII did not differ between young and mature leaves.

### Statistical Analysis

All data are displayed as means of five leaves from five independent plants. A *T*-test was used to determine whether significant differences existed between different treatments ( $\alpha = 0.05$ ).

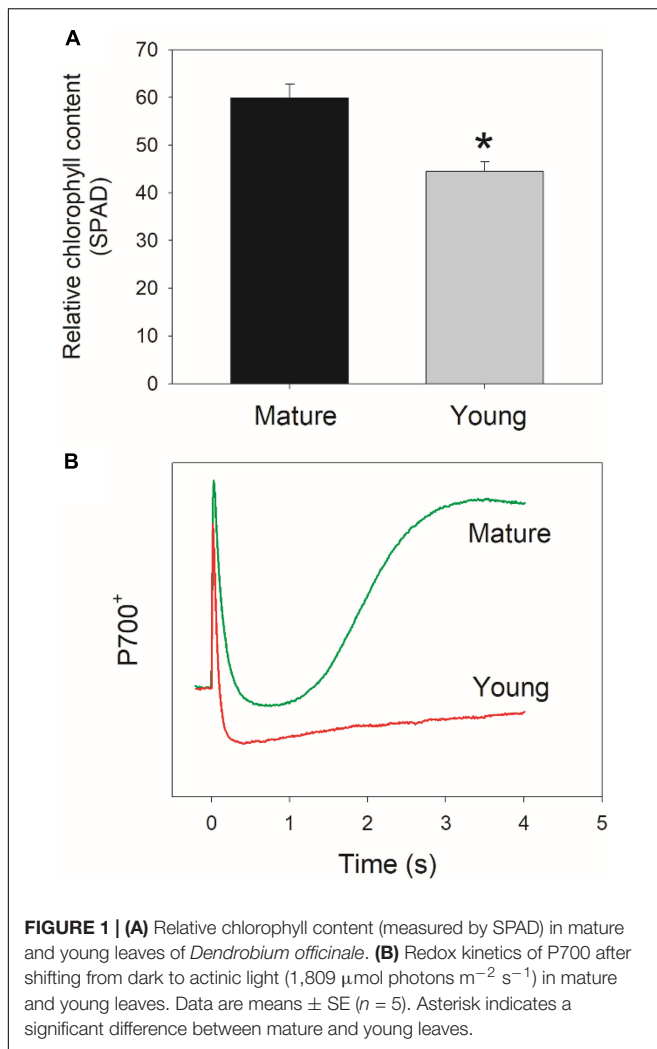
## RESULTS

### The Activity of Water-Water Cycle Differed Between Young and Mature Leaves

For plants of *D. officinale*, the young leaves are reddish and the mature leaves are green. The relative chlorophyll content, as demonstrated by SPAD value, was significantly lower in young leaves than mature leaves (Figure 1A). After shifting from dark to  $1,809 \mu\text{mol photons m}^{-2} \text{s}^{-1}$ , mature leaves showed the rapid re-oxidation of P700 in 3 s (Figure 1B). However, such rapid P700 re-oxidation was not observed in young leaves (Figure 1B). Many previous studies have indicated that this rapid re-oxidation of P700 in angiosperms is caused by the fast outflow of electrons from PSI to  $O_2$  mediated by the WWC activity (Shirao et al., 2013; Huang et al., 2019b, 2021; Sun et al., 2020; Yang et al., 2020). Therefore, WWC activity was present in mature leaves but was lacking in young leaves.

### Photosynthetic Performances Upon Transition From Low to High Light Differed Between Young and Mature Leaves

Under FL, the responses of PSI and PSII to a sudden increase in illumination significantly affected the extent of photoinhibition (Suorsa et al., 2012; Huang et al., 2019a; Yamamoto and Shikanai, 2019; Tan et al., 2021). Therefore, we examined the performances of PSI and PSII under FL alternating between 59 and  $1,809 \mu\text{mol photons m}^{-2} \text{s}^{-1}$  in young and mature leaves. The PSI parameters included  $Y(I)$  (the quantum yield of PSI photochemistry),  $Y(ND)$  (the oxidation ratio of P700), and  $Y(NA)$  {the extent of PSI over-reduction}; and the PSII parameters included the quantum yield of PSII photochemistry ( $Y(II)$ ), non-photochemical quenching in PSII [ $Y(NPQ)$ ], and quantum yield of non-regulatory energy dissipation in PSII [ $Y(NO)$ ].



At low light, mature leaves had similar  $Y(I)$  (Figure 2A), lower  $Y(ND)$  (Figure 2B), and higher  $Y(NA)$  (Figure 2C) when compared with young leaves. After transition to high light for 10 s,  $Y(ND)$  rapidly increased to high levels ( $>0.8$ ) and  $Y(NA)$  rapidly decreased to low levels ( $<0.15$ ) in mature leaves, indicating that PSI over-reduction was prevented in mature leaves when exposed to FL (Figures 2B,C). By comparison,  $Y(ND)$  increased more slowly in young leaves (Figure 2B). Concomitantly,  $Y(NA)$  abruptly increased to a peak in 10 s, followed by its gradual decrease, indicating the transient PSI over-reduction in young leaves under FL (Figure 2C). Therefore, the response of PSI redox state to FL largely differed between young and mature leaves.

At low light, mature leaves displayed higher  $Y(II)$ , lower  $Y(NPQ)$ , and similar  $Y(NO)$ , when compared with young leaves (Figure 3), suggesting the lower light use efficiency in young leaves. After an abrupt increase in illumination,  $Y(II)$  largely decreased and  $Y(NPQ)$  gradually increased in mature and young leaves (Figures 3A,B). Concomitantly,  $Y(NO)$  first increased and then gradually decreased during the prolonged exposure to high light. The young leaves displayed higher  $Y(NPQ)$  capacity

than mature leaves (Figure 3B), leading to lower  $Y(NO)$  under high light in young leaves (Figure 3C). The enhancement of  $Y(NPQ)$  in young leaves can dissipate the excess light energy harmlessly as heat and diminish the production of ROS. Therefore, young leaves upregulated NPQ to compensate the limitation of light use efficiency.

Mature and young leaves showed similar ETRI under low light (Figure 4A). Upon the transition to high light, ETRI rapidly increased within 10 s in mature leaves, followed by its decrease and re-increase (Figure 4A). By comparison, ETRI peaked in the first 10 s and then gradually decreased over time in young leaves. The performance of ETRII under FL was largely different from ETRI. By transitioning to high light, ETRII gradually increased in mature and young leaves (Figure 4B). After exposure to high light for 2 min, mature leaves displayed much higher ETRII than young leaves (Figure 4B). Since the operation of ETRII is largely determined by  $\text{CO}_2$  assimilation rate, this result indicates that under high light mature leaves have much higher  $\text{CO}_2$  assimilation rate than young leaves.

## Regulation of Cyclic Electron Flow Activation Under High Light

Cyclic electron flow (CEF) contributes to the total photosynthetic electron transport and thus helps  $\Delta\text{pH}$  formation (Wang et al., 2015; Shikanai and Yamamoto, 2017). Upon the transition to high light, ETRI–ETRII rapidly increased to the peaks in mature and young leaves within the first 10 s (Figure 5A). Subsequently, ETRI–ETRII gradually decreased in parallel. Because the difference between ETRI and ETRII is an indicator of CEF activation, these results indicated that CEF was highly activated within the first 10 s upon transition to high light. Furthermore, the CEF activation under FL was enhanced in young leaves than mature leaves. After this light transition for 2 min, ETRI–ETRII decreased to similar level in mature and young leaves. During this process, young leaves displayed much higher ETRI–ETRII values than mature leaves. Since an important role of CEF activation under FL is to alleviate PSI over-reduction, we examined the relationship between ETRI–ETRII and  $Y(NA)$ , and found that the ETRI–ETRII value was strongly correlated to  $Y(NA)$  (Figure 5B). At the same ETRI–ETRII value, the  $Y(NA)$  was higher in young leaves than in mature leaves, indicating that young leaves enhanced CEF activity to protect PSI from the FL-induced over-reduction.

## DISCUSSION

Generally, the induction speed of PSII electron flow is faster than that of  $\text{CO}_2$  assimilation in photosynthetic organisms, leading to the accumulation of excited states in PSI when light intensity abruptly changes from low to high (Gerotto et al., 2016; Yamori et al., 2016; Li et al., 2021). Meanwhile, photosynthetic angiosperms cannot generate a sufficient  $\Delta\text{pH}$  (Huang et al., 2019a; Yang et al., 2021a), leading to a temporary uncontrolled electron flow from PSII to PSI through the Cyt b6f complex (Tikkanen and Aro, 2014; Armbruster et al., 2017). If the excess reducing power in PSI cannot be immediately

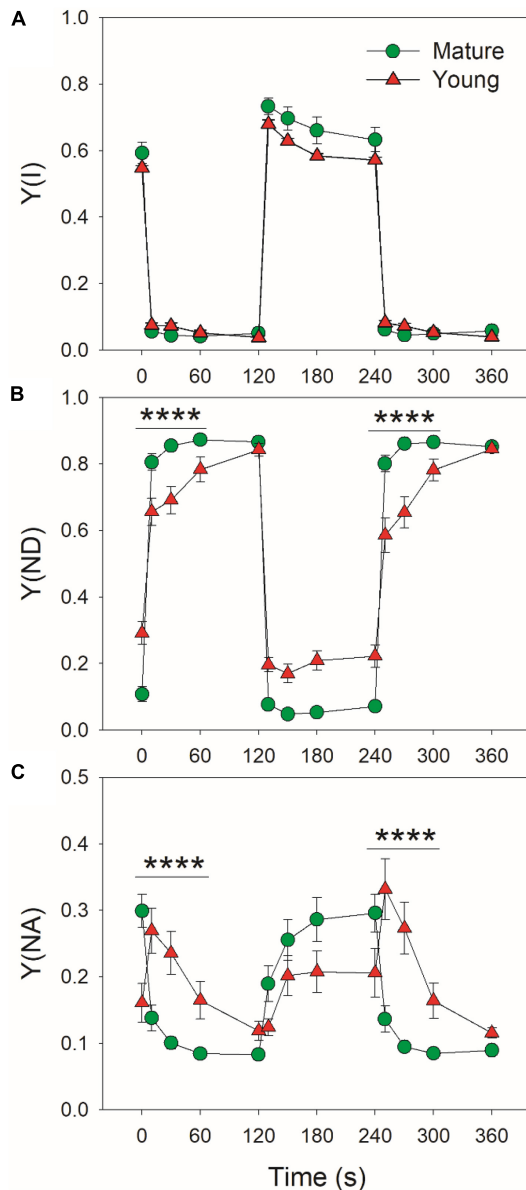


**FIGURE 2** | Changes in PSI parameters under fluctuating light alternating between 59 and 1809  $\mu\text{mol photons m}^{-2} \text{s}^{-1}$  for mature and young leaves of *Dendrobium officinale*. **(A)**  $Y(I)$ , the quantum yield of PSI photochemistry; **(B)**  $Y(ND)$ , the oxidation ratio of P700; **(C)**  $Y(NA)$ , the extent of PSI over-reduction. Data are means  $\pm$  SE ( $n = 5$ ). Asterisk indicates a significant difference between mature and young leaves.

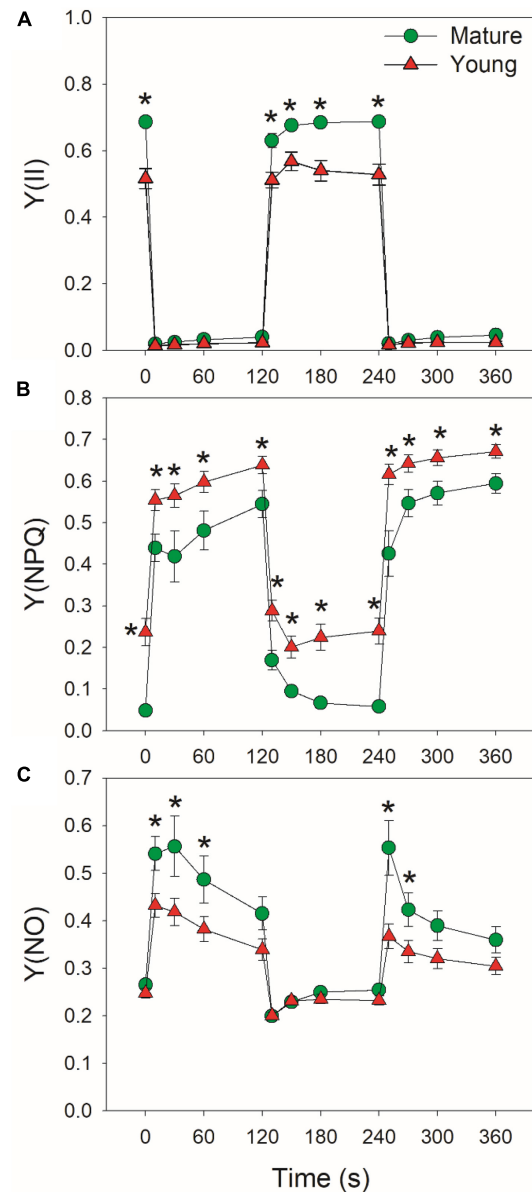
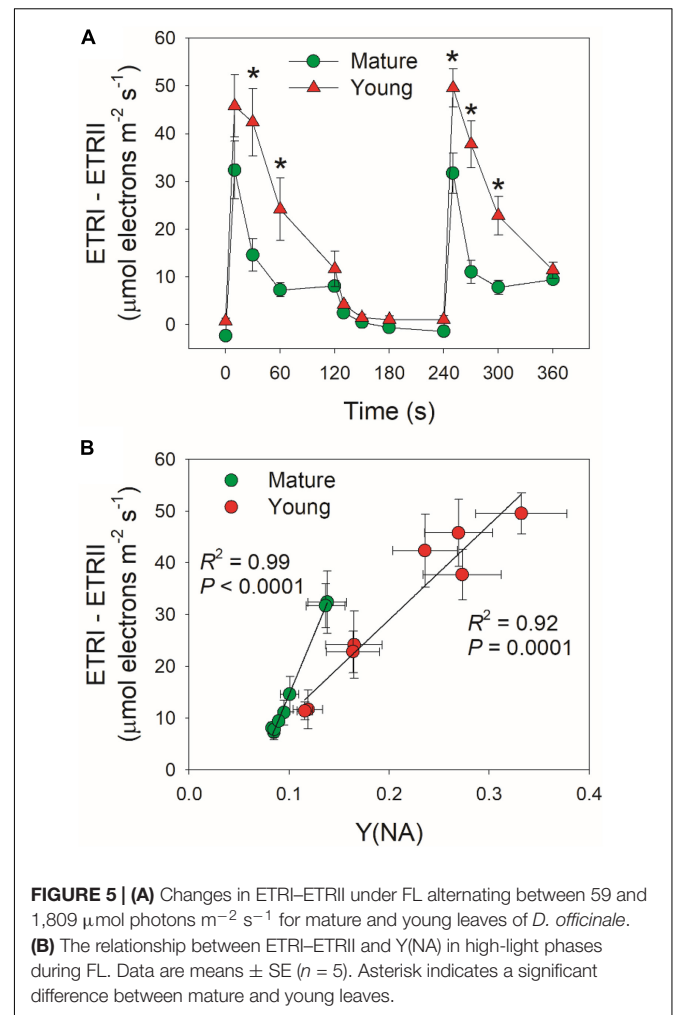
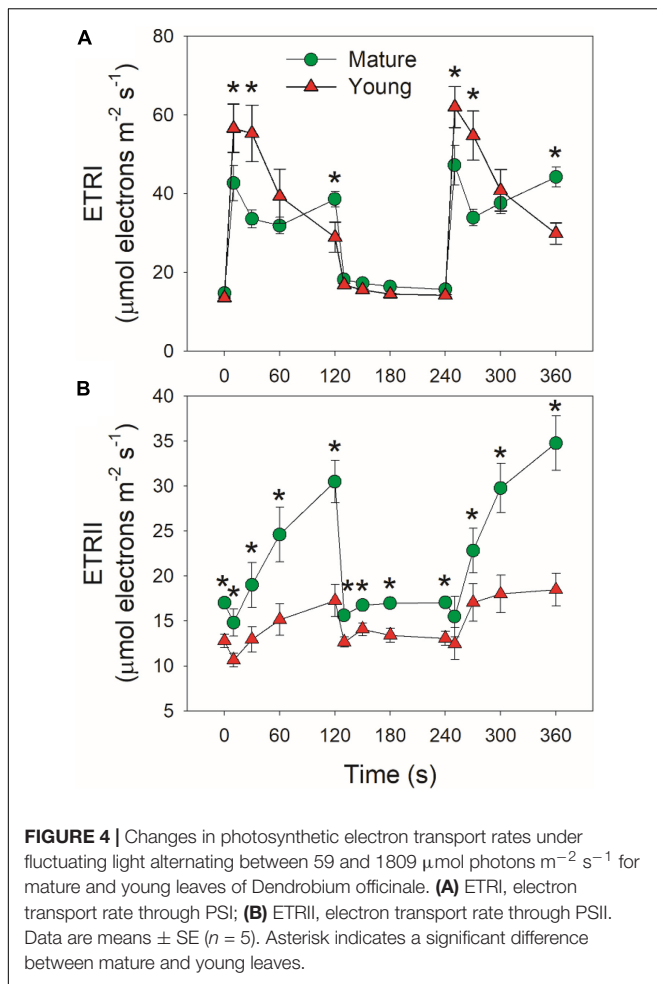


**FIGURE 3** | Changes in PSII parameters under fluctuating light alternating between 59 and 1809  $\mu\text{mol photons m}^{-2} \text{s}^{-1}$  for mature and young leaves of *Dendrobium officinale*. **(A)**  $Y(II)$ , the quantum yield of PSII photochemistry; **(B)**  $Y(NPQ)$ , the quantum yield of non-photochemical quenching in PSII; **(C)**  $Y(NO)$ , the quantum yield of non-regulatory energy dissipation in PSII. Data are means  $\pm$  SE ( $n = 5$ ). Asterisk indicates a significant difference between mature and young leaves.

consumed by downstream sinks of PSI, FL can induce a transient PSI over-reduction and thus causes PSI photoinhibition (Allahverdiyeva et al., 2013; Gerotto et al., 2016; Jokel et al., 2018; Yamamoto and Shikanai, 2019). To avoid FL-induced PSI photoinhibition, both flavodiiron proteins and CEF are employed by non-angiosperms to avoid PSI photoinhibition, in which flavodiiron proteins are the main players (Gerotto et al., 2016; Chaux et al., 2017; Shimakawa et al., 2017; Jokel et al., 2018). However, the genes of flavodiiron proteins are lacking in

angiosperms (Ilík et al., 2017). Therefore, many angiosperms, such as *Arabidopsis*, rice, and tobacco display transient PSI over-reduction upon a sudden increase in irradiance (Yamamoto et al., 2016; Wada et al., 2018). Our results supported this notion by showing the transient increase in  $Y(NA)$  in young leaves after transition from low to high light (**Figures 2A–C**). To prevent an uncontrolled PSI over-reduction under high light, CEF around PSI is employed by angiosperms to help the rapid  $\Delta\text{pH}$  formation





(Suorsa et al., 2012; Kono et al., 2014; Tazoe et al., 2020). An increased  $\Delta\text{pH}$  not only strengthens the downregulation of plastoquinone oxidation at the Cyt b6f but also enhances the electron sink downstream of PSI *via* providing additional ATP (Armbruster et al., 2017; Yamamoto and Shikanai, 2019). Consistently, we here observed the highly stimulation of CEF within the first 10 s after transition from low to high light in both young and mature leaves (Figure 5A). Additionally, an interesting phenomenon is that some angiosperms do not display PSI over-reduction under FL, which is caused by the operation of a pseudo-CEF pathway called WWC (Huang et al., 2019b; Sun et al., 2020; Yang et al., 2020). Therefore, angiosperms can use diverse strategies for protecting the PSI against FL-induced photoinhibition.

Both strategies are effective in protecting the PSI against photoinhibition under FL in angiosperms as demonstrated by their normal growth under natural FL conditions. However, CEF is a universal protective mechanism while the activity of WWC in angiosperms largely varies among angiosperms (Driever and Baker, 2011; Shirao et al., 2013; Huang et al., 2019b; Yang et al., 2020). The operation of WWC can consume excess light energy and favors the regulation of photosynthetic electron flow (Asada, 1999; Miyake and Yokota, 2000; Makino et al., 2002;

Miyake, 2010; Alric and Johnson, 2017). The WWC activity in plants can be affected by environmental conditions, such as chilling temperature, drought stress, and high light (Zhou et al., 2004; Zivcak et al., 2013; Yi et al., 2014; Ferroni et al., 2021). It is unclear whether the activity of WWC is also affected by the ontogenetic stage of leaf in a given species. In the studied species *D. officinale*, WWC is documented to be operational in PSI photoprotection under FL in mature leaves. To test the effect of leaf ontogenetic stage on photosynthetic strategies coping with FL, the photosynthetic performance under FL was compared between mature and young leaves of *D. officinale*. We found that in mature leaves, WWC rapidly consumed excess reducing power in PSI and thus avoided the PSI over-reduction after any increase in illumination (Figure 1). In contrast, the WWC activity was negligible in young leaves as indicated by the clearly missing of rapid P700 re-oxidation upon transition from dark to actinic light. These results indicate that the establishment of WWC activity is largely dependent on the leaf ontogenetic stage. Furthermore, young leaves significantly displayed PSI over-reduction within the first 30 s after shifting from low to high light (Figure 2C), which was similar to the phenomenon observed in other angiosperms lacking

WWC pathway (Yamamoto et al., 2016; Yamamoto and Shikanai, 2019). Therefore, the differential response of PSI to FL in mature and young leaves in *D. officinale* is largely caused by their difference in WWC activity.

It has been indicated that CEF and WWC have large functional overlap but can cooperate to protect PSI from photoinhibition under FL (Alboresi et al., 2019; Storti et al., 2019, 2020). In mature leaves of *D. officinale*, WWC was enhanced more strongly than CEF when exposed to FL at high temperature (Yang et al., 2021b). At low temperature, WWC activity was largely inhibited and CEF was highly activated to regulate the PSI redox state under FL (Huang et al., 2021). Upon the transition to high light at 25°C, WWC functioned to prevent the PSI over-reduction in the mature leaves. Meanwhile, CEF was stimulated moderately within the first 10 s. Therefore, WWC and CEF cooperate to fine-tune photosynthesis in mature leaves under FL at normal growth temperature (Sun et al., 2021). When light intensity abruptly shifted from low to high for 10 s, CEF was highly stimulated as indicated by the rapid increase of ETRI–ETR<sub>II</sub> value, and the CEF activation was stronger in young leaves than mature leaves (Figure 5A). Concomitantly, the PSI over-reduction was not completely avoided in young leaves. These results indicated that in young leaves, the lack of WWC activity was partially compensated by the enhancement of CEF. Therefore, mature and young leaves of *D. officinale* employed different strategies to adjust PSI redox state under FL. Furthermore, we observed positive relationship between CEF activation and PSI over-reduction (Figure 5B), suggesting that the CEF activation is affected by Y(NA). Compared with mature leaves, CEF was enhanced in young leaves to prevent the PSI over-reduction under FL. The PSI over-reduction indicates the insufficient ΔpH across the thylakoid membranes (Munekage et al., 2002, 2004; Yamamoto et al., 2016; Kanazawa et al., 2017; Takagi et al., 2017). Under such condition, the rapid stimulation of CEF helped ΔpH formation and thus prevented an uncontrolled PSI over-reduction in young leaves. By comparison, mature leaves mainly used WWC to prevent the PSI over-reduction and the major role of CEF was to balance ATP/NADPH production ratio via additional ATP synthesis. Therefore, the role of CEF in photosynthetic regulation under FL is flexible and can be affected by the operation of WWC.

In addition to the electron sink downstream, the redox state of PSI is affected by the PSII electron flow (Tikkanen et al., 2014; Suorsa et al., 2016; Terashima et al., 2021). At moderate PSII photoinhibition, the PSI over-reduction under high light is alleviated in *Arabidopsis pgr5* mutant (Tikkanen et al., 2014). Furthermore, the minimal activity of oxygen-evolving complex can rescue the lethal phenotype of *pgr5* when grown under FL (Suorsa et al., 2016). Therefore, when the capacity of CO<sub>2</sub> assimilation rate is low, a low activity of oxygen-evolving complex

is beneficial for protecting the PSI under FL. In young leaves of *D. officinale*, the maximum ETR<sub>II</sub> was much lower than mature leaves. Furthermore, the maximum value of Y(NA) under FL in young leaves was approximately 0.3, which was much lower than those in *Arabidopsis*, tobacco, and rice. These results indicated that the transient PSI over-reduction was slighter than the high-photosynthesis plants lacking WWC activity. Therefore, the relatively lower PSII activity in young leaves acts as a safety valve for alleviating the FL-induced PSI over-reduction.

## CONCLUSION

The response of PSI to FL varied among different plants and can be affected by environmental conditions. In this study, we examine the impacts of leaf ontogenetic stage on photosynthetic strategies used by *D. officinale* plants to cope with the FL. In mature leaves, WWC is mainly employed to avoid PSI over-reduction upon any increase in illumination. Concomitantly, CEF is stimulated to regulate the photosynthesis by adjusting the ATP/NADPH production ratio. In contrast, young leaves display PSI over-reduction under FL because WWC activity is absent. To compensate for the lacking of WWC activity, CEF is enhanced under FL to protect the PSI against photoinhibition. Therefore, the response of PSI to FL and the related photoprotective mechanisms are affected by leaf ontogenetic stage.

## DATA AVAILABILITY STATEMENT

The original contributions presented in the study are included in the article/supplementary material, further inquiries can be directed to the corresponding authors.

## AUTHOR CONTRIBUTIONS

WH and R-QM designed the study. Y-JY, QS, and HS performed the photosynthetic measurements. Y-JY, R-QM, and WH performed the data analysis. WH wrote first draft of the manuscript, which was extensively edited and approved the submitted version by all authors.

## FUNDING

This work was supported by the National Natural Science Foundation of China (No. 31971412), Digitalization, Development, and Application of Biotic Resource (202002 AA100007), and Beijing DR PLANT Biotechnology Co., Ltd.

## REFERENCES

- Acevedo-Siaca, L. G., Coe, R., Wang, Y., Kromdijk, J., Quick, W. P., and Long, S. P. (2020). Variation in photosynthetic induction between rice accessions and its potential for improving productivity. *New Phytol.* 227, 1097–1108.
- Alboresi, A., Storti, M., and Morosinotto, T. (2019). Balancing protection and efficiency in the regulation of photosynthetic electron transport across plant evolution. *New Phytol.* 221, 105–109. doi: 10.1111/nph.15372
- Allahverdiyeva, Y., Mustila, H., Ermakova, M., Bersanini, L., Richaud, P., Ajlani, G., et al. (2013). Flavodiiron proteins Flv1 and Flv3 enable cyanobacterial growth

- and photosynthesis under fluctuating light. *Proc. Natl. Acad. Sci. U.S.A.* 110, 4111–4116. doi: 10.1073/pnas.1221194110
- Allahverdiyeva, Y., Suorsa, M., Tikkanen, M., and Aro, E. M. (2015). Photoprotection of photosystems in fluctuating light intensities. *J. Exp. Bot.* 66, 2427–2436. doi: 10.1093/jxb/eru463
- Alric, J., and Johnson, X. (2017). Alternative electron transport pathways in photosynthesis: a confluence of regulation. *Curr. Opin. Plant Biol.* 37, 78–86. doi: 10.1016/j.pbi.2017.03.014
- Armbruster, U., Correa Galvis, V., Kunz, H. H., and Strand, D. D. (2017). The regulation of the chloroplast proton motive force plays a key role for photosynthesis in fluctuating light. *Curr. Opin. Plant Biol.* 37, 56–62. doi: 10.1016/j.pbi.2017.03.012
- Asada, K. (1999). The water-water cycle in chloroplasts: scavenging of active oxygens and dissipation of excess photons. *Annu. Rev. Plant Physiol. Plant Mol. Biol.* 50, 601–639. doi: 10.1146/annurev.arplant.50.1.601
- Asada, K. (2000). The water-water cycle as alternative photon and electron sinks. *Philos. Trans. R. Soc. Lond. B. Biol. Sci.* 355, 1419–1431. doi: 10.1098/rstb.2000.0703
- Brestic, M., Zivcak, M., Kunderlikova, K., and Allakhverdiev, S. I. (2016). High temperature specifically affects the photoprotective responses of chlorophyll b-deficient wheat mutant lines. *Photosynth. Res.* 130, 251–266. doi: 10.1007/s1120-016-0249-7
- Brestic, M., Zivcak, M., Kunderlikova, K., Sytar, O., Shao, H., Kalaji, H. M., et al. (2015). Low PSI content limits the photoprotection of PSI and PSII in early growth stages of chlorophyll b-deficient wheat mutant lines. *Photosynth. Res.* 125, 151–166. doi: 10.1007/s1120-015-0093-1
- Chaux, F., Burlacot, A., Mekhalfi, M., Auroy, P., Blangy, S., Richaud, P., et al. (2017). Flavodiiron proteins promote fast and transient O<sub>2</sub> photoreduction in *Chlamydomonas*. *Plant Physiol.* 174, 1825–1836. doi: 10.1104/pp.17.00421
- Chovancek, E., Zivcak, M., Botyanszka, L., Hauptvogel, P., Yang, X., Misheva, S., et al. (2019). Transient heat waves may affect the photosynthetic capacity of susceptible wheat genotypes due to insufficient photosystem I photoprotection. *Plants* 8:282. doi: 10.3390/plants8080282
- Chovancek, E., Zivcak, M., Brestic, M., Hussain, S., and Allakhverdiev, S. I. (2021). The different patterns of post-heat stress responses in wheat genotypes: the role of the transthylakoid proton gradient in efficient recovery of leaf photosynthetic capacity. *Photosynth. Res.* 150, 179–193. doi: 10.1007/s1120-020-00812-0
- Dąbrowski, P., Baczewska-Dąbrowska, A. H., Kalaji, H. M., Goltsev, V., Paunov, M., Rapacz, M., et al. (2019). Exploration of chlorophyll a fluorescence and plant gas exchange parameters as indicators of drought tolerance in perennial ryegrass. *Sensors* 19:2736. doi: 10.3390/s19122736
- De Souza, A. P., Wang, Y., Orr, D. J., Carmo-Silva, E., and Long, S. P. (2020). Photosynthesis across African cassava germplasm is limited by rubisco and mesophyll conductance at steady state, but by stomatal conductance in fluctuating light. *New Phytol.* 225, 2498–2512. doi: 10.1111/nph.16142
- Driever, S. M., and Baker, N. R. (2011). The water-water cycle in leaves is not a major alternative electron sink for dissipation of excess excitation energy when CO<sub>2</sub> assimilation is restricted. *Plant Cell Environ.* 34, 837–846. doi: 10.1111/j.1365-3040.2011.02288.x
- Ferroni, L., Brestic, M., Živčák, M., Cantelli, R., and Pancaldi, S. (2021). Increased photosynthesis from a deep-shade to high-light regime occurs by enhanced CO<sub>2</sub> diffusion into the leaf of *Selaginella martensii*. *Plant Physiol. Biochem.* 160, 143–154. doi: 10.1016/j.plaphy.2021.01.012
- Ferroni, L., Živčák, M., Sytar, O., Kovár, M., Watanabe, N., Pancaldi, S., et al. (2020). Chlorophyll-depleted wheat mutants are disturbed in photosynthetic electron flow regulation but can retain an acclimation ability to a fluctuating light regime. *Environ. Exp. Bot.* 178:104156. doi: 10.1016/j.envexpbot.2020.104156
- Gerotto, C., Alboresi, A., Meneghesso, A., Jokel, M., Suorsa, M., Aro, E.-M., et al. (2016). Flavodiiron proteins act as safety valve for electrons in physcomitrella patens. *Proc. Natl. Acad. Sci. U.S.A.* 113, 12322–12327. doi: 10.1073/pnas.1606685113
- Grieco, M., Roustan, V., Dermendjiev, G., Rantala, S., Jain, A., Leonardelli, M., et al. (2020). Adjustment of photosynthetic activity to drought and fluctuating light in wheat. *Plant. Cell Environ.* 43, 1484–1500. doi: 10.1111/pce.13756
- Hepworth, C., Wood, W. H. J., Emrich-Mills, T. Z., Proctor, M. S., Casson, S., and Johnson, M. P. (2021). Dynamic thylakoid stacking and state transitions work synergistically to avoid acceptor-side limitation of photosystem I. *Nat. Plants* 7, 87–98. doi: 10.1038/s41477-020-00828-3
- Hirotsu, N., Makino, A., Ushio, A., and Mae, T. (2004). Changes in the thermal dissipation and the electron flow in the water-water cycle in rice grown under conditions of physiologically low temperature. *Plant Cell Physiol.* 45, 635–644. doi: 10.1093/pcp/pch075
- Huang, W., Sun, H., Tan, S.-L., and Zhang, S.-B. (2021). The water-water cycle is not a major alternative sink in fluctuating light at chilling temperature. *Plant Sci.* 305:110828. doi: 10.1016/j.plantsci.2021.110828
- Huang, W., Yang, Y.-J., and Zhang, S.-B. (2019b). The role of water-water cycle in regulating the redox state of photosystem I under fluctuating light. *Biochim. Biophys. Acta - Bioenerg.* 1860, 383–390. doi: 10.1016/j.bbabi.2019.03.007
- Huang, W., Yang, Y.-J., and Zhang, S.-B. (2019a). Photoinhibition of photosystem I under fluctuating light is linked to the insufficient ΔpH upon a sudden transition from low to high light. *Environ. Exp. Bot.* 160, 112–119. doi: 10.1016/j.envexpbot.2019.01.012
- Ilik, P., Pavlović, A., Kouřil, R., Alboresi, A., Morosinotto, T., Allahverdiyeva, Y., et al. (2017). Alternative electron transport mediated by flavodiiron proteins is operational in organisms from cyanobacteria up to gymnosperms. *New Phytol.* 214, 967–972. doi: 10.1111/nph.14536
- Johnson, G. N. (2011). Reprint of: physiology of PSI cyclic electron transport in higher plants. *Biochim. Biophys. Acta Bioenerg.* 1807, 906–911. doi: 10.1016/j.bbabi.2011.05.008
- Jokel, M., Johnson, X., Peltier, G., Aro, E. M., and Allahverdiyeva, Y. (2018). Hunting the main player enabling *Chlamydomonas reinhardtii* growth under fluctuating light. *Plant J.* 94, 822–835. doi: 10.1111/tpj.13897
- Kanazawa, A., Ostendorf, E., Kohzuma, K., Hoh, D., Strand, D. D., Sato-Cruz, M., et al. (2017). Chloroplast ATP synthase modulation of the thylakoid proton motive force: implications for photosystem I and photosystem II photoprotection. *Front. Plant Sci.* 8:719. doi: 10.3389/fpls.2017.00719
- Kimura, H., Hashimoto-Sugimoto, M., Iba, K., Terashima, I., and Yamori, W. (2020). Improved stomatal opening enhances photosynthetic rate and biomass production in fluctuating light. *J. Exp. Bot.* 71, 2339–2350. doi: 10.1093/jxb/eraa090
- Kono, M., Noguchi, K., and Terashima, I. (2014). Roles of the cyclic electron flow around PSI (CEF-PSI) and O<sub>2</sub>-dependent alternative pathways in regulation of the photosynthetic electron flow in short-term fluctuating light in *Arabidopsis thaliana*. *Plant Cell Physiol.* 55, 990–1004. doi: 10.1093/pcp/pcu033
- Li, T., Shi, Q., Sun, H., Yue, M., Zhang, S., and Huang, W. (2021). Diurnal response of photosystem I to fluctuating light is affected by stomatal conductance. *Cells* 10:3128. doi: 10.3390/cells10113128
- Lima-Melo, Y., Gollan, P. J., Tikkanen, M., Silveira, J. A. G., and Aro, E. M. (2019). Consequences of photosystem-I damage and repair on photosynthesis and carbon use in *Arabidopsis thaliana*. *Plant J.* 97, 1061–1072. doi: 10.1111/tpj.14177
- Makino, A., Miyake, C., and Yokota, A. (2002). Physiological functions of the water-water cycle (mehler reaction) and the cyclic electron flow around PSI in rice leaves. *Plant Cell Physiol.* 43, 1017–1026. doi: 10.1093/pcp/pcf124
- Miyake, C. (2010). Alternative electron flows (water-water cycle and cyclic electron flow around PSI) in photosynthesis: molecular mechanisms and physiological functions. *Plant Cell Physiol.* 51, 1951–1963. doi: 10.1093/pcp/pcq173
- Miyake, C., and Yokota, A. (2000). Determination of the rate of photoreduction of O<sub>2</sub> in the water-water cycle in watermelon leaves and enhancement of the rate by limitation of photosynthesis. *Plant Cell Physiol.* 41, 335–343. doi: 10.1093/pcp/41.3.335
- Munekage, Y., Hashimoto, M., Miyake, C., Tomizawa, K., Endo, T., Tasaka, M., et al. (2004). Cyclic electron flow around photosystem I is essential for photosynthesis. *Nature* 429, 579–582. doi: 10.1038/nature02598
- Munekage, Y., Hojo, M., Meurer, J., Endo, T., Tasaka, M., and Shikanai, T. (2002). PGR5 is involved in cyclic electron flow around photosystem I and is essential for photoprotection in *Arabidopsis*. *Cell* 110, 361–371. doi: 10.1016/S0092-8674(02)00867-X
- Nishikawa, Y., Yamamoto, H., Okegawa, Y., Wada, S., Sato, N., Taira, Y., et al. (2012). PGR5-dependent cyclic electron transport around PSI contributes to the redox homeostasis in chloroplasts rather than CO<sub>2</sub> fixation and biomass production in rice. *Plant Cell Physiol.* 53, 2117–2126. doi: 10.1093/pcp/pcs153

- Pearcy, R. W. (1990). Sunflecks and photosynthesis in plant canopies. *Annu. Rev. Plant Physiol. Plant Mol. Biol.* 41, 421–453. doi: 10.1146/annurev.pp.41.060190.002225
- Rantala, S., Lempiäinen, T., Gerotto, C., Tiwari, A., Aro, E.-M., and Tikkanen, M. (2020). PGR5 and NDH-1 systems do not function as protective electron acceptors but mitigate the consequences of PSI inhibition. *Biochim. Biophys. Acta Bioenerg.* 1861:148154. doi: 10.1016/j.bbabo.2020.148154
- Rizhsky, L., Liang, H., and Mittler, R. (2003). The water-water cycle is essential for chloroplast protection in the absence of stress. *J. Biol. Chem.* 278, 38921–38925. doi: 10.1074/jbc.M304987200
- Roberty, S., Bailleul, B., Berne, N., Franck, F., and Cardol, P. (2014). PSI meher reaction is the main alternative photosynthetic electron pathway in *Symbiodinium* sp., symbiotic dinoflagellates of cnidarians. *New Phytol.* 204, 81–91. doi: 10.1111/nph.12903
- Schreiber, U., and Klughammer, C. (2008). Non-photochemical fluorescence quenching and quantum yields in PS I and PS II: analysis of heat-induced limitations using maxi-imaging- PAM and dual-PAM-100. *PAM Appl. Notes* 1, 15–18. doi: 10.13140/2.1.3517.0083
- Sejima, T., Takagi, D., Fukayama, H., Makino, A., and Miyake, C. (2014). Repetitive short-pulse light mainly inactivates photosystem i in sunflower leaves. *Plant Cell Physiol.* 55, 1184–1193. doi: 10.1093/pcp/pcu061
- Shikanai, T., and Yamamoto, H. (2017). Contribution of cyclic and pseudo-cyclic electron transport to the formation of proton motive force in chloroplasts. *Mol. Plant* 10, 20–29. doi: 10.1016/j.molp.2016.08.004
- Shimakawa, G., Ishizaki, K., Tsukamoto, S., Tanaka, M., Sejima, T., and Miyake, C. (2017). The liverwort, marchantia, drives alternative electron flow using a flavodiiron protein to protect PSI. *Plant Physiol.* 173, 1636–1647. doi: 10.1104/pp.16.01038
- Shimakawa, G., and Miyake, C. (2019). What quantity of photosystem I is optimum for safe photosynthesis? *Plant Physiol.* 179, 1479–1485. doi: 10.1104/pp.18.01493
- Shirao, M., Kuroki, S., Kaneko, K., Kinjo, Y., Tsuyama, M., Förster, B., et al. (2013). Gymnosperms have increased capacity for electron leakage to oxygen (mehler and PTOX reactions) in photosynthesis compared with angiosperms. *Plant Cell Physiol.* 54, 1152–1163. doi: 10.1093/pcp/pct066
- Slattery, R. A., Walker, B. J., Weber, A. P. M., and Ort, D. R. (2018). The impacts of fluctuating light on crop performance. *Plant Physiol.* 176, 990–1003. doi: 10.1104/pp.17.01234
- Storti, M., Alboresi, A., Gerotto, C., Aro, E., Finazzi, G., and Morosinotto, T. (2019). Role of cyclic and pseudo-cyclic electron transport in response to dynamic light changes in *Physcomitrella patens*. *Plant. Cell Environ.* 42, 1590–1602. doi: 10.1111/pce.13493
- Storti, M., Segalla, A., Mellon, M., Alboresi, A., and Morosinotto, T. (2020). Regulation of electron transport is essential for photosystem I stability and plant growth. *New Phytol.* 228, 1316–1326. doi: 10.1111/nph.16643
- Sun, H., Shi, Q., Zhang, S.-B., and Huang, W. (2021). Coordination of cyclic electron flow and water–water cycle facilitates photoprotection under fluctuating light and temperature stress in the epiphytic orchid *Dendrobium officinale*. *Plants* 10:606. doi: 10.3390/plants10030606
- Sun, H., Yang, Y.-J., and Huang, W. (2020). The water-water cycle is more effective in regulating redox state of photosystem I under fluctuating light than cyclic electron transport. *Biochim. Biophys. Acta - Bioenerg.* 1861:148235. doi: 10.1016/j.bbabo.2020.148235
- Suorsa, M., Jarvi, S., Grieco, M., Nurmi, M., Pietrzykowska, M., Rantala, M., et al. (2012). Proton gradient regulation5 is essential for proper acclimation of Arabidopsis photosystem I to naturally and artificially fluctuating light conditions. *Plant Cell* 24, 2934–2948. doi: 10.1105/tpc.112.097162
- Suorsa, M., Rossi, F., Tadini, L., Labs, M., Colombo, M., Jahns, P., et al. (2016). PGR5-PGRL1-dependent cyclic electron transport modulates linear electron transport rate in *Arabidopsis thaliana*. *Mol. Plant* 9, 271–288. doi: 10.1016/j.molp.2015.12.001
- Takagi, D., Amako, K., Hashiguchi, M., Fukaki, H., Ishizaki, K., Goh, T., et al. (2017). Chloroplastic ATP synthase builds up a proton motive force preventing production of reactive oxygen species in photosystem I. *Plant J.* 91, 306–324. doi: 10.1111/tpj.13566
- Takahashi, S., Milward, S. E., Fan, D.-Y., Chow, W. S., and Badger, M. R. (2009). How does cyclic electron flow alleviate photoinhibition in arabidopsis? *Plant Physiol.* 149, 1560–1567. doi: 10.1104/pp.108.134122
- Tan, S.-L., Huang, J.-L., Zhang, F.-P., Zhang, S.-B., and Huang, W. (2021). Photosystem I photoinhibition induced by fluctuating light depends on background low light irradiance. *Environ. Exp. Bot.* 181:104298. doi: 10.1016/j.envexpbot.2020.104298
- Tazoe, Y., Ishikawa, N., Shikanai, T., Ishiyama, K., Takagi, D., Makino, A., et al. (2020). Overproduction of PGR5 enhances the electron sink downstream of photosystem I in a C 4 plant. *Flaveria bidentis*. *Plant J.* 103, 814–823. doi: 10.1111/tpj.14774
- Terashima, I., Matsuo, M., Suzuki, Y., Yamori, W., and Kono, M. (2021). Photosystem I in low light-grown leaves of *Alocasia odora*, a shade-tolerant plant, is resistant to fluctuating light-induced photoinhibition. *Photosynth. Res.* 149, 69–82. doi: 10.1007/s11120-021-00832-4
- Tikkanen, M., and Aro, E. M. (2014). Integrative regulatory network of plant thylakoid energy transduction. *Trends Plant Sci.* 19, 10–17. doi: 10.1016/j.tplants.2013.09.003
- Tikkanen, M., Grieco, M., Nurmi, M., Rantala, M., Suorsa, M., and Aro, E.-M. (2012). Regulation of the photosynthetic apparatus under fluctuating growth light. *Philos. Trans. R. Soc. B Biol. Sci.* 367, 3486–3493. doi: 10.1098/rstb.2012.0067
- Tikkanen, M., Mekala, N. R., and Aro, E.-M. (2014). Photosystem II photoinhibition-repair cycle protects photosystem I from irreversible damage. *Biochim. Biophys. Acta Bioenerg.* 1837, 210–215. doi: 10.1016/j.bbabo.2013.10.001
- Tikkanen, M., Rantala, S., Grieco, M., and Aro, E. M. (2017). Comparative analysis of mutant plants impaired in the main regulatory mechanisms of photosynthetic light reactions - from biophysical measurements to molecular mechanisms. *Plant Physiol. Biochem.* 112, 290–301. doi: 10.1016/j.plaphy.2017.01.014
- Wada, S., Yamamoto, H., Suzuki, Y., Yamori, W., Shikanai, T., and Makino, A. (2018). Flavodiiron protein substitutes for cyclic electron flow without competing CO<sub>2</sub> assimilation in rice. *Plant Physiol.* 176, 1509–1518. doi: 10.1104/pp.17.01335
- Wang, C., Yamamoto, H., and Shikanai, T. (2015). Role of cyclic electron transport around photosystem I in regulating proton motive force. *Biochim. Biophys. Acta Bioenerg.* 1847, 931–938. doi: 10.1016/j.bbabo.2014.11.013
- Yamamoto, H., and Shikanai, T. (2019). PGR5-dependent cyclic electron flow protects photosystem I under fluctuating light at donor and acceptor sides. *Plant Physiol.* 179, 588–600. doi: 10.1104/pp.18.01343
- Yamamoto, H., Takahashi, S., Badger, M. R., and Shikanai, T. (2016). Artificial remodelling of alternative electron flow by flavodiiron proteins in arabidopsis. *Nat. Plants* 2:16012. doi: 10.1038/nplants.2016.12
- Yamori, W., Kusumi, K., Iba, K., and Terashima, I. (2020). Increased stomatal conductance induces rapid changes to photosynthetic rate in response to naturally fluctuating light conditions in rice. *Plant. Cell Environ.* 43, 1230–1240. doi: 10.1111/pce.13725
- Yamori, W., Makino, A., and Shikanai, T. (2016). A physiological role of cyclic electron transport around photosystem I in sustaining photosynthesis under fluctuating light in rice. *Sci. Rep.* 6:20147. doi: 10.1038/srep20147
- Yamori, W., Sakata, N., Suzuki, Y., Shikanai, T., and Makino, A. (2011). Cyclic electron flow around photosystem I via chloroplast NAD(P)H dehydrogenase (NDH) complex performs a significant physiological role during photosynthesis and plant growth at low temperature in rice. *Plant J.* 68, 966–976. doi: 10.1111/j.1365-313X.2011.04747.x
- Yamori, W., and Shikanai, T. (2016). Physiological functions of cyclic electron transport around photosystem I in sustaining photosynthesis and plant growth. *Annu. Rev. Plant Biol.* 67, 81–106. doi: 10.1146/annurev-arplant-043015-112002
- Yang, Y.-J., Ding, X.-X., and Huang, W. (2019a). Stimulation of cyclic electron flow around photosystem I upon a sudden transition from low to high light in two angiosperms *Arabidopsis thaliana* and *bletilla striata*. *Plant Sci.* 287:110166. doi: 10.1016/j.plantsci.2019.110166
- Yang, Y.-J., Zhang, S.-B., and Huang, W. (2019b). Photosynthetic regulation under fluctuating light in young and mature leaves of the CAM plant *Bryophyllum pinnatum*. *Biochim. Biophys. Acta Bioenerg.* 1860, 469–477. doi: 10.1016/j.bbabo.2019.04.006
- Yang, Y.-J., Zhang, S.-B., Wang, J.-H., and Huang, W. (2019c). Photosynthetic regulation under fluctuating light in field-grown *Cerasus cerasoides*: a



- comparison of young and mature leaves. *Biochim. Biophys. Acta Bioenerg.* 1860:148073. doi: 10.1016/j.bbapbio.2019.148073
- Yang, Y.-J., Tan, S.-L., Sun, H., Huang, J.-L., Huang, W., and Zhang, S.-B. (2021b). Photosystem I is tolerant to fluctuating light under moderate heat stress in two orchids *dendrobium officinale* and *bletilla striata*. *Plant Sci.* 303:110795. doi: 10.1016/j.plantsci.2020.110795
- Yang, Y.-J., Sun, H., Zhang, S.-B., and Huang, W. (2021a). Roles of alternative electron flows in response to excess light in ginkgo biloba. *Plant Sci.* 312:111030. doi: 10.1016/j.plantsci.2021.111030
- Yang, Y.-J., Tan, S.-L., Huang, J.-L., Zhang, S.-B., and Huang, W. (2020). The water-water cycle facilitates photosynthetic regulation under fluctuating light in the epiphytic orchid *dendrobium officinale*. *Environ. Exp. Bot.* 180:104238. doi: 10.1016/j.envexpbot.2020.104238
- Yi, X. P., Zhang, Y. L., Yao, H. S., Zhang, X. J., Luo, H. H., Gou, L., et al. (2014). Alternative electron sinks are crucial for conferring photoprotection in field-grown cotton under water deficit during flowering and boll setting stages. *Funct. Plant Biol.* 41, 737–747. doi: 10.1071/FP13269
- Zhang, S., and Scheller, H. V. (2004). Photoinhibition of photosystem I at chilling temperature and subsequent recovery in *Arabidopsis thaliana*. *Plant Cell Physiol.* 45, 1595–1602. doi: 10.1093/pcp/pch180
- Zhou, Y., Lam, H. M., and Zhang, J. (2007). Inhibition of photosynthesis and energy dissipation induced by water and high light stresses in rice. *J. Exp. Bot.* 58, 1207–1217. doi: 10.1093/jxb/erl291
- Zhou, Y. H., Yu, J. Q., Huang, L. F., and Nogue, S. (2004). The relationship between CO<sub>2</sub> assimilation, photosynthetic electron transport and water-water cycle in chill-exposed cucumber leaves under low light and subsequent recovery. *Plant Cell Environ.* 27, 1503–1514. doi: 10.1111/j.1365-3040.2004.01255.x
- Zhu, J. J., Zhang, J. L., Liu, H. C., and Cao, K. F. (2009). Photosynthesis, non-photochemical pathways and activities of antioxidant enzymes in a resilient evergreen oak under different climatic conditions from a valley-savanna in Southwest China. *Physiol. Plant.* 135, 62–72. doi: 10.1111/j.1399-3054.2008.01171.x
- Zivcak, M., Brestic, M., Balatova, Z., Drevenakova, P., Olsovska, K., Kalaji, H. M., et al. (2013). Photosynthetic electron transport and specific photoprotective responses in wheat leaves under drought stress. *Photosynth. Res.* 117, 529–546. doi: 10.1007/s11120-013-9885-3
- Zivcak, M., Brestic, M., Botyanszka, L., Chen, Y. E., and Allakhverdiev, S. I. (2019). Phenotyping of isogenic chlorophyll-less bread and durum wheat mutant lines in relation to photoprotection and photosynthetic capacity. *Photosynth. Res.* 139, 239–251. doi: 10.1007/s11120-018-0559-z
- Zivcak, M., Brestic, M., Kunderlikova, K., Sytar, O., and Allakhverdiev, S. I. (2015). Repetitive light pulse-induced photoinhibition of photosystem I severely affects CO<sub>2</sub> assimilation and photoprotection in wheat leaves. *Photosynth. Res.* 126, 449–463. doi: 10.1007/s11120-015-0121-1
- Zivcak, M., Kalaji, H. M., Shao, H. B., Olsovska, K., and Brestic, M. (2014). Photosynthetic proton and electron transport in wheat leaves under prolonged moderate drought stress. *J. Photochem. Photobiol. B Biol.* 137, 107–115. doi: 10.1016/j.jphotobiol.2014.01.007

**Conflict of Interest:** The authors declare that the research was conducted in the absence of any commercial or financial relationships that could be construed as a potential conflict of interest.

**Publisher's Note:** All claims expressed in this article are solely those of the authors and do not necessarily represent those of their affiliated organizations, or those of the publisher, the editors and the reviewers. Any product that may be evaluated in this article, or claim that may be made by its manufacturer, is not guaranteed or endorsed by the publisher.

Copyright © 2022 Yang, Shi, Sun, Mei and Huang. This is an open-access article distributed under the terms of the Creative Commons Attribution License (CC BY). The use, distribution or reproduction in other forums is permitted, provided the original author(s) and the copyright owner(s) are credited and that the original publication in this journal is cited, in accordance with accepted academic practice. No use, distribution or reproduction is permitted which does not comply with these terms.



# Photosynthetic Induction Under Fluctuating Light Is Affected by Leaf Nitrogen Content in Tomato

Hu Sun<sup>1,2</sup>, Yu-Qi Zhang<sup>3</sup>, Shi-Bao Zhang<sup>1</sup> and Wei Huang<sup>1\*</sup>

<sup>1</sup> Kunming Institute of Botany, Chinese Academy of Sciences, Kunming, China, <sup>2</sup> University of Chinese Academy of Sciences, Beijing, China, <sup>3</sup> Institute of Environment and Sustainable Development in Agriculture, Chinese Academy of Agriculture Sciences, Beijing, China

## OPEN ACCESS

### Edited by:

Marian Brestic,  
Slovak University of Agriculture,  
Slovakia

### Reviewed by:

Xinghong Yang,  
Shandong Agricultural University,  
China

Alfred Holzwarth,  
Max Planck Institute for Chemical  
Energy Conversion, Germany

### \*Correspondence:

Wei Huang  
huangwei@mail.kib.ac.cn

### Specialty section:

This article was submitted to  
Plant Abiotic Stress,  
a section of the journal  
Frontiers in Plant Science

Received: 14 December 2021

Accepted: 17 January 2022

Published: 17 February 2022

### Citation:

Sun H, Zhang Y-Q, Zhang S-B  
and Huang W (2022) Photosynthetic  
Induction Under Fluctuating Light Is  
Affected by Leaf Nitrogen Content  
in Tomato.  
Front. Plant Sci. 13:835571.  
doi: 10.3389/fpls.2022.835571

The response of photosynthetic CO<sub>2</sub> assimilation to changes of illumination affects plant growth and crop productivity under natural fluctuating light conditions. However, the effects of nitrogen (N) supply on photosynthetic physiology after transition from low to high light are seldom studied. To elucidate this, we measured gas exchange and chlorophyll fluorescence under fluctuating light in tomato (*Solanum lycopersicum*) seedlings grown with different N conditions. After transition from low to high light, the induction speeds of net CO<sub>2</sub> assimilation ( $A_N$ ), stomatal conductance ( $g_s$ ), and mesophyll conductance ( $g_m$ ) delayed with the decline in leaf N content. The time to reach 90% of maximum  $A_N$ ,  $g_s$  and  $g_m$  was negatively correlated with leaf N content. This delayed photosynthetic induction in plants grown under low N concentration was mainly caused by the slow induction response of  $g_m$  rather than that of  $g_s$ . Furthermore, the photosynthetic induction upon transfer from low to high light was hardly limited by photosynthetic electron flow. These results indicate that decreased leaf N content declines carbon gain under fluctuating light in tomato. Increasing the induction kinetics of  $g_m$  has the potential to enhance the carbon gain of field crops grown in infertile soil.

**Keywords:** fluctuating light, nitrogen, photosynthesis, mesophyll conductance, photosynthetic limitation

## INTRODUCTION

Plants capture light energy to produce chemical energy ATP and NADPH, which are used to drive nitrogen assimilation and the conversion of CO<sub>2</sub> to sugar. Enhancing net CO<sub>2</sub> assimilation rate ( $A_N$ ) is thought to be one of the most important targets for improving plant growth and crop productivity (Kromdijk et al., 2016; Yamori et al., 2016a; South et al., 2019; Ferroni et al., 2020). Many previous studies indicated that increasing  $A_N$  under constant high light can boost plant biomass (Kebeish et al., 2007; Timm et al., 2012, 2015). Recently, some studies reported that the response of  $A_N$  to the increases of illumination significantly affects the carbon gain and thus influences plant growth (Slattery et al., 2018; Adachi et al., 2019; Kimura et al., 2020; Yamori et al., 2020; Zhang et al., 2020). Therefore, altering the photosynthetic performance under dynamic illumination is a promising way to improve photosynthesis under natural fluctuating light (FL) conditions.

Plants grown under high nitrogen (N) concentration usually have higher biomass than plants grown under low N concentration (Makino, 2011). An important explanation for this is that leaf photosynthetic capacity is related to the leaf N content in many higher plants (Yamori et al., 2011; Fan et al., 2020; Li et al., 2020), since stromal enzymes and thylakoid proteins account for

the majority of leaf N (Makino and Osmond, 1991; Sudo et al., 2003; Takashima et al., 2004). Furthermore, stomatal conductance ( $g_s$ ) and mesophyll conductance ( $g_m$ ) under constant high light are also increased in plants grown under high N concentration, which speeds up  $\text{CO}_2$  diffusion from atmosphere to chloroplast carboxylation sites and thus favors the operation of  $A_N$  under constant high light (Yamori et al., 2011). However, few is known about the effects of leaf N content on non-steady-state photosynthetic performances under FL.

Under natural field conditions, light intensity exposed on leaf surface dynamically changes on timescales from milliseconds to hours (Percy, 1990; Slattery et al., 2018). Furthermore, FL and N deficiency usually occurs concomitantly, but how FL and N deficiency interacts to influence photosynthetic physiology in crop plants is poorly understood. After a sudden transitioning from low to high light, the gradual increase of  $A_N$  is termed “photosynthetic induction.” Recent studies indicated that the induction response of  $A_N$  was significantly affected by the induction speed of  $g_s$  (De Souza et al., 2020; Kimura et al., 2020). Gene expression plays a crucial role in the induction response of  $g_s$  under FL. For example, the *slow anion channel-associated 1* (*slac1*), *open stomata 1* (*ost1*) and abscisic acid-deficient *flacca* mutants, and the *proton ATPase translocation control 1* (*PATROL1*) overexpression line had faster stomatal opening responses than WT types in *Arabidopsis thaliana*, rice and tomato (De Souza et al., 2020; Kaiser et al., 2020; Kimura et al., 2020; Yamori et al., 2020). Furthermore, the stomatal opening during photosynthetic induction can be affected by environment conditions such as drought, target light intensity, magnitude of change,  $g_s$  at low light, the time of day, and vapor pressure deficit (Zivcak et al., 2013; Kaiser et al., 2020; Sakoda et al., 2020; Eyland et al., 2021). However, there have been few studies that examined the effect of leaf N content on the induction response of  $g_s$  after transition from low to high light (Li et al., 2020).

In addition to  $g_s$ ,  $g_m$  is a major factor that affects  $\text{CO}_2$  concentration in chloroplast, because  $g_m$  determines the  $\text{CO}_2$  diffusion from intercellular space into the chloroplast (Flexas et al., 2013; Carriqui et al., 2015). In general,  $g_m$  can be determined by structure across leaf profiles, genetic types, biochemical components, and environmental conditions (Yamori et al., 2011; Xiong et al., 2015; Thérout-Rancourt and Gilbert, 2017; Ferroni et al., 2021). Previous studies have highlighted that  $g_m$  is the most important limiting factor for  $A_N$  in many angiosperms (Peguero-Pina et al., 2017; Xiong et al., 2018; Yang Z.-H. et al., 2018, Yang et al., 2021; Gago et al., 2020). Short-term response of  $g_m$  to light intensity has been determined and found that it varies between plant species (Tazoe et al., 2009; Yamori et al., 2010a; Xiong et al., 2018; Yang et al., 2020). However, the induction response of  $g_m$  after transition from low to high light is less known. The  $g_m$  level under constant light is also significantly affected by leaf N content (Yamori et al., 2011). Furthermore, the rapid responses of  $g_m$  to  $\text{CO}_2$  concentration and temperature were also affected by leaf N content (Xiong et al., 2015). However, no studies have elucidated the effect of leaf N content on induction response of  $g_m$  upon transfer from low to high light.

In this study, we aimed to characterize the effects of leaf N content on induction kinetics of  $A_N$ ,  $g_s$ , and  $g_m$  after a sudden transition from low to high light. Gas exchange and chlorophyll fluorescence were measured in tomato plants grown under contrasting N concentrations. The dynamic limitations of  $g_s$ ,  $g_m$ , and biochemical factors imposed on  $A_N$  were analyzed based on the biochemical model for C3 photosynthesis (Farquhar et al., 1980). The effects of leaf N content on photosynthetic performances during photosynthetic induction were revealed.

## MATERIALS AND METHODS

### Plant Materials and Growth Conditions

Tomato (*Solanum lycopersicum* cv. Hupishizi) plants were grown in a greenhouse with the light condition of 40% full sunlight. The day or night air temperatures were approximately 30 or 20°C, the relative air humidity was approximately 60–70%, and the maximum light intensity exposed to leaves was approximately 800  $\mu\text{mol photons m}^{-2} \text{s}^{-1}$ . Plants were grown in 19-cm plastic pots with humus soil, and the initial soil N content was 2.1 mg/g. Plants were fertilized with Peters professional water solution (N:P:K = 15:4.8:24.1, quality ratio) or water as follows: high nitrogen (HN, 0.15 g N/plant every 2 days), middle nitrogen (MN, 0.05 g N/plant once a week), and low nitrogen (LN, 0 mM N/plant). The fertilizer was dissolved in 0.3% water solution and subsequently was used for fertilization, and the nitrogen sources were 24%  $(\text{NH}_4)_3\text{PO}_4$ , 65%  $\text{KNO}_3$ , and 9.5%  $\text{CH}_4\text{N}_2\text{O}$ . To prevent any water stress, these plants were watered every day. After cultivation for 1 month, youngest fully developed leaves were used for measurements. For each N treatment, five leaves from five independent plants were used for gas exchange and chlorophyll fluorescence measurements.

### Gas Exchange and Chlorophyll Fluorescence Measurements

An open gas exchange system (LI-6400XT; Li-Cor Biosciences, Lincoln, NE, United States) was used to simultaneously measure gas exchange and chlorophyll fluorescence. Measurements were taken at a leaf temperature of approximately 25°C, leaf-to-air vapor pressure deficit of 1.2–1.4 kPa, and flow rate of air through the system of 300  $\text{mmol min}^{-1}$ . To measure photosynthetic induction after a short-term shade-fleck, leaves were first adapted to a light intensity of 1,500  $\mu\text{mol photons m}^{-2} \text{s}^{-1}$  and air  $\text{CO}_2$  concentration of 400  $\mu\text{mol mol}^{-1}$  for > 20 min until  $A_N$  and  $g_s$  reached steady state. Then, leaves were subjected to 5 min of low light (50  $\mu\text{mol photons m}^{-2} \text{s}^{-1}$ ) followed by 30 min of high light (1,500  $\mu\text{mol photons m}^{-2} \text{s}^{-1}$ ), and gas exchange and chlorophyll fluorescence were logged every minute. iWUE was calculated as  $\text{iWUE} = A_N/g_s$ . The relative  $A_N$ ,  $g_s$ , and  $g_m$  curves were obtained from the standardization against the maximum values after 30 min photosynthetic induction at high light. The time required to reach 90% of the maximum  $A_N$ ,  $g_s$ , and  $g_m$  was estimated by the first time at which the relative values were higher than 90%. After photosynthetic induction measurement, the response of  $\text{CO}_2$  assimilation rate to incident intercellular  $\text{CO}_2$  concentration ( $A/C_i$ ) curves was measured by decreasing

the CO<sub>2</sub> concentration to a lower limit of 50 μmol mol<sup>-1</sup> and then increasing stepwise to an upper limit of 1,500 μmol mol<sup>-1</sup>. For each CO<sub>2</sub> concentration, photosynthetic measurement was completed in 3 min. Using the A/C<sub>i</sub> curves, the maximum rates of RuBP regeneration (*J<sub>max</sub>*) and carboxylation (*V<sub>cmax</sub>*) were calculated (Long and Bernacchi, 2003).

The quantum yield of PSII photochemistry was calculated as  $\Phi_{PSII} = (F_m' - F_s)/F_m'$  (Genty et al., 1989), where *F<sub>m</sub>'* and *F<sub>s</sub>* represent the maximum and steady-state fluorescence after light adaptation, respectively (Baker, 2004). The total electron transport rate (ETR) through PSII (*J<sub>PSII</sub>*) was calculated as follows (Krall and Edwards, 1992):

$$J_{PSII} = \Phi_{PSII} \times PPFD \times L_{abs} \times 0.5 \quad (1)$$

where PPFD is the photosynthetic photon flux density, and leaf absorbance (*L<sub>abs</sub>*) is assumed to be 0.84. We applied the constant of 0.5 based on the assumption that photons were equally distributed between PSI and PSII.

## Estimation of Mesophyll Conductance and Chloroplast CO<sub>2</sub> Concentration

Mesophyll conductance was calculated according to the following equation (Harley et al., 1992):

$$g_m = \frac{A_N}{C_i - \Gamma^* (J_{PSII} + 8(A_N + R_d)) / (J_{PSII} - 4(A_N + R_d))} \quad (2)$$

where *A<sub>N</sub>* represents the net rate of CO<sub>2</sub> assimilation; *C<sub>i</sub>* is the intercellular CO<sub>2</sub> concentration;  $\Gamma^*$  is the CO<sub>2</sub> compensation point in the absence of daytime respiration (Yamori et al., 2010b; von Caemmerer and Evans, 2015). We used a typical value of 40 μmol mol<sup>-1</sup> in our current study (Xiong et al., 2018). Respiration rate in the dark (*R<sub>d</sub>*) was considered to be half of the dark-adapted mitochondrial respiration rate as measured after 10 min of dark adaptation (Carriquí et al., 2015).

Based on the estimated *g<sub>m</sub>*, the chloroplast CO<sub>2</sub> concentration (*C<sub>c</sub>*) was calculated according to the following equation (Long and Bernacchi, 2003; Warren and Dreyer, 2006):

$$C_c = C_i - \frac{A_N}{g_m} \quad (3)$$

## Quantitative Limitation Analysis of *A<sub>N</sub>*

Relative photosynthetic limitations were assessed as follows (Grassi and Magnani, 2005):

$$L_s = \frac{g_{tot}/g_s \times A_N/C_c}{g_{tot} + A_N/C_c} \quad (4)$$

$$L_{mc} = \frac{g_{tot}/g_m \times A_N/C_c}{g_{tot} + A_N/C_c} \quad (5)$$

$$L_b = \frac{g_{tot}}{g_{tot} + A_N/C_c} \quad (6)$$

where *L<sub>s</sub>*, *L<sub>mc</sub>*, and *L<sub>b</sub>* represent the relative limitations of stomatal conductance, mesophyll conductance, and biochemical

capacity, respectively, in setting the observed value of *A<sub>N</sub>*. *g<sub>tot</sub>* is the total conductance of CO<sub>2</sub> between the leaf surface and sites of RuBP carboxylation (calculated as  $1/g_{tot} = 1/g_s + 1/g_m$ ).

## SPAD Index and Nitrogen Content Measurements

A handy chlorophyll meter (SPAD-502 Plus; Minolta, Tokyo, Japan) was used to nondestructively measure the SPAD index (relative content of chlorophyll per unit leaf area) of leaves used for photosynthetic measurements. Thereafter, leaf area was measured using a LI-3000A portable leaf area meter (Li-Cor, Lincoln, NE, United States). After leaf material was dried at 80°C for 48 h, dry weight was measured and leaf N content was determined with a Vario MICRO Cube Elemental Analyzer (Elementar Analysensysteme GmbH, Langenselbold, Germany) (Sakowska et al., 2018).

## Statistical Analysis

For each N treatment, five leaves from five independent plants were used for gas exchange and chlorophyll fluorescence measurements. One-way ANOVA and *t*-tests were used to determine whether significant differences existed between different treatments ( $\alpha = 0.05$ ). The software SigmaPlot 10.0 was used for graphing and fitting.

## RESULTS

### Effect of Leaf N Content on Steady-State Physiological Characteristics Under High Light

The leaf N content in LN-, MN-, and HN-plants was  $0.42 \pm 0.03$ ,  $0.71 \pm 0.3$ , and  $1.2 \pm 0.07$  g m<sup>-2</sup>, respectively (Table 1). The HN-plants displayed the highest relative chlorophyll content, measured by SPAD value, followed by MN- and LN-plants. After 30 min light adaptation at 1,500 μmol photons m<sup>-2</sup> s<sup>-1</sup> and 400 μmol mol<sup>-1</sup> CO<sub>2</sub> concentration, HN-plants had the highest net CO<sub>2</sub> assimilation rate (*A<sub>N</sub>*), stomatal conductance (*g<sub>s</sub>*), mesophyll conductance (*g<sub>m</sub>*), and ETR. Therefore, the steady-state photosynthetic capacities were significantly affected by leaf N content. Furthermore, HN-, MN-, and LN-plants showed slight difference in *g<sub>s</sub>* but significant difference in *g<sub>m</sub>*, which indicates that *g<sub>m</sub>* is more responsive to leaf N content than *g<sub>s</sub>* in tomato.

### Effects of Leaf N Content on Photosynthetic Induction Upon Transfer From Low to High Light

During this photosynthetic induction after 5 min of shade-fleck, HN-plants showed the highest induction speeds of *A<sub>N</sub>*, *g<sub>s</sub>*, and *g<sub>m</sub>*, followed by MN- and LN-plants (Figure 1). The time required to reach 90% of the maximum *A<sub>N</sub>* (*t<sub>90AN</sub>*) significantly increased with the decrease in leaf N content (Figure 1G). The time required to reach 90% of the maximum *g<sub>s</sub>* and *g<sub>m</sub>* (*t<sub>90gs</sub>* and *t<sub>90gm</sub>*, respectively) was significantly shorter in HN-plants than MN- and LN-plants, whereas *t<sub>90gs</sub>* and *t<sub>90gm</sub>* did



not differ significantly between MN- and LN-plants (**Figure 1G**). Interestingly,  $t_{90g_m}$  was lower than  $t_{90g_s}$  in all plants. The higher  $t_{90g_s}$  and  $t_{90A_N}$  in MN- and LN-plants were

partially related to the relatively lower initial  $g_s$  prior to light change (**Supplementary Figure 1**). Within the first 15 min after transition from low to high light, all plants showed similar intrinsic water use efficiency (iWUE) (**Supplementary Figure 2**). However, during prolonged photosynthetic induction, HN-plants displayed much higher iWUE than MN- and LN-plants (**Supplementary Figure 2**). Further analysis found that leaf N content was negatively correlated with  $t_{90A_N}$ ,  $t_{90g_s}$ , and  $t_{90g_m}$  (**Figure 2**). Therefore, leaf N content plays a crucial role in affecting the induction responses of  $A_N$ ,  $g_s$ , and  $g_m$  after transition from low to high light. The comparative extent of the reductions of  $t_{90A_N}$  was more correlated to  $t_{90g_m}$  than  $t_{90g_s}$  (**Figure 3A**). Furthermore, the change in  $A_N$  during photosynthetic induction was more related to  $g_m$  than  $g_s$  (**Figures 3B,C**). These results suggest that, upon transfer from low to high light,  $g_m$  plays a more important role in determining the induction response of  $A_N$  than  $g_s$ .

## Effects of Leaf N Content on Intercellular and Chloroplast $\text{CO}_2$ Concentrations Upon Transfer From Low to High Light

We calculated the response kinetics of intercellular ( $C_i$ ) and chloroplast  $\text{CO}_2$  concentration ( $C_c$ ) using  $A_N$ ,  $g_s$ , and  $g_m$ . After transitioning from low to high light,  $C_i$  and  $C_c$  gradually increased in all plants (**Figure 4**). HN-plants had the lowest values of  $C_i$  and  $C_c$  after photosynthetic sufficient photosynthetic induction. The change in  $A_N$  during photosynthetic induction was tightly and positively correlated with  $C_c$  in all plants, which suggests the importance of  $C_c$  in determining  $A_N$ . Because  $C_c$  can be affected by  $g_s$  and  $g_m$ , we analyzed the relationships between  $C_c$ ,  $g_s$ , and  $g_m$ . Compared with  $g_s$ , a smaller change in  $g_m$  could result in a larger change in  $C_c$  (**Figure 5**), which suggests that the change of  $C_c$  upon transfer from low to high light was more determined by  $g_m$  than  $g_s$ .

## Effects of Leaf N Content on Relative Limitations of Photosynthesis Upon Transfer From Low to High Light

After transition from low to high light, the limitations of photosynthesis by  $g_s$  ( $L_{gs}$ ),  $g_m$  ( $L_{gm}$ ), and biochemical factors ( $L_b$ ) changed slightly in HN-plants (**Figure 6**). In MN- and LN-plants,

$L_{gs}$  gradually decreased over time. Within the first 15 min,  $L_{gs}$  was lower in HN-plants than MN- and LN-plants. However, the LN-plants had the lowest  $L_{gs}$  after sufficient photosynthetic induction.  $L_{gm}$  was also maintained stable during whole photosynthetic induction in MN- and LN-plants, but  $L_b$  gradually increased from 0.3 to 0.5 in them. Therefore, leaf N content could affect the kinetics of relative limitations of photosynthesis during photosynthetic induction after transfer from low to high light. To explore whether the induction of  $A_N$  is limited by photosynthetic electron transport, we estimated the dynamic change in ETR. Upon a sudden increase in illumination, ETR rapidly increased and the  $\text{ETR}/(A_N + R_d)$  ratio first increased and then gradually decreased in all plants (**Figure 7**). These results indicated that the activation speed of ETR was much faster than that of  $A_N$ . Therefore, during photosynthetic induction, the limitation of ETR imposed to  $A_N$  was negligible in all samples.

## DISCUSSION

Leaf N content plays an important role in determining photosynthesis, plant growth, and crop productivity (Makino, 2011). Under natural field conditions, FL and N deficiency usually occurs concomitantly. However, it is unknown how FL and N deficiency interacts to influence photosynthetic physiology in crop plants. In this study, we here for the first time examined the effects of leaf N content on photosynthetic induction after transition from low to high light in tomato. We found that leaf N content significantly affected the induction responses of  $g_s$  and  $g_m$  and thus affected induction kinetics of  $A_N$ . However, the activation speed of photosynthetic electron flow was not influenced by leaf N content. Therefore, the effect of leaf N content on photosynthetic induction was more attributed to the induction kinetics of diffusional conductance rather than the activation speed of electron transport.

In addition to steady-state photosynthetic capacity under high light, the photosynthetic responses to the changes in illumination significantly affect the carbon gain and plant biomass (Adachi et al., 2019; Kimura et al., 2020; Zhang et al., 2020). Many previous studies have documented that leaf N content influences the steady-state photosynthetic performances under high light (Evans and Terashima, 1988; Makino and Osmond, 1991), but few is known about the influence of leaf N content on photosynthetic induction under FL conditions. Similar to previous studies, the maximum steady-state  $A_N$  under high

**TABLE 1** | Physiological characteristics of leaves from plants grown under three different nutrient concentrations (low, medium and high nitrogen).

	Low N	Medium N	High N
Leaf N content ( $\text{g m}^{-2}$ )	$0.42 \pm 0.03a$	$0.71 \pm 0.3b$	$1.2 \pm 0.07c$
SPAD value	$29.2 \pm 1.2a$	$40.2 \pm 1.7b$	$50.1 \pm 1.7c$
$A_N$ ( $\mu\text{mol m}^{-2} \text{s}^{-1}$ )	$5.9 \pm 0.3a$	$10.2 \pm 0.29b$	$19.1 \pm 0.67c$
$g_s$ ( $\text{mol m}^{-2} \text{s}^{-1}$ )	$0.22 \pm 0.02a$	$0.25 \pm 0.01a$	$0.31 \pm 0.01b$
$g_m$ ( $\text{mol m}^{-2} \text{s}^{-1}$ )	$0.045 \pm 0.002a$	$0.09 \pm 0.007b$	$0.19 \pm 0.01c$
ETR ( $\mu\text{mol m}^{-2} \text{s}^{-1}$ )	$44 \pm 2.7c$	$80 \pm 2.0b$	$156 \pm 3.9a$

All parameters were measured at  $1,500 \mu\text{mol photons m}^{-2} \text{s}^{-1}$  and  $400 \mu\text{mol mol}^{-1} \text{CO}_2$  concentration. Values are means  $\pm$  SE ( $n = 5$ ). Different letters indicate significant differences among different treatments.

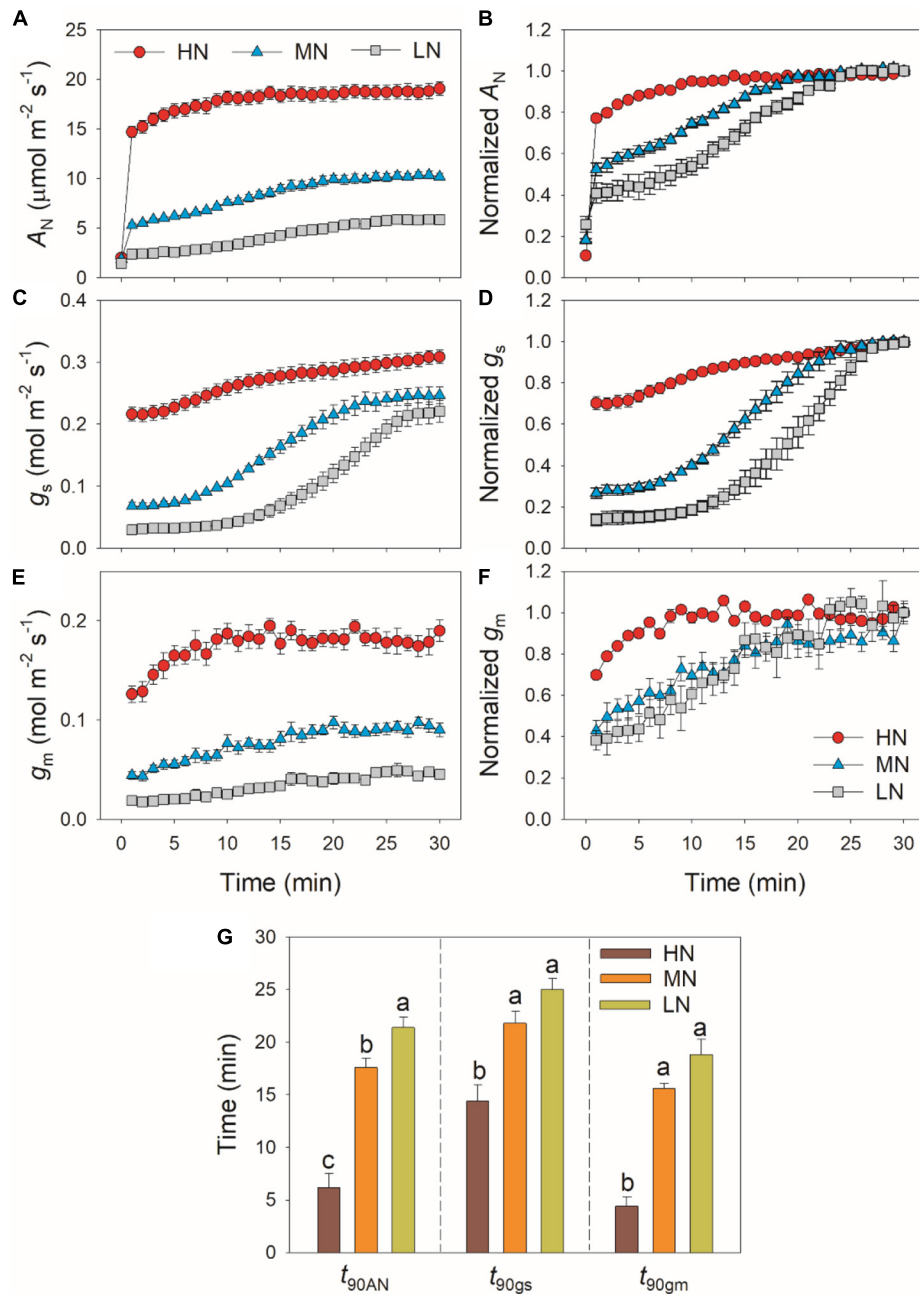
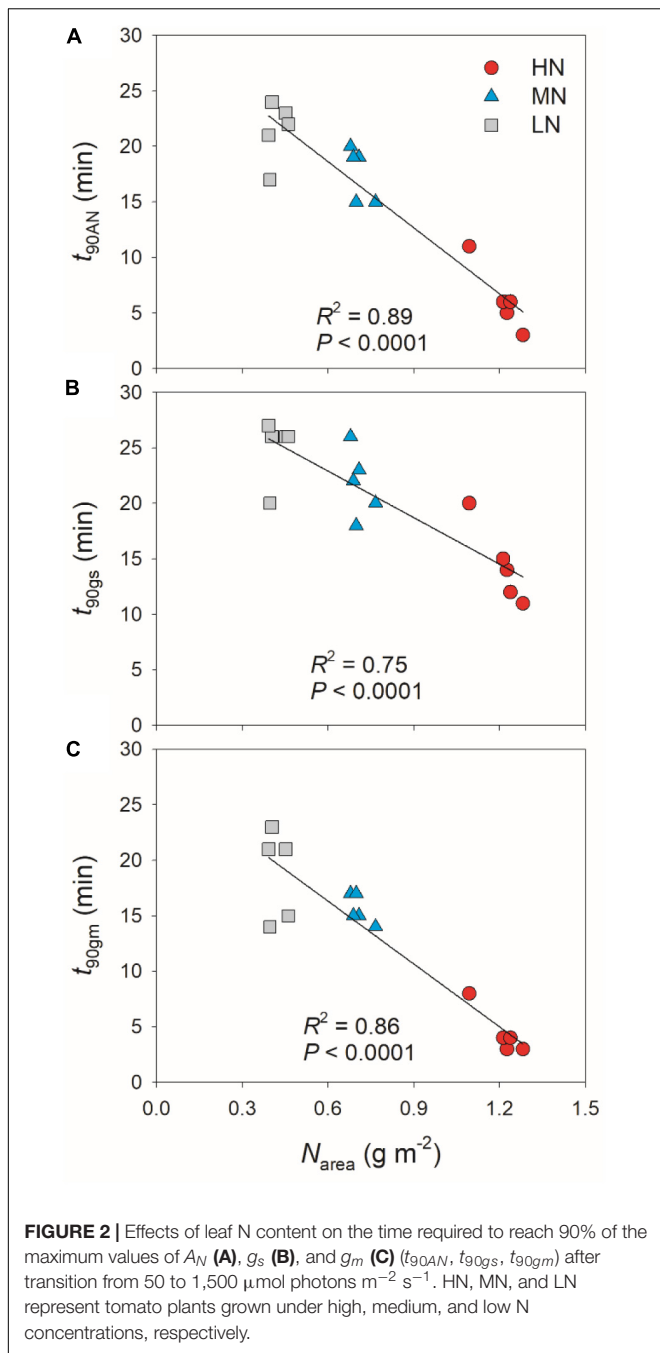


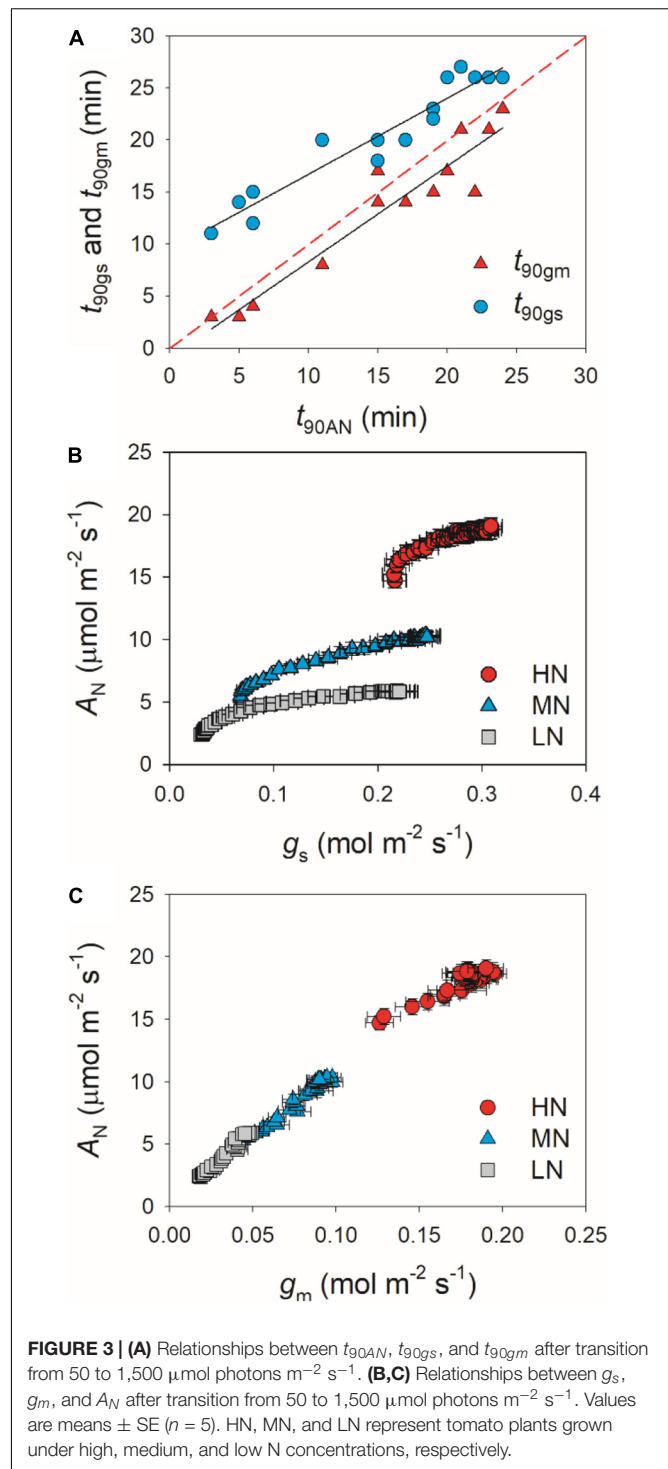
**FIGURE 1 |** Induction response of net CO<sub>2</sub> assimilation rate ( $A_N$ ) (A,B), stomatal conductance ( $g_s$ ) (C,D) and mesophyll conductance ( $g_m$ ) (E,F), and the time required to reach 90% of the maximum values of  $A_N$ ,  $g_s$  and  $g_m$  ( $t_{90AN}$ ,  $t_{90gs}$ ,  $t_{90gm}$ ) (G) after transition from 50 to 1,500  $\mu\text{mol photons m}^{-2} \text{s}^{-1}$ .  $A_N$ ,  $g_s$ , and  $g_m$  were measured every 1 min. Values are means  $\pm$  SE ( $n = 5$ ). Different letters indicate significant differences among different treatments. The relative  $A_N$ ,  $g_s$ , and  $g_m$  curves were obtained from the standardization against the maximum values after 30 min photosynthetic induction at high light. HN, MN, and LN represent tomato plants grown under high, medium, and low N concentrations, respectively.

light significantly declined with the decrease in leaf N content (Table 1). Moreover, we here found that, after transition from low to high light, the HN-plants showed much faster induction response of  $A_N$  than MN- and LN-plants (Figure 1). The time required to reach 90% of the steady state of photosynthesis ( $t_{90AN}$ ) was negatively correlated to leaf N content (Figure 2).

Therefore, leaf N content significantly affects the photosynthetic induction after transition from low to high light in tomato. This finding is similar to the photosynthetic induction of dark-adapted leaves among canola genotypes (*Brassica napus* L.) (Liu et al., 2021), but was inconsistent with the phenomenon in soybean (Li et al., 2020) and *Panax notoginseng* (Chen et al., 2014). In

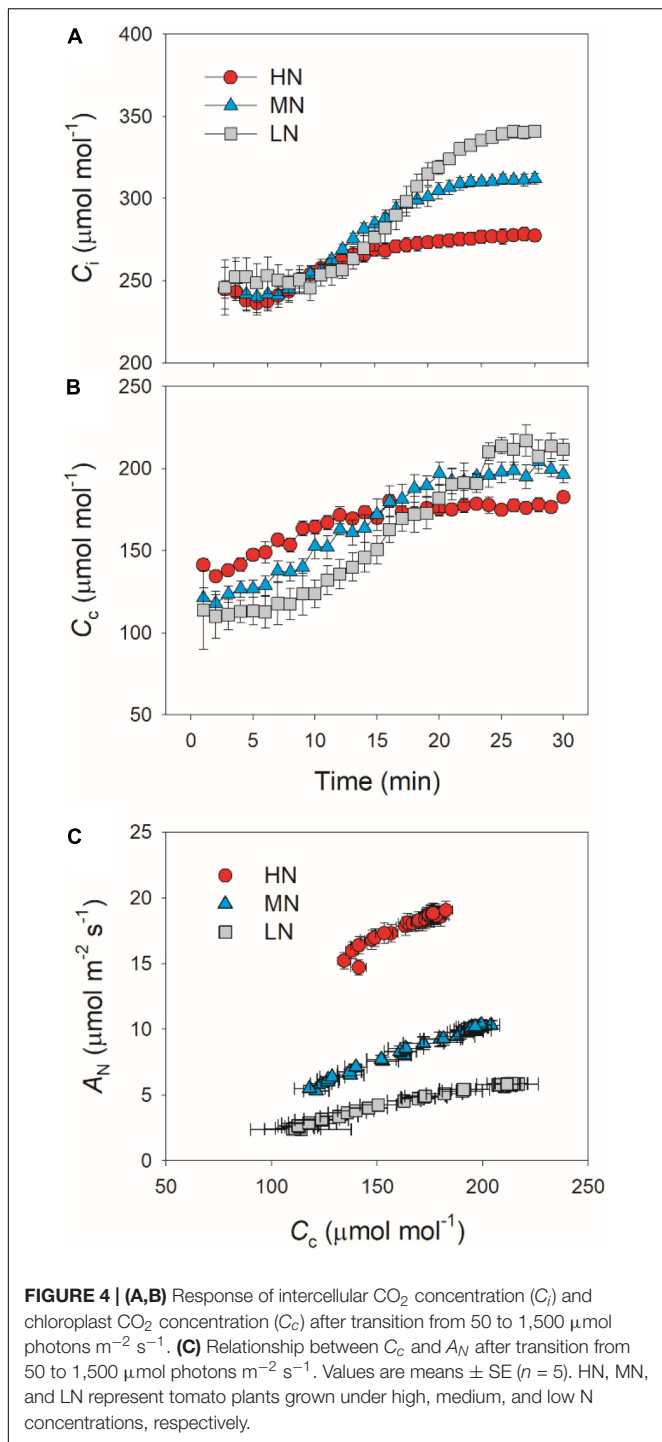


soybean, the induction rate of  $A_N$  under high light after shading for 5 min was very fast (Pearcy et al., 1996; Li et al., 2020). Furthermore, this fast photosynthetic induction in soybean was not affected by leaf N content (Li et al., 2020). In the shade-establishing plant *Panax notoginseng*, the higher leaf N content in shade leaves was accompanied with slower photosynthetic induction rate than sun leaves (Chen et al., 2014). Therefore, the effect of leaf N content on fast photosynthetic induction following shade fleck depends on the species and on growth conditions. In MN- and LN-plants of tomato, the delayed induction of  $A_N$  caused a larger loss of carbon gain under FL.

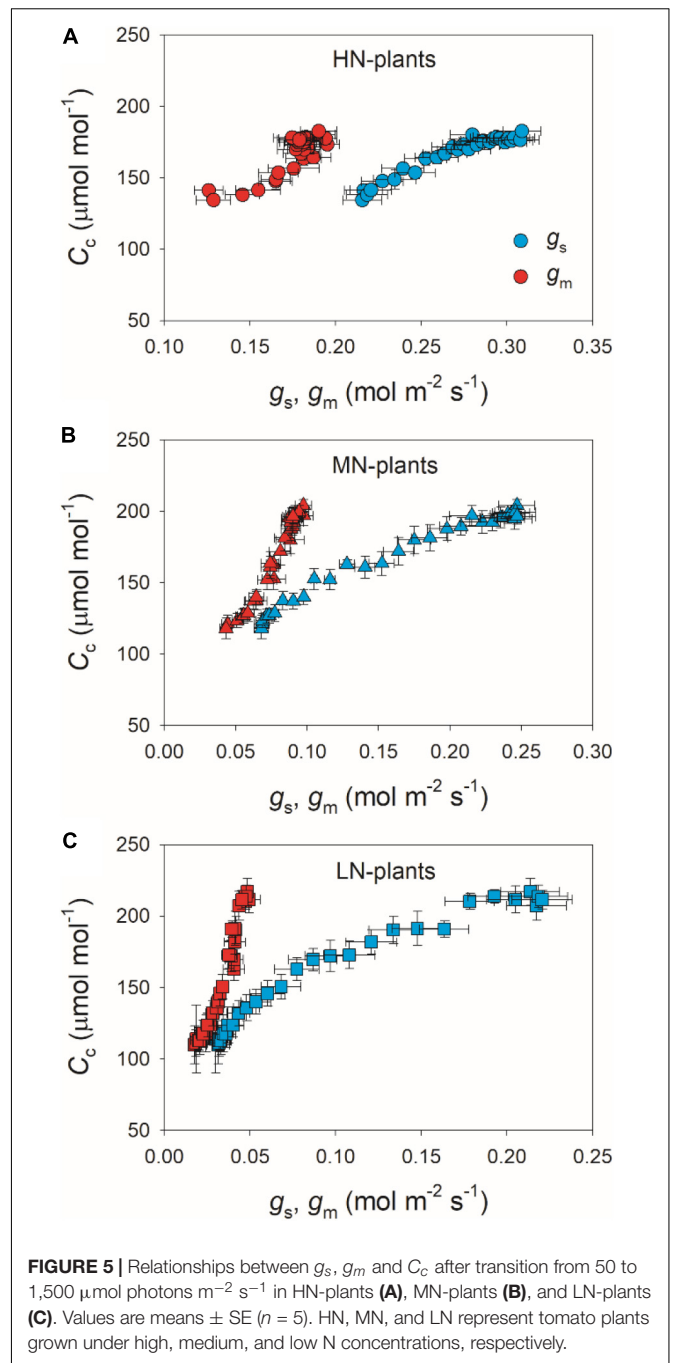


This finding provides insight into why plants grown under low N concentrations display reduction in plant biomass under natural field FL conditions.

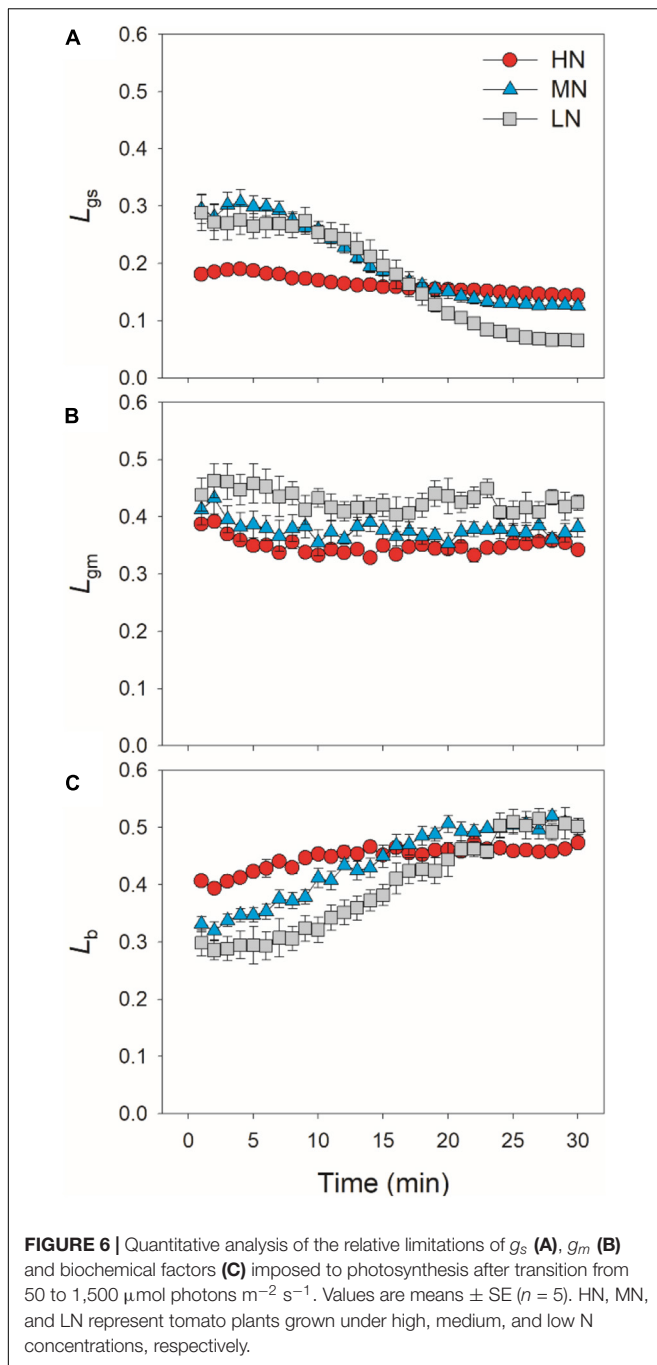
After transition from low to high light, the time to reach the maximum  $C_c$  was less in HN-plants than MN- and LN-plants (Figure 4). Furthermore, tight and positive relationships were found between  $C_c$  and  $A_N$  in all plants (Figure 4). These



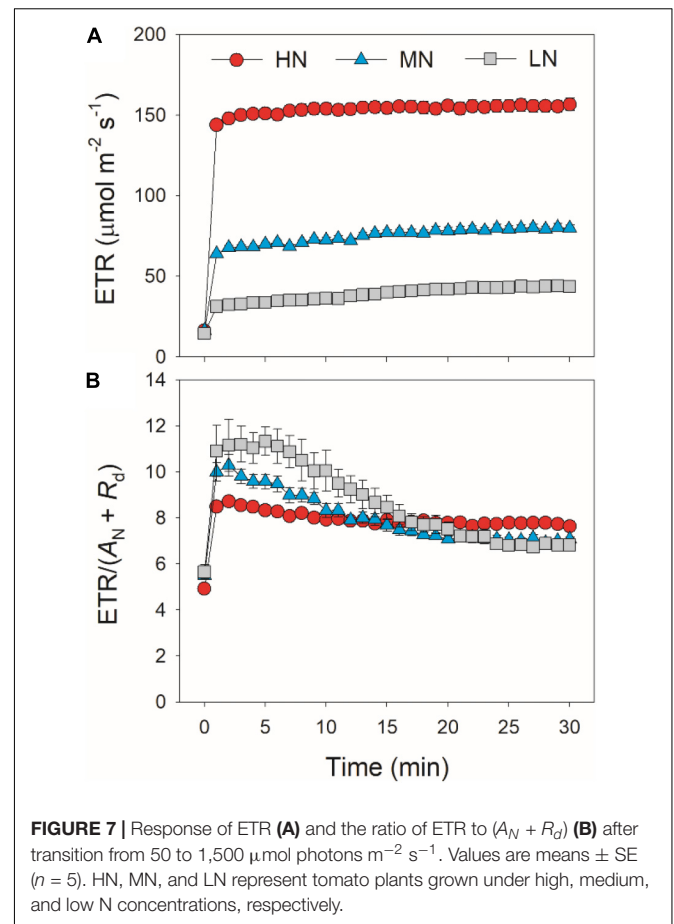
results suggested that the induction response of  $A_N$  was largely determined by the change of  $\text{CO}_2$  concentration in the site of RuBP carboxylation. The value of  $C_c$  in a given leaf is largely affected by  $\text{CO}_2$  diffusional conductance, which includes  $g_s$  and  $g_m$  (Sagardoy et al., 2010; Carriqui et al., 2015; Yang Z.-H. et al., 2018). However, it is unclear whether the photosynthetic induction of  $A_N$  upon transfer from low to high light is more determined by the induction response of  $g_s$  or  $g_m$ . We found that



the induction responses of  $g_s$  and  $g_m$  were largely delayed in MN- and LN-plants than HN-plants (Figure 1), and the induction rates of  $g_s$  and  $g_m$  were negatively correlated with leaf N content (Figure 2). Furthermore, the change of  $C_c$  during photosynthetic induction was more related to  $g_m$  rather than  $g_s$  (Figure 5), which pointing out the important role of  $g_m$  response in determining  $C_c$  upon transfer from low to high light. Therefore, the delayed photosynthetic induction of  $A_N$  in plants grown under low N concentrations was more attributed to the slower induction response of  $g_m$  than  $g_s$ .



In HN-plants of tomato, photosynthetic limitations by  $g_s$ ,  $g_m$ , and biochemical factors changed slightly upon transfer from low to high light. Meanwhile,  $g_s$  imposed to the smallest limitation to  $A_N$ , owing to the high levels of  $g_s$  (Figure 6). Therefore, improving the induction response of  $g_s$  might have a minor factor for improving photosynthesis under FL in HN-plants of tomato under optimal conditions (Kaiser et al., 2020). By comparison, increased  $g_s$  has a significant effect on photosynthetic  $\text{CO}_2$  assimilation under FL in *Arabidopsis thaliana* and rice (Kimura et al., 2020; Yamori et al., 2020). These results indicate that



the effects of altered  $g_s$  kinetics on photosynthesis under FL are species-dependent. In MN- and LN-plants, the relatively slower kinetics of  $g_s$  led to a higher  $L_{g_s}$  of  $A_N$  during the initial 15 min after transition from low to high light (Figure 6). Therefore, altered  $g_s$  kinetics would have more significant effects on photosynthetic carbon gain in crop plants grown under low N concentrations.

Many previous studies have indicated that  $g_m$  act as a major limitation for steady-state  $A_N$  under high light in many angiosperms (Peguero-Pina et al., 2017; Thérout-Rancourt and Gilbert, 2017; Yang Y.-J. et al., 2018; Huang et al., 2019). Increasing  $g_m$  has been thought to be a potential target for improving crop productivity and water use efficiency under constant high light (Flexas et al., 2013; Gago et al., 2016). However, the limitation of  $g_m$  imposed to  $A_N$  under FL is poorly understood. Upon transition from dark to light, the induction response of  $g_m$  was much faster than that of  $g_s$ , which leads to the smallest limitation of  $g_m$  imposed to  $A_N$  in *Arabidopsis thaliana* and tobacco (Sakoda et al., 2021). Consequently, one concluded that altering  $g_m$  kinetics would have less impact on  $A_N$  under FL. However, we found that, after transfer from low to high light,  $L_{g_m}$  was higher than  $L_{g_s}$  in tomato plants (Figure 6). Furthermore, the time to reach 90% of  $A_N$  was closer to that of  $g_m$  rather than that of  $g_s$  (Figure 3). Therefore, altering  $g_m$  kinetics would significantly influence  $A_N$  upon transfer from low



to high light, at least in tomato. These results suggested that the photosynthetic limitation upon transfer from low to high light was largely different from the photosynthetic induction during illumination of dark-adapted leaves. Improving the induction rate of  $g_m$  has a potential to enhance carbon gain and plant biomass under natural FL conditions.

A recent study reported that, if RuBP regeneration limitation was assumed, electron transport imposed the greatest limitation to  $A_N$  during illumination of dark-adapted leaves (Sakoda et al., 2021). Based on this result, it is hypothesized that increased activation of electron transport has the potential to enhance carbon gain under naturally FL environments. Controversially, this study indicated that electron transport was rapidly activated upon transfer from low to high light. After transition from low to high light, the  $ETR/(A_N + R_d)$  value rapidly increased to the peak within 1–2 min and then gradually decreased over time (Figure 7). These results indicated that, upon transfer from low to high light, the induction response of electron transport was much faster than that of  $A_N$ , which was consistent with the photosynthetic performance in rice (Yamori et al., 2016b). Therefore, induction response of  $A_N$  after transition from low to high light was hardly limited by electron transport in tomato. The effect of electron transport on  $A_N$  upon transition from low to high light is largely different from that upon transition from dark to light. Therefore, to improve photosynthesis under FL in tomato, more attention should be focused on the induction kinetics of  $CO_2$  diffusional conductance rather than the activation of electron transport.

## CONCLUSION

We studied the effects of leaf N content on photosynthetic induction after transfer from low to high light in tomato. The induction speeds of  $A_N$ ,  $g_s$ , and  $g_m$  significantly decreased with the decrease in leaf N content. Such delayed photosynthetic induction in plants grown under low N concentration caused a larger loss of carbon gain under FL conditions, which further explained why N deficiency reduced plant biomass under natural FL environments. After transition from low to high light, increasing the induction responses of  $g_s$  and  $g_m$  has the potential

to improve  $A_N$  in tomato, especially when plants are grown under low N concentration, whereas photosynthetic induction of  $A_N$  was hardly limited by electron transport. Therefore, altering induction kinetics of  $CO_2$  diffusional conductance is likely the most effective target for improving photosynthesis under FL conditions in tomato.

## DATA AVAILABILITY STATEMENT

The raw data supporting the conclusions of this article will be made available by the authors, without undue reservation.

## AUTHOR CONTRIBUTIONS

WH and S-BZ designed the study. HS performed the photosynthetic measurements. HS, Y-QZ, and WH performed the data analysis. WH wrote the first draft of the manuscript, which was extensively edited by all authors.

## FUNDING

This work was supported by the National Natural Science Foundation of China (grant nos. 31971412 and 32171505) and the Project for Innovation Team of Yunnan Province (202105AE160012).

## SUPPLEMENTARY MATERIAL

The Supplementary Material for this article can be found online at: <https://www.frontiersin.org/articles/10.3389/fpls.2022.835571/full#supplementary-material>

**Supplementary Figure 1** | Relationships between  $t_{90AN}$  (A),  $t_{90gs}$  (B), and the initial  $g_s$  prior to light change. HN, MN, and LN represent tomato plants grown under high, medium, and low N concentrations, respectively.

**Supplementary Figure 2** | Response of intrinsic water use efficiency (iWUE) after transition from 50 to 1,500  $\mu\text{mol photons m}^{-2} \text{s}^{-1}$ . Values are means  $\pm$  SE ( $n = 5$ ). HN, MN, and LN represent tomato plants grown under high, medium, and low N concentrations, respectively.

## REFERENCES

- Adachi, S., Tanaka, Y., Miyagi, A., Kashima, M., Tezuka, A., Toya, Y., et al. (2019). High-yielding rice Takanari has superior photosynthetic response to a commercial rice Koshihikari under fluctuating light. *J. Exp. Bot.* 70, 5287–5297. doi: 10.1093/jxb/erz304
- Baker, N. R. (2004). Applications of chlorophyll fluorescence can improve crop production strategies: an examination of future possibilities. *J. Exp. Bot.* 55, 1607–1621. doi: 10.1093/jxb/erh196
- Carriqui, M., Cabrera, H. M., Conesa, M., Coopman, R. E., Douthe, C., Gago, J., et al. (2015). Diffusional limitations explain the lower photosynthetic capacity of ferns as compared with angiosperms in a common garden study. *Plant Cell Environ.* 38, 448–460. doi: 10.1111/pce.12402
- Chen, J.-W., Kuang, S.-B., Long, G.-Q., Meng, Z.-G., Li, L.-G., Chen, Z.-J., et al. (2014). Steady-state and dynamic photosynthetic performance and nitrogen partitioning in the shade-demanding plant *Panax notoginseng* under different levels of growth irradiance. *Acta Physiol. Plant.* 36, 2409–2420. doi: 10.1007/s11738-014-1614-9
- De Souza, A. P., Wang, Y., Orr, D. J., Carmo-Silva, E., and Long, S. P. (2020). Photosynthesis across African cassava germplasm is limited by Rubisco and mesophyll conductance at steady state, but by stomatal conductance in fluctuating light. *New Phytol.* 225, 2498–2512. doi: 10.1111/nph.16142
- Evans, J. R., and Terashima, I. (1988). Photosynthetic characteristics of spinach leaves grown with different nitrogen treatments. *Plant Cell Physiol.* 29, 157–165. doi: 10.1093/oxfordjournals.pcp.a077462
- Eyland, D., van Wesemael, J., Lawson, T., and Carpentier, S. (2021). The impact of slow stomatal kinetics on photosynthesis and water use efficiency under fluctuating light. *Plant Physiol.* 186, 998–1012. doi: 10.1093/PLPHYS/KIA B114
- Fan, X., Cao, X., Zhou, H., Hao, L., Dong, W., He, C., et al. (2020). Carbon dioxide fertilization effect on plant growth under soil water stress associates with changes in stomatal traits, leaf photosynthesis, and foliar nitrogen of bell

- pepper (*Capsicum annuum* L.). *Environ. Exp. Bot.* 179:104203. doi: 10.1016/j.envexpbot.2020.104203
- Farquhar, G. D., von Caemmerer, S., and Berry, J. A. (1980). A biochemical model of photosynthetic CO<sub>2</sub> assimilation in leaves of C<sub>3</sub> species. *Planta* 149, 78–90. doi: 10.1007/BF00386231
- Ferroni, L., Brestì, M., Živěak, M., Cantelli, R., and Pancaldi, S. (2021). Increased photosynthesis from a deep-shade to high-light regime occurs by enhanced CO<sub>2</sub> diffusion into the leaf of *Selaginella martensii*. *Plant Physiol. Biochem.* 160, 143–154. doi: 10.1016/j.plaphy.2021.01.012
- Ferroni, L., Živěak, M., Sytar, O., Kovár, M., Watanabe, N., Pancaldi, S., et al. (2020). Chlorophyll-depleted wheat mutants are disturbed in photosynthetic electron flow regulation but can retain an acclimation ability to a fluctuating light regime. *Environ. Exp. Bot.* 178:104156. doi: 10.1016/j.envexpbot.2020.104156
- Flexas, J., Niinemets, Ü., Gallé, A., Barbour, M. M., Centritto, M., Diaz-Espejo, A., et al. (2013). Diffusional conductances to CO<sub>2</sub> as a target for increasing photosynthesis and photosynthetic water-use efficiency. *Photosynth. Res.* 117, 45–59. doi: 10.1007/s11120-013-9844-z
- Gago, J., Daloso, D. M., Carriqui, M., Nadal, M., Morales, M., Araújo, W. L., et al. (2020). The photosynthesis game is in the “inter-play”: mechanisms underlying CO<sub>2</sub> diffusion in leaves. *Environ. Exp. Bot.* 178:104174. doi: 10.1016/j.envexpbot.2020.104174
- Gago, J., Daloso, D., de, M., Figueroa, C. M., Flexas, J., Fernie, A. R., et al. (2016). Relationships of Leaf Net photosynthesis, stomatal conductance, and mesophyll conductance to primary metabolism: a multispecies meta-analysis approach. *Plant Physiol.* 171, 265–279. doi: 10.1104/pp.15.01660
- Genty, B., Briantais, J.-M., and Baker, N. R. (1989). The relationship between the quantum yield of photosynthetic electron transport and quenching of chlorophyll fluorescence. *Biochim. Biophys. Acta Gen. Subj.* 990, 87–92. doi: 10.1016/S0304-4165(89)80016-9
- Grassi, G., and Magnani, F. (2005). Stomatal, mesophyll conductance and biochemical limitations to photosynthesis as affected by drought and leaf ontogeny in ash and oak trees. *Plant Cell Environ.* 28, 834–849. doi: 10.1111/j.1365-3040.2005.01333.x
- Harley, P. C., Loreto, F., Di Marco, G., and Sharkey, T. D. (1992). Theoretical considerations when estimating the mesophyll conductance to CO<sub>2</sub> flux by analysis of the response of photosynthesis to CO<sub>2</sub>. *Plant Physiol.* 98, 1429–1436. doi: 10.1104/pp.98.4.1429
- Huang, W., Yang, Y.-J., Wang, J.-H., and Hu, H. (2019). Photorespiration is the major alternative electron sink under high light in alpine evergreen sclerophyllous *Rhododendron* species. *Plant Sci.* 289:110275. doi: 10.1016/j.plantsci.2019.110275
- Kaiser, E., Morales, A., Harbinson, J., Heuvelink, E., and Marcelis, L. F. M. (2020). High stomatal conductance in the tomato flacca mutant allows for faster photosynthetic induction. *Front. Plant Sci.* 11:1317. doi: 10.3389/fpls.2020.01317
- Kebeish, R., Niessen, M., Thiruveedhi, K., Bari, R., Hirsch, H.-J., Rosenkranz, R., et al. (2007). Chloroplastic photorespiratory bypass increases photosynthesis and biomass production in *Arabidopsis thaliana*. *Nat. Biotechnol.* 25, 593–599. doi: 10.1038/nbt1299
- Kimura, H., Hashimoto-Sugimoto, M., Iba, K., Terashima, I., and Yamori, W. (2020). Improved stomatal opening enhances photosynthetic rate and biomass production in fluctuating light. *J. Exp. Bot.* 71, 2339–2350. doi: 10.1093/jxb/eraa090
- Krall, J. P., and Edwards, G. E. (1992). Relationship between photosystem II activity and CO<sub>2</sub> fixation in leaves. *Physiol. Plant.* 86, 180–187. doi: 10.1111/j.1399-3054.1992.tb01328.x
- Kromdijk, J., Glowacka, K., Leonelli, L., Gabilly, S. T., Iwai, M., Niyogi, K. K., et al. (2016). Improving photosynthesis and crop productivity by accelerating recovery from photoprotection. *Science* 354, 857–861. doi: 10.1126/science.aai8878
- Li, Y.-T., Li, Y., Li, Y.-N., Liang, Y., Sun, Q., Li, G., et al. (2020). Dynamic light caused less photosynthetic suppression, rather than more, under nitrogen deficit conditions than under sufficient nitrogen supply conditions in soybean. *BMC Plant Biol.* 20:339. doi: 10.1186/s12870-020-02516-y
- Liu, J., Zhang, J., Estavillo, G. M., Luo, T., and Hu, L. (2021). Leaf N content regulates the speed of photosynthetic induction under fluctuating light among canola genotypes (*Brassica napus* L.). *Physiol. Plant.* 172, 1844–1852. doi: 10.1111/ppl.13390
- Long, S. P., and Bernacchi, C. J. (2003). Gas exchange measurements, what can they tell us about the underlying limitations to photosynthesis? Procedures and sources of error. *J. Exp. Bot.* 54, 2393–2401. doi: 10.1093/jxb/erg262
- Makino, A. (2011). Photosynthesis, grain yield, and nitrogen utilization in rice and wheat. *Plant Physiol.* 155, 125–129. doi: 10.1104/pp.110.165076
- Makino, A., and Osmond, B. (1991). Effects of nitrogen nutrition on nitrogen partitioning between chloroplasts and mitochondria in pea and wheat. *Plant Physiol.* 96, 355–362. doi: 10.1104/pp.96.2.355
- Pearcy, R. W. (1990). Sunflecks and photosynthesis in plant canopies. *Annu. Rev. Plant Physiol. Plant Mol. Biol.* 41, 421–453. doi: 10.1146/annurev.pp.41.060190.002225
- Pearcy, R. W., Krall, J. P., and Sassenrath-Cole, G. F. (1996). “Photosynthesis in fluctuating light environments,” in *Photosynthesis and the Environment*, ed. N. R. Baker (Dordrecht: Kluwer Academic Publishers), 321–346. doi: 10.1007/0-306-48135-9\_13
- Peguero-Pina, J. J., Sisó, S., Flexas, J., Galmés, J., García-Nogales, A., Niinemets, Ü., et al. (2017). Cell-level anatomical characteristics explain high mesophyll conductance and photosynthetic capacity in sclerophyllous Mediterranean oaks. *New Phytol.* 214, 585–596. doi: 10.1111/nph.14406
- Sagardoy, R., Vázquez, S., Florez-Sarasa, I. D., Albacete, A., Ribas-Carbo, M., Flexas, J., et al. (2010). Stomatal and mesophyll conductances to CO<sub>2</sub> are the main limitations to photosynthesis in sugar beet (*Beta vulgaris*) plants grown with excess zinc. *New Phytol.* 187, 145–158. doi: 10.1111/j.1469-8137.2010.03241.x
- Sakoda, K., Yamori, W., Groszmann, M., and Evans, J. R. (2021). Stomatal, mesophyll conductance, and biochemical limitations to photosynthesis during induction. *Plant Physiol.* 185, 146–160. doi: 10.1093/plphys/kiaa011
- Sakoda, K., Yamori, W., Shimada, T., Sugano, S. S., Hara-Nishimura, I., and Tanaka, Y. (2020). Higher stomatal density improves photosynthetic induction and biomass production in *Arabidopsis* under fluctuating light. *Front. Plant Sci.* 11:1308. doi: 10.3389/fpls.2020.589603
- Sakowska, K., Alberti, G., Genesio, L., Peressotti, A., Delle Vedove, G., Gianelle, D., et al. (2018). Leaf and canopy photosynthesis of a chlorophyll deficient soybean mutant. *Plant. Cell Environ.* 41, 1427–1437. doi: 10.1111/pce.13180
- Slattery, R. A., Walker, B. J., Weber, A. P. M., and Ort, D. R. (2018). The impacts of fluctuating light on crop performance. *Plant Physiol.* 176, 990–1003. doi: 10.1104/pp.17.01234
- South, P. F., Cavanagh, A. P., Liu, H. W., and Ort, D. R. (2019). Synthetic glycolate metabolism pathways stimulate crop growth and productivity in the field. *Science* 363:eaa9077. doi: 10.1126/science.aat9077
- Sudo, E., Makino, A., and Mae, T. (2003). Differences between rice and wheat in ribulose-1,5-bisphosphate regeneration capacity per unit of leaf-N content. *Plant Cell Environ.* 26, 255–263. doi: 10.1046/j.1365-3040.2003.00955.x
- Takahashi, T., Hikosaka, K., and Hirose, T. (2004). Photosynthesis or persistence: nitrogen allocation in leaves of evergreen and deciduous *Quercus* species. *Plant Cell Environ.* 27, 1047–1054. doi: 10.1111/j.1365-3040.2004.01209.x
- Tazoe, Y., Von Caemmerer, S., Badger, M. R., and Evans, J. R. (2009). Light and CO<sub>2</sub> do not affect the mesophyll conductance to CO<sub>2</sub> diffusion in wheat leaves. *J. Exp. Bot.* 60, 2291–2301. doi: 10.1093/jxb/erp035
- Thérault-Rancourt, G., and Gilbert, M. E. (2017). The light response of mesophyll conductance is controlled by structure across leaf profiles. *Plant Cell Environ.* 40, 726–740. doi: 10.1111/pce.12890
- Timm, S., Florian, A., Arrivault, S., Stitt, M., Fernie, A. R., and Bauwe, H. (2012). Glycine decarboxylase controls photosynthesis and plant growth. *FEBS Lett.* 586, 3692–3697. doi: 10.1016/j.febslet.2012.08.027
- Timm, S., Wittmiß, M., Gamliel, S., Ewald, R., Florian, A., Frank, M., et al. (2015). Mitochondrial dihydrolipoyl dehydrogenase activity shapes photosynthesis and photorespiration of *Arabidopsis thaliana*. *Plant Cell* 27, 1968–1984. doi: 10.1105/tpc.15.00105
- von Caemmerer, S., and Evans, J. R. (2015). Temperature responses of mesophyll conductance differ greatly between species. *Plant Cell Environ.* 38, 629–637. doi: 10.1111/pce.12449
- Warren, C. R., and Dreyer, E. (2006). Temperature response of photosynthesis and internal conductance to CO<sub>2</sub>: results from two independent approaches. *J. Exp. Bot.* 57, 3057–3067. doi: 10.1093/jxb/erl067



- Xiong, D., Douthe, C., and Flexas, J. (2018). Differential coordination of stomatal conductance, mesophyll conductance, and leaf hydraulic conductance in response to changing light across species. *Plant. Cell Environ.* 41, 436–450. doi: 10.1111/pce.13111
- Xiong, D., Liu, X., Liu, L., Douthe, C., Li, Y., Peng, S., et al. (2015). Rapid responses of mesophyll conductance to changes of CO<sub>2</sub> concentration, temperature and irradiance are affected by N supplements in rice. *Plant Cell Environ.* 38, 2541–2550. doi: 10.1111/pce.12558
- Yamori, W., Evans, J. R., and Von Caemmerer, S. (2010a). Effects of growth and measurement light intensities on temperature dependence of CO<sub>2</sub> assimilation rate in tobacco leaves. *Plant Cell Environ.* 33, 332–343. doi: 10.1111/j.1365-3040.2009.02067.x
- Yamori, W., Noguchi, K., Hikosaka, K., and Terashima, I. (2010b). Phenotypic plasticity in photosynthetic temperature acclimation among crop species with different cold tolerances. *Plant Physiol.* 152, 388–399. doi: 10.1104/pp.109.145862
- Yamori, W., Kondo, E., Sugiura, D., Terashima, I., Suzuki, Y., and Makino, A. (2016a). Enhanced leaf photosynthesis as a target to increase grain yield: insights from transgenic rice lines with variable Rieske FeS protein content in the cytochrome b6/f complex. *Plant Cell Environ.* 39, 80–87. doi: 10.1111/pce.12594
- Yamori, W., Makino, A., and Shikanai, T. (2016b). A physiological role of cyclic electron transport around photosystem I in sustaining photosynthesis under fluctuating light in rice. *Sci. Rep.* 6:20147. doi: 10.1038/srep20147
- Yamori, W., Kusumi, K., Iba, K., and Terashima, I. (2020). Increased stomatal conductance induces rapid changes to photosynthetic rate in response to naturally fluctuating light conditions in rice. *Plant Cell Environ.* 43, 1230–1240. doi: 10.1111/pce.13725
- Yamori, W., Nagai, T., and Makino, A. (2011). The rate-limiting step for CO<sub>2</sub> assimilation at different temperatures is influenced by the leaf nitrogen content in several C3 crop species. *Plant Cell Environ.* 34, 764–777. doi: 10.1111/j.1365-3040.2011.02280.x
- Yang, K., Yang, J., Lv, C., Cao, P., Deng, X., Wang, Y., et al. (2021). Reduced mesophyll conductance induces photosynthetic acclimation of japonica rice under elevated CO<sub>2</sub>. *Environ. Exp. Bot.* 190:104590. doi: 10.1016/j.envexpbot.2021.104590
- Yang, Y.-J., Hu, H., and Huang, W. (2020). The light dependence of mesophyll conductance and relative limitations on photosynthesis in evergreen Sclerophyllous *Rhododendron* species. *Plants* 9:1536. doi: 10.3390/plants9111536
- Yang, Y.-J., Tong, Y.-G., Yu, G.-Y., Zhang, S.-B., and Huang, W. (2018). Photosynthetic characteristics explain the high growth rate for *Eucalyptus camaldulensis*: implications for breeding strategy. *Ind. Crops Prod.* 124, 186–191. doi: 10.1016/j.indcrop.2018.07.071
- Yang, Z.-H., Huang, W., Yang, Q.-Y., Chang, W., and Zhang, S.-B. (2018). Anatomical and diffusional determinants inside leaves explain the difference in photosynthetic capacity between *Cypripedium* and *Paphiopedilum*, Orchidaceae. *Photosynth. Res.* 136, 315–328. doi: 10.1007/s11120-017-0466-8
- Zhang, Y., Kaiser, E., Marcelis, L. F. M., Yang, Q., and Li, T. (2020). Salt stress and fluctuating light have separate effects on photosynthetic acclimation, but interactively affect biomass. *Plant Cell Environ.* 43, 2192–2206. doi: 10.1111/pce.13810
- Zivcak, M., Brestic, M., Balatova, Z., Drevenakova, P., Olsovska, K., Kalaji, H. M., et al. (2013). Photosynthetic electron transport and specific photoprotective responses in wheat leaves under drought stress. *Photosynth. Res.* 117, 529–546. doi: 10.1007/s11120-013-9885-3

**Conflict of Interest:** The authors declare that the research was conducted in the absence of any commercial or financial relationships that could be construed as a potential conflict of interest.

**Publisher's Note:** All claims expressed in this article are solely those of the authors and do not necessarily represent those of their affiliated organizations, or those of the publisher, the editors and the reviewers. Any product that may be evaluated in this article, or claim that may be made by its manufacturer, is not guaranteed or endorsed by the publisher.

Copyright © 2022 Sun, Zhang, Zhang and Huang. This is an open-access article distributed under the terms of the Creative Commons Attribution License (CC BY). The use, distribution or reproduction in other forums is permitted, provided the original author(s) and the copyright owner(s) are credited and that the original publication in this journal is cited, in accordance with accepted academic practice. No use, distribution or reproduction is permitted which does not comply with these terms.



# Cold Stress Resistance of Tomato (*Solanum lycopersicum*) Seedlings Is Enhanced by Light Supplementation From Underneath the Canopy

Tao Lu<sup>1†</sup>, Yangfan Song<sup>2,3†</sup>, Hongjun Yu<sup>1†</sup>, Qiang Li<sup>1†</sup>, Jingcheng Xu<sup>1,4</sup>, Yong Qin<sup>2</sup>, Guanhua Zhang<sup>5</sup>, Yuhong Liu<sup>6</sup> and Weijie Jiang<sup>1\*</sup>

<sup>1</sup> Institute of Vegetables and Flowers, Chinese Academy of Agricultural Sciences, Beijing, China, <sup>2</sup> College of Horticulture, Xinjiang Agricultural University, Ürümqi, China, <sup>3</sup> Natural Resources Bureau of Hutubi County in Xinjiang Province, Changji, China, <sup>4</sup> Taizhou Academy of Agricultural Sciences, Taizhou, China, <sup>5</sup> Agriculture and Animal Husbandry Comprehensive Inspection and Testing Center of Chifeng, Chifeng, China, <sup>6</sup> Tibet Academy of Agriculture and Animal Husbandry Sciences Vegetable Research Institute, Lhasa, China

## OPEN ACCESS

### Edited by:

Marian Brestic,  
Slovak University of Agriculture,  
Slovakia

### Reviewed by:

Shokoofeh Hajhashemi,  
Behbahan Khatam Alanbia University  
of Technology, Iran  
Milan Skalicky,  
Czech University of Life Sciences  
Prague, Czechia

### \*Correspondence:

Weijie Jiang  
jiangweijie@caas.cn

<sup>†</sup>These authors have contributed  
equally to this work and share first  
authorship

### Specialty section:

This article was submitted to  
Plant Abiotic Stress,  
a section of the journal  
Frontiers in Plant Science

Received: 08 December 2021

Accepted: 24 February 2022

Published: 12 April 2022

### Citation:

Lu T, Song YF, Yu HJ, Li Q, Xu JC,  
Qin Y, Zhang GH, Liu YH and  
Jiang WJ (2022) Cold Stress  
Resistance of Tomato (*Solanum  
lycopersicum*) Seedlings Is Enhanced  
by Light Supplementation From  
Underneath the Canopy.  
Front. Plant Sci. 13:831314.  
doi: 10.3389/fpls.2022.831314

Adverse environmental conditions, such as low temperature (LT), greatly limit the growth and production of tomato. Recently, light-emitting diodes (LEDs) with specific spectra have been increasingly used in horticultural production facilities. The chosen spectrum can affect plant growth, development, and resistance, but the physiological regulatory mechanisms are largely unknown. In this study, we investigated the effects of LED light supplementation (W:B = 2:1, light intensity of 100  $\mu\text{mol}\cdot\text{m}^{-2}\cdot\text{s}^{-1}$ , for 4 h/day from 9:00 to 13:00) from above and below the canopy on tomato resistance under sub-LT stress (15/8°C). The results showed that supplemental lighting from underneath the canopy (USL) promoted the growth of tomato seedlings, as the plant height, stem diameter, root activity, and plant biomass were significantly higher than those under LT. The activity of the photochemical reaction center was enhanced because of the increase in the maximal photochemical efficiency ( $F_v/F_m$ ) and photochemical quenching (qP), which distributed more photosynthetic energy to the photochemical reactions and promoted photosynthetic performance [the maximum net photosynthetic rate ( $P_{max}$ ) was improved]. USL also advanced the degree of stomatal opening, thus facilitating carbon assimilation under LT. Additionally, the relative conductivity (RC) and malondialdehyde (MDA) content were decreased, while the soluble protein content and superoxide dismutase (SOD) activity were increased with the application of USL under LT, thereby causing a reduction in membrane lipid peroxidation and alleviation of stress damage. These results suggest that light supplementation from underneath the canopy improves the cold resistance of tomato seedlings mainly by alleviating the degree of photoinhibition on photosystems, improving the activity of the photochemical reaction center, and enhancing the activities of antioxidant enzymes, thereby promoting the growth and stress resistance of tomato plants.

**Keywords:** photosynthetic efficiency, light responsiveness, stomatal traits, antioxidant enzyme, abiotic stress

## INTRODUCTION

Under natural conditions, plants often encounter various stresses, including biotic and abiotic stresses, which impede plant growth and development and have adverse impacts on quality and productivity (Domenico et al., 2013; Zhou et al., 2020). As one of the main determinants of plant propagation and production, low temperature (LT) often occurs during late autumn, winter, and early spring in northern China (Shi et al., 2016; Nievola et al., 2017), causing a series of molecular, physiological, biochemical, and morphological changes to occur in plants (Khan et al., 2019). Previous studies have reported that cold stress reduces the net photosynthesis rate and maximal efficiency of photosystem (PS) II photochemistry (Devacht et al., 2011; Kalisz et al., 2016), increases cell relative electrical conductivity (Kim and Tai, 2011), increases the accumulation of soluble sugars that originate from starch metabolism (Lin et al., 2019), and promotes the activity of superoxide dismutase and catalase (Petrić et al., 2013). Several photoreceptors, such as phytochromes (phy) and cryptochromes (cry), have developed in plants to sense changing environments. Phy A is the predominant photoreceptor of far-red (FR) light and phy B is the primary photoreceptor of red (R) light (Chen and Chory, 2011). In addition, the transcription factor ELONGATED HYPOCOTYL5 (HY5) can be activated by photoreceptors to promote downstream photomorphogenesis (Li et al., 2021). Many studies have shown that the above molecules play key roles in cold tolerance (Chen and Chory, 2011; Li et al., 2021; Wang et al., 2021). It has been shown that light signals regulate chloroplast avoidance movement through phy to reduce photodamage in plants (Kasahara et al., 2002; Jaedicke et al., 2012; Suetsugu et al., 2017). Wang et al. (2018) found that phy is involved in photoprotection through the PROTON GRADIENT REGULATION5 (PGR5)-dependent cyclic electron flow pathway during cold stress and they suggested that phy A and phy B function antagonistically to regulate cold tolerance via abscisic acid-dependent jasmonate signaling (Wang et al., 2016). SIFHY3 and SIHY5 act together to enhance cold tolerance through the integration of myoinositol and light signaling in tomato (Wang et al., 2021). Bu et al. (2021) characterized 31 *B-BOX* (*BBX*) genes in tomato that play important roles in the plant response to cold and light signaling. Plants must maintain membrane fluidity at the cellular level in progressively cold and oxidized environments to overcome cold stress. As membranes are sensitive to damage, improved cold resistance helps to maintain membrane stability and, thus, minimize electrolyte leakage (Raju et al., 2018). In addition, reactive oxygen species (ROS), calcium ( $\text{Ca}^{2+}$ ), and plant hormones such as abscisic acid, brassinosteroids, and strigolactone all play key roles in plant cold tolerance (Demidchik et al., 2018; Khan et al., 2019; Lu et al., 2019; Cao et al., 2021). Hydrogen peroxide ( $\text{H}_2\text{O}_2$ ) is the most stable ROS and previous studies have revealed that elevated levels of apoplastic  $\text{H}_2\text{O}_2$  and increased respiratory burst oxidase homolog (RBOH)-encoded NADPH oxidase activity are related to acclimation-induced cross-tolerance (Zhou et al., 2014). Recently, the glutamate receptor-like (GLR) genes such as *GLR3.3* and *GLR3.5* were shown to mediate chilling tolerance by regulating apoplastic  $\text{H}_2\text{O}_2$  production and redox homeostasis

(Li et al., 2019). These various pathways work together to alter cold resistance.

As an energy source and signaling factor, light affects photosynthesis through complex and diverse photosensitive systems and regulates the structure and permeability of the membrane system, thereby changing the structure of cells and ultimately affecting their growth and metabolism (Molina et al., 1997; Grieco et al., 2012). In plant cultivation and production, metal-halide lamps and high-pressure sodium lamps are generally used to extend light duration or increase light intensity. However, these light sources also provide wavelengths that cannot be utilized efficiently or may not support photosynthesis and plant growth at all (Olive et al., 2013). Besides, one another disadvantage of these artificial lights is the reduction of light intensity with increasing the distance between lamps with leaves (Poorter et al., 2012). The positions of leaves at the top of the canopy vary as the plants increase in size. To maintain constant light intensity at the top of the canopy, the height of the lamp needs to be adjusted constantly; however, light at the bottom of the canopy is inevitably reduced (Rowse et al., 2016). These light sources also produce heat that is conducive to crop growth, but as thermal light sources, they cannot be placed very close to the plant surface or they will easily burn young tissues and cause leaf photoinhibition (Niinemets and Keenan, 2012; Li et al., 2021). In comparison, light-emitting diodes (LEDs) are considered to be a suitable light source for interlighting because of their low heat production (less likely to burn leaves), non-residual and non-toxic effects, and long operating lifetimes. In addition, LED lighting offers a specific monochromatic spectrum, thus favoring photomorphogenic responses such as the morphology and metabolite content of the leaves (Taulavuori et al., 2017). Commercial LED lamps typically combine blue and red wavelengths, as these wavelengths are highly absorbed by chlorophyll and, thus, promote photosynthesis and biomass production (Okamoto et al., 1996).

Improving the distribution of light in the canopy can improve the utilization efficiency of light and, thus, improve canopy photosynthesis. In the plant canopy, leaves at the top of the canopy usually absorb more light energy than it is necessary and the excess light energy is dissipated as heat and may result in photoinhibition. However, leaves at the bottom of the canopy usually have limited available light, which can also lead to photoinhibition (Keren and Krieger, 2011; Huang et al., 2018; Hikosaka, 2021). To improve the light use efficiency of the canopy, a variety of schemes have been proposed (Zhu et al., 2010; Long et al., 2015). Among these schemes, supplementary light from underneath the canopy has been proposed as a viable option. A comparison of light supplies placed above, inside, and underneath the canopy showed that light above the canopy only increased the light intensity of the plant tip, while the other two light positions improved the light distribution in the middle and bottom parts of the tomato plant; this was especially true for light supplied underneath the canopy, which made the whole light environment of the plant more uniform (Shao, 2019). Improving the distribution of light inside the canopy can increase light use efficiency and, hence, increase canopy photosynthesis. Several studies have shown that in the case of limited sunshine,

supplemental lighting above or within the canopy promoted the growth of tomato plants and shortened the flowering time, thus increasing yield and economic efficiency (Na et al., 2012). Moreover, researchers found that supplemental light within the cowpea canopy delayed the senescence of interior leaves (Frantz et al., 2000). Additionally, supplying upward lighting from underneath retarded the senescence of outer leaves of lettuce and improved plant growth (Zhang et al., 2015). Therefore, lighting different parts of the plant canopy can be beneficial.

Seedlings cultivated under supplementary light are robust and have good resistance to adversity; moreover, the fruit quality of these plants is improved at the harvest stage (Lu et al., 2012). Studies also show that LED lighting application increases the resistance of strawberry to *Botrytis cinerea* and cucumber to root knot nematodes; it can also increase the stress resistance of gourd seedlings and pomegranate saplings (Meng et al., 2018; Khan and Siddiqui, 2021). Hence, using light manipulation to improve seedling resistance is regarded as a green energy technology. Tomato is the second most important vegetable crop grown in protected facilities worldwide and it has been reported that temperatures below sub-LT (15°C) must be avoided with most cultivars (Dominguez et al., 2005). It is necessary to enhance the cold resistance of tomato plants to minimize economic losses from low-temperature injury. However, to the best of our knowledge, no information is available about LED light application on the growth and development of tomato plants under LT. Our objective was to investigate how supplemental LED from underneath the canopy improves the resistance of tomato seedlings under sub-LT stress.

## MATERIALS AND METHODS

### Plant Material and Growth Conditions

Tomato (*Solanum lycopersicum* “Moneymaker”) seeds were soaked in 55°C water for 30 min and pregerminated in a 28°C thermostat incubator. The germinated seeds were then sown in 72-cell trays filled with vermiculite. Seedlings at the two-leaf stage were cultivated in 15 cm × 13 cm pots with regular cultivation management and irrigated with half-Hoagland’s nutrient solution in a glasshouse. Seedlings at the six-leaf stage were separated into the five groups of 45 pots each and transferred to a phytotron (plant growth sodium lamps were used as the light source with approximately 300  $\mu\text{mol}\cdot\text{m}^{-2}\cdot\text{s}^{-1}$ ) for 3 days to adapt to the following environment: a relative humidity of 60%, a photoperiod of 12 h (7:00–19:00), and a 25/15°C (day/night) air temperature.

### Supplemental Lighting and Sub-Low Temperature Treatments

Light-emitting diode lighting systems (Philips, Eindhoven, Netherlands) were applied as supplemental light sources. The polychromatic light was combined white and blue light (W:B = 2:1) with a photosynthetic photon flux density (PPFD) of 100  $\mu\text{mol}\cdot\text{m}^{-2}\cdot\text{s}^{-1}$  measured at 10 cm from the LED module. Seedlings were divided into different phytotrons for the following treatments: CK, seedlings under natural temperature (25/15°C); CK + USL, seedlings under natural temperature

with supplemental lighting from underneath the canopy; LT, seedlings under sub-LT (15/8°C); LT + USL, seedlings under LT with supplemental lighting from underneath the canopy; and LT + TSL, seedlings under LT with supplemental lighting from above the canopy. Light was provided from 9:00 to 13:00. The fifth fully expanded leaves and roots were collected for physiological and biochemical analysis.

### Measurement of Gas Exchange and Chlorophyll Fluorescence

The gas exchange, chlorophyll fluorescence, and P700 redox state were measured *in vivo* by using the LI-6400XT Photosynthesis System (Li-Cor Incorporation, United States) and the Dual PAM-100F (Heinz Walz, Effeltrich, Germany) as described in previous reports (Grieco et al., 2012; Pietrzykowska et al., 2014). The light-adapted curves were recorded after 2 min of exposure to various PPFDs (Lu et al., 2019; Li et al., 2021).

### Determination of Plant Growth and Root Morphology

Plant growth was evaluated by measuring plant height, stem diameter, and wet and dry weight. Root morphology was scanned using an “Epson Perfection V168” photo flatbed scanner (Epson, Long Beach, United States) and root activity was measured with the triphenyltetrazolium chloride (TTC) method (Ou et al., 2011).

### Observation of Leaf Stomatal Microstructure

To observe the microstructure of the stomata, the torn leaf epidermis was immersed in a transparent nail polish buffer and sectioned onto slides for microimaging. Images of each strip were taken under a Leica microscope (Leica Microsystems AG, Solms, Germany) equipped with a Nikon NIS-F1 CCD camera and a Nikon DS-U3 controller (Nikon, Tokyo, Japan). Enumeration and measurement of stomatal parameters were conducted with 20 and 100× objective lenses (Lu et al., 2017a).

### Analysis of Chlorophyll, Malondialdehyde, and Soluble Protein Content

The chlorophyll content was measured with the lixiviating method (Muneer et al., 2020). The contents of Malondialdehyde (MDA) and soluble protein were measured based on the thiobarbituric acid (TBA) assay and Bradford method, respectively (Chang et al., 2016).

### Estimation of Relative Conductivity and Cell Damage Rate

The estimations of Relative Conductivity (RC) and cell damage rate were carried out according to Yang et al. (1996) report. Fresh leaf samples were washed and cut into 1 cm strips. Leaves (0.1 g) were soaked in 20 ml deionized water for 12 h at room temperature (RT) and the initial conductivity was



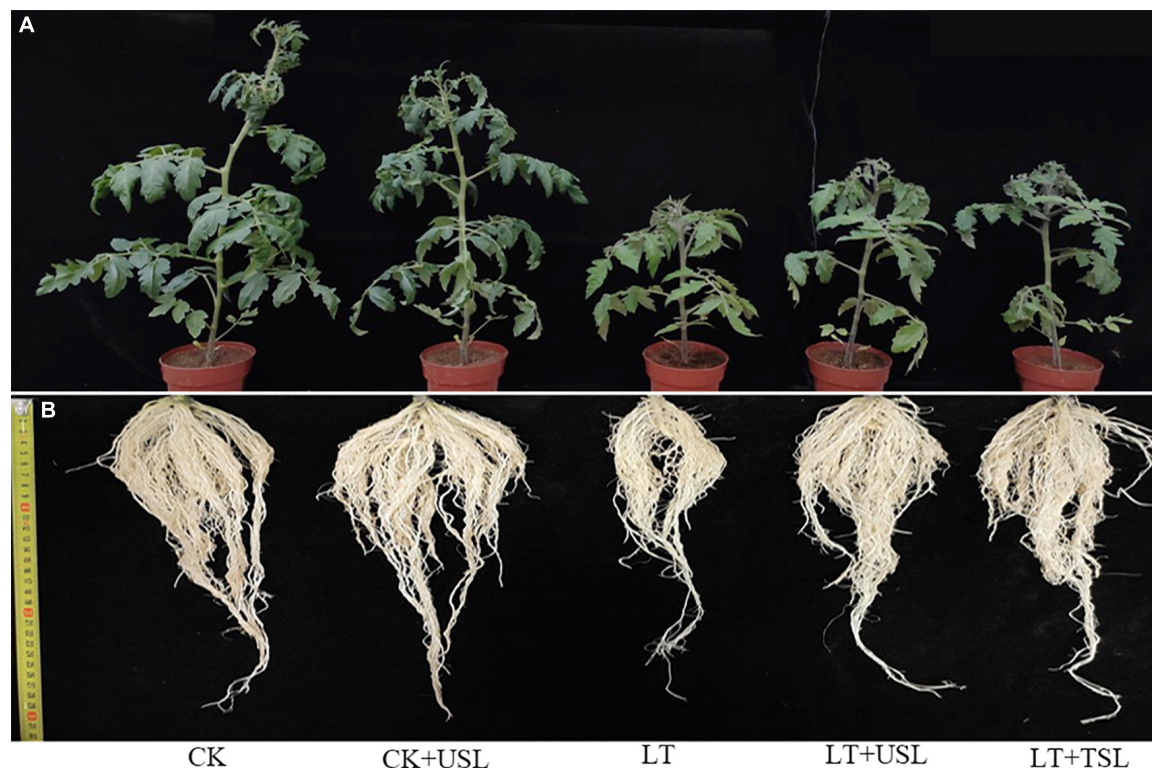


**FIGURE 1 |** Phenotypic observation of the aboveground **(A)** and underground **(B)** morphology of tomato seedlings under low temperature (LT) stress with light supplementation from underneath the canopy. CK, seedlings under natural temperature; CK + USL, seedlings under natural temperature with supplemental lighting from underneath the canopy; LT, seedlings under sub-LT; LT + USL, seedlings under sub-LT with supplemental lighting from underneath the canopy; and LT + TSL, seedlings under sub-LT with supplemental lighting from above the canopy.

measured as R1. Then, leaves were heated in boiling water for 30 min and cooled to RT. After shaking, the conductivity was measured as R2.  $RC = R1/R2 \times 100\%$ . Cell damage rate =  $[1 - (R1/R2)/(C1/C2)] \times 100\%$ . C1 and C2 are the conductivities of the blank controls.

## Assessment of Antioxidant Enzyme Activity

The activities of superoxide dismutase (SOD), peroxidase (POD), and catalase (CAT) were measured with plant physiology kits (Jiancheng Biotechnology Corporation Ltd., Nanjing, China). Half gram of fresh leaves were ground into a fine powder with liquid nitrogen and extracted with ice-cold 50 mM phosphate buffer (pH 7.8). The extracts were centrifuged at 4°C and  $10,000 \times g$  for 15min and the supernatants were used to evaluate the enzyme activity based on the enzyme assay with a Multiskan Sky Visible Spectrophotometer (Thermo Fisher Scientific, Massachusetts, United States) (Zhao et al., 2017).

## Statistical Analysis and Visualization

Five treatments were setup in this experiment with three replicates for each treatment. Related indicators were measured for three separate plants for each replication. The data were the mean  $\pm$  SD of three replicates. Values were compared between

the five treatments with Duncan's multiple comparison test at a probability level of 0.05 in SPSS version 20 software (SPSS Incorporation, IBM Armonk, New York, United States). Figures were drawn with GraphPad Prism version 6.01 (GraphPad Software Incorporation, La Jolla, United States).

## RESULTS

### Supplemental Lighting From Underneath Promotes the Growth and Development of Tomato Seedlings Under Low Temperature Stress

Supplemental lighting from underneath (USL) promoted the growth of aboveground and underground parts of tomato seedlings and improved their morphological structure under sub-LT stress (**Figures 1A,B**). Compared with the CK, the plant heights of CK + USL, LT, LT + USL, and LT + TSL plants were significantly decreased. LT + USL and LT + TSL effectively increased plant height by 27 and 24% compared to LT, respectively, and there was no significant difference between them. In addition, root length was significantly increased by supplementary light. The effect of LT + USL was better than that of LT + TSL, as both produced longer roots than LT by 26 and



**TABLE 1** | Effects of USL on the plant and root growth indices, biomass allocation, and root activity of tomato seedlings under low temperature (LT).

Treatment	Plant height cm	Stem diameter mm	Dry weight				Root activity mg·g <sup>-1</sup> ·h <sup>-1</sup>	Total root length m	Average root diameter mm
			Leaf g	Stem g	Root g	Total g			
CK	65 ± 2 <sup>a</sup>	8.0 ± 0.1 <sup>b</sup>	6.2 ± 0.2 <sup>b</sup>	3.2 ± 0.1 <sup>b</sup>	1.1 ± 0.1 <sup>bc</sup>	10.5 ± 0.5 <sup>b</sup>	1.50 ± 0.03 <sup>b</sup>	13.5 ± 0.5 <sup>b</sup>	0.42 ± 0.02 <sup>b</sup>
CK + USL	56 ± 4 <sup>b</sup>	8.4 ± 0.1 <sup>a</sup>	6.9 ± 0.3 <sup>a</sup>	3.6 ± 0.1 <sup>a</sup>	1.4 ± 0.1 <sup>a</sup>	11.8 ± 0.4 <sup>a</sup>	1.65 ± 0.02 <sup>a</sup>	16.2 ± 0.9 <sup>a</sup>	0.46 ± 0.02 <sup>a</sup>
LT	33 ± 3 <sup>d</sup>	7.5 ± 0.1 <sup>d</sup>	4.1 ± 0.2 <sup>d</sup>	1.6 ± 0.1 <sup>d</sup>	0.7 ± 0.1 <sup>d</sup>	6.4 ± 0.3 <sup>d</sup>	1.20 ± 0.01 <sup>d</sup>	8.6 ± 0.2 <sup>e</sup>	0.33 ± 0.01 <sup>d</sup>
LT + USL	42 ± 4 <sup>c</sup>	7.8 ± 0.1 <sup>c</sup>	4.8 ± 0.2 <sup>c</sup>	1.9 ± 0.1 <sup>c</sup>	0.9 ± 0.1 <sup>c</sup>	7.6 ± 0.3 <sup>c</sup>	1.30 ± 0.01 <sup>c</sup>	10.8 ± 0.3 <sup>c</sup>	0.37 ± 0.01 <sup>c</sup>
LT + TSL	41 ± 4 <sup>c</sup>	7.8 ± 0.1 <sup>c</sup>	4.5 ± 0.1 <sup>d</sup>	1.8 ± 0.1 <sup>c</sup>	0.8 ± 0.1 <sup>c</sup>	7.1 ± 0.2 <sup>c</sup>	1.29 ± 0.02 <sup>c</sup>	9.6 ± 0.4 <sup>d</sup>	0.36 ± 0.01 <sup>c</sup>

Data represent the means ± SE (n = 9). Different superscript letters in the same column indicate significant difference ( $P < 0.05$ ), and the same letter indicates no significant difference ( $P > 0.05$ ).

**TABLE 2** | Effects of USL on the leaf chlorophyll content of tomato seedlings under LT stress.

Treatment	Chl a content	Chl b content	Total chlorophyll content	Ratio of Chl a/Chl b
	mg·g <sup>-1</sup> FW	mg·g <sup>-1</sup> FW	mg·g <sup>-1</sup> FW	
CK	1.63 ± 0.01 <sup>b</sup>	0.38 ± 0.02 <sup>b</sup>	2.01 ± 0.02 <sup>b</sup>	4.30 ± 0.29 <sup>d</sup>
CK + USL	1.72 ± 0.04 <sup>a</sup>	0.33 ± 0.02 <sup>a</sup>	2.05 ± 0.03 <sup>a</sup>	5.24 ± 0.22 <sup>b</sup>
LT	1.29 ± 0.02 <sup>e</sup>	0.26 ± 0.02 <sup>c</sup>	1.55 ± 0.01 <sup>d</sup>	4.95 ± 0.34 <sup>c</sup>
LT + USL	1.41 ± 0.04 <sup>c</sup>	0.22 ± 0.01 <sup>d</sup>	1.63 ± 0.03 <sup>c</sup>	6.41 ± 0.45 <sup>a</sup>
LT + TSL	1.34 ± 0.02 <sup>d</sup>	0.23 ± 0.01 <sup>d</sup>	1.57 ± 0.02 <sup>cd</sup>	5.83 ± 0.33 <sup>a</sup>

Different superscript letters in the same column indicate significant difference ( $P < 0.05$ ), and the same letter indicates no significant difference ( $P > 0.05$ ).

12%, respectively, and there was a significant difference between these treatments. Other growth indices, such as stem and root diameter, as well as root activity, showed the same trend: LT resulted in the diameter of stems and roots becoming thinner. After supplemental lighting, both the indices became larger (as shown in **Table 1**). Additionally, plant biomass was significantly decreased by LT and the dry weights of roots, stems, and leaves were lower than those under CK by 34, 50, and 36%, respectively. When seedlings were given USL, these weights were improved by 17, 19, and 29%, which were significantly higher than those under LT. Supplemental lighting from above the canopy had a similar, but weaker improvement effect.

## Supplemental Lighting From Underneath Improves Leaf Photosynthetic Capacity Under Low Temperature Stress

As shown in **Table 2**, the contents of Chl *a*, Chl *b*, and total chlorophyll were significantly increased by CK + USL. LT caused the above contents to decrease by 21, 32, and 23% and Chl *a*/Chl *b* to decrease by 17%. Compared with LT, LT + USL significantly increased the contents of Chl *a*, total chlorophyll, and Chl *a*/Chl *b* by 9, 5, and 29%, respectively; however, the Chl *b* content was decreased by 16%.

The chlorophyll content affects photosynthesis and light supplementation significantly increased the apparent quantum efficiency (AQE) and light saturation point (LSP). Compared with

LT, the AQE and LSP under LT + USL were significantly increased by 20 and 6%, respectively, while the light compensation point (LCP) was significantly decreased by 76% (**Figure 2A**). In addition, the carboxylation efficiency (CE) and CO<sub>2</sub> saturation point (CSP) significantly increased by 15 and 4%, respectively, while the CO<sub>2</sub> compensation point (CCP) significantly decreased by 11% (**Figure 2B**). Additionally, the maximum net photosynthetic rate (*P*<sub>max</sub>) of the Pn-light and Pn-CO<sub>2</sub> response curves were both improved by USL under LT stress.

## Supplemental Lighting From the Underneath Relieves the Photoinhibition Degree and Enhances the Energy Distribution in Photosystem II and Photosystem I Under Low Temperature Stress

Photoinhibition occurred in tomato leaves under LT stress. As shown in **Figures 3A,B,D** LT caused a significant decrease in the maximal photochemical efficiency of PS II (*F<sub>v</sub>/F<sub>m</sub>*), the potential photochemical activity of PS II (*F<sub>v</sub>/F<sub>o</sub>*), and photochemical quenching (qP); however, USL significantly increased these values by 78, 54, and 71%, respectively. In addition, non-photochemical quenching (NPQ) of LT was increased by 68%, which was significantly higher than that of the CK, while LT + USL significantly decreased NPQ by 25% (**Figure 3C**). Thus, USL could effectively alleviate the PS II photoinhibition in tomato leaves caused by LT stress and the activity of the PS II reaction center was greatly improved.

The maximal P700 changes (*P*<sub>m</sub>) as well as the effective quantum yield of PS I [*Y*(I)] decreased from day 4 after LT stress and the decrease in the amplitude increased with prolonged stress duration. Hence, PS I activity was inhibited. Compared with LT, at day 16, LT + USL significantly increased the values of *P*<sub>m</sub> and *Y*(I) by 43 and 54%, respectively (**Figure 4**). Therefore, USL is good for tomato PS I.

In this study, we measured the direct energy flow across both the PS II and PS I. As shown in **Figure 5**, the difference in quantum yields increased over time. Compared to the CK, the regulatory and non-regulatory quantum yields of energy dissipation [*Y*(NPQ) and *Y*(NO)] were both significantly

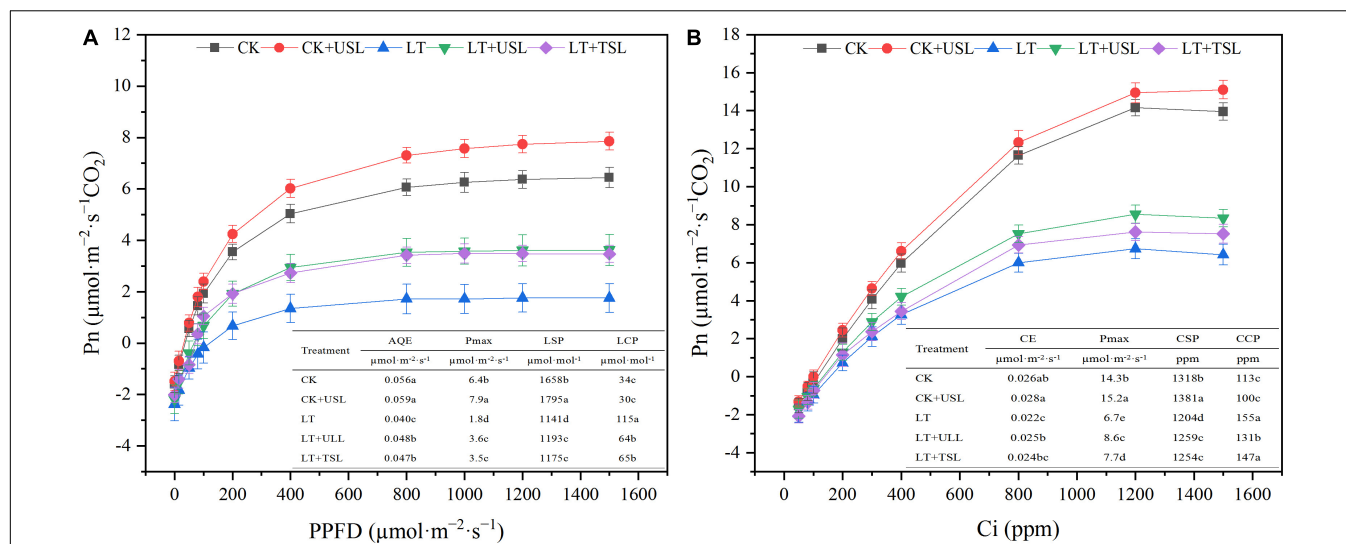


**FIGURE 2 |** Effects of USL on the Pn-light response curve (A) and Pn-CO<sub>2</sub> response curve (B) of tomato leaves under LT. AQE, apparent quantum efficiency; LSP, light saturation point; LCP, light compensation point; CE, carboxylation efficiency; CSP, CO<sub>2</sub> saturation point; CCP, CO<sub>2</sub> compensation point; Pmax, maximum net photosynthetic rate.

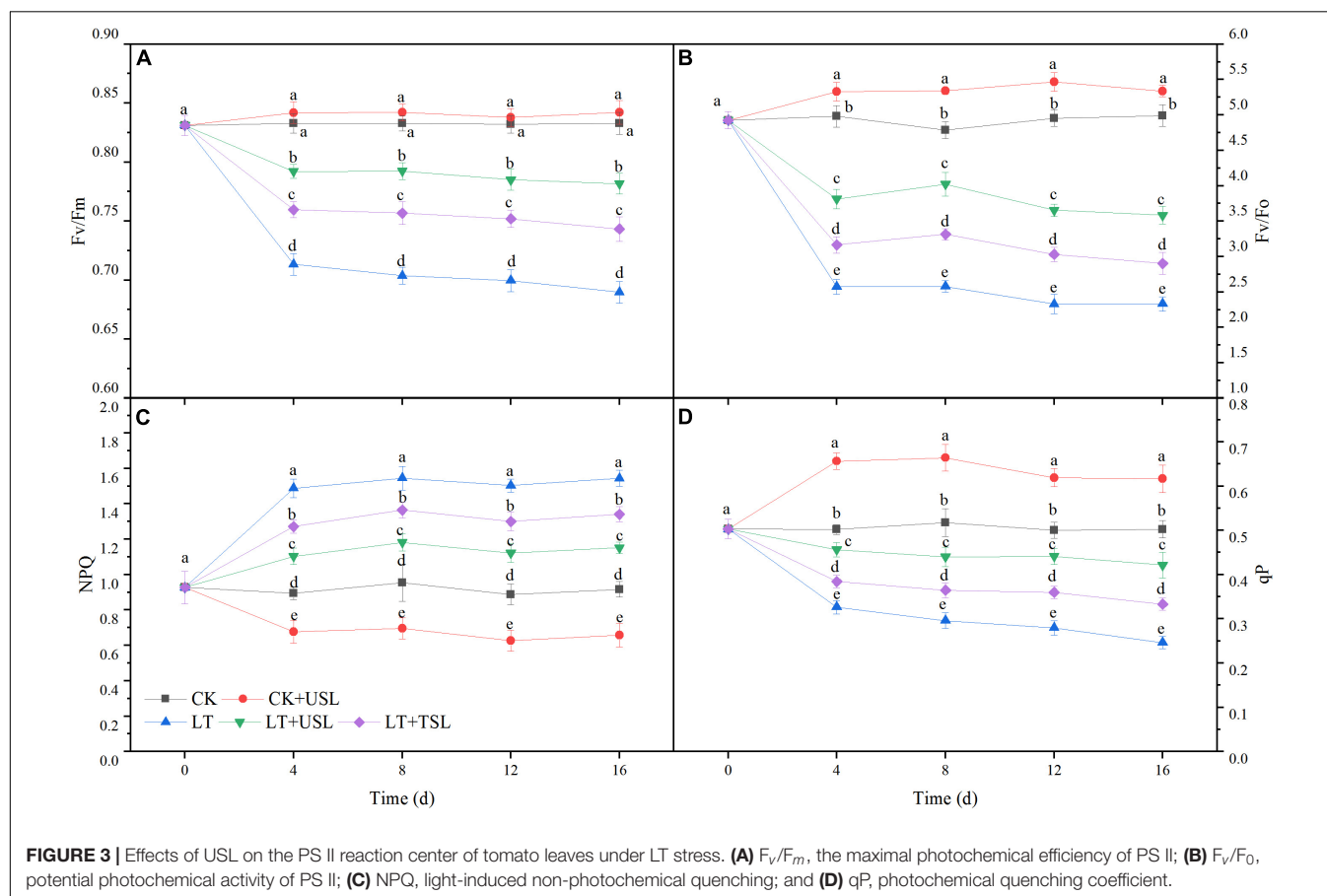


**FIGURE 3 |** Effects of USL on the PS II reaction center of tomato leaves under LT stress. (A)  $F_v/F_m$ , the maximal photochemical efficiency of PS II; (B)  $F_v/F_0$ , potential photochemical activity of PS II; (C) NPQ, light-induced non-photochemical quenching; and (D)  $qP$ , photochemical quenching coefficient.

increased by LT. Once USL was applied,  $Y(NPQ)$  and  $Y(NO)$  were both decreased significantly compared with LT (Figures 5A,B). The  $Y(I)$  of LT decreased gradually due to

an increase in the acceptor-side limitation of PS I [ $Y(NA)$ ] and an increase in the donor-side limitation of PS I [ $Y(ND)$ ]. However, the  $Y(NA)$  and  $Y(ND)$  values of LT + USL were

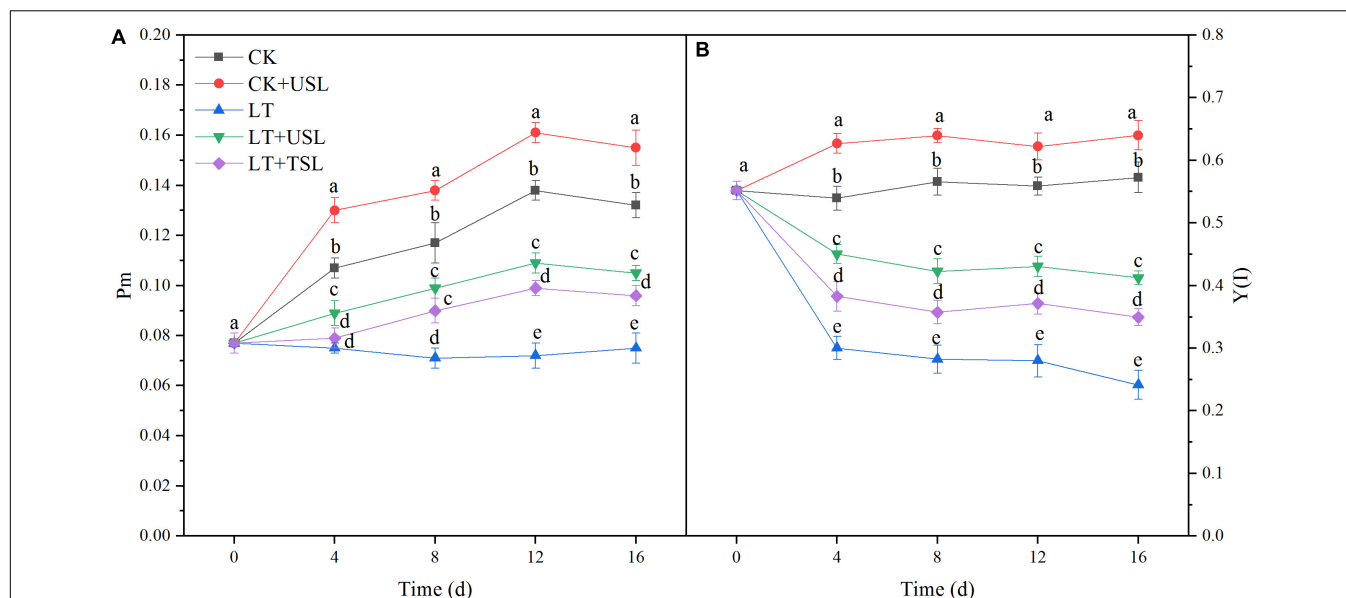


**FIGURE 4 |** Effects of USL on the PS I reaction center of tomato seedlings under LT stress. **(A)** Pm, the maximal P700 changes and **(B)** Y(I), the effective quantum yield of PS I.

significantly lower than those of LT (**Figures 5C,D**). These results suggested that applying USL enhanced the energy fluxes between PS II and PS I.

### Effects of Supplemental Lighting From Underneath on Leaf Stomatal Density and Morphology Under Low Temperature Stress

Compared with the CK, LT decreased the density of stomata by 13% (**Figures 6A,C** and **Table 3**). Supplementation with light increased the density of stomata in the leaves; for example, the stomatal number of CK + USL was 36% higher than that of the CK (**Figure 6B** and **Table 3**). In addition, the stomatal numbers of LT + USL and LT + TSL were 41 and 16% higher than those of LT (**Figures 6D,E** and **Table 3**). In addition, USL effectively improved the stomatal aperture of tomato leaves under LT stress. By observing stomatal morphology and analyzing apparent characteristics, we found that stomatal area was significantly decreased by LT, but with USL or TSL, it was significantly elevated. The stomatal area of LT + USL was the largest because both the vertical diameter and transverse diameter were increased (**Figures 6F,G** and **Table 3**).

### Effects of Supplemental Lighting From Underneath on Membrane Lipid Peroxidation and Antioxidant Enzyme Activity Under Low Temperature Stress

Stress conditions will increase the permeability of the cell membrane, leading to electrolyte extravasation in cells. In this study, LT gradually increased the RC with the extension of stress duration and the cell damage rate was seriously aggravated.

Compared with the CK, these values were increased by 128 and 228%. However, supplemental lighting reduced the damage degree and the RC and cell damage rate of LT + USL were decreased by 13 and 11%, respectively (**Figures 7A,B**). Soluble protein is an important osmotic regulator in plants and the MDA content directly affects lipid peroxidation. In contrast to RC, the soluble protein content showed an initial increasing trend and then a decreasing trend under LT; after 16 days, this content had decreased by 23%. Compared with LT, the soluble protein content of LT + USL was significantly increased by 10%, while the MDA content was significantly decreased by 20%, indicating that USL alleviated the stress degree.

Plants rely on a variety of antioxidant enzymes, such as SOD, CAT, and POD, to remove ROS. As shown in **Table 4**, SOD activity was significantly increased and CAT activity was significantly decreased by LT. Compared with LT, the activities of both the SOD and CAT activities were significantly increased; however, the activity of POD showed no significant differences among the treatments, except CK + USL.

## DISCUSSION

Low temperature represents an important environmental factor affecting vegetable growth to a great extent. Under LT, plant height, stem diameter, and the growth of leaves of eggplant and tomato are inhibited (Cui et al., 2016; Shi et al., 2019). The key negative effect of chilling on cucumber and pepper is a reduction in biomass and photosynthetic capacity (Yong et al., 2003; Ikkonen et al., 2018). LT also induces chloroplast damage and affects photosynthetic physiological metabolism in thylakoid membranes (Shi et al., 2016; Yang et al., 2018), where the

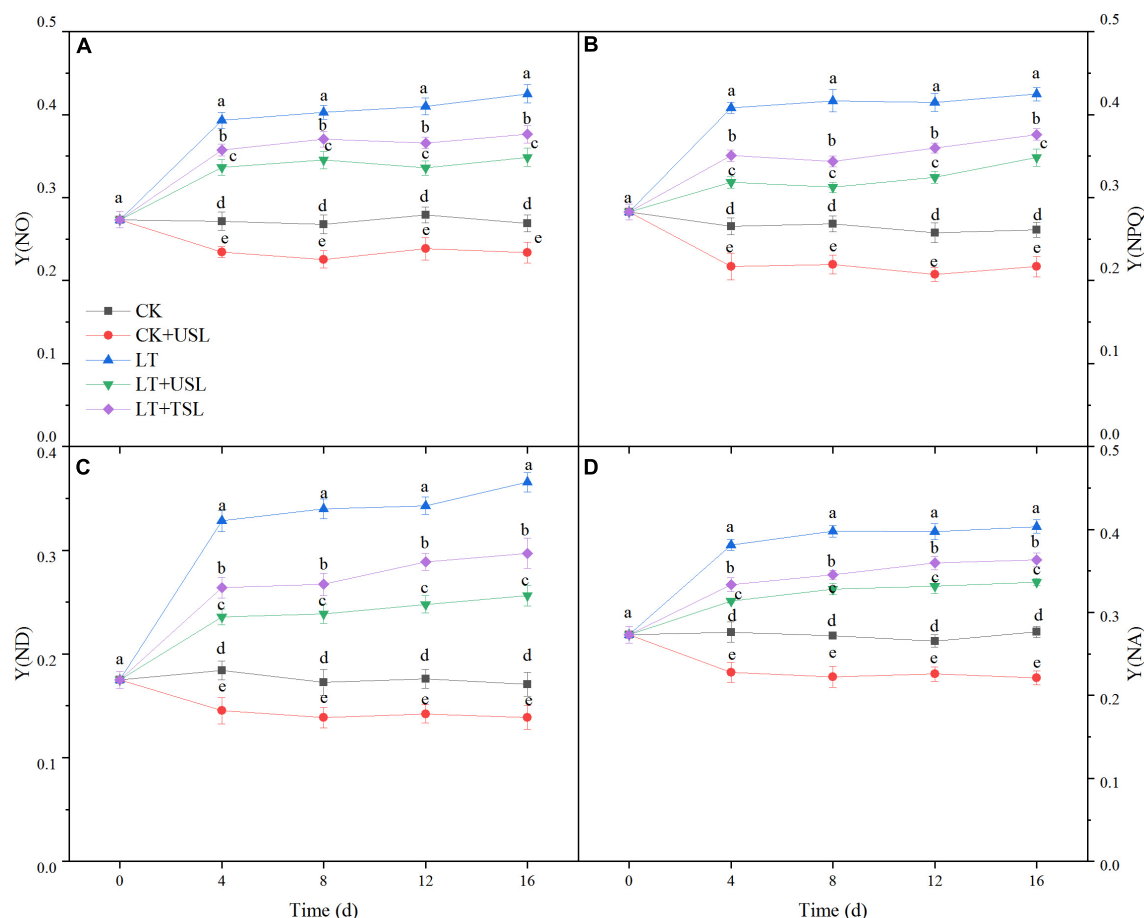


**FIGURE 5 |** Effects of USL on the energy fluxes between photosystems in tomato leaves under LT stress. **(A)** Y(NO), the quantum yield of non-regulated energy dissipation; **(B)** Y(NPQ), the quantum yield of regulated energy dissipation; **(C)** Y(ND), PS I donor side limitation; and **(D)** Y(NA), PS I acceptor side limitation.

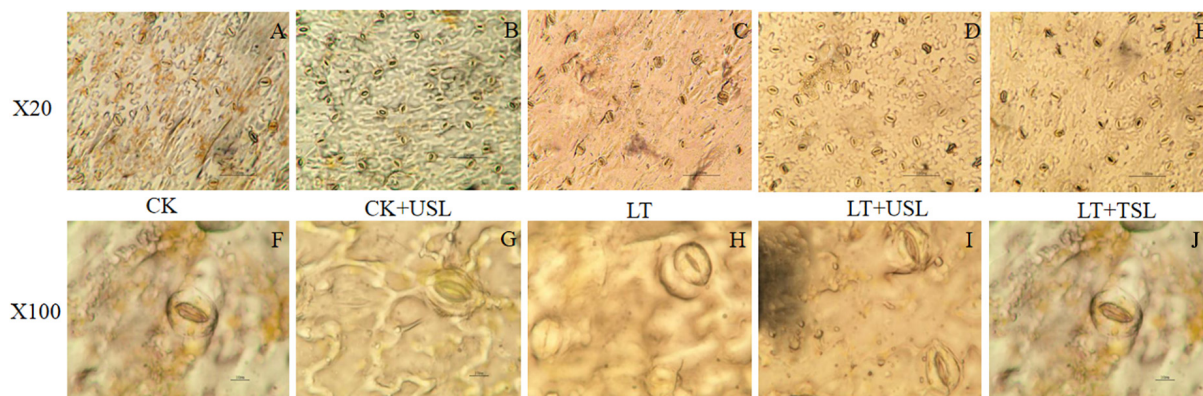


**FIGURE 6 |** Effects of USL on the stomatal morphology of tomato leaves under LT stress. **(A-E,F-J)** are the stomatal morphology observed under 20 and 100X objective lenses, respectively.

functions of sunlight capture, electron transmission, and energy conversion occur. Light is an energy and signaling factor that influences photosynthesis through complex plant photosystems and changes cell structure by regulating the

permeability of biofilm systems, ultimately affecting plant growth and metabolism. To solve the shortage of sunlight in greenhouse cultivation and alleviate plant stress, artificial light supplementation technology has become one of the



**TABLE 3 |** Effects of USL on the characteristics of the tomato stomatal apparatus under LT stress.

Treatments	Vertical diameter	Transverse diameter	Area	Number
	$\mu\text{m}$	$\mu\text{m}$	$\mu\text{m}^2$	
CK	16.48 $\pm$ 0.06 <sup>b</sup>	5.14 $\pm$ 0.27 <sup>c</sup>	66.54 $\pm$ 3.29 <sup>c</sup>	30.33 $\pm$ 1.53 <sup>c</sup>
CK + USL	19.72 $\pm$ 0.52 <sup>a</sup>	9.56 $\pm$ 0.36 <sup>a</sup>	148.03 $\pm$ 8.55 <sup>a</sup>	41.33 $\pm$ 1.53 <sup>a</sup>
LT	12.43 $\pm$ 0.72 <sup>c</sup>	3.59 $\pm$ 0.12 <sup>d</sup>	34.96 $\pm$ 0.97 <sup>d</sup>	26.33 $\pm$ 1.53 <sup>d</sup>
LT + USL	16.71 $\pm$ 0.23 <sup>b</sup>	6.08 $\pm$ 0.45 <sup>b</sup>	79.82 $\pm$ 6.18 <sup>b</sup>	37.00 $\pm$ 2.00 <sup>b</sup>
LT + TSL	16.72 $\pm$ 0.78 <sup>b</sup>	4.99 $\pm$ 0.08 <sup>c</sup>	65.48 $\pm$ 3.71 <sup>c</sup>	30.67 $\pm$ 1.15 <sup>c</sup>

One slice was made for each plant, and nine slices were made for each treatment. The number of stoma in 3 non-adjacent visual fields in each slice was counted under a 20 $\times$  objective lens. To measure stomatal vertical and transverse diameters, 6 complete and clear stomata were chosen for each slice under a 100 $\times$  objective lens, with a total of 54 stomata for each treatment. Different superscript letters in the same column indicate significant difference ( $P < 0.05$ ), and the same letter indicates no significant difference ( $P > 0.05$ ).

important ways to improve the production efficiency of facility agriculture. Thus, it is crucial to choose the best method of light supplementation and understand the physiological mechanism of stress resistance enhancement.

Stomatal characteristics are closely related to stomatal conductance and a higher stomatal conductance is always accompanied by greater photosynthesis (Zhang et al., 2019). Kim et al. (2004) found that the stomatal opening and Pn of *Chrysanthemum* tissue-cultured seedlings with red and

blue mixed LEDs were largely enhanced. Previous studies in *Arabidopsis* also showed that the existence of blue light increased the number of stomata and stimulated stomatal opening (Yang et al., 2020). Under LT stress, USL not only increased the stomatal density, but also promoted stomatal opening by increasing the vertical and transverse diameters (Figure 6 and Table 3), which might partly explain the significant increase in  $P_{\text{max}}$  observed in LT + USL plants. Moreover, USL may contributed to the activation of Rubisco (Wu et al., 2020), which can be reflected by the improved CE in LT + UTL seedlings (Figure 2B). Kinoshita et al. (2001) suggested that blue light promoted the absorption of the carotenoid zeaxanthin, thus promoting the opening of stomata. Li et al. (2020) believed that a blue LED light source directly promoted stomatal opening. Kang et al. (2009) and Yang et al. (2020) considered that stomatal opening was regulated by phy and cry. Although not definitive, most studies show that blue light can stimulate the expansion of stomatal opening and improve plant photosynthesis. Our physiological data also revealed that  $P_{\text{max}}$ , AQE, LSP, CE, CSP, Chl *a*, and Chl *b* in tomato leaves were decreased by LT (Figures 2–4 and Table 2). However, USL significantly increased these parameters. As the main photosynthetic pigment, chlorophyll is capable of capturing, transmitting, and converting light energy (Jian et al., 2016). The reduction in chlorophyll content in tomato leaves by LT stress affected photosynthetic efficiency and aggravated photoinhibition (Table 2); however, LT + USL treatment effectively reduced the degradation of chlorophyll to improve leaf chlorophyll content and, thereby, maintain the high

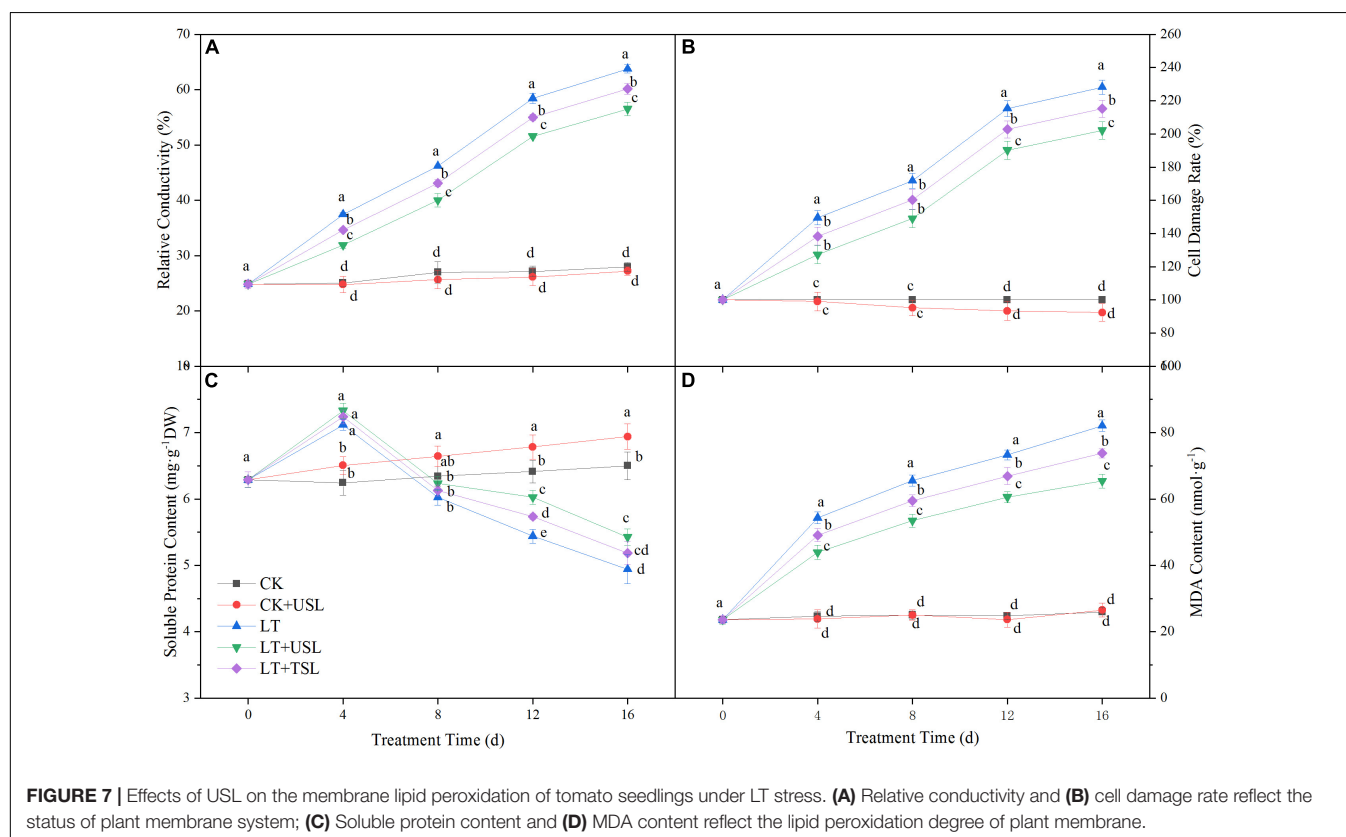




**TABLE 4 |** Effects of USL on the activities of antioxidant enzymes in tomato leaves under LT stress.

Treatments	SOD	POD	CAT
	U·g <sup>-1</sup> FW·min <sup>-1</sup>	U·g <sup>-1</sup> FW·min <sup>-1</sup>	U·g <sup>-1</sup> FW·min <sup>-1</sup>
CK	123 ± 7 <sup>d</sup>	215 ± 18 <sup>b</sup>	315 ± 10 <sup>b</sup>
CK + USL	161 ± 6 <sup>c</sup>	365 ± 23 <sup>a</sup>	377 ± 13 <sup>a</sup>
LT	216 ± 12 <sup>b</sup>	210 ± 23 <sup>b</sup>	160 ± 7 <sup>d</sup>
LT + USL	257 ± 11 <sup>a</sup>	213 ± 25 <sup>b</sup>	178 ± 8 <sup>c</sup>
LT + TSL	237 ± 12 <sup>ab</sup>	212 ± 28 <sup>b</sup>	170 ± 10 <sup>cd</sup>

Different superscript letters in the same column indicate significant difference ( $P < 0.05$ ), and the same letter indicates no significant difference ( $P > 0.05$ ).

photosynthetic capacity of chloroplasts. LT + UTL-grown plants displayed lower LCP and CCP, which are characteristics that are conducive to the accumulation of organic matter and indicate stronger photosynthetic capacity (Cui et al., 2016; Rasmusson et al., 2020).

Photoinhibition is defined as a decrease in photosynthetic efficiency under strong light conditions, in which the photon input exceeds the requirements of photosynthesis (Barber and Andersson, 1992; Lu et al., 2017b). Photoinhibition may occur under other stresses as long as the light intensity and duration reach a certain photon threshold (Meng et al., 2017). In this study, we found that LT stress exacerbated the photoinhibition degree, as evidenced by a decrease in Fv/Fm, Fv/F0, and Pm (Figures 3A, 4A), resulting in reduced light energy utilization (Sultana et al., 1999). USL significantly attenuated these parameters by increasing Y(I) and decreasing Y(NO) (Figures 4B, 5A). Recent studies suggest that moderate phosphorylation of LHC II and PS II makes PS I complexes move to the edge of the grana, which transfers sufficient excitation energy to PS I and alleviates the photoinhibition of PS II (Grieco et al., 2012; Pietrzykowska et al., 2014; Lima-Melo et al., 2019). Conversely, the photoinhibition of PS II within a controllable range can protect PS I from photoinhibition by preventing ROS production and regulating the electron transport chain (Takagi et al., 2016; Lima-Melo et al., 2019). According to Wang et al. (2020), LT destroys PQ and electron transport from PQH<sub>2</sub> to PS I, which leads to an imbalance in electron consumption and light reactions, resulting in an increased degree of membrane lipid peroxidation and cell damage (Figures 7B,D). Fortunately, USL significantly decreased Y(NA), indicating that the PS I acceptor side limitation under LT was alleviated (Figure 5D). Recent studies suggest that this alleviation is due to the promotion of the NADP<sup>+</sup>/NADPH ratio and the number of available oxidized forms of NADP (Grieco et al., 2012; Lima-Melo et al., 2019; Wang et al., 2020). In this study, a large decrease in Pm and an increase in Y(ND) and Y(NO) under LT showed that the photoinhibition of PS I occurred rapidly upon the onset of an imbalance between the donor and acceptor side of PS I (Figures 4A, 5C,D). However, USL not only stimulated the photoprotection mechanism on the donor side, but also reduced the photodamage on the acceptor side to reduce PSI photoinhibition and enhance the Calvin cycle. Moreover, as the PS I activity cannot be restored to the control level, these

results supported other findings suggesting that chloroplast antioxidant scavengers cannot prevent PS I photoinhibition in the case of donor/acceptor side imbalance (Takagi et al., 2016; Lima-Melo et al., 2019; Lu et al., 2020). Y(NPQ) and Y(NO) represent the activity and energy distribution of the PS II reaction center. In this study, they were both increased by USL under LT stress (Figures 5A,B), implying that LT + USL treatment increased the quantity of light absorbed by the reaction center and partially promoted PS II opening of tomato seedlings under LT stress (Klughammer and Schreiber, 2008). However, the excess light energy still could not dissipate through the regulatory mechanism of seedlings, which was reflected by the higher Y(NO) compared with the CK and the damage to the photosynthetic system was caused by LT stress. In addition, USL effectively diminished the Y(NO) proportion and enhanced the photochemical energy conversion, as Y(NPQ) remained higher than that under LT. These results suggested that the application of USL to plants under LT stress could enhance photosynthesis due to the enhancement of light harvesting efficiency caused by heightening of the response of the Mg branch through USL, which mainly increased the chlorophyll content (Wu et al., 2018).

Photosynthetic activity is highly affected by ROS; excess ROS production caused by disordered photosynthetic redox homeostasis will damage the cell membrane, leading to intracellular ion efflux (Lima-Melo et al., 2019). Under LT stress, ROS accumulation resulted in the peroxidation of cell membrane lipids, as reflected by the significant increase in the MDA content (Figure 7D) and the decrease in the soluble protein content (Figure 7C), which led to disruption of the physiological function of tomato plants and could even cause cell death (Figures 7A,B; Fahrenstich et al., 2008; Cao et al., 2021). The change in ion exosmosis and the level of cell damage can be reflected by electrolyte leakage measurements. The values of RC increased in stressed plants under LT; however, supplemental lighting significantly decreased this value and that of the cell damage degree rate (Figures 7A,B). Many studies use 50% electrolyte leakage as the critical survival threshold, although many plants die after more than 30% electrolyte leakage (Helena et al., 2017). A lower RC value below 50% was measured for USL compared to TSL. According to Helena et al. (2017) and Demidchik et al. (2018), the increase in the concentration of soluble protein, an osmotically active substance, by USL (Figure 7C) results in a decrease in the osmotic potential, which is a cold tolerance strategy that protects the structural integrity of cell membranes and proteins.

Plants have evolved many photoprotective mechanisms to reduce ROS formation and mitigate photooxidative damage (Fahrenstich et al., 2008). The increase in NPQ reflects the energy dissipation mechanism that protects the photosynthetic system by dissipating excess energy as heat and preventing oxidative damage (Jia et al., 2019). The decrease in qP suggests that the redox state of QA, which is a PS II primary electron receptor, is not good for electron transfer (Maxwell and Johnson, 2000). In this study, NPQ was decreased and qP was increased by LT + USL treatment throughout the entire LT stress duration (Figures 3C,D), indicating a decrease in the level of energy

dissipation and an increase in the electron transfer activity. According to a previous study, the impairment of *SIBBX7*, *SIBBX9*, and *SIBBX20* suppresses the photosynthetic response and NPQ immediately after cold stress; thus, these genes positively regulate cold tolerance in tomato plants by preventing photoinhibition and enhancing photoprotection (Bu et al., 2021). The antioxidative mechanism is another important regulatory balance between the production and scavenging of ROS. Previous studies have shown that in stressed plants, the generated ROS induce antioxidant enzymes such as SOD, POD, and CAT to scavenge harmful compounds (Yu et al., 2016). These key enzymes work together to maintain the steady-state level of free radicals in plants and prevent the disorders of plant physiology and biochemistry caused by free radicals. Under cold stress, the high accumulation of H<sub>2</sub>O<sub>2</sub> was accompanied by upregulation of Ca<sup>2+</sup>-dependent protein kinases (CPKs) (Lv et al., 2018) and was responsible for the activation of antioxidant systems, such as SOD, CAT, ascorbate peroxidase, phenols, and anthocyanins (Hajihashemi et al., 2020). In this study, higher SOD, CAT, and POD activities were observed in LT + USL-treated tomato plants than in LT-treated plants (Table 4), indicating that USL reduced LT-induced damage to the cell membrane of tomato leaves (Moura et al., 2018; Cao et al., 2021). Maintaining the integrity of membrane and organelle is closely related to ROS scavenging capacity and is considered to be a particular challenge under cold stress (Pennycooke et al., 2005; Nievola et al., 2017; Hajihashemi et al., 2020).

There is a balance and exchange between the plant defense response and plant growth promotion. Researchers have reported that plant height, stem diameter, and biomass production are external indicators of plant aboveground development (Kang and Kong, 2016). In this study, the lower shoot height, thinner stem diameter, and lighter shoot biomass of LT-treated plants (Figure 1A and Table 1) indicated that shoot growth was sensitive to sub-LT stress, which was consistent with the results of Helena et al. (2017). However, once tomato plants under LT were given USL, the leaves became larger, the chlorophyll content increased, and the photosynthetic activity increased, accordingly producing more photosynthetic products, which could promote the growth of plants (Zhang et al., 2017). The utilization of USL benefited not only shoot growth, but also root growth, which was clearly greater than that under LT (Figure 1B and Table 1), suggesting improved rooting. Generally, the growth of underground roots is closely related to the rhizosphere environment. After the application of USL to the aboveground leaves, the stress degree of LT was alleviated and the underground root absorption (especially

nitrate nitrogen) was improved, which might promote the root growth of tomato seedlings, as confirmed by a large number of studies where nitrate nitrogen stimulated lateral root formation and increased root length (Jampeetong and Brix, 2009; Zhou et al., 2020).

## CONCLUSION

Cold resistance in plants is a multifaceted physiological trait. We present a way to effectively enhance the LT tolerance of tomato seedlings, i.e., supplemental lighting from underneath canopies. In line with physiological observations, the adaptation of tomato seedlings to sub-LT stress mainly depends on the enhancement of osmotic regulation, improvement of antioxidant enzyme activities, promotion of photosystem photochemical activities, and improvement of plant and root development. This study suggests a positive role for supplemental lighting from underneath the leaf canopy in protecting the plant against the hazards of cold stress. Moreover, the integration of light and temperature signals by plants to adapt to adverse stress remains to be further studied.

## DATA AVAILABILITY STATEMENT

The original contributions presented in the study are included in the article/supplementary material, further inquiries can be directed to the corresponding author/s.

## AUTHOR CONTRIBUTIONS

WJ, YQ, and HY made the study plan. YS, TL, QL, and JX performed the experiments. QL, HY, and YL collected the materials. TL, HY, GZ, YL, and WJ analyzed the data. TL, YS, GZ, and HY wrote the manuscript. All authors discussed the results and commented on the manuscript and gave final approval for publication.

## FUNDING

This study was financially supported by the China's National Key R&D Program 2019YFD1000300 and the National Natural Science Foundation of China, 32002115.

## REFERENCES

- Barber, J., and Andersson, B. (1992). Too much of a good thing - light can be bad for photosynthesis. *Trends Biochem. Sci.* 17, 61–66. doi: 10.1016/0968-0004(92)90503-2
- Bu, X., Wang, X., Yan, J., Zhang, Y., Zhou, S., Sun, X., et al. (2021). Genome-wide characterization of B-box gene family and its roles in responses to light quality and cold stress in tomato. *Front. Plant Sci.* 12:13455. doi: 10.3389/fpls.2021.698525
- Cao, L., Lu, X., Wang, G., Zhang, Q., Zhang, X., Fan, Z., et al. (2021). Maize ZmbZIP33 is involved in drought resistance and recovery ability through an abscisic acid-dependent signaling pathway. *Front. Plant Sci.* 12:629903. doi: 10.3389/fpls.2021.629903
- Chang, S., Li, C., Yao, X., Chen, S., Jiao, X., Liu, X., et al. (2016). Morphological, photosynthetic, and physiological responses of rapeseed leaf to different combinations of red and blue lights at the rosette stage. *Front. Plant Sci.* 7:771. doi: 10.3389/fpls.2016.01144
- Chen, M., and Chory, J. (2011). Phytochrome signaling mechanisms and the control of plant development. *Trends Cell Biol.* 21, 664–671. doi: 10.1016/j.tcb.2011.07.002
- Cui, L., Zou, Z., Zhang, J., Zhao, Y., and Yan, F. (2016). 24-Epibrassinolide enhances plant tolerance to stress from low temperatures and poor light

- intensities in tomato (*Lycopersicon esculentum* Mill.). *Funct. Integr. Genom.* 16, 29–35. doi: 10.1007/s10142-015-0464-x
- Demidchik, V., Shabala, S., Isayenkov, S., Cuin, T. A., and Pottosin, I. (2018). Calcium transport across plant membranes: mechanisms and functions. *New Phytol.* 220, 49–69. doi: 10.1111/nph.15266
- Devacht, S., Lootens, P., Baert, J., Van Waes, J., Van Bockstaele, E., and Roldan-Ruiz, I. (2011). Evaluation of cold stress of young industrial chicory (*Cichorium intybus* L.) plants by chlorophyll a fluorescence imaging. I. Light induction curve. *Photosynthetica* 49, 161–171. doi: 10.1007/s11099-011-0015-1
- Domenico, P., Gianluca, B., Wouter, G., and Van, D. (2013). Effects of low temperature storage and sucrose pulsing on the vase life of *Lilium* cv. Brindisi inflorescences. *Posthar. Biol. Technol.* 1, 26–37.
- Dominguez, E., Cuartero, J., and Fernandez-Munoz, R. (2005). Breeding tomato for pollen tolerance to low temperatures by gametophytic selection. *Euphytica* 142, 253–263. doi: 10.1007/s10681-005-2042-0
- Fahnenstich, H., Scarpeci, T., Valle, E., Flugge, U., and Maurino, V. (2008). Generation of hydrogen peroxide in chloroplasts of *Arabidopsis* overexpressing glycolate oxidase as an inducible system to study oxidative stress. *Plant Physiol.* 148, 719–729. doi: 10.1104/pp.108.126789
- Frantz, J., Joly, R., and Mitchell, C. (2000). Intracanopy lighting influences radiation capture, productivity, and leaf senescence in cowpea canopies. *J. Am. Soc. Hortic. Sci.* 125, 694–701. doi: 10.21273/jashs.125.6.694
- Grieco, M., Tikkanen, M., Paakkanen, V., Kangasjarvi, S., and Aro, E. M. (2012). Steady-state phosphorylation of light-harvesting complex II proteins preserves photosystem I under fluctuating white light. *Plant Physiol.* 160, 1896–1910. doi: 10.1104/pp.112.206466
- Hajhashemi, S., Brestic, M., Landi, M., and Skalicky, M. (2020). Resistance of *Fritillaria imperialis* to freezing stress through gene expression, osmotic adjustment and antioxidants. *Sci. Rep.* 10, 1–13. doi: 10.1038/s41598-020-63006-7
- Helena, H., Václav, H., Lenka, N., Jaroslava, M., Milan, S., František, H., et al. (2017). The effect of freezing temperature on physiological traits in sunflower. *Plant Soil Environ.* 63, 375–380. doi: 10.17221/214/2017-pse
- Hikosaka, K. (2021). Photosynthesis, chlorophyll fluorescence and photochemical reflectance index in photoinhibited leaves. *Funct. Plant Biol.* 48, 815–826. doi: 10.1071/FP20365
- Huang, W., Zhang, S., and Liu, T. (2018). Moderate photoinhibition of photosystem II significantly affects linear electron flow in the shade-demanding plant *panax notoginseng*. *Front. Plant Sci.* 9:637. doi: 10.3389/fpls.2018.00637
- Ikkonen, E., Shibaeva, T., and Titov, A. (2018). Influence of daily short-term temperature drops on respiration to photosynthesis ratio in chilling-sensitive plants. *Russ. J. Plant Physiol.* 65, 78–83. doi: 10.1134/s1021443718010041
- Jaedicke, K., Lichtenthaler, A. L., Meyberg, R., Zeidler, M., and Hughes, J. (2012). A phytochrome-phototropin light signaling complex at the plasma membrane. *Proc. Natl. Acad. Sci. U. S. A.* 109, 12231–12236. doi: 10.1073/pnas.1120203109
- Jampeetong, A., and Brix, H. (2009). Oxygen stress in *Salvinia natans*: interactive effects of oxygen availability and nitrogen source. *Environ. Exp. Bot.* 66, 153–159. doi: 10.1016/j.envexpbot.2009.01.006
- Jia, X., Zhu, Y., Hu, Y., Zhang, R., and Wang, Y. (2019). Integrated physiologic, proteomic, and metabolomic analyses of *Malus halliana* adaptation to saline-alkali stress. *Hortic. Res.* 6, 91–100. doi: 10.1038/s41438-019-0172-0
- Jian, L., Huang, J., Yan, X., Hong, T., Cheng, W., and Hong, W. (2016). Effects of low phosphorus stress on photosynthetic characteristics of *Tripterygium wilfordii* seedlings. *J. For. Environ.* 44, 256–270.
- Kalisz, A., Jezdinsky, A., Pokluda, R., Sekara, A., Grabowska, A., and Gil, J. (2016). Impacts of chilling on photosynthesis and chlorophyll pigment content in juvenile *Basil* Cultivars. *Hortic. Environ. Biotechnol.* 57, 330–339. doi: 10.1007/s13580-016-0095-8
- Kang, C., Lian, H., Wang, F., Huang, J., and Yang, H. (2009). Cryptochromes, phytochromes, and COP1 regulate light-controlled stomatal development in *Arabidopsis*. *Plant Cell* 21, 2624–2641. doi: 10.1105/tpc.109.069765
- Kang, I., and Kong, I. (2016). Effects of properties of metal-contaminated soils on bacterial bioluminescence activity, seed germination, and root and shoot growth. *Springerplus* 5, 272–284. doi: 10.1186/s40064-016-1774-8
- Kasahara, M., Kagawa, T., Oikawa, K., Suetsugu, N., Miyao, M., and Wada, M. (2002). Chloroplast avoidance movement reduces photodamage in plants. *Nature* 420, 829–832. doi: 10.1038/nature01213
- Keren, N., and Krieger, L. A. (2011). Photoinhibition: molecular mechanisms and physiological significance. *Physiol. Plantar.* 142, 1–5. doi: 10.1111/j.1399-3054.2011.01467.x
- Khan, M., and Siddiqui, Z. (2021). Role of zinc oxide nanoparticles in the management of disease complex of beetroot (*Beta vulgaris* L.) caused by *pectobacterium betavascularum*, *melioidogone incognita* and *rhizoctonia solani*. *Hortic. Environ. Biotechnol.* 62, 225–241. doi: 10.1007/s13580-020-00312-z
- Khan, T. A., Yusuf, M., Ahmad, A., Bashir, Z., Saeed, T., Fariduddin, Q., et al. (2019). Proteomic and physiological assessment of stress sensitive and tolerant variety of tomato treated with brassinosteroids and hydrogen peroxide under low-temperature stress. *Food Chem.* 289, 500–511. doi: 10.1016/j.foodchem.2019.03.029
- Kim, S. I., and Tai, T. H. (2011). Evaluation of seedling cold tolerance in rice cultivars: a comparison of visual ratings and quantitative indicators of physiological changes. *Euphytica* 178, 437–447. doi: 10.1007/s10681-010-0343-4
- Kim, S., Hahn, E., Heo, J., and Paek, K. (2004). Effects of LEDs on net photosynthetic rate, growth and leaf stomata of chrysanthemum plantlets in vitro. *Sci. Hortic.* 101, 143–151. doi: 10.1016/j.scienta.2003.10.003
- Kinoshita, T., Doi, M., Suetsugu, N., Kagawa, T., Wada, M., and Shimazaki, K.-I. (2001). Phot1 and phot2 mediate blue light regulation of stomatal opening. *Nature* 414, 656–660. doi: 10.1038/414656a
- Klughammer, C., and Schreiber, U. (2008). Complementary PS II quantum yields calculated from simple fluorescence parameters measured by PAM fluorometry and the Saturation Pulse method. *Pam Appl. Notes* 5, 77–79.
- Li, H., Jiang, X., Lv, X., Ahammed, G. J., Guo, Z., Qi, Z., et al. (2019). Tomato GLR3.3 and GLR3.5 mediate cold acclimation-induced chilling tolerance by regulating apoplastic H<sub>2</sub>O<sub>2</sub> production and redox homeostasis. *Plant Cell Environ.* 42, 3326–3339. doi: 10.1111/pce.13623
- Li, J., Wu, T., Huang, K., Liu, Y., Liu, M., and Wang, J. (2021). Effect of LED Spectrum on the quality and nitrogen metabolism of lettuce under recycled hydroponics. *Front. Plant Sci.* 12:678197. doi: 10.3389/fpls.2021.678197
- Li, R., Sun, S., Wang, H., Wang, K., Yu, H., Zhou, Z., et al. (2020). FIS1 encodes a GA2-oxidase that regulates fruit firmness in tomato. *Nat. Commun.* 11:1. doi: 10.1038/s41467-020-19705-w
- Lima-Melo, Y., Alencar, V., Lobo, A., Sousa, R., Tikkanen, M., Aro, E., et al. (2019). Photoinhibition of photosystem I provides oxidative protection during imbalanced photosynthetic electron transport in *Arabidopsis thaliana*. *Front. Plant Sci.* 10:916. doi: 10.3389/fpls.2019.00916
- Lin, Q., Xie, Y., Guan, W., Duan, Y., Wang, Z., and Sun, C. (2019). Combined transcriptomic and proteomic analysis of cold stress induced sugar accumulation and heat shock proteins expression during postharvest potato tuber storage. *Food Chem.* 297:124991. doi: 10.1016/j.foodchem.2019.124991
- Long, S., Marshall-Colon, A., and Zhu, X. (2015). Meeting the global food demand of the future by engineering crop photosynthesis and yield potential. *Cell* 161, 56–66. doi: 10.1016/j.cell.2015.03.019
- Lu, J., Yin, Z., Lu, T., Yang, X., Wang, F., Qi, M., et al. (2020). Cyclic electron flow modulate the linear electron flow and reactive oxygen species in tomato leaves under high temperature. *Plant Sci.* 292:110387. doi: 10.1016/j.plantsci.2019.110387
- Lu, N., Maruo, T., Johkan, M., Hohjo, M., Tsukagoshi, S., Ito, Y., et al. (2012). Effects of supplemental lighting within the canopy at different developing stages on tomato yield and quality of single-truss tomato plants grown at high density. *Environ. Control Biol.* 50, 1–11. doi: 10.2525/ecb.50.1
- Lu, T., Meng, Z., Zhang, G., Qi, M., Sun, Z., Liu, Y., et al. (2017a). Sub-high temperature and high light intensity induced irreversible inhibition on photosynthesis system of tomato plant (*Solanum lycopersicum* L.). *Front. Plant Sci.* 8:365. doi: 10.3389/fpls.2017.00365
- Lu, T., Shi, J., Sun, Z., Qi, M., Liu, Y., and Li, T. (2017b). Response of linear and cyclic electron flux to moderate high temperature and high light stress in tomato. *J. Zhejiang Univ.-Sci. B* 18, 635–648. doi: 10.1631/jzus.B1600286
- Lu, T., Yu, H., Li, Q., Chai, L., and Jiang, W. (2019). Improving plant growth and alleviating photosynthetic inhibition and oxidative stress from low-light stress



- with exogenous GR24 in tomato (*Solanum lycopersicum* L.) seedlings. *Front. Plant Sci.* 10:490. doi: 10.3389/fpls.2019.00490
- Lv, X., Li, H., Chen, X., Xiang, X., Guo, Z., Yu, J., et al. (2018). The role of calcium-dependent protein kinase in hydrogen peroxide, nitric oxide and ABA-dependent cold acclimation. *J. Exp. Bot.* 69, 4127–4139. doi: 10.1093/jxb/er/y212
- Maxwell, K., and Johnson, G. (2000). Chlorophyll fluorescence—a practical guide. *J. Exp. Bot.* 51, 659–668. doi: 10.1093/jxb/51.345.659
- Meng, L., Höfte, M., and Labeke, M. (2018). Leaf age and light quality influence the basal resistance against *Botrytis cinerea* in strawberry leaves. *Environ. Exp. Bot.* 157, 35–45. doi: 10.1016/j.envexpbot.2018.09.025
- Meng, Z., Lu, T., Zhang, G., Qi, M., Tang, W., Li, L., et al. (2017). Photosystem inhibition and protection in tomato leaves under low light. *Sci. Hortic.* 217, 145–155. doi: 10.1016/j.scienta.2017.01.039
- Molina, C., Arenas, A., Victoria, L., and Ibanez, J. A. (1997). Characterization of a membrane system. Complex character of the permeability from an electrical model. *J. Phys. Chem. B* 101, 10323–10331. doi: 10.1021/jp9711104
- Moura, F. S., Vieira, M. N., Simões, A., Ferreira-Silva, S. L., Souza, C., Souza, E., et al. (2018). Physiological effect of kinetin on the photosynthetic apparatus and antioxidant enzymes activities during production of anthurium. *Hortic. Plant J.* 4, 12–22.
- Muneer, M., Wang, P., Zhang, J., Li, Y., Munir, M., and Ji, B. (2020). Formation of common mycorrhizal networks significantly affects plant biomass and soil properties of the neighboring plants under various nitrogen levels. *Microorganisms* 8, 230–246. doi: 10.3390/microorganisms8020230
- Na, L., Maruo, T., Johkan, M., Hohjo, M., and Shinohara, Y. (2012). Effects of supplemental lighting with light-emitting diodes (LEDs) on tomato yield and quality of single-truss tomato plants grown at high planting density. *Environ. Control Biol.* 50, 63–74. doi: 10.2525/ecb.50.63
- Nievol, C., Carvalho, C., Carvalho, V., and Rodrigues, E. (2017). Rapid responses of plants to temperature changes. *Temperature* 4, 371–405. doi: 10.1080/23328940.2017.1377812
- Niinemet, Ü, and Keenan, T. (2012). Measures of light in studies on light-driven plant plasticity in artificial environments. *Front. Plant Sci.* 3:156. doi: 10.3389/fpls.2012.00156
- Okamoto, K., Yanagi, T., Takita, S., Tanaka, M., and Watanabe, H. (1996). Development of plant growth apparatus using blue and red LED as artificial light source. *Acta Hortic.* 440, 111–116. doi: 10.17660/actahortic.1996.440.20
- Olive, I., Vergara, J., and Perez-Llorens, J. (2013). Photosynthetic and morphological photoacclimation of the seagrass *Cymodocea nodosa* to season, depth and leaf position. *Mar. Biol.* 160, 285–297. doi: 10.1007/s00227-012-2087-2
- Ou, L., Dai, X., Zhang, Z., and Zou, X. (2011). Responses of pepper to waterlogging stress. *Photosynthetica* 49, 339–345. doi: 10.1186/s12864-021-08183-z
- Pennycooke, J., Cox, S., and Stushnoff, C. (2005). Relationship of cold acclimation, total phenolic content and antioxidant capacity with chilling tolerance in petunia (*Petunia × hybrida*). *Environ. Exp. Bot.* 53, 225–232. doi: 10.1016/j.envexpbot.2004.04.002
- Petrić, M., Jevremović, S., Trifunović, M., Tadić, V., and Subotić, A. (2013). The effect of low temperature and GA3 treatments on dormancy breaking and activity of antioxidant enzymes in *Fritillaria meleagris* bulblets cultured in vitro. *Acta Physiol. Plantar.* 35, 3223–3236. doi: 10.1007/s11738-013-1357-z
- Pietrzykowska, M., Suorsa, M., Semchonok, D., Tikkanen, M., Boekema, E., Aro, E., et al. (2014). The light-harvesting chlorophyll a/b binding proteins Lhcb1 and Lhcb2 play complementary roles during state transitions in *Arabidopsis*. *Plant Cell* 26, 3646–3660. doi: 10.1105/tpc.114.127373
- Poorter, H., Fiorani, F., Stitt, M., Schurr, U., Finck, A., Gibon, Y., et al. (2012). The art of growing plants for experimental purposes: a practical guide for the plant biologist. *Funct. Plant Biol.* 39, 821–838. doi: 10.1071/FP12028
- Raju, S. K. K., Barnes, A. C., Schnable, J. C., and Roston, R. L. (2018). Low-temperature tolerance in land plants: Are transcript and membrane responses conserved? *Plant Sci.* 276, 73–86. doi: 10.1016/j.plantsci.2018.08.002
- Rasmusson, L., Buapet, P., George, R., Gullstrom, M., Gunnarsson, P., and Bjork, M. (2020). Effects of temperature and hypoxia on respiration, photorespiration, and photosynthesis of seagrass leaves from contrasting temperature regimes. *Ices J. Mar. Sci.* 77, 2056–2065. doi: 10.1093/icesjms/fsaa093
- Rowse, E., Harris, S., and Jones, G. (2016). The switch from low-pressure sodium to light emitting diodes does not affect bat activity at street lights. *PLoS One* 11:e0150884. doi: 10.1371/journal.pone.0150884
- Shao, L. (2019). *Analysis on the Effect of LED Supplemental Lighting Position on Tomato in Winter Solar Greenhouse*. China: Shenyang Agricultural University.
- Shi, D., Wei, X., and Chen, G. (2016). Effects of low temperature on photosynthetic characteristics in the super-high-yield hybrid rice 'Liangyoupeijiu' at the seedling stage. *Genet. Mol. Res.* 15, 4–18. doi: 10.4238/gmr15049021
- Shi, J., Zuo, J., Xu, D., Gao, L., and Wang, Q. (2019). Effect of low-temperature conditioning combined with methyl jasmonate treatment on the chilling resistance of eggplant (*Solanum melongena* L.) fruit. *J. Food Sci. Technol.* 56, 4658–4666. doi: 10.1007/s13197-019-03917-0
- Suetsugu, N., Higa, T., and Wada, M. (2017). Ferns, mosses and liverworts as model systems for light-mediated chloroplast movements. *Plant Cell Environ.* 40, 2447–2456. doi: 10.1111/pce.12867
- Sultana, N., Ikeda, T., and Itoh, R. (1999). Effect of NaCl salinity on photosynthesis and dry matter accumulation in developing rice grains. *Environ. Exp. Bot.* 42, 211–220. doi: 10.1016/s0098-8472(99)00035-0
- Takagi, D., Takumi, S., Hashiguchi, M., Sejima, T., and Miyake, C. (2016). Superoxide and singlet oxygen produced within the thylakoid membranes both cause photosystem I photoinhibition. *Plant Physiol.* 171, 1626–1634. doi: 10.1104/pp.16.00246
- Taulavuori, E., Taulavuori, K., Holopainen, J., Julkunen-Tiitto, R., Acar, C., and Dincer, I. (2017). Targeted use of LEDs in improvement of production efficiency through phytochemical enrichment. *J. Sci. Food Agric.* 97, 5059–5064. doi: 10.1002/jsfa.8492
- Wang, F., Guo, Z. X., Li, H. Z., Wang, M. M., Onac, E., Zhou, J., et al. (2016). Phytochrome A and B function antagonistically to regulate cold tolerance via abscisic acid-dependent jasmonate signaling. *Plant Physiol.* 170, 459–471. doi: 10.1104/pp.15.01171
- Wang, F., Wang, X., Zhang, Y., Yan, J., Ahammed, G. J., Bu, X., et al. (2021). SIFHY3 and SIHY5 act compliantly to enhance cold tolerance through the integration of myo-inositol and light signaling in tomato. *New Phytol.* 4:17934. doi: 10.1111/nph.17934
- Wang, F., Wu, N., Zhang, L. Y., Ahammed, G. J., Chen, X. X., Xiang, X., et al. (2018). Light signaling-dependent regulation of photoinhibition and photoprotection in tomato. *Plant Physiol.* 176, 1311–1326. doi: 10.1104/pp.17.01143
- Wang, F., Yan, J., Ahammed, G. J., Wang, X., Bu, X., Xiang, H., et al. (2020). PGR5/PGR1 and NDH mediate far-red light-induced photoprotection in response to chilling stress in tomato. *Front. Plant Science* 11:669. doi: 10.3389/fpls.2020.00669
- Wu, P., Xiao, C., Cui, J., Hao, B., Zhang, W., Yang, Z., et al. (2020). Nitric oxide and its interaction with hydrogen peroxide enhance plant tolerance to low temperatures by improving the efficiency of the calvin cycle and the ascorbate–glutathione cycle in cucumber seedlings. *J. Plant Growth Regul.* 22, 1–19.
- Wu, Y., Jin, X., Liao, W., Hu, L., Dawuda, M. M., Zhao, X., et al. (2018). 5-Aminolevulinic Acid (ALA) alleviated salinity stress in cucumber seedlings by enhancing chlorophyll synthesis pathway. *Front. Plant Sci.* 9:635. doi: 10.3389/fpls.2018.00635
- Yang, G., Rhodes, D., and Joly, R. (1996). Effects of high temperature on membrane stability and chlorophyll fluorescence in glycinebetaine-deficient and glycinebetaine-containing maize lines. *Austr. J. Plant Physiol.* 23, 437–443. doi: 10.1071/pp9960437
- Yang, J., Li, C., Kong, D., Guo, F., and Wei, H. (2020). Light-mediated signaling and metabolic changes coordinate stomatal opening and closure. *Front. Plant Sci.* 11:601478. doi: 10.3389/fpls.2020.601478
- Yang, X., Xu, H., Li, D., Gao, X., Li, T., and Wang, R. (2018). Effect of melatonin priming on photosynthetic capacity of tomato leaves under low-temperature stress. *Photosynthetica* 56, 884–892. doi: 10.1007/s11099-017-0748-6
- Yong, I., Lee, J., Han, Y., Chung, S., Chung, G., Guh, J., et al. (2003). Relationships of cold acclimation and antioxidative enzymes with chilling tolerance in cucumber (*Cucumis sativus* L.). *J. Am. Soc. Hortic. Sci.* 12, 36–47.
- Yu, Y., Zhen, S., Wang, S., Wang, Y., Cao, H., Zhang, Y., et al. (2016). Comparative transcriptome analysis of wheat embryo and endosperm responses to ABA

- and H<sub>2</sub>O<sub>2</sub> stresses during seed germination. *BMC Genom.* 17:97. doi: 10.1186/s12864-016-2416-9
- Zhang, G., Shen, S., Michiko, T., Toyoki, K., and Wataru, Y. (2015). Supplemental upward lighting from underneath to obtain higher marketable lettuce (*Lactuca sativa*) leaf fresh weight by retarding senescence of outer leaves. *Front. Plant Sci.* 6:1110. doi: 10.3389/fpls.2015.01110
- Zhang, J., Zhu, C., and Chen, J. (2019). Photosynthetic performance and photosynthesis-related gene expression coordinated in a shade-tolerant species *Panax notoginseng* under nitrogen regimes. *BMC Plant Biol.* 20:273. doi: 10.1186/s12870-020-02434-z
- Zhang, Q., Liu, N., Xiang, Z., Yang, Z., and Hu, L. (2017). Effects of neutral and alkaline salt stresses on the growth and physiological metabolism of Kentucky bluegrass. *Acta Pratac. Sin.* 44, 56–70.
- Zhao, D., Wang, R., Meng, J., Li, Z., Wu, Y., and Tao, J. (2017). Ameliorative effects of melatonin on dark-induced leaf senescence in gardenia (*Gardenia jasminoides* Ellis): leaf morphology, anatomy, physiology and transcriptome. *Sci. Rep.* 7:10423. doi: 10.1038/s41598-017-10799-9
- Zhou, J., Xia, X., Zhou, Y., Shi, K., Chen, Z., and Yu, J. (2014). RBOH1-dependent H<sub>2</sub>O<sub>2</sub> production and subsequent activation of MPK1/2 play an important role in acclimation-induced cross-tolerance in tomato. *J. Exp. Bot.* 65, 595–607. doi: 10.1093/jxb/ert404
- Zhou, W., Chen, J., Qi, Z., Wang, C., and Yi, Z. (2020). Effects of applying ramie fiber nonwoven films on root-zone soil nutrient and bacterial community of rice seedlings for mechanical transplanting. *Sci. Rep.* 10:16842.
- Zhu, X., Long, S., and Ort, D. (2010). Improving photosynthetic efficiency for greater yield. *Annu. Rev. Plant Biol.* 61, 235–261. doi: 10.1146/annurev-arplant-042809-112206
- Conflict of Interest:** The authors declare that the research was conducted in the absence of any commercial or financial relationships that could be construed as a potential conflict of interest.
- Publisher's Note:** All claims expressed in this article are solely those of the authors and do not necessarily represent those of their affiliated organizations, or those of the publisher, the editors and the reviewers. Any product that may be evaluated in this article, or claim that may be made by its manufacturer, is not guaranteed or endorsed by the publisher.

Copyright © 2022 Lu, Song, Yu, Li, Xu, Qin, Zhang, Liu and Jiang. This is an open-access article distributed under the terms of the Creative Commons Attribution License (CC BY). The use, distribution or reproduction in other forums is permitted, provided the original author(s) and the copyright owner(s) are credited and that the original publication in this journal is cited, in accordance with accepted academic practice. No use, distribution or reproduction is permitted which does not comply with these terms.





# Integrated Analyses of Transcriptome and Chlorophyll Fluorescence Characteristics Reveal the Mechanism Underlying Saline–Alkali Stress Tolerance in *Kosteletzkya pentacarpos*

Jian Zhou<sup>1,2\*</sup>, Anguo Qi<sup>1,2</sup>, Baoquan Wang<sup>1,2</sup>, Xiaojing Zhang<sup>1</sup>, Qidi Dong<sup>1</sup> and Jinxiu Liu<sup>1</sup>

<sup>1</sup> School of Horticulture and Landscape Architecture, Henan Institute of Science and Technology, Xinxiang, China, <sup>2</sup> Henan Province Engineering Center of Horticulture Plant Resource Utilization and Germplasm Enhancement, Xinxiang, China

## OPEN ACCESS

### Edited by:

Marcin Rapacz,  
University of Agriculture in Krakow,  
Poland

### Reviewed by:

Muhammad Ali Raza,  
Sichuan Agricultural University, China  
Ji-Hong Liu,  
Huazhong Agricultural University,  
China

### \*Correspondence:

Jian Zhou  
zj200102@163.com

### Specialty section:

This article was submitted to  
Plant Abiotic Stress,  
a section of the journal  
Frontiers in Plant Science

**Received:** 30 January 2022

**Accepted:** 28 March 2022

**Published:** 06 May 2022

### Citation:

Zhou J, Qi A, Wang B, Zhang X,  
Dong Q and Liu J (2022) Integrated  
Analyses of Transcriptome  
and Chlorophyll Fluorescence  
Characteristics Reveal  
the Mechanism Underlying  
Saline–Alkali Stress Tolerance in  
*Kosteletzkya pentacarpos*.  
Front. Plant Sci. 13:865572.  
doi: 10.3389/fpls.2022.865572

In recent years, soil salinization has become increasingly severe, and the ecological functions of saline–alkali soils have deteriorated because of the lack of plants. Therefore, understanding the tolerance mechanisms of saline–alkali-tolerant plants has become crucial to restore the ecological functions of saline–alkali soils. In this study, we evaluated the molecular mechanism underlying the tolerance of *Kosteletzkya pentacarpos* L. (seashore mallow) seedlings treated with 0.05 or 0.5% saline–alkali solution (NaCl: NaHCO<sub>3</sub> = 4:1 mass ratio) for 1 and 7 days. We identified the key genes involved in tolerance to saline–alkali stress using orthogonal partial least squares regression analysis (OPLS-RA) based on both chlorophyll fluorescence indexes and stress-responsive genes using transcriptome analysis, and, finally, validated their expression using qRT-PCR. We observed minor changes in the maximum photochemical efficiency of the stressed seedlings, whose photosynthetic performance remained stable. Moreover, compared to the control, other indicators varied more evidently on day 7 of 0.5% saline–alkali treatment, but no variations were observed in other treatments. Transcriptome analysis revealed a total of 54,601 full-length sequences, with predominantly downregulated differentially expressed gene (DEG) expression. In the high concentration treatment, the expression of 89.11 and 88.38% of DEGs was downregulated on days 1 and 7, respectively. Furthermore, nine key genes, including *KpAGO4*, *KpLARP1C*, and *KpPUB33*, were involved in negative regulatory pathways, such as siRNA-mediated DNA methylation, inhibition of 5'-terminal oligopyrimidine mRNA translation, ubiquitin/proteasome degradation, and other pathways, including programmed cell death. Finally, quantitative analysis suggested that the expression of key genes was essentially downregulated. Thus, these genes can be used in plant molecular breeding in the future to generate efficient saline–alkali-tolerant plant germplasm resources to improve the ecological functions of saline–alkali landscapes.

**Keywords:** soil salinization, seashore mallow, photosynthetic function, sequencing, gene analysis

## INTRODUCTION

Population growth and environmental degradation have caused soil salinization to become a global problem (Munns and Tester, 2008). Approximately 7% of the world's land (over 900 million hectares) is threatened by salinization (Fang et al., 2021), among which northwest, north, and northeast China have significant distribution of saline-alkali soils. Unlike coastal saline soils, saline-alkali soils contain alkaline salts (such as  $\text{NaHCO}_3$ ), in addition to the neutral salt  $\text{NaCl}$  (Wang et al., 2008). Plants growing in saline-alkali soils are affected by factors, such as high pH, low water potential, high  $\text{Na}^+$  concentration, and drought, which cause biological toxicity (Alhdad et al., 2013) and severely hinder plant development.

Sowing saline-alkali-tolerant plants is a useful approach for improving the ecological functions of saline-alkali soils. Presently, plants with the potential of improving the quality of saline-alkali soils include *Puccinellia tenuiflora* (Guo et al., 2010), *Kochia scoparia* (Zhao, 2018), *Tamarix hispida* (Wang et al., 2014), and *Populus euphratica* (An et al., 2018).

*Kosteletzkya pentacarpos* L. (seashore mallow), formerly known as *Kosteletzkya virginica* (Liu et al., 2020, 2021), is a perennial halophyte belonging to the *Malva* genus of the *Malvaceae* family. It is naturally distributed on the salt marshy coasts of eastern United States, and is commercially used for the production of oil (Ruan et al., 2008), feed (Sun et al., 2019), medicines (Bai et al., 2015), and beauty products (Qin et al., 2015). The plant was introduced in China in 1993 as a candidate species for the development of coastal tidal flats (Xu et al., 1996). Previous studies on *K. pentacarpos* have focused on its saline-tolerance characteristics and mechanism (Blits and Gallagher, 1990a; Hasson and Poljakoff-Mayber, 1995; Guo et al., 2009b; Tang et al., 2015, 2020).

Several physiological adaptations add to the tolerance of *K. pentacarpos* to salt stress. Cations in *K. pentacarpos* are reverse transported across membranes, which establishes a favorable  $\text{K}^+$ - $\text{Na}^+$  relationship (Blits and Gallagher, 1990b,c). Its root system has a mechanism for  $\text{Na}^+$  repulsion and absorption (Blits and Gallagher, 1990c), endowing the plant with considerably high levels of salinity tolerance; Its hypocotyl callus can even grow in 240 mmol/L  $\text{NaCl}$  environments (Hasson and Poljakoff-Mayber, 1995). Under high-salinity stress, *K. pentacarpos* reduces biological toxicity by enhancing its ability to remove reactive oxygen species (Zhang et al., 2007).

In the early salinity stress stage, the expression of *K. pentacarpos* genes is upregulated and re-induced in the root system (Guo et al., 2009b). This involves ionic balance, plant growth and development, and signal transduction, which are mediated by peroxisome membrane proteins and ornithine transferase genes (Guo et al., 2009a). Wang et al. (2015a) cloned *KvP5CS1* from *K. pentacarpos* leaves, whose function in improving salinity tolerance by synthesizing proline to regulate cellular osmotic pressure was verified using a transgenic tobacco model (Wang H. Y. et al., 2019). Under 300 and 400 mmol/L  $\text{NaCl}$  conditions, proline concentrations in *K. pentacarpos* leaves were 9 and 27 times higher than that in the control, respectively, indicating that the regulation of

osmotic pressure was closely related to its salinity tolerance (Wang et al., 2015b).

The heat shock protein gene *KvHSP70* is sensitive to  $\text{NaCl}$  stress and significantly improves the salinity tolerance of transgenic tobacco plants (Tang et al., 2020). Subsequently, the salinity stress-sensitive genes cloned from *K. pentacarpos*, such as the chloroplast small heat shock protein gene *KvHSP26* and the tonoplast intrinsic protein gene *KvTIP3*, are potential candidates for molecular plant breeding (Liu et al., 2020, 2021).

In 2011, *K. pentacarpos* was introduced in the saline-alkali beachhead soils of the Yellow River in northern China (Xu et al., 2013). However, there were major differences between the saline-alkali soils along the river and coastal saline soils. To date, studies on the saline tolerance of *K. pentacarpos* mainly focused on saline soils alone or salt-stressed environments. There have been no studies on the effects of mixed saline-alkali conditions and saline-alkali stress-mediating pathways, and the limited investigations have been restricted to the physiological level (Yan and Zhou, 2019; Zhou and Zhang, 2019; Dai and Zhou, 2020), which failed to fundamentally examine the tolerance mechanism of *K. pentacarpos* to mixed saline-alkali stress.

To address this issue, this study aimed to determine the key genes of *K. pentacarpos* that respond to saline-alkali stress using transcriptome sequencing, weighted gene co-expression network analysis (WGCNA), and orthogonal partial least squares regression analysis (OPLS-RA). The findings of this study will provide insights into the use of *K. pentacarpos* to improve saline-alkali soils and molecular plant breeding in the future.

## MATERIALS AND METHODS

### Experimental Materials and Design

Seeds of *K. pentacarpos* were obtained from the Halophyte Research Laboratory of Nanjing University, which introduced *K. pentacarpos* from the Halophyte Biotechnology Center, University of Delaware, United States, in 1993.

Uniform and plump *K. pentacarpos* seeds were selected and soaked in concentrated sulfuric acid for 30 min, followed by rinsing with clean water and soaking for 24 h. Next, the seeds were placed on a wet towel and covered to induce germination. When one-third of the germinated seeds exhibited approximately 1 mm-long sprouts, they were sown in plastic cultivation bowls (diameter: 11 cm; height: 10 cm), with five seeds per bowl. Common garden soil (0.6 kg per bowl) was used for cultivation. A tray was arranged at the bottom of each bowl, and the bowls were placed in a greenhouse with day/night temperatures of 28/25°C. Then, 120 mL of water, based on specialized experimental determination, was added to each bowl per week. After all the seeds germinated, 120 mL of 25% Hoagland's nutrient solution was added to provide nutrition once every 2 weeks. Furthermore, the water and the nutrient solution evenly permeated throughout the cultivation soil from the tray in this experiment.

According to the classification of China's saline-alkali soil, the salt content of severe saline-alkali soil is 0.4–0.6% (Zhang, 2019). Therefore, in this study, salt concentration of the cultivation soil

was set at 0.05 and 0.5%. Before the seedlings reached the age of 90 days, they were separately subjected to saline-alkali stress treatments for 1 and 7 days. Using the amount of cultivation soil in the bowls as the basis, NaCl and NaHCO<sub>3</sub> were accurately weighed to a mass ratio of 4:1 to obtain total concentrations of 0.5 g/kg (0.05%) and 5 g/kg (0.5%). The saline-alkali mixture was dissolved in 120 mL of distilled water, placed in the tray at the base of each bowl, and allowed to permeate evenly throughout the cultivation soil. All seedlings were sampled and measured at 90 days of age. In this experiment, seedlings cultivated using ordinary garden soil served as the control (CK). The treatment groups were as follows: (i) Tr1: 0.05% saline-alkali solution for 1 day; (ii) Tr2: 0.05% saline-alkali solution for 7 days; (iii) Tr3: 0.5% saline-alkali solution for 1 day; and (iv) Tr4: 0.5% saline-alkali solution for 7 days. Each treatment group consisted of six cultivation bowls.

## Measurement of Chlorophyll Fluorescence Characteristics

The chlorophyll fluorescence parameters were measured using a YAXIN 1161G chlorophyll fluorometer (Beijing Yaxinliyi Science and Technology Co., Ltd., Beijing, China). Intact leaves from the middle-upper section of the seedlings were selected and darkened for 30 min using clamping blade clips before testing. The leaves were treated with saturated pulsed light at  $3,000 \mu\text{mol}\cdot\text{m}^{-2}\cdot\text{s}^{-1}$  for 1 s followed by actinic light at  $1,000 \mu\text{mol}\cdot\text{m}^{-2}\cdot\text{s}^{-1}$  for 9 s. The light-induced curve was then used to measure the initial fluorescence ( $F_0$ ) and other indicators of chlorophyll fluorescence. From each treatment group, three cultivation bowls were randomly selected, and each bowl was tested five times to obtain the average value. Indicators were measured thrice.

## RNA Extraction and Analysis

Leaves from the middle-upper section of the seedlings and some tender stems were collected and immediately frozen using liquid nitrogen at  $-80^\circ\text{C}$  for storage. From each treatment group, three cultivation bowls were selected for analyses. After extracting total RNA using a Takara RNA Preparation Kit (Takara Bio, Dalian, China), RNA concentration and quality were determined using a Nanodrop ND-1000 spectrophotometer (NanoDrop Technologies, DE, United States) and Agilent 2100 Bioanalyzer system (Agilent Technologies, CA, United States), respectively.

## Full-Length Transcriptome Sequencing and Data Analysis

Full-length (FL) cDNAs were synthesized using a SMARTer™ PCR cDNA Synthesis Kit (Takara Bio, Dalian, China), and cDNA length (1–6 kb) was determined and screened using a BluePippin™ Size-Selection System (Sage Science, Beverly, MA, United States). Next, a DNA Template Prep Kit 2.0 (Pacific Biosciences, Menlo Park, California, United States) was used to establish the SMRTbell library before performing single-molecule real-time (SMRT) sequencing on the PacBio RSII platform (Pacific Biosciences, Menlo Park, California, United States).

The polymerase reads that the length is less than 50 bp, and the accuracy is less than 0.90, were filtered according to the standard procedures of the SMRT Analysis Software package, and sub-sequences shorter than 50 bp were removed to obtain insert reads. The Iso-Seq module of the SMRT Link software was used to iteratively cluster similar full-length (FL) non-chimeric (FLNC) sequences. Consensus isoforms were obtained and further corrected to obtain high-quality transcriptomes with accuracies above 99%. Subsequently, the corresponding Illumina RNA-seq data were input in the Proovread 2.13.841 software to correct for low-quality consensus sequences, thereby increasing sequence accuracy. Finally, the CD-HIT 4.6.142 software was used to eliminate redundant sequences (Li and Godzik, 2006), resulting in a high-quality transcriptome database.

## Second-Generation Transcriptome Sequencing and Data Analysis

The operating instructions of the NEBNext® Ultra™ RNA Library Preparation Kit (NEB, Beverly, MA, United States) were followed to generate a second-generation sequencing cDNA library. After purification of the cDNA fragments using the AMPure XP system, the Agilent 2100 Bioanalyzer was used to evaluate the quality of the library. After the quality was ascertained, cDNA library sequencing was performed on the Illumina HiSeq 2500 platform (Illumina, San Diego, CA, United States) to derive paired-end reads.

The raw data were processed to eliminate the sequencing adapters and primer sequences to obtain clean reads before the value of fragments per kilobase of exon per million fragments mapped (FPKM) was used to measure the level of gene expression. The DESeq R software package of the Bioconductor platform was then run to analyze the differential expression between the transcriptomes of the various treatment groups (Anders and Huber, 2010). Differentially expressed genes (DEGs) were screened using fold change  $\geq 2$  and false discovery rate (FDR)  $< 0.01$  as the standards.

The identified DEGs were clustered using k-means method, and then used for KEGG enrichment analysis. The KOBAS software was used to test the statistical enrichment of DEGs in KEGG pathways (Mao et al., 2005). The hypergeometric test was used to analyze pathway enrichment based on the KEGG pathway database as the unit. The results were compared with the transcriptome background to identify enriched pathways from the differentially expressed transcriptomes.

Using the NCBI database,<sup>1</sup> a homology search and comparison ( $E\text{-value} \leq 1\text{e-}5$ ) of the key genes (FL sequences) selected from the DEGs was performed. Based on query coverage, identity percentage, and E-value of matched nucleobases, the comparison result ranked first in the database were then screened.

## Weighted Gene Co-expression Network Analysis of Differential Genes

The WGCNA R software package (Langfelder and Horvath, 2008) was used to construct a weighted gene co-expression

<sup>1</sup><https://www.ncbi.nlm.nih.gov/genome>

network. The WGCNA analysis was performed on the DEGs with FPKM values  $\geq 1$  and coefficient of variation between treatments  $\geq 0.5$  for a total of 15 transcriptome samples (5 treatments, each with 3 replicates). After threshold screening and determination of the weighting coefficient  $\beta$ , the original scaled relationship matrix was subjected to power processing to obtain an unscaled adjacency matrix. Considering the correlation of expression patterns between a gene and other genes in WGCNA analysis, the adjacency matrix was further transformed into a topological overlap matrix (TOM). Based on topological dissimilarity matrix (diss TOM = 1-TOM), dynamic shearing algorithm was used for gene clustering and module division. Furthermore, the minimum number of genes in a module was 30 (min Module Size = 30), the threshold for merging similar modules was 0.1327 (minimum Height for Merging Modules = 0.1327), and the network type was “Unsigned” in this analysis.

The genes were selected as module members according to the kME value  $> 0.7$ . Some modules, which exhibited high correlations with sample traits, were selected from the heatmap, and their gene co-expression visualization network diagrams were constructed using the Cytoscape 3.7.2 software.

## Quantitative Expression of Real-Time Fluorescence in Selected Genes

Leaves from the middle-upper section and tender stems were mixed following the aforementioned experimental design. Next, a SteadyPure Plant RNA Extraction Kit (Hunan Accurate Bio-Medical Co., Ltd., Changsha, China) was used to extract RNA for quality inspection according to the manufacturer's instructions. After quality testing, a PrimeScript<sup>TM</sup> RT reagent kit with gDNA Eraser (Perfect Real Time) (Takara Bio, Dalian, China) was used to synthesize cDNA by reverse transcription.

A CFX96 real-time fluorescence quantitative PCR system (Bio-Rad Laboratories, Inc., California, United States) was used for qRT-PCR analysis. The reagent test kit used was the TB Green<sup>®</sup> Premix EX Taq<sup>TM</sup> II (Tli RNase H Plus) (Takara Bio, Dalian, China), the dye was TB Green, and the internal reference gene was  $\beta$ -actin. The primer designing tool of NCBI was used to design the fluorescence quantitative PCR primers. Relative gene expression was analyzed using the  $2^{-\Delta\Delta CT}$  method (Livak and Schmittgen, 2001) with three replicates.

## Statistics

SPSS 21.0 was used to perform Duncan's multiple range test at a significance level ( $\alpha$ ) of 0.05; SIMCA 14.1 was used to perform OPLS-RA.

## RESULTS

### Fluorescence Characteristics of *Kosteletzkya pentacarpos* Seedlings Under Saline-Alkali Stress

The  $F_0$  of seedlings increased with prolonged treatment with 0.05 and 0.5% saline-alkali solutions. All treatments exhibited

$F_0$  values greater than that of the control, and the  $F_0$  value was 32.85% higher than that of the control, with a significant difference under the high-concentration condition ( $P = 0.001$ , see **Figure 1A**) on day 7. Compared to the control, the maximum photochemical efficiency ( $F_v/F_m$ ) was relatively stable and changed slightly under saline-alkali conditions (see **Figure 1B**). However,  $F_v/F_m$  significantly decreased under prolonged high-concentration condition ( $P = 0.022$ ), and the value on day 7 was 5.02% lower than that on day 1. The photochemical quenching coefficient (qP) and PSII quantum yield ( $\Phi$ PSII) also presented similar patterns (see **Figures 1C,D**): under the 0.05 and 0.5% saline-alkali conditions, both parameters decreased with prolonged treatment. The variations in qP and  $\Phi$ PSII were significant under the 0.5% saline-alkali condition after 7 days ( $P = 0.010$ ,  $P = 0.000$ ), and qP and  $\Phi$ PSII values decreased by 68.94 and 33.80%, respectively, compared with the respective control groups.

### Analysis of *Kosteletzkya pentacarpos* Transcriptome Characteristics Under Saline-Alkali Stress

The SMRT sequencing technique was used to determine the FL transcriptomes of *K. pentacarpos* seedlings. An SMRT cell was used to establish an FL cDNA library with a sequence length of 1–6 kb (**Table 1**). Subreads smaller than 50 bp in length were filtered, yielding 18.95 G of clean data. A total of 410,351 circular consensus sequences (CCS) were extracted based on the criteria of full passes  $\geq 3$  and sequencing accuracy  $> 0.9$ , with sequence length distributed between 1 and 3 kb (**Supplementary Figure 1A**). After removing the cDNA primer and polyA sequences from the CCS, 383,234 FLNC sequences were obtained, most of which were 1–3 kb in length (**Supplementary Figure 1B**). Following iterative clustering, 96,419 consensus isoforms were obtained, with the majority of the transcriptomes being approximately 2-kb long (**Supplementary Figure 1C**). Further correction yielded 93,218 high-quality consensus isoforms, the accuracies of which were above 99%. Finally, highly similar sequences were merged, and redundancies were removed, leaving 54,601 non-redundant sequences.

In this experiment, differential expression in the transcriptomes of *K. pentacarpos* seedlings was not evident following 0.05% saline-alkali treatment (**Figures 2A,B**). The number of DEGs on day 1 and 7 were 185 and 203, respectively. Under 0.5% saline-alkali treatment, differential expression in their transcriptomes became evident, with 1,588 and 1,764 DEGs on days 1 and 7, respectively. Among these, downregulated DEGs were predominant (**Figures 2C,D**) and accounted for 89.11 and 88.38% of the total expression on days 1 and 7 of 0.5% saline-alkali treatment, respectively. These results revealed that saline-alkali concentrations considerably affected *K. pentacarpos* seedlings than treatment duration.

The top 20 pathways with the smallest q values are shown in **Figures 2E–H** for the four treatments. Under 0.05% saline-alkali treatment, the enrichment factors of each pathway were small, but the q value was larger on day 1. The pathways were mainly enriched in the biosynthesis and endocytosis of ubiquinone and



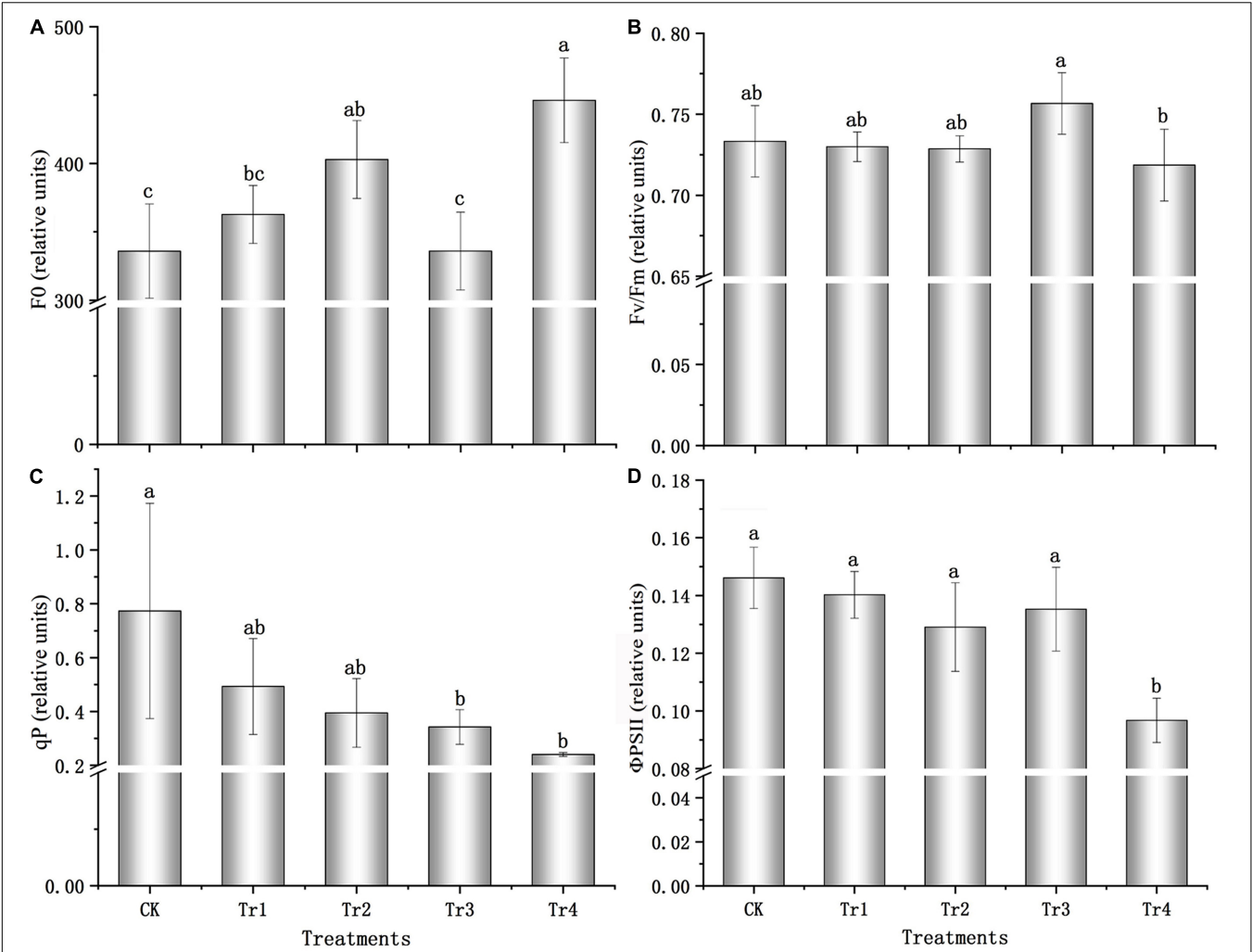
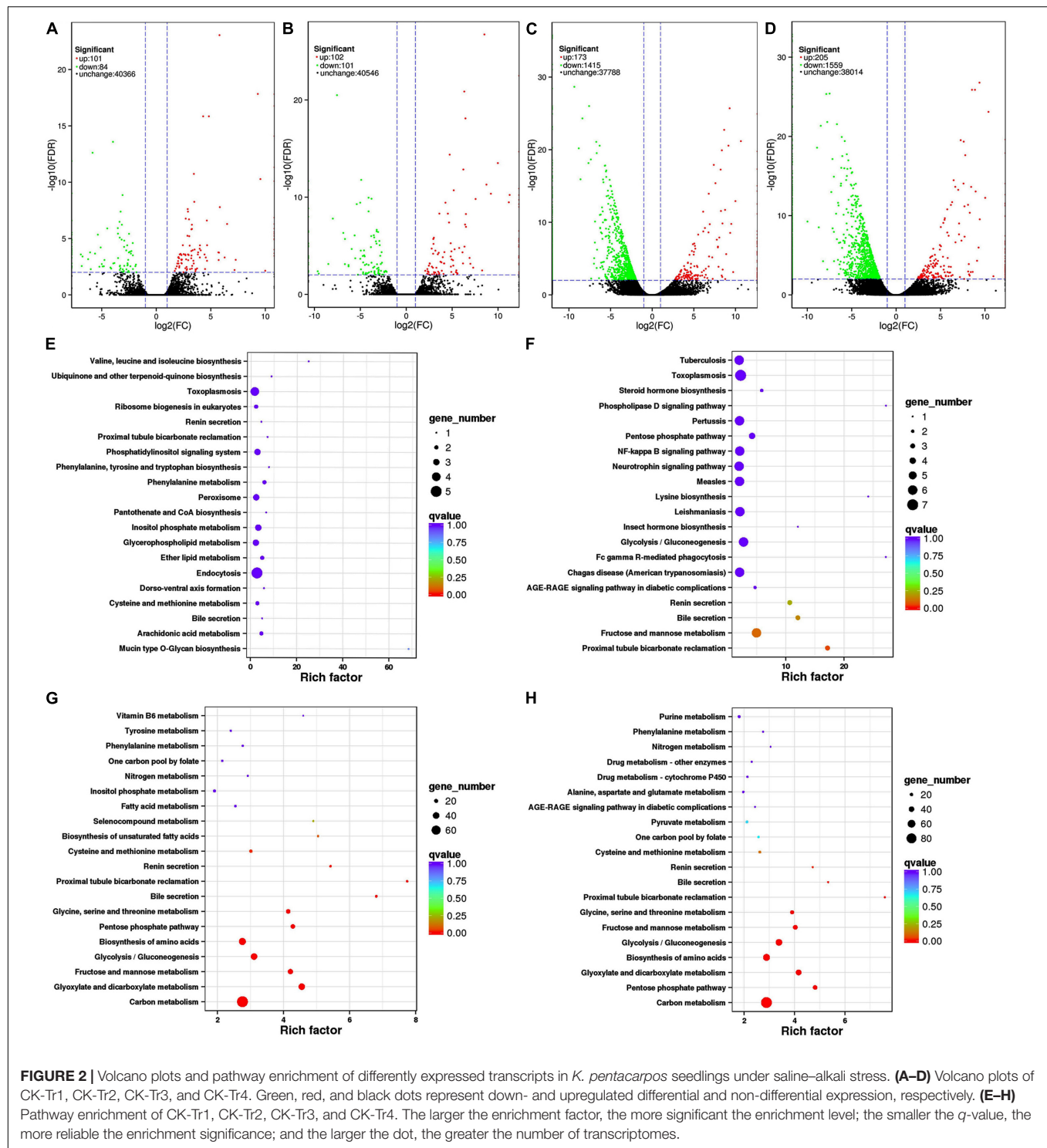


**FIGURE 1 |** Chlorophyll fluorescence characteristics of *K. pentacarpus* seedlings under saline-alkali stress. **(A)** Initial fluorescence ( $F_0$ ). **(B)** Maximum photochemical efficiency ( $F_v/F_m$ ). **(C)** Photochemical quenching coefficient (qP). **(D)** PSII quantum yield ( $\Phi_{PSII}$ ). Vertical bars in the figure indicate mean  $\pm$  SD ( $n = 3$ ). Different letters indicate significant differences at  $P < 0.05$ .

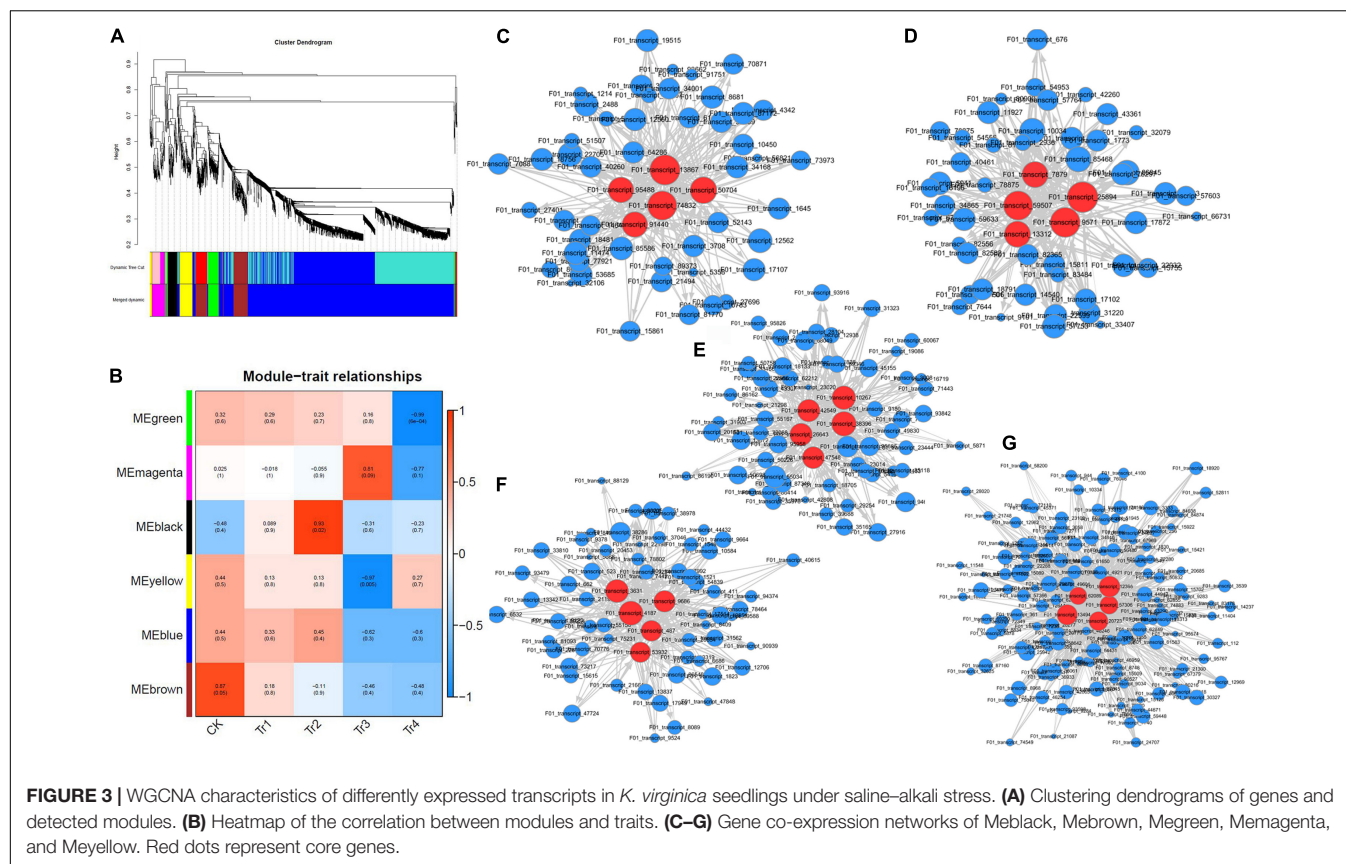
**TABLE 1 |** PacBio iso-seq output statistics for *K. pentacarpus* seedlings.

CCS data					
Samples	cDNA size	CCS number	Read bases of CCS	Mean read length of CCS	Mean number of passes
F01	1–6K	410351	831995069	2027	24
FLNC data					
Samples	Number of CCS	Number of undesired primer reads	Number of filtered short reads	Number of FLNC reads	FLNC%
F01	410351	19467	33	383234	93.39%
Clustering and redundance removal					
Samples	Number of consensus isoforms	Average consensus isoforms read length	Number of polished HQ isoforms	Percent of polished HQ isoforms (%)	Non-redundant consensus isoforms
F01	96419	2109	93218	96.68%	54601



terpenoid-ubiquinone (Figure 2E). When the seedlings were subjected to stress for 7 days, a small portion of the pathway enrichment factors increased, while the *q* value became smaller. Most pathways were similar to those on day 1 and were mainly enriched in pathways, such as phagocytosis and metabolism of fructose and mannose (Figure 2F). The pathway enrichment

conditions on days 1 and 7 were similar with 0.5% saline-alkali treatment. The enrichment factors of the various pathways increased significantly compared with that of low-concentration treatment, but the *q* value was small. The number of enriched transcriptomes also increased significantly. Enrichment occurred in various pathways, including those of carbon metabolism,



amino acid biosynthesis, and fructose and mannose metabolism (Figures 2G,H).

## Weighted Gene Co-expression Network Analysis of Differential Genes in *Kosteletzkya pentacarpos* Under Saline-Alkali Stress

We used kME values to evaluate the existence of effective connectivity between key genes and identify module members. In this experiment, DEGs with kME > 0.7 were selected as module members, and similar modules were merged after their eigenvectors were calculated, resulting in six gene co-expression modules (Figure 3A). The modules had 52 (Memagenta) to 1,370 (Meblue) DEGs. The expression patterns of DEGs in the same module were similar and downregulated.

The modules–traits correlation heatmap (Figure 3B) reflected the correlation between genes in samples with related traits and the modules to which they belonged. The greater the absolute value, the stronger the correlation. Red and blue colors indicate positive and negative correlations, respectively. In this experiment, five gene modules were highly correlated with the saline-alkali stress in *K. pentacarpos*, with all their correlation coefficients being > 0.80. Among them, Memagenta ( $r = 0.81$ ), Mebrown ( $r = 0.87$ ), and Meblack ( $r = 0.92$ ) were positively correlated with CK, Tr2, and Tr3, respectively; Meyellow ( $r = -0.97$ ) and Megreen ( $r = -0.99$ ) were negatively correlated with Tr3 and Tr4, respectively. The WGCNA visualization

diagrams for the five modules were generated (Figures 3C–G), and the top five genes with the highest kME values in each module were selected as key genes for that module (marked in red, see Supplementary Table 1).

## Screening of Key Genes in *Kosteletzkya pentacarpos* Seedlings That Responded to Saline-Alkali Stress

$F_v/F_m$  reflects the potential maximum light conversion efficiency of plants, and can indicate their overall health status (Bjorkman and Demming, 1987). Therefore, it is an important indicator of the impact of environmental stress on photosynthetic performance. In this study, OPLS-RA was performed on the  $F_v/F_m$  (Y) of *K. pentacarpos* and the FPKM value (X) of the selected 25 key genes. The degree of influence of each factor over photosynthetic performance was analyzed using the VIP value, which was the basis for screening the key genes. After fitting the principal component analysis model ( $R^2X = 0.504$ ,  $Q^2 = 0.149$ ), the score chart of the samples (Figure 4A) revealed that the 15 sample groups were normally distributed with no abnormalities. The regression model was established using OPLS-RA fitting ( $R^2X = 0.625$ ,  $R^2Y = 0.921$ ,  $Q^2 = 0.542$ ).

The VIP value of the model indicated the degree of influence that the relevant factors exhibited on Y. The selection criterion, based on the requirements stipulated in the SIMCA user guide, was that the VIP value must be > 1. After evaluation, nine DEGs in the *K. pentacarpos* seedlings were found to have VIP values > 1

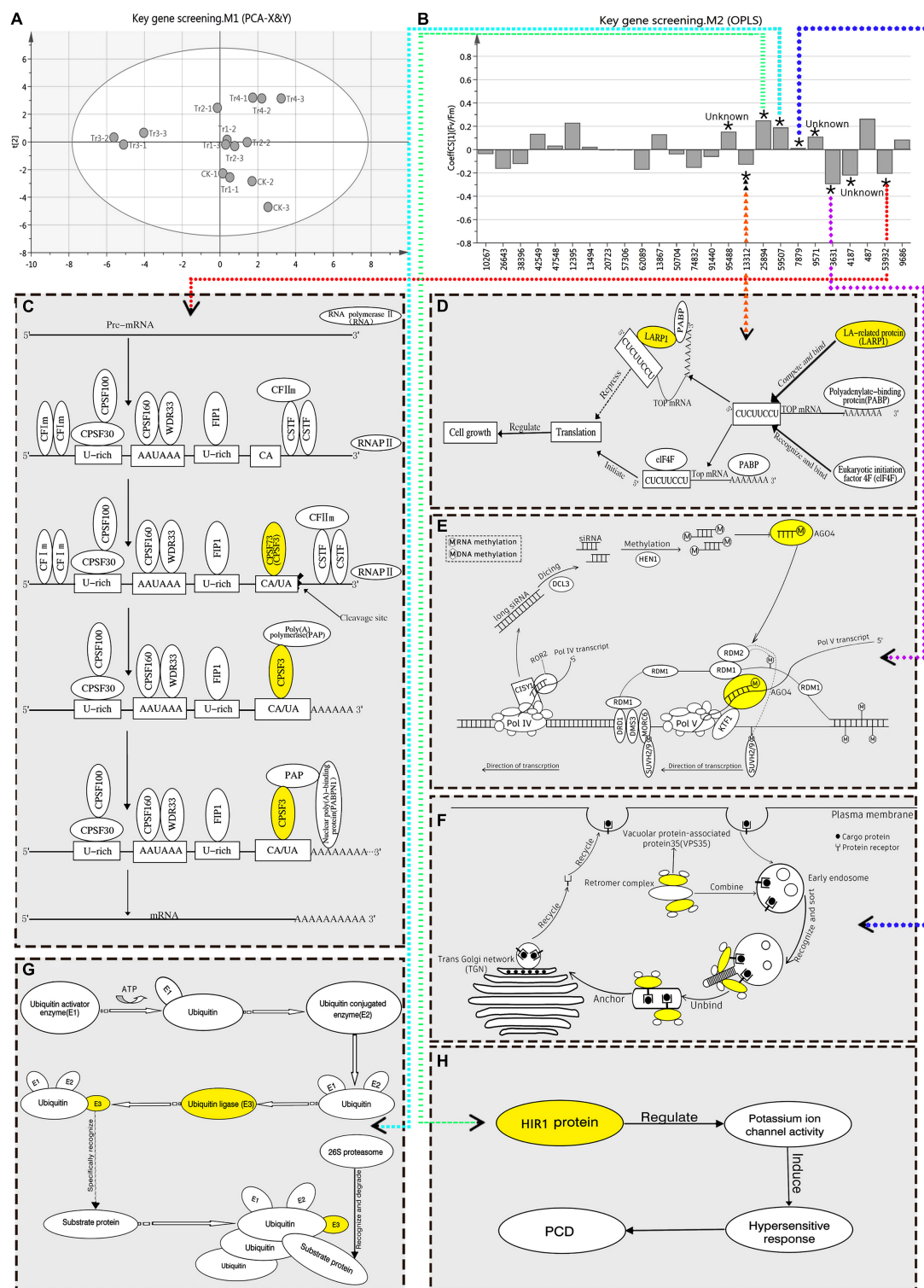


**FIGURE 4** | OPLS-RA conduction and filtration of key genes responsive to saline-alkali stress in *K. pentacarpus* seedlings. **(A)** Sample score chart of PCA.

**(B)** OPLS-RA model diagram. In this model, “\*” indicates that the VIP value of the corresponding transcript is > 1 in this model, “Unknown” indicates that function of the corresponding gene is not clear, the numbers on the x-axis represent transcript ID of 25 core genes, and dotted arrows in different colors point to functional maps of the corresponding genes. **(C–H)** Function diagrams of the key genes filtered using the OPLS-RA model, including *KpCPSF3* (**C**, diagram **C** refers to this literature; Xu et al., 2021), *KpLARP1C* (**D**, diagram **D** refers to this literature; Philippe et al., 2018), *KpAGO4* (**E**, diagram **E** refers to the literatures; Pikaard et al., 2012; Matzke and Mosher, 2014), *KpVPS35A* (**F**, diagram **F** refers to this literature; Song et al., 2016), *KpPUB33* (**G**), *KpHIR1* (**H**).



(Supplementary Table 2) and were selected as key genes that responded to saline-alkali treatments (Figure 4B).

The FL cDNA sequences (Supplementary Table 3) were used to perform homology comparisons with the NCBI database. Among them, the functions of three genes was unknown, while those of the remaining six were known. The IDs of their transcriptome sequence were F01\_transcript\_53932, F01\_transcript\_13312, F01\_transcript\_3631, F01\_transcript\_7879, F01\_transcript\_59507, and F01\_transcript\_25894. After comparison, these six genes were highly homologous to plants, such as *Hibiscus syriacus* and *Gossypium hirsutum*, both of which belong to the Malvaceae family. These genes were predicted to be *KpCPSF3*, *KpLARP1C*, *KpAGO4*, *KpVPS35A*, *KpPUB33*, and *KpHIR1* (Figures 4C–H). The specific comparisons are given in Table 2.

Functional analysis revealed that the key genes were involved in regulating pathways, such as vesicular transport (*KpVPS35A*), programmed cell death (PCD; *KpHIR1*) induction, transcription levels (*KpCPSF3* and *KpAGO4*), translation levels (*KpLARP1C*), and post-translational protein levels (*KpPUB33*) (see Table 2). Most genes exhibited negative regulatory effects.

### qRT-PCR Analysis of Key Genes of *Kosteletzkya pentacarpos*

Specific primers were designed according to the FL transcriptome sequences (Supplementary Table 4) for qRT-PCR analysis of the nine key genes. For most treatments, the expression levels of the key genes were significantly lower than those of the control and were downregulated (Figure 5); this was consistent with the transcriptome results.

Among the nine genes, the expression patterns of five genes—F01\_transcript\_53932, F01\_transcript\_7879, F01\_transcript\_59507, F01\_transcript\_25894, and F01\_transcript\_9571—were similar. Compared to the control, gene expression gradually decreased under Tr1 and Tr2 (low saline-alkali treatments). Nonetheless, gene expression initially decreased but recovered under Tr3 and Tr4 (high saline-alkali treatments), despite being lower than that of the control (Figures 5A,D–H). However, their expression levels under Tr2 was the lowest among all treatments, and significantly decreased by 56.65, 53.80, 67.16, and 87.51% compared with those of their corresponding controls ( $P = 0.000$ ).

The expression patterns of F01\_transcript\_13312, F01\_transcript\_95488, and F01\_transcript\_4187 were similar; under prolonged saline-alkali treatments, the expression levels of these three genes decreased. The expression levels of these genes in most treatment groups were lower than those in the control, and only few genes exhibited expression levels greater than the control for the treatment groups on day 1 (Figures 5B,G,I), which under the Tr2 treatment were the lowest and 95.54, 55.92, and 44.14% lower than those of their respective controls ( $P = 0.000$ ). This anomaly might be caused by an emergency response to saline-alkali stress. Under Tr1 and Tr2, the expression of F01\_transcript\_3631 increased with time, and the value under Tr1 significantly decreased by 50.90% compared with that of the control ( $P = 0.000$ ), whereas under Tr3 and Tr4,

its expression levels were relatively stable but consistently lower than that of the control (Figure 5C).

## DISCUSSION

### Characteristics of the Photosynthetic Functions of *Kosteletzkya pentacarpos* Seedlings Under Saline-Alkali Stress

In this study, the Fv/Fm of seashore mallow was stable under saline-alkali stress, and the Fv/Fm value of each treatment was not significantly different from that of control plants. However, F0, qP, and  $\Phi$ PSII changed significantly in the later stages of high-concentration saline-alkali treatment compared with their respective controls, and the variations were relatively small in other treatments.

The decrease in Fv/Fm of the stressed seedlings can be attributed to the inactivation of the PSII reaction center (Dąbrowski et al., 2015) or blockage of the photosynthetic electron transport chain (Tuba et al., 2010). However, the difference between the Fv/Fm values of the treated plants and the control was not significant under Tr4, indicating that the photosynthetic performance of the *K. pentacarpos* seedlings was relatively stable under saline-alkali stress conditions. However, qP was used to reflect the photosystem pressure due to the excess excitation energy of PSII (Öquist and Huner, 1993). With increasing saline-alkali concentrations, the qP of the *K. pentacarpos* seedlings decreased with time, indicating that the pressure of excitation energy gradually increased on photosystem and the photosynthetic function was affected (Öquist and Huner, 1993). As for the electron transport chain, the  $\Phi$ PSII reflected the working status of PSII (Li and Feng, 2004). In this study, the variation was similar to that of Fv/Fm, indicating that the PSII electron transport chain was relatively normal in the early stage, but electron transfer was blocked to weaken photosynthetic function in the later stage. Based on chlorophyll fluorescence characteristics, photosynthetic performance of the seedlings was relatively stable, and *K. pentacarpos* showed strong tolerance to saline-alkali stress.

### Impact of Negative Regulation on *Kosteletzkya pentacarpos* Response to Saline-Alkali Stress

Plants must finely regulate their gene expression in response to environmental stress. Although previous studies have focused on positive regulatory mechanisms (Cao et al., 2017; Pang et al., 2017; Lu et al., 2019), recent studies have paid increasing attention to negative regulation. In this study, downregulated DEGs accounted for 89.11 and 88.38% of the expression under Tr3 and Tr4, respectively, with negative regulation being predominant. Three negative regulatory pathways, involving the key genes of *K. pentacarpos*, were involved in responding to saline-alkali stress: (i) LARP1 inhibited the translation of 5'-terminal oligopyrimidine mRNAs (TOP mRNAs) (Philippe et al., 2018); (ii) AGO4-mediated DNA methylation through siRNA interaction (Pikaard et al., 2012; Matzke and Mosher, 2014); and

**TABLE 2 |** Sequence match in NCBI database and functional analysis of key differentially expressed genes in *K. pentacarpos* seedlings under saline-alkali stress.

Transcript ID	Gene type	Functional description	Matching species	Query coverage (%)	Identity percentage (%)	E-value	Accession
F01_transcript_53932	<i>KpCPSF3</i>	The encoded protein binds to pre-mRNA, performs precise cleavage, and assists in the polymerization of poly(A) to complete the processing of mature mRNA.	<i>Hibiscus syriacus</i>	78.00	92.48	0.00	XM_039209821.1
F01_transcript_13312	<i>KpLARP1C</i>	The encoded protein competes with eukaryotic initiation factor 4F to bind to 5' terminal oligopyrimidine mRNA (TOP mRNA), inhibit its translation, and then regulate cell growth.	<i>Gossypium hirsutum</i>	40.00	86.57	0.00	XM_016852313.2
F01_transcript_3631	<i>KpAGO4</i>	AGO4 protein binding to siRNA (short interfering RNA) mediates histone methylation and non-CG site DNA methylation in chromatin	<i>H. syriacus</i>	92.00	91.95	0.00	XM_039136791.1
F01_transcript_7879	<i>KpVPS35A</i>	This gene is mainly involved in endocytosis, where VPS35 binds to cargo proteins and transports them to the trans -Golgi network region.	<i>H. syriacus</i>	91.00	94.18	0.00	XM_039152238.1
F01_transcript_59507	<i>KpPUB33</i>	After binding to ubiquitin, U-box protein can specifically recognize and bind to substrate proteins, and these proteins are marked by ubiquitin chains and then degraded by the 26S proteome.	<i>H. syriacus</i>	83.00	91.81	0.00	XM_039139593.1
F01_transcript_25894	<i>KpHIR1</i>	The protein encoded by this gene can induce hypersensitivity response to external stress by regulating activity of potassium channels, and thus initiates programmed cell death.	<i>H. syriacus</i>	92.00	89.44	0.00	XM_039207218.1

(iii) the plant U-box33 recognized and labeled target proteins for degradation by the 26S proteasome in the ubiquitin pathway (Jin et al., 2007).

The 5'-TOP mRNAs, a class of eukaryotic mRNA family, contains proteins that regulate cell growth (Philippe et al., 2018), whose translation is regulated by the eukaryotic promoter 4F (eIF4F). Its translational abilities can be inhibited by LARP1, which competes to bind with TOP mRNAs (Tcherkezian et al., 2014). Fonseca et al. (2015) used RNA interference techniques to reduce the levels of LARP1, thereby alleviating its inhibitory effects on TOP mRNA translation. However, target of rapamycin (TOR) specifically controls the translation of 5'-TOP mRNAs by the putative TOR substrate, LARP1. Furthermore, the regulatory pathway of TOR-LARP1-5'-TOP is conserved in plants (Scarpin et al., 2020). In this study, *KpLARP1C* expression decreased with prolonged saline-alkali treatment, and its expression in most treatment groups was lower than that of the control. It is speculated that the decreased expression of *KpLARP1C* may reduce competition and the inhibition of TOP mRNA translation and promote cell growth, thereby enhancing the tolerance of *K. pentacarpos* seedlings to saline-alkali stress.

AGO4 has been mainly reported in studies of plant resistance to diseases (Brosseau et al., 2016). AGO4 achieves transcriptional silencing of genes through DNA methylation (Raja et al., 2008; Duan et al., 2015), leading to the regulation of plant responses to biotic and abiotic stress (Pu et al., 2021). *Arabidopsis thaliana* mutant, which over-expresses *AtAGO4*, is more likely to be infected by *Pseudomonas syringae* (Agorio and Vera, 2007), while the double mutant of *AtAGO4* and *AtAGO2* is susceptible to the tobacco rattle virus (Ma et al., 2015). AGO4 induces nucleic

chromatin modifications and prevents recessive transcription to maintain or activate the expression of stress-responsive genes (Al et al., 2017), which regulate physiological pathways, such as jasmonic acid signaling pathway (Prashanm et al., 2020). As for hypoxia, AGO1 in *Arabidopsis* coordinates AGO4, which represses the expression of HR4 by DNA methylation to regulate stress tolerance (Loreti et al., 2020). Under saline-alkali stress, the expression of *KpAGO4* was lower than that of the control plants., indicating that the decreased expression of *KpAGO4* may weaken the inhibition of DNA methylation and transcriptional gene silencing. Then, the function of related genes mediated by *KpAGO4* could be activated to respond to stress (Al et al., 2017), thereby improving the tolerance of *K. pentacarpos* seedlings to saline-alkali stress. This, in turn, maintained the stability of their photosynthetic function.

The ubiquitin system can selectively degrade proteins related to stress response, growth, and development of plants to adapt to environmental stress (Varshavsky, 1997). The plant U-box (PUB) protein is a type of ubiquitin-linked enzyme, E3, that specifically identifies target proteins (Zhou and Zeng, 2017), enabling plants to respond to stress. Sixty-six *StPUB* genes have been identified in potato, and 200 proteins are modified, including 25 differential ubiquitination modification sites under PEG-induced drought (Tang et al., 2022). *Arabidopsis thaliana* proteins, PUB22 and PUB23, act on RPN12a and cooperate to negatively regulate drought-stress responses through the drought signaling pathway (Cho et al., 2008; Seo et al., 2012). Similarly, *AtPUB11* is a negative regulator of drought tolerance, which degrades LRR1 and KIN7 (Chen et al., 2021). *Capsicum frutescens* *CaPUB1* gene, which was heterologously transferred into rice, negatively regulated

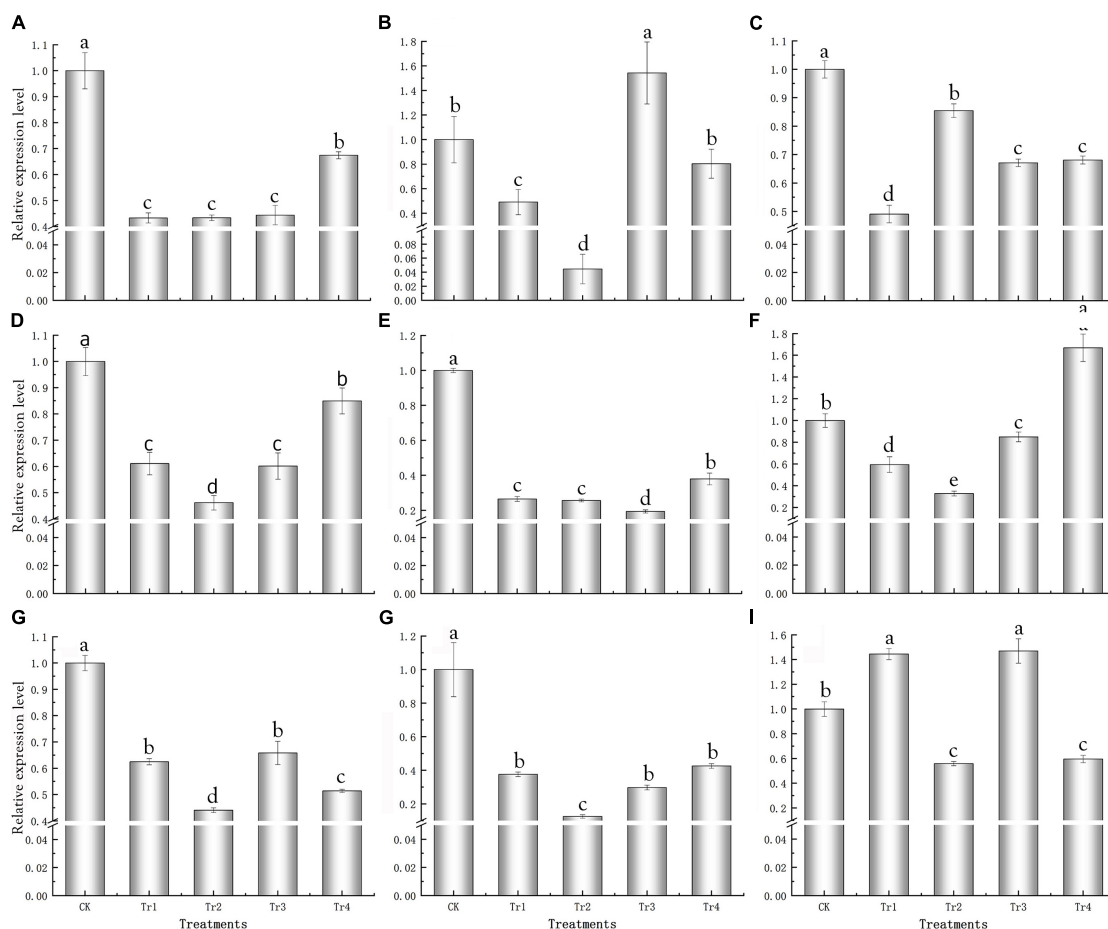


**FIGURE 5 |** qRT-PCR analysis of key genes responsive to saline-alkali stress in *K. pentacarpos* seedlings. **(A)** F01\_transcript\_53932 (*KpCPSF3*), **(B)** F01\_transcript\_13312 (*KpLARP1C*), **(C)** F01\_transcript\_3631 (*KpAGO4*), **(D)** F01\_transcript\_7879 (*KpVPS35A*), **(E)** F01\_transcript\_59507 (*KpPUB33*), **(F)** F01\_transcript\_25894 (*KpHIR1*), and **(G–I)** F01\_transcript\_95488, F01\_transcript\_9571, and F01\_transcript\_4187 (their function is unknown).

rice response to drought-stress and decreased drought-tolerance of rice (Min et al., 2016). Under salinity stress, *A. thaliana* protein PUB30 degraded BKI1 through ubiquitination and negatively regulated the salinity tolerance of plants (Zhang et al., 2017). After the *Pohlia nutans* *PnSAG1* gene was heterologously overexpressed in *A. thaliana*, the sensitivity of transformed plants to salinity stress increased, indicating negative regulation (Wang J. et al., 2019). In this study, *KpPUB33* expression was significantly downregulated in stressed *K. pentacarpos* plants. This indicates that a decrease in *KpPUB33* expression maybe alleviate the ubiquitin-mediated degradation of target proteins, and then maintain the normal functions of the target proteins, thereby improving saline-alkali tolerance of *K. pentacarpos*.

### Significance of Programmed Cell Death in *Kosteletzkya pentacarpos* Response to Saline-Alkali Stress

Plant PCD can be classified as apoptotic or autophagic (Huang and Fu, 2010). Apoptotic PCD often occurs in stress-induced hypersensitivity reaction (HR), such as heavy metal or salinity

stress (Pan et al., 2001; Liu et al., 2007). Hypersensitivity-induced response (HIR) genes can induce HR responses and participate in the regulation of ion channels and cell death (Zhou et al., 2010). Overexpression of the *C. frutescens* *CaHIR1* in *A. thaliana* led to tissue necrosis similar to HR and improved plant resistance to bacterial and fungal infections (Jung and Hwang, 2007). The expression of *Arachis hypogaea* *AhHIR* was significantly decreased under low-temperature stress, which increased with time (Liu et al., 2014). This observation was similar to that of *K. pentacarpos* *KpHIR1* under saline-alkali stress. The expression of *KpHIR1* decreased under Tr3 but increased to 66.91% compared to the control value under Tr4 ( $P = 0.000$ ), whereas its expression continuously decreased under Tr1 and Tr2. Downregulation of the expression of HIR gene was conducive to reducing cell mortality (Liu et al., 2014), whereas the upregulation of its expression promoted apoptosis-like PCD to form a barrier of dead cells (Liu et al., 2007), which prevented further tissue damage by the salt ions (Liu et al., 2007). This is the potential mechanism by which *K. pentacarpos* seedlings increase tolerance to saline-alkali stress.

Autophagic PCD is induced by stress, such as drought, salinity, and nutrient deficiency, where the endoplasmic reticulum is involved in regulating and inducing cell death (Huang and Fu, 2010). During PCD, endoplasmic reticulum recycles nutrients of damaged cells to supply them to other cells for survival. Phagocytes, however, reuse these nutrients through autophagy and vesicular transport (Song et al., 2016). The VPS35 protein in the vesicular transport complex Retromer specifically identifies the cargo protein, transports it to the vesicles of the Golgi reverse membranes, and then packages and exports it (Song et al., 2016), thereby ensuring reuse of the protein. Therefore, the Retromer complex could regulate the identification of dead cells by phagocytes through the cargo protein CED-1, and to recycle more nutrients (Yamanaka and Ohno, 2008). Under high-concentration saline-alkali stress, *KpVPS35A* expression increased with time, indicating that the ability to identify and transport the cargo protein was improved by VPS35. This led to improved precise identification of the PCD cells, which facilitated the recycle and reuse of their nutrients and maintained the vitality of other cells to help *K. pentacarpos* seedlings survive saline-alkali conditions.

## CONCLUSION

Based on the results in this study, we conclude that under saline-alkali stress, the photosynthetic performance of seashore mallow was relatively stable, the seedlings exhibited strong tolerance, and the saline-alkali concentration was more influential than the duration of exposure. The expression of the DEGs was mainly downregulated, indicating that *K. pentacarpos* responded to saline-alkali stress through a negative regulatory pathway. Nine key genes in saline-alkali-stressed *K. pentacarpos* seedlings were screened using WGCNA and OPLS-RA, six of which had known functions and were mainly involved in negative regulatory pathways, such as ubiquitin degradation, siRNA-mediated DNA methylation, and inhibition of TOP mRNAs translation, and other pathways, including vesicle transport and PCD. Using qRT-PCR analysis, the expression of the nine key genes showed a declining trend, which was consistent with the transcriptomic data.

The key genes screened in this study need further functional studies in model plants. Besides functional tests, both degraded

target proteins and methylated target genes require further investigations to determine their roles in regulatory pathways. Additionally, the key genes can also be used for plant molecular breeding to generate more saline-alkali-tolerant plant germplasm resources in the future. This will help restore saline-alkali lands to improve their ecological functions and alleviate the development of soil salinization in China and other countries.

## DATA AVAILABILITY STATEMENT

The datasets presented in this study can be found in online repositories. The names of the repository/repositories and accession number(s) can be found below: <https://www.ncbi.nlm.nih.gov/>, PRJNA771942; <https://www.ncbi.nlm.nih.gov/>, PRJNA771922.

## AUTHOR CONTRIBUTIONS

JZ designed the research and wrote the original draft of the manuscript. AQ contributed to the data analyses. BW provided technical guidance. XZ and QD conducted the experiments. JL contributed to the experimental-figure-drawing. All authors have read and agreed to the published version of the manuscript.

## FUNDING

This work was supported by the Science and Technology Project of Xinxiang City (CXGG17010) and the Henan Province Key R&D and Promotion Special Project (Science and Technology) (212102310843), China.

## SUPPLEMENTARY MATERIAL

The Supplementary Material for this article can be found online at: <https://www.frontiersin.org/articles/10.3389/fpls.2022.865572/full#supplementary-material>

**Supplementary Figure 1** | Read length distribution of transcriptome sequences. (A) CCS sequence. (B) FLNC sequences. (C) Consensus isoforms.

## REFERENCES

- Agorio, A., and Vera, P. (2007). Argonate 4 is required for resistance to *Pseudomonas syringae* in Arabidopsis. *Plant Cell* 19, 3778–3790. doi: 10.1105/tpc.107.054494
- Al, P. C. K., Dennis, E. S., and Wang, M. B. (2017). Analysis of Argonaute 4-associated long non-coding RNA in *Arabidopsis thaliana* sheds novel insights into gene regulation through RNA-directed DNA methylation. *Genes* 8:198. doi: 10.3390/genes8080198
- Alhdad, G. M., Seal, C. E., Al-Azzawi, M. J., and Flowers, T. J. (2013). The effect of combined salinity and waterlogging on the halophyte *Suaeda maritima*: the role of antioxidants. *Environ. Exp. Bot.* 87, 120–125. doi: 10.1016/j.envexpbot.2012.10.010
- An, S. H., Wang, X. L., Duan, J. J., Wang, X. K., and Xia, D. (2018). Advances in biotechnology research on soil remediation and improvement. *Hans. J. Soil Sci.* 6, 100–107. doi: 10.12677/HJSS.2018.64013
- Anders, S., and Huber, W. (2010). Differential expression analysis for sequence count data. *Genom. Biol.* 11:R106. doi: 10.1186/gb-2010-11-10-r106
- Bai, B., Gu, X. W., Chen, Y., Guan, F. Q., Shan, Y., and Xu, F. (2015). Virginicin, a new naphthalene from *Kosteletzkya virginica* (Malvaceae). *J. Braz. Chem. Soc.* 26, 723–728. doi: 10.5935/0103-5053.20150032
- Bjorkman, O., and Demming, B. (1987). Photon yield of O<sub>2</sub> evolution and chlorophyll fluorescence characteristics at 77K among vascular plants of diverse origins. *Planta* 170, 489–504. doi: 10.1007/BF00402983
- Blits, K. C., and Gallagher, J. L. (1990a). Effect of NaCl on lipid content of plasma membranes isolated from roots and cell suspension cultures of the dicot halophyte *Kosteletzkya virginica* (L.) Presl. *Plant Cell Rep.* 9, 156–159. doi: 10.1007/BF00232094



- Blits, K. C., and Gallagher, J. L. (1990b). Salinity tolerance of *Kosteletzkya virginica*. I. Shoot growth, lipid content, ion and water relations. *Plant Cell Environ.* 13, 409–418. doi: 10.1111/j.1365-3040.1990.tb01317.x
- Blits, K. C., and Gallagher, J. L. (1990c). Salinity tolerance of *Kosteletzkya virginica*. II. Root growth, ion and water relations. *Plant Cell Environ.* 13, 419–425. doi: 10.1111/j.1365-3040.1990.tb01318.x
- Brosseau, C., Oirdi, M. E., Adurogbangba, A., Ma, X. F., and Moffett, P. (2016). Antiviral defense involves AGO4 in an Arabidopsis-potextvirus interaction. *Mol. Plant Microbe Interact.* 29, 878–888. doi: 10.1094/MPMI-09-16-0188-R
- Cao, H. L., Wang, L., Qian, W. J., Hao, X. Y., Yang, Y. J., and Wang, X. C. (2017). Positive regulation of *CsbZIP4* transcription factor on salt stress response in transgenic Arabidopsis. *Acta Agronom. Sin.* 43, 1012–1020. doi: 10.3724/SP.J.1006.2017.01012
- Chen, X. X., Wang, T. T., Rehman, A. U., Wang, J., Qi, J. S., and Li, Z. (2021). Arabidopsis U-box E3 ubiquitin ligase PUB11 negatively regulates drought tolerance by degrading the receptor-like protein kinases LRR1 and KIN7. *J. Integr. Plant Biol.* 63, 494–509. doi: 10.1111/jipb.13058
- Cho, S. K., Ryu, M. Y., Song, C., Kwak, J. M., and Kim, W. T. (2008). Arabidopsis PUB 22 and PUB 23 are homologous U-box E3 ubiquitin ligases that play combinatory roles in response to drought stress. *Plant Cell* 20, 1899–1914. doi: 10.1105/tpc.108.060699
- Dąbrowski, P., Pawluśkiewicz, B., Baczewska, A. H., Ogłęcki, P., and Kalaji, H. M. (2015). Chlorophyll a fluorescence of perennial ryegrass (*Lolium perenne* L.) varieties under long term exposure to shade. *Zemdirbyste* 102, 305–312. doi: 10.13080/z-a.2015.102.039
- Dai, Y. M., and Zhou, J. (2020). Regulating effect of exogenous Ascorbic acid on *Kosteletzkya virginica* under saline-alkali stress. *Modern Agric. Sci. Technol.* 3, 171–174. doi: 10.3969/j.issn.1007-5739.2020.03.104
- Duan, C. G., Zhang, H. M., Kai, T., Zhu, X. H., Qian, W. Q., Hou, Y. J., et al. (2015). Specific but interdependent functions for *Arabidopsis* AGO4 and AGO6 in RNA directed DNA methylation. *EMBO J.* 34, 581–592. doi: 10.15252/embj.201489453
- Fang, S., Hou, X., and Liang, X. (2021). Response mechanisms of plants under saline-alkali stress. *Front Plant Sci.* 12:667458. doi: 10.3389/fpls.2021.667458
- Fonseca, B. D., Zakaria, C., Jia, J. J., Graber, T. E., Svitkin, Y., Tahmasebi, S., et al. (2015). La-related protein 1 (LAR1) represses terminal oligopyrimidine (TOP) mRNA translation downstream of mTOR complex 1 (mTORC1). *J. Biol. Chem.* 290, 15996–16020. doi: 10.1074/jbc.M114.621730
- Guo, L. Q., Wang, H. Y., Ma, Y., and Shi, D. C. (2010). Mechanism of osmotic adjustment and ionic balance in *Puccinellia tenuiflora* in response to salt and alkali stresses. *J. Northeast Norm. Univ.* 42, 120–125.
- Guo, Y. Q., Tian, Z. Y., Yan, D. L., and Qin, P. (2009b). Gene expression of *Kosteletzkya virginica* in response to salt stress at early stage. *J. Wuhan Univ.* 5, 340–347. doi: 10.3321/j.issn:1671-8836.2009.03.016
- Guo, Y. Q., Tian, Z. Y., Yan, D. L., Zhang, J., Zhou, W. Z., and Qin, P. (2009a). Gene expression of halophyte *Kosteletzkya virginica* seedlings under salt stress at early stage. *Genetica* 137, 189–199. doi: 10.1007/s10709-009-9384-9
- Hasson, E., and Poljakoff-Mayber, A. (1995). Callus culture from hypocotyls of *Kosteletzkya virginica* (L.) seedlings-Its growth, salt tolerance and response to abscisic acid. *Plant Cell Tissue Organ. Cult.* 43, 279–285. doi: 10.1007/BF00039956
- Huang, L. Y., and Fu, B. Y. (2010). Mechanism of Programmed Cell Death (PCD) responding to abiotic stresses in plant. *Mol. Plant Breed.* 8, 764–770.
- Jin, M. J., Liu, G. Z., Liu, Q., and Li, L. Y. (2007). Advancement of U-box protein structure and function. *CHIN. Agric. Sci. Bull.* 23, 119–123.
- Jung, H. W., and Hwang, B. K. (2007). The leucine-rich repeat (LRR) protein, CaLRR1, interacts with the hypersensitive induced reaction (HIR) protein, CaHIR1, and suppresses cell death induced by the CaHIR1 protein. *Mol. Plant Pathol.* 8, 503–514. doi: 10.1111/J.1364-3703.2007.00410.X
- Langfelder, P., and Horvath, S. (2008). WGCNA: an R package for weighted correlation network analysis. *BMC Bioinform.* 9:559. doi: 10.1186/1471-2105-9-559
- Li, W. Z., and Godzik, A. (2006). Cd-hit: a fast program for clustering and comparing large sets of protein or nucleotide sequences. *Bioinformatics* 22, 1658–1659. doi: 10.1093/bioinformatics/btl158
- Li, Z., and Feng, Y. L. (2004). Photosynthesis and oxidative stress of leaves at different positions in *Amomum villosum* Lour. *J. Plant Physiol. Mol. Biol.* 30, 546–552.
- Liu, S. H., Fu, B. Y., Xu, H. X., Zhu, L. H., Zhai, H. Q., and Li, Z. K. (2007). Cell death in response to osmotic and salt stresses in two rice (*Oryza sativa* L.) ecotypes. *Plant Sci.* 172, 897–902. doi: 10.1016/j.plantsci.2006.12.017
- Liu, X. H., Cheng, J. G., Jiang, F. H., Liang, M. X., Han, J. J., Zhang, J., et al. (2020). The tonoplast intrinsic protein gene *KvTIP3* is responsive to different abiotic stresses in *Kosteletzkya virginica*. *Int. J. Genom.* 2020:2895795. doi: 10.1155/2020/2895795
- Liu, X. H., Zhao, L. Z., Li, J. Z., Duan, L. J., Zhang, K., Qiao, X. Q., et al. (2021). The chloroplastic small heat shock protein gene *KvHSP26* is induced by various abiotic stresses in *Kosteletzkya virginica*. *Int. J. Genom.* 2021:6652445. doi: 10.1155/2021/6652445
- Liu, Y., Zhao, C. Z., Li, C. S., Li, C., and Wang, X. J. (2014). Cloning, expression and evolution analysis of peanut HIR gene. *Shandong Agric. Sci.* 46, 1–6. doi: 10.3969/j.issn.1001-4942.2014.05.001
- Livak, K. J., and Schmittgen, T. D. (2001). Analysis of relative gene expression data using real-time quantitative PCR and the  $2^{-\Delta\Delta CT}$  method. *Methods* 25, 402–408. doi: 10.1006/meth.2001.1262
- Loreti, E., Betti, F., Ladera-Carmona, M. J., Fontana, F., and Novi, G., Valeri, M. C., Perata, P. (2020). Agonaute1 and Agonaute4 regulate gene expression and hypoxia Tolerance. *Plant Physiol.* 182, 287–300. doi: 10.1104/pp.19.00741
- Lu, L. L., Feng, X. F., Li, K., and Li, W. (2019). *SmCCoAOMT* positively regulates the peel coloring in eggplant under high temperature stress. *CHIN. J. Trop. Crops* 40, 2091–2096. doi: 10.3969/j.issn.1000-2561.2019.10.025
- Ma, X., Nicole, M. C., Metegnier, L. V., Hong, N., Wang, G. P., and Moffett, P. (2015). Different roles for RNA silencing and RNA processing components in virus recovery and virus-induced gene silencing in plants. *J. Exp. Bot.* 66, 919–932. doi: 10.1093/jxb/eru447
- Mao, X., Cai, T., Olyarchuk, J. G., and Wei, L. (2005). Automated genome annotation and pathway identification using the KEGG Orthology (KO) as a controlled vocabulary. *Bioinformatics* 21, 3787–3793. doi: 10.1093/bioinformatics/bti430
- Matzke, M. A., and Mosher, R. A. (2014). RNA-directed DNA methylation: an epigenetic pathway of increasing complexity. *Nat. Rev. Genet.* 15, 394–408. doi: 10.1038/nrg3683
- Min, H. J., Jung, Y. J., Kang, B. G., and Kim, W. T. (2016). Ca PUB 1, a hot pepper U-box E3 ubiquitin ligase, confers enhanced cold stress tolerance and decreased drought stress tolerance in transgenic rice (*Oryza sativa* L.). *Mol. Cells* 39, 250–257. doi: 10.14348/molcells.2016.2290
- Munns, R., and Tester, M. (2008). Mechanisms of salinity tolerance. *Plant Biol.* 59, 651–681. doi: 10.1146/annurev.arplant.59.032607.092911
- Öquist, G., and Huner, N. P. A. (1993). Cold-hardening-induced resistance to photoinhibition of photosynthesis in winter rye is dependent upon an increased capacity for photosynthesis. *Planta* 189, 150–156. doi: 10.1007/BF00201355
- Pan, J. W., Zhu, M. Y., and Chen, H. (2001). Aluminum-induced cell death in root-tip cells of barley. *Environ. Exp. Bot.* 46, 71–79. doi: 10.1016/S0098-8472(01)00083-1
- Pang, X., Zhao, Y. T., Fan, J. T., Xing, H. X., Zhang, J., Xing, J. H., et al. (2017). AtMYB73 gene positively regulates the response to salt stress in Arabidopsis. *J. Agric. Univ. Hebei* 40, 44–48. doi: 10.13320/j.cnki.jauh.2017.0101
- Philippe, L., Vasseur, J. J., Debart, F., and Thoreen, C. C. (2018). La-related protein 1 (LAR1) repression of TOP mRNA translation is mediated through its cap-binding domain and controlled by an adjacent regulatory region. *Nucleic Acids Res.* 46, 1457–1469. doi: 10.1093/nar/gkx1237
- Pikaard, C. S., Haag, J. R., Pontes, O. M. F., Blevins, T., and Cocklin, R. (2012). A transcription fork model for Pol IV and Pol V-dependent RNA-directed DNA methylation. *Cold Spring Harb. Symp. Quant. Biol.* 77, 205–212. doi: 10.1101/sqb.2013.77.014803
- Prashanm, M., Pandey, P., Baldwin, I. T., and Pandey, S. P. (2020). Argonaute 4 modulates resistance to *Fusarium brachygybbsum* infection by regulating jasmonic acid signaling. *Plant Physiol.* 184, 1128–1152. doi: 10.1104/pp.20.00171
- Pu, W. J., Tan, B. L., and Zhu, L. (2021). Progress on the biological functions of argonaute proteins in response to stress in plants. *J. Agric. Sci. Technol.* 23, 17–26. doi: 10.13304/j.nykjdb.2020.0670
- Qin, P., Han, R. M., Zhou, M. X., Zhang, H. S., Fan, L. S., Seliskar, D. M., et al. (2015). Ecological engineering through the biosecure introduction of *Kosteletzkya virginica* (seashore mallow) to saline lands in China: a review

- of 20 years of activity. *Ecol. Eng.* 74, 174–186. doi: 10.1016/j.ecoleng.2014.10.021
- Raja, P., Sanville, B. C., Buchmann, R. C., and Bisaro, D. M. (2008). Viral genome methylation as an epigenetic defense against geminiviruses. *J. Virol.* 82, 8997–9007. doi: 10.1128/JVI.00719-08
- Ruan, C. J., Li, H., Guo, Y. Q., Qin, P., Gallagher, J. L., Seliskarc, D. M., et al. (2008). *Kosteletzkya virginica*, an agrocoengineering halophytic species for alternative agricultural production in China's east coast: ecological adaptation and benefits, seed yield, oil content, fatty acid and biodiesel properties. *Ecol. Eng.* 32, 320–328. doi: 10.1016/j.ecoleng.2007.12.010
- Scarpin, M. R., Leiboff, S., and Brunkard, J. O. (2020). Parallel global profiling of plant TOR dynamics reveals a conserved role for LARP1 in translation. *eLife* 9:e58795. doi: 10.7554/eLife.58795
- Seo, D. H., Ryu, M. Y., Jammes, F., Hwang, J. H., Turek, M., Kang, B. G., et al. (2012). Roles of retromer complex and SNX protein family in negative regulation of abscisic acid-mediated drought stress responses. *Plant Physiol.* 160, 556–568. doi: 10.1104/pp.112.202143
- Song, Y. Z., Shen, C. H., Li, X., Su, L. B., Lin, X. H., and Wu, Y. H. (2016). Roles of retromer complex and SNX protein family in development and diseases. *Sci. Sin. Vitae* 46, 36–51. doi: 10.1360/N052015-00221
- Sun, J. G., Zhang, H. S., Fu, S. Y., Bu, Z., and Qin, P. (2019). Effects of *Kosteletzkya virginica* root flour on growth performance, slaughter performance, immunity performance and antioxidant ability of broilers. *Jiangsu Agric. Sci.* 47, 176–179. doi: 10.15889/j.issn.1002-1302.2019.17.043
- Tang, X., Ghimire, S., Liu, W. G., Fu, X., Zhang, H. H., and Sun, F. J. (2022). Genome-wide Identification of U-box Genes and Protein Ubiquitination under PEG-induced Drought Stress in Potato. *Physiol. Plantarum* 174:e13475. doi: 10.1111/ppl.13475
- Tang, X. L., Shao, H. B., Jiang, F. D., Amr, S., Mohamed, S., Yang, R. P., et al. (2020). Molecular cloning and functional analyses of the salt-responsive gene KVHSP70 from *Kosteletzkya virginica*. *Land Degrad. Dev.* 31, 773–782. doi: 10.1002/ldr.3503
- Tang, X. L., Wang, H. Y., Shao, C. Y., and Shao, H. B. (2015). Global gene expression of *Kosteletzkya virginica* seedlings responding to salt stress. *PLoS One* 10:e0124421. doi: 10.1371/journal.pone.0124421
- Tcherkezian, J., Cargnello, M., Romeo, Y., Huttlin, E. L., Lavoie, G., Gygi, S. P., et al. (2014). Proteomic analysis of cap-dependent translation identifies LARP1 as a key regulator of 5' TOP mRNA translation. *Genes Dev.* 28, 357–371. doi: 10.1101/gad.231407.113
- Tuba, Z., Saxena, D. K., Srivastava, K., Singh, S., Czebol, S., and Kalaji, M. H. (2010). Chlorophyll a fluorescence measurements for validating the tolerant bryophytes for heavy metal (Pb) biomapping. *Curr. Sci. India* 98, 1505–1508.
- Varshavsky, A. (1997). The ubiquitin system. *Trends Biochem. Sci.* 22, 383–387. doi: 10.1016/S0968-0004(97)01122-5
- Wang, C., Gao, C. Q., Wang, L. Q., Zheng, L., Yang, C. P., and Wang, Y. C. (2014). Comprehensive transcriptional profiling of NaHCO<sub>3</sub>-stressed *Tamarix hispida* roots reveals networks of responsive genes. *Plant Mol. Biol.* 84, 145–157. doi: 10.1007/s11103-013-0124-2
- Wang, H. Y., Ding, Q., Shao, H. B., and Wang, H. L. (2019). Overexpression of KVP5CS1 increases salt tolerance in transgenic tobacco. *Pak. J. Bot.* 51, 831–836. doi: 10.30848/PJB2019-3(9)
- Wang, H. Y., Tang, X. L., Wang, H. L., and Shao, H. B. (2015a). Proline accumulation and metabolism-related genes expression profiles in *Kosteletzkya virginica* seedlings under salt stress. *Front. Plant Sci.* 6:792. doi: 10.3389/fpls.2015.00792
- Wang, H. Y., Tang, X. L., Wang, H. L., and Shao, H. B. (2015b). Physiological responses of *Kosteletzkya virginica* to coastal wetland soil. *Sci. World J.* 2015:354581. doi: 10.1155/2015/354581
- Wang, J., Liu, S., Liu, H., Chen, K., and Zhang, P. (2019). PnSAG1, an E3 ubiquitin ligase of the Antarctic moss *Pohlia nutans*, enhanced sensitivity to salt stress and ABA. *Plant Physiol. Biochem.* 141, 343–352. doi: 10.1016/j.plaphy.2019.06.002
- Wang, Z. C., Yang, F., Chen, Y., and Liang, Z. W. (2008). Sodium and potassium responses to sodicity stress in rice. *Ecol. Environ.* 17, 1198–1203. doi: 10.3969/j.issn.1674-5906.2008.03.063
- Xu, A. H., Tian, Z. Y., Cui, W. L., Li, J., and Guo, Y. Q. (2013). Molecular classification and introduction of *Kosteletzkya pentacarpos* germplasm at streamside of the Yellow River in Zhengzhou. *J. Plant Genet. Resour.* 14, 1045–1052.
- Xu, G. W., Qin, P., Xie, M., Lv, W. L., and Zhong, C. X. (1996). A study on the trial planting ecology of *Kosteletzkya virginica* in China. *Nanjing Univ.* 32, 268–274.
- Xu, H. D., Ning, B. L., Mu, F., Li, H., and Wang, N. (2021). Advances of functional consequences and regulation mechanisms of alternative cleavage and polyadenylation. *Hereditas* 43, 4–15. doi: 10.16288/j.ycz.20-200
- Yamanaka, T., and Ohno, S. (2008). Role of Lgl/Dlg/Scribble in the regulation of epithelial junction, polarity and growth. *Front. Biosci.* 13:6693–6707. doi: 10.2741/3182
- Yan, G. G., and Zhou, J. (2019). Effects of exogenous salicylic acid on growth characteristics, Na<sup>+</sup> accumulation and transferring coefficient in *Kosteletzkya virginica* plants under saline-alkali stress. *J. Henan Inst. Sci. Technol.* 47, 9–14.
- Zhang, H. L. (2019). *Study on Forestry Quality Improvement Planning of Coastal Saline-Alkali Land in Hekou District of Dongying City, Shandong Province*. [PhD thesis]. Beijing: Beijing Forestry University.
- Zhang, M., Zhao, J. F., Li, L., Gao, Y. N., Zhao, L. L., Patil, S. B., et al. (2017). The *Arabidopsis* U-box E3 ubiquitin ligase PUB 30 negatively regulates salt tolerance by facilitating BRI1 kinase inhibitor 1 (BKI1) degradation. *Plant Cell Environ.* 40, 2831–2843. doi: 10.1111/pce.13064
- Zhang, Y., Lin, Y., Liu, Y. H., and Fan, H. (2007). Effects of salt stress on the metabolism of reactive oxygen species in *Kosteletzkya virginica* L. *J. Shandong Norm. Univ.* 22, 117–119.
- Zhao, L. (2018). *Physiological and Molecular Mechanisms Underlying Salt Tolerance in Halophyte Kochia Sieversiana*. [PhD thesis]. Changchun: Northeast Normal University.
- Zhou, B. J., and Zeng, L. R. (2017). Conventional and unconventional ubiquitination in plant immunity. *Mol. Plant Pathol.* 18, 1313–1330. doi: 10.1111/mpp.12521
- Zhou, J., and Zhang, X. (2019). Growth, sodium ions' absorption and sub-cell distribution in saline-alkali stressed seedlings of *Kosteletzkya virginica* under potassium ion regulation. *J. Henan Inst. Sci. Technol.* 47, 1–8.
- Zhou, L., Cheung, M. Y., Li, M. W., Fu, Y. P., Sun, Z. X., Sun, S. M., et al. (2010). Rice Hypersensitive Induced Reaction Protein 1 (OsHIR1) associates with plasma membrane and triggers hypersensitive cell death. *BMC Plant Biol.* 10:290. doi: 10.1186/1471-2229-10-290

**Conflict of Interest:** The authors declare that the research was conducted in the absence of any commercial or financial relationships that could be construed as a potential conflict of interest.

**Publisher's Note:** All claims expressed in this article are solely those of the authors and do not necessarily represent those of their affiliated organizations, or those of the publisher, the editors and the reviewers. Any product that may be evaluated in this article, or claim that may be made by its manufacturer, is not guaranteed or endorsed by the publisher.

Copyright © 2022 Zhou, Qi, Wang, Zhang, Dong and Liu. This is an open-access article distributed under the terms of the Creative Commons Attribution License (CC BY). The use, distribution or reproduction in other forums is permitted, provided the original author(s) and the copyright owner(s) are credited and that the original publication in this journal is cited, in accordance with accepted academic practice. No use, distribution or reproduction is permitted which does not comply with these terms.



# NaCl Pretreatment Enhances the Low Temperature Tolerance of Tomato Through Photosynthetic Acclimation

Xiaolong Yang<sup>1,2†</sup>, Fengyu Zou<sup>1†</sup>, Yumeng Zhang<sup>1</sup>, Jiali Shi<sup>1,3</sup>, Mingfang Qi<sup>1</sup>, Yufeng Liu<sup>1\*</sup> and Tianlai Li<sup>1\*</sup>

<sup>1</sup> Key Laboratory of Protected Horticulture of Ministry of Education, National and Local Joint Engineering Research Center of Northern Horticultural Facilities Design and Application Technology (Liaoning), College of Horticulture, Shenyang Agricultural University, Shenyang, China, <sup>2</sup> College of Horticulture, South China Agricultural University, Guangzhou, China, <sup>3</sup> Jiuquan Academy of Agricultural Sciences, Jiuquan, China

## OPEN ACCESS

### Edited by:

Vasilij Goltsev,  
Sofia University, Bulgaria

### Reviewed by:

Antoaneta Popova,  
Bulgarian Academy of  
Sciences, Bulgaria  
Nan Xu,  
Nature and Ecology Institute of  
Heilongjiang Academy of  
Sciences, China

### \*Correspondence:

Yufeng Liu  
yufengliu@syau.edu.cn  
Tianlai Li  
ltl@syau.edu.cn

<sup>†</sup>These authors have contributed  
equally to this work

### Specialty section:

This article was submitted to  
Plant Abiotic Stress,  
a section of the journal  
Frontiers in Plant Science

**Received:** 08 March 2022

**Accepted:** 23 May 2022

**Published:** 13 June 2022

### Citation:

Yang X, Zou F, Zhang Y, Shi J, Qi M,  
Liu Y and Li T (2022) NaCl  
Pretreatment Enhances the Low  
Temperature Tolerance of Tomato  
Through Photosynthetic Acclimation.  
Front. Plant Sci. 13:891697.  
doi: 10.3389/fpls.2022.891697

Plants often need to withstand multiple types of environmental stresses (e.g., salt and low temperature stress) because of their sessile nature. Although the physiological responses of plants to single stressor have been well-characterized, few studies have evaluated the extent to which pretreatment with non-lethal stressors can maintain the photosynthetic performance of plants in adverse environments (i.e., acclimation-induced cross-tolerance). Here, we studied the effects of sodium chloride (NaCl) pretreatment on the photosynthetic performance of tomato plants exposed to low temperature stress by measuring photosynthetic and chlorophyll fluorescence parameters, stomatal aperture, chloroplast quality, and the expression of stress signaling pathway-related genes. NaCl pretreatment significantly reduced the carbon dioxide assimilation rate, transpiration rate, and stomatal aperture of tomato leaves, but these physiological acclimations could mitigate the adverse effects of subsequent low temperatures compared with non-pretreated tomato plants. The content of photosynthetic pigments decreased and the ultra-microstructure of chloroplasts was damaged under low temperature stress, and the magnitude of these adverse effects was alleviated by NaCl pretreatment. The quantum yield of photosystem I (PSI) and photosystem II (PSII), the quantum yield of regulatory energy dissipation, and non-photochemical energy dissipation owing to donor-side limitation decreased following NaCl treatment; however, the opposite patterns were observed when NaCl-pretreated plants were exposed to low temperature stress. Similar results were obtained for the electron transfer rate of PSI, the electron transfer rate of PSII, and the estimated cyclic electron flow value (CEF). The production of reactive oxygen species induced by low temperature stress was also significantly alleviated by NaCl pretreatment. The expression of ion channel and tubulin-related genes affecting stomatal aperture, chlorophyll synthesis genes, antioxidant enzyme-related genes, and abscisic acid (ABA) and low temperature signaling-related genes was up-regulated in NaCl-pretreated plants under low temperature stress. Our findings indicated that CEF-mediated photoprotection, stomatal movement, the maintenance of chloroplast quality, and ABA and low temperature signaling pathways all play key roles in maintaining the photosynthetic capacity of NaCl-treated tomato plants under low temperature stress.

**Keywords:** tomato, salt stress, cross-tolerance, cyclic electron transport, non-photochemical quenching, photosynthetic acclimation

## INTRODUCTION

Because of their sessile nature, plants are often exposed to unfavorable environmental conditions, such as high soil salinity and low temperatures. The abiotic stress has deleterious effects on the photosynthesis efficiency and redistribution the energy from growth to stress resistance, which can drastically decrease crop yield and quality (Zhang et al., 2020). Plants employ a sensitive and complex regulatory system to ensure survival in unpredictable environments (Bailey-Serres et al., 2019; Morales and Kaiser, 2020). Photosynthetic efficiency is maintained in plant leaves through various photoprotective pathways, including the rapid induction and relaxation of non-photochemical quenching (NPQ) and cyclic electron transport around photosystem I (PSI), to prevent oxidative damage to the photosynthetic apparatus caused by reactive oxygen species (ROS) (Pinnola and Bassi, 2018; Park et al., 2019). Soil salinization affects large areas of agricultural land used for crop production worldwide. The main effects of soil salinization on plants include the creation of a hyperosmotic state, which can lead to ion toxicity, and oxidative damage associated with the accumulation of ROS, which can slow growth and result in developmental and metabolic abnormalities (Yang and Guo, 2018; Saddhe et al., 2019). Salt stress induces downstream signaling pathways that trigger a series of cellular responses that mediate the re-establishment of homeostasis and the alleviation of stress-induced damage (Zhao et al., 2020).

Plants often experience multiple abiotic stresses simultaneously or successively; the unique response and specific pathways play a critical role in the acclimation of plants to multifactorial stress combination (Zandalinas et al., 2021). Exposure to a single non-lethal stressor can sometimes confer resistance to various adverse conditions in plants, and this phenomenon is referred to as cross-tolerance (Bowler and Fluhr, 2000). Acclimation to specific stresses in plants is achieved by triggering a regulatory cascade or network that includes the stress stimulus, perception, signal transduction, transcriptional regulation of target genes, and physiological responses (Tombesi et al., 2018). Generally, the action of specific signaling pathways early in the stress response is critically important for the maintenance of cell functions, and common or overlapping signaling pathways and components often act near the end of stress response cascades (Pastori and Foyer, 2002; Locato et al., 2018). The resistance of tomato plants to low temperature and drought stress can be induced by mild low temperature, paraquat, and drought pretreatment, and this cross-tolerance mechanism involves the activation of ROS-mediated signal transduction pathways (Zhou et al., 2014). Pretreatment of soil with salt has been shown to result in higher leaf mass per area, total chlorophyll (Chl) and carotenoid (Car) content, and photosynthetic activity in tomato plants fumigated with sulfur (Jiang et al., 2017). In addition, drought pretreatment can induce resistance to heat in tall fescue and *Arabidopsis*, and heat shock and NaCl treatment can induce resistance to UV-B radiation in barley (Çakırlar et al., 2008; Zhang et al., 2019).

A particularly effective strategy for improving crop yields under abiotic stress is to enhance the photosynthetic capacity of

crops (Gururani et al., 2015). Extensive studies have characterized the effects of single stressors on photosynthesis using plant genetic engineering techniques and photosynthetic fluorescence analysis (Guidi et al., 2019). Soil salinity pretreatment can alleviate the damage to photosynthetic capacity induced by drought treatment in tomato plants; however, the cross-tolerance mechanism mediating the photosynthetic capacity response remains unclear (Yang et al., 2020). Salt stress is a very common abiotic stress in vegetable production, especially the accumulation of salt in the soil surface due to the frequent irrigation. In addition, plants are still hard to avoid the adverse effects of low temperature even growth in energy-saving solar greenhouse in northern China. Salt stress and low temperature are considered to be the major factors limiting vegetable production to a certain extent, there is thus a need to determine how exposure to soil salinity affects the tradeoff between photoprotection, photochemistry, and chloroplast quality and confers tolerance to low temperature stress. The aim of this study was to explore the photosynthetic performance of tomato plants pretreated with sodium chloride (NaCl) under low temperature stress. Generally, the results of this study provide new insights that enhance our understanding of acclimation-induced cross-tolerance and have implications for environmental management during vegetable production.

## MATERIALS AND METHODS

### Plant Materials and Treatments

Experiments were conducted in the solar climate chamber at Shenyang Agricultural University from May to October 2019. The tomato (*Solanum lycopersicum* L.) variety “Liao Yuan Duo Li” was used in experiments, and seeds were germinated in seedling trays and transferred to plastic pots at the two-leaf stage. The growth temperature was controlled at approximately 25/15°C (day/night, 12 h/12 h), the humidity was ~50% during the day and 80% at night, and the light intensity was approximately 800  $\mu\text{mol}\cdot\text{photons}\cdot\text{m}^{-2}\cdot\text{s}^{-1}$  natural solar radiation at noon. Before the experiment, ~50–100 mL of water was applied to each seedling per day to ensure consistent growth. Plants were exposed to the NaCl pretreatment and the low temperature stress treatment when they had reached the five-leaf stage. For the NaCl pretreatment, 100 mL of water and 100 mL of 100 mM NaCl solution were applied every morning for 5 days. The plants were then divided into the normal temperature group (CK, NaCl) and low temperature group (CK+LT, NaCl+LT). Plants in the normal temperature group were exposed to 25/15°C (day/night) for 5 days, and plants in the low temperature group were exposed to 15/6°C for 5 days. Measurements were taken on the first (T1) and fifth (T5) day after NaCl pretreatment and the fifth day (T10) after low temperature treatment.

### Measurement of Leaf Photosynthesis Gas Exchange

A synchronous measurement system with a GFS-3000 photosynthesizer and Dual-PAM-100 fluorescence analyzer (Heinz Walz, Effeltrich, Germany) was used to analyze the



photosynthetic gas exchange and Chl fluorescence of plant leaves *in vivo* using standard measurement procedures and settings but with various modifications (Zhang et al., 2014; Lu et al., 2017; Yang et al., 2018, 2020). All measurements were made using the fourth functional leaf from the top of each plant; the area of the measuring head was 1.3 cm<sup>2</sup>. During measurements, the air inlet of the photosynthetic apparatus was connected to a 10-L air buffer bottle so that the ambient atmospheric carbon dioxide (CO<sub>2</sub>) concentration could be taken as a reference; the indoor temperature was approximately 25°C, and the light intensity was 1,100  $\mu\text{mol}\cdot\text{photos}\cdot\text{m}^{-2}\cdot\text{s}^{-1}$ . When leaf photosynthesis gas exchange reached a stable state after full photoadaptation, the net photosynthetic rate (Pn), intercellular CO<sub>2</sub> concentration (Ci), stomatal conductance (GH<sub>2</sub>O), transpiration rate (E), water use efficiency (WUE), stomatal limit value (Ls), and other parameters were measured.

### Measurement of Pigment Content and Observations of Stomatal Aperture

The content of photosynthetic pigments in tomato leaves was determined by the ethanol and acetone extraction method. Specifically, 0.2 g of fresh leaf samples were placed into a 20-mL test tube; 10 mL of a 1:1 mixture of 95% ethanol and 80% acetone was then added, and the mixture was left to stand in a dark environment for 24 h. The optical density (OD) was measured using a UV 1200 ultraviolet spectrophotometer (Shimadzu, Kyoto, Japan), and calculated by the following equations: the content of Chlorophyll a ( $\text{mg}\cdot\text{g}^{-1}$ ) =  $(12.72 \text{ OD}_{663} - 2.59 \text{ OD}_{645}) \text{ V} / 1,000 \text{ W}$ ; the content of Chlorophyll b ( $\text{mg}\cdot\text{g}^{-1}$ ) =  $(22.88 \text{ OD}_{645} - 4.67 \text{ OD}_{663}) \text{ V} / 1,000 \text{ W}$ ; the content of Carotenoid ( $\text{mg}\cdot\text{g}^{-1}$ ) =  $(1,000 \text{ OD}_{470} - 3.27 \text{ Chl a} - 104 \text{ Chl b}) \text{ V} / (229 \times 1,000 \text{ W})$ . Where V is the total volume of ethanol and acetone extract (mL), and W is the fresh weight (g) of the sample (Fan et al., 2013; Yang et al., 2018). The lower epidermis of tomato was removed with tweezers and placed on a microscope slide, and appropriate distilled water was placed on the slide to ensure that samples were completely immersed in fluid. Each treatment was repeated six times. Observations and photography of the stomata aperture were carried out using a fluorescence inverted microscope (Axio Observer A1, Zeiss, Germany); 10 photographs of each leaf were taken at random times for measurements of stomatal parameters.

### Chloroplast Ultramicrostructure Observations

Veinless strips (1 × 2 mm) from tomato leaves were fixed with 2.5% glutaraldehyde and 1% acetic acid and dehydrated with ethanol; they were then embedded with epoxy resin, sliced, and stained (Hao et al., 2016). An ultra-thin slicing machine (Leica EM UC7, Germany) was used to make ultra-thin slices. The ultramicrostructure of the chloroplast was observed and photographed using transmission electron microscope (Hitachi HT-7700, Japan) under 1,500×, 6,000×, and 20,000× magnification. Ten photos were taken of each sample for measurements of chloroplast ultramicrostructure parameters.

### Measurement of the OJIP Induction Curve and the P700 Redox Status

A saturation pulse (300 ms, 10,000  $\mu\text{mol}\cdot\text{photons}\cdot\text{m}^{-2}\cdot\text{s}^{-1}$ ) was used to determine the OJIP induction curve of the Chl a fluorescence per the automated routines provided by Dual-PAM software following dark adaptation for at least 30 min (Zhang et al., 2014; Lu et al., 2017; Yang et al., 2018, 2020). The redox state of P700 was determined *in vivo* using the dual-beam 870–830 nm signal difference provided by the Dual-PAM-100 system. Single-turnover flash (ST, 50 ms) induction of the oxidation of PQ pools and multiple-turnover flash (MT, 50 ms) induction of the full reduction of PQ pools in the presence of far-red light were used to measure the redox kinetics of P700. The complementary areas of ST and MT excitation signal change were used to calculate the functional pool sizes of intersystem electrons on a P700 reaction center as follows:  $\text{PQ size} = \text{MT-areas} / \text{ST-areas}$  (Zhang et al., 2014; Lu et al., 2017; Yang et al., 2018, 2020).

### Measurement of Light Energy Conversion and the Electron Transfer Rate

All measurements were conducted on plants following dark adaptation for more than 30 min. The slow Chl fluorescence induction curve was then recorded for 520 s. A low intensity measuring light was used to detect the minimum fluorescence, F<sub>0</sub>; a saturating pulse (10,000  $\mu\text{mol}\cdot\text{photons}\cdot\text{m}^{-2}\cdot\text{s}^{-1}$ ) was then applied to detect the maximum fluorescence, F<sub>m</sub>. A saturation pulse after illumination with far-red light was used to measure the maximum change in the P700 signal, P<sub>m</sub>. A saturating pulse (300 ms, 10,000  $\mu\text{mol}\cdot\text{photons}\cdot\text{m}^{-2}\cdot\text{s}^{-1}$ ) was applied every 20 s after the actinic light (191  $\mu\text{mol}\cdot\text{photons}\cdot\text{m}^{-2}\cdot\text{s}^{-1}$ , 635 nm) was turned on to determine the maximum fluorescence signal (F<sub>m</sub>') and maximum P700<sup>+</sup> signal (P<sub>m</sub>') under light adaptation for 8 min. The rapid light response curves (RLCs) were determined using the standard measurement program immediately after slow induction curve measurements. The light intensity of the RLC changed every 30 s in the sequence 29, 37, 55, 113, 191, 213, 349, 520, 778, 1,197, and 1,474  $\mu\text{mol}\cdot\text{photons}\cdot\text{m}^{-2}\cdot\text{s}^{-1}$ , and a saturating pulse was used to measure F<sub>m</sub>' and P<sub>m</sub>' after each period of actinic light. The parameters measured in this study were as follows: maximum photochemical quantum yield of PSII, F<sub>v</sub>/F<sub>m</sub>; effective quantum yield of PSII, Y(II); quantum yield of non-regulatory energy dissipation, Y(NO); quantum yield of regulatory energy dissipation, Y(NPQ); non-photochemical quenching in PSII, NPQ; quantum yield of PSI, Y(I); quantum yield of non-photochemical energy dissipation owing to acceptor-side limitation, Y(NA); quantum yield of PSI non-photochemical energy dissipation owing to donor-side limitation, Y(ND); electron transfer rate of PSI, ETR(I); electron transfer rate of PSII, ETR(II); and estimated cyclic electron flow value (CEF), which was determined by ETR(I)–ETR(II) (Zhang et al., 2014; Lu et al., 2017; Yang et al., 2018, 2020; Sun et al., 2022).

### Analysis of ROS Production and Antioxidant Enzyme Activity

The O<sub>2</sub><sup>-</sup> production rate and H<sub>2</sub>O<sub>2</sub> content were determined by the hydroxylamine oxidation method (Ibrahim and Jaafar, 2012;

Lu et al., 2020b). Briefly, 0.2 g of tomato leaves were placed in a mortar, and 3 mL of 50 mM PBS buffer (pH 7.8) was added three times; the mixture was then fully ground and centrifuged at 10,000 g and 4°C for 20 min, and the supernatant, which comprised the enzyme extract, was collected. The methods of Lu (2020) were used to determine the superoxide dismutase (SOD) and peroxidase (POD) activities.

## Quantitative Real-Time Polymerase Chain Reaction

Fresh leaf samples (0.2 g) were taken, quick-frozen with liquid nitrogen, and then stored at −80°C. Total RNA was extracted per the instructions of the RNA extraction kit (Kangwei, Biotech, Beijing, China). The quality of RNA was evaluated using 1% agarose gel electrophoresis, and the concentration and purity (28SrRNA/18SrRNA) were measured using a NanoDrop spectrophotometer ND-1000 (NanoDrop, USA). 1 µg of RNA was reverse-transcribed into cDNA using Prime Script™ RT Master Mix (Perfect Real Time, Takara) and stored at −20°C. Real-time quantitative fluorescence polymerase chain reaction (PCR) was conducted following the instructions in the Super Real PreMix Plus (SYBR Green) (TaKaRa, Dalian, China) kit, and the amplification procedure was conducted using a real-time quantitative fluorescence PCR instrument; the primers used are shown in **Supplementary Table 1**.

## Statistical Analysis

Student's *t*-tests were conducted in SPSS version 22 (SPSS, Armonk, NY, USA) to evaluate the significance of differences between treatments. The mean values of three to six independent biological replicates were calculated and presented as mean ± standard deviation (SD), and the threshold for significance was  $P \leq 0.05$ . All graphs were made using Origin Version 12.0 (Systat, San Jose, CA, USA).

## RESULTS

### Stomatal Aperture and Photosynthetic Gas Exchange in Tomato Leaves

The growth potential of NaCl-pretreated plants was greater than that of plants in the CK+LT treatment under low temperature stress (**Figure 1A**). The stomatal width of tomato leaves was significantly reduced by NaCl treatment at room temperature and under low temperature treatment; however, NaCl+LT treatment significantly increased the stomatal width and reduced the stomatal length and the ratio of Length/Width compared with CK+LT treatment (**Figure 1C**, **Table 1**). The relative expression levels of the ion channel-related genes *SIQuAC1-1*, *SIQuAC1-2* and *SISLAC1* and tubulin-related genes *SIMAP56-1* and *SITUB1-1* were significantly up-regulated at low temperatures in NaCl-pretreated plants compared with plants in the CK+LT treatment (**Figure 1D**). These findings indicate that NaCl pretreatment affects the expression of ion channel and tubulin-related genes in leaves at low temperature, which might affect the concentrations of ions inside and outside the guard cells and thus stomatal opening. The photosynthesis gas exchange parameters have no significantly differences between treatments

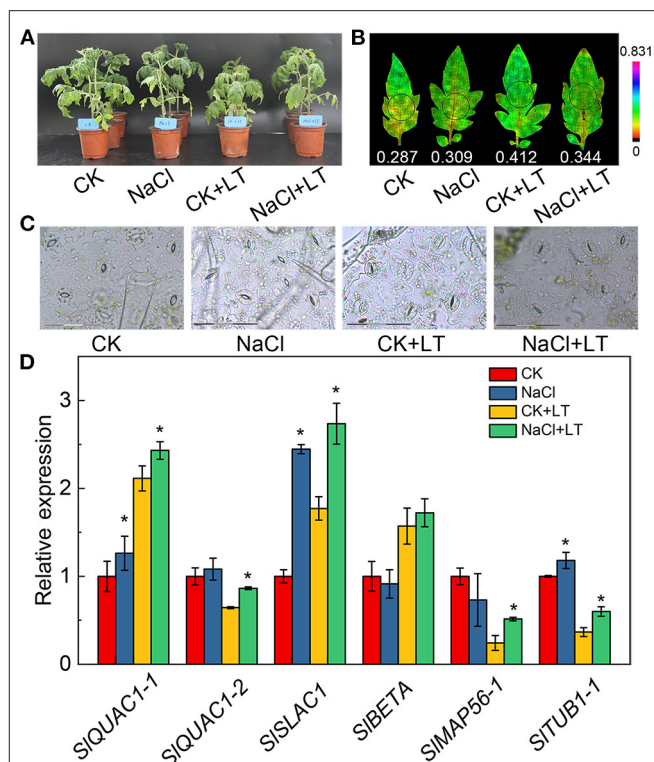


**FIGURE 1** | Effects of NaCl pretreatment on the phenotype, stomatal movements, and expression of ion transport-related genes of tomato leaves under low temperature treatment. The growth state of tomato plants under different treatments at different stages (**A**); Chl fluorescence imaging of Y(NPQ) (**B**); images of the stomata on tomato leaves under different treatments (**C**); and relative expression of ion channel and tubulin-related genes (**D**). The results are shown as mean values of three to five independent biological replicates ± SD, \* indicate significant differences between CK and NaCl and between CK+LT and NaCl+LT ( $P < 0.05$ , Student's *t*-test).

**TABLE 1** | Effects of NaCl pretreatment on the stomatal aperture of tomato leaves under low temperature stress.

Treatments	Length (µm)	Width (µm)	Length/width
CK	11.27 ± 0.43a	5.61 ± 0.81a	2.03 ± 0.23d
NaCl	11.72 ± 0.27a	3.46 ± 0.18b	3.39 ± 0.18c
CK+LT	11.30 ± 0.20a	2.49 ± 0.18d	4.55 ± 0.26a
NaCl+LT	10.59 ± 0.47b	2.97 ± 0.63c	3.72 ± 1.04b

The results are shown as mean values of six independent biological replicates ± SD, different letters in the same column indicate significant differences according to Student's *t*-test ( $P < 0.05$ ).

at T1; NaCl-pretreated significantly reduced the parameters E, Pn, gH<sub>2</sub>O, Ls, and WUE of plants than CK at T5. After 5 days of low temperature treatment, E, Pn, gH<sub>2</sub>O, and WUE were significantly higher in NaCl-treated plants (NaCl+LT) than in plants in the CK+LT treatment, indicating that NaCl pretreatment enhances the CO<sub>2</sub> assimilation efficiency under low temperature stress (**Figure 2**). This result might be related to the effect of NaCl pretreatment on the regulation of stomatal opening and the water use of plants.

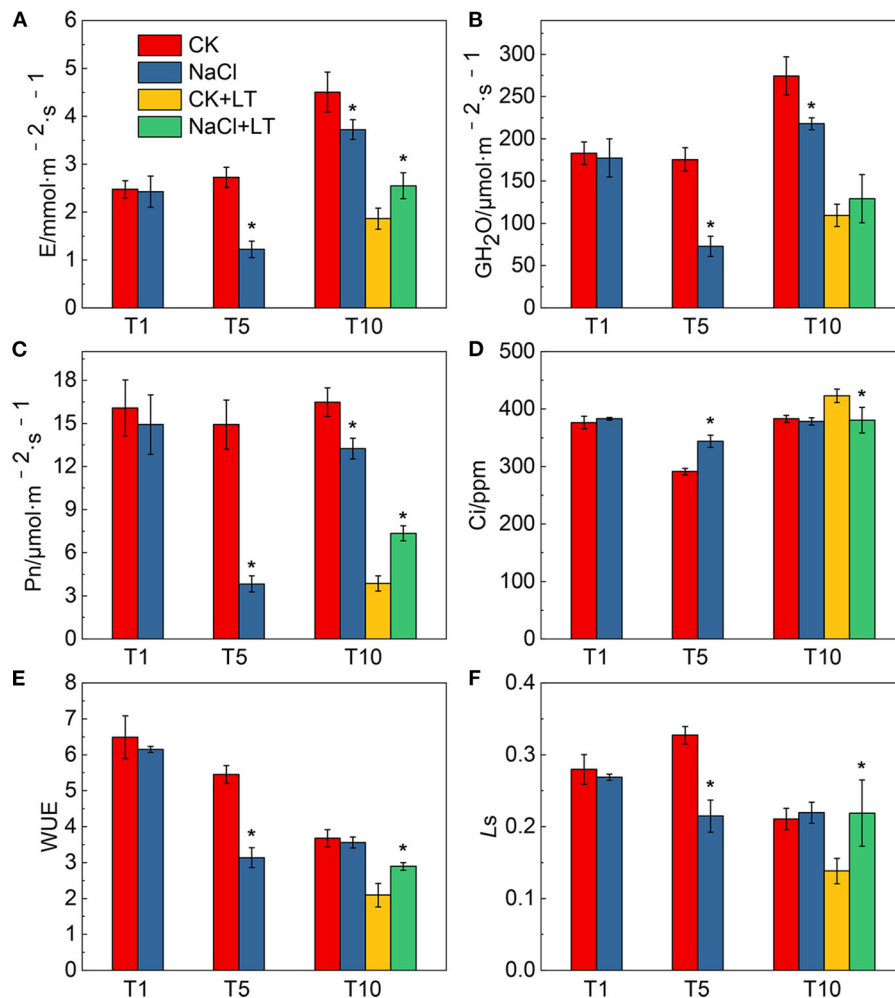


**FIGURE 2 |** Effects of NaCl pretreatment on the photosynthetic gas exchange parameters of tomato leaves under low temperature stress. The effect of NaCl pretreatment on the transpiration rate (A,E), stomatal conductance ( $\text{GH}_2\text{O}$ ) (B), net photosynthetic rate (Pn) (C), intercellular  $\text{CO}_2$  concentration (Ci) (D), water use efficiency (WUE) (E), and stomatal limitation value (Ls) (F) in tomato leaves under low temperature stress. The results are shown as the mean values of six independent biological replicates  $\pm$  SD, \* indicate significant differences between CK and NaCl and between CK+LT and NaCl+LT ( $P < 0.05$ , Student's  $t$ -test).

## Chl Metabolism and Chloroplast Ultrastructure

The ultrastructure of the chloroplasts was not significantly affected by the NaCl treatment. However, low temperature stress resulted in the destruction of the chloroplast membrane, significantly reduced the chloroplast length-to-width ratio, and significantly increased the number of starch grains per chloroplast. In the NaCl+LT treatment, the ultrastructure of the chloroplasts was more complete, the chloroplast membrane was intact, the crenellate structure of the thylakoid was clear, the chloroplast length-to-width ratio was significantly increased, and the number of starch grains and glutathione grains in chloroplasts was significantly reduced compared with the CK+LT treatment (Figure 3A, Table 2). These results suggested that NaCl pretreatment might enhance the photosynthetic capacity of tomato by alleviating the

damage of low temperature on chloroplast structure. Low temperature treatment significantly reduced the content of photosynthetic pigments, and the content of Chl *a*, Chl *b*, Car, and total Chl was significantly higher in the NaCl+LT treatment than in the CK+LT treatment (Table 3). The relative expression levels of the Chl synthesis genes *SICA01*, *SICHLG*, *SICHLI*, *SIDVR*, *SIHMD*, *SIHEMA1*, and *SIHEME1* were significantly up-regulated by NaCl pretreatment; in addition, the relative expression levels of the Chl decomposition-related genes *SIEEL*, *SIHCAR*, *SIPAO*, and *SINYC1* were significantly down-regulated under low temperatures stress compared with the CK+LT treatment (Figures 3B,C). These findings indicate that NaCl pretreatment can maintain the content of photosynthetic pigments by enhancing the photosynthetic capacity of tomato under low temperature stress.

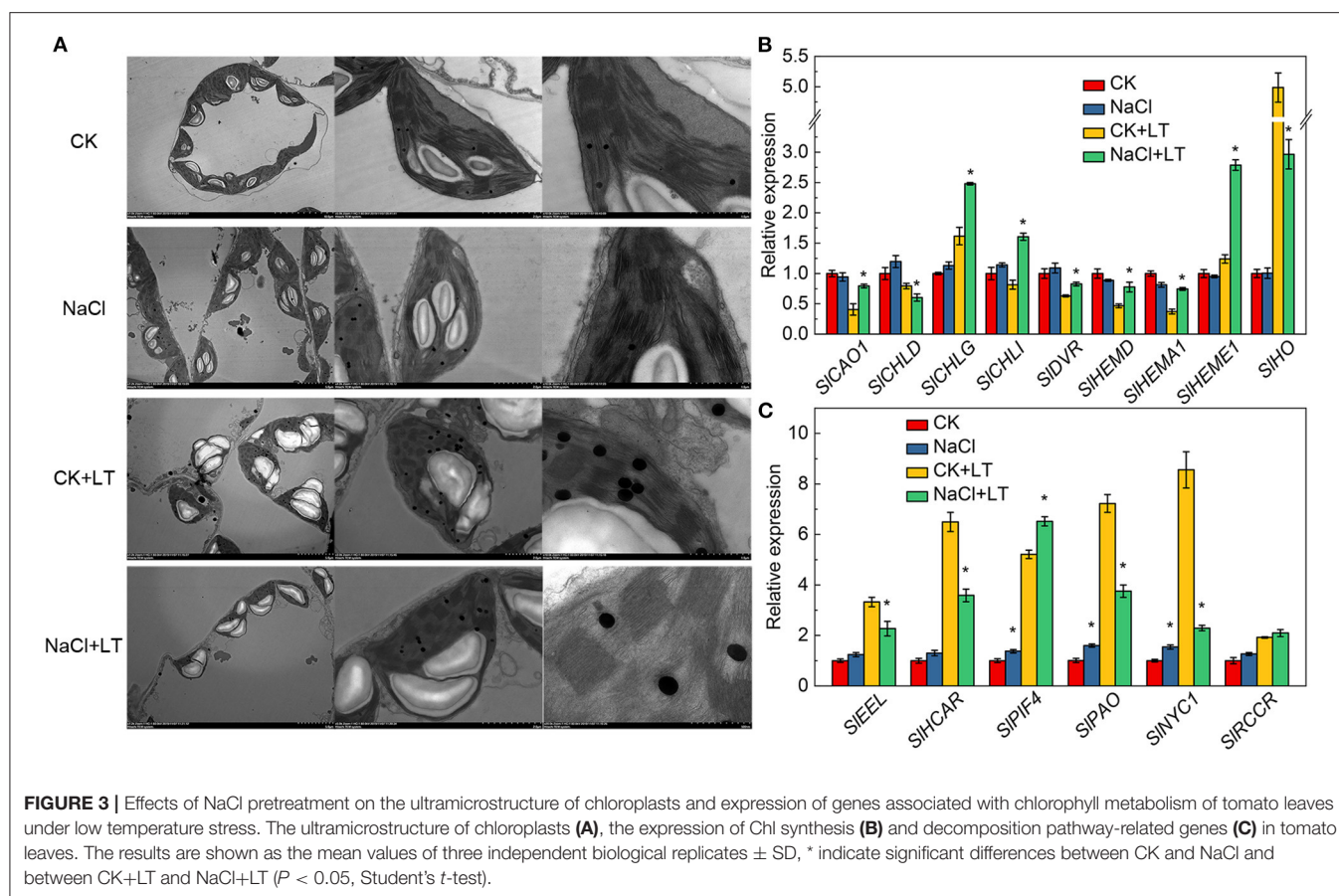


**TABLE 2 |** Effect of NaCl pretreatment on the chloroplast ultrastructure in tomato leaves under low temperature treatment.

Types	Chloroplast length/ $\mu\text{m}$	Chloroplast width/ $\mu\text{m}$	Chloroplast length/width
CK	5.47 $\pm$ 0.21a	2.86 $\pm$ 0.07c	1.94 $\pm$ 0.05a
NaCl	5.37 $\pm$ 0.22a	2.92 $\pm$ 0.06c	1.84 $\pm$ 0.06a
LT	4.28 $\pm$ 0.06c	3.43 $\pm$ 0.08a	1.25 $\pm$ 0.04c
LT+NaCl	4.81 $\pm$ 0.05b	3.18 $\pm$ 0.05b	1.51 $\pm$ 0.04b

The results are shown as mean values of three independent biological replicates  $\pm$  SD, different letters in the same column indicate significant differences according to Student's  $t$ -test ( $P < 0.05$ ).

**TABLE 3 |** Effect of NaCl pretreatment on the Chl content in tomato leaves under low temperature treatment.

Types	Chlorophyll a / $\text{mg}\cdot\text{g}^{-1}\text{FW}$	Chlorophyll b / $\text{mg}\cdot\text{g}^{-1}\text{FW}$	Carotenoid / $\text{mg}\cdot\text{g}^{-1}\text{FW}$
CK	8.08 $\pm$ 0.10a	1.89 $\pm$ 0.03a	2.13 $\pm$ 0.07a
NaCl	7.80 $\pm$ 0.04b	1.80 $\pm$ 0.01ab	2.06 $\pm$ 0.01a
LT	6.37 $\pm$ 0.05d	1.41 $\pm$ 0.02c	1.78 $\pm$ 0.01b
LT+NaCl	7.30 $\pm$ 0.03c	1.64 $\pm$ 0.01b	1.94 $\pm$ 0.01ab

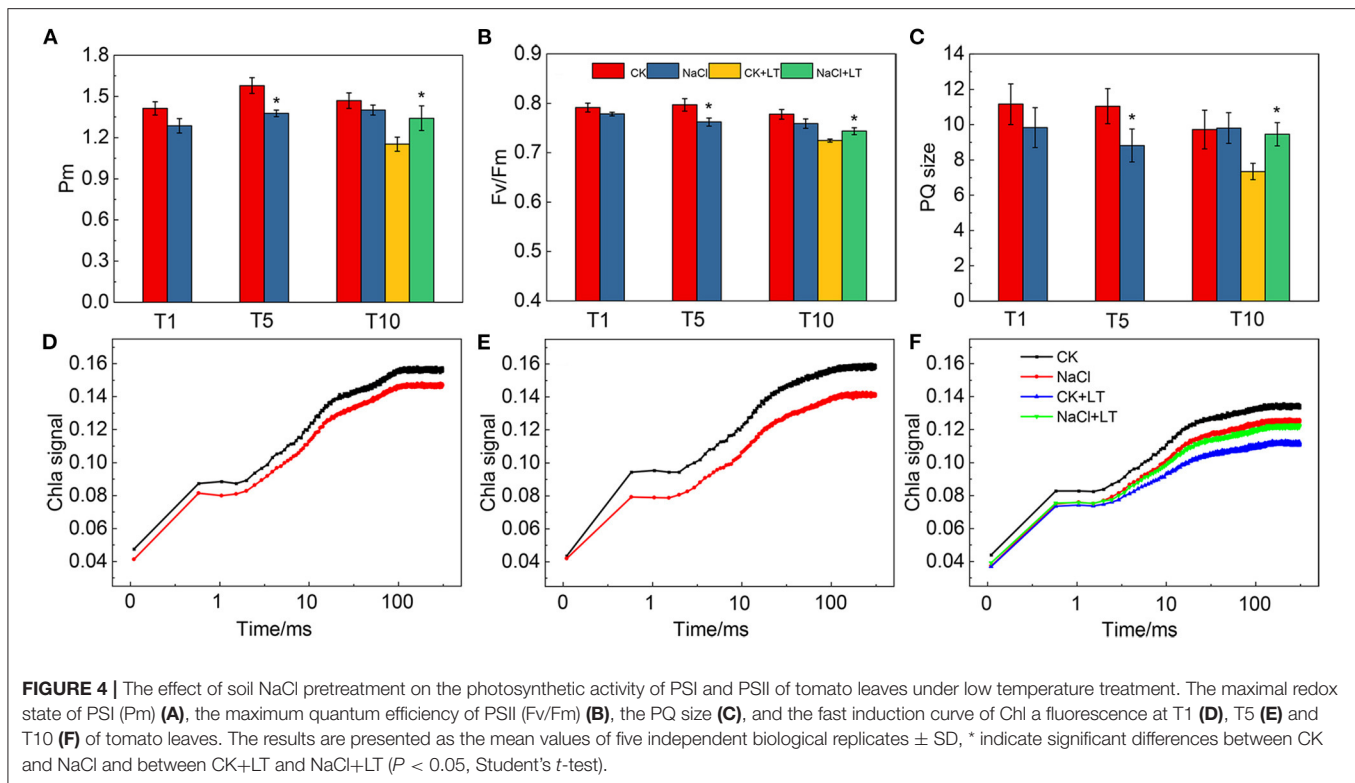
The results are shown as mean values of six independent biological replicates  $\pm$  SD, different letters in the same column indicate significant differences according to Student's  $t$ -test ( $P < 0.05$ ).

## Photochemical Efficiency of PSI and PSII

Pm reflects the maximum oxidation state that P700 can reach in the PSI reaction center of leaves; it thus reflects the activity of PSI to a certain extent. Pm was sensitive to NaCl treatment, the results shown 5 days NaCl treatment significantly reduced Pm of tomato leaves compared with CK, while it was significantly lower in CK+LT than in NaCl+LT at T10 (Figure 4A). The results of Fv/Fm were similar to Pm, indicating that NaCl pre-treatment can alleviate the damage to PSI and PSII induced by subsequent low temperature stress (Figure 4B). The ratio between the area of the MT flash/ST flash was used for determination of the relative

functional pool size of the intersystem electrons able to reduce PSI reaction center ( $\text{P700}^+$ ), the results shown PQ size was significantly lower in NaCl-pretreated plants than in CK plants at T5; at T10, the PQ size was significantly lower in plants in the CK+LT treatment than in plants in the NaCl+LT treatment, indicating that NaCl pretreatment can alleviate the deleterious effects of low temperature stress on PQ electron carriers and maintain high electron transport capacity (Figure 4C). The OJIP kinetics curve of leaves under NaCl treatment decreased slightly at T1 and significantly at T5, indicating that NaCl treatment had an effect on the electron transfer of the donor and acceptor





sides of PSII. Following low temperature stress, the signal intensity significantly decreased in the CK+LT treatment; the OJIP signal remained strong in the NaCl+LT treatment relative to the CK+LT treatment, suggesting that NaCl pretreatment can alleviate the damage to the PSII reaction center induced by low temperature stress (Figures 4D–F).

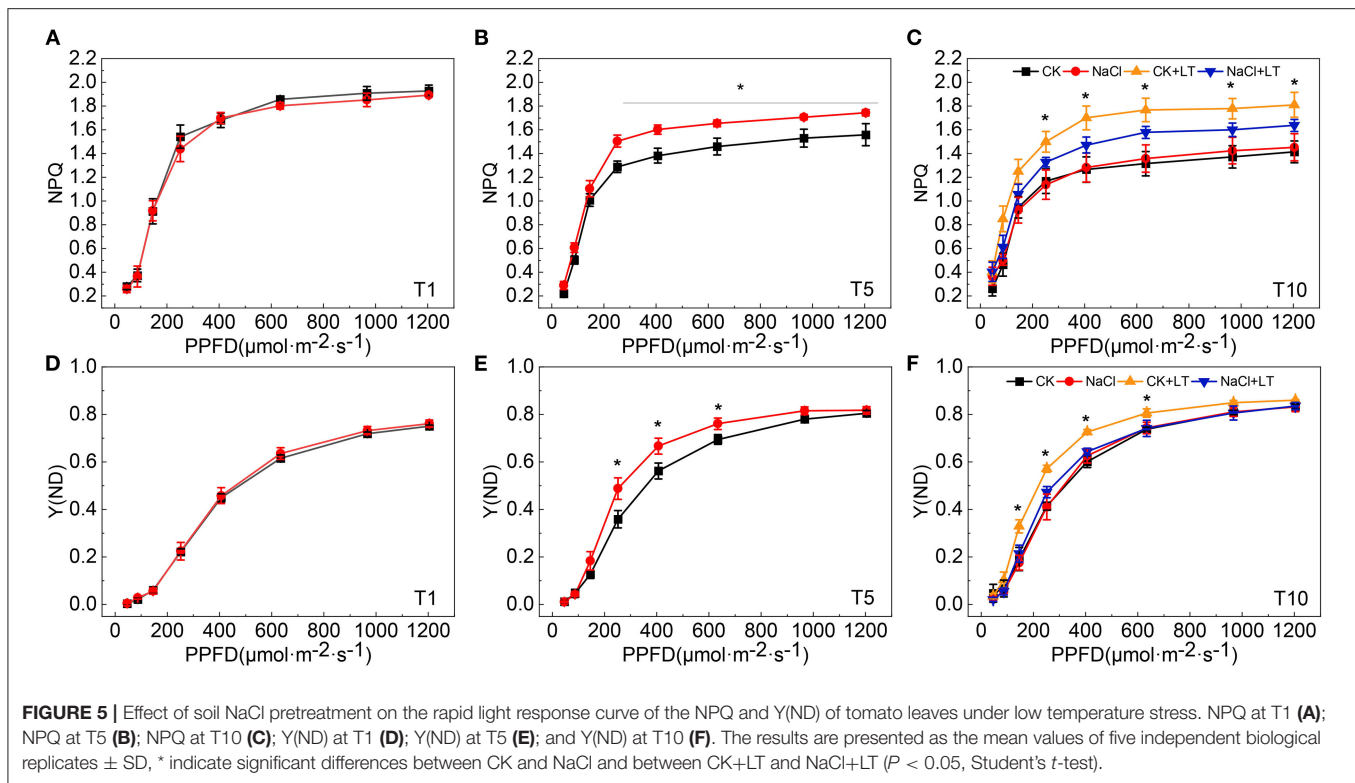
### Light Energy Distribution in PSI and PSII

When plants are subjected to stress, the excessive light energy absorbed can be dissipated in the form of heat to protect the photosystems from damage. The NPQ of the antenna pigments in PSII and the energy dissipation on the PSI donor side are important regulatory strategies. Both NPQ and Y(ND) increased as the light intensity increase, at T1, NPQ and Y(ND) did not significantly differ between NaCl-pretreated leaves and control leaves; at T5, the NPQ and Y(ND) were significantly higher in NaCl-pretreated leaves than in CK leaves under high light intensity. The NPQ and Y(ND) were significantly higher in the CK+LT treatment than in the NaCl+LT treatment following low temperature stress (Figure 5). The distribution of captured light energy between photosystems plays an important role in regulating the photochemical reactions of photosynthesis. At T1, the fluorescence parameters did not differ between NaCl-pretreated leaves and CK leaves. At T5, Y(I) and Y(II) were significantly reduced and Y(ND) and Y(NPQ) were significantly increased under NaCl pretreatment, and no differences were observed in Y(NA) and Y(NO) among treatments. After exposure to low temperature stress, Y(I) and Y(II) decreased rapidly

and were significantly lower in the CK+LT treatment than in the NaCl+LT treatment; Y(NPQ) and Y(ND) increased rapidly and were significantly higher in the CK+LT treatment than in the NaCl+LT treatment following low temperature exposure, indicating that NaCl pretreatment increased the photochemical reaction efficiency of PSI and PSII (Figures 1B, 6).

### Photosynthetic Linear and Cyclic Electron Transport in Tomato Leaves

Analysis of the light intensity-dependent linear and cyclic electron transport rate revealed that the ETR(I), ETR(II), and CEF increased rapidly as the light intensity increased. At T1, there was no difference between treatments. At T5, when the electron transfer rate reached a steady-state, ETR(I), ETR(II), and CEF were significantly lower in NaCl-pretreated leaves than in control leaves, indicating that NaCl treatment reduced both the photosynthetic linear and cyclic electron transfer rate of tomato leaves (Figure 7). The linear and cyclic electron transport rate of plants subjected to low temperature stress were lower than those not subjected to low temperature stress, and the electron transfer rate was significantly higher in NaCl-pretreated leaves than in leaves subjected to low temperature stress that had not been pretreated with NaCl. These findings indicate that despite the reduction in the electron transfer rate caused by NaCl pretreatment, the linear and cyclic electron transport rate remained high under low temperature stress, and these patterns were consistent with the phenotypes observed in each treatment.



## ROS Metabolism and Antioxidant Enzyme Activity

The content of  $H_2O_2$  and  $O_2^-$  production rate was greatly increased after low temperature treatment, while it was significantly alleviated in the NaCl+LT treatment compared with the CK+LT treatment, this indicates that NaCl pretreatment could significantly reduce the accumulation of ROS in tomato plants under low temperature stress (Figures 8A,B). POD activity was significantly increased in tomato leaves in the NaCl+LT treatment compared with the CK+LT treatment, but no difference was observed in SOD activity (Figures 8C,D). NaCl pretreatment significantly increased the relative expression levels of *SIPOD*, *SICAT*, and *SIGR* in tomato leaves under low temperature stress, indicating that NaCl pretreatment could increase the expression of antioxidase-related genes under low temperature stress. By contrast, the relative expression levels of *SIMnSOD*, *SIDHAR*, and *SIMDHAR* were significantly down-regulated by NaCl pretreatment under low temperature stress (Figure 8E).

## Expression of ABA Signaling Pathway and Cold Stress-Related Genes

The effects of NaCl pretreatment on the expression of ABA signal transduction and low temperature stress-related genes in tomato leaves were determined. The relative expression levels of the ABA synthesis-related genes *SINCE1* and the ABA decomposition-related genes *SICYP707A1* were significantly increased in the NaCl+LT treatment relative to the CK+LT treatment. The relative expression levels of the ABA signal transduction-related

genes *SIMYB1* and *SIABRE* were significantly up-regulated in the NaCl+LT treatment compared with the CK+LT treatment of tomato leaves under low temperature stress (Figure 9A). The cold stress-related genes *SIICE1*, *SIICEa*, *SISnRK2.6a*, *SISnRK2.6b*, *SICBF1*, *SICBF2*, and *SICBF3* were significantly up-regulated under low temperature stress. The relative expression levels of these genes were significantly increased in the NaCl+LT treatment compared with the CK+LT treatment (Figure 9B). These findings indicate that NaCl pretreatment affected the expression of ABA signal transduction and low temperature signaling-related genes in tomato leaves under low temperature stress, which might enhance the resistance of tomato to low temperature stress.

## DISCUSSION

Tomato is a popular vegetable worldwide, and obtaining high-yield and high-quality tomato plants requires a suitable environment. Plants, both in the wild and under controlled conditions (e.g., greenhouses), are often exposed to non-lethal stresses (Zandalinas et al., 2021). These stresses can promote resistance to future lethal stresses and ensure survival in unpredictable environments (Katam et al., 2020). One effective strategy for increasing crop yields in adverse environments that has been successfully applied in recent studies is enhancing the photosynthetic capacity of crops. Crops are often subjected to salt and low temperature stress, and these stresses can lead to stomatal closure, photoinhibition, and reductions in photosynthetic efficiency, which can eventually damage plants.

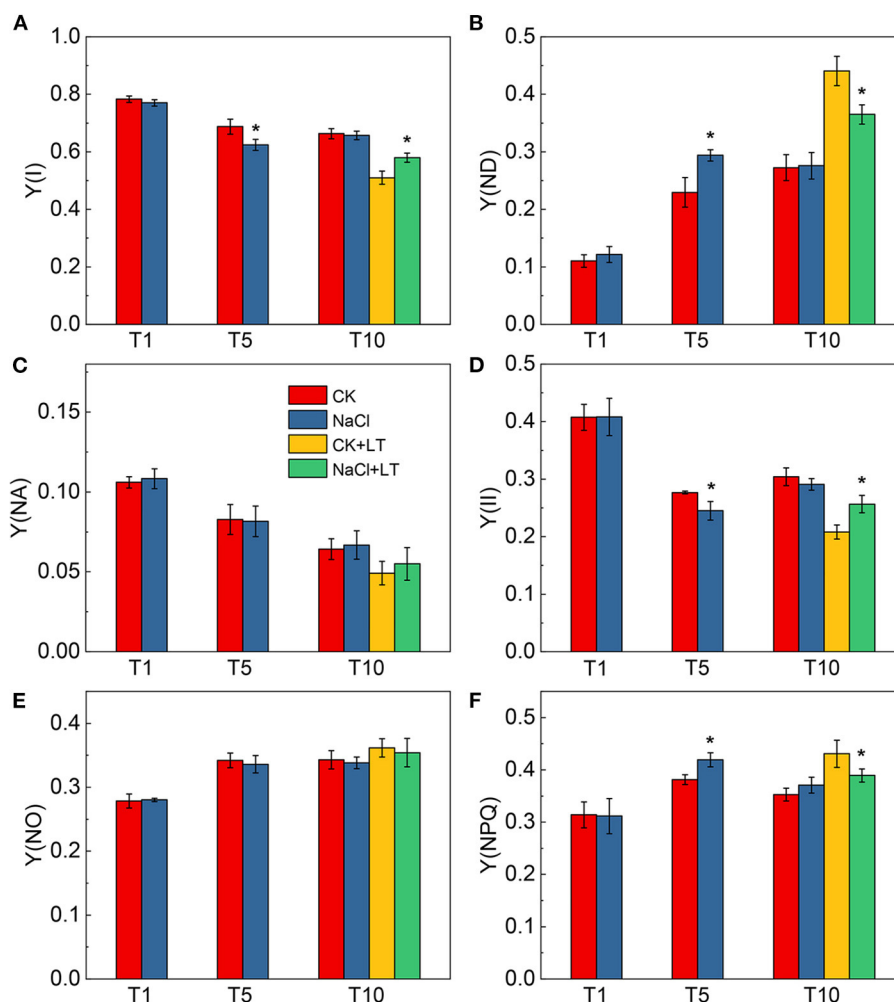
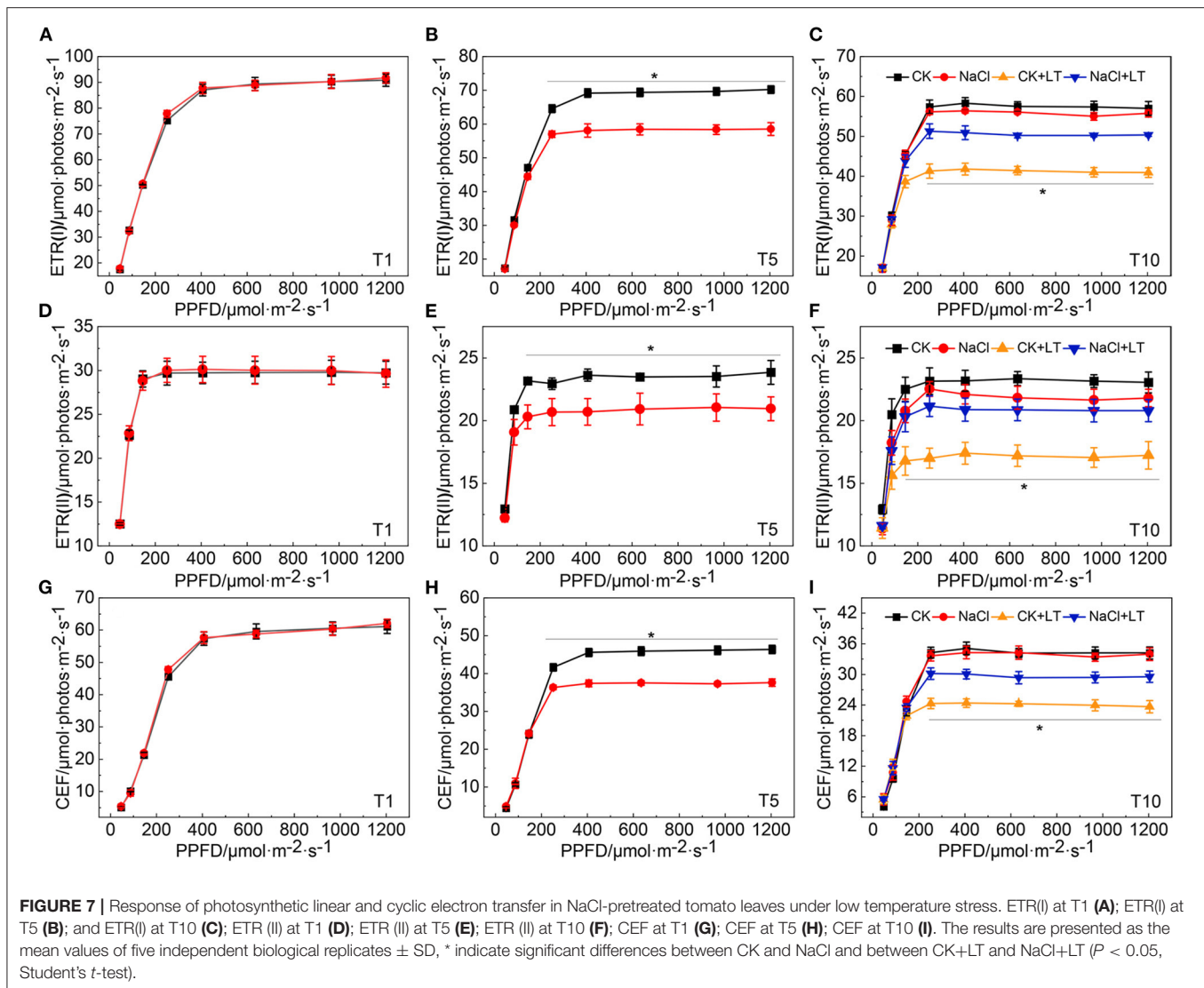


**FIGURE 6 |** Effect of soil NaCl pretreatment on the energy conversion in PSI and PSII of tomato leaves under drought stress. Y(I) (A); Y(ND) (B); Y(NA) (C); Y(II) (D); Y(NO) (E); and Y(NPQ) (F). The results are presented as the mean values of five independent biological replicates  $\pm$  SD, \* indicate significant differences between CK and NaCl and between CK+LT and NaCl+LT ( $P < 0.05$ , Student's  $t$ -test).

The effects of single stressors on photosynthetic capacity have been extensively studied; by contrast, few studies have examined the effects of multiple stressors on photosynthetic capacity. The results of this study revealed that pretreatment with NaCl and low temperature treatment significantly reduced the photosynthetic carbon assimilation rate and photosystem activity, which is consistent with the results of previous studies; however, we found that NaCl pretreatment could induce tolerance of low temperature stress through photosynthetic acclimation (Figures 1, 2, 4). This acclimation-induced cross-tolerance equips plants with tolerance to multiple stresses following exposure to a specific stimulus; this phenomenon has major agricultural implications given the difficulty of controlling the environments in which many crops are grown (Locato et al., 2018).

Salt and low temperature have deleterious effects on the photosynthetic electron transport and cause excessive light

energy to be absorbed by photosynthetic pigments. The severe adversity can substantially exacerbate photoinhibition and induce damage to the photosynthetic apparatus through the production of ROS (Lima-Melo et al., 2019; Yang et al., 2020). The decreases in Fv/Fm and Pm indicate the photoinhibition of PSII and PSI, respectively. Fv/Fm, Pm, PQ size, Y(I), and Y(II) were significantly reduced and Pm, Y(I), and Y(II) were significantly increased in NaCl-pretreated tomato leaves under low temperature stress compared with tomato leaves without pretreated with NaCl. This indicates that NaCl pretreatment can alleviate photoinhibition caused by subsequent low temperature (Figure 4). Previous studies have shown that PSI in many crops, such as *Arabidopsis*, peanut, and cucumber, tends to experience photoinhibition under low temperature and fluctuating light conditions, which limits crop production (Lima-Melo et al., 2019; Wu et al., 2019; Song et al., 2020; Muhammad et al., 2021; Tan et al., 2021). In contrast to PSII photoinhibition, photoinhibition



of PSI cannot be effectively repaired; consequently, recovery of PSI photoinhibition is extremely slow (Kudoh and Sonoike, 2002). The distribution of light energy between photosystems not only determines the amount of excess light energy dissipated by plants in the form of heat but also determines the efficiency of the photochemical reaction. NaCl pretreatment significantly increased  $Y(I)$  and  $Y(II)$  and significantly decreased  $Y(NPQ)$  and  $Y(ND)$  of tomato plants suffer subsequent low temperature relative to the plants without NaCl pretreatment. These results might stem from the fact that NaCl pretreatment contributed to induce heat dissipation at both PSI and PSII, which enhanced photosynthetic adaptability of tomato plants and further alleviate the damage caused by low temperature stress (Figures 5, 6).

A range of photoprotective mechanisms can decrease the damage of the PSII and PSI reaction centers, such as chloroplast avoidance movement, dissipation of absorbed light energy as thermal energy (i.e., NPQ), CEF around PSI, and the

photorespiratory pathway (Guidi et al., 2019; Bassi and Dall'Osto, 2021). Stomata control the entry of  $CO_2$  into the cell and the transpiration of leaves and are sensitive to environmental fluctuations. In this study, salt stress caused the stomata to close, and this stomatal adaptation can alleviate the adverse effects of subsequent low temperatures and contributes to the entry of  $CO_2$ , thus maintaining a relatively high net photosynthetic rate (Figure 1). We found that NaCl pretreatment can effectively reduce low temperature-induced chloroplast damage (Figure 3). The degradation of chloroplast proteins is initiated by ROS and involves the action of proteolytic enzymes such as cysteine and serine proteases (Li et al., 2018). Photosynthetic electron transfer is thought to play a major role in controlling chloroplast quality, because of the excessive ROS accumulation caused by photoinhibition can damage chloroplast proteins, and subsequently, the expression of nuclear genes involved in the regulation of the import and degradation of chloroplast proteins



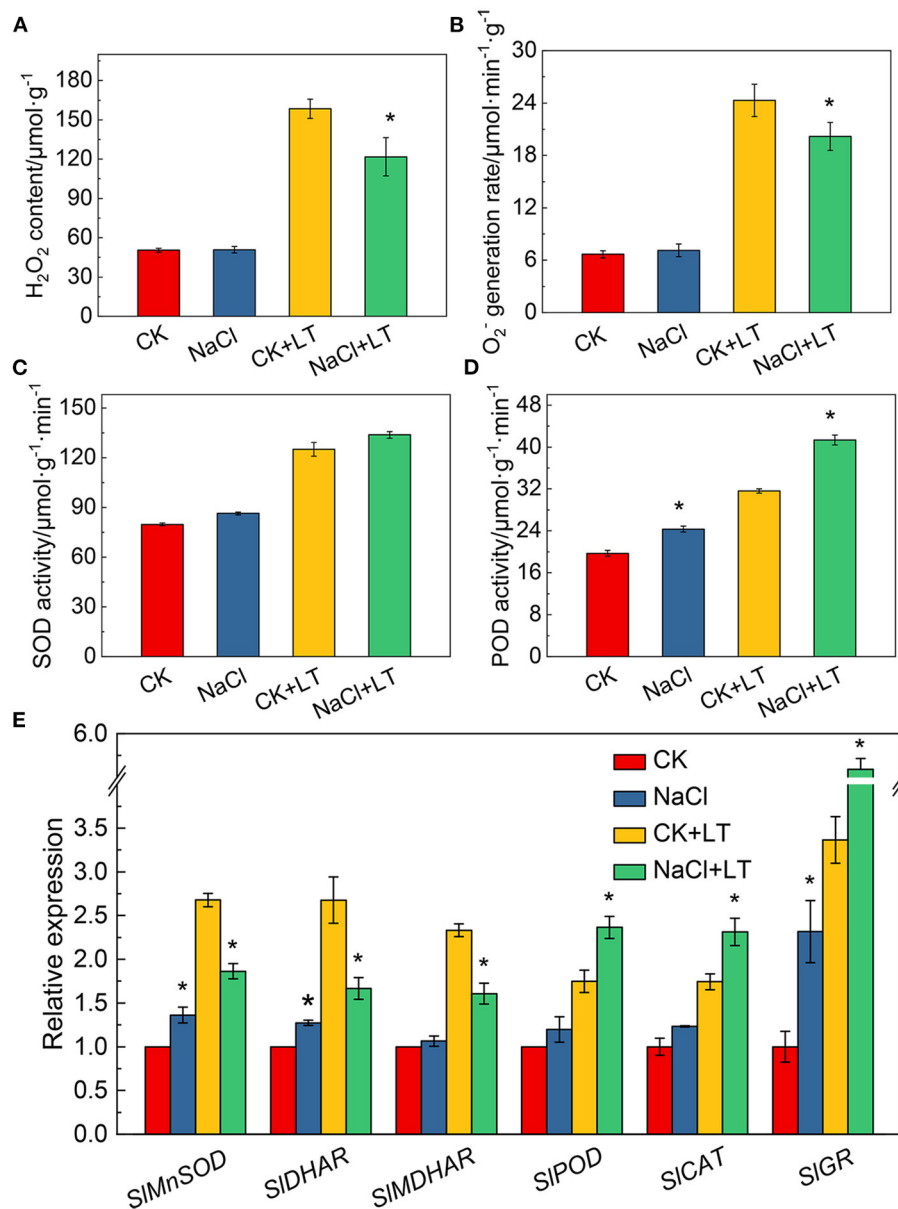
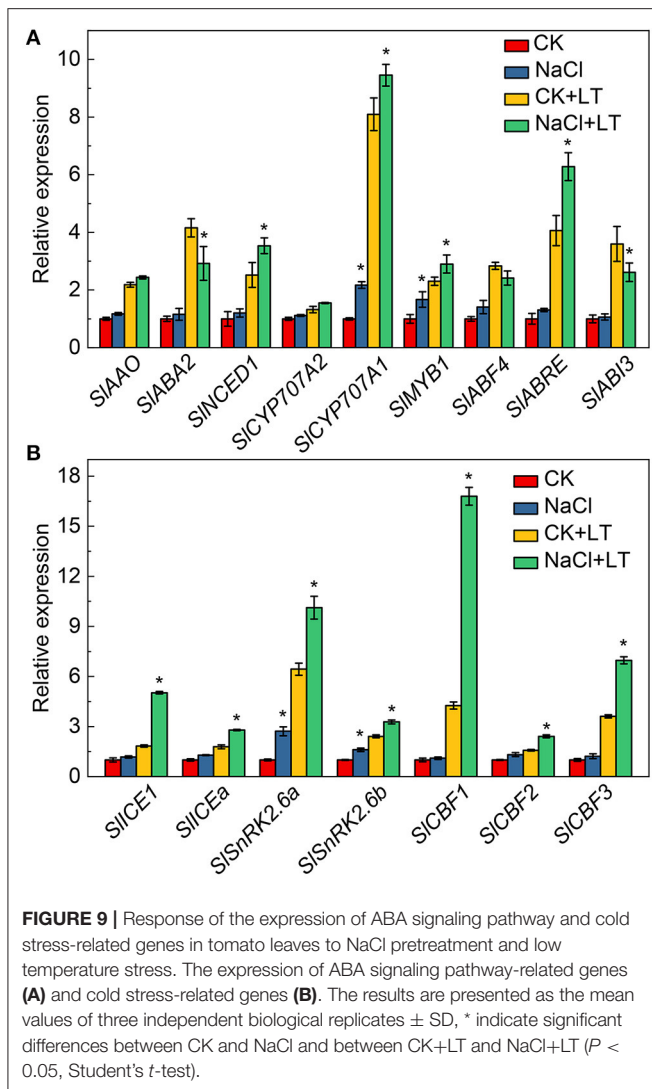


**FIGURE 8 |** Response of reactive oxygen species production, antioxidant enzyme activity, and the expression of related genes in tomato leaves to salt pretreatment and low temperature stress. H<sub>2</sub>O<sub>2</sub> content (A); O<sub>2</sub><sup>-</sup> generation rate (B); superoxide dismutase (SOD) activity (C); peroxidase (POD) activity (D); and antioxidant-related gene expression (E). The results are presented as the mean values of three independent biological replicates  $\pm$  SD, \* indicate significant differences between CK and NaCl and between CK+LT and NaCl+LT ( $P < 0.05$ , Student's *t*-test).

were induced through plastid retrograde signaling (Yang et al., 2020).

The CEF-mediated NPQ was increased in NaCl-pretreated tomato plants under low temperature stress, which alleviated photoinhibition and kept photosynthetic performance high (Figures 6, 7). NPQ, which is closely related to CEF, is the most important component of the photoprotection response; the photoprotection of CEF-induced NPQ during the response of plants to stress has been widely studied (Murchie and Ruban,

2020; Bassi and Dall'Osto, 2021). We have previously shown that CEF can modulate linear electron flow and ROS in response to high temperature, and it mainly protects the donor side of PSI under low night temperature stress (Zhang et al., 2014; Lu et al., 2017, 2020a,b). CEF is thought to be closely related to proton gradient production when linear electron transport does not produce sufficient proton gradients across thylakoid membranes. The proton gradient across the thylakoid membrane can induce the protonation of the PSII protein subunit PsbS,



which dynamically regulates NPQ (Ikeuchi et al., 2014; Nicol and Croce, 2021). In addition, proton gradients can also down-regulate the electron transfer rate of Cytb6f and activate NPQ through the acidification of the thylakoid lumen. The down-regulation of the electron transport rate through Cytb6f is essential for protecting PSI from damage caused by fluctuations in light (Höhner et al., 2016; Zhou et al., 2022).

Salt stress signal cascades can activate downstream overlapping transduction pathways that enhance the photosynthetic acclimation of plants under low temperature stress, which is consistent with the mechanisms of cross-tolerance (Hossain et al., 2018; Gong et al., 2020). Plants adapt to environmental stresses through photosynthetic acclimation, which involves ROS production, antioxidant defense, ABA, and low temperature signaling pathways. In this study, NaCl stress induced the production of ROS, which activated the oxidative response and the activity of antioxidant enzymes, and these physiological changes could alleviate low temperature-induced damage to plants (Figure 8). In addition, the ABA and low

temperature stress signaling were investigated in this study, we found that ABA signal transduction and the low temperature signal pathway contribute to increase the resistance of tomato to low temperature stress (Figure 9). Our results indicates that ROS metabolism, ABA signal transduction, and low temperature signaling pathways can alleviate photoinhibition by activating photoprotection mechanisms, and they also play an important role in regulating salt acclimation-induced cross-tolerance to low temperature stress of tomato. Researches over the past decades have revealed the major functional of apoplastic ROS production and ABA signaling pathway in plants responses to salt and low temperature stress, suggesting that they might be crucial signal molecules mediating cross-tolerance (Van Zelm et al., 2020; Chen et al., 2021). Nevertheless, additional researches are needed to clarify the relationship between stress signaling pathways and photosynthetic acclimation.

## CONCLUSION

In this study, the photosynthetic mechanism underlying cross-tolerance was characterized through analysis of the photosynthetic performance of tomato plants under NaCl pretreatment and low temperature stress. NaCl treatment reduced the CO<sub>2</sub> assimilation rate and photochemical reaction efficiency of tomato leaves and induced non-photochemical quenching at PSI and PSII. This, in turn, affected the photosynthetic adaptability of tomato plants and alleviated damage induced by low temperature stress. CEF-mediated photoprotection, stomatal movement, and chloroplast quality maintenance, as well as ABA signal transduction and low temperature stress-related signaling pathways, play a key role in this acclimation process. The results of our study provide new insights into photosynthetic acclimation mechanisms and have implications for environmental management during crop cultivation.

## DATA AVAILABILITY STATEMENT

The original contributions presented in the study are included in the article/**Supplementary Material**, further inquiries can be directed to the corresponding authors.

## AUTHOR CONTRIBUTIONS

XY, YL, and TL conceived and designed the experiment. XY and FZ conducted the experiment analyzed the data. XY prepared the manuscript. YZ and JS participated in the experiment and revised the manuscript. MQ participated in the guidance of the experiment. All authors contributed to the article and approved the submitted version.

## FUNDING

This study was supported by the National Key Research and Development Program of China (2019YFD1000300), the National Natural Science Foundation of China (Grant No.

31772356), China Agriculture Research System of MOF and MARA (CARS-23), the joint fund for innovation enhancement of Liaoning Province (2021-NLTS-11-01), and the support program of young and middle-aged scientific and technological innovation talents (RC210293).

## REFERENCES

- Bailey-Serres, J., Parker, J. E., Ainsworth, E. A., Oldroyd, G. E., and Schroeder, J. I. (2019). Genetic strategies for improving crop yields. *Nature* 575, 109–118. doi: 10.1038/s41586-019-1679-0
- Bassi, R., and Dall'Osto, L. (2021). Dissipation of light energy absorbed in excess: the molecular mechanisms. *Annu. Rev. Plant. Boil.* 72, 47–76. doi: 10.1146/annurev-arplant-071720-015522
- Bowler, C., and Fluhr, R. (2000). The role of calcium and activated oxygens as signals for controlling cross-tolerance. *Trends. Plant. Sci.* 5, 241–246. doi: 10.1016/S1360-1385(00)01628-9
- Çakırlar, H., Çiçek, N., Fedina, I., Georgieva, K., Dogru, A., and Velitchkova, M. (2008). NaCl induced cross-acclimation to UV-B radiation in four Barley (*Hordeum vulgare* L.) cultivars. *Acta. Physiol. Plant.* 30, 561–567. doi: 10.1007/s11738-008-0155-5
- Chen, X., Ding, Y., Yang, Y., Song, C., Wang, B., Yang, S., et al. (2021). Protein kinases in plant responses to drought, salt, and cold stress. *J. Integr. Plant. Boil.* 63, 53–78. doi: 10.1111/jipb.13061
- Fan, X., Zang, J., Xu, Z., Guo, S., Jiao, X., Liu, X., et al. (2013). Effects of different light quality on growth, chlorophyll concentration and chlorophyll biosynthesis precursors of non-heading Chinese cabbage (*Brassica campestris* L.). *Acta. Physiol. Plant.* 35, 2721–2726. doi: 10.1007/s11738-013-1304-z
- Gong, Z., Xiong, L., Shi, H., Yang, S., Herrera-Estrella, L. R., Xu, G., et al. (2020). Plant abiotic stress response and nutrient use efficiency. *Sci. China Life. Sci.* 63, 635–674. doi: 10.1007/s11427-020-1683-x
- Guidi, L., Lo Piccolo, E., and Landi, M. (2019). Chlorophyll fluorescence, photoinhibition and abiotic stress: does it make any difference the fact to be a C3 or C4 species? *Front. Plant. Sci.* 10, 174. doi: 10.3389/fpls.2019.00174
- Gururani, M. A., Venkatesh, J., and Tran, L. S. P. (2015). Regulation of photosynthesis during abiotic stress-induced photoinhibition. *Mol. Plant.* 8, 1304–1320. doi: 10.1016/j.molp.2015.05.005
- Hao, J., Gu, F., Zhu, J., Lu, S., Liu, Y., Li, Y., et al. (2016). Low night temperature affects the phloem ultrastructure of lateral branches and raffinose family oligosaccharide (RFO) accumulation in RFO-transporting plant melon (*Cucumis melo* L.) during fruit expansion. *PLoS ONE* 11, e0160909. doi: 10.1371/journal.pone.0160909
- Höhner, R., Aboukila, A., Kunz, H. H., and Venema, K. (2016). Proton gradients and proton-dependent transport processes in the chloroplast. *Front. Plant. Sci.* 7, 218. doi: 10.3389/fpls.2016.00218
- Hossain, M. A., Li, Z. G., Hoque, T. S., Burritt, D. J., Fujita, M., and Munné-Bosch, S. (2018). Heat or cold priming-induced cross-tolerance to abiotic stresses in plants: key regulators and possible mechanisms. *Protoplasma.* 255, 399–412. doi: 10.1007/s00709-017-1150-8
- Ibrahim, M. H., and Jaafar, H. Z. (2012). Primary, secondary metabolites, H<sub>2</sub>O<sub>2</sub>, malondialdehyde and photosynthetic responses of *Orthosiphon stamineus* Benth to different irradiance levels. *Molecules* 17, 1159–1176. doi: 10.3390/molecules17021159
- Ikeuchi, M., Uebayashi, N., Sato, F., and Endo, T. (2014). Physiological functions of PsbS-dependent and PsbS-independent NPQ under naturally fluctuating light conditions. *Plant. Cell. Physiol.* 55, 1286–1295. doi: 10.1093/pcp/pcu069
- Jiang, Y., Ding, X., Zhang, D., Deng, Q., Yu, C. L., Zhou, S., et al. (2017). Soil salinity increases the tolerance of excessive sulfur fumigation stress in tomato plants. *Environ. Exp. Bot.* 133, 70–77. doi: 10.1016/j.envexpbot.2016.10.002
- Katam, R., Shokri, S., Murthy, N., Singh, S. K., Suravajhala, P., Khan, M. N., et al. (2020). Proteomics, physiological, and biochemical analysis of cross tolerance mechanisms in response to heat and water stresses in soybean. *PLoS ONE* 15, e0233905. doi: 10.1371/journal.pone.0233905
- Kudoh, H., and Sonoike, K. (2002). Irreversible damage to photosystem I by chilling in the light: cause of the degradation of chlorophyll after returning to normal growth temperature. *Planta* 215, 541–548. doi: 10.1007/s00425-002-0790-9
- Li, L., Aro, E. M., and Millar, A. H. (2018). Mechanisms of photodamage and protein turnover in photoinhibition. *Trends. Plant. Sci.* 23, 667–676. doi: 10.1016/j.tplants.2018.05.004
- Lima-Melo, Y., Alencar, V. T., Lobo, A. K., Sousa, R. H., Tikkanen, M., Aro, E. M., et al. (2019). Photoinhibition of photosystem I provides oxidative protection during imbalanced photosynthetic electron transport in *Arabidopsis thaliana*. *Front. Plant. Sci.* 10, 916. doi: 10.3389/fpls.2019.00916
- Locato, V., Cimini, S., and De Gara, L. (2018). ROS and redox balance as multifaceted players of cross-tolerance: epigenetic and retrograde control of gene expression. *J. Exp. Bot.* 69, 3373–3391. doi: 10.1093/jxb/ery168
- Lu, J., Wang, Z., Yang, X., Wang, F., Qi, M., Li, T., et al. (2020a). Cyclic electron flow protects photosystem I donor side under low night temperature in tomato. *Environ. Exp. Bot.* 177, 104151. doi: 10.1016/j.envexpbot.2020.104151
- Lu, J., Yin, Z., Lu, T., Yang, X., Wang, F., Qi, M., et al. (2020b). Cyclic electron flow modulate the linear electron flow and reactive oxygen species in tomato leaves under high temperature. *Plant. Sci.* 292, 110387. doi: 10.1016/j.plantsci.2019.110387
- Lu, T., Meng, Z., Zhang, G., Qi, M., Sun, Z., Liu, Y., et al. (2017). Sub-high temperature and high light intensity induced irreversible inhibition on photosynthesis system of tomato plant (*Solanum lycopersicum* L.). *Front. Plant. Sci.* 8, 365. doi: 10.3389/fpls.2017.00365
- Morales, A., and Kaiser, E. (2020). Photosynthetic acclimation to fluctuating irradiance in plants. *Front. Plant. Sci.* 11, 268. doi: 10.3389/fpls.2020.00268
- Muhammad, I., Shalmani, A., Ali, M., Yang, Q. H., Ahmad, H., and Li, F. B. (2021). Mechanisms regulating the dynamics of photosynthesis under abiotic stresses. *Front. Plant. Sci.* 11, 2310. doi: 10.3389/fpls.2020.615942
- Murchie, E. H., and Ruban, A. V. (2020). Dynamic non-photochemical quenching in plants: from molecular mechanism to productivity. *Plant. J.* 101, 885–896. doi: 10.1111/tpj.14601
- Nicol, L., and Croce, R. (2021). The PsbS protein and low pH are necessary and sufficient to induce quenching in the light-harvesting complex of plants LHCII. *Sci. Rep.* 11, 1–8. doi: 10.1038/s41598-021-86975-9
- Park, S., Steen, C. J., Lyska, D., Fischer, A. L., Endelman, B., Iwai, M., et al. (2019). Chlorophyll–carotenoid excitation energy transfer and charge transfer in Nannochloropsis oceanica for the regulation of photosynthesis. *P. Nat. Acad. Sci. USA.* 116, 3385–3390. doi: 10.1073/pnas.1819011116
- Pastori, G. M., and Foyer, C. H. (2002). Common components, networks, and pathways of cross-tolerance to stress. The central role of “redox” and abscisic acid-mediated controls. *Plant Physiol.* 129, 460–468. doi: 10.1104/pp.011021
- Pinnola, A., and Bassi, R. (2018). Molecular mechanisms involved in plant photoprotection. *Biochem. Soc. T.* 46, 467–482. doi: 10.1042/BST20170307
- Saddhe, A. A., Malvankar, M. R., Karle, S. B., and Kumar, K. (2019). Reactive nitrogen species: paradigms of cellular signaling and regulation of salt stress in plants. *Environ. Exp. Bot.* 161, 86–97. doi: 10.1016/j.envexpbot.2018.11.010
- Song, Q., Liu, Y., Pang, J., Yong, J. W. H., Chen, Y., Bai, C., et al. (2020). Supplementary calcium restores peanut (*Arachis hypogaea*) growth and photosynthetic capacity under low nocturnal temperature. *Front. Plant Sci.* 10, 1637. doi: 10.3389/fpls.2019.01637
- Sun, H., Shi, Q., Zhang, S. B., and Huang, W. (2022). The response of photosystem I to fluctuating light is influenced by leaf nitrogen content in tomato. *Environ. Exp. Bot.* 193, 104665. doi: 10.1016/j.envexpbot.2021.104665
- Tan, S. L., Huang, J. L., Zhang, F. P., Zhang, S. B., and Huang, W. (2021). Photosystem I photoinhibition induced by fluctuating light depends on background low light irradiance. *Environ. Exp. Bot.* 181, 104298. doi: 10.1016/j.envexpbot.2020.104298

## SUPPLEMENTARY MATERIAL

The Supplementary Material for this article can be found online at: <https://www.frontiersin.org/articles/10.3389/fpls.2022.891697/full#supplementary-material>

- Tombesi, S., Frioni, T., Poni, S., and Palliotti, A. (2018). Effect of water stress “memory” on plant behavior during subsequent drought stress. *Environ. Exp. Bot.* 150, 106–114. doi: 10.1016/j.envexpbot.2018.03.009
- Van Zelm, E., Zhang, Y., and Testerink, C. (2020). Salt tolerance mechanisms of plants. *Annu. Rev. Plant. Biol.* 71, 403–433. doi: 10.1146/annurev-arplant-050718-100005
- Wu, X., Shu, S., Wang, Y., Yuan, R., and Guo, S. (2019). Exogenous putrescine alleviates photoinhibition caused by salt stress through cooperation with cyclic electron flow in cucumber. *Photosynth. Res.* 141, 303–314. doi: 10.1007/s11120-019-00631-y
- Yang, X., Li, Y., Chen, H., Huang, J., Zhang, Y., Qi, M., et al. (2020). Photosynthetic response mechanism of soil salinity-induced cross-tolerance to subsequent drought stress in tomato plants. *Plants* 9, 363. doi: 10.3390/plants9030363
- Yang, X., Xu, H., Shao, L., Li, T., Wang, Y., and Wang, R. (2018). Response of photosynthetic capacity of tomato leaves to different LED light wavelength. *Environ. Exp. Bot.* 150, 161–171. doi: 10.1016/j.envexpbot.2018.03.013
- Yang, Y., and Guo, Y. (2018). Elucidating the molecular mechanisms mediating plant salt-stress responses. *New. Phytol.* 217, 523–539. doi: 10.1111/nph.14920
- Zandalinas, S. I., Sengupta, S., Fritschi, F. B., Azad, R. K., Nechushtai, R., and Mittler, R. (2021). The impact of multifactorial stress combination on plant growth and survival. *New. Phytol.* 230, 1034–1048. doi: 10.1111/nph.17232
- Zhang, G., Liu, Y., Ni, Y., Meng, Z., Lu, T., and Li, T. (2014). Exogenous calcium alleviates low night temperature stress on the photosynthetic apparatus of tomato leaves. *PLoS ONE* 9, e97322. doi: 10.1371/journal.pone.0097322
- Zhang, H., Zhao, Y., and Zhu, J. K. (2020). Thriving under stress: how plants balance growth and the stress response. *Dev. Cell.* 55, 529–543. doi: 10.1016/j.devcel.2020.10.012
- Zhang, X., Xu, Y., and Huang, B. (2019). Lipidomic reprogramming associated with drought stress priming-enhanced heat tolerance in tall fescue (*Festuca arundinacea*). *Plant. Cell. Environ.* 42, 947–958. doi: 10.1111/pce.13405
- Zhao, C., Zhang, H., Song, C., Zhu, J. K., and Shabala, S. (2020). Mechanisms of plant responses and adaptation to soil salinity. *Innovation* 1, 100017. doi: 10.1016/j.xinn.2020.100017
- Zhou, J., Xia, X. J., Zhou, Y. H., Shi, K., Chen, Z., and Yu, J. Q. (2014). RBOH1-dependent H<sub>2</sub>O<sub>2</sub> production and subsequent activation of MPK1/2 play an important role in acclimation-induced cross-tolerance in tomato. *J. Exp. Bot.* 65, 595–607. doi: 10.1093/jxb/ert404
- Zhou, Q., Wang, C., Yamamoto, H., and Shikanai, T. (2022). PTOX-dependent safety valve does not oxidize P700 during photosynthetic induction in the *Arabidopsis* *pgr5* mutant. *Plant. Physiol.* 188, 1264–1276. doi: 10.1093/plphys/kiab541

**Conflict of Interest:** The authors declare that the research was conducted in the absence of any commercial or financial relationships that could be construed as a potential conflict of interest.

**Publisher’s Note:** All claims expressed in this article are solely those of the authors and do not necessarily represent those of their affiliated organizations, or those of the publisher, the editors and the reviewers. Any product that may be evaluated in this article, or claim that may be made by its manufacturer, is not guaranteed or endorsed by the publisher.

Copyright © 2022 Yang, Zou, Zhang, Shi, Qi, Liu and Li. This is an open-access article distributed under the terms of the Creative Commons Attribution License (CC BY). The use, distribution or reproduction in other forums is permitted, provided the original author(s) and the copyright owner(s) are credited and that the original publication in this journal is cited, in accordance with accepted academic practice. No use, distribution or reproduction is permitted which does not comply with these terms.





# The Transcription Factor MYB37 Positively Regulates Photosynthetic Inhibition and Oxidative Damage in Arabidopsis Leaves Under Salt Stress

Yuanyuan Li<sup>1†</sup>, Bei Tian<sup>1†</sup>, Yue Wang<sup>1</sup>, Jiechen Wang<sup>1</sup>, Hongbo Zhang<sup>1</sup>, Lu Wang<sup>1</sup>, Guangyu Sun<sup>1</sup>, Yongtao Yu<sup>2\*</sup> and Huihui Zhang<sup>1\*</sup>

## OPEN ACCESS

### Edited by:

Marcin Rapacz,  
University of Agriculture in Krakow,  
Poland

### Reviewed by:

Wei Huang,  
Kunming Institute of Botany, Chinese  
Academy of Sciences (CAS), China  
Sumaira Rasul,  
Bahauddin Zakariya University,  
Pakistan

### \*Correspondence:

Yongtao Yu  
yuyongtao@nercv.org  
Huihui Zhang  
zhang\_hh@nefu.edu.cn

<sup>†</sup>These authors have contributed  
equally to this work

### Specialty section:

This article was submitted to  
Plant Abiotic Stress,  
a section of the journal  
Frontiers in Plant Science

**Received:** 13 May 2022

**Accepted:** 21 June 2022

**Published:** 12 July 2022

### Citation:

Li Y, Tian B, Wang Y, Wang J,  
Zhang H, Wang L, Sun G, Yu Y and  
Zhang H (2022) The Transcription  
Factor MYB37 Positively Regulates  
Photosynthetic Inhibition and  
Oxidative Damage in Arabidopsis  
Leaves Under Salt Stress.  
Front. Plant Sci. 13:943153.  
doi: 10.3389/fpls.2022.943153

<sup>1</sup>Key Laboratory of Saline-alkali Vegetation Ecology Restoration, Ministry of Education, College of Life Sciences, Northeast Forestry University, Harbin, China, <sup>2</sup>National Watermelon and Melon Improvement Center, Beijing Academy of Agriculture and Forestry Sciences, Key Laboratory of Biology and Genetic Improvement of Horticultural Crops (North China), Beijing Key Laboratory of Vegetable Germplasm Improvement, Beijing, China

MYB transcription factors (TFs) mediate plant responses and defenses to biotic and abiotic stresses. The effects of overexpression of MYB37, an R2R3 MYB subgroup 14 transcription factors in *Arabidopsis thaliana*, on chlorophyll content, chlorophyll fluorescence parameters, reactive oxygen species (ROS) metabolism, and the contents of osmotic regulatory substances were studied under 100 mM NaCl stress. Compared with the wild type (Col-0), MYB37 overexpression significantly alleviated the salt stress symptoms in *A. thaliana* plants. Chlorophyll a (Chl a) and chlorophyll b (Chl b) contents were significantly decreased in OE-1 and OE-2 than in Col-0. Particularly, the Chl a/b ratio was also higher in OE-1 and OE-2 than in Col-0 under NaCl stress. However, MYB37 overexpression alleviated the degradation of chlorophyll, especially Chl a. Salt stress inhibited the activities of PSII and PSI in Arabidopsis leaves, but did not affect the activity of PSII electron donor side oxygen-evolving complex (OEC). MYB37 overexpression increased photosynthesis in Arabidopsis by increasing PSII and PSI activities. MYB37 overexpression also promoted the transfer of electrons from Q<sub>A</sub> to Q<sub>B</sub> on the PSII receptor side of Arabidopsis under NaCl stress. Additionally, MYB37 overexpression increased Y(II) and Y(NPQ) of Arabidopsis under NaCl stress and decreased Y(NO). These results indicate that MYB37 overexpression increases PSII activity and regulates the proportion of energy dissipation in Arabidopsis leaves under NaCl stress, thus decreasing the proportion of inactivated reaction centers. Salt stress causes excess electrons and energy in the photosynthetic electron transport chain of Arabidopsis leaves, resulting in the release of reactive oxygen species (ROS), such as superoxide anion and hydrogen peroxide, leading to oxidative damage. Nevertheless, MYB37 overexpression reduced accumulation of malondialdehyde in Arabidopsis leaves under NaCl stress and alleviated the degree of membrane lipid peroxidation caused by ROS. Salt stress also enhanced the accumulation of soluble sugar (SS) and proline (Pro) in Arabidopsis leaves, thus reducing salt stress damage to plants. Salt stress also degraded

soluble protein (SP). Furthermore, the accumulation of osmoregulation substances SS and Pro in OE-1 and OE-2 was not different from that in Col-0 since *MYB37* overexpression in *Arabidopsis* OE-1, and OE-2 did not significantly affect plants under NaCl stress. However, SP content was significantly higher in OE-1 and OE-2 than in Col-0. These results indicate that *MYB37* overexpression can alleviate the degradation of *Arabidopsis* proteins under NaCl stress, promote plant growth and improve salt tolerance.

**Keywords:** salt stress, *Arabidopsis thaliana*, transcription factor MYB37, photosynthesis, reactive oxygen species

## INTRODUCTION

Abiotic stress, especially salt stress, has gradually become the primary factor affecting the survival and distribution of plants due to the change in global climate conditions (Shaheen et al., 2013). Salt stress mainly affects plants in three aspects: (I) Excessive salt in the soil produces osmotic stress. As a result, the water potential becomes lower in soil than in plant root cells, thus inhibiting water absorption (Rana and Mark, 2008). (II) Gradual accumulation of Na<sup>+</sup> inhibits the absorption of K<sup>+</sup> in plants, thus affecting some physiological and biochemical reactions that are dependent on K<sup>+</sup>, including enzymatic reactions, protein synthesis, and photosynthesis. Excessive Na<sup>+</sup> and Cl<sup>-</sup> also significantly increase intracellular Ca<sup>2+</sup>, resulting in metabolic disorder and even death (Tsugane et al., 1999). (III) Salt stress causes secondary stresses on plants, including oxidative stress and the inhibition of photosynthesis. Excessive reactive oxygen species (ROS) can produce oxidative stress on plants, and damage DNA, enzymes, and biofilm, thus affecting cell structure and metabolism (Dorothea and Ramanjulu, 2005). For instance, salt stress decreases the stability of thylakoid membranes by increasing the rate of chlorophyll degradation in plants, thus hindering the electron transport chain and energy transport of the photosynthetic system and inhibiting photosynthesis (Zhao et al., 2019; Zhang et al., 2020b). Photosynthesis, particularly the photoinhibition of photosystem II (PSII) and photosystem I (PSI), is closely related to ROS production (Che et al., 2018). Excessive ROS disturbs the redox balance in cells, leading to oxidative damage (Jithesh et al., 2006). Therefore, excessive accumulation of ROS in plants under salt stress can significantly affect plant biomass (Klaus and Heribert, 2004). The adaptation of plants to abiotic stress is a complex process involving cell adaptation at the molecular, biochemical and physiological levels (Pushp et al., 2015). The transcriptional machinery associated with stress responses maintains the growth, metabolism, and development of plants through an intricate network of transcription factors (TFs; Agarwal et al., 2013).

Related studies have found that TFs play crucial roles in plant signal regulatory networks. TFs receive the perceived signals and regulate the expression of downstream genes. TFs also act as a node to coordinate the interaction between different signaling pathways. TFs provide complex control mechanisms for plants to manage abiotic and biological stresses, thus regulating developmental processes (Mitsuda and Ohme, 2009). Therefore, the functional study of stress response of transcription factors may provide insights into how plants adapt to severe environments

at the molecular level. More than 1,600 TFs have been identified in *Arabidopsis* (Riechmann et al., 2000; Chen et al., 2006). These TFs can help plants rapidly adapt to changing environments by regulating gene transcription (Zhu, 2002; Kazuo et al., 2003; Chinnusamy et al., 2004). The MYB domain TFs are characterized by a conserved MYB domain with about 52 amino acids involved in DNA binding and are present in all eukaryotes (Yu et al., 2016b). The MYB TF family in *Arabidopsis* contains 200 genes. It is the largest TF family in *Arabidopsis*, accounting for 9% of all the TFs in this plant (Riechmann et al., 2000; Søren et al., 2013). Many members of the MYB TF family play a role in tolerance to abiotic stress (Li et al., 2015; Zhang et al., 2020e), regulation of nitrogen absorption and utilization (Liu et al., 2022), and defense responses to pathogens (Mengiste et al., 2003; Liu et al., 2013). The MYB proteins are divided into four subfamilies based on the number of adjacent repeats in the MYB domain (R1-MYB, R2R3-MYB, 3R-MYB, and 4R-MYB; Dubos et al., 2010). The R2R3-MYB family is common in plants (Jiang and Rao, 2020; Wu et al., 2022), with about 126 of these TFs found in *Arabidopsis* (Chen et al., 2006). Many members of the MYB TF family participate in *Arabidopsis* response to salt stress (Mengiste et al., 2003; Xie et al., 2010; Cui et al., 2013; Xu et al., 2015; Wang et al., 2016). However, only a few studies have assessed how MYB regulates plant photosynthesis and oxidative damage under salt stress. Previous studies have shown that MYB37, R2R3 MYB subgroup 14 TF in *Arabidopsis*, affects the phenotypic changes of plant hairy roots by mediating plant hormone signaling pathway. MYB37 also positively regulates plant response to abscisic acid (ABA) and drought stress, thus improving the seed setting rate of *Arabidopsis* (Dubos et al., 2010; Yu et al., 2016a; Zheng et al., 2020). This study evaluated the effects of *MYB37* overexpression on chlorophyll content, PSII and PSI functions in light reactions, ROS metabolism, and osmotic regulation in *Arabidopsis* leaves under salt stress. Therefore, this study may provide new insights into how MYB37 alleviates salt stress and provides a theoretical basis for improving the genes related to stress resistance.

## MATERIALS AND METHODS

### Experimental Materials

The *Arabidopsis* seeds were disinfected, then sown on MS solid medium. The seeds were vernalized at 4°C for 2 days and cultured in a greenhouse at 21°C, light intensity of 400 μmol·m<sup>-2</sup>·s<sup>-1</sup>, photoperiod of 16/8 h (light/dark), and relative

humidity of 60%. *Agrobacterium tumefaciens* containing the recombinant plasmid p MDC85-35s::MYB37-GFP was used to genetically transform wild-type *A. thaliana* (Col-0) via inflorescence infection. The positive transgenic lines were screened based on their resistance to hygromycin. The transgenic plants were verified using PCR and real-time quantitative reverse transcription PCR (qRT-PCR). Genotypic lines (OE-1 and OE-2) with high expression levels of MYB37 in the third generation (T3) homozygous lines were used as the experimental materials. NaCl (100 mmol·L<sup>-1</sup>) and an equal volume of water were used to irrigate Arabidopsis transgenic lines (OE-1 and OE-2) and Arabidopsis wild type (Col-0) when the seedlings had grown for 4 weeks. A plastic tray was placed under each basin to prevent the loss of salt solution. The solution was poured back into the tray when the matrix was slightly dry. Arabidopsis leaves of each treatment group were randomly sampled on after 7 d irrigation for the following analyses.

## Parameter Measurements and Methods

### Real-Time PCR Analysis

The 10-day-old seedlings were used to determine the MYB37 transcript levels in the wild-type Col-0 and the plants overexpressing MYB37. Total RNA was extracted from about 100 mg of plant tissue using a Total RNA Rapid Extraction Kit (BioTeke Co., Ltd., Wuxi, China). The total RNA was treated with RNase-free DNaseI (NEB, Ipswich, MA, United States) at 37°C for 1 h to degrade the genomic DNA, then purified using an RNA Purification Kit (BioTeke Co., Ltd.). The total RNA (2 µg) was used to synthesize first-strand cDNA via a Roche Transcriptor First Strand cDNA Synthesis Kit (Roche, Basel, Switzerland) and an oligo (dT18) primer. A Bio-Rad Real-Time System CFX96TM C1000 Thermal Cycler (Bio-Rad, Singapore, Singapore) was used for the analysis. ACTIN2/8 genes were amplified and used as the internal control. The cDNA was amplified using SYBR Premix Ex Taq (TaKaRa, Dalian, China) with a DNA Engine Opticon 2 thermal cycler in a 10 µl. All the experiments were repeated at least thrice. The gene-specific primer sequences (5'-3') were as follows:

MYB37: forward primer: CGACAAGACAAAAGTGAAGCGA.  
: reverse primer: TGGCAGCGAAGAGACTAAAAATG.  
ACTIN2/8: forward primer: GGTAACATTGTGCTCAGTGG  
TGG.  
: reverse primer: AACGACCTTAATCTTCATGCTGC.

### Subcellular Localization of MYB37

The roots of 1-week-old MYB37-overexpressing seedlings (OE-2) were immersed in 2 µg/ml 4',6-diamidino-2-phenylindole (DAPI) solution for 10–15 min for nucleus labeling. The roots were visualized using fluorescence microscopy (EVOS™ FL Auto; Thermo Fisher Scientific, Waltham, MA, United States).

### Determination of the OJIP Curve and 820 nm Light Reflection Curve ( $MR_{820}$ )

The leaves of Arabidopsis plants were used for a dark adaptation experiment for 30 min using a dark adaptation clip. The OJIP and 820 nm light reflection curves ( $MR_{820}$ ) were measured five

times using a Hansatech multifunctional plant efficiency instrument (M-PEA; Hansatech Instruments, Ltd., King's Lynn, United Kingdom) after dark adaptation. The corresponding time points at O, J, I, and P points were 0.01, 2, 30, and 1,000 ms, respectively (represented as  $F_o$ ,  $F_p$ ,  $F_i$ , and  $F_m$ , respectively). Points L and K represent the corresponding points on the curve at 0.15 ms and 0.3 ms, respectively. O-P and O-J were standardized on the OJIP curve. The relative fluorescence intensity ( $F_o$ ) of the O point was set to 0, while the relative fluorescence intensity ( $F_p$ ) of the P, J and K points was set to 1 as follows:  $V_{O-P} = (F_i - F_o) / (F_p - F_o)$  and  $V_{O-J} = (F_i - F_o) / (F_j - F_o)$ , where  $F_i$  represents the relative fluorescence intensity of each time point. The relative variable fluorescence intensities of the K and J points on the standardization curve were expressed as  $V_K$  and  $V_J$ , respectively [ $V_K = (F_K - F_o) / (F_j - F_o)$  and  $V_J = (F_j - F_o) / (F_p - F_o)$ ]. A JIP test analysis was conducted as described by Strasser and Strasser (1995). The PSII maximum photochemical efficiency ( $F_v/F_m$ ) and photosynthetic performance index were determined based on light absorption ( $PI_{ABS}$ ). The slope of the initial section of  $MR_{820}$  curve ( $\Delta I/I_o$ , where  $I_o$  and  $\Delta I$  represent the maximum value and the difference between the maximum value and the minimum value of the reflected signal in 820 nm light reflection curve, respectively) represented the activity of the PSI reaction center (Oukarroum et al., 2018).

### Determination of Energy Distribution Parameters of the PSII Reaction Center

The maximum fluorescence ( $F_m$ ) was measured using an FMS-2 pulse modulated fluorometer (Hansatech) after dark adaptation. The steady-state fluorescence ( $F_s$ ) and maximum steady-state fluorescence ( $F_m'$ ) were treated at light intensity (PFD) of 1,000 µmol·m<sup>-2</sup>·s<sup>-1</sup> for light adaptation. The data measured were used to calculate the energy distribution parameters of the PSII reaction center, such as the PSII effective quantum yield Y(II), PSII non-regulated energy dissipation Y(NO), and the PSII regulated energy dissipation yield Y(NPQ) [ $Y(II) = (F_m' - F_s)/F_m'$ ,  $Y(NO) = F_s/F_m$  and  $Y(NPQ) = 1 - Y(II) - Y(NO)$ ] (Kramer et al., 2004).

### Determination of Chlorophyll Content

Fresh leaves without main veins were soaked in a 1:1 solution of acetone and ethanol (v/v) to extract the pigments [Chlorophyll a (Chl a), Chlorophyll b (Chl b), total chlorophyll (Chl a + b) and chlorophyll a/b (Chl a/b)] (Porra, 2002).

### Histochemical Staining of Superoxide Anion ( $O_2^-$ ) and Hydrogen Peroxide ( $H_2O_2$ )

The superoxide anions ( $O_2^-$ ) and hydrogen peroxide ( $H_2O_2$ ) in fresh leaves were stained using nitro blue tetrazolium chloride (NBT) and 3, 3'-diaminobenzidine tetrahydrochloride (DAB), respectively, as described by Mostofa et al. (2015).

### Determination of Reactive Oxygen Species (ROS) and Malondialdehyde (MDA) Contents

The rate of production of superoxide anion ( $O_2^-$ ) and the content of hydrogen peroxide ( $H_2O_2$ ) were determined as

described by Zhang et al. (2006) and Alexieva et al. (2001). The content of MDA was determined using thiobarbituric acid (TBA) colorimetry (Ernster et al., 1968).

### Determination of Osmotic Regulatory Substances Content

The contents of soluble sugar (SS), soluble protein (SP), and free proline (Pro) were determined using anthrone colorimetry (Bradford, 1976). Coomassie brilliant blue G-250 staining (Bradford, 1976), acid ninhydrin colorimetry (Bates et al., 1973), respectively.

### Statistical Analysis

Microsoft Excel 2016 (Redmond, WA, United States) and GraphPad Prism 6 software (GraphPad, San Diego, CA, United States) were used for statistical analyses. Data are expressed as mean  $\pm$  SD. A one-way analysis of variance (ANOVA) and least significant difference (LSD) tests were used to compare the treatments.

## RESULTS AND ANALYSIS

### Expression and Subcellular Localization of MYB37 in Arabidopsis

Arabidopsis overexpressing MYB37 was obtained *via* transgenic technology to clarify the function of MYB37 in Arabidopsis under NaCl stress. Real-time quantitative reverse transcription PCR (qRT-PCR) results showed that MYB37 was significantly expressed in the OE-1 and OE-2 lines than in the other overexpression lines (the expression was more than 100-fold higher than that in Col-0; **Figure 1A**). Therefore, the OE-1 and OE-2 lines were selected for further functional verification

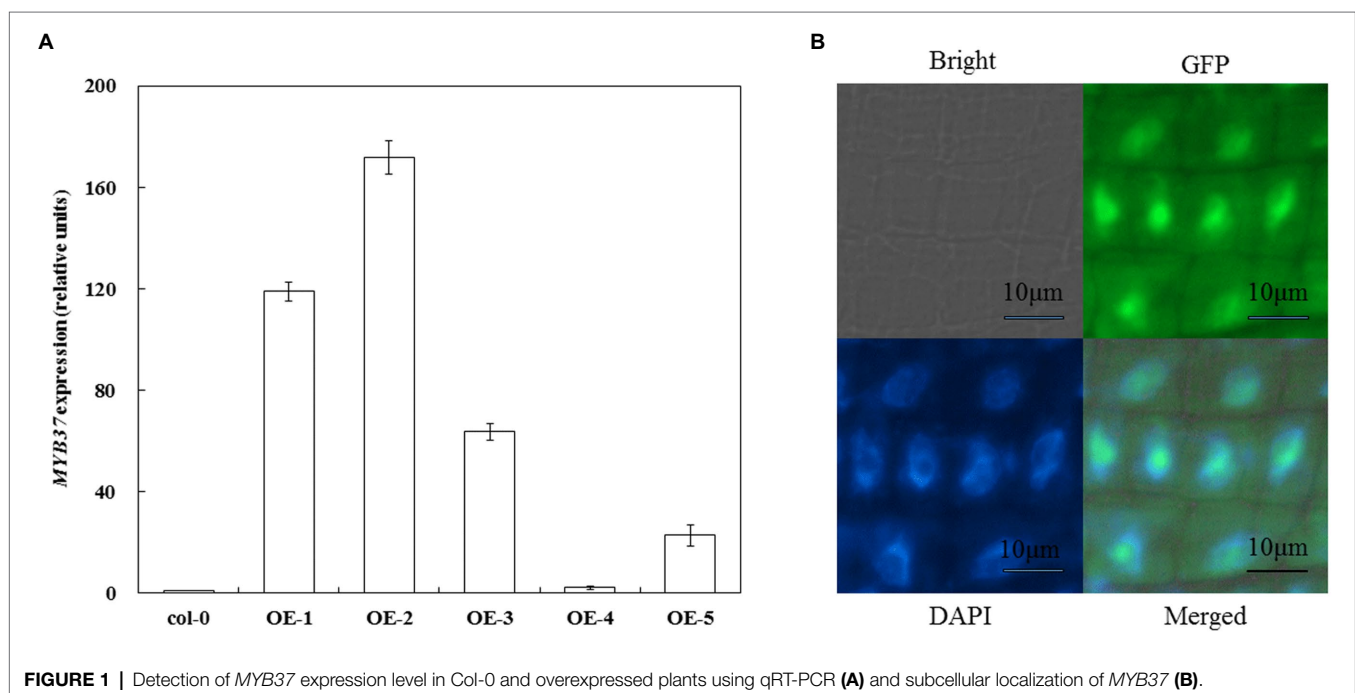
tests. The OE-2 lines with the highest MYB37 expression were selected to determine the subcellular localization of MYB37-GFP fusion protein. High green fluorescent protein (GFP) activity was observed in the nuclear region of the elongation region of Arabidopsis root tips (**Figure 1B**), indicating that MYB37 is located in the nucleus.

### Overexpression of the MYB37 Transcription Factor Improves Salt Stress Tolerance

The growth of taproots was not significantly different among Col-0, OE-1, and OE-2 Arabidopsis seedlings in normal media. Elongation of the taproots was inhibited in  $\frac{1}{2}$  MS media with NaCl. Although there were fewer yellow leaves in OE-1 and OE-2, the root length and number of leaves in the OE-1 and OE-2 plants were significantly higher than Col-0 (**Figures 2A,C**). The crown width of OE-2 line was slightly lower than that of Col-0 at the 4-week-old adult stage. However, the crown width was not significantly different between OE-1 and Col-0. MYB37 overexpression significantly relieved the salt damage symptoms of the OE-1 and OE-2 plants aged 4 weeks compared with the Col-0 plants. For instance, MYB37 overexpression changed the color of the leaves of Col-0 plants from yellow to green (**Figure 2B**).

### Effects of MYB37 Overexpression on the Chlorophyll Content in Arabidopsis Leaves Under NaCl Stress

Quantitative analysis showed that the contents of Chl *a*, Chl *b*, and Chl *a* + *b* and the Chl *a/b* ratio of Col-0, OE-1, and OE-2 Arabidopsis leaves were not significantly different under normal conditions (**Figure 3**). NaCl stress degraded chlorophyll





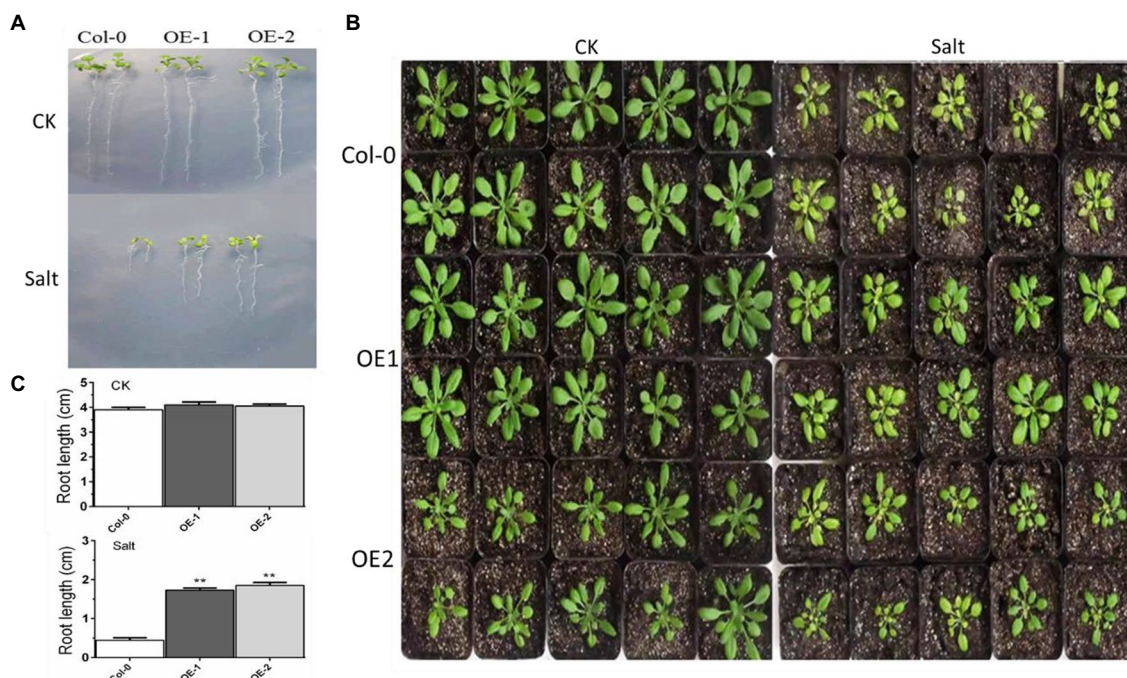


**FIGURE 2 |** Effects of *MYB37* overexpression on phenotypes of *Arabidopsis* seedlings (A) and 4-week-old adult (B) under NaCl stress. **Figure 2A** shows the phenotype of *Arabidopsis* seedlings grown on MS medium for 3 days, then transferred to 1/2MS medium with 0 mM or 100 mM NaCl for 7 days. **Figure 2B** shows the phenotype of *Arabidopsis* seedlings cultured in the soil after watering with an equal volume of distilled water and 100 mM NaCl solution for 2 weeks. **Figure 2C** shows statistics of the primary root lengths of the plants as described in (A). Student's *t*-test was used to compare the primary root lengths of transgenic line with WT plants (with significant differences at \*\* $p < 0.01$ ).

and decreased Chl *a/b* ratio in *Arabidopsis* leaves. However, the contents of Chl *a*, Chl *b*, and Chl *a + b* were significantly higher in OE-1 and OE-2 lines than in Col-0 under NaCl stress, except for the Chl *b* content, which was not significantly different between the OE-2 lines and Col-0 (Figures 3A–C). Additionally, the Chl *a/b* ratio was higher in the OE-1 and OE-2 lines under NaCl stress [20.97 and 7.52% ( $p > 0.05$ ), respectively] than in Col-0 (Figure 3D).

### Effects of *MYB37* Overexpression on the PSII and PSI Activities in *Arabidopsis* Leaves Under NaCl Stress

Although the relative fluorescence intensity from point J to point P on the OJIP curve was lower in Col-0 *Arabidopsis* leaves than in OE-1 and OE-2 lines (Figure 4A),  $F_v/F_m$  was not significantly different (Figure 4C). The relative fluorescence intensity of point O slightly changed in Col-0 *Arabidopsis* leaves. However, the relative fluorescence intensity from point J to point P significantly decreased, and the OJIP curve became relatively flat. The relative fluorescence intensity of OE-1 and OE-2 lines slightly changed (Figure 4B). Compared with OE-1 and OE-2 lines, NaCl stress significantly decreased  $F_v/F_m$  in Col-0 (Figure 4C). Similarly, although the amplitude of  $MR_{820}$  curve was slightly lower in Col-0 *Arabidopsis* leaves than in the OE-1 and OE-2 lines under non-stress conditions (Figure 4D),  $\Delta I/I_0$  was not significantly different. Moreover, the amplitude of  $MR_{820}$  curve and  $\Delta I/I_0$  of *Arabidopsis* leaves

decreased under NaCl stress (Figure 4E). However,  $\Delta I/I_0$  was significantly decreased in Col-0 compared with OE-1 and OE-2 lines under salt stress (Figure 4F).

### Effects of *MYB37* Overexpression on the PSII Receptor Side and Donor Side Electron Transport in *Arabidopsis* Leaves Under NaCl Stress

O-P normalization of the original OJIP curve showed that the relative fluorescence intensity of each point on the OJIP curve was not significantly different among Col-0 *Arabidopsis* leaves, OE-1, and OE-2 lines under non-stress conditions (Figure 5A). However, the relative fluorescence intensity of point J on the OJIP curve of Col-0 *Arabidopsis* leaves substantially changed under NaCl stress compared with OE-1 and OE-2 lines (Figure 5B). The O-P normalized curves of Col-0, OE-1, and OE-2 leaves under NaCl stress were compared with the O-P normalized curves under non-stress. The relative fluorescence intensity at point J on Col-0 curve significantly increased, while it decreased on OE-1 and OE-2 curves (Figure 5C). However, the relative fluorescence intensity was not significant in the quantitative analysis of  $V_j$ . Only the  $V_j$  of Col-0 increased by 26.12% under NaCl stress ( $p < 0.05$ ; Figure 5G). Furthermore, the O-J normalized curve of the Col-0, OE-1, and OE-2 leaves were not significantly different under non-stress and NaCl stress conditions (Figures 5D,E). The O-J standardization

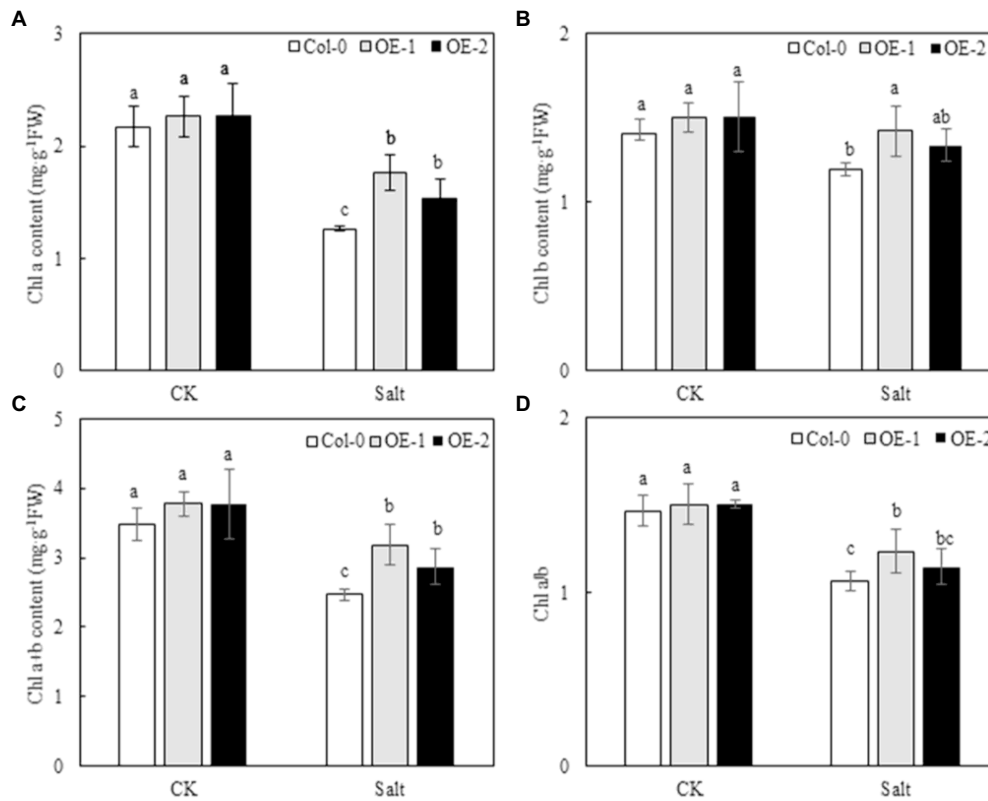


**FIGURE 3 |** Effects of MYB37 overexpression on Chl a content (A), Chl b content (B), Chl a+b content (C), and Chl a/b ratio (D) in Arabidopsis leaves under NaCl stress. Data are expressed as means  $\pm$  SE of three replicated experiments (n=3). Different small letters indicate significant differences (p < 0.05).

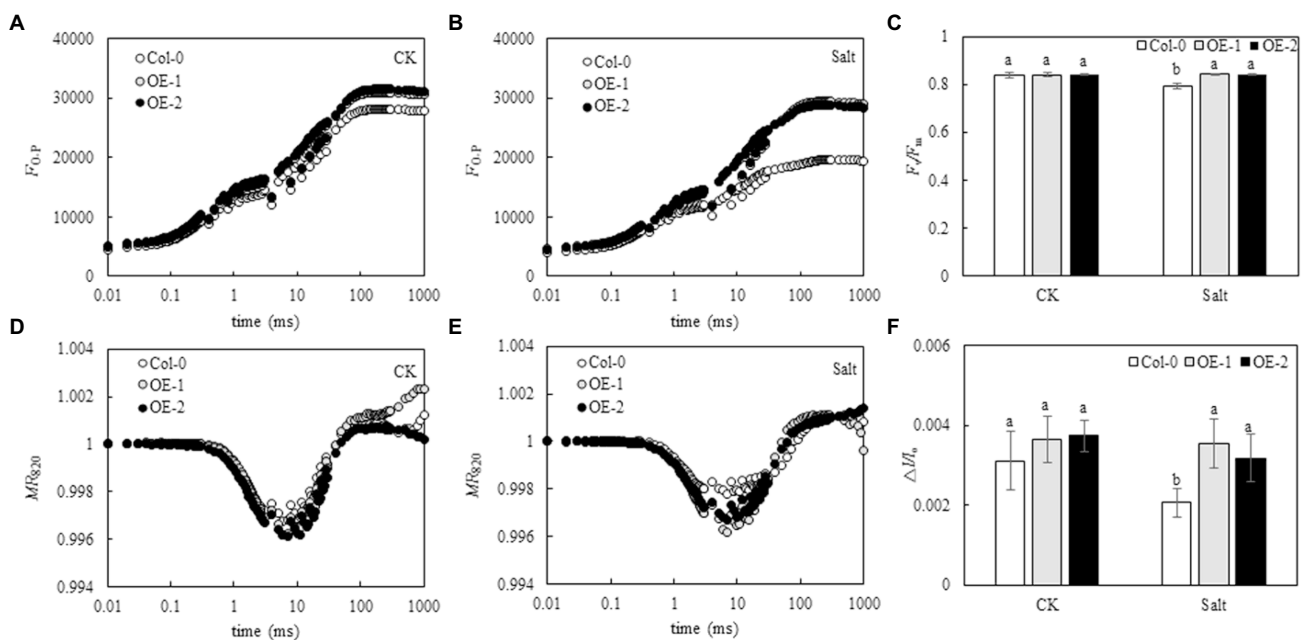
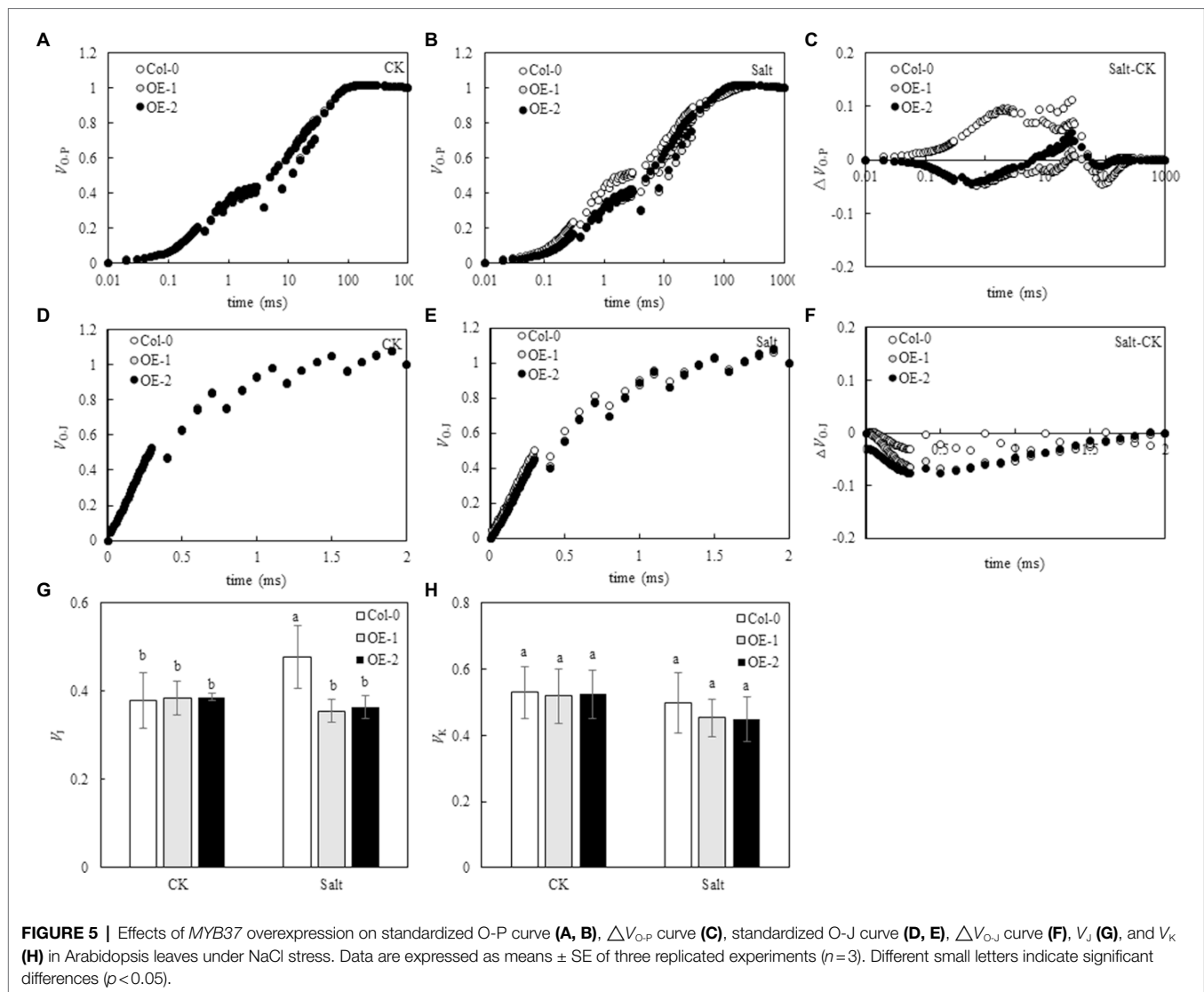


**FIGURE 4 |** Effects of MYB37 overexpression on OJIP curve (A, B), MR<sub>620</sub> curve (D, E), F<sub>v</sub>/F<sub>m</sub> (C), and ΔMn (F) in Arabidopsis leaves under NaCl stress. Data are expressed as means  $\pm$  SE of three replicated experiments (n=3). Different small letters indicate significant differences (p < 0.05).



curves of Col-0, OE-1, and OE-2 Arabidopsis leaves under NaCl stress were compared with those under non-stress conditions. The relative fluorescence intensity at point K of Col-0, OE-1, and OE-2 curves slightly decreased under NaCl stress (Figures 5F,H).

### Effects of MYB37 Overexpression on the Energy Distribution Parameters of the PSII Reaction Center in Arabidopsis Leaves Under Salt Stress

Compared with Col-0, MYB37 overexpression did not significantly affect the energy allocation parameters Y(II), Y(NO), and Y(NPQ) of the PSII reaction center in Arabidopsis leaves under non-stress conditions (Figure 6). NaCl stress reduced the proportion of Y(II) in Arabidopsis leaves while it increased the proportion of Y(NO) and Y(NPQ). However, Y(II) and Y(NPQ) were significantly higher in the OE-1, and OE-2 Arabidopsis leaves than in Col-0 under NaCl stress. In contrast,

Y(NO) was significantly lower in OE-1, and OE-2 Arabidopsis leaves than in Col-0.

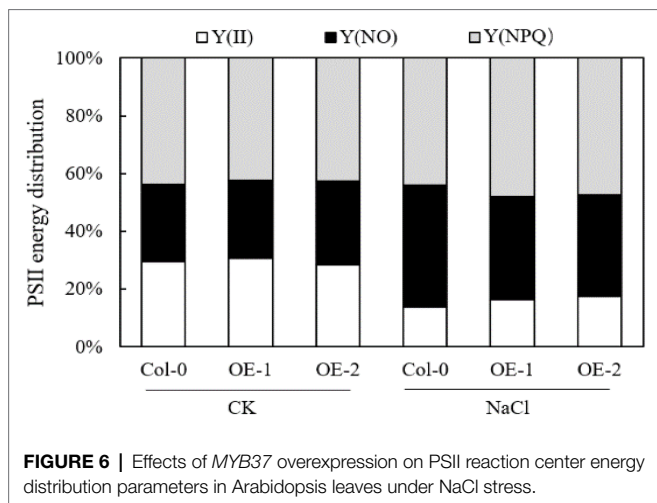
### Effects of MYB37 Overexpression on the Contents of ROS and MDA in Arabidopsis Leaves Under Salt Stress

NBT and DAB staining were used to detect the accumulation of  $O_2^-$  and  $H_2O_2$  in Arabidopsis leaves. Less blue sediment accumulated in the OE-1 and OE-2 leaves than in Col-0 under NaCl stress, similar to the accumulation of  $H_2O_2$  (yellowish-brown sediment; Figures 7A,B). However, the rate of  $O_2^-/H_2O_2$  production and MDA contents was not significantly different among Col-0, OE-1, and OE-2 lines under non-stress conditions. In contrast, NaCl stress significantly increased the rate of  $O_2^-$  and  $H_2O_2$  production and MDA contents of Arabidopsis. Nevertheless,  $O_2^-$ ,  $H_2O_2$ , and MDA contents were significantly lower in OE-1 and OE-2 lines than in Col-0 (Figures 7C-E), consistent with the *in situ* staining results of  $O_2^-$  and  $H_2O_2$ .

## Effects of MYB37 Overexpression on Osmotic Regulatory Substances in Arabidopsis Leaves Under Salt Stress

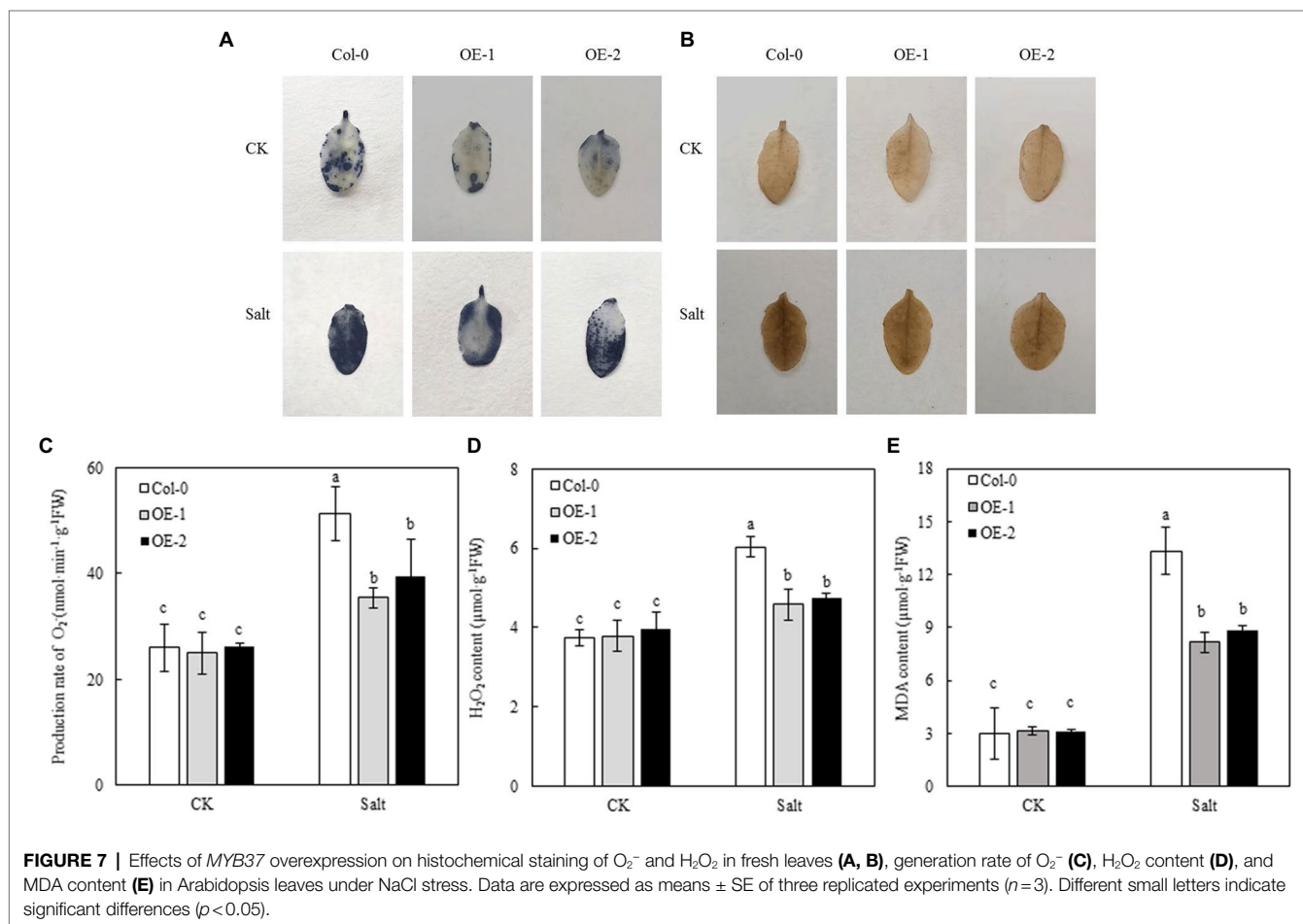
The SS, SP, and Pro contents of OE-1, OE-2, and Col-0 were not significantly different under non-stress conditions (Figures 8A–C). However, NaCl stress significantly increased

the contents of SS and Pro in Arabidopsis leaves, while it significantly decreased SP contents. Moreover, SS and Pro contents were significantly lower in OE-1 and OE-2 Arabidopsis leaves than in Col-0 under NaCl stress (Figures 8A–C), while SP content was significantly higher than that of Col-0 (Figure 8B).

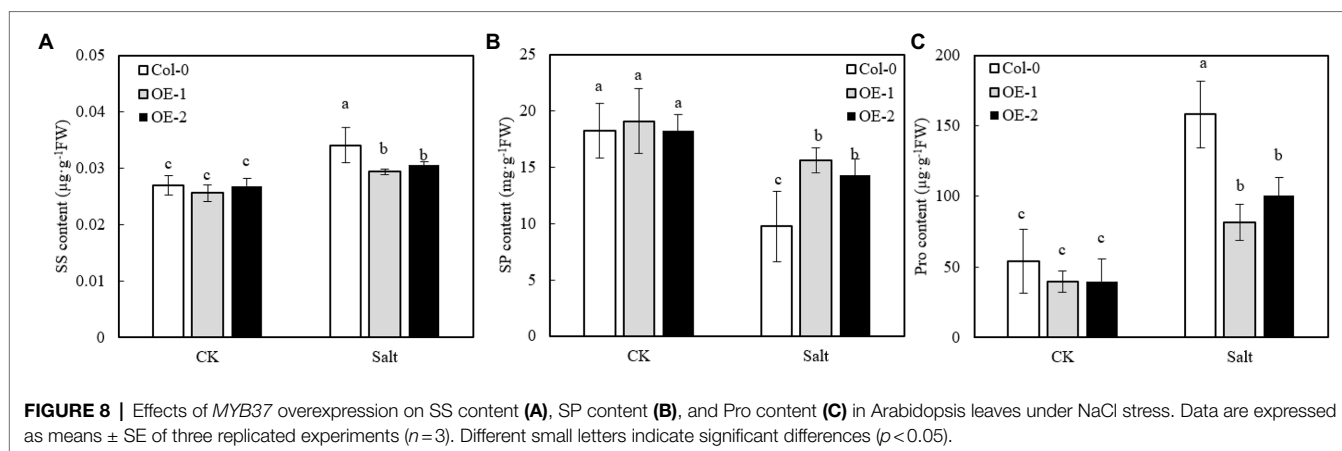


## DISCUSSION

The ability of transgenic overexpression lines or the loss of function mutants to tolerate abiotic stress is associated with reduced growth or loss of seed productivity (Yu et al., 2016a, 2016b). For instance, although MYB52/MYB96 overexpression confers a dwarf phenotype, while MYB44/MYB61 overexpression reduces seed productivity, the overexpression of these genes improves tolerance to drought or salt stress (Jung et al., 2008; Seo et al., 2009; Park et al., 2011; Romano et al., 2012). In this study, the crown width was slightly lower in Arabidopsis OE-2 line overexpressing MYB37 than in the wild type. However, MYB37 overexpression in *A. thaliana* maintained green leaves under NaCl stress and significantly alleviated salt stress symptoms. Photosynthesis promotes plant growth and development by providing energy. The photosynthesis of green plants primarily







depends on the absorption of light energy by chlorophyll. Therefore, chlorophyll degradation directly reduces the photosynthetic capacity of plants (Zhang et al., 2020d; Siddiqui et al., 2022). Studies have shown that salt stress can inhibit chlorophyll synthesis or degradation in plant leaves (Alaghabary et al., 2005; Ahanger et al., 2019). Herein, salt stress reduced the chlorophyll content of *Arabidopsis* leaves. Yang et al. (2011) showed that salt stress reduces chlorophyll content in plants through the disruption of  $\text{Na}^+$  ion balance and activity of some proteases. Tulay et al. (2015) also found that salt stress increases the activity of chlorophyllase in *Spergularia marina* (Caryophyllaceae), decreases the content of  $\text{Mg}^{2+}$  ions, accelerates the degradation of chlorophyll, inhibits the function of pigment protein complex, and the leaves become yellow or even fall off. Herein, *MYB37* overexpression delayed chlorophyll degradation under salt stress and alleviated chlorophyll reduction effect, especially Chl *a*, similar to the results of Bundó et al. (2022). *MYB37* overexpression can excrete or compartmentalize  $\text{Na}^+$  in the cytoplasm into vacuoles, regulate the concentration of  $\text{Na}^+$  in cells and maintain intracellular ion homeostasis by increasing the expression of  $\text{Na}^+/\text{H}^+$  antiporter NHX1 in the vacuolar membrane, thus delaying chlorophyll degradation and enhancing salt tolerance (Zhao et al., 2019). The *MYB* transcription factor also reduces chlorophyll degradation in birch (*Betula* sp.) leaves (Zhou and Li., 2016) and tobacco (*Nicotiana benthamiana*) leaves (Pushp et al., 2015).

Chlorophyll fluorescence can be used to analyze the absorption and utilization of light energy by photosynthesis (Dimitrova et al., 2020; Zhang et al., 2020c). In this study, chlorophyll fluorescence curves (OJIP and  $\text{MR}_{820}$  curves) were used to study the PSII and PSI activities of wild-type *Arabidopsis* Col-0 and *Arabidopsis* overexpressing *MYB37* under salt stress.  $F_v/F_m$  and  $\Delta I/I_0$  are key indexes of photochemical activity in PSII (Giannakoula and Ilias, 2007) and the activity of PSI (Wang et al., 2019), respectively. Herein, salt stress significantly reduced the  $F_v/F_m$  and  $\Delta I/I_0$  levels in wild-type *A. thaliana* Col-0 compared with normal growth conditions. However,  $F_v/F_m$  and  $\Delta I/I_0$  levels were not significantly changed in the OE-1 and OE-2 lines of *A. thaliana* overexpressing *MYB37*. Additionally,  $F_v/F_m$  and  $\Delta I/I_0$  were significantly higher in the OE-1 and OE-2 lines than in Col-0 under salt stress. Salt

stress inhibits the activities of PSII and PSI in the leaves of sorghum (*Sorghum bicolor* L.; Zhang et al., 2018b) and halophytic soybean (*Glycine soja*; Yan et al., 2020). Sudhir and Murthy (2004) showed that salt stress inhibits PSII and PSI activities in leaves due to the accumulation of  $\text{Na}^+$  in chloroplasts. In this study,  $F_v/F_m$  and  $\Delta I/I_0$  were significantly higher in the OE-1 and OE-2 lines than in the wild type, indicating that *MYB37* can improve photosynthesis by increasing the activities of PSII and PSI, thus enhancing salt tolerance. Pushp et al. (2015) also found that *SbMYB15* improves salt tolerance and dehydration in *Salicornia brachia* (highly tolerant to salt) by increasing PSII activity. The electron donor and acceptor sides of the PSII reaction center inhibit photosynthetic electron transport in plants under adverse environmental conditions (Zhang et al., 2020a).  $V_i$  on the OJIP curve can reflect the accumulation of  $Q_A$ . The enhancement of  $V_i$  indicates that the electron transfer from  $Q_A$  to  $Q_B$  on the PSII receptor side is blocked (Zhang et al., 2016). The change of  $V_K$  is a specific marker of whether the oxygen-evolving complex (OEC) activity of the PSII electron donor side oxygen release complex is damaged (Zhang et al., 2020d). In this study, salt stress only increased the  $V_i$  value of wild-type *Arabidopsis* Col-0 curve while slightly changing the  $V_K$  value, indicating that salt stress inhibited the electron transfer from  $Q_A$  to  $Q_B$  on the PSII receptor side of wild-type *Arabidopsis* leaves. Salt stress did not affect the activity of OEC on the PSII electron donor side. Zhang et al. (2019) also found that salt stress affects OEC activity on the electron donor side of PSII in leaves of mulberry (*Morus alba* L.) after salt and alkali stress treatment. Lu and Vonshak (2002) also found that salt stress reduces the reception of upstream  $Q_A$  electrons by plastoquinone  $Q_B$  (connecting the PSII and PSI reaction centers) in cyanobacteria (*Spirulina platensis*), thus decreasing the electron transfer speed of the entire photosynthetic electron transport chain. Previous studies have also shown that increased  $\text{Na}^+$  content in the cytoplasm and extracellular tissues under salt stress affects the activity of the photosynthetic electron transport chain (Kao et al., 2003). Herein, *MYB37* overexpression alleviated the electron transfer from  $Q_A$  to  $Q_B$  on the PSII receptor side of *Arabidopsis* under salt stress. Pushp et al. (2015) also proposed that *SbMYB15* could improve the photoprotection

mechanism of transgenic lines under salt stress by enhancing electron transfer from the PSII reaction center to the primary quinone receptor. Although stress inhibits the activity of PSII and even leads to the inactivation of PSII response centers, plants adapt to stress by regulating the energy distribution of PSII response centers, such as by increasing energy dissipation (Dimitrova et al., 2020; Sun et al., 2021). In this study, salt stress significantly decreased Y(II) of leaves of *A. thaliana*, while it significantly increased Y(NO) and Y(NPQ). These results indicate that *A. thaliana* adapts to salt stress by increasing its energy dissipation mechanisms. Bashir et al. (2021) showed that salt stress decreases Y(II) in moringa (*Moringa oleifera*), while it increases Y(NO) and Y(NPQ), consistent with this study. Herein, *MYB37* overexpression increased Y(II) and Y(NPQ) of Arabidopsis under salt stress but decreased the Y(NO). These results indicate that *MYB37* overexpression increases the activity of PSII and regulates energy dissipation in Arabidopsis leaves under salt stress, thus decreasing the proportion of inactivated reaction centers.

Photosynthesis inhibition produces excess electrons and energy in the photosynthetic electron transport chain, resulting in an ROS burst and peroxidation damage (Kalaji et al., 2014; Wang et al., 2021b). Wang et al. (2021a) found that salt stress significantly increases O<sub>2</sub> production rate and the contents of H<sub>2</sub>O<sub>2</sub> and MDA of alfalfa (*Medicago sativa*) leaves. Zhang et al. (2018a) also found that salt stress increases the rate of O<sub>2</sub> production and H<sub>2</sub>O<sub>2</sub> content of mulberry leaves. In this study, salt stress significantly increased the rate of O<sub>2</sub> production and the contents of H<sub>2</sub>O<sub>2</sub> and MDA of Arabidopsis leaves. However, ROS and MDA contents were lower in Arabidopsis OE-1 and OE-2 overexpressing *MYB37* than in the wild type under salt stress, consistent with the results of Zhang et al. (2020e) and Huang et al. (2018) in Arabidopsis, tobacco (Pushp et al., 2015) and *Tamarix hispida* (Liu et al., 2021). The overexpression of stress tolerance genes can inhibit membrane damage and significantly reduce the accumulation of ROS and MDA under stress conditions. The content of osmotic regulators changes under osmotic stress, thus improving plant tolerance to abiotic stress (Li et al., 2019). Plants adapt to saline-alkali stress by regulating the accumulation of proline (Pro) and soluble sugar (SS; Ren et al., 2020). Previous studies have shown that Pro and SS regulate plant osmotic balance and improve salt or alkali tolerance (Kanu et al., 2019). Guo et al. (2011, 2017) showed that Pro is significantly accumulated in maize (*Zea mays* L.) under salt stress. Wang et al. (2021a, 2021b) also found that alfalfa leaves can adapt to salt stress by increasing the content of SS and Pro. This experiment also found similar findings described above. In summary, the contents of SS and Pro were significantly increased in Arabidopsis leaves under salt stress, thus reducing salt stress damage to plants. Moreover, *MYB37* overexpression enhanced Arabidopsis OE-1 and OE-2 resistance to salt stress and decreased SS and Pro contents. Pushp et al. (2015) also found similar results in tobacco overexpressing *SbMYB15* under salt stress. Soluble protein (SP) is also a key osmoregulatory substance. Relevant studies have shown that the SP content is substantially accumulated in plant leaves under salt stress (Zhuang et al.,

2010; Bai et al., 2013; Hong et al., 2014). In this experiment, salt stress degraded SP in Arabidopsis leaves, similar to Gulen et al. (2006) (strawberry, *Fragaria x ananassa*), Liu et al. (2006) (rice and *Oryza sativa*). However, the accumulation of SP was higher in OE-1 and OE-2 leaves than in the wild type under salt stress, indicating that *MYB37* overexpression promotes protein synthesis of Arabidopsis plant under salt stress and maintains water transport and photosynthetic function of leaves, thus promoting plant growth and salt tolerance (Cernusak et al., 2007).

## CONCLUSION

Compared with the wild-type (Col-0) Arabidopsis, the overexpression of *MYB37* significantly alleviated the symptoms of salt injury in plants under NaCl stress and alleviated chlorophyll degradation (particularly Chl *a*) under NaCl stress. *MYB37* overexpression also alleviated the photoinhibition of PSII and PSI in Arabidopsis under NaCl stress, particularly by alleviating the electron transfer from Q<sub>A</sub> to Q<sub>B</sub> on the PSII receptor side. *MYB37* overexpression increased the PSII activity, and regulated energy dissipation in Arabidopsis leaves under salt stress, thus decreasing the proportion of inactivated reaction centers. *MYB37* overexpression also reduced the accumulation of ROS and MDA in Arabidopsis leaves under NaCl stress, thus alleviating the oxidative damage. In addition, *MYB37* overexpression alleviated SP degradation in Arabidopsis leaves under salt stress. However, *MYB37* overexpression did not enhance plant adaption to NaCl stress by accumulating SS and Pro due to the strong resistance to NaCl stress.

## DATA AVAILABILITY STATEMENT

The original contributions presented in the study are included in the article/supplementary material, further inquiries can be directed to the corresponding authors.

## AUTHOR CONTRIBUTIONS

HZ and YY conceived and designed the experiments. YL, BT, and YW wrote the manuscript and prepared the figures and tables. All the authors performed the experiments and analyzed the data. YL, HZ, and YY reviewed drafts of the paper. Sun Guangyu supervised the work. All authors contributed to the article and approved the submitted version.

## FUNDING

This research was supported by the Project Funded by China Postdoctoral Science Foundation (2022M710023), Fundamental Research Funds for the Central Universities (2572022BD01), National Natural Science Foundation of China (NSFC grant no. 31900228, 31901088, 52004067).

## REFERENCES

- Agarwal, P. K., Shukla, P. S., Gupta, K., and Jha, B. (2013). Bioengineering for salinity tolerance in plants: state of the art. *Mol. Biotechnol.* 54, 102–123. doi: 10.1007/s12033-012-9538-3
- Ahanger, M. A., Qin, C., Begum, N., Maodong, Q., Dong, X. X., El-Esawi, M., et al. (2019). Nitrogen availability prevents oxidative effects of salinity on wheat growth and photosynthesis by up-regulating the antioxidants and osmolytes metabolism, and secondary metabolite accumulation. *BMC Plant Biol.* 19:479. doi: 10.1186/s12870-019-2085-3
- Alaghabary, K., Zhu, Z., and Shi, Q. (2005). Influence of silicon supply on chlorophyll content, chlorophyll fluorescence, and antioxidative enzyme activities in tomato plants under salt stress. *J. Plant Nutr.* 27, 2101–2115. doi: 10.1081/PLN-200034641
- Alexieva, V., Sergiev, I., Mapelli, S., and Karanov, E. (2001). The effect of drought and ultraviolet radiation on growth and stress markers in pea and wheat. *Plant Cell Environ.* 24, 1337–1344. doi: 10.1046/j.1365-3040.2001.00778.x
- Bai, Q., Yang, R., Zhang, L., and Gu, Z. (2013). Salt stress induces accumulation of  $\gamma$ -aminobutyric acid in germinated foxtail millet (*Setaria italica* L.). *Cereal Chem.* 90, 145–149. doi: 10.1094/CCHEM-06-12-0071-R
- Bashir, S., Amir, M., Bashir, F., Javed, M., Hussain, A., Fatima, S., et al. (2021). Structural and functional stability of photosystem-II in *Moringa oleifera* under salt stress. 5, 676–682.
- Bates, L. B., Waldren, R. P., and Teare, I. D. (1973). Rapid determination of free proline for water-stress studies. *Plant Soil* 39, 205–207. doi: 10.1007/BF00018060
- Bradford, M. M. (1976). A rapid and sensitive method for the quantitation of microgram quantities of protein utilizing the principle of protein-dye binding. *Anal. Biochem.* 72, 248–254. doi: 10.1016/0003-2697(76)90527-3
- Bundó, M., Martín, C. H., Pesenti, M., Gómez, A. J., Castillo, L., Frouin, J., et al. (2022). Integrative approach for precise genotyping and transcriptomics of salt tolerant introgression Rice lines. *Front. Plant Sci.* 12:797141. doi: 10.3389/fpls.2021.797141
- Cernusak, L. A., Aranda, J., Marshall, J. D., and Winter, K. (2007). Large variation in whole-plant water-use efficiency among tropical tree species. *New Phytol.* 173, 294–305. doi: 10.1111/j.1469-8137.2006.01913.x
- Che, X., Ding, R., Li, Y., Zhang, Z., Gao, H., and Wang, W. (2018). Mechanism of long-term toxicity of CuO NPs to microalgae. *Nanotoxicology* 12, 923–939. doi: 10.1080/17435390.2018.1498928
- Chen, Y., Yang, X., He, K., Liu, M., Li, J., Gao, Z., et al. (2006). The MYB transcription factor superfamily of Arabidopsis: expression analysis and phylogenetic comparison with the rice MYB family. *Plant Mol. Biol.* 60, 107–124. doi: 10.1007/s11103-005-2910-y
- Chinnusamy, V., Schumaker, K., and Zhu, J. K. (2004). Molecular genetic perspectives on cross-talk and specificity in abiotic stress signalling in plants. *J. Exp. Bot.* 55, 225–236. doi: 10.1093/jxb/erh005
- Cui, M. H., Yoo, K. S., Hyoun, S., Nguyen, H. T. K., Kim, Y. Y., Kim, H. J., et al. (2013). An Arabidopsis R2R3-MYB transcription factor, AtMYB20, negatively regulates type 2C serine/threonine protein phosphatases to enhance salt tolerance. *FEBS Lett.* 587, 1773–1778. doi: 10.1016/j.febslet.2013.04.028
- Dimitrova, S., Paunov, M., Pavlova, B., Dankov, K., Kouzmanova, M., Velikova, V., et al. (2020). Photosynthetic efficiency of two *Platanus orientalis* L. ecotypes exposed to moderately high temperature: JIP-test analysis. *Photosynthetica* 58, 657–670. doi: 10.32615/ps.2020.012
- Dorothea, B., and Ramanjulu, S. (2005). Drought and salt tolerance in plants. *Crit. Rev. Plant Sci.* 24, 23–58. doi: 10.1080/07352680590910410
- Dubos, C., Stracke, R., Grotewold, E., Weisshaar, B., Martin, C., and Lepiniec, L. (2010). MYB transcription factors in Arabidopsis. *Trends Plant Sci.* 15, 573–581. doi: 10.1016/j.tplants.2010.06.005
- Ernster, L., Nordenbrand, K., Orrenius, S., and Das, M. L. (1968). Microsomal lipid peroxidation. *Biol. Chem.* 349, 1604–1605.
- Giannakoula, A., and Ilias, I. F. (2007). Chlorophyll fluorescence and photosystem II activity of tomato leaves as affected by irradiance and prohexadione-calcium. *Proc. WSEAS Int. Conf. Renew. Energy Sources* 91, 49–56.
- Gulen, H., Turhan, E., and Eris, A. (2006). Changes in peroxidase activities and soluble proteins in strawberry varieties under salt-stress. *Acta Physiol. Plant.* 28, 109–116. doi: 10.1007/s11738-006-0037-7
- Guo, R., Shi, L. X., Yan, C., Zhong, X., Gu, F. X., Liu, Q., et al. (2017). Ionic and metabolic responses to neutral salt or alkaline salt stresses in maize (*Zea mays* L.) seedlings. *BMC Plant Biol.* 17:41. doi: 10.1186/s12870-017-0994-6
- Guo, R., Zhou, J., Hao, W. P., Gong, D. Z., Zhong, X. L., Gu, F. X., et al. (2011). Germination, growth, photosynthesis and ionic balance in *Setaria viridis* seedlings subjected to saline and alkaline stress. *Can. J. Plant Sci.* 91, 1077–1088. doi: 10.4141/cjps10167
- Hong, C. T., Guo, H. P., Fang, J., Ren, W., Wang, T. F., Ji, M. C., et al. (2014). Physiological and biochemical responses of *miscanthus sacchariflorus* to salt stress. *Adv. Mater. Res.* 1051, 333–340. doi: 10.4028/www.scientific.net/AMR.1051.333
- Huang, Y., Zhao, H., Gao, F., Yao, P., Deng, R., Li, C., et al. (2018). A R2R3-MYB transcription factor gene, FtMYB13, from Tartary buckwheat improves salt/drought tolerance in Arabidopsis. *Plant Physiol. Biochem.* 132, 238–248. doi: 10.1016/j.plaphy.2018.09.012
- Jiang, C. K., and Rao, G. Y. (2020). Insights into the diversification and evolution of R2R3-MYB transcription factors in plants. *Plant Physiol.* 183, 637–655. doi: 10.1104/pp.19.01082
- Jithesh, M. N., Prashanth, S. R., Sivaprakash, K. R., and Parida, A. K. (2006). Antioxidative response mechanisms in halophytes: their role in stress defence. *J. Genet.* 85, 237–254. doi: 10.1007/BF02935340
- Jung, C., Seo, J. S., Han, S. W., Koo, Y. J., Kim, C. H., Song, S. I., et al. (2008). Overexpression of AtMYB44 enhances stomatal closure to confer abiotic stress tolerance in transgenic Arabidopsis. *Plant Physiol.* 146, 623–635. doi: 10.1104/pp.107.110981
- Kalaji, H. M., Oukarroum, A., Alexandrov, V., Kouzmanova, M., Brestic, M., Zivcak, M., et al. (2014). Identification of nutrient deficiency in maize and tomato plants by in vivo chlorophyll a fluorescence measurement. *Plant Physiol. Biochem.* 81, 16–25. doi: 10.1016/j.plaphy.2014.03.029
- Kanu, A. S., Ashraf, U., Mo, Z., Sabir, S. U. R., Baggie, I., Charley, C. S., et al. (2019). Calcium amendment improved the performance of fragrant rice and reduced metal uptake under cadmium toxicity. *Environ. Sci. Pollut. Res.* 26, 24748–24757. doi: 10.1007/s11356-019-05779-7
- Kao, W. Y., Tsai, T. T., and Shih, C. N. (2003). Photosynthetic gas exchange and chlorophyll a fluorescence of three wild soybean species in response to NaCl treatments. *Photosynthetica* 41, 415–419. doi: 10.1023/B:PHOT.0000015466.22288.23
- Kazuo, S., Kazuko, Y. S., and Motoaki, S. (2003). Regulatory network of gene expression in the drought and cold stress responses. *Curr. Opin. Plant Biol.* 6, 410–417. doi: 10.1016/S1369-5266(03)00092-X
- Klaus, A., and Heribert, H. (2004). Reactive oxygen species: metabolism, oxidative stress, and signal transduction. *Annu. Rev. Plant Biol.* 55, 373–399. doi: 10.1146/annurev.arplant.55.031903.141701
- Kramer, D. M., Johnson, G., Kiirats, O., and Edwards, G. E. (2004). New fluorescence parameters for the determination of  $Q_A$  redox state and excitation energy fluxes. *Photosynth. Res.* 79, 209–218. doi: 10.1023/B:PRES.0000015391.99477.0d
- Li, Z., Fu, X., Tian, Y., Xu, J., Gao, J., Wang, B., et al. (2019). Overexpression of a trypanothione synthetase gene from *Trypanosoma cruzi*, TcTrys, confers enhanced tolerance to multiple abiotic stresses in rice. *Gene* 710, 279–290. doi: 10.1016/j.gene.2019.06.018
- Li, C., Ng, C. K. Y., and Fan, L. M. (2015). MYB transcription factors, active players in abiotic stress signaling. *Environ. Exp. Bot.* 114, 80–91. doi: 10.1016/j.envexpbot.2014.06.014
- Liu, Z. Y., Li, X. P., Zhang, T. Q., Wang, Y. Y., Wang, C., and Gao, C. Q. (2021). Overexpression of ThMYB8 mediates salt stress tolerance by directly activating stress-responsive gene expression. *Plant Sci.* 302:110668. doi: 10.1016/j.plantsci.2020.110668
- Liu, X., Liu, H. F., Li, H. L., An, X. H., Song, L. Q., You, C. X., et al. (2022). MdMYB10 affects nitrogen uptake and reallocation by regulating the nitrate transporter MdNRT2.4–1 in the red flesh apple. *Horticulture Research* 9, 1–13. doi: 10.1093/hr/uhac016
- Liu, K., Xu, S., Xuan, W., Ling, T. F., Cao, Z., Huang, B., et al. (2006). Carbon monoxide counteracts the inhibition of seed germination and alleviates oxidative damage caused by salt stress in *Oryza sativa*. *Plant Sci.* 172, 544–555. doi: 10.1016/j.plantsci.2006.11.007
- Liu, X., Yang, L., Zhou, X., Zhou, M., Lu, Y., Ma, L., et al. (2013). Transgenic wheat expressing *Thinopyrum intermedium* MYB transcription factor TiMYB2R-1 shows enhanced resistance to the take-all disease. *J. Exp. Bot.* 64, 2243–2253. doi: 10.1093/jxb/ert084

- Lu, C., and Vonshak, A. (2002). Effects of salinity on photosystem II function in cyanobacterial *Spirulina platensis* cells. *Physiol Plant. Physiologia Plantarum* 114, 405–413. doi: 10.1034/j.1399-3054.2002.1140310.x
- Mengiste, T., Chen, X., Salmeron, J., and Dietrich, R. (2003). The BOTRYTIS SUSCEPTIBLE1 gene encodes an R2R3MYB transcription factor protein that is required for biotic and abiotic stress responses in Arabidopsis. *Plant Cell* 15, 2551–2565. doi: 10.1105/tpc.014167
- Mitsuda, N., and Ohme, T. M. (2009). Functional analysis of transcription factors in Arabidopsis. *Plant Cell Physiol.* 50, 1232–1248. doi: 10.1093/pcp/pcp075
- Mostofa, M. G., Rahman, A., Ansary, M. M. U., Watanabe, A., Fujita, M., and Tran, L. S. P. (2015). Hydrogen sulfide modulates cadmium-induced physiological and biochemical responses to alleviate cadmium toxicity in rice. *Sci. Rep.* 5:14078. doi: 10.1038/srep14078
- Oukarroum, A., Goltsev, V., and Strasser, R. J. (2018). Temperature effects on pea plants probed by simultaneous measurements of the kinetics of prompt fluorescence, delayed fluorescence and modulated 820 nm reflection. *PLoS One* 8:e59433. doi: 10.1371/journal.pone.0059433
- Park, M. Y., Kang, J. Y., and Kim, S. Y. (2011). Overexpression of AtMYB52 confers ABA hypersensitivity and drought tolerance. *Mol. Cells* 31, 447–454. doi: 10.1007/s10059-011-0300-7
- Porra, R. J. (2002). The chequered history of the development and use of simultaneous equations for the accurate determination of chlorophylls a and b. *Photosynth. Res.* 73, 149–156. doi: 10.1023/A:1020470224740
- Pushp, S. S., Kamil, G., Parinita, A., Bhavanath, J., and Pradeep, K. A. (2015). Overexpression of a novel SbMYB15 from *Salicornia brachiata* confers salinity and dehydration tolerance by reduced oxidative damage and improved photosynthesis in transgenic tobacco. *Planta* 242, 1291–1308. doi: 10.1007/s00425-015-2366-5
- Rana, M., and Mark, T. (2008). Mechanisms of salinity tolerance. *Annu. Rev. Plant Biol.* 59, 651–681. doi: 10.1146/annurev.arplant.59.032607.092911
- Ren, Y., Wang, W., He, J., Zhang, L., Wei, Y., and Yang, M. (2020). Nitric oxide alleviates salt stress in seed germination and early seedling growth of pakchoi (*Brassica chinensis* L.) by enhancing physiological and biochemical parameters. *Ecotoxicol. Environ. Saf.* 187:109785. doi: 10.1016/j.ecoenv.2019.109785
- Riechmann, J. L., Heard, J., Martin, G., Reuber, L., Jiang, C., Keddie, J., et al. (2000). Arabidopsis transcription factors: genome-wide comparative analysis among eukaryotes. *Science* 290, 2105–2110. doi: 10.1126/science.290.5499.2105
- Romano, J. M., Dubos, C., Prouse, M. B., Wilkins, O., Hong, H., Poole, M., et al. (2012). AtMYB61, an R2R3-MYB transcription factor, functions as a pleiotropic regulator via a small gene network. *New Phytol.* 195, 774–786. doi: 10.1111/j.1469-8137.2012.04201.x
- Seo, P. J., Xiang, F., Qiao, M., Park, J. Y., Lee, Y. N., Kim, S. G., et al. (2009). The MYB96 transcription factor mediates abscisic acid signaling during drought stress response in Arabidopsis. *Plant Physiol.* 151, 275–289. doi: 10.1104/pp.109.144220
- Shaheen, S., Naseer, S., Ashraf, M., and Akram, N. A. (2013). Salt stress affects water relations, photosynthesis, and oxidative defense mechanisms in *Solanum melongena* L. *J. Plant Interact.* 8, 85–96. doi: 10.1080/17429145.2012.718376
- Siddiqui, M. H., Mukherjee, S., Al-Munqedhi, B. M. A., Kumar, R., and Kalaji, H. M. (2022). Salicylic acid and silicon impart resilience to lanthanum toxicity in *Brassica juncea* L. seedlings. *Plant Growth Regul.* 1–14. doi: 10.1007/s10725-021-00787-5
- Søren, L., Charlotte, O., Michael, J., and Karen, S. (2013). Structure, function and networks of transcription factors involved in abiotic stress responses. *Int. J. Mol. Sci.* 14, 5842–5878. doi: 10.3390/ijms14035842
- Strasser, B., and Strasser, R. 1995. Measuring fast fluorescence transients to address environmental questions: the JIP-test. Photosynthesis: from light to biosphere, Volume V, Proceedings of the Xth International Photosynthesis Congress, Montpellier, France, 20–25 August 1995, 977–980.
- Sudhir, P., and Murthy, S. D. S. (2004). Effects of salt stress on basic processes of photosynthesis. *Photosynthetica* 42, 481–486. doi: 10.1007/S11099-005-0001-6
- Sun, H. W., Zhang, H. B., Xu, Z. S., Wang, Y., Liu, X. Q., Li, Y. Y., et al. (2021). TMT-based quantitative proteomic analysis of the effects of *Pseudomonas syringae* pv. *Tabaci* (Pst) infection on photosynthetic function and the response of the MAPK signaling pathway in tobacco leaves. *Plant Physiol. Biochem.* 166, 657–667. doi: 10.1016/j.plaphy.2021.06.049
- Tsugane, K., Kobayashi, K., Niwa, Y., Ohba, Y., Wada, K., and Kobayashi, H. (1999). A recessive Arabidopsis mutant that grows photoautotrophically under salt stress shows enhanced active oxygen detoxification. *Plant Cell* 11, 1195–1206. doi: 10.1105/tpc.11.7.1195
- Tulay, A. A., Adnan, A., and Erkan, Y. (2015). Anatomical adaptations to salinity in *Spergularia marina* (Caryophyllaceae) from Turkey. *Proc. Natl. Acad. Sci. India* 85, 625–634. doi: 10.1007/s40011-014-0386-8
- Wang, Y., Jin, W. W., Che, Y. H., Huang, D., Wang, J. C., Zhao, M. C., et al. (2019). Atmospheric nitrogen dioxide improves photosynthesis in mulberry leaves via effective utilization of excess absorbed light energy. *Forests* 10:312. doi: 10.3390/f10040312
- Wang, F., Kong, W., Wong, G., Fu, L., Peng, R., Li, Z., et al. (2016). AtMYB12 regulates flavonoids accumulation and abiotic stress tolerance in transgenic *Arabidopsis thaliana*. *Mol. Gen. Genomics.* 291, 1545–1559. doi: 10.1007/s00438-016-1203-2
- Wang, Y., Wang, J. C., Guo, D. D., Zhang, H. B., Che, Y. H., Li, Y. Y., et al. (2021a). Physiological and comparative transcriptome analysis of leaf response and physiological adaption to saline alkali stress across pH values in alfalfa (*Medicago sativa*). *Plant Physiol. Biochem.* 167, 140–152. doi: 10.1016/j.plaphy.2021.07.040
- Wang, Y., Yu, Y. T., Zhang, H. B., Huo, Y. Z., Liu, X. Q., Che, Y. H., et al. (2021b). The phytotoxicity of exposure to two polybrominated diphenyl ethers (BDE47 and BDE209) on photosynthesis and the response of the hormone signaling and ROS scavenging system in tobacco leaves. *J. Hazard. Mater.* 426:128012. doi: 10.1016/j.jhazmat.2021.128012
- Wu, Y., Wen, J., Xia, Y., Zhang, L., and Du, H. (2022). Author notes evolution and functional diversification of R2R3-MYB transcription factors in plants. *Hortic. Res.* 9:uhac058. doi: 10.1093/hr/uhac058
- Xie, Z., Li, D., Wang, L., Sack, F. D., and Grotewold, E. (2010). Role of the stomatal development regulators FLP/MYB88 in abiotic stress responses. *Plant J.* 64, 731–739. doi: 10.1111/j.1365-313X.2010.04364.x
- Xu, R., Wang, Y., Zheng, H., Lu, W., Wu, C., Huang, J., et al. (2015). Salt-induced transcription factor MYB74 is regulated by the RNA-directed DNA methylation pathway in Arabidopsis. *J. Exp. Bot.* 66, 5997–6008. doi: 10.1093/jxb/erv312
- Yan, K., He, W., Bian, L., Zhang, Z., Tang, X., An, M., et al. (2020). Salt adaptability in a halophytic soybean (*Glycine soja*) involves photosystems coordination. *BMC Plant Biol.* 20:155. doi: 10.1186/s12870-020-02371-x
- Yang, J. Y., Zheng, W., Tian, Y., Wu, Y., and Zhou, D. W. (2011). Effects of various mixed salt-alkaline stresses on growth, photosynthesis, and photosynthetic pigment concentrations of *Medicago ruthenica* seedlings. *Photosynthetica* 49, 275–284. doi: 10.1007/s11099-011-0037-8
- Yu, Y. T., Wu, Z., Lu, K., Bi, C., Liang, S., Wang, X. F., et al. (2016a). Overexpression of the MYB37 transcription factor enhances abscisic acid sensitivity, and improves both drought tolerance and seed productivity in *Arabidopsis thaliana*. *Plant Mol. Biol.* 90, 267–279. doi: 10.1007/s11103-015-0411-1
- Yu, Y. T., Wu, Z., Lu, K., Bi, C., Liang, S., Wang, X. F., et al. (2016b). Overexpression of the MYB transcription factor MYB28 or MYB99 confers hypersensitivity to abscisic acid in arabidopsis. *J. Plant Biol.* 59, 152–161. doi: 10.1007/s12374-016-0463-z
- Zhang, C. G., Leung, K. K., Wong, Y. S., and Tam, N. F. Y. (2006). Germination, growth and physiological responses of mangrove plant (*Bruguiera gymnorhiza*) to lubricating oil pollution. *Environ. Exp. Bot.* 60, 127–136. doi: 10.1016/j.envexpbot.2006.09.002
- Zhang, H. H., Li, X., Xu, Z. S., Wang, Y., Teng, Z. Y., An, M. J., et al. (2020a). Toxic effects of heavy metals Pb and Cd on mulberry (*Morus alba* L.) seedling leaves: photosynthetic function and reactive oxygen species (ROS) metabolism responses. *Ecotoxicol. Environ. Saf.* 195:110469. doi: 10.1016/j.ecoenv.2020.110469
- Zhang, H. H., Li, X., Zhang, S. B., Yin, Z. P., Zhu, W. X., Li, J. B., et al. (2018a). Rootstock alleviates salt stress in grafted mulberry seedlings: physiological and PSII function responses. *Front. Plant Sci.* 9:1806. doi: 10.3389/fpls.2018.01806
- Zhang, H. H., Shi, G. L., Shao, J. Y., Li, X., Li, M. B., Meng, L., et al. (2019). Photochemistry and proteomics of mulberry (*Morus alba* L.) seedlings under NaCl and NaHCO<sub>3</sub> stress. *Ecotoxicol. Environ. Saf.* 184:109624.
- Zhang, H. H., Wang, Y., Li, X., He, G. Q., Che, Y. H., Teng, Z. Y., et al. (2020b). Chlorophyll synthesis and the photoprotective mechanism in leaves



- of mulberry (*Morus alba* L.) seedlings under NaCl and NaHCO<sub>3</sub> stress revealed by TMT-based proteomics analyses. *Ecotoxicol. Environ. Saf.* 190:110164. doi: 10.1016/j.ecoenv.2020.110164
- Zhang, P., Wang, R., Yang, X., Ju, Q., Li, W., Lü, S., et al. (2020e). The R2R3-MYB transcription factor AtMYB49 modulates salt tolerance in Arabidopsis by modulating the cuticle formation and antioxidant defence. *Plant Cell Environ.* 43, 1925–1943. doi: 10.1111/pce.13784
- Zhang, H. H., Xu, Z. S., Guo, K. W., Huo, Y. Z., He, G. Q., Sun, H. W., et al. (2020d). Toxic effects of heavy metal Cd and Zn on chlorophyll, carotenoid metabolism and photosynthetic function in tobacco leaves revealed by physiological and proteomics analysis. *Ecotoxicol. Environ. Saf.* 202:110856. doi: 10.1016/j.ecoenv.2020.110856
- Zhang, H. H., Xu, Z. S., Huo, Y. Z., Guo, K. W., Wang, Y., He, G. Q., et al. (2020c). Overexpression of Trx CDS32 gene promotes chlorophyll synthesis and photosynthetic electron transfer and alleviates cadmium-induced photoinhibition of PSII and PSI in tobacco leaves. *J. Hazard. Mater.* 398:122899. doi: 10.1016/j.jhazmat.2020.122899
- Zhang, H. H., Xu, N., Wu, X. Y., Wang, J. R., Ma, S. L., Li, X., et al. (2018b). Effects of four types of sodium salt stress on plant growth and photosynthetic apparatus in sorghum leaves. *J. Plant Interact.* 13, 506–513. doi: 10.1080/17429145.2018.1526978
- Zhang, H. H., Zhong, H. X., Wang, J. F., Sui, X., and Xu, N. (2016). Adaptive changes in chlorophyll content and photosynthetic features to low light in *Physocarpus amurensis* Maxim and *Physocarpus opulifolius* “Diabolo”. *Peer J.* 4:e2125.
- Zhao, Y., Yang, Z., Ding, Y., Liu, L., Han, X., Zhan, J., et al. (2019). Overexpression of an R2R3 MYB gene, GhMYB73, increases tolerance to salt stress in transgenic Arabidopsis. *Plant Sci.* 286, 28–36. doi: 10.1016/j.plantsci.2019.05.021
- Zheng, X., Li, H., Chen, M., Zhang, J., Tan, R., Zhao, S., et al. (2020). *Sm-miR396b* targeted SmGRFs, SmHDT1, and SmMYB37/4 synergistically regulates cell growth and active ingredient accumulation in *Salvia miltiorrhiza* hairy roots. *Plant Cell Rep.* 39, 1263–1283. doi: 10.1007/s00299-020-02562-8
- Zhou, C., and Li, C. (2016). A novel R2R3-MYB transcription factor BpMYB106 of birch (*Betula platyphylla*) confers increased photosynthesis and growth rate through up-regulating photosynthetic gene expression. *Front. Plant Sci.* 7:315. doi: 10.3389/fpls.2016.00315
- Zhu, J. K. (2002). Salt and drought stress signal transduction in plants. *Annu. Rev. Plant Biol.* 53, 247–273. doi: 10.1146/annurev.arplant.53.091401.143329
- Zhuang, W. W., Li, J., Cao, M. H., Feng, W. J., and Li, Y. P. (2010). Changes of osmotic adjusting substances in leaves of *ammodendron argenteum* seedlings under salt and drought stress. *Acta Botan. Boreali-Occiden. Sin.* 30, 2010–2015.

**Conflict of Interest:** The authors declare that the research was conducted in the absence of any commercial or financial relationships that could be construed as a potential conflict of interest.

**Publisher’s Note:** All claims expressed in this article are solely those of the authors and do not necessarily represent those of their affiliated organizations, or those of the publisher, the editors and the reviewers. Any product that may be evaluated in this article, or claim that may be made by its manufacturer, is not guaranteed or endorsed by the publisher.

Copyright © 2022 Li, Tian, Wang, Wang, Zhang, Wang, Sun, Yu and Zhang. This is an open-access article distributed under the terms of the Creative Commons Attribution License (CC BY). The use, distribution or reproduction in other forums is permitted, provided the original author(s) and the copyright owner(s) are credited and that the original publication in this journal is cited, in accordance with accepted academic practice. No use, distribution or reproduction is permitted which does not comply with these terms.



## OPEN ACCESS

## EDITED BY

Vasilij Goltsev,  
Sofia University,  
Bulgaria

## REVIEWED BY

Krishna Niyogi,  
University of California,  
Berkeley, United States  
Alexei E. Solovchenko,  
Lomonosov Moscow State University,  
Russia

## \*CORRESPONDENCE

Shu Yuan  
roundtree318@hotmail.com  
Jun Zhao  
zhaojun01@caas.cn

## SPECIALTY SECTION

This article was submitted to  
Plant Abiotic Stress,  
a section of the journal  
Frontiers in Plant Science

RECEIVED 28 February 2022

ACCEPTED 27 June 2022

PUBLISHED 14 July 2022

## CITATION

Liu W-J, Liu H, Chen Y-E, Yin Y, Zhang Z-W,  
Song J, Chang L-J, Zhang F-L, Wang D,  
Dai X-H, Wei C, Xiong M, Yuan S and  
Zhao J (2022) Chloroplastic  
photoprotective strategies differ between  
bundle sheath and mesophyll cells in maize  
(*Zea mays* L.) Under drought.  
*Front. Plant Sci.* 13:885781.  
doi: 10.3389/fpls.2022.885781

## COPYRIGHT

© 2022 Liu, Liu, Chen, Yin, Zhang, Song,  
Chang, Zhang, Wang, Dai, Wei, Xiong, Yuan  
and Zhao. This is an open-access article  
distributed under the terms of the [Creative  
Commons Attribution License \(CC BY\)](#). The  
use, distribution or reproduction in other  
forums is permitted, provided the original  
author(s) and the copyright owner(s) are  
credited and that the original publication in  
this journal is cited, in accordance with  
accepted academic practice. No use,  
distribution or reproduction is permitted  
which does not comply with these terms.

# Chloroplastic photoprotective strategies differ between bundle sheath and mesophyll cells in maize (*Zea mays* L.) Under drought

Wen-Juan Liu<sup>1</sup>, Hao Liu<sup>2</sup>, Yang-Er Chen<sup>3</sup>, Yan Yin<sup>4</sup>,  
Zhong-Wei Zhang<sup>5</sup>, Jun Song<sup>1</sup>, Li-Juan Chang<sup>1</sup>, Fu-Li Zhang<sup>1</sup>,  
Dong Wang<sup>1</sup>, Xiao-Hang Dai<sup>1</sup>, Chao Wei<sup>1</sup>, Mei Xiong<sup>1</sup>,  
Shu Yuan<sup>5\*</sup> and Jun Zhao<sup>2\*</sup>

<sup>1</sup>Institute of Quality Standard and Testing Technology Research, Sichuan Academy of Agricultural Sciences, Chengdu, China, <sup>2</sup>Biotechnology Research Institute, Chinese Academy of Agricultural Sciences, Beijing, China, <sup>3</sup>College of Life Sciences, Sichuan Agricultural University, Ya'an, China, <sup>4</sup>Plant Science Facility of the Institute of Botany, Chinese Academy of Sciences, Beijing, China, <sup>5</sup>College of Resources Science and Technology, Sichuan Agricultural University, Chengdu, China

Bundle sheath cells play a crucial role in photosynthesis in C<sub>4</sub> plants, but the structure and function of photosystem II (PSII) in these cells is still controversial. Photoprotective roles of bundle sheath chloroplasts at the occurrence of environmental stresses have not been investigated so far. Non-photochemical quenching (NPQ) of chlorophyll a fluorescence is the photoprotective mechanism that responds to a changing energy balance in chloroplasts. In the present study, we found a much higher NPQ in bundle sheath chloroplasts than in mesophyll chloroplasts under a drought stress. This change was accompanied by a more rapid dephosphorylation of light-harvesting complex II (LHCII) subunits and a greater increase in PSII subunit S (PsbS) protein abundance than in mesophyll cell chloroplasts. Histochemical staining of reactive oxygen species (ROS) suggested that the high NPQ may be one of the main reasons for the lower accumulation of ROS in bundle sheath chloroplasts. This may maintain the stable functioning of bundle sheath cells under drought condition. These results indicate that the superior capacity for dissipation of excitation energy in bundle sheath chloroplasts may be an environmental adaptation unique to C<sub>4</sub> plants.

## KEYWORDS

bundle sheath chloroplast, drought stress, maize (*Zea mays* L.), non-photochemical quenching, photoprotection, reactive oxygen species

## Introduction

Plant growth and productivity are adversely affected by various abiotic and biotic stress factors in both natural and agricultural ecosystems. Photosynthesis is the primary physiological process that drives plant growth and crop productivity and influences many other plant processes. Studies have indicated that the photosynthetic apparatus

of higher plants is highly susceptible to environmental stresses such as high light intensity, cold, UV radiation, high salinity, and water deficit. Soil drought is an important limitation that severely impairs plant growth, development, crop yield, and various morphological, anatomical, physiological, and biochemical processes. Inhibition of photosynthesis is one of the primary physiological consequences of drought stress. Reports show that during water deficit, plants experience a number of metabolic changes that affect photosynthesis, including stomatal closure (Campos et al., 2014), decline in the content of photosynthetic pigments (Hsu et al., 2003), production of reactive oxygen species (ROS; Chen et al., 2016), and limitation of photosynthetic carbon metabolism (Dias and Brüggemann, 2010).

The photosynthetic apparatus of higher plants comprises two chlorophyll-protein complexes photosystem I (PSI) and photosystem II (PSII), which are located in the thylakoid membranes. PSII catalyzes the light-driven electron transfer from water to plastoquinone. When the energetic balance of chloroplasts changes, there are two major mechanisms in PSII to sense and respond. One is the strong and reversible phosphorylation of several proteins in the PSII-light-harvesting complex II (LHCII) supercomplexes, and the other is non-photochemical quenching (NPQ) of chlorophyll a (Chl a) fluorescence (Tikkanen and Aro, 2012). Together, these regulatory mechanisms maintain the energetic balance of the electron transfer reactions, prevent excess energy from damaging photosynthetic apparatus, and lead to the migration and reorganization of the PSII-LHCII complexes along the thylakoid membrane. It has been demonstrated that PSII can dissipate excess absorbed light energy into heat through enhancing NPQ in response to water deficit (Liu et al., 2009; Chen et al., 2016). However, the regulatory mechanism of NPQ *in vivo* under drought stress remains to be elucidated. The reversible phosphorylation and metabolism of PSII functional proteins in *Arabidopsis thaliana* and barley (*Hordeum vulgare* L.) cultivars under water stress were discovered in our previous research. The repair cycle process of damaged reaction centers of PSII (RCII) under water stress appeared to be different from that under high-light treatment (Yuan et al., 2005; Liu et al., 2009; Chen et al., 2016). Furthermore, in nature, drought conditions are frequently accompanied by other environmental stressors such as irradiation, elevated temperature, and nutrient deficiency, which can result in more complicated photoprotection responses of the photosynthetic apparatus.

Some pathways that regulate the responses of photosynthesis to environmental stress have been established in C3 plants such as *Arabidopsis*, beans, and cereal crops (wheat, barley, and rice). C4 plants have two distinct chloroplast types, mesophyll and bundle sheath chloroplasts, which cooperate to accomplish photosynthesis. There has been controversy surrounding the structure and function of PSII in the bundle sheath chloroplasts of C4 plants. Some earlier reports considered that bundle sheath

chloroplasts of C4 plants lack grana and display depleted PSII activity owing to the absence of polypeptides participating in the water oxidation or light harvesting of PSII (Hatch, 1987). However, some opposing reports have revealed that the bundle sheath chloroplasts of some C4 plants did contain a significant capacity for O<sub>2</sub> evolution and NADP<sup>+</sup> reduction linked with PSII (Chapman et al., 1980). Additionally, the excitation energy of PSII has been shown to be efficiently transferred to PSI in the bundle sheath thylakoids of many C4 plants (Pfündel et al., 1996). Maize is a typical C4 plant and is one of the most cultivated crops worldwide. In 2006, Romanowska et al. effectively isolated the mesophyll and bundle sheath chloroplasts of maize. They then revealed that PSII in the bundle sheath thylakoids contained all the polypeptides involved in photosynthetic electron transport and oxygen evolution, albeit the abundance and activity of the PSII complex were very low. Moreover, the reversible phosphorylation of PSII-LHCII proteins and the degradation of damaged D1 proteins were observed in isolated mesophyll and bundle sheath chloroplasts of maize under high light conditions (Pokorska et al., 2009). This demonstrated that the repair cycle of RCII could exist in the two cell types.

In this paper, we report on the NPQ mechanism of PSII in the bundle sheath chloroplasts of maize. Additionally, we demonstrate the superior capacity for excess energy dissipation of bundle sheath chloroplasts compared to that of mesophyll chloroplasts, under progressive drought stress. In both mesophyll and bundle sheath chloroplasts, the NPQ increased with the intensity of the drought treatment. This was accompanied by the dephosphorylation of LHCII and an increase in PSII subunit S (PsbS) content. The comparison of the two types of chloroplasts showed that under drought conditions, there was less accumulation of ROS in bundle sheath cells, and the PSII complexes and chloroplast structures were more stable. The photoprotection in bundle sheath chloroplasts may be beneficial for maintaining the photosynthetic efficiency and the capacity for transporting nutrients in maize leaves subjected to drought stress.

## Materials and methods

### Plant materials and stress treatments

Maize (*Zea mays* L.) inbred line Zheng 58 was used in this work. Maize plants were potted in a growth chamber under a 14 h photoperiod, with relative humidity 70%, an irradiance of 300  $\mu\text{mol photons m}^{-2} \text{s}^{-1}$ , and a day/night regime of 24/22°C. Maize seeds were surface sterilized in 1% sodium hypochlorite for 10 min. Before sowing, the seeds were imbibed and incubated on moisture filter paper at 24°C in dark for 48 h, then were sown into pots (60 cm  $\times$  20 cm  $\times$  16 cm) filled with compost soil. Ten maize plants were grown in each pot. Loamy soil (pH 6.2–6.9) was used in this study. Soil organic matter,

alkali-hydrolyzed nitrogen, available phosphorus, and available potassium were  $18.7 \text{ g kg}^{-1}$ ,  $157 \text{ mg kg}^{-1}$ ,  $9.7 \text{ mg kg}^{-1}$ , and  $177 \text{ mg kg}^{-1}$ , respectively. When grown to the fourth-leaf stage, drought stress was imposed on maize plants through withholding water. The experiment consisted of four soil moisture regimes with four replications. (i) Well-watered control (CK): pots were irrigated sufficiently to maintain soil water content at 80%–85% of field water capacity (FWC). (ii) Mild drought stress (S1): water content in the entire soil profile was maintained at 70%–75% FWC. (iii) Moderate drought stress (S2): water content in the entire soil profile was maintained at 50%–55% FWC. (iv) Severe drought stress (S3): water content in the entire soil profile was maintained at 30%–35% FWC. To measure the FWC, experimental soil was taken by ring knife and subjected to water absorption water for 24 h. The soil of saturated water absorption was weighted ( $w_1$ ), and dried at  $105^\circ\text{C}$  for more than 10 h, after which, dry soil was determined ( $w_2$ ). Field water capacity was calculated as:  $\text{FWC} = (w_1 - w_2) / w_2 \times 100\%$ . The FWC of the soil in the experiment was 87.83%. During withholding irrigation, the soil relative water content in each pot was measured every 3 days till the individual moisture regimes were achieved. Then, the soil moisture was maintained by measuring gravimetrically every day. After 7 days of drought stress, the first developed leaf at the top of maize plant was harvested for following experiments.

## Leaf water status and chlorophyll contents

The results of stress to plants were characterized by the relative water content (RWC) of leaves. RWC was measured according to the method of [Tambussi et al. \(2005\)](#) with minor modifications. Leaves of maize were weighed ( $w_i$ ), floated on distilled water at  $4^\circ\text{C}$  overnight, weighed again ( $w_f$ ), and dried at  $80^\circ\text{C}$ – $90^\circ\text{C}$  for 4–6 h, after which, dry mass was determined ( $w_d$ ). Relative water content was calculated as:  $\text{RWC} = (w_i - w_d) / (w_f - w_d) \times 100\%$ .

Chlorophyll (Chl) a and b content was measured according to the method of [Lichtenthaler \(1987\)](#) with some modifications. Fifteen fresh leaf disks ( $1 \text{ cm}^2$  each) were taken with hole punch from each sample leaf, then were cut into filaments ( $5 \text{ mm} \times 1 \text{ mm}$ ) and put into tubes with 5 ml of 80% acetone. The leaf and acetone were incubated at room temperature for 24 h in darkness to allow for complete extraction of chlorophyll into the solution. The absorbance of the extract was measured in microtiter plate using a microplate reader (Synergy H1, BioTek, Vermont, United States) at 645 and 663 nm. Calculate the concentration of Chl a and Chl b in the cuvette using the equations:  $\text{Chl a } (\mu\text{g ml}^{-1}) = 12.7 A_{663} - 2.69 A_{645}$ ,  $\text{Chl b } (\mu\text{g ml}^{-1}) = 22.9 A_{645} - 4.68 A_{663}$ . The total chlorophyll content based on leaf area in original suspension was calculated as:  $\text{Chl } (\mu\text{g cm}^{-2}) = (\text{Chl a} + \text{Chl b}) \times 5/S$ , where  $S \text{ (cm}^2\text{)}$  was the value of leaf area.

## Assay of reactive oxygen species

Superoxide anion radicals ( $\text{O}_2^-$ ) and hydrogen peroxide ( $\text{H}_2\text{O}_2$ ) levels were visually detected with nitro-blue tetrazolium (NBT) and 3,3-diaminobenzidine (DAB), respectively, as described in [Chen et al. \(2016\)](#) with some modifications. Leaf tissues were excised into segments (8 cm) without the tip and base parts and then immersed into 6 mM NBT solution containing 50 mM Hepes buffer (pH 7.5) for 2 h or 1  $\text{mg ml}^{-1}$  DAB solution (pH 3.8) 1 day in the dark. Leaves stained by NBT or DAB solution were decolorized in boiling ethanol (80%) or  $70^\circ\text{C}$  ethanol (95%) respectively for chlorophyll removal. Finally, leaves-segments stained by NBT and DAB solution were crosscut with a razor blade (avoiding the thick midrib), and the transection sections were observed and imaged through the microscope (Biological microscope L1800, Guangzhou LISS Optical Instrument Co., Ltd., Guangzhou, China). The microscopic images in mesophyll and bundle sheath cells after staining with NBT and DAB were quantitative analyzed using the Image J software. More than five “Kranz structure” cell regions were selected from leaf transection to analyze the depth of staining per unit area.

The production of  $\text{O}_2^-$  was determined using the method of [Elstner and Heupel \(1976\)](#) by monitoring the nitrite formation from hydroxyl amine. The content of  $\text{H}_2\text{O}_2$  was measured according to the method of [Okuda et al. \(1991\)](#). Approximately 0.5 g of fresh leaf tissues was cut into small pieces and homogenized in an ice bath with 5 ml of 0.1% (w/v) TCA. After centrifugation at  $12,000 \times g$  for 20 min at  $4^\circ\text{C}$ , 0.5 ml of supernatant plant extract was added to 0.5 ml of 10 mM potassium phosphate buffer (pH 7.0) and 1 ml of 1 M KI. The absorbance of the supernatant was recorded at 390 nm. Finally, the concentration of  $\text{H}_2\text{O}_2$  was calculated using a standard curve plotted with known concentrations of  $\text{H}_2\text{O}_2$ .

## Lipid peroxidation measurements

The level of lipid peroxidation in maize leaves from each treatment was estimated by measuring electrolyte leakage and malondialdehyde (MDA) contents. To determine electrolyte leakage, 0.5 g fresh leaf samples were cut into 5–10 mm length and put in test tubes containing 25 ml deionized water. The tubes were covered with caps and placed in a vacuum-pumping equipment for 20 min, to measure the initial electrical conductivity (EC1) of leaves using an electrical conductivity meter (DDS-307, RuiZi, Chengdu, China). The samples were heated at  $100^\circ\text{C}$  for 30 min to completely kill the tissues and release all electrolytes. After cooling to room temperature, the final electrical conductivity (EC2) of leaves was measured. Electrolyte leakage (EL) was expressed following the formula  $\text{EL} = \text{EC1}/\text{EC2} \times 100\%$ .

The thiobarbituric acid (TBA) method was applied to measure MDA concentration in leaf cells or in mesophyll and bundle sheath chloroplasts. Fresh leaf tissues (1.0 g) were homogenized in 10 ml of 10% (w/v) trichloroacetic acid (TCA). The homogenate



was centrifuged at 4°C for 10 min at 4,000 r min<sup>-1</sup>. To 2 ml of the supernatant, 2 ml of 0.6% TBA was added. The assay mixture was heated at 95°C for 15 min and then quickly cooled in an ice bath. The mixture was centrifuged at 4,000 r min<sup>-1</sup> for 15 min at 4°C. The concentration of leaf total MDA was calculated from the difference of the absorbance of the supernatant at 532 and 600 nm. For measuring plastid MDA, mesophyll and bundle sheath chloroplasts of maize leaves were isolated mechanically according to Romanowska and Parys (2011). Before homogenization in 10% TCA, the Chl concentrations of two chloroplasts preparations were measured in 80% (v/v) acetone.

## Gas exchange

Gas exchange analysis of maize leaves was made using an open system (CIRAS-3, PP system, Hitchin, United Kingdom) from 9 AM to 12 AM each day for 3 days. All measurements were taken at a constant airflow rate of 300 ml min<sup>-1</sup> under the artificial light condition of 1,200  $\mu\text{mol m}^{-2} \text{s}^{-1}$ . The reference concentration of ambient CO<sub>2</sub> was about 400  $\mu\text{mol mol}^{-1}$ , the temperature was 25°C, and the relative humidity was 30%. Photosynthetic parameters including stomatal conductance, transpiration rate, intercellular CO<sub>2</sub> concentration, and net photosynthetic rate were measured.

## In vivo chlorophyll fluorescence measurements

Chlorophyll a fluorescence induction kinetics and imaging of intact leaves were measured at room temperature with a pulse-amplitude-modulated imaging fluorometer (the Imaging PAM M-Series Chlorophyll Fluorescence system, Heinz Walz GmbH, Effeltrich, Germany). Maize plants were dark adapted for 30 min prior to fluorescence measurements. The minimal fluorescence yield (F<sub>o</sub>) and maximal fluorescence yield (F<sub>m</sub>) were measured with dark-adapted leaves when all RCII are fully opened and closed. F<sub>m</sub> was induced by a saturating pulse of white light (0.8 s, 8,000  $\mu\text{mol m}^{-2} \text{s}^{-1}$ ). The fluorescence in stable state (F<sub>s</sub>) was measured after actinic light (1,000  $\mu\text{mol m}^{-2} \text{s}^{-1}$ ) was applied for 30 min. Then the maximal fluorescence yield after light adaption (F<sub>m'</sub>) was attained with a pulse of saturating light with 0.8 s interval while leaves were illuminated by actinic light. After the actinic light was turned off, a far-red light was applied to excite PSI preferentially, leaving the electron transport of PSII in an oxidized state, to obtain the minimum fluorescence of the light-adaptive leaves (F<sub>o'</sub>). By using fluorescence parameters determined in both light- and dark-adapted leaves, the maximal photochemical quantum yield of PSII in darkness [ $F_v/F_m = (F_m - F_o)/F_m$ ], the maximal photochemical quantum yield of PSII under light [ $F_v'/F_m' = (F_m' - F_o')/F_m'$ ], the effective photochemical quantum yield of PSII under light [ $\Phi_{\text{PSII}} = (F_m' - F_s)/F_m'$ ], and the non-photochemical fluorescence quenching under light

[ $\text{NPQ} = (F_m - F_m')/F_m'$ ] were calculated. Among these parameters, F<sub>v</sub>/F<sub>m</sub> is used to monitor the potential efficiency of PSII photochemistry,  $\Phi_{\text{PSII}}$  represents light use efficiency at a given light intensity, and NPQ reflects heat-dissipation of excitation energy in the antenna system. The image data averaged in each experiment were normalized to a false color scale. Light responses curves (LRCs) analysis was performed using light steps between 0 and 1,500  $\mu\text{mol m}^{-2} \text{s}^{-1}$ . During light-to-dark shifts, NPQ kinetics of intact maize leaves was measured according to Chen et al. (2019).

## Chlorophyll fluorescence kinetic microscope measurements

In maize, a typical C<sub>4</sub> plant, it was demonstrated that bundle sheath chloroplast contained about half the amount of PSII complexes compared with mesophyll one (Romanowska et al., 2006). Nevertheless, it is impossible to distinguish chlorophyll fluorescence of bundle sheath chloroplasts from mesophyll chloroplasts, on the intact leaves, due to leaf anatomy in which a few layers of mesophyll cells tightly surround one layer of bundle sheath cells. In this study, the chlorophyll fluorescence kinetic microscope (FKM) system (Micro-FluorCam FC2000, Photon Systems Instruments, Brno, Czech Republic) was applied to analyze the fluorescence parameters at the cellular level *in vivo*.

Fresh leaves with different treatments were carefully crosscut, and the transection of slices (more than three slices of each sample) were imaged and measured under microscope. The FKM was operated by the FluorCam software, and the modules of slow kinetics, light responses curves, and light-to-dark shifts were applied. Blue excitation (470 nm) was used and Chlorophyll fluorescence was detected from 695 to 770 nm. Measuring saturating and actinic light were 3,000 and 180  $\mu\text{mol m}^{-2} \text{s}^{-1}$ , respectively. From the microscopic imaging of the leaf transection, different types of cell regions were selected to individually analyze the fluorescence parameters of mesophyll or bundle sheath chloroplasts, in which more than five “Kranz structure” cell regions were selected from each slice. Consistent with the experiment of intact leaves, parameters such as F<sub>o</sub>, F<sub>m</sub>, F<sub>o'</sub>, F<sub>m'</sub>, and F<sub>s</sub> were measured. F<sub>v</sub>/F<sub>m</sub>, F<sub>v'</sub>/F<sub>m'</sub>,  $\Phi_{\text{PSII}}$  and NPQ of mesophyll and bundle sheath chloroplasts were calculated.

## Electron microscopy

Leaves of maize plants with differently drought treatments were cut into pieces about 2 mm × 3 mm, and three of which were fixed immediately with 3% glutaraldehyde in 0.1 M sodium cacodylate buffer (pH 6.9) at 4°C over night. The fixed leaves pieces were then post-fixed with 1% osmium tetroxide, dehydrated in series acetone and embedded in Epon 812, as described previously (Liu et al., 2009). Ultrathin sections, cut with an ultramicrotome (EM UC6, Leica Microsystem GmbH, Wetzlar,

Germany), were observed with a transmission electron microscope (H-7500, Hitachi, Tokyo, Japan) operating at 75 kV. Three visual field of each section were selected to observe.

## Thylakoid isolation

Mesophyll and bundle sheath thylakoids were isolated according to Romanowska and Parys (2011). Isolation procedures were carried out at 4°C, under dim green light. All the isolation buffers were supplemented with 10 mM NaF to inhibit thylakoid protein dephosphorylation. Maize leaves were homogenized in a medium containing 400 mM mannitol, 50 mM HEPES-NaOH (pH 8.0), 5 mM MgCl<sub>2</sub>, 10 mM NaCl, 10 mM sodium isoascorbate, 2 mM PMSF, 5 mM amino-n-caproic acid (EACA), 1 mM benzamidine (BA), 2 mM EDTA, 10 mM NaF, and 0.2% (w/v) BSA. The homogenate was filtered through six layers of Miracloth (20 mm) and the filtrate was used for preparation of mesophyll chloroplasts. The residue continued to be homogenized, then filtered and the residue on the cloth was washed briefly with cold distilled water until the filtrate was clear. The residue was microscopically examined to ensure that the bundle sheath strands were completely free of mesophyll contamination. The final bundle sheath residue was homogenized and filtered through six layers of nylon (20 mm). The filtrates obtained during isolation of mesophyll chloroplasts and bundle sheath chloroplasts were centrifuged at 8,000 × g for 15 min. Isolated thylakoid samples were immediately frozen in liquid nitrogen and stored at −80°C until use. The effective isolation of mesophyll and bundle sheath cells was monitored by immuno detection of anti-phosphoenolpyruvate carboxylase (PEPC) and anti-Ribulose-1,5-bisphosphate carboxylase/oxygenase (Rubisco), which are key enzymes of CO<sub>2</sub> assimilation process located in mesophyll and bundle sheath cells, respectively.

## Sds-page and immunoblot analysis

According to the method of Pokorska et al. (2009) and Betterle et al. (2015) with minor modification, isolated thylakoid samples were solubilized in the denaturing buffer containing 0.05 M Tris-HCl (pH 6.8), 5% (w/v) SDS, 8 M urea, 5% (v/v) 2-mercaptoethanol, and 20% (v/v) glycerol. The polypeptides were separated by SDS-PAGE using 15% (w/v) acrylamide gels with 3 or 6 M urea. The amount of protein loaded was equivalent to 0.5–1.5 µg of Chl depending on the protein abundance in thylakoid membranes. For western blotting, separated proteins were electro-transferred onto a PVDF membrane (Immobilon, Millipore, Massachusetts, United States). Then antibodies against D1, D2, CP43, CP47, Lhcb1, Lhcb2, Lhcb4, PsbS (Agrisera, Vännas, Sweden), and a polyclonal anti-phosphothreonine antibody (Cell Signaling Technology, Boston, United States) were applied. The signals were revealed by using a chemiluminescent detection system (ECL, GE Healthcare,

Buckinghamshire, United Kingdom). Quantification of the immunoblots was done using Lane 1D analysis software (SAGE Creation, Beijing, China).

## *In vivo* dephosphorylation of thylakoid proteins

According to Rokka et al. (2000) and Liu et al. (2009), maize plants were illuminated under a PFD of 1,000 µmol photons m<sup>−2</sup> s<sup>−1</sup> at 25°C for 60 min to phosphorylate RCII proteins. To induce maximal LHCII phosphorylation, maize leaves were illuminated at low light (a PFD of 80 µmol photons m<sup>−2</sup> s<sup>−1</sup>) for 60 min. Metal halide lamps were served as light source. After light treatment the maize leaves were transferred to darkness and incubated at 25°C for up to 120 min for gradual dephosphorylation. Samples for mesophyll and bundle sheath thylakoids isolation were taken during the time course of incubation, frozen in liquid nitrogen, and stored at −80°C.

## Blue native page

Thylakoid protein solubilization and BN-PAGE analysis was performed as described by Pokorska et al. (2009) with slight modification. Thylakoid membranes, corresponding to 15 µg Chl, were sedimented at 7,000 g for 5 min at 4°C and resuspended in 25 mM Bis Tris-HCl (pH 7.0), 20% (v/v) glycerol. Membrane proteins were solubilized by the addition of n-dodecyl β-D-maltoside (DDM) in 25 mM imidazole-HCl (pH 7.0), 20% glycerol, to a final concentration of 1% (w/v) for mesophyll thylakoid and 2% (w/v) for bundle sheath one. Final chlorophyll concentration was 0.5 mg/ml. Samples were incubated on ice for 10 min followed by centrifugation at 18,000 × g for 15 min. The supernatant was supplemented with 1/10 volume of BN sample buffer (5% w/v Serva Blue G, 100 mM Bis Tris-HCl pH 7.0, 30% w/v sucrose and 500 mM ε-amino-n-caproic acid) and loaded directly onto a 4%–12% acrylamide (w/v) gradient gel. Electrophoresis was performed at 4°C by increasing the voltage gradually from 50 to 200 V during the 3–4 h run. After the BN-PAGE run, the immunoblotting of thylakoid membrane proteins was performed according to the method of Wittig et al. (2006). The quantitative analysis of thylakoid membrane complexes was performed using Lane 1D software.

## Statistical analysis

At least four independent replicates were conducted for each determination. Data analysis was performed using the statistical software SPSS 17.0, and the means were compared using Duncan's multiplication range test. A difference was considered to be statistically significant when  $p < 0.05$ . Error bars in figures represent SD of the means.

## Results

### Response of the water status, chlorophyll content, and gas exchange to drought stress in maize leaves

Drought stress was induced by withholding water according to four different soil moisture regimes. These included a well-watered control (CK), mild drought stress (S1), moderate drought stress (S2), and severe drought stress (S3). The relative water content (RWC) of the maize leaves decreased gradually with increasing drought stress (Supplementary Figure 1A). This indicated that the decrease in soil moisture led to the water deficit in maize leaves.

A decrease in chlorophyll content is commonly observed under drought stress (Yuan et al., 2005; Liu et al., 2009; Chen et al., 2016). As shown in Supplementary Figure 1B, mild drought stress did not have an obvious effect on the Chl a and b contents, but the total chlorophyll content was markedly reduced under moderate and severe drought conditions.

The stomatal conductance ( $g_s$ ), transpiration rate ( $E$ ), intercellular  $\text{CO}_2$  concentration ( $C_i$ ), and  $\text{CO}_2$  assimilation rate ( $A$ ) were measured in maize leaves under different drought conditions (Supplementary Figures 1C–F). Compared with the control,  $g_s$  and  $E$  gradually declined under progressive drought stress. Mild or moderate drought stress did not have an obvious influence on  $C_i$ , but  $C_i$  increased significantly under severe drought stress.  $A$  displayed a slight decrease under mild drought stress; this was not statistically significant. However, moderate and severe drought stress dramatically reduced  $A$  in maize leaves.

### Drought stress induced significant ROS accumulation and lipid peroxidation in maize mesophyll cells

The accumulation of ROS can be detected in plants under environmental stress (Foyer and Noctor, 2005; Rao and Chaitanya, 2016). To identify the influence of drought stress on ROS production, in this experiment, the levels of the two major ROS,  $\text{O}_2^-$  and  $\text{H}_2\text{O}_2$ , were measured by quantitative analysis and histochemical staining of maize leaves. To further compare the differences in ROS accumulation between mesophyll and bundle sheath cells in maize leaves under drought stress, the transverse sections of stained leaves were observed under a light microscope. As shown in Supplementary Figures 2A,B, both  $\text{O}_2^-$  and  $\text{H}_2\text{O}_2$  levels increased when the maize plant was exposed to drought stress, particularly when exposed to severe drought stress. Interestingly, compared with bundle sheath cells, ROS accumulation in mesophyll cells of maize leaves increased more obviously, especially under moderate and severe drought conditions (Figures 1A–D).

ROS accumulation can damage membrane lipids. Hence, in this experiment, electrolyte leakage and malondialdehyde (MDA)

contents were examined to estimate the amount of lipid peroxidation and to further determine the degree of oxidative damage on the plants. As shown in Supplementary Figures 2C,D, the electrolyte leakage and the total leaf MDA content increased significantly under moderate and severe drought stress. This indicated that ROS accumulation increased the lipid peroxidation in maize leaves under serious drought conditions. Notably, the MDA content in the mesophyll chloroplasts displayed a clear increase under drought stress, whereas the MDA content in bundle sheath chloroplasts was less affected by the drought treatments (Figure 1E).

### The npq in bundle sheath chloroplasts increased more markedly than in mesophyll chloroplasts under drought stress

The ratio obtained from chlorophyll fluorescence parameters,  $F_v/F_m$ , reflects the primary conversion efficiency of light energy in PSII. It is also an excellent indicator for measuring the degree of photoinhibition. As shown in Figure 2, there were no statistically significant changes in the  $F_v/F_m$  value when plants were subjected to mild drought stress. After severe drought, the  $F_v/F_m$  value decreased from 0.81 to 0.73. This resulted from the reduction in the proportion of open RCII's under severe drought stress. The changes observed in  $F_v'/F_m'$  and  $\Phi_{\text{PSII}}$  of PSII further indicated that severe drought stress suppressed the electron transfer capability of PSII. Thermal energy dissipation from the antenna pigments of PSII, as an important mechanism that protects against excessive excitation, increased when plants were subjected to the drought stress.

Fluorescence Kinetic Microscope (FKM) measurements have been applied to analyze the *in vivo* photosynthetic activity of individual cells in algae (Ferimazova et al., 2013) and plants (Jacobs et al., 2016). In recent years, the application of FKM measurements to determine the Chl a fluorescence of plant mesophyll and bundle sheath cells has also been reported (Gorecka et al., 2014). In this study, Chl a fluorescence in the mesophyll and bundle sheath cells of maize leaves was detected by FKM measurement. Consistent with the results of previous studies (Ferimazova et al., 2013; Gorecka et al., 2014; Jacobs et al., 2016), at the microscopic level, the values of chlorophyll fluorescence, including  $F_v/F_m$ ,  $\Phi_{\text{PSII}}$  and NPQ, were all much lower than those measured on intact leaves. The reasons for the low values of chlorophyll fluorescence, especially NPQ values, measured with FKM in this study may be the low chlorophyll contents per unit area in leaf slices, and the low actinic light intensity applied to avoid photoinhibition to leaf slices. As shown in Figure 3, under severe drought stress, the Kranz structure of the maize leaves was looser compared to that of the control plants. Mild drought stress did not significantly affect the photochemical efficiency of PSII in

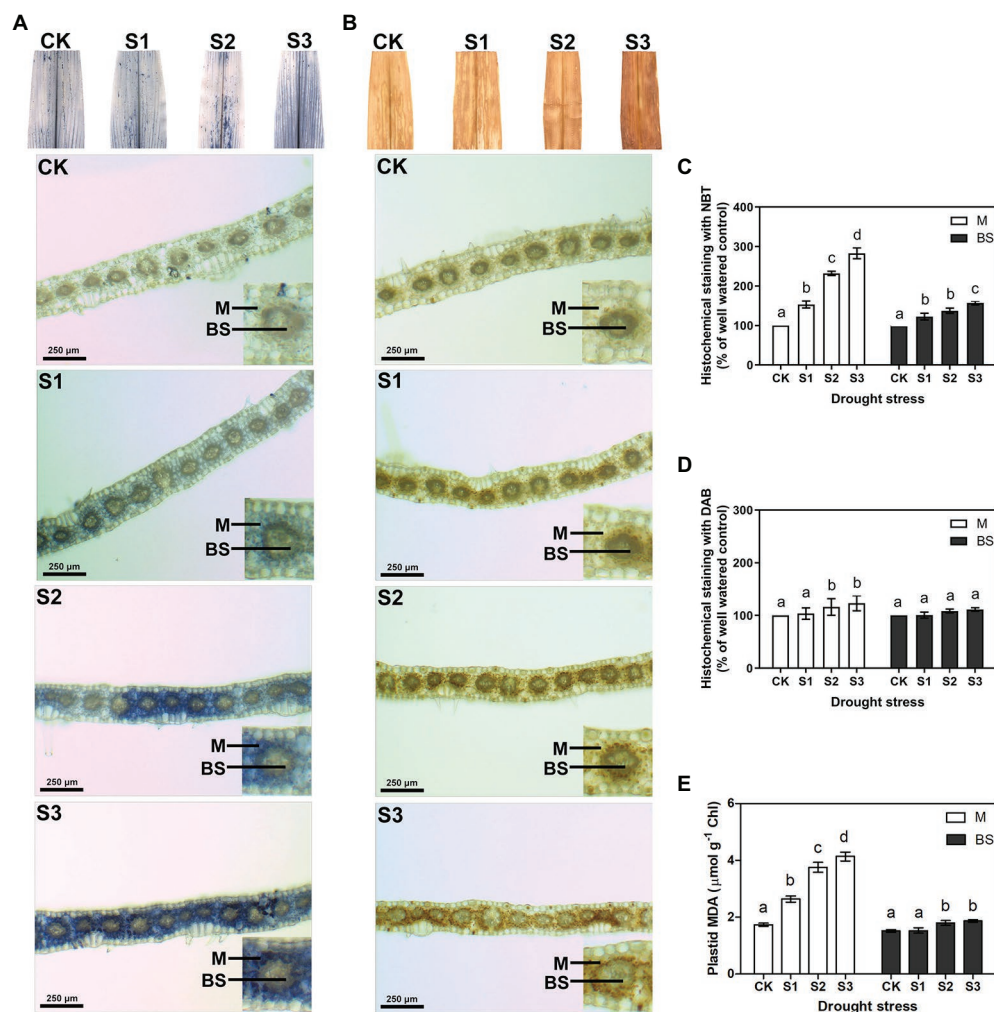


FIGURE 1

Measurement of reactive oxygen species (ROS) and lipid peroxidation in mesophyll (M) and bundle sheath (BS) cells of maize leaves under drought stress. Histochemical assays for  $\text{O}_2^-$  and  $\text{H}_2\text{O}_2$  in leaves by nitro-blue tetrazolium (NBT; **A**) and 3,3-diaminobenzidine (DAB; **B**) staining, respectively. Distribution of  $\text{O}_2^-$  and  $\text{H}_2\text{O}_2$  in M and BS cells were imaged in microscope. The microscopic images in M and BS cells were quantitative analyzed (**C,D**). Plastid malondialdehyde (MDA) content (**E**) in M and BS chloroplasts of maize leaves were detected. CK, S1, S2, and S3 represent, respectively, the soil moisture regimes of well-watered, mild drought stress, moderate drought stress and severe drought stress. Values are expressed as the means  $\pm$  SD from four independent biological replicates ( $n=4$ ). Different letters depict significant differences between the treatments ( $p<0.05$ ) according to Duncan's multiplication range test.

mesophyll or bundle sheath cells. However, the Fv/Fm and  $\Phi\text{PSII}$  values in the two classes of chloroplasts declined markedly when plants were exposed to moderate and severe drought conditions. These results were consistent with those of the intact leaf (Figure 2). NPQ in mesophyll and bundle sheath chloroplasts increased with increasing water deficit to dissipate excess excitation energy. Interestingly, the NPQ in bundle sheath chloroplasts was higher than in mesophyll chloroplasts when the plants were well watered. Furthermore, with increasing drought stress, the NPQ in bundle sheath chloroplasts displayed a greater increase than in mesophyll chloroplasts. As shown in light response curves (LRCs) analysis, compared with mesophyll chloroplasts, the primary energy conversion of bundle sheath chloroplasts decreased

more slightly, while the NPQ of bundle sheath chloroplasts increased more obviously.

The above results seemed to indicate that bundle sheath chloroplasts of maize leaves may be highly capable of thermal dissipation, especially under drought conditions. NPQ kinetic studies were performed in intact leaves and leaf transections with a light ( $1,500 \text{ mmol m}^{-2} \text{ s}^{-1}$ ) over a time period of 0–2,000 s. Under the high-light periods, drought treatment induced a typical rapid increase in NPQ followed by a slower increase, both in intact leaves and microstructure samples. The increasing trend of NPQ was positively correlated with the degree of drought stress (Figure 4). In particularly, as shown in Figure 4B, mesophyll chloroplasts exhibited a significantly weaker increase of NPQ than bundle sheath chloroplasts.



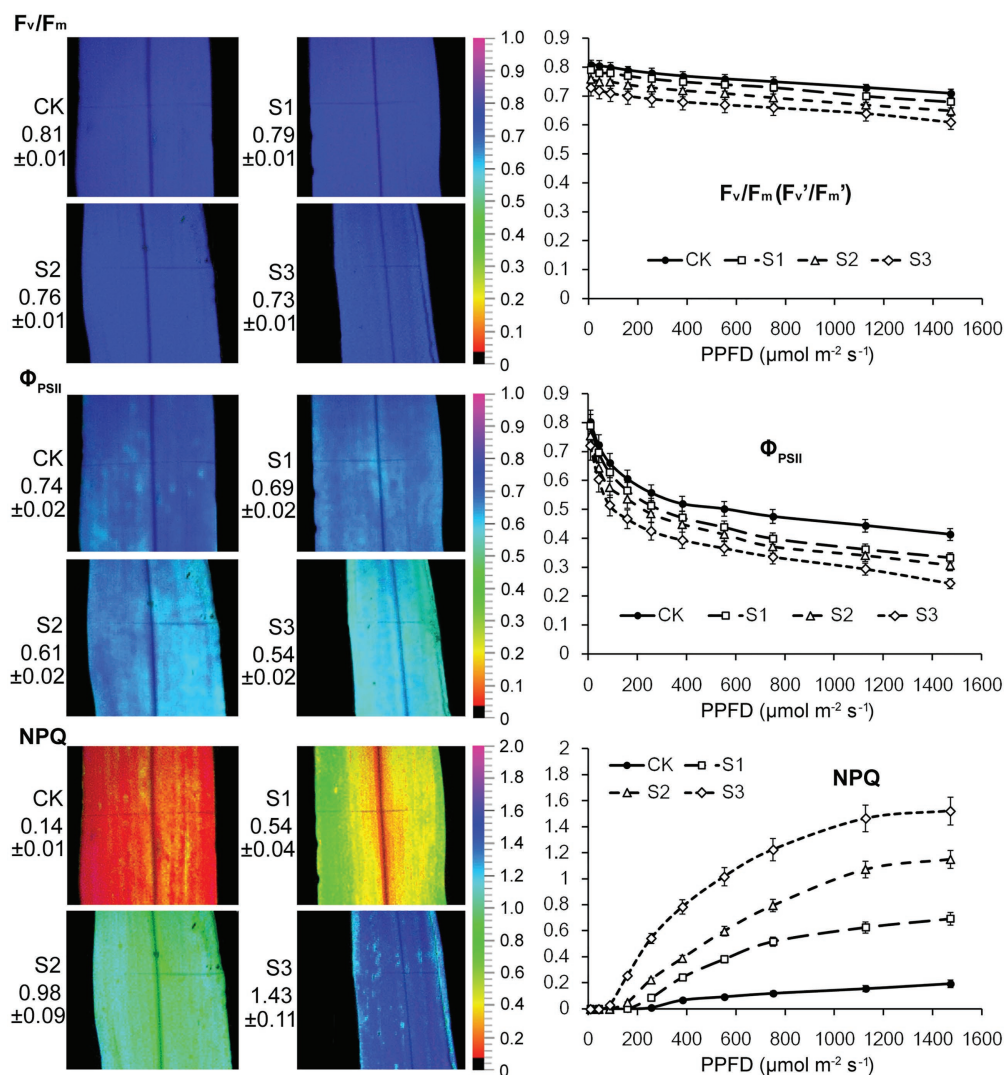


FIGURE 2

Chlorophyll fluorescence imaging and light response curves (LRCs) in intact maize leaves under drought stress.  $F_v/F_m$ , the maximal photochemical quantum yield of PSII in darkness;  $F_v/F_m'$ , the maximal photochemical quantum yield of PSII under light;  $\Phi_{PSII}$ , the effective photochemical quantum yield of PSII under light; NPQ, the non-photochemical fluorescence quenching under light. CK, well-watered control; S1, mild drought stress; S2, moderate drought stress; and S3, severe drought stress. Values beside the individual images present quantitative means  $\pm$  SD ( $n=4$ ). Vertical bars represent SD of the mean ( $n=4$ ).

## Drought stress decreased phospho-lhcbii level, especially in bundle sheath chloroplasts

The accumulation of PSII proteins in bundle sheath chloroplasts can be determined when cross-contamination with mesophyll cells is avoided. The mesophyll and bundle sheath chloroplasts of maize leaves exposed to drought stress were obtained through mechanical isolation. To determine the separation efficiency, isolated mesophyll and bundle sheath cell samples were immuno-blotted with the antibodies against mesophyll-specific enzyme PEPC and bundle sheath-specific enzyme Rubisco. The result is shown in [Supplementary Figure 3A](#), almost no PEPC was detected in bundle sheath cells, and Rubisco was detected only in bundle sheath

chloroplasts. Under drought stress, especially severe drought, the steady-state levels of PEPC and Rubisco declined. Thus, the used procedure effectively isolated mesophyll and bundle sheath cells, and was suitable for our investigation.

As shown in [Figure 5A](#), the steady-state levels of phosphorylated CP43, D1, and D2 in the mesophyll and bundle sheath cells increased significantly under drought stress. On the contrary, the levels of phospho-LHCII decreased dramatically during drought treatment, especially in bundle sheath chloroplasts. The reversible phosphorylation of Lhcb4 (CP29) during water stress has been reported in our previous studies ([Liu et al., 2009](#)). In this experiment, phospho-CP29 was not detected in mesophyll chloroplasts but was detected in bundle sheath chloroplasts when the maize plants were well watered. Drought

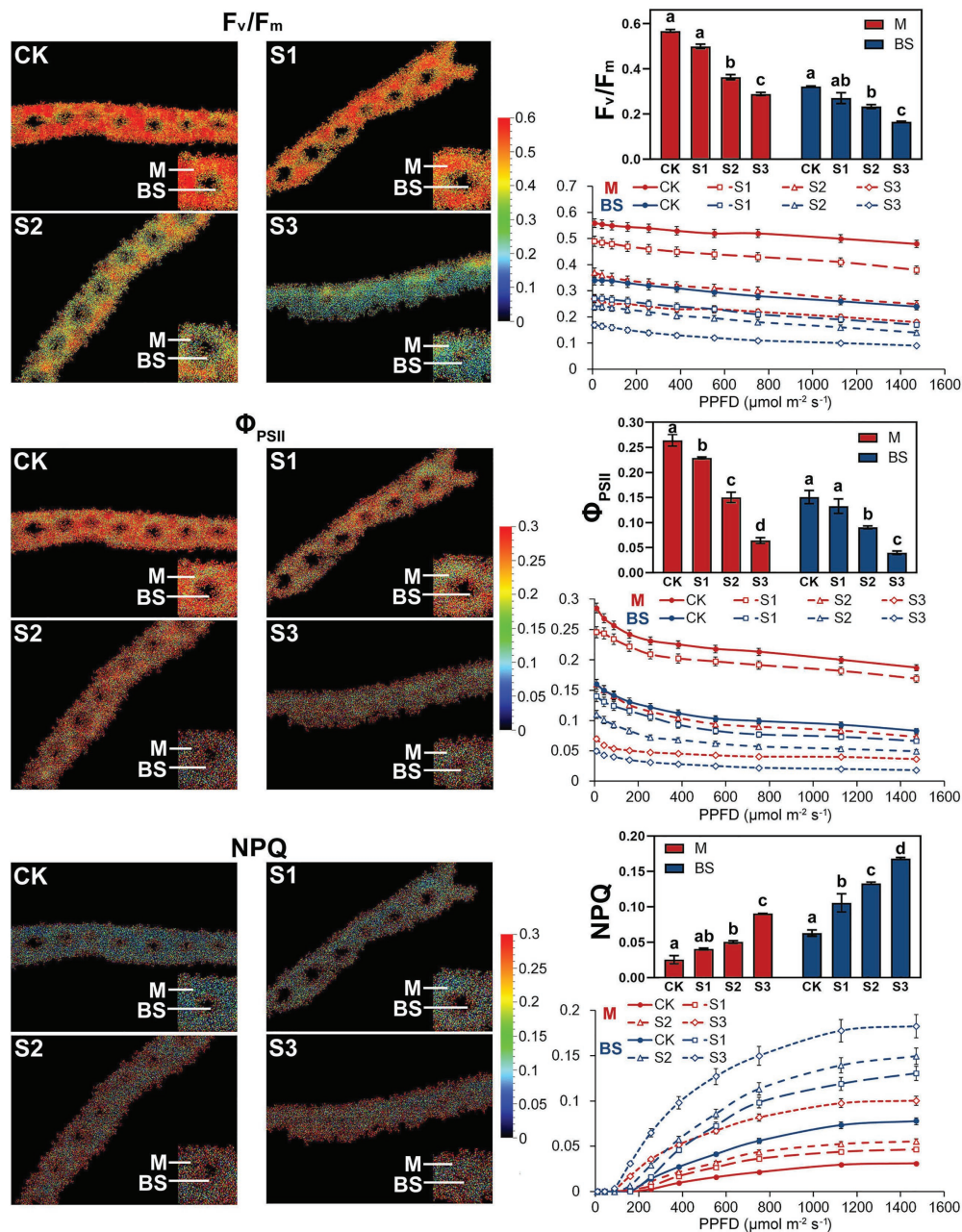


FIGURE 3

Chlorophyll fluorescence imaging and LRCs in M and BS chloroplasts of maize leaves under drought stress. Fv/Fm, the maximal photochemical quantum yield of PSII in darkness; Fv/Fm', the maximal photochemical quantum yield of PSII under light; Φ<sub>PSII</sub>, the effective photochemical quantum yield of PSII under light; NPQ, the non-photochemical fluorescence quenching under light. CK, well-watered control; S1, mild drought stress; S2, moderate drought stress; and S3, severe drought stress. Vertical bars represent SD of the mean (*n*=4). Different letters mean significant differences at the 0.05 level according to Duncan's multiplication range test.

stress increased CP29 phosphorylation, in both mesophyll and bundle sheath chloroplasts.

The dephosphorylation rates of the core PSII proteins and LHCII were investigated in this study to better understand the dynamic changes in the phosphorylation status of the PSII proteins under drought stress. The dephosphorylation rates of the core PSII proteins (CP43, D1, and D2) in maize plants under

severe drought stress were lower than in well-watered plants (Figures 5C,D). In contrast, drought treatment led to an obvious increase in the dephosphorylation rate of LHCII (Figure 5E). Under severe drought, the half-times of phospho-LHCII decreased from 74 and 94 min to 48 and 34 min in mesophyll and bundle sheath chloroplasts, respectively. This indicated that the dephosphorylation of LHCII proteins was more accelerated in

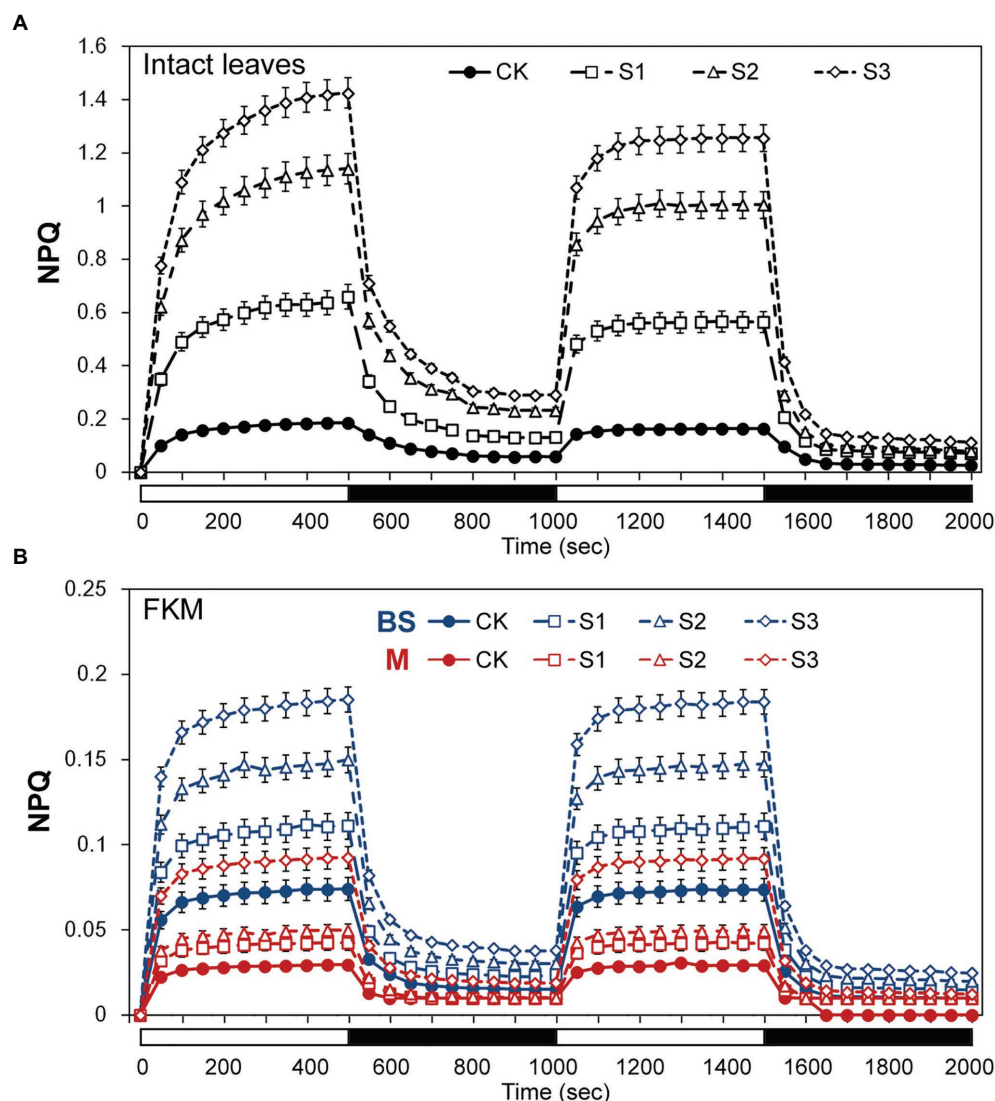


FIGURE 4

Assays of non-photochemical quenching (NPQ) kinetics under drought stress. (A) Measurement of NPQ kinetics in intact maize leaves. (B) Measurement of NPQ kinetics in M and BS chloroplasts of maize leaves. The two consecutive periods of illumination with  $1,500 \text{ molm}^{-2} \text{ s}^{-1}$  for 500s with a 500s period of darkness in between, as indicated by the white (light on) and black (dark) bars at the bottom of figure. CK, well-watered control; S1, mild drought stress; S2, moderate drought stress; and S3, severe drought stress. Vertical bars represent SD of the mean ( $n=4$ ).

bundle sheath chloroplasts than in mesophyll chloroplasts under drought treatment (Table 1).

## The changes in steady-state levels of psii proteins differed between mesophyll and bundle sheath chloroplasts in response to drought stress

The steady-state levels of PSII proteins in mesophyll and bundle sheath chloroplasts of maize leaves subjected to drought stress were investigated by immunoblot analysis (Figure 6). In general, PSII protein levels in bundle sheath were much lower than those in mesophyll cells, which is consistent with the

previous reports (Majeran et al., 2005, 2008). In mesophyll chloroplasts, the levels of the core PSII proteins were all markedly reduced under drought stress (Supplementary Figures 4A–F). Similar trends were not observed in bundle sheath chloroplasts under drought conditions. Interestingly, the LHCI content in bundle sheath chloroplasts increased when plants were subjected to drought stress.

It is considered that the PSII protein, PsbS, could play a crucial role in enabling the rapidly reversible component of NPQ (Li et al., 2000). Therefore, the response of the PsbS level upon drought stress was investigated in this experiment. As shown in Figure 6, the steady-state levels of PsbS in both mesophyll and bundle sheath chloroplasts increased under drought stress. Furthermore, this increase was greater in



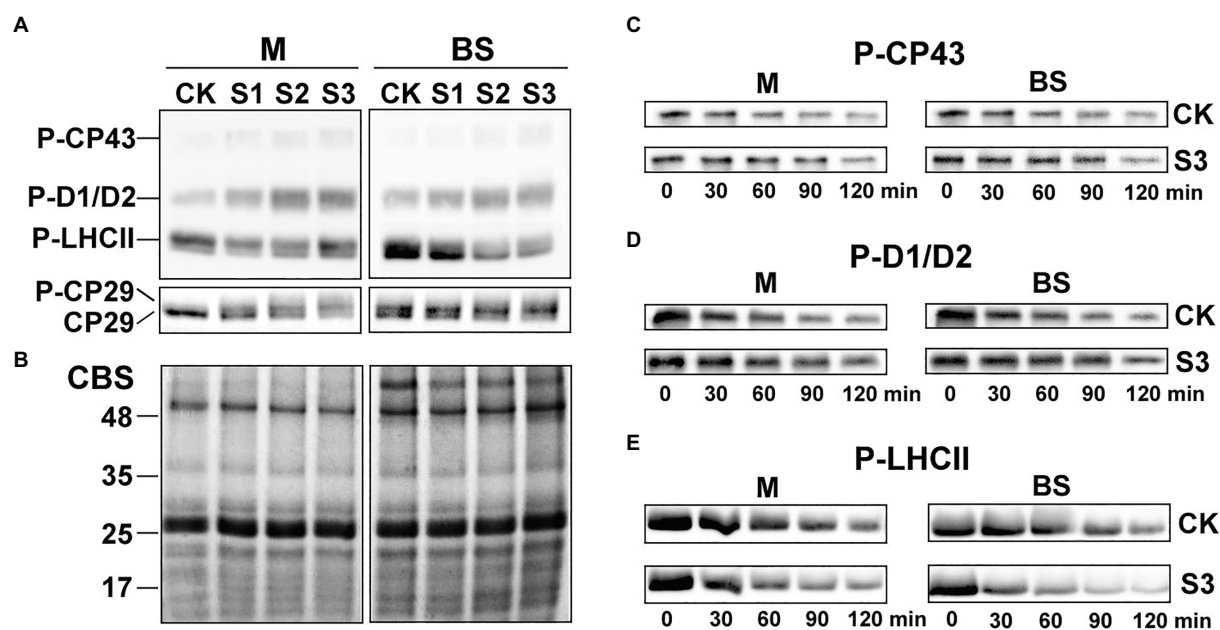


FIGURE 5

Reversible phosphorylation of PSII proteins in M and BS chloroplasts of maize leaves under drought stress. (A) Immunoblot analysis of the PSII proteins phosphorylation in M and BS chloroplasts under drought stress. Proteins in M (1.0  $\mu\text{g}$  Chl) and BS chloroplasts (1.5  $\mu\text{g}$  Chl), were detected with anti-PThr antibody. (B) Coomassie staining of protein samples (CBS) was shown as a control. The positions of detected phosphoproteins and molecular masses of protein markers (in kDa) are indicated. (C–E) Dephosphorylation of PSII proteins *in vivo* under severe drought stress. Maize leaves were illuminated 120 min at 25°C and then transferred to darkness and incubated at 25°C. Dephosphorylation was terminated at the indicated time points by freezing the leaves in liquid nitrogen. Thylakoid membranes in M and BS cells were isolated and the extent of protein phosphorylation was determined using anti-PThr antibody. Before conducting the dephosphorylation experiments, different light intensities were used for induction of higher *in vivo* phosphorylation levels of either core proteins or LHCII. Maize leaves were illuminated under a PFD 1,000  $\mu\text{mol photons m}^{-2} \text{ s}^{-1}$  for more effective phosphorylation of PSII core proteins (C,D) or under a PFD 80  $\mu\text{mol photons m}^{-2} \text{ s}^{-1}$  for induction of LHCII phosphorylation (E). CK, well-watered control; S1, mild drought stress; S2, moderate drought stress; and S3, severe drought stress. The results shown are representative of those obtained in at least three independent experiments. Thylakoids were isolated in the presence of 10 mM NaF.

bundle sheath chloroplasts than in mesophyll chloroplasts. After severe drought, the levels of PsbS in the mesophyll and bundle sheath chloroplasts increased by 28.20% and 124.87%, respectively, compared with the control (Supplementary Figure 4G).

## The organization of psii complexes in mesophyll and bundle sheath thylakoids varied under drought stress

PSII is present in thylakoid membranes both as a dimer and a monomer. The functional dimeric PSII complexes bind at least two LHCII trimers, thus forming the PSII-LHCII supercomplexes in the appressed grana regions. Some evidence suggests that, during NPQ, PsbS controls the dissociation of the portion of PSII-LHCII supercomplexes and aggregation of LHCII antenna (Betterle et al., 2009; Johnson and Ruban, 2011; Goral et al., 2012). In our study, the aim was to gain an insight into the organizational changes of the PSII complexes in thylakoid membranes in the leaves of maize plants subjected to drought stress. To do this, the thylakoid membranes in mesophyll and bundle sheath chloroplasts were solubilized with 1% and 2% DM, respectively. The thylakoids

were then analyzed using the blue native PAGE (BN-PAGE) technique.

Protein analysis of crosslinked thylakoids using BN-PAGE revealed that the composition of protein complexes in mesophyll and bundle sheath thylakoids were similar to those described by Pokorska et al. (2009) and Rogowski et al. (2018). Bands corresponding to major protein complexes were identified on BN-gels (Figure 7). These complexes included the PSII-LHCII and PSI-LHCI supercomplexes, PSII dimers and monomers, ATP synthase, PSI core complex, and LHCII trimers. The relative level of the supercomplexes was lower in bundle sheath thylakoids compared with mesophyll thylakoids, and the abundance of the LHCII trimers was lower in bundle sheath membranes. As expected, drought stress induced different changes to the steady-state levels of protein complexes in mesophyll and bundle sheath thylakoids. There were reductions in the amount of PSII dimers, PSII monomers, and LHCII trimers in mesophyll thylakoids isolated from maize leaves under drought stress when compared to the well-watered control (Figure 7A). These reductions were greater in thylakoids isolated from maize subjected to severe drought stress. Nevertheless, no such changes were observed in bundle sheath membranes. When maize leaves were exposed to drought stress, almost all the protein complexes in the bundle sheath thylakoids



TABLE 1 Dephosphorylation rates for CP43, D1/D2, and LHClI phosphoproteins in isolated mesophyll (M) and bundle sheath (BS) thylakoids under drought stress.

Phosphoprotein	Mesophyll				Bundle sheath			
	$t_{1/2}$ (min)				$t_{1/2}$ (min)			
	CK	S1	S2	S3	CK	S1	S2	S3
CP43	96 ± 5 <sup>d</sup>	112 ± 9 <sup>c</sup>	132 ± 11 <sup>b</sup>	164 ± 15 <sup>a</sup>	64 ± 5 <sup>e</sup>	88 ± 7 <sup>d</sup>	103 ± 9 <sup>c</sup>	139 ± 13 <sup>b</sup>
D1/D2	76 ± 6 <sup>d</sup>	93 ± 8 <sup>c</sup>	111 ± 10 <sup>b</sup>	143 ± 16 <sup>a</sup>	52 ± 3 <sup>e</sup>	75 ± 7 <sup>d</sup>	98 ± 10 <sup>bc</sup>	131 ± 12 <sup>a</sup>
LHCII	74 ± 4 <sup>b</sup>	66 ± 5 <sup>bc</sup>	57 ± 4 <sup>c</sup>	48 ± 4 <sup>d</sup>	94 ± 8 <sup>a</sup>	78 ± 7 <sup>b</sup>	55 ± 5 <sup>c</sup>	34 ± 2 <sup>e</sup>

The data are presented as the half-times (minutes). The half-times were calculated from the first-order rate fitting of the dephosphorylation versus time curves obtained from four experiments at each treatment. CK, well-watered control; S1, mild drought stress; S2, moderate drought stress; and S3, severe drought stress. Results are expressed as means ± SD of four independent experiments, different letters mean significant differences at the 0.05 level according to Duncan's multiplication range test.

were stable (Figure 7B). Interestingly, severe drought stress markedly increased the relative abundance of LHCII trimers in bundle sheath membranes (Supplementary Figure 5).

Drought stress accelerated the destacking of grana in mesophyll thylakoids

To further investigate the effects of drought stress on thylakoid structures, the ultrastructure of mesophyll and bundle sheath chloroplasts in maize leaves were analyzed (Figure 8). Transmission electron microscopy showed that the length-to-width ratio and area of mesophyll chloroplasts tended to decrease in response to drought stress. The stacking of the grana in mesophyll chloroplasts gradually loosened as drought stress increased. The number of grana also reduced. The bundle sheath chloroplasts appeared to lack grana, which is in accordance with the conclusion reported by Edwards et al. (2001). As shown in Figure 8, the unstacked thylakoid lamellae in bundle sheath chloroplasts were not obviously damaged after drought treatment. However, the starch granules were reduced both in size and in number under severe drought stress.

Discussion

There are many notable photosynthetic structures and functions that differ between C4 and C3 plants. These include the Kranz anatomy, the higher optimum temperature and irradiance saturation for maximum photosynthetic rates, the lower CO<sub>2</sub> compensation point, and the higher instantaneous water use efficiency of leaves of C4 plants (El-Sharkawy, 2009). These characteristics may provide C4 plants with a superior capacity for environmental adaptation. In our previous work, water deficit reduced stomatal opening in wheat and barley leaves to reduce water transpiration. This directly affected CO<sub>2</sub> uptake and led to reduced CO<sub>2</sub> assimilation and a corresponding decrease in energy conversion in PSII, even under mild water stress. Furthermore, excess excitation energy led to the production of ROS (including O<sub>2</sub><sup>-</sup>, <sup>1</sup>O<sub>2</sub>, H<sub>2</sub>O<sub>2</sub>, and OH). ROS accumulation has been shown to impair cell structure and damage photosynthetic apparatus, which further reduces the net photosynthetic rate and plant growth (Yuan et al., 2005; Liu et al., 2006, 2009). Nevertheless, in this study, reduced stomatal conductance in maize leaves only slightly affected the net photosynthetic rate under mild drought stress (Supplementary Figure 1). Significant increases in C<sub>i</sub> (Supplementary Figure 1E) and reductions in net photosynthetic rate (Supplementary Figure 1F) only occurred in leaves subjected to severe drought conditions. These results suggest that maize may have a mechanism for maintaining photosynthetic assimilation efficiency, thereby limiting the negative feedback of stomatal and non-stomatal influences under drought stress.

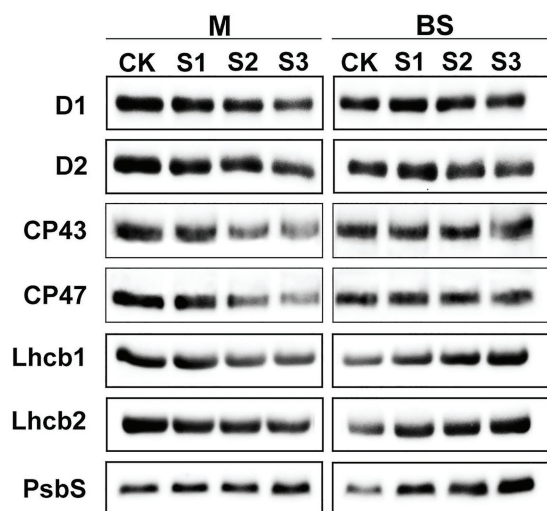


**FIGURE 6**  
Steady-state levels of PSII proteins in M and BS thylakoids of maize leaves under drought stress. Immunoblot analyses of PSII proteins in M thylakoids (1.0  $\mu$ g Chl) and BS thylakoids (1.5  $\mu$ g Chl) were performed using antibodies specific for D1, D2, CP43, CP47, Lhcb1, Lhcb2, and PsbS. The results shown are representative of those obtained in at least three independent experiments. CK, S1, S2, and S3 represent, respectively, the well-watered, mild drought, moderate drought and severe drought treatments.

The discovery of functional PSII complexes in bundle sheath chloroplasts of maize provided a new insight into the photosynthetic mechanism of C4 plants (Romanowska et al., 2006; Pokorska et al., 2009; Rogowski et al., 2018). In this study, the presence of an NPQ mechanism in the bundle sheath chloroplasts of maize was determined through physiological and biochemical experiments. Importantly, more significant enhancement of NPQ was detected in bundle sheath chloroplasts under drought stress than in mesophyll chloroplasts (Figures 3, 4). NPQ is considered as the most rapid molecular response of PSII in higher plants for protecting photosynthetic apparatus. However, many aspects of the NPQ mechanism such as the quenching site and its regulation are still debated currently. Ruban (2016) summarized that the minimum requirements for NPQ *in vivo* are the proton gradient ( $\Delta$ pH), LHCII complexes, and the PsbS protein. When light intensities change,  $\Delta$ pH, as the trigger, results in PsbS being protonated. This leads to concomitant rearrangements of the antenna system, which switches the antenna into their dissipative state. In this quenched state, LHCII is dephosphorylated and dissociates from PSII-LHCII complexes. This favors thermal dissipation of excitation energy over energy transfer to RCII (Tikkanen and Aro, 2012). In the above model, PsbS protein functions as a switch. The PSII-LHCII pool and aggregated LHCII antenna participate in the energy-dependent quenching (qE; Ruban, 2016; Rogowski et al., 2018), in which dephosphorylation of LHCII may occur (Rintamäki et al., 1997).

PsbS content can be adjusted to the intensity of the growth light conditions (Ballottari et al., 2007). When grown in high light,

plants have a faster induction and relaxation rate for qE, which is correlated with a higher abundance of the PsbS protein (Kromdijk et al., 2016). Our previous research has also shown that NPQ and PsbS content in Arabidopsis leaves increased under long-term (6–15 days) drought stress (Chen et al., 2016). In this study on maize, increasing drought stress led to an increase in NPQ (Figures 2–4), which was accompanied by accelerated dephosphorylation of the LHCII subunits (Figure 5) and enhanced PsbS content (Figure 6). These results were consistent with previous findings in C3 plants and were observed in both mesophyll and bundle sheath chloroplasts. Therefore, it can be concluded that LHCII antenna and the PsbS protein may play roles in regulating excess energy dissipation in PSII in maize leaves. The accumulation of PsbS may be positively correlated with the NPQ capacity when maize plants encounter drought stress.

More significantly, it can be deduced that the photoprotection capacity (*via* thermal dissipation) of bundle sheath chloroplasts is superior to that of mesophyll chloroplasts in response to drought stress. This may be significantly correlated with the dephosphorylation of LHCII (Table 1) and the PsbS levels (Supplementary Figure 4G) in bundle sheath chloroplasts. This superior capacity of bundle sheath cells was also reflected by the NPQ displayed in the two types of chloroplasts under drought stress. Additionally, the phosphorylation of core proteins (CP43, D1, and D2) and CP29 in both mesophyll and bundle sheath chloroplasts increased under drought stress. Interestingly, phospho-CP29 was found in bundle sheath chloroplasts but not mesophyll chloroplasts, when maize plants were well watered (Figure 5A). The phosphorylation of core proteins has been shown to have a role in facilitating the disassembly and migration of the PSII-LHCII supercomplexes under changing light intensities (Goral et al., 2010; Tikkanen and Aro, 2012; Chen et al., 2018a). The significance of the phosphorylation of CP29 is still controversial. Some researchers have suggested that the phosphorylation of CP29 is associated with NPQ (Betterle et al., 2015). It has even been proposed that the quencher is localized within CP29 (Ahn et al., 2008). Whether the NPQ mechanism in mesophyll and bundle sheath chloroplasts of maize under drought stress involves the reversible phosphorylation of CP29 requires further study.

Previous studies have shown that bundle sheath cells exhibit predominantly PSI cyclic electron flow, which generates a trans-thylakoid  $\Delta$ pH (Ivanov et al., 2005, 2007). This feature of bundle sheath cells may be also correlated with the higher NPQ bundle sheath cells and may be not attributed into a greater need for photoprotection under drought. The roles of higher PSI cyclic electron flow in bundle sheath cells under environmental stresses require further investigations.

Inspection of the histochemical staining of  $O_2^-$  and  $H_2O_2$  indicated that drought stress resulted in higher ROS accumulation in mesophyll cells than in bundle sheath cells (Figures 1A,B). The results of measuring the plastid MDA also showed that the lipid peroxidation of chloroplast membranes in mesophyll cells was more severe than in bundle sheath cells under drought conditions (Figure 1C). The homeostasis between the formation and removal

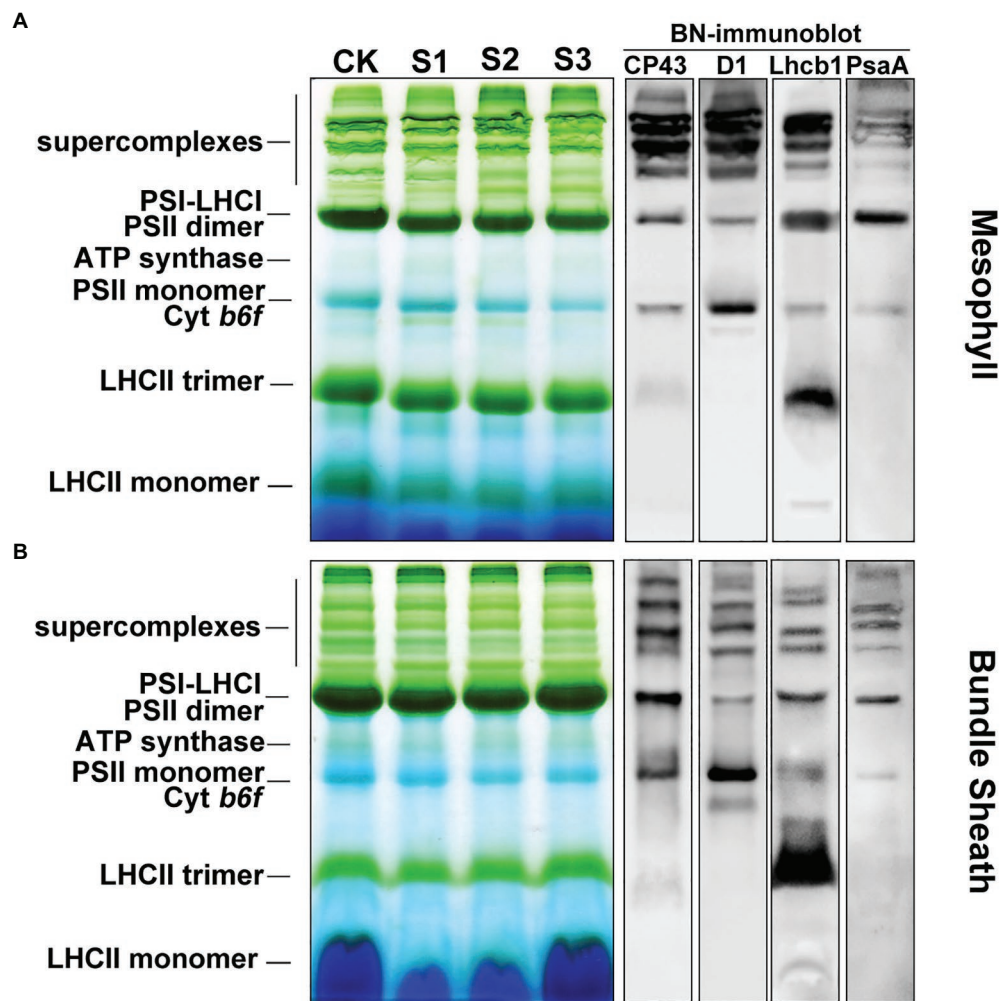


FIGURE 7

The composition of protein complexes in M and BS thylakoids of maize leaves under drought stress. **(A)** Membranes (15µg Chl) in M thylakoids were solubilized with 1% *n*-dodecyl β-D-maltoside (DDM) and loaded onto 4%–12% acrylamide Blue-Native gel. **(B)** Membranes (15µg Chl) in BS thylakoids were solubilized with 2% DDM and loaded onto 4%–12% acrylamide Blue-Native gel. The bands of BN-PAGE were confirmed by immunoblotting with CP43, D1, Lhcb1, and PsaA specific antibodies (on the right). The control line of the BN gel was selected for immunodetection. The results shown are representative of those obtained in at least three independent experiments. CK, S1, S2, and S3 represent, respectively, the well-watered, mild drought, moderate drought and severe drought treatments.

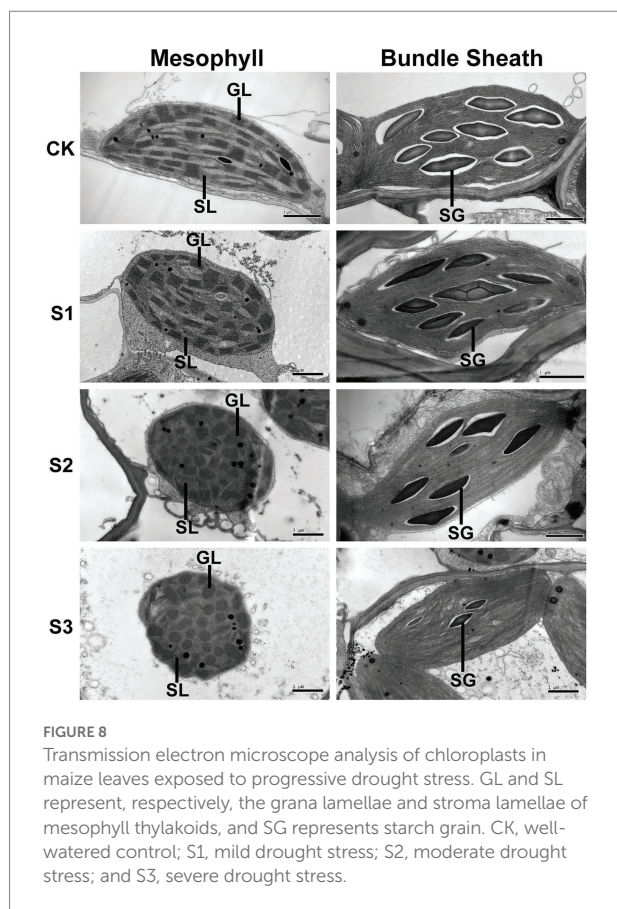
of ROS in plant cells is regulated through enzymatic pathways and antioxidants. Increased ROS accumulation under environmental stress can damage proteins, membrane lipids, DNA, and other cellular components. NPQ, as the first defense and photoprotection mechanism of PSII, exerts control over the CO<sub>2</sub> assimilation rate in fluctuating light conditions (Hubbart et al., 2012; Roach and Krieger-Liszkay, 2012; Zulfugarov et al., 2014).

Consistent with our previous findings in wheat, barley, and Arabidopsis (Liu et al., 2006, 2009; Chen et al., 2016), ROS accumulation may be one of the main reasons for the increase in lipid peroxidation (Figure 1C), downregulation of photosynthetic proteins (Figures 6, 7), and destacking of grana (Figure 8) in mesophyll chloroplasts of maize under drought stress. In bundle sheath cells, after drought treatment, there was no obvious peroxidative damage or reductions in protein abundance.

Interestingly, the steady-state levels of LHCII (including the levels of the LHCII monomer and the LHCII trimer) in the bundle sheath chloroplasts increased with increasing drought stress (Figures 6, 7B). This may have contributed to maintaining the higher NPQ, as LHCII may be important to the NPQ mechanism (Rintamäki et al., 1997; Iliaia et al., 2011). Therefore, our data indicate that the lower accumulation of ROS in bundle sheath chloroplasts under drought conditions compared to that in the mesophyll chloroplasts may be related to the superior capacity of bundle sheath cells to dissipate excess energy.

Maize, as an NADP-dependent malic enzyme (NADP-ME) type of C<sub>4</sub> plants, has a CO<sub>2</sub> concentrating mechanism in its bundle sheath cells coupled with high stomatal resistances. This results in improved water conservation in leaves when the CO<sub>2</sub> assimilation efficiency is equal to or higher than that of C<sub>3</sub> plants





(El-Sharkawy, 2009). Therefore, when environmental factors change, it is crucial for maize to maintain photosynthetic efficiency by ensuring the CO<sub>2</sub> assimilation capacity in bundle sheath chloroplasts and limiting CO<sub>2</sub> diffusion from bundle sheath cells to mesophyll cells (Langdale, 2011). The superior NPQ mechanism in bundle sheath cells inhibits the release of ROS to an extent, which may have positive consequences for maintaining the structure and function of bundle sheath cells. This enables the bundle sheath cells to retain high CO<sub>2</sub> concentrations and improves the water use efficiency of leaves under drought conditions. In addition, the lower accumulation of ROS under drought stress could reduce the risk of oxidative damage to the transitory starch stored in bundle sheath chloroplasts. This starch can be utilized as a stored energy source for glucose metabolism in maize cells (Figure 8). Currently, there are no suitable instruments or methods to separately measure the water potential or osmotic pressure in mesophyll and bundle sheath cells of plants with dense veins such as maize. Here, we presume that the structural integrity and functional stability of bundle sheath cells under drought stress may contribute to the ability of vascular tissues to transport water, mineral salts, and organic compounds produced by photosynthesis.

Many studies on photosynthesis in C4 plants focus on the CO<sub>2</sub> assimilation process; researchers attempt to improve the photosynthetic efficiency, especially under environmental stress, through modifications such as the enhancement of PEPC content

and activity. There are many strategies for improving the photosynthetic capacity of C3 plants that have been put into practice. These include the introduction of Rubisco or PEPC from C4 species, the introduction of carbon concentrating mechanisms, and the engineering of a full C4 Kranz pathway using the existing evolutionary progression observed in C3–C4 intermediates as a blueprint (Leegood, 2013; Qin et al., 2015).

The effect of PsbS expression on NPQ has been well-documented (Peterson and Havir, 2001, 2003). C3 plants such as Arabidopsis, tobacco, and rice overexpressing PsbS have been shown to display increased photoprotection compared with wild-type plants under high light or other fluctuating environmental conditions (Roach and Krieger-Liszka, 2012; Glowacka et al., 2018). However, this can be at the expense of CO<sub>2</sub> fixation under less stressful conditions (Hubbart et al., 2012; Kromdijk et al., 2016). In this study in maize, the significant correlation between PsbS content and NPQ was found in both mesophyll and bundle sheath chloroplasts. The superior photoprotection observed in bundle sheath cells may be beneficial to stabilizing their function. Therefore, it is suggested that overexpression of PsbS in C4 plants such as maize may improve environmental adaptation. Moreover, the PsbS protein, particularly in bundle sheath chloroplasts, is hypothesized to be a useful marker for assessing chlorophyll fluorescence and field yield when breeding stress-resistant maize varieties. This hypothesis has recently been discussed in the context of wheat (Chen et al., 2018b).

## Data availability statement

The original contributions presented in the study are included in the article/Supplementary Material; further inquiries can be directed to the corresponding authors.

## Author contributions

W-JL, SY, and JZ planned and designed the research and wrote the manuscript with contribution of all authors. W-JL, HL, Y-EC, YY, Z-WZ, JS, L-JC, F-LZ, and DW performed experiments. W-JL, HL, X-HD, CW, MX, SY, and JZ analyzed data. All authors contributed to the article and approved the submitted version.

## Funding

This work was supported by Beijing Municipal Joint Research Program for Germplasm Innovation and New Variety Breeding (to JZ), the National Natural Science Foundation of China (31770322 to SY), the National Special Program for GMO Development of China (2016ZX08003-004 to JZ), the Natural Science Foundation of Sichuan Province (2022NSFSC0140 to W-JL), the Fund of Talent Project of Sichuan Academy of Agricultural Sciences (2021LJRC to W-JL), and the Fund of “1+9” Science and Technology Project of



Sichuan Academy of Agricultural Sciences (1+9 KJGG 006), Advanced technology for biosafety.

## Acknowledgments

The authors acknowledge LetPub ([www.letpub.com](http://www.letpub.com)) for its linguistic assistance during the preparation of this manuscript.

## Conflict of interest

The authors declare that the research was conducted in the absence of any commercial or financial relationships that could be construed as a potential conflict of interest.

## References

- Ahn, T. K., Avenson, T. J., Ballottari, M., Cheng, Y. C., Niyogi, K. K., Bassi, R., et al. (2008). Architecture of a charge-transfer state regulating light harvesting in a plant antenna protein. *Science* 320, 794–797. doi: 10.1126/science.1154800
- Ballottari, M., Dall'Osto, L., Morosinotto, T., and Bassi, R. (2007). Contrasting behavior of higher plant photosystem I and II antenna systems during acclimation. *J. Biol. Chem.* 282, 8947–8958. doi: 10.1074/jbc.M606417200
- Betterle, N., Ballottari, M., Baginsky, S., and Bassi, R. (2015). High light-dependent phosphorylation of photosystem II inner antenna CP29 in monocots is STN7 independent and enhances nonphotochemical quenching. *Plant Physiol.* 167, 457–471. doi: 10.1104/pp.114.252379
- Betterle, N., Ballottari, M., Zorzan, S., de Bianchi, S., Cazzaniga, S., Dall'osto, L., et al. (2009). Light-induced dissociation of an antennahetero-oligomer is needed for non-photochemical quenching induction. *J. Biol. Chem.* 284, 15255–15266. doi: 10.1074/jbc.M808625200
- Campos, H., Trejob, C., Peña-Valdivia, C. B., García-Nava, R., Conde-Martínez, F. V., and Cruz-Ortega, M. R. (2014). Stomatal and non-stomatal limitations of bell pepper (*Capsicum annuum* L.) plants under water stress and re-watering: delayed restoration of photosynthesis during recovery. *Environ. Exp. Bot.* 98, 56–64. doi: 10.1016/j.envexpbot.2013.10.015
- Chapman, K. S., Berry, J. A., and Hatch, M. D. (1980). Photosynthetic metabolism in bundle sheath cells of the C4 species *Zea mays*: sources of ATP and NADPH and the contribution of photosystem II. *Arch. Biochem. Biophys.* 202, 330–341. doi: 10.1016/0003-9861(80)90435-x
- Chen, Y. E., Liu, W. J., Su, Y. Q., Cui, J. M., Zhang, Z. W., Yuan, M., et al. (2016). Different response of photosystem II to short and long term drought stress in *Arabidopsis thaliana*. *Physiol. Plant.* 158, 225–235. doi: 10.1111/ppl.12438
- Chen, Y. E., Su, Y. Q., Mao, H. T., Wu, N., Zhu, F., Yuan, M., et al. (2018a). Terrestrial plant evolve highly assembled photosystem complexes in adaptation to light shifts. *Front. Plant Sci.* 9:1811. doi: 10.3389/fpls.2018.01811
- Chen, Y. E., Su, Y. Q., Zhang, C. M., Ma, J., Mao, H. T., Yang, Z. H., et al. (2018b). Comparison of photosynthetic characteristics and antioxidant systems in Different Wheat Strains. *J. Plant Growth Regul.* 37, 347–359. doi: 10.1007/s00344-017-9731-5
- Chen, Y. E., Yuan, S., Lezhneva, L., Meurer, J., Schwenkert, S., Mamedov, F., et al. (2019). The low molecular mass photosystem II protein psbTn is important for light acclimation. *Plant Physiol.* 179, 1739–1753. doi: 10.1104/pp.18.01251
- Dias, M. C., and Brüggemann, W. (2010). Limitations of photosynthesis in *Phaseolus vulgaris* under drought stress: gas exchange, chlorophyll fluorescence and Calvin cycle enzymes. *Photosynthetica* 48, 96–102. doi: 10.1007/s11099-010-0013-8
- Edwards, G. E., Franceschi, V. R., Ku, M. S., Voznesenskaya, E. V., Pyankov, V. I., and Andreo, C. S. (2001). Compartmentation of photosynthesis in cells and tissues of C4 plants. *J. Exp. Bot.* 52, 577–590. doi: 10.1093/jexbot/52.356.577
- El-Sharkawy, M. A. (2009). Pioneering research on C4 leaf anatomical, physiological, and agronomic characteristics of tropical monocot and dicot plant species: implications for crop water relations and productivity in comparison to C3 cropping systems. *Photosynthetica* 47, 163–183. doi: 10.1007/s11099-009-0030-7
- Elstner, E. F., and Heupel, A. (1976). Inhibition of nitrite formation from hydroxylammoniumchloride: a simple assay for superoxide dismutase. *Anal. Biochem.* 70, 616–620. doi: 10.1016/0003-2697(76)90488-7
- Ferimazova, N., Felcmanová, K., Šetliková, E., Küpper, H., Maldener, I., Hauska, G., et al. (2013). Regulation of photosynthesis during heterocyst differentiation in *Anabaena* sp. strain PCC 7120 investigated in vivo at single-cell level by chlorophyll fluorescence kinetic microscopy. *Photosynth. Res.* 116, 79–91. doi: 10.1007/s11120-013-9897-z
- Foyer, C. H., and Noctor, G. (2005). Redox homeostasis and antioxidant signaling: a metabolic interface between stress perception and physiological responses. *Plant Cell* 17, 1866–1875. doi: 10.1105/TPC.105.033589
- Glowacka, K., Kromdijk, J., Kucera, K., Xie, J., Cavanagh, A. P., Leonelli, L., et al. (2018). Photosystem II subunit S overexpression increases the efficiency of water use in a field-grown crop. *Nat. Commun.* 9:868. doi: 10.1038/s41467-018-03231-x
- Goral, T. K., Johnson, M. P., Brain, A. P. R., Kirchhoff, H., Ruban, A. V., and Mullineaux, C. W. (2010). Visualising the mobility and distribution of chlorophyll-proteins in higher plant thylakoid membranes: effects of photoinhibition and protein phosphorylation. *Plant J.* 62, 948–959. doi: 10.1111/j.1365-313x.2010.04207.x
- Goral, T. K., Johnson, M. P., Duffy, C. D. P., Brain, A. P. R., Ruban, A. V., and Mullineaux, C. W. (2012). Light-harvesting antenna composition controls the macrostructure and dynamics of thylakoid membranes in *Arabidopsis*. *Plant J.* 69, 289–301. doi: 10.1111/j.1365-313x.2011.04790.x
- Gorecka, M., Alvarez-Fernandez, R., Slattery, K., McAusland, L., Davey, P. A., Karpinski, S., et al. (2014). Abscisic acid signalling determines susceptibility of bundle sheath cells to photoinhibition in high light-exposed *Arabidopsis* leaves. *Philos. Trans. R. Soc. Lond. Ser. B Biol. Sci.* 369:20130234. doi: 10.1098/rstb.2013.0234
- Hatch, M. D. (1987). C4 photosynthesis: a unique blend of modified biochemistry, anatomy and ultrastructure. *Biochim. Biophys. Acta - Bioenerg.* 895, 81–106. doi: 10.1016/S0304-4173(87)80009-5
- Hsu, S. Y., Hsu, Y. T., and Kao, C. K. (2003). Ammonium ion, ethylene, and abscisic acid in polyethylene glycol-treated rice leaves. *Biol. Plant.* 46, 239–242. doi: 10.1023/a:1022854728064
- Hubbart, S., Ajigboye, O. O., Horton, P., and Murchie, E. H. (2012). The photoprotective protein PsbS exerts control over CO<sub>2</sub> assimilation rate in fluctuating light in rice. *Plant J.* 71, 402–412. doi: 10.1111/j.1365-313x.2012.04995.x
- Ilioaia, C., Johnson, M. P., Liao, P.-N., Pascal, A. A., van Grondelle, R., Walla, P. J., et al. (2011). Photoprotection in plants involves a change in lutein 1 binding domain in the major light-harvesting complex of photosystem II. *J. Biol. Chem.* 286, 27247–27254. doi: 10.1074/jbc.M111.234617
- Ivanov, B., Asada, K., and Edwards, G. E. (2007). Analysis of donors of electrons to photosystem I and cyclic electron flow by redox kinetics of P700 in chloroplasts of isolated bundle sheath strands of maize. *Photosynth. Res.* 92, 65–74. doi: 10.1007/s11120-007-9166-0
- Ivanov, B., Asada, K., Kramer, D. M., and Edwards, G. (2005). Characterization of photosynthetic electron transport in bundle sheath cells of maize. I. Ascorbate effectively stimulates cyclic electron flow around PSI. *Planta* 220, 572–581. doi: 10.1007/s00425-004-1367-6

## Publisher's note

All claims expressed in this article are solely those of the authors and do not necessarily represent those of their affiliated organizations, or those of the publisher, the editors and the reviewers. Any product that may be evaluated in this article, or claim that may be made by its manufacturer, is not guaranteed or endorsed by the publisher.

## Supplementary materials

The Supplementary materials for this article can be found online at: <https://www.frontiersin.org/articles/10.3389/fpls.2022.885781/full#supplementary-material>

- Jacobs, M., Lopez-Garcia, M., Phrathep, O. P., Lawson, T., Oulton, R., and Whitney, H. M. (2016). Photonic multilayer structure of Begonia chloroplasts enhances photosynthetic efficiency. *Nat. Plants* 2:16162. doi: 10.1038/nplants.2016.162
- Johnson, M. P., and Ruban, A. V. (2011). Restoration of rapidly reversible photo-protective energy dissipation in the absence of PsbS protein by enhanced pH. *J. Biol. Chem.* 286, 19973–19981. doi: 10.1074/jbc.M111.237255
- Kromdijk, J., Glowacka, K., Leonelli, L., Gabilly, S. T., Iwai, M., Niyogi, K. K., et al. (2016). Improving photosynthesis and crop productivity by accelerating recovery from photoprotection. *Science* 354, 857–861. doi: 10.1126/science.aai8878
- Langdale, J. A. (2011). C4 cycles: past, present, and future research on C4 photosynthesis. *Plant Cell* 23, 3879–3892. doi: 10.1105/tpc.1111.092098
- Leegood, R. C. (2013). Strategies for engineering C4 photosynthesis. *J. Plant Physiol.* 170, 378–388. doi: 10.1016/j.jplph.2012.10.011
- Li, X. P., Olle, B., Shih, C., Grossman, A. R., Rosenquist, M., Jansson, S., et al. (2000). A pigment-binding protein essential for regulation of photosynthetic light harvesting. *Nature* 403, 391–395. doi: 10.1038/35000131
- Lichtenthaler, H. K. (1987). Chlorophyll fluorescence signatures of leaves during the autumnal chlorophyll breakdown. *J. Plant Physiol.* 131, 101–110. doi: 10.1016/S0176-1617(87)80271-7
- Liu, W. J., Chen, Y. E., Tian, W. J., Du, J. B., Zhang, Z. W., Xu, F., et al. (2009). Dephosphorylation of photosystem II proteins and phosphorylation of CP29 in barley photosynthetic membranes as a response to water stress. *Biochim. Biophys. Acta - Bioenerg* 1787, 1238–1245. doi: 10.1016/j.bbabo.2009.04.012
- Liu, W. J., Yuan, S., Zhang, N. H., Lei, T., Duan, H. G., Liang, H. G., et al. (2006). Effect of water stress on photosystem 2 in two wheat cultivars. *Biol. Plant.* 50, 597–602. doi: 10.1007/s10535-006-0094-1
- Majeran, W., Cai, Y., Sun, Q., and van Wijk, K. J. (2005). Functional differentiation of bundle sheath and mesophyll maize chloroplasts determined by comparative proteomics. *Plant Cell* 17, 3111–3140. doi: 10.1105/tpc.105.035519
- Majeran, W., Zybaïlov, B., Ytterberg, A. J., Dunsmore, J., Sun, Q., and van Wijk, K. J. (2008). Consequences of C4 differentiation for chloroplast membrane proteomes in maize mesophyll and bundle sheath cells. *Mol. Cell. Proteomics* 7, 1609–1638. doi: 10.1074/mcp.M800016-MCP200
- Okuda, T., Masuda, Y., Yamanka, A., and Sagisaka, S. (1991). Abrupt increase in the level of hydrogen peroxide in leaves of winter wheat is caused by cold treatment. *Plant Physiol.* 97, 1265–1267. doi: 10.1104/pp.97.3.1265
- Peterson, R. B., and Havir, E. A. (2001). Photosynthetic properties of an *Arabidopsis thaliana* mutant possessing a defective PsbS gene. *Planta* 214, 142–152. doi: 10.1007/s004250100601
- Peterson, R. B., and Havir, E. A. (2003). Contrasting modes of regulation of PS II light utilization with changing irradiance in normal and psbS mutant leaves of *Arabidopsis thaliana*. *Photosynth. Res.* 75, 57–70. doi: 10.1023/A:1022458719949
- Pfündel, E., Nagel, E., and Meister, A. (1996). Analyzing the light energy distribution in the photosynthetic apparatus of C4 plants using highly purified mesophyll and bundle-sheath thylakoids. *Plant Physiol.* 112, 1055–1070. doi: 10.1104/pp.112.3.1055
- Pokorska, B., Zienkiewicz, M., Powikrowska, M., Drozak, A., and Romanowska, E. (2009). Differential turnover of the photosystem II reaction Centre D1 protein in mesophyll and bundle sheath chloroplasts of maize. *Biochim. Biophys. Acta - Bioenerg* 1787, 1161–1169. doi: 10.1016/j.bbabo.2009.05.002
- Qin, N., Xu, W., Hu, L., Li, Y., Wang, H., Qi, X., et al. (2015). Drought tolerance and proteomics studies of transgenic wheat containing the maize C4 phosphoenolpyruvate carboxylase (PEPC) gene. *Protoplasma* 253, 1503–1512. doi: 10.1007/s00709-015-0906-2
- Rao, D. E., and Chaitanya, K. V. (2016). Photosynthesis and antioxidative defense mechanisms in deciphering drought stress tolerance of crop plants. *Biol. Plant.* 60, 201–218. doi: 10.1007/s10535-016-0584-8
- Rintamäki, E., Salonen, M., Suoranta, U. M., Carlberg, I., Andersson, B., and Aro, E. M. (1997). Phosphorylation of light-harvesting complex II and photosystem II core proteins shows different irradiance-dependent regulation in vivo. Application of phosphothreonine antibodies to analysis of thylakoid phosphoproteins. *J. Biol. Chem.* 272, 30476–30482. doi: 10.1074/jbc.272.48.30476
- Roach, T., and Krieger-Liszka, A. (2012). The role of the PsbS protein in the protection of photosystems I and II against high light in *Arabidopsis thaliana*. *Biochim. Biophys. Acta - Bioenerg* 1817, 2158–2165. doi: 10.1016/j.bbabo.2012.09.011
- Rogowski, P., Wasilewska, W., Urban, A., and Romanowska, E. (2018). Maize bundle sheath chloroplasts – a unique model of permanent state 2. *Environ. Exp. Bot.* 155, 321–331. doi: 10.1016/j.envexpbot.2018.07.012
- Rokka, A., Aro, E. M., Herrmann, R. G., Andersson, B., and Vener, A. V. (2000). Dephosphorylation of photosystem II reaction center proteins in plant photosynthetic membranes as an immediate response to abrupt elevation of temperature. *Plant Physiol.* 123, 1525–1536. doi: 10.2307/4279386
- Romanowska, E., Drozak, A., Pokorska, B., Shiell, B. J., and Michalski, W. P. (2006). Organization and activity of photosystems in the mesophyll and bundle sheath chloroplasts of maize. *J. Plant Physiol.* 163, 607–618. doi: 10.1016/j.jplph.2005.06.007
- Romanowska, E., and Parys, E. (2011). “Photosynthesis research protocols, methods in molecular biology,” in *Mechanical Isolation of Bundle Sheath Cell Strands and Thylakoids From Leaves of C4 Grasses*. ed. R. Carpentier (New York: Springer Science+Business Media), 327–337.
- Ruban, A. V. (2016). Nonphotochemical chlorophyll fluorescence quenching: mechanism and effectiveness in protecting plants from photodamage. *Plant Physiol.* 170, 1903–1916. doi: 10.1104/pp.15.01935
- Tambussi, E. A., Nogués, S., and Araus, J. L. (2005). Ear of durum wheat under water stress: water relations and photosynthetic metabolism. *Planta* 221, 446–458. doi: 10.1007/s00425-004-1455-7
- Tikkanen, M., and Aro, E. M. (2012). Thylakoid protein phosphorylation in dynamic regulation of photosystem II in higher plants. *Biochim. Biophys. Acta - Bioenerg* 1817, 232–238. doi: 10.1016/j.bbabo.2011.05.005
- Wittig, I., Braun, H. P., and Schägger, H. (2006). Blue native PAGE. *Nat. Protoc.* 1, 418–428. doi: 10.1038/nprot.2006.62
- Yuan, S., Liu, W. J., Zhang, N. H., Wang, M. B., Liang, H. G., and Lin, H. H. (2005). Effects of water stress on major photosystem II gene expression and protein metabolism in barley leaves. *Physiol. Plant.* 125, 464–473. doi: 10.1111/j.1399-3054.2005.00577.x
- Zulfugarov, I. S., Tovuu, A., Eu, Y. J., Dogsom, B., Poudyal, R. S., Nath, K., et al. (2014). Production of superoxide from photosystem II in a rice (*Oryza sativa* L.) mutant lacking PsbS. *BMC Plant Biol.* 14:242. doi: 10.1186/s12870-014-0242-2



## OPEN ACCESS

EDITED BY  
Vasilij Goltsev,  
Sofia University, Bulgaria

REVIEWED BY  
Grażyna Mastalerczuk,  
Warsaw University of Life Sciences,  
Poland  
Abdallah Oukarroum,  
Mohammed VI Polytechnic University,  
Morocco

\*CORRESPONDENCE  
Kun Yan  
kyan@ldu.edu.cn;  
yankunacademic@163.com

†These authors have contributed  
equally to this work and share first  
authorship

SPECIALTY SECTION  
This article was submitted to  
Plant Abiotic Stress,  
a section of the journal  
Frontiers in Plant Science

RECEIVED 26 March 2022  
ACCEPTED 06 July 2022  
PUBLISHED 27 July 2022

CITATION  
Yan K, Mei H, Dong X, Zhou S, Cui J  
and Sun Y (2022) Dissecting  
photosynthetic electron transport  
and photosystems performance  
in Jerusalem artichoke (*Helianthus  
tuberosus* L.) under salt stress.  
*Front. Plant Sci.* 13:905100.  
doi: 10.3389/fpls.2022.905100

COPYRIGHT  
© 2022 Yan, Mei, Dong, Zhou, Cui and  
Sun. This is an open-access article  
distributed under the terms of the  
Creative Commons Attribution License  
(CC BY). The use, distribution or  
reproduction in other forums is  
permitted, provided the original  
author(s) and the copyright owner(s)  
are credited and that the original  
publication in this journal is cited, in  
accordance with accepted academic  
practice. No use, distribution or  
reproduction is permitted which does  
not comply with these terms.

# Dissecting photosynthetic electron transport and photosystems performance in Jerusalem artichoke (*Helianthus tuberosus* L.) under salt stress

Kun Yan<sup>1\*†</sup>, Huimin Mei<sup>2†</sup>, Xiaoyan Dong<sup>3</sup>, Shiwei Zhou<sup>1</sup>,  
Jinxin Cui<sup>1</sup> and Yanhong Sun<sup>4</sup>

<sup>1</sup>School of Agriculture, Ludong University, Yantai, China, <sup>2</sup>School of Life Sciences, Liaoning University, Shenyang, China, <sup>3</sup>CAS Key Laboratory of Coastal Environmental Processes and Ecological Remediation, Yantai Institute of Coastal Zone Research, Chinese Academy of Sciences (CAS), Yantai, China, <sup>4</sup>School of Environmental and Material Engineering, Yantai University, Yantai, China

Jerusalem artichoke (*Helianthus tuberosus* L.), a vegetable with medical applications, has a strong adaptability to marginal barren land, but the suitability as planting material in saline land remains to be evaluated. This study was envisaged to examine salt tolerance in Jerusalem artichoke from the angle of photosynthetic apparatus stability by dissecting the photosynthetic electron transport process. Potted plants were exposed to salt stress by watering with a nutrient solution supplemented with NaCl. Photosystem I (PSI) and photosystem II (PSII) photoinhibition appeared under salt stress, according to the significant decrease in the maximal photochemical efficiency of PSI ( $\Delta MR/MR_0$ ) and PSII. Consistently, leaf hydrogen peroxide ( $H_2O_2$ ) concentration and lipid peroxidation were remarkably elevated after 8 days of salt stress, confirming salt-induced oxidative stress. Besides photoinhibition of the PSII reaction center, the PSII donor side was also impaired under salt stress, as a K step emerged in the prompt chlorophyll transient, but the PSII acceptor side was more vulnerable, considering the decreased probability of an electron movement beyond the primary quinone (ETo/TRo) upon depressed upstream electron donation. The declined performance of entire PSII components inhibited electron inflow to PSI, but severe PSI photoinhibition was not averted. Notably, PSI photoinhibition elevated the excitation pressure of PSII (1-qP) by inhibiting the PSII acceptor side due to the negative and positive correlation of  $\Delta MR/MR_0$  with 1-qP and ETo/TRo, respectively. Furthermore, excessive reduction of PSII acceptors side due to PSI photoinhibition was simulated by applying a specific inhibitor blocking electron transport beyond primary quinone, demonstrating that PSII photoinhibition was actually accelerated by PSI photoinhibition under salt stress. In conclusion, PSII and PSI vulnerabilities were proven in Jerusalem artichoke under salt stress, and PSII inactivation, which

was a passive consequence of PSI photoinhibition, hardly helped protect PSI. As a salt-sensitive species, Jerusalem artichoke was recommended to be planted in non-saline marginal land or mild saline land with soil desalination measures.

#### KEYWORDS

chlorophyll fluorescence, delayed chlorophyll fluorescence, malondialdehyde, modulated 820 nm reflection, photoinhibition

## Introduction

As a major abiotic stress endangering agricultural production, soil salinity usually lies in farmland with irrational irrigation and saline land in inland arid and coastal regions (Nikalje et al., 2017). Under salt stress, plants are first confronted with osmotic stress and then have to endure ionic toxicity; however, the damages to biological macromolecules often resulted from the salt-induced excess generation of reactive oxygen species (ROS) in plant cells (Gill and Tuteja, 2010; Hossain and Dietz, 2016; Chen et al., 2018). In photosynthetic organisms, ROS can be considered a by-product of photosynthetic electron transport in the chloroplast (Asada, 2006; Gill and Tuteja, 2010; Foyer, 2018).

Photosynthetic electron transport from water to  $\text{NADP}^+$  is powered by photosystem II (PSII) and photosystem I (PSI), and this electron transport chain also involves other electron carriers such as oxygen-evolving complex, primary and secondary quinone ( $\text{Q}_\text{A}$  and  $\text{Q}_\text{B}$ ), and plastoquinone (PQ). In contrast to the equilibrium state of ROS in plants under normal growth condition, depressed  $\text{CO}_2$  assimilation will inhibit photosynthetic electron transport in a feedback way and then elevate excitation pressure in the chloroplast under abiotic stress (Murata et al., 2007; Takahashi and Murata, 2008; Zhang et al., 2014; Yan et al., 2015, 2018b). As a consequence, a great number of photosynthetic electrons tend to be transferred to  $\text{O}_2$  rather than  $\text{NADP}^+$  to generate superoxide anion ( $\text{O}_2^-$ ). Hydrogen peroxide ( $\text{H}_2\text{O}_2$ ) is generated from  $\text{O}_2^-$  through dismutation reaction, and then hydroxyl radical, the most dangerous ROS, may be synthesized by the Fenton reaction finally (Gill and Tuteja, 2010; Foyer, 2018). In addition, the

elevated excitation pressure can also cause greater production of singlet oxygen in PSII reaction centers (Foyer, 2018). The excess generation of these ROS may bring about PSII and PSI photoinhibition by impairing photosynthetic membrane proteins or lipids. In particular, Oukarroum et al. (2015) illustrated that PSI and PSII photochemical capacities were negatively correlated with ROS production. At present, salt-induced PSII photoinhibition has been extensively documented. Traditionally, PSII is considered more vulnerable than PSI under abiotic stresses, and rapid PSII photoinhibition can protect PSI by reducing ROS production at its acceptor side by restricting electron flow to PSI under light stress or high temperature (Yan et al., 2013a,b; Zivcak et al., 2014; Zhang et al., 2016). In contrast, limited restriction on PSII electron donation is liable to induce PSI photoinhibition under chilling stress (Zhang et al., 2011, 2014; Yang et al., 2014). PSI was also demonstrated to be a possible photoinhibition site under salt stress in our recent study, as PSII photoinhibition hardly prevented PSI photoinhibition in a salt-sensitive honeysuckle cultivar (Yan et al., 2015). Compared with PSII photoinhibition, PSI photoinhibition is more harmful in light of its difficult recovery (Sonoike, 2011), and particularly, PSI vulnerability poses a big threat to PSII by aggravating feedback inhibition at the PSII acceptor side. Therefore, PSII and PSI interaction is very important for plants to adapt to abiotic stress. To date, less attention has been paid to the salt tolerance of PSI than PSII, and moreover, PSII and PSI interaction remain largely unknown under salt stress. In other words, the characterization of photosynthetic electron transport has not been thoroughly dissected in plants under salt-induced oxidative stress, since PSII and PSI interaction relies on this electron transport process.

The Jerusalem artichoke (*Helianthus tuberosus* L.) is a vegetable native to North America. The Jerusalem artichoke can be used for medical applications and ethanol production because the tubers contain quantities of fructose and inulin (Baldini et al., 2004; Saengthongpinit and Saijaanantakul, 2005). In recent years, we have analyzed photosynthetic characteristics at various leaf expansion stages, verified PSII susceptibility to high temperature, and particularly demonstrated the sensitivity to waterlogging from aspects of PSI vulnerability and photosynthesis in Jerusalem artichoke

**Abbreviations:** ETo/TRo, the probability for an electron movement beyond primary quinone;  $g_s$ , stomatal conductance; MDA, malondialdehyde; Pn, photosynthetic rate; PSI, photosystem I; PSII, photosystem II; RC/ABS, primary quinone reducing reaction centers per PSII antenna chlorophyll; PQ, plastoquinone; REo/ETo, the probability with which an electron from the intersystem electron carriers is transferred to reduce end electron acceptors at the PSI acceptor side;  $\text{Q}_\text{A}$ , primary quinone; ROS, reactive oxygen species;  $V_k$ , variable fluorescence intensity at K step;  $\Delta\text{MR}/\text{MR}_0$ , the maximal photochemical capacity of PSI;  $\Phi\text{PSII}$ , actual photochemical efficiency of PSII; 1-qP, excitation pressure of PSII.



(Yan et al., 2012, 2013b, 2018b). Notably, Jerusalem artichoke has been selected for an attempt to utilize marginal land in the coastal zone in China, considering its high capacity to acclimate to barren soil (Long et al., 2016). It has been reported that salt stress can decrease CO<sub>2</sub> assimilation and induce oxidative injury with chlorophyll loss in Jerusalem artichoke (Long et al., 2009; Huang et al., 2012; Li et al., 2017). However, the stability of photosystems has not been paid enough attention in Jerusalem artichoke under salt-induced oxidative stress, let alone the characterization of photosynthetic electron transport.

A new technique has been recently developed to simultaneously detect prompt chlorophyll fluorescence (PF), modulated 820 nm reflection (MR), and delayed chlorophyll fluorescence (DF) (Goltsev et al., 2009; Strasser et al., 2010; Gao et al., 2014; Yan et al., 2018a). In this study, we aimed to investigate photosystems performance and interaction by analyzing the photosynthetic electron transport process in Jerusalem artichoke under salt-induced oxidative stress using this technique. This study can deeply unveil the mechanism of plant resistance to salt stress and may aid in the exploitation of marginal abandoned land.

## Materials and methods

### Plant material and treatment

In Laizhou Bay, China, Jerusalem artichoke tubers were gathered and cultivated in the room as in the previous study (Yan et al., 2018b). The tubers were planted in plastic pots (20 cm in diameter and 25 cm high) filled with vermiculite and cultured in an artificial climatic room (Qiushi, China). There was one tuber in each pot, and the vermiculite was kept wet by watering. The photon flux density, day/night temperature, and humidity were controlled at 400  $\mu\text{mol m}^{-2} \text{s}^{-1}$  (12 h/day from 07:00 to 19:00), 25/18°C, and 70% in the room, respectively. After 1 month, the germinated seedlings appeared, and their growth was ensured by daily watering with Hoagland nutrient solution (pH 5.7). After 1 month, 45 uniform seedling plants were chosen and divided into three groups. In the first group, the control plants were not subjected to NaCl stress. In the second group, plants were subjected to 100 mM NaCl stress. In the third group, plants were subjected to 200 mM NaCl stress. NaCl was added to the nutrient solution gradually by 50 mM step every day to the final treatment concentrations (100 and 200 mM) on the same day, and thereafter, the salt stress persisted for 8 days. During the salt treatment experiment, the solution was refreshed every 2 days, and before refreshing the solution, the culture substrate was thoroughly leached using the nutrient solution to avoid ion accumulation. The newest fully expanded leaves were sampled to measure physiological and biochemical parameters.

### Assay of Na<sup>+</sup>, H<sub>2</sub>O<sub>2</sub>, malondialdehyde, and relative water contents

Fresh leaf tissues were sampled for measuring MDA, H<sub>2</sub>O<sub>2</sub>, Na<sup>+</sup>, and relative water contents using colorimetric methods, and the detailed procedure was reported in our previous studies (Yan et al., 2015, 2018b).

### Test of gas exchange with modulated chlorophyll fluorescence

An open photosynthetic system (LI-6400XTR, Li-Cor, Lincoln, NE, United States) equipped with a fluorescence leaf chamber (6400-40 LCF, Li-Cor) was utilized, and the same measuring procedure in our previous study was adopted for measuring the photosynthetic rate (Pn) and stomatal conductance (g<sub>s</sub>) (Yan et al., 2018b). The actual photochemical efficiency of PSII ( $\Phi\text{PSII}$ ) and photochemical quenching coefficient were also recorded, and then PSII excitation pressure (1-qP) was calculated.

### Detection of prompt chlorophyll fluorescence, modulated 820 nm reflection transients, and delayed chlorophyll fluorescence

The detection of PF, DF, and MR transients was simultaneously conducted using a multifunctional plant efficiency analyzer (MPEA, Hansatech, Norfolk, United Kingdom) with the same illumination procedure as in our previous study (Yan et al., 2018a). According to Schansker et al. (2003) and Strasser et al. (2010), the maximal photochemical efficiencies of PSII (Fv/Fm) and PSI ( $\Delta\text{MR}/\text{MR}_0$ ), Q<sub>A</sub> reducing reaction centers per PSII antenna chlorophyll (RC/ABS), variable fluorescence intensity at K step (V<sub>k</sub>), the probability with which an electron moves beyond Q<sub>A</sub> (ETo/TRo), and from the intersystem electron carriers to reduce PSI end electron acceptors (REo/ETo) were calculated.

### Statistical analysis

One-way ANOVA was performed using SPSS 16.0 (SPSS Inc., Chicago, IL, United States) for all data, which are the average value from five replicate plants. The average value was compared through the LSD test. Regression analysis of  $\Delta\text{MR}/\text{MR}_0$  with 1-qP and ETo/TRo was also performed using SPSS 16.0.

## Results

### Lipid peroxidation, $\text{H}_2\text{O}_2$ , $\text{Na}^+$ , and relative water contents

The level of lipid peroxidation in plant tissues can be reflected by MDA content. After 8 days of 100 mM NaCl stress,  $\text{H}_2\text{O}_2$ , and MDA contents were significantly elevated by 48.89 and 14.86% in the leaves of Jerusalem artichoke, and the increase was up to 152.46 and 46.42% under 200 mM NaCl stress (Figures 1A,B). Leaf  $\text{Na}^+$  was significantly increased by 2.65- and 5.92-fold after 8 days of 100 and 200 mM NaCl stress, respectively (Figure 1C). Leaf relative water content remarkably decreased on day 8 under 100 and 200 mM NaCl stress, and there was no significant difference in leaf relative water content between the two salt treatments (Figure 1D).

### Photosynthetic rate, stomatal conductance, photosystem II actual quantum yield, and excitation pressure

After 2 days of 100 mM NaCl stress,  $\text{Pn}$ ,  $g_s$ , and  $\Phi\text{PSII}$  were significantly reduced, and the reduction was up to 52.51,

68.09, and 37.66% on day 8 (Figures 2A–C). In comparison, the reduction of  $\text{Pn}$ ,  $g_s$ , and  $\Phi\text{PSII}$  was far greater under 200 mM NaCl stress (Figures 2A–C). Under 100 mM NaCl stress, 1-qP was significantly elevated on day 2, and the elevation reached 27.67% on day 8, whereas the elevation of 1-qP was greater under 200 mM NaCl stress (Figure 2D).

### Prompt chlorophyll fluorescence, modulated 820 nm reflection transients, and delayed chlorophyll fluorescence

J and I steps indicate the accumulation of reduced  $\text{Q}_\text{A}$  and PQ (Schansker et al., 2003, 2005; Yan et al., 2013b). J and I steps obviously rose under salt stress on day 8, suggesting that PQ and  $\text{Q}_\text{A}$  re-oxidation were inhibited (Figure 3A). The occurrence of K step around 300  $\mu\text{s}$  suggests the injury on OEC at the PSII donor side (Oukarroum et al., 2013, 2016). After 8 days of 200 mM NaCl stress, the PSII donor side was damaged, as indicated by the occurrence of the K step (Figure 3A). In contrast, J and I steps were less elevated, and the K step did not appear under 100 mM NaCl stress (Figure 3A).

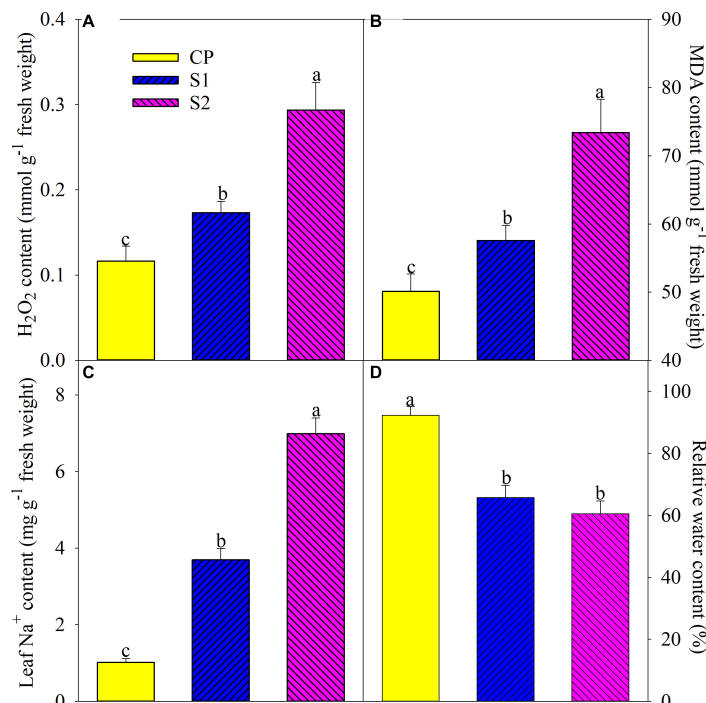


FIGURE 1

Changes in leaf  $\text{H}_2\text{O}_2$  (A), malondialdehyde (MDA) (B),  $\text{Na}^+$  (C), and relative water (D) contents in Jerusalem artichoke after 8 days of 100 and 200 mM NaCl stress. Data in the figure are the average value of five replicates ( $\pm\text{SD}$ ), and the different letters on error bars indicate remarkable differences among salt treatments at  $P < 0.05$ . CP, T1, and T2 indicate control plants, plants exposed to 100 and 200 mM NaCl, respectively, and these symbols are also used in the following figures.

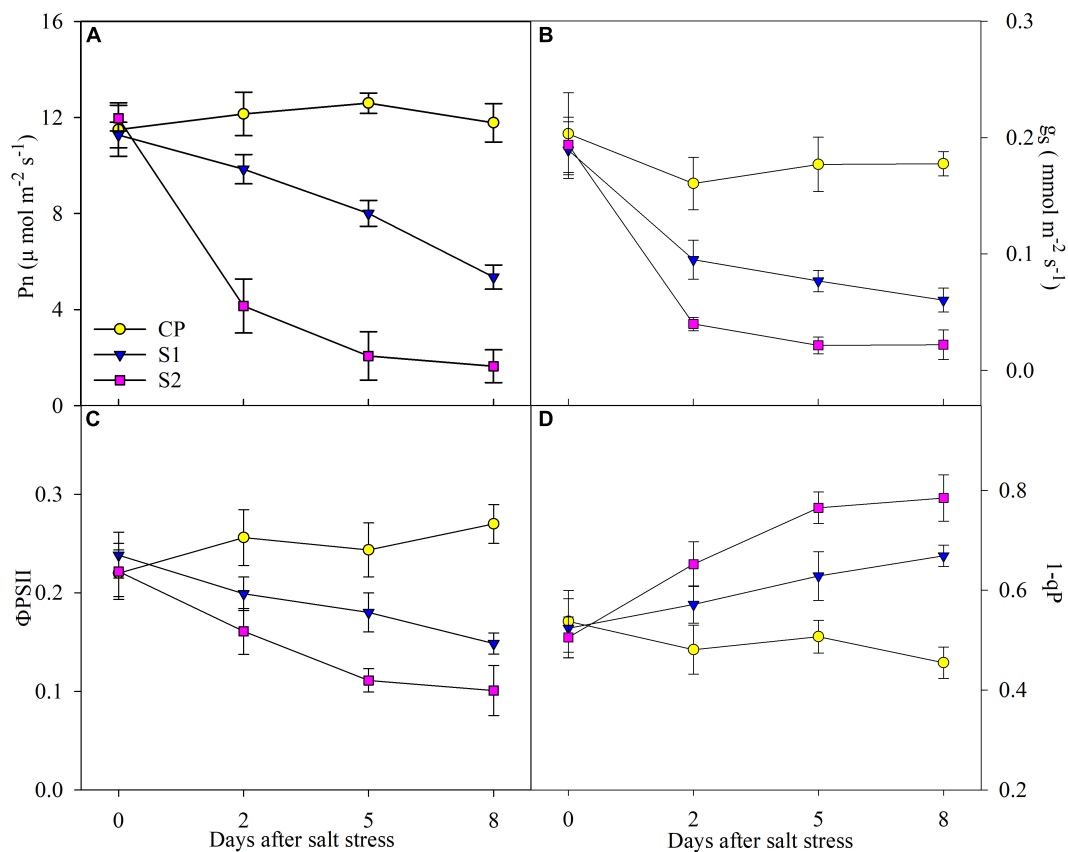


FIGURE 2

Changes in photosynthetic rate (Pn) (A), stomatal conductance ( $g_s$ ) (B), actual photochemical efficiency of photosystem II (PSII) ( $\Phi_{PSII}$ ) (C), and PSII excitation pressure (1-qP) (D) in Jerusalem artichoke under 100 and 200 mM NaCl stress. Data in the figure are the average value of five replicates ( $\pm$ SD), and the different letters on error bars indicate remarkable differences among salt treatments at  $P < 0.05$ .

During PSI oxidation,  $MR_0$  decreased to the minimal value ( $MR_{min}$ ). Subsequently, PSI re-reduction was initiated, and  $MR/MR_0$  increased to the maximal level ( $MR_{max}$ ). MR transient was remarkably changed by salt stress, as  $MR_0-MR_{min}$  and  $MR_{max}-MR_{min}$  significantly decreased (Figures 3C,D), suggesting the negative effect on both PSI oxidation and re-reduction, and the variations were greater in plants under 200 mM NaCl stress than 100 mM NaCl stress (Figures 3C,D). Under salt stress, DF transient was prominently suppressed in line with lowered  $I_1$  and  $I_2$  peaks, and obviously, the influence was less in plants under 100 mM NaCl stress than 200 mM NaCl stress (Figure 3B).

## Photosynthetic electron transport process

After 200 mM NaCl stress for 5 days,  $\Delta MR/MR_0$  and  $Fv/Fm$  were significantly reduced, and the reduction was up to 54.31 and 9.06% on day 8 (Figures 4A,B). After 8 days of 100 mM NaCl stress, the obvious decrease of 32.15 and 2.94%

appeared in  $\Delta MR/MR_0$  and  $Fv/Fm$ , respectively (Figures 4A,B). The greater decrease in  $\Delta MR/MR_0$  than  $Fv/Fm$  implied that PSI photoinhibition was more severe than PSII photoinhibition under NaCl stress. After 5 days of 200 mM NaCl stress,  $ET_o/Tro$ , and  $RE_o/ET_o$  significantly declined, while the marked decrease in them was not found until 8 days of 100 mM NaCl stress (Figures 4E,F). No obvious effect on  $V_k$  was noted under 100 mM NaCl stress, but it was significantly increased after 200 mM NaCl stress for 5 days (Figure 4C). Under salt stress, only a mild decrease was observed in  $RC/ABS$  (Figure 4D).

## The coordination between photosystem I and photosystem II

According to the regression analysis,  $\Delta MR/MR_0$  had a significant positive correlation with  $ET_o/Tro$ , whereas, the correlation between 1-qP and  $\Delta MR/MR_0$  was markedly negative (Figures 5A,C). DCMU functioned as a specific inhibitor for intervening electron transport from  $Q_A^-$  to  $Q_B^-$ , and  $Fv/Fm$  and  $ET_o/Tro$  were significantly decreased in plants applied with

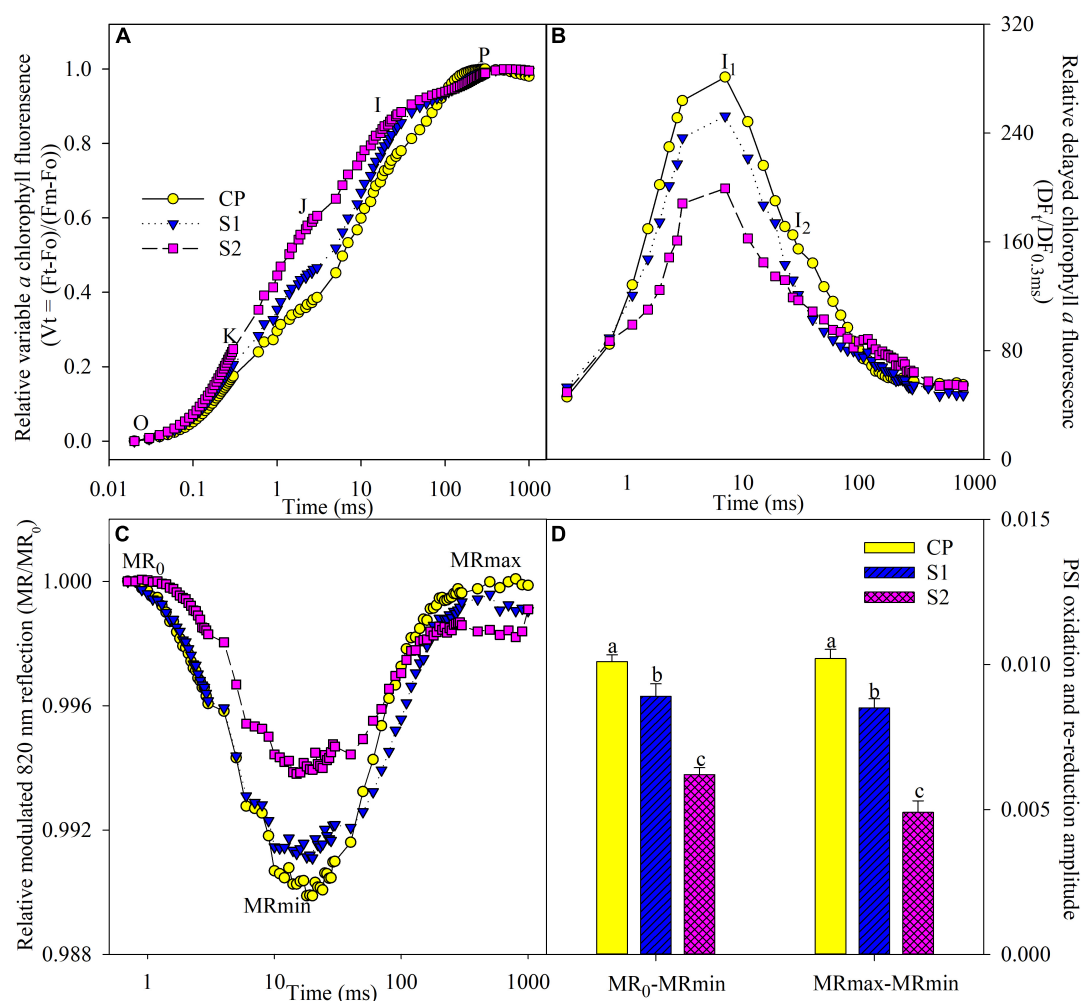


FIGURE 3

Transients of prompt chlorophyll fluorescence (A), delayed chlorophyll fluorescence (B), modulated 820 nm reflection (C), and photosystem I (PSI) oxidation and re-reduction amplitude (D) in Jerusalem artichoke after 8 days of 100 and 200 mM NaCl stress. The specific steps in chlorophyll fluorescence transient are O, K, J, I, and P. The value of modulated 820 nm at the onset of red light illumination [0.7 ms, the first reliable modulated reflection (MR) measurement] is  $MR_0$ . PSI oxidation and re-reduction amplitude were represented by  $MR_0 - MR_{min}$  and  $MR_{max} - MR_{min}$ , respectively. Data of  $MR_0 - MR_{min}$  and  $MR_{max} - MR_{min}$  indicate the average value of five replicates ( $\pm$ SD), and the different letters on error bars indicate significant differences at  $P < 0.05$ . In delayed chlorophyll fluorescence curves, D0, I1, I2, and D2 are the initial point, the first (7 ms) and second (50 ms) maximal peaks, and the minimum point. The initial microsecond delayed fluorescence signal at 0.3 ms is indicated by  $DF_{0.3ms}$ . The signals were plotted on a logarithmic timescale, and each curve is the mean of five replicate plants.

DCMU than those without DCMU application after 8 days of salt stress (Figures 5B,D).

## Discussion

As an ordinary finding, photosynthesis was depressed by salt stress in line with stomatal closure in Jerusalem artichoke (Figures 2A,B). The inhibited  $CO_2$  fixation can cause feedback inhibition on photosynthetic electron transport and accelerate ROS production as more photosynthetic electrons are diverged to oxygen (Gill and Tuteja, 2010; Foyer, 2018). Exactly, the elevated leaf lipid peroxidation

and  $H_2O_2$  concentration proved salt-induced oxidative stress on Jerusalem artichoke (Figures 1A,B). Elevated ROS generation in photosynthetic organisms is usually associated with the inhibited photosynthetic electron transport and can cause photosystems photoinhibition with oxidative damage to photosynthetic membranes lipids and proteins (Murata et al., 2007; Sonoike, 2011; Oukarroum et al., 2015). Therefore, photosystem photoinhibition seems to be a feasible proxy for the oxidative threat to the plant (Zhang et al., 2012, 2014; Yan et al., 2015, 2018b). Under salt stress,  $Na^+$  toxicity may induce more severe oxidative stress on photosystems than osmotic pressure (Muranaka et al., 2002; Allakhverdiev and Murata, 2008; Cha-um and Kirdmanee, 2010; Hossain et al., 2017). In



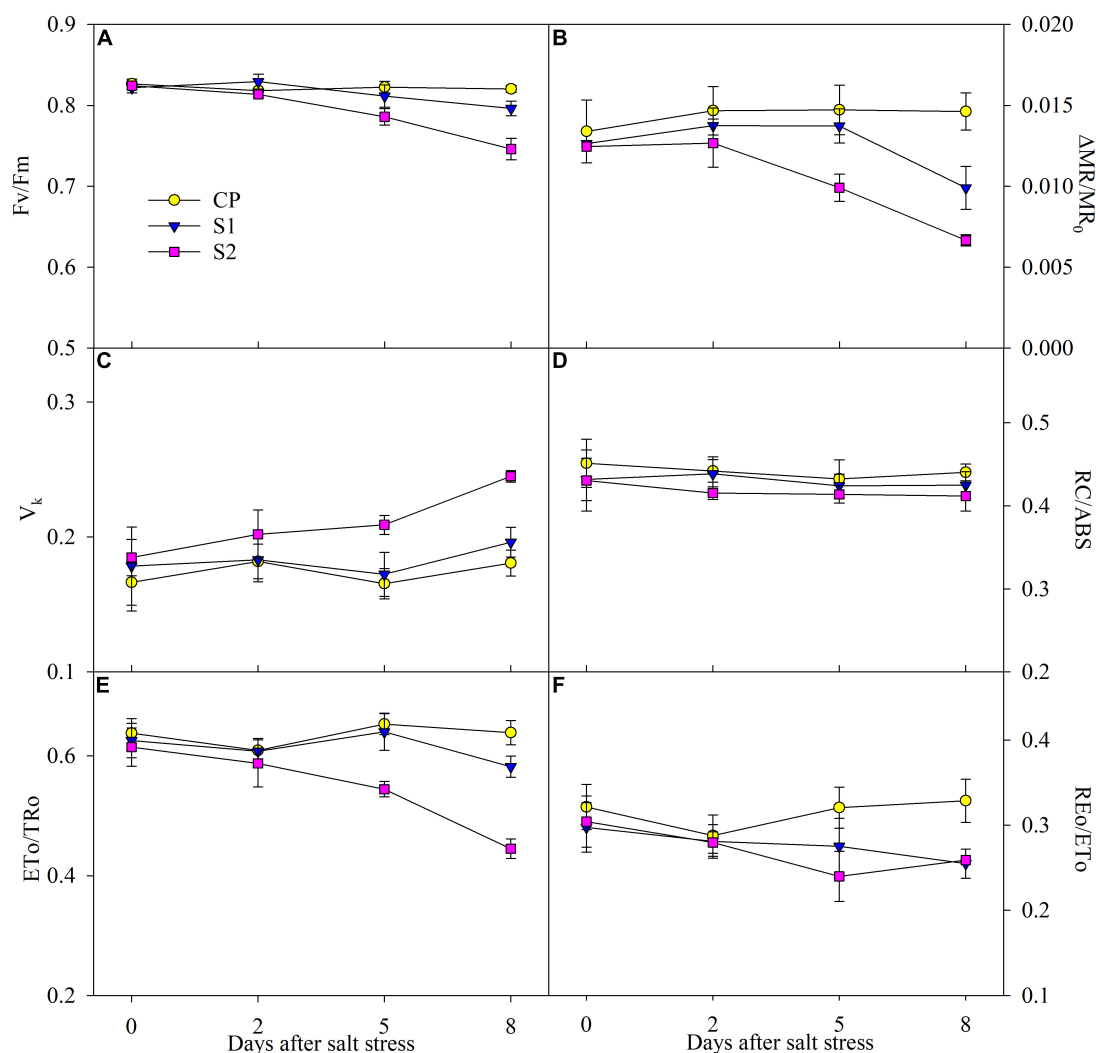


FIGURE 4

Changes in the maximal photochemical efficiency of photosystem II (PSII) ( $F_v/F_m$ ) (A), photosystem I (PSI) ( $\Delta MR/MR_0$ ) (B), variable fluorescence intensity at K step ( $V_k$ ) (C), primary quinone reducing reaction centers per PSII antenna chlorophyll (RC/ABS) (D), probability that an electron moves beyond primary quinone (ETo/TRo) (E), and probability with which an electron from the intersystem electron carriers is transferred to reduce end electron acceptors at the PSI acceptor side (REo/ETo) (F) in Jerusalem artichoke under 100 and 200 mM NaCl stress. Data in the figure are the average value of five replicates ( $\pm$ SD), and the different letters on error bars indicate remarkable differences among salt treatments at  $P < 0.05$ .

this study, leaf oxidative damage also resulted from  $Na^+$  toxicity rather than osmotic pressure to a greater extent, as severe lipid peroxidation appeared with greater leaf  $Na^+$  accumulation rather than leaf water deficit under salt stress with 200 mM NaCl than 100 mM NaCl (Figures 1C,D).

Consistent with leaf ROS burst, salt stress actually caused PSI and PSII photoinhibition according to the significantly lowered  $F_v/F_m$  and  $\Delta MR/MR_0$  in Jerusalem artichoke (Figures 4A,B). The classic proxy for the photochemical capability of the PSII reaction center,  $F_v/F_m$  rarely reflects PSII whole performance (Li et al., 2009). Under 200 mM NaCl stress, the elevated J step and declined ETo/TRo suggested the inhibited electron transport beyond  $Q_A$  with accumulated  $Q_A^-$ ,

while electron donation from the oxygen-evolving complex was also constrained due to the increased  $V_k$  (Figures 3A, 4C,E).  $I_1$  peak indicating the accumulation of  $S3Z^+P680Q_A^-$  can comprehensively reflect the state of the whole PSII, including active reaction centers and electron transporters at both donor and acceptor sides (Goltsev et al., 2009; Gao et al., 2014). Depressed  $I_1$  corroborated salt-induced damage on PSII (Figure 3B). The value of ETo/TRo is dependent not only on electrons transferred beyond  $Q_A$  but also on electrons donation from upstream electron carriers. Thus, the PSII acceptor side exhibited greater salt susceptibility than the reaction center and donor side in view of the significant reduction in ETo/TRo on the premise of lowered electron donation from the upstream

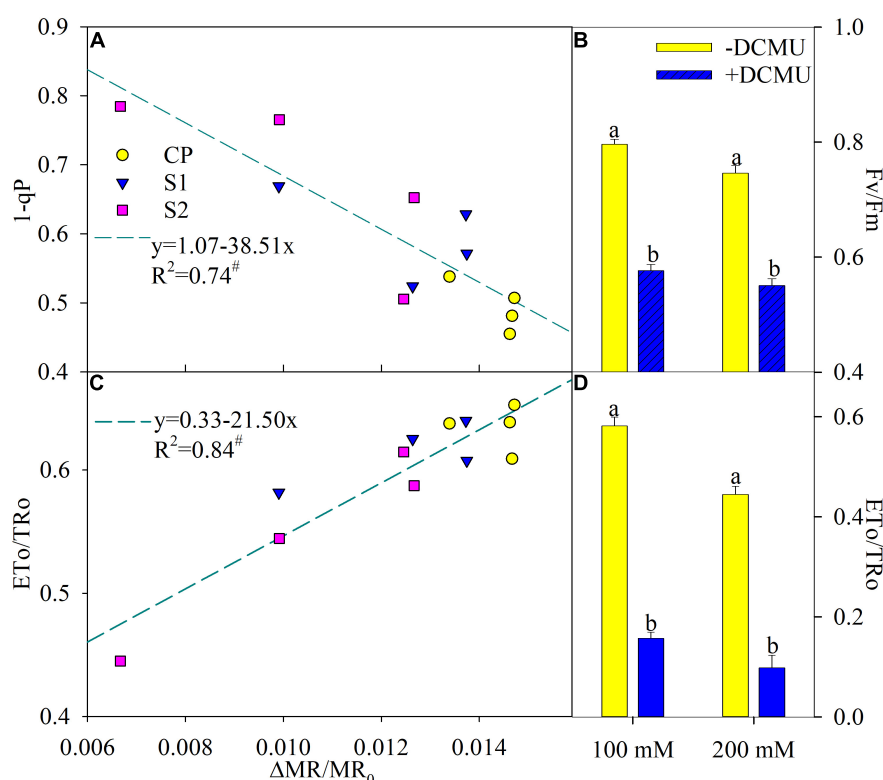


FIGURE 5

Regression of the maximal photochemical efficiency of photosystem II (PSII) ( $\Delta MR/MR_0$ ) with PSII excitation pressure (1-qP) (A) and probability that an electron moves beyond primary quinone (ETo/TRo) (C) in Jerusalem artichoke. The significant correlation at  $P < 0.05$  was indicated by #. Effects of applying DCMU on the maximal photochemical efficiency of PSII (Fv/Fm) (B) and ETo/TRo (D) in Jerusalem artichoke after 8 days of 100 and 200 mM NaCl stress. For reagent treatment, the leaves after 5 days of 100 and 200 mM NaCl stress were immersed in 0 or 70  $\mu M$  DCMU for 3 h in the dark. Data of Fv/Fm and ETo/TRo indicate the average value of five replicates ( $\pm SD$ ), and the different letters on error bars indicate remarkable differences between the leaves with and without DCMU treatment at  $P < 0.05$ .

under 200 mM NaCl stress. Consistently, the similar variations of ETo/TRo, Fv/Fm, and  $V_k$  under 100 mM NaCl stress also verified the greater susceptibility of the PSII acceptor side (Figures 4A,C,E). In addition, unchanged  $V_k$  and K step with lowered Fv/Fm under 100 mM NaCl stress suggested that salt sensitivity of the PSII donor side was lower than the PSII reaction center (Figures 4A,C). In summary, the salt sensitivity of PSII components gradually rose along with the direction of photosynthetic electron transport. The responses of whole PSII components also implied PSII vulnerability in Jerusalem artichoke under salt stress.

The declined PSII performance was consistent with the elevated PSII excitation pressure upon declined  $CO_2$  assimilation and restricted electron flow to PSI when photosynthesis reached a steady-state (Figures 2A,C,D). In MR transients, the lowered PSI re-reduction amplitude also suggested the restricted electron donation from PSII (Figures 3C,D). The restricted electron donation from PSII can help protect PSI against photoinhibition by decreasing the probability of ROS generation at the PSI acceptor side. However, PSI photoinhibition was never prevented under salt

stress and was even more severe than PSII photoinhibition, considering the greater decreased amplitude of  $\Delta MR/MR_0$  than Fv/Fm (Figures 4A,B). Limited electron inflow should improve PSI oxidation by blocking its re-reduction in MR transients; however, PSI oxidation was curtailed with decreased PSI oxidative amplitude, confirming that PSI encounters greater damage than PSII (Figures 3C,D). Because the reopening of PSII reaction centers is prolonged by electron transfer from reduced quinone to plastoquinone before the plastoquinone pool is fully reduced, an  $I_2$  phase appears in DF transient (Goltsev et al., 2009). Salt-induced decrease in  $I_2$  coincided with decreased REo/ETo and elevated I step, and all these changes pointed to that salt-induced PSI damage led to inhibition of PQ re-oxidation (Figures 3A,B, 4F). To summarize, PSI was more vulnerable to salt stress than PSII in Jerusalem artichoke, but in disagreement with the traditional viewpoint, PSII inactivation offered scarce protection to PSI.

In accordance with the negative correlation of  $\Delta MR/MR_0$  with 1-qP and the positive correlation of  $\Delta MR/MR_0$  with ETo/TRo (Figures 5A,C), PSI photoinhibition led to feedback inhibition on PSII electron outflow at the acceptor side and

then elevated exciting pressure of PSII in Jerusalem artichoke upon salt stress. In addition, over-reduction of PSII acceptor side due to PSI photoinhibition was simulated by the experiment of DCMU application, and the result demonstrated that PSII photoinhibition was actually accelerated by PSI photoinhibition in Jerusalem artichoke under salt stress (Figures 5B,D). Thus, salt-induced depression on PSII performance should be interpreted as a result of PSI photoinhibition, and the passive PSII inactivation was rarely capable of defending PSI oxidative injury. Invalid PSII and PSI interaction has been found with PSI vulnerability in sensitive plants under abiotic stress and can bring about detrimental effects on the entire photosynthetic apparatus (Zhang et al., 2014; Yan et al., 2018b). Accordingly, Jerusalem artichoke should be classified as a salt-sensitive plant.

## Conclusion

Photosystem II and PSI vulnerability to salt stress were illustrated in Jerusalem artichoke, and PSII inactivation, which was a passive consequence of PSI photoinhibition, hardly helped defend PSI. Given the salt sensitivity of Jerusalem artichoke, it is better to select non-saline marginal land for planting in agricultural practice, or the mild saline land in the coastal zone can also be used in combination with some desalination measures such as freshwater leaching and applying salt separation layer.

## Data availability statement

The raw data supporting the conclusions of this article will be made available by the authors, without undue reservation.

## References

- Allakhverdiev, S. I., and Murata, N. (2008). Salt stress inhibits photosystems II and I in cyanobacteria. *Photosynth. Res.* 98, 529–539. doi: 10.1007/s11120-008-9334-x
- Asada, K. (2006). Production and scavenging of reactive oxygen species in chloroplasts and their functions. *Plant Physiol.* 141, 391–396. doi: 10.1104/pp.106.082040
- Baldini, M., Danuso, F., Turi, M., and Vannozzi, P. (2004). Evaluation of new clones of Jerusalem artichoke (*Helianthus tuberosus* L.) for inulin and sugar yield from stalks and tubers. *Ind. Crop. Prod.* 19, 25–40. doi: 10.1016/S0926-6690(03)00078-5
- Cha-um, S., and Kirdmanee, C. (2010). Effects of water stress induced by sodium chloride and mannitol on proline accumulation, photosynthetic abilities and growth characters of eucalyptus (*Eucalyptus camaldulensis* Dehnh.). *New For.* 40, 349–360. doi: 10.1007/s11056-010-9204-1
- Chen, M., Yang, Z., Liu, J., Zhu, T., Wei, X., Fan, H., et al. (2018). Adaptation mechanism of salt excluders under saline conditions and its applications. *Int. J. Mol. Sci.* 19:3668. doi: 10.3390/ijms19113668
- Foyer, C. H. (2018). Reactive oxygen species, oxidative signaling and the regulation of photosynthesis. *Environ. Exp. Bot.* 154, 134–142. doi: 10.1016/J.ENVEXPBOT.2018.05.003
- Gao, J., Li, P., Ma, F., and Goltsev, V. (2014). Photosynthetic performance during leaf expansion in *Malus micromalus* probed by chlorophyll a fluorescence and modulated 820nm reflection. *J. Photochem. Photobiol. B Biol.* 137, 144–150. doi: 10.1016/J.JPHOTOBIO.2013.12.005
- Gill, S. S., and Tuteja, N. (2010). Reactive oxygen species and antioxidant machinery in abiotic stress tolerance in crop plants. *Plant Physiol. Biochem.* 48, 909–930. doi: 10.1016/J.PLAPHY.2010.08.016
- Goltsev, V., Zaharieva, I., Chernev, P., and Strasser, R. J. (2009). Delayed fluorescence in photosynthesis. *Photosynth. Res.* 101, 217–232. doi: 10.1007/S11120-009-9451-1
- Hossain, M. S., Alam, M. U., Rahman, A., Hasanuzzaman, M., Nahar, K., Al Mahmud, J., et al. (2017). Use of iso-osmotic solution to understand salt stress responses in lentil (*Lens culinaris* Medik.). *S. Afr. J. Bot.* 113, 346–354. doi: 10.1016/j.sajb.2017.09.007

## Author contributions

KY designed and performed the experiment and wrote the manuscript. HM, JC, and YS participated in the experiment. XD and SZ participated in the data analysis. All authors have read the manuscript and approved the final version of the manuscript.

## Funding

This study was jointly financed by the National Key Research and Development Project in China (2019YFD1002702), the Joint Funds of the National Natural Science Foundation of China (U2106214), and the Yantai Science and Technology Innovation Development Plan (2020MSGY065).

## Conflict of interest

The authors declare that the research was conducted in the absence of any commercial or financial relationships that could be construed as a potential conflict of interest.

## Publisher's note

All claims expressed in this article are solely those of the authors and do not necessarily represent those of their affiliated organizations, or those of the publisher, the editors and the reviewers. Any product that may be evaluated in this article, or claim that may be made by its manufacturer, is not guaranteed or endorsed by the publisher.

- Hossain, M. S., and Dietz, K. J. (2016). Tuning of redox regulatory mechanisms, reactive oxygen species and redox homeostasis under salinity stress. *Front. Plant Sci.* 7:548. doi: 10.3389/FPLS.2016.00548
- Huang, Z., Long, X., Wang, L., Kang, J., Zhang, Z., Zed, R., et al. (2012). Growth, photosynthesis and H<sup>+</sup>-ATPase activity in two Jerusalem artichoke varieties under NaCl-induced stress. *Process Biochem.* 47, 591–596. doi: 10.1016/J.PROCBIO.2011.12.016
- Li, L., Shao, T., Yang, H., Chen, M., Gao, X., Long, X., et al. (2017). The endogenous plant hormones and ratios regulate sugar and dry matter accumulation in Jerusalem artichoke in salt-soil. *Sci. Total Environ.* 578, 40–46. doi: 10.1016/J.SCITOTENV.2016.06.075
- Li, P. M., Cheng, L. L., Gao, H. Y., Jiang, C. D., and Peng, T. (2009). Heterogeneous behavior of PSII in soybean (*Glycine max*) leaves with identical PSII photochemistry efficiency under different high temperature treatments. *J. Plant Physiol.* 166, 1607–1615. doi: 10.1016/j.jplph.2009.04.013
- Long, X., Huang, Z., Zhang, Z., Li, Q., Zed, R., and Liu, Z. (2009). Seawater stress differentially affects germination, growth, photosynthesis, and ion concentration in genotypes of Jerusalem Artichoke (*Helianthus tuberosus* L.). *J. Plant Growth Regul.* 29, 223–231. doi: 10.1007/S00344-009-9125-4
- Long, X. H., Liu, L. P., Shao, T. Y., Shao, H. B., and Liu, Z. P. (2016). Developing and sustainably utilize the coastal mudflat areas in China. *Sci. Total Environ.* 569–570, 1077–1086. doi: 10.1016/J.SCITOTENV.2016.06.170
- Muranaka, S., Shimizu, K., and Kato, M. (2002). Ionic and osmotic effects of salinity on single-leaf photosynthesis in two wheat cultivars with different drought tolerance. *Photosynthetica* 40, 201–207. doi: 10.1023/A:1021337522431
- Murata, N., Takahashi, S., Nishiyama, Y., and Allakhverdiev, S. I. (2007). Photoinhibition of photosystem II under environmental stress. *Biochim. Biophys. Acta* 1767, 414–421. doi: 10.1016/J.BBABIO.2006.11.019
- Nikalje, G. C., Srivastava, A. K., Pandey, G. K., and Suprasanna, P. (2017). Halophytes in biosaline agriculture: mechanism, utilization, and value addition. *Land Degrad. Dev.* 29, 1081–1095. doi: 10.1002/LDR.2819
- Oukarroum, A., Bussotti, F., Goltsev, V., and Kalaji, H. M. (2015). Correlation between reactive oxygen species production and photochemistry of photosystems I and II in Lemna gibba L. plants under salt stress. *Environ. Exp. Bot.* 109, 80–88. doi: 10.1016/J.ENVEXPBOT.2014.08.005
- Oukarroum, A., El Madidi, S., and Strasser, R. J. (2016). Differential heat sensitivity index in barley cultivars (*Hordeum vulgare* L.) monitored by chlorophyll a fluorescence OKJIP. *Plant Physiol. Biochem.* 105, 102–108. doi: 10.1016/J.PLAPHY.2016.04.015
- Oukarroum, A., Goltsev, V., and Strasser, R. J. (2013). Temperature effects on pea plants probed by simultaneous measurements of the kinetics of prompt fluorescence, delayed fluorescence and modulated 820 nm reflection. *PLoS One* 8:e59433. doi: 10.1371/JOURNAL.PONE.0059433
- Saengthongpinit, W., and Saijaanantakul, T. (2005). Influence of harvest time and storage temperature on characteristics of inulin from Jerusalem artichoke (*Helianthus tuberosus* L.) tubers. *Postharvest Biol. Technol.* 37, 93–100. doi: 10.1016/J.POSTHARVIBIO.2005.03.004
- Schansker, G., Srivastava, A., Govindjee, and Strasser, R. J. (2003). Characterization of the 820-nm transmission signal paralleling the chlorophyll a fluorescence rise (OJIP) in pea leaves. *Funct. Plant Biol.* 30, 785–796. doi: 10.1071/FP03032
- Schansker, G., Toth, S. Z., and Strasser, R. J. (2005). Methylviologen and dibromothymoquinone treatments of pea leaves reveal the role of photosystem I in the Chl a fluorescence rise OJIP. *Biochim. Biophys. Acta* 1706, 250–261. doi: 10.1016/J.BBABIO.2004.11.006
- Sonoike, K. (2011). Photoinhibition of photosystem I. *Physiol. Plant.* 142, 56–64. doi: 10.1111/J.1399-3054.2010.01437.X
- Strasser, R. J., Tsimilli-Michael, M., Qiang, S., and Goltsev, V. (2010). Simultaneous in vivo recording of prompt and delayed fluorescence and 820 nm reflection changes during drying and after rehydration of the resurrection plant *Haberlea rhodopensis*. *Biochim. Biophys. Acta* 1797, 1313–1326. doi: 10.1016/J.BBABIO.2010.03.008
- Takahashi, S., and Murata, N. (2008). How do environmental stresses accelerate photoinhibition? *Trends Plant Sci.* 13, 178–182. doi: 10.1016/J.TPLANTS.2008.01.005
- Yan, K., Chen, P., Shao, H., Zhao, S., Zhang, L., Zhang, L., et al. (2012). Photosynthetic characterization of Jerusalem artichoke during leaf expansion. *Acta Physiol. Plant.* 34, 353–360. doi: 10.1007/s11738-011-0834-5
- Yan, K., Chen, P., Shao, H. B., Shao, C. Y., Zhao, S. J., and Brestic, M. (2013a). Dissection of photosynthetic electron transport process in sweet sorghum under heat stress. *PLoS One* 8:e62100. doi: 10.1371/JOURNAL.PONE.0062100
- Yan, K., Chen, P., Shao, H. B., and Zhao, S. J. (2013b). Characterization of photosynthetic electron transport chain in bioenergy crop Jerusalem artichoke (*Helianthus tuberosus* L.) under heat stress for sustainable cultivation. *Ind. Crop. Prod.* 50, 809–815. doi: 10.1016/J.INDCROP.2013.08.012
- Yan, K., Zhao, S., Cui, M., Han, G., and Wen, P. (2018b). Vulnerability of photosynthesis and photosystem I in Jerusalem artichoke (*Helianthus tuberosus* L.) exposed to waterlogging. *Plant Physiol. Biochem.* 125, 239–246. doi: 10.1016/J.PLAPHY.2018.02.017
- Yan, K., Han, G., Ren, C., Zhao, S., Wu, X., and Bian, T. (2018a). *Fusarium solani* infection depressed photosystem performance by inducing foliage wilting in apple seedlings. *Front. Plant Sci.* 9:479. doi: 10.3389/FPLS.2018.00479
- Yan, K., Wu, C., Zhang, L., and Chen, X. (2015). Contrasting photosynthesis and photoinhibition in tetraploid and its autodiploid honeysuckle (*Lonicera japonica* Thunb.) under salt stress. *Front. Plant Sci.* 6:227. doi: 10.3389/FPLS.2015.00227
- Yang, C., Zhang, Z. S., Gao, H. Y., Fan, X. L., Liu, M. J., and Li, X. D. (2014). The mechanism by which NaCl treatment alleviates PSI photoinhibition under chilling-light treatment. *J. Photochem. Photobiol. B Biol.* 140, 286–291. doi: 10.1016/J.PHOTOBIO.2014.08.012
- Zhang, L. T., Zhang, Z. S., Gao, H. Y., Meng, X. L., Yang, C., Liu, J. G., et al. (2012). The mitochondrial alternative oxidase pathway protects the photosynthetic apparatus against photodamage in Rumex K-1 leaves. *BMC Plant Biol.* 12:40. doi: 10.1186/1471-2229-12-40
- Zhang, Z. S., Jia, Y. J., Gao, H. Y., Zhang, L. T., Li, H. D., and Meng, Q. W. (2011). Characterization of PSI recovery after chilling-induced photoinhibition in cucumber (*Cucumis sativus* L.) leaves. *Planta* 234, 883–889. doi: 10.1007/S00425-011-1447-3
- Zhang, Z. S., Jin, L. Q., Li, Y. T., Tikkanen, M., Li, Q. M., Ai, X. Z., et al. (2016). Ultraviolet-B radiation (UV-B) relieves chilling-light-induced PSI photoinhibition and accelerates the recovery of CO<sub>2</sub> assimilation in cucumber (*Cucumis sativus* L.) leaves. *Sci. Rep.* 6:34455. doi: 10.1038/SREP34455
- Zhang, Z. S., Yang, C., Gao, H. Y., Zhang, L. T., Fan, X. L., and Liu, M. J. (2014). The higher sensitivity of PSI to ROS results in lower chilling-light tolerance of photosystems in young leaves of cucumber. *J. Photochem. Photobiol. B Biol.* 137, 127–134. doi: 10.1016/J.PHOTOBIO.2013.12.012
- Zivcak, M., Brestic, M., Kalaji, H. M., and Govindjee. (2014). Photosynthetic responses of sun- and shade-grown barley leaves to high light: Is the lower PSII connectivity in shade leaves associated with protection against excess of light? *Photosynth. Res.* 119, 339–354. doi: 10.1007/S11120-014-9969-8





## OPEN ACCESS

## EDITED BY

Marian Brestic,  
Slovak University of Agriculture,  
Slovakia

## REVIEWED BY

Stefan Timm,  
University of Rostock, Germany  
Xiangnan Li,  
Northeast Institute of Geography  
and Agroecology (CAS), China

## \*CORRESPONDENCE

Ying-Jie Yang  
yangyingjie@mail.kib.ac.cn  
Wei Huang  
huangwei@mail.kib.ac.cn

## SPECIALTY SECTION

This article was submitted to  
Plant Abiotic Stress,  
a section of the journal  
Frontiers in Plant Science

RECEIVED 11 April 2022

ACCEPTED 11 July 2022

PUBLISHED 03 August 2022

## CITATION

Sun H, Wang X-Q, Zeng Z-L, Yang Y-J  
and Huang W (2022) Exogenous  
melatonin strongly affects dynamic  
photosynthesis and enhances  
water-water cycle in tobacco.  
*Front. Plant Sci.* 13:917784.  
doi: 10.3389/fpls.2022.917784

## COPYRIGHT

© 2022 Sun, Wang, Zeng, Yang and  
Huang. This is an open-access article  
distributed under the terms of the  
[Creative Commons Attribution License](#)  
(CC BY). The use, distribution or  
reproduction in other forums is  
permitted, provided the original  
author(s) and the copyright owner(s)  
are credited and that the original  
publication in this journal is cited, in  
accordance with accepted academic  
practice. No use, distribution or  
reproduction is permitted which does  
not comply with these terms.

# Exogenous melatonin strongly affects dynamic photosynthesis and enhances water-water cycle in tobacco

Hu Sun<sup>1,2</sup>, Xiao-Qian Wang<sup>1,3</sup>, Zhi-Lan Zeng<sup>1,2</sup>,  
Ying-Jie Yang<sup>1\*</sup> and Wei Huang<sup>1\*</sup>

<sup>1</sup>Kunming Institute of Botany, Chinese Academy of Sciences, Kunming, China, <sup>2</sup>University of Chinese Academy of Sciences, Beijing, China, <sup>3</sup>School of Life Sciences, Northwest University, Xi'an, China

Melatonin (MT), an important phytohormone synthesized naturally, was recently used to improve plant resistance against abiotic and biotic stresses. However, the effects of exogenous melatonin on photosynthetic performances have not yet been well clarified. We found that spraying of exogenous melatonin (100  $\mu$ M) to leaves slightly affected the steady state values of CO<sub>2</sub> assimilation rate ( $A_N$ ), stomatal conductance ( $g_s$ ) and mesophyll conductance ( $g_m$ ) under high light in tobacco leaves. However, this exogenous melatonin strongly delayed the induction kinetics of  $g_s$  and  $g_m$ , leading to the slower induction speed of  $A_N$ . During photosynthetic induction,  $A_N$  is mainly limited by biochemistry in the absence of exogenous melatonin, but by CO<sub>2</sub> diffusion conductance in the presence of exogenous melatonin. Therefore, exogenous melatonin can aggravate photosynthetic carbon loss during photosynthetic induction and should be used with care for crop plants grown under natural fluctuating light. Within the first 10 min after transition from low to high light, photosynthetic electron transport rates (ETR) for  $A_N$  and photorespiration were suppressed in the presence of exogenous melatonin. Meanwhile, an important alternative electron sink, namely water-water cycle, was enhanced to dissipate excess light energy. These results indicate that exogenous melatonin upregulates water-water cycle to facilitate photoprotection. Taking together, this study is the first to demonstrate that exogenous melatonin inhibits dynamic photosynthesis and improves photoprotection in higher plants.

## KEYWORDS

melatonin, photosynthesis, fluctuating light, stomatal conductance, mesophyll conductance, photoprotection

## Introduction

Melatonin (MT) is an important hormone synthesized naturally in both plants and animals. Many recent studies have documented that MT is critical in several metabolic processes, including ROS scavenging systems (Siddiqui et al., 2020a,b), secondary metabolism (Farouk and Al-Amri, 2019; Jahan et al., 2020), and modulation of nitrogen metabolism (Qiao et al., 2019; Chen et al., 2021; Meng et al., 2021; Kaya et al., 2022). Therefore, MT plays a significant role in plants to cope with biotic and abiotic stresses (Arnao and Hernández-Ruiz, 2015, 2019, 2020). For example, MT promotes plant growth under harsh environmental conditions such as pollution of harmful elements (Farouk and Al-Amri, 2019; Kaya et al., 2019, 2022; Ahammed et al., 2020; Jahan et al., 2020; Seleiman et al., 2020; Hoque et al., 2021; Li S. et al., 2021; Bhat et al., 2022), heat (Ahammed et al., 2018; Jahan et al., 2019), low temperature (Bajwa et al., 2014; Li et al., 2018; Zhang et al., 2021), salinity (Liang et al., 2015; Qi et al., 2020; Siddiqui et al., 2020a), drought (Sharma and Zheng, 2019; Dai et al., 2020; Imran et al., 2021), high light (Ding et al., 2018; Lee and Back, 2018), ultraviolet radiation (Yao et al., 2021), and herbicides (Park et al., 2013; Giraldo Acosta et al., 2022). Therefore, MT is a plant master regulator with great potential for increasing crop yield in agriculture (Wang et al., 2018; Arnao and Hernández-Ruiz, 2019; Bose and Howlader, 2020). Spraying of melatonin to leaves with a moderate concentration of 100  $\mu$ M was usually used in previous studies, and the photosynthetic capacity was hardly affected by the spraying of MT (Jahan et al., 2020; Kaya et al., 2022). Naturally, plant growth is not only determined by the photosynthetic capacity but also can be affected by the dynamic photosynthesis under fluctuating light (Adachi et al., 2019; Kimura et al., 2020; Yamori et al., 2020). In nature, fluctuating light can affect plant growth by restricting photosynthesis. However, it is unclear whether the spraying of MT can affect the dynamic photosynthesis in healthy leaves. If the spraying of MT improves photosynthetic induction in crops, it can be used as a potential growth promoter. However, if the dynamic photosynthesis in higher plants is inhibited by the spraying of MT, MT should be used with care to avoid environmental pollution.

Under high light, stomatal conductance ( $g_s$ ) and mesophyll conductance ( $g_m$ ) are elevated to increase CO<sub>2</sub> diffusion from air to the sites of Rubisco carboxylation in chloroplasts and thus contribute to the high level of net CO<sub>2</sub> assimilation rate ( $A_N$ ) (Oguchi et al., 2003; Xiong et al., 2015, 2018; Ferroni et al., 2021). Under low light, relative low levels of  $g_s$  and/or  $g_m$  can satisfy the low  $A_N$  (Xiong et al., 2018; Qiao et al., 2020; Zhang et al., 2020). Most crop plants cultivated under natural field conditions usually experience dramatic fluctuations of illumination (Pearcy, 1990; Slattey et al., 2018). When light intensity increased abruptly, the low  $g_s$  and/or  $g_m$  restricted CO<sub>2</sub> diffusion rate and thus made  $A_N$  to be limited by the

low chloroplast CO<sub>2</sub> concentration (De Souza et al., 2020; Liu et al., 2022; Sun et al., 2022). Improved stomatal opening or increased  $g_s$  could significantly accelerate the response speed of  $A_N$  and thus enhance biomass production in fluctuating light (Kimura et al., 2020; Yamori et al., 2020). Under salinity or nitrogen deficiency conditions, the decreased induction speeds of  $g_s$  and  $g_m$  restricted  $A_N$  during photosynthetic induction, leading to the decline of biomass production under fluctuating light (Zhang et al., 2020; Sun et al., 2022). Therefore, if MT increases the induction speeds of  $g_s$  and  $g_m$ , it can be used as a growth promoter for crop plants under natural fluctuating light. In the other hand, if MT decreases the response kinetics of  $g_s$  and  $g_m$  under fluctuating light, MT should be used with care to prevent negative effect on plant growth. Therefore, it is necessary to clarify the effects of MT on dynamic changes in  $g_s$  and  $g_m$ .

When CO<sub>2</sub> assimilation is restricted under environmental stresses, the excess light energy should be finely dissipated harmlessly to avoid photodamage to photosystem I and II (PSI and PSII). For example, fluctuating light causes selective photoinhibition of PSI in angiosperms (Kono et al., 2014; Yamamoto et al., 2016; Huang et al., 2019a; Yamamoto and Shikanai, 2019). When light intensity abruptly increases, electron transport from PSII immediately increases (Sun et al., 2020b; Tan et al., 2021). This rapid change in PSII electron flow is accompanied by much slower kinetics of  $A_N$  (Yamamoto et al., 2016). The resulting PSI over-reduction produces reactive oxygen species within PSI and thus causes PSI photoinhibition (Yamamoto and Shikanai, 2019). Owing to the key role of PSI in regulation of photosynthetic electron flow, PSI photoinhibition strongly suppresses  $A_N$ , photoprotection and plant growth (Sejima et al., 2014; Brestic et al., 2015; Zivcak et al., 2015; Lima-Melo et al., 2019; Shimakawa and Miyake, 2019). Under high light, the inhibition of  $A_N$  increases the electron transfer from PSI to oxygen, resulting in the production of reactive oxygen species in chloroplast stroma (Takahashi and Murata, 2005, 2006). Reactive oxygen species inhibit the *de novo* synthesis of PSII proteins, primarily the D1 protein at the translation elongation step in *psbA* expression (Nishiyama et al., 2001, 2005). Under such conditions, the higher rate of PSII photodamage relative to PSII repair accelerates PSII photoinhibition (Murata et al., 2007). If moderate PSII photoinhibition occurred, the oxidation of water at PSII and linear electron flow would be suppressed, restricting regeneration of ATP and NADPH and thus impairing  $A_N$  and plant growth (Takahashi and Murata, 2008; Huang et al., 2018; Kaya et al., 2022).

Plants have several photoprotective mechanisms to deal with environmental stress (Takahashi and Badger, 2011; Allahverdiyeva et al., 2015; Shikanai and Yamamoto, 2017; Alboresi et al., 2019). In angiosperms, cyclic electron flow plays the key role in protecting PSI and PSII under excess light (Munekage et al., 2002, 2008; Takahashi et al., 2009;

Suorsa et al., 2012; Yamamoto and Shikanai, 2019). In addition, water-water cycle can significantly prevent PSI photoinhibition under fluctuating light (Huang et al., 2019b; Sun et al., 2020a; Yang et al., 2020) and protect PSII under high light (Asada, 1999, 2000; Hirotsu et al., 2004; Yi et al., 2014; Huang et al., 2016). During water-water cycle, electrons splitting from water are transported through photosynthetic electron transport chains and ultimately to oxygen. The resulting reactive oxygen species are converted into water by superoxide dismutase (SOD) and ascorbate peroxidase (APX). The operation of water-water cycle can dissipate excess light energy, increase  $\Delta pH$  formation and balance ATP/NADPH production ratio (Miyake, 2010; Shikanai and Yamamoto, 2017). Consequently, water-water cycle favors photosynthetic regulation when  $CO_2$  assimilation is restricted under harsh environmental conditions. As reported in previous studies, exogenous MT can increase the expression of SOD and APX in leaves of higher plants (Kaya et al., 2019; Jahan et al., 2020; Li X. et al., 2021). Because SOD and APX are the two key enzymes in charge of water-water cycle (Asada, 2000), the positive effect of exogenous MT on plant growth under environmental stresses might be related to the enhancement of water-water cycle. However, no study has investigated the effect of exogenous MT on the capacity of water-water cycle.

In the present study, we studied the effect of exogenous MT on dynamic photosynthetic performances in leaves of tobacco. The aims were to (1) understand whether exogenous MT is beneficial or detrimental to dynamic photosynthesis; and (2) explore whether exogenous MT enhances the capacity of water-water cycle. We found that spraying of exogenous MT strongly inhibited the dynamic photosynthesis in healthy leaves of tobacco, suggesting that abuse of MT can restrict the photosynthetic carbon gain under natural fluctuating light. Furthermore, exogenous MT upregulated water-water cycle to favor photoprotection especially when  $CO_2$  assimilation was restricted.

## Materials and methods

### Plant materials and treatments

Tobacco (*Nicotiana tabacum* cv. K326) plants were grown in an open field with full sunlight. Plants were grown in 19-cm plastic pots with humus soil (the initial soil nitrogen content was 2.1 mg/g). Plants were fertilized with Peters Professional's water solution (0.15 g N/plant every 2 days) and were watered every day to prevent any nutrient or water stress. After cultivation for 1 month, melatonin solution (MT, 100  $\mu M$ ) or water were sprayed to youngest fully developed leaves. This MT concentration was chosen based on previous studies (Kaya et al., 2019, 2022; Jahan et al., 2020). After spraying twice with the interval of 3 days, photosynthetic measurements were conducted. During the period of treatment, the day/night

air temperatures were approximately 30/20 °C, the relative air humidity was approximately 60–70%, and the maximum light intensity exposed to leaves was approximately 2,000  $\mu mol$  photons  $m^{-2} s^{-1}$ .

### Gas exchange and chlorophyll fluorescence measurements

Gas exchange and chlorophyll fluorescence were measured using a LI-6400XT coupled with a fluorometer (LI-6400-40; Li-Cor Inc., Lincoln, NE, United States). For all measurements, air temperature was approximately 25°C and the vapor pressure deficit was approximately 1.3 kPa. The flow rate within the chamber was set at 300  $mmol$  air  $min^{-1}$ . After pre-illumination at high light (1,500  $\mu mol$  photons  $m^{-2} s^{-1}$ , 90–10% red-blue light) and 400  $\mu mol$   $CO_2$   $mol^{-1}$  air to reach steady-state photosynthesis, leaves were exposed to low light (50  $\mu mol$  photons  $m^{-2} s^{-1}$ , 90–10% red-blue light) for 5 min to simulate natural shade-fleck. Afterward, photosynthetic induction phases were conducted again at high light (1,500  $\mu mol$  photons  $m^{-2} s^{-1}$ ), and the steady-state conditions were achieved after 30 min illumination.

During photosynthesis induction, the steady-state fluorescence ( $F_s$ ) and the maximum fluorescence ( $F_m'$ ) were measured for further analysis.  $F_m'$  was measured by application of a saturating white light flash of 8,000  $\mu mol$   $m^{-2} s^{-1}$ , and the quantum efficiency of photosystem II ( $\Phi_{PSII}$ ) was calculated as follows (Genty et al., 1989):

$$\Phi_{PSII} = \frac{(F_m' - F_s)}{F_m'}$$

The electron transport rate (ETR) through PSII was calculated as

$$ETR = \Phi_{PSII} \times PPFD \times \alpha \times \beta$$

where the PPFD value corresponded to the light intensity stated above, the typical value 0.45 was assumed for the product of  $\alpha \times \beta$  (Kaiser et al., 2017).

### Estimation of mesophyll conductance, chloroplast $CO_2$ concentration, and maximum velocity of rubisco for carboxylation

Based on the combination of gas exchange and ETR,  $g_m$  is calculated (Harley et al., 1992):

$$g_m = \frac{A_N}{C_i - \Gamma^* (ETR + 8(A_N + R_d)) / (ETR - 4(A_N + R_d))}$$

where  $A_N$  represents the area-based net  $CO_2$  assimilation rate and  $\Gamma^*$  represents the  $CO_2$  compensation point in the absence

of respiration (Farquhar et al., 1980; von Caemmerer and Evans, 2015). The average  $\Gamma^*$  for C3 species at 25°C, 41.2  $\mu\text{mol/mol}$  (Hermida-Carrera et al., 2016), was used in this study. In the current study, the day respiration rate ( $R_d$ ) was calculated as half of the dark respiration rate as measured after dark adaptation for 10 min (Carriqui et al., 2015).

Based on the estimated  $g_m$ , the chloroplast  $\text{CO}_2$  concentration ( $C_c$ ) was calculated (Long and Bernacchi, 2003; Warren and Dreyer, 2006):

$$C_c = C_i - \frac{A_N}{g_m}$$

The maximum velocity of Rubisco for carboxylation ( $V_{\text{cmax}}$ ) at steady-state conditions was calculated with following equation (Farquhar et al., 1980; Eyland et al., 2021):

$$V_{\text{cmax}} = \frac{(A_N + R_d)(C_i + K_m)}{(C_i - \Gamma^*)}$$

where  $K_m$  is the effective the Rubisco Michaelis–Menten constant for  $\text{CO}_2$  under 21%  $\text{O}_2$ , and the average value for C3 species at 25°C, 529.4  $\mu\text{mol mol}^{-1}$  (Hermida-Carrera et al., 2016; Eyland et al., 2021), was used in this study.

## Quantitative limitation analysis of assimilation rate

In general, photosynthesis can be limited by stomatal conductance, mesophyll conductance, and biochemical capacity. The relative photosynthetic limitations  $l_s$ ,  $l_m$ , and  $l_b$  represent the relative importance of stomatal conductance, mesophyll conductance, and biochemical capacity, respectively, in determining the observed value of  $A_N$ . The values of  $l_s$ ,  $l_m$ , and  $l_b$  were calculated using the following equations (Grassi and Magnani, 2005):

$$l_s = \frac{g_{\text{tot}}/g_s \times \partial A_N/C_c}{g_{\text{tot}} + \partial A_N/C_c}$$

$$l_m = \frac{g_{\text{tot}}/g_m \times \partial A_N/C_c}{g_{\text{tot}} + \partial A_N/C_c}$$

$$l_b = \frac{g_{\text{tot}}}{g_{\text{tot}} + \partial A_N/C_c}$$

where the total  $\text{CO}_2$  diffusion conductance ( $g_{\text{tot}}$ ) was calculated as  $1/g_{\text{tot}} = 1/g_s + 1/g_m$  (Grassi and Magnani, 2005), and the slope of the  $A_N$  vs.  $C_c$  response curve ( $\partial A_N/\partial C_c$ ) was calculated according to the method of Xiong et al. (2018).

## Analysis of photosynthetic electron transport

From gas exchange parameters, the ETR for Rubisco carboxylation and oxygenation ( $J_G$ )

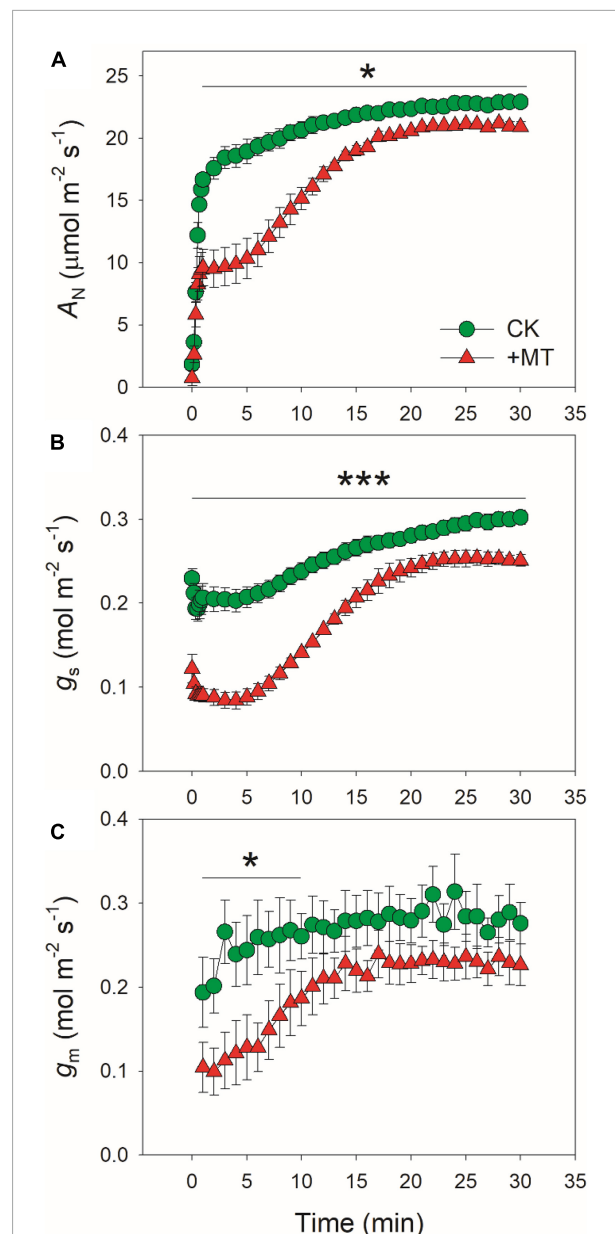


FIGURE 1

Effects of exogenous melatonin (MT, 100  $\mu\text{M}$ ) on the induction response of net  $\text{CO}_2$  assimilation rate [ $A_N$ , (A)], stomatal conductance [ $g_s$ , (B)], and mesophyll conductance [ $g_m$ , (C)] after transition from 50 to 1500  $\mu\text{mol photons m}^{-2} \text{s}^{-1}$ . Values are means  $\pm$  SE ( $n = 5$ ). Asterisk indicates a significant difference between CK and MT-treated leaves.

was calculated as follows (Zivcak et al., 2013; Walker et al., 2014):

$$J_G = \frac{4 \times (A_N + R_d) \times (C_i + 2\Gamma^*)}{(C_i - \Gamma^*)}$$

The alternative electron sink ( $J_A$ ) was calculated by subtracting  $J_G$  from ETR:

$$J_A = \text{ETR} - J_G$$



Because  $J_G$  represents the ETR for NADPH production, it was further divided into the two components devoted to RuBP carboxylation ( $J_C$ ) or RuBP oxygenation ( $J_O$ ) (Valentini et al., 1995):

$$J_C = \frac{1}{3} \times [J_G + 8 \times (A_N + R_d)]$$

$$J_O = \frac{2}{3} \times [J_G - 4 \times (A_N + R_d)]$$

where  $J_C$  indicates the rate of electron flow consumed by the Calvin-Benson cycle, and  $J_O$  indicates the rate of electron flow consumed by photorespiration.

## Statistical analysis

All data are displayed as mean values of five leaves from five independent plants. *T*-test was used to determine whether significant differences existed between different treatments ( $\alpha = 0.05$ ).

## Results

### Exogenous melatonin affects gas exchange during photosynthetic induction

The changing kinetics of  $A_N$ ,  $g_s$ , and  $g_m$  during photosynthetic induction were measured by transitioning from low light ( $50 \mu\text{mol photons m}^{-2} \text{s}^{-1}$ ) to high light ( $1,500 \mu\text{mol photons m}^{-2} \text{s}^{-1}$ ) (Figure 1). The initial values of  $A_N$  at low light were 1.8 and  $0.7 \mu\text{mol photons m}^{-2} \text{s}^{-1}$  in CK and MT-treated leaves, respectively. After this photosynthetic induction for 1 min,  $A_N$  rapidly increased to  $16.7 \mu\text{mol photons m}^{-2} \text{s}^{-1}$  in CK leaves but just increased to  $9.6 \mu\text{mol photons m}^{-2} \text{s}^{-1}$  in the MT-treated leaves (Figure 1A). After this photosynthetic induction for 5 and 10 min,  $A_N$  in CK leaves increased to 18.9 and  $20.7 \mu\text{mol photons m}^{-2} \text{s}^{-1}$ , respectively (Figure 1A). By comparison,  $A_N$  in MT-treated leaves increased to 10.3 and  $15.2 \mu\text{mol photons m}^{-2} \text{s}^{-1}$ , respectively (Figure 1A). Therefore, the induction of  $A_N$  after transition from low light was largely delayed by the application of exogenous melatonin. After illumination at high light for 30 min,  $A_N$  reached 22.9 and  $20.9 \mu\text{mol photons m}^{-2} \text{s}^{-1}$  in CK and MT-treated leaves, respectively (Figure 1A), indicating that exogenous melatonin just slightly affected the steady-state  $A_N$  in tobacco leaves.

Because the induction kinetics of  $A_N$  under fluctuating light is largely affected by  $g_s$  and  $g_m$ , we further analyzed the effects of exogenous melatonin on the changing kinetics of  $g_s$  and  $g_m$  during photosynthetic induction. Under low light,  $g_s$  was much lower in the MT-treated leaves when compared with the CK

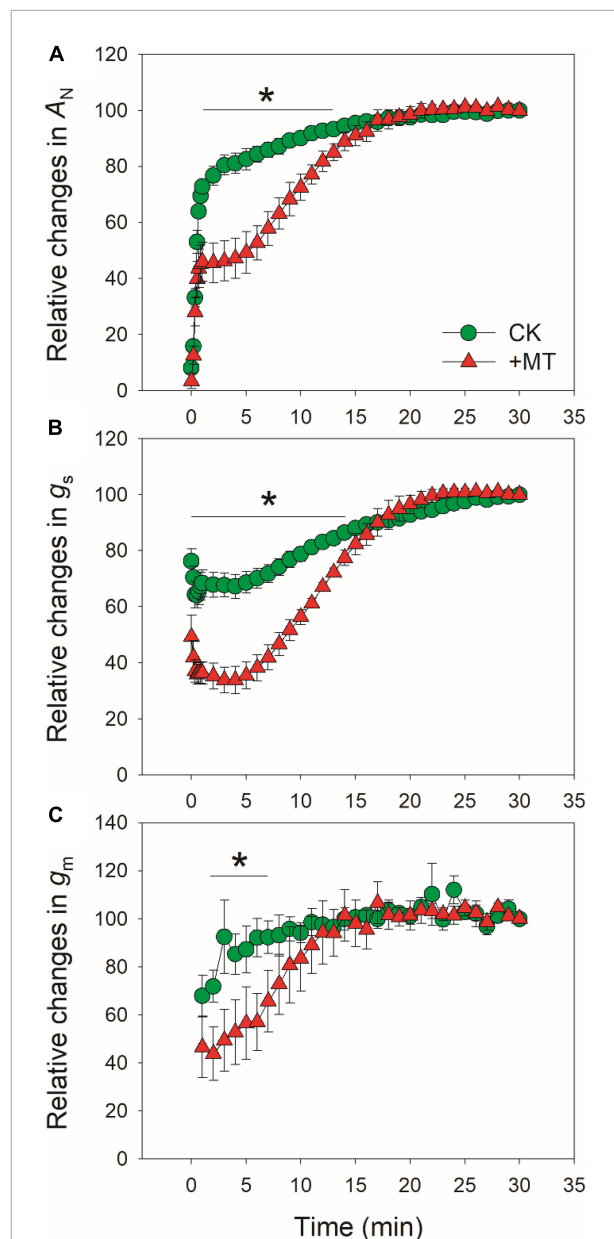


**FIGURE 2**  
Effects of exogenous melatonin (MT,  $100 \mu\text{M}$ ) on the relative changes in  $A_N$  (A),  $g_s$  (B), and  $g_m$  (C) after transition from 50 to  $1500 \mu\text{mol photons m}^{-2} \text{s}^{-1}$ . Values are means  $\pm$  SE ( $n = 5$ ). Asterisk indicates a significant difference between CK and MT-treated leaves.

leaves (Figure 1B). Within the first 5 min after photosynthetic induction,  $g_s$  in CK leaves was two-fold than that in the MT-treated leaves (Figure 1B). After photosynthetic induction for 10 min,  $g_s$  reached  $0.24$  and  $0.14 \text{ mol m}^{-2} \text{s}^{-1}$  in CK and MT-treated leaves, respectively (Figure 1B). Consistently, the transpiration rate within the first minutes after light increased was also lower in the MT-treated leaves than CK leaves (Supplementary Figure 1). Therefore, exogenous melatonin not

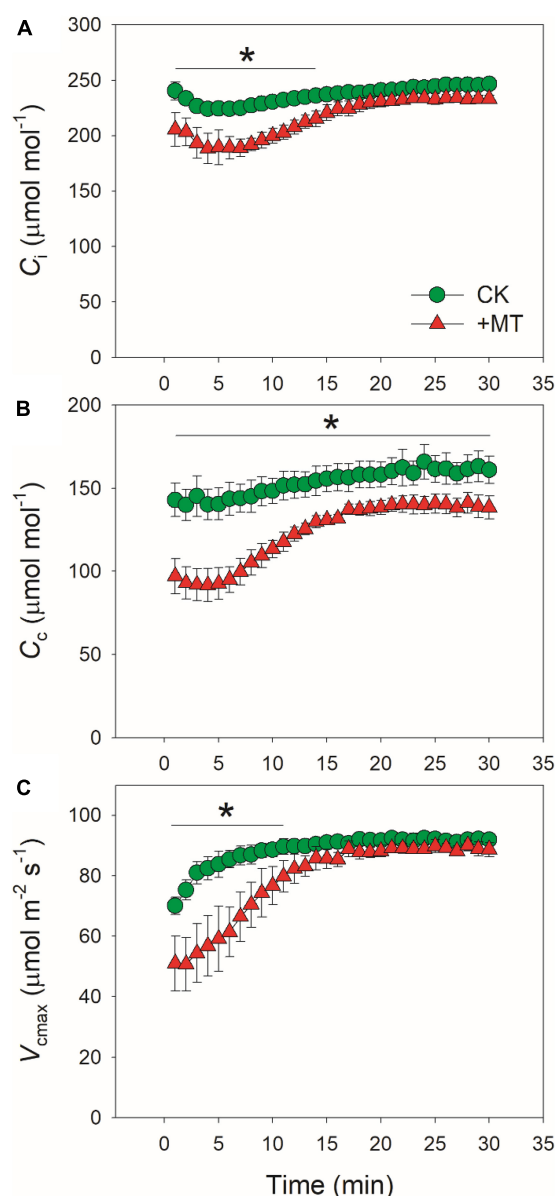


**FIGURE 3**  
Effects of exogenous melatonin (MT, 100  $\mu\text{M}$ ) on the induction response of intercellular  $\text{CO}_2$  concentration [ $C_i$ , (A)], chloroplast  $\text{CO}_2$  concentration [ $C_c$ , (B)], and the maximum velocity of Rubisco for carboxylation [ $V_{cmax}$ , (C)] after transition from 50 to 1500  $\mu\text{mol photons m}^{-2} \text{s}^{-1}$ . Values are means  $\pm$  SE ( $n = 5$ ). Asterisk indicates a significant difference between CK and MT-treated leaves.

only lowered  $g_s$  under low light but also delayed the stomatal opening under fluctuating light. After photosynthetic induction for 30 min, the values for  $g_s$  were 0.30 and 0.25  $\text{mol m}^{-2} \text{s}^{-1}$  in CK and MT-treated leaves, respectively (Figure 1B), suggesting the slight effect of exogenous melatonin on steady-state  $g_s$ . Similar to the performance of  $g_s$ , the MT-treated leaves showed significantly lower  $g_m$  than CK leaves within the first 5 min

after transition to high light (Figure 1C). However, the steady-state value of  $g_m$  was just slightly affected by the application of exogenous melatonin (Figure 1C).

After standardization against the maximum values after 30 min photosynthetic induction at high light, the relative changes in  $A_N$ ,  $g_s$ , and  $g_m$  after transition from low to high were analyzed (Figure 2). The time required to reach 80% of the maximum  $A_N$  was approximately 3 min in CK leaves, which was much shorter than that in the MT-treated leaves (12 min) (Figure 2A). Similarly, the time required to reach 70% of the maximum  $g_s$  was much lower in CK leaves (6 min) than in the MT-treated leaves (13 min) (Figure 2B). The increase in relative  $g_m$  was faster than  $g_s$  in both the CK and MT-treated leaves. However, the time required to reach 90% of the maximum  $g_m$  was much lower in CK leaves (3 min) than in the MT-treated leaves (12 min) (Figure 2C). These results indicated that the induction speeds of  $A_N$ ,  $g_s$ , and  $g_m$  during photosynthetic induction were largely delayed upon the application of exogenous melatonin.

## Exogenous melatonin alters photosynthetic limitations during photosynthetic induction

Because  $\text{CO}_2$  diffusion conductance determines photosynthesis through affecting intercellular ( $C_i$ ) and chloroplast  $\text{CO}_2$  concentration ( $C_c$ ), we calculated the response kinetics of  $C_i$  and  $C_c$  using  $A_N$ ,  $g_s$  and  $g_m$ . During the initial 10 min after transition to high light,  $C_i$  and  $C_c$  were much lower in the MT-treated leaves when compared with CK leaves (Figures 3A,B). Therefore, the delayed induction kinetics of  $g_s$  and  $g_m$  in the MT-treated leaves led to the lowering of  $C_c$  under fluctuating light. Furthermore, the maximum velocity of Rubisco carboxylation ( $V_{cmax}$ ) was inhibited by the exogenous melatonin (Figure 3C), suggesting that the activation state of Rubisco was also decreased by the exogenous melatonin. During photosynthetic induction, the relative limitations of  $A_N$  by  $g_s$  ( $l_s$ ),  $g_m$  ( $l_m$ ), and biochemical factors ( $l_b$ ) changed slightly in CK plants (Figure 4). By comparison,  $l_s$  gradually decreased and  $l_b$  gradually increased in the MT-treated leaves. As shown in Figure 4D, the value of  $(l_s + l_m)/l_b$  was almost lower than 1.0 in CK leaves, indicating that  $l_b$  was the major limiting factor of  $A_N$  after transition from low to high light. In contrast, the value of  $(l_s + l_m)/l_b$  in the MT-treated leaves was higher than 1.0 within the initial 10 min of photosynthetic induction (Figure 4D), pointing out that during this period  $A_N$  was mainly limited by diffusional conductance. Therefore, exogenous melatonin altered the relative limitations of  $A_N$  during photosynthetic induction. This conclusion was further supported by the ratios of  $V_{cmax}$  and ETR to gross  $\text{CO}_2$  assimilation rate ( $A_N + R_d$ ). During photosynthetic induction,  $V_{cmax}/(A_N + R_d)$  and  $\text{ETR}/(A_N + R_d)$  were maintained stable in CK leaves (Figure 5). However, the MT-treated leaves had

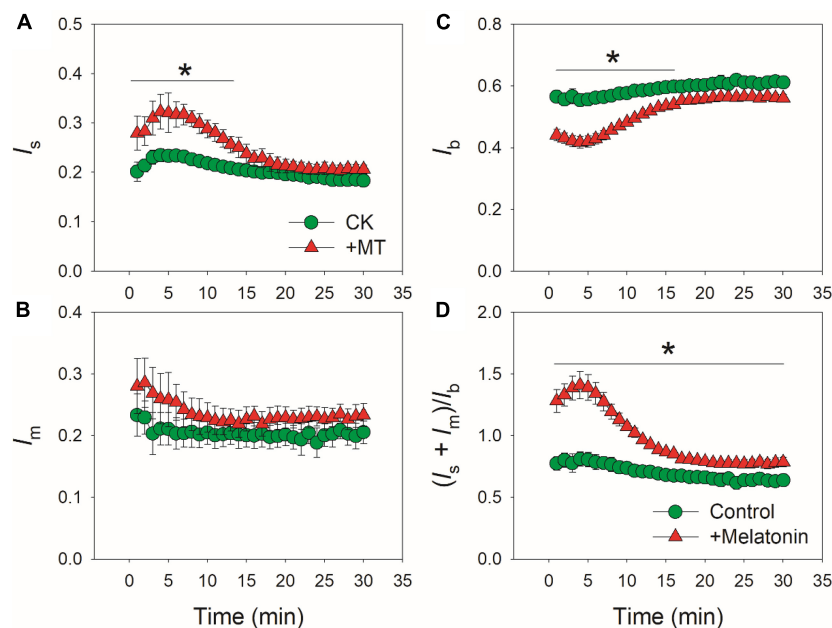


FIGURE 4

Effects of exogenous melatonin (MT, 100  $\mu\text{M}$ ) on the induction response of the relative limitations of  $g_s$  [ $l_s$ , (A)],  $g_m$  [ $l_m$ , (B)], biochemical factors [ $l_b$ , (C)] and the ratio of  $(l_s + l_m)/l_b$  (D) imposed to photosynthesis after transition from 50 to 1500  $\mu\text{mol photons m}^{-2} \text{s}^{-1}$ . Values are means  $\pm$  SE ( $n = 5$ ). Asterisk indicates a significant difference between CK and MT-treated leaves.

higher values of  $V_{cmax}/(A_N + R_d)$  and  $\text{ETR}/(A_N + R_d)$  during the initial 10 min of photosynthetic induction (Figure 5). After fully photosynthetic induction, the CK and MT-treated leaves showed similar values of  $V_{cmax}/(A_N + R_d)$  and  $\text{ETR}/(A_N + R_d)$  (Figure 5). These results indicated that during photosynthetic induction the limitations of Rubisco activity and electron flow imposed to  $A_N$  were lowered in the MT-treated leaves compared with CK leaves.

## Exogenous melatonin enhances the capacity of alternative electron sinks

When  $\text{CO}_2$  was restricted under fluctuating light, alternative electron sinks might protect photosynthetic apparatus against photoinhibition. We analyzed the response kinetics of total PSII ETR, ETR for Rubisco carboxylation ( $J_C$ ), for Rubisco oxygenation ( $J_O$ ), and for alternative sinks ( $J_A$ ) (Figure 6). After transition from low to high light, CK and MT-treated leaves showed similar values of ETR (Figure 6A). However, the MT-treated leaves showed much lower  $J_C$  and  $J_O$  during the initial phase of photosynthetic induction (Figures 6B,C). Concomitantly,  $J_A$  was increased in the MT-treated leaves (Figure 6D). The maximum  $J_A$  in CK and the MT-treated leaves were 48.6 and 74.5  $\mu\text{mol electrons m}^{-2} \text{s}^{-1}$ , respectively. During photosynthetic induction,  $J_A$  in the MT-treated leaves was maintained at high levels in the initial 6 min but

subsequently decreased gradually. By comparison,  $J_A$  in CK leaves was maintained stable. Therefore, the MT-treated leaves had a higher  $J_A$  to compensate for the restriction of  $J_C$  and  $J_O$  during the initial phase of photosynthetic induction. After fully photosynthetic induction for 30 min, CK and the MT-treated leaves showed similar ETR. However, a higher  $J_A$  was observed in the MT-treated leaves. These results strongly indicated that exogenous melatonin enhanced the capacity of  $J_A$  without altering the total ETR.

## Discussion

Recently, melatonin has been used as a plant master regulator for improving resistance to abiotic stresses (Wang et al., 2018; Arnao and Hernández-Ruiz, 2019). Generally, exogenous melatonin has the potential to modulate oxidative activity, nitrogen metabolism, secondary metabolism under these stresses, leading to the improvement of plant growth under abiotic and biotic stresses (Kaya et al., 2019, 2022; Ahammed et al., 2020; Jahan et al., 2020; Yao et al., 2021). Spraying of melatonin to the leaves is one of the most popular methods used in agriculture (Kaya et al., 2019, 2022; Jahan et al., 2020). This measure gives rise a question that whether exogenous melatonin has side effects on photosynthesis on healthy leaves. Furthermore, in view of evolutionary story of plants, it is surprising that why melatonin is not highly expressed in wild

plants to enhance their resistance to environmental stresses. A possible explanation is that the content of melatonin in leaves should be controlled to a moderate level to avoid side effect on photosynthesis (Arnao and Hernández-Ruiz, 2015, 2019). However, the effects of exogenous melatonin on photosynthesis in higher plants have not yet been well known.

Under natural field conditions, plants usually experience fluctuations of light intensity on timescales of seconds, minutes, and hours owing to cloud, wind, and shading from upper leaves (Valladares et al., 1997; Slaterry et al., 2018). In this study, we investigated the effects of exogenous melatonin on gas exchange and photosynthetic electron flow in tobacco plants grown under natural fluctuating light conditions. We found that the maximum  $A_N$  at  $1,500 \mu\text{mol photons m}^{-2} \text{s}^{-1}$  was similar between the CK and MT-treated leaves (Figure 1A), indicating that the spraying of moderate concentration of melatonin ( $100 \mu\text{M}$ ) to the leaves hardly affected the steady-state photosynthetic capacity in tobacco. However, exogenous melatonin strongly affected photosynthesis during the photosynthetic induction (Figure 1A). For example, after transitioning from 50 to  $1500 \mu\text{mol photons m}^{-2} \text{s}^{-1}$  for 1 min,  $A_N$  increased to  $16.7 \mu\text{mol CO}_2 \text{ m}^{-2} \text{s}^{-1}$  in CK leaves but just increased to  $9.6 \mu\text{mol CO}_2 \text{ m}^{-2} \text{s}^{-1}$  in the MT-treated leaves. During prolonged illumination at high light for 10 min,  $A_N$  increased to  $20.7 \mu\text{mol CO}_2 \text{ m}^{-2} \text{s}^{-1}$  in CK leaves but just increased to  $15.2 \mu\text{mol CO}_2 \text{ m}^{-2} \text{s}^{-1}$  in the MT-treated leaves. Therefore, during the initial 10 min of photosynthetic induction, exogenous melatonin strongly decreased the photosynthetic carbon gain of tobacco leaves. Recent studies have documented that the rate of photosynthetic induction is an important factor affecting carbon gain and plant growth when plants grown under natural and artificial fluctuating light (Kaiser et al., 2020; Kimura et al., 2020; Yamori et al., 2020). Accelerated induction speed of  $A_N$  significantly enhanced biomass production in *Arabidopsis thaliana* and rice under fluctuating light (Kimura et al., 2020; Sakoda et al., 2020; Yamori et al., 2020). In tomato (*Lycopersicon esculentum*) plants treated with moderate salinity ( $80 \text{ mM NaCl}$ ), the induction speed of  $A_N$  was lowered, impairing plant growth and reducing biomass production under fluctuating light (Zhang et al., 2020). Therefore, spraying of exogenous melatonin to leaves might impair the plant growth of crops cultivated under natural fluctuating light conditions.

The induction speed of  $A_N$  can be affected by diffusional conductance ( $g_s$  and  $g_m$ ) and biochemical factors ( $V_{\text{cmax}}$  and ETR) (Kaiser et al., 2017, 2020; Acevedo-Siaca et al., 2020; De Souza et al., 2020; Sakoda et al., 2021; Liu et al., 2022). We found that the MT-treated leaves displayed much lower  $g_s$  during initial 10 min of photosynthetic induction (Figure 1B), and  $g_s$  required more time to reach the maximum value in the MT-treated leaves compared with CK leaves (Figure 2B). Furthermore, induction speed of  $g_m$  was also delayed in the MT-treated leaves (Figures 1C, 2C). Such lowering of  $g_s$  and  $g_m$

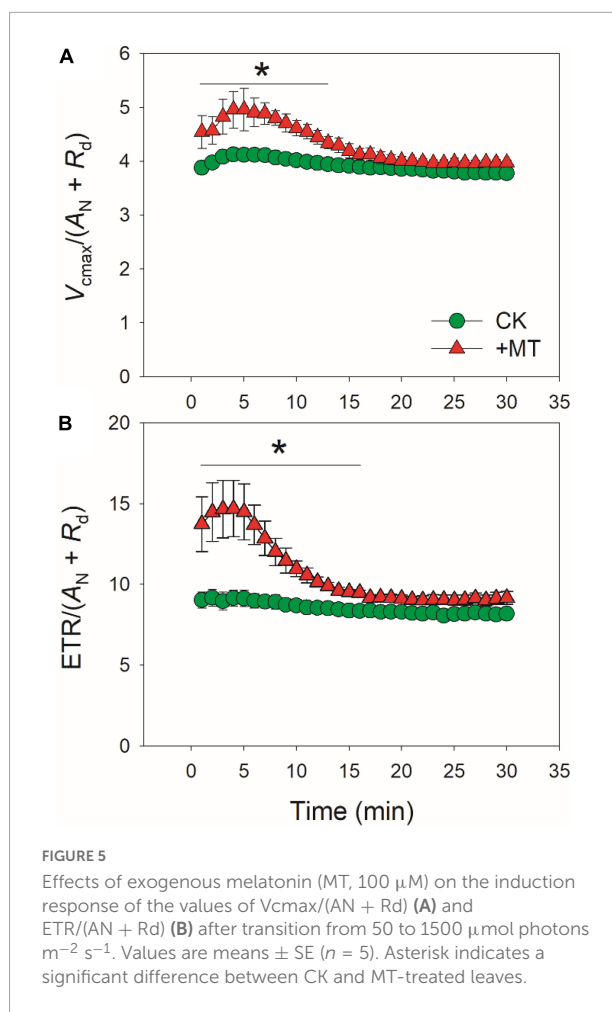


**FIGURE 5**  
Effects of exogenous melatonin (MT,  $100 \mu\text{M}$ ) on the induction response of the values of  $V_{\text{cmax}}/(A_N + R_d)$  (A) and  $\text{ETR}/(A_N + R_d)$  (B) after transition from 50 to  $1500 \mu\text{mol photons m}^{-2} \text{s}^{-1}$ . Values are means  $\pm$  SE ( $n = 5$ ). Asterisk indicates a significant difference between CK and MT-treated leaves.

decreased  $C_i$  and  $C_c$  during the initial phase of photosynthetic induction (Figure 3). Although the induction speed of  $V_{\text{cmax}}$  was lowered by exogenous melatonin (Figure 3C), the MT-treated leaves showed higher values of  $V_{\text{cmax}}/(A_N + R_d)$  during the initial phase of photosynthetic induction (Figure 5A), suggesting that exogenous melatonin did not increase the limitation of  $V_{\text{cmax}}$  imposed to photosynthesis. Similarly, the MT-treated leaves showed higher values of  $\text{ETR}/(A_N + R_d)$  during the initial phase after transition to high light (Figure 5B), indicating that the limitation of ETR imposed to photosynthesis was decreased in the MT-leaves. After quantitative analysis of relative photosynthetic limitations, we found that during the initial 10 min of photosynthetic induction,  $A_N$  was mainly limited by diffusional conductance in the WT-treated leaves but was mainly limited by biochemical factors in CK plants (Figure 4). This altered relative photosynthetic limitation by exogenous melatonin was largely caused by the increased limitation of  $g_s$  imposed on  $A_N$ . Therefore, the inhibition effect of exogenous melatonin on  $A_N$  during photosynthetic induction was primarily caused by the decreased induction speed of  $g_s$ .



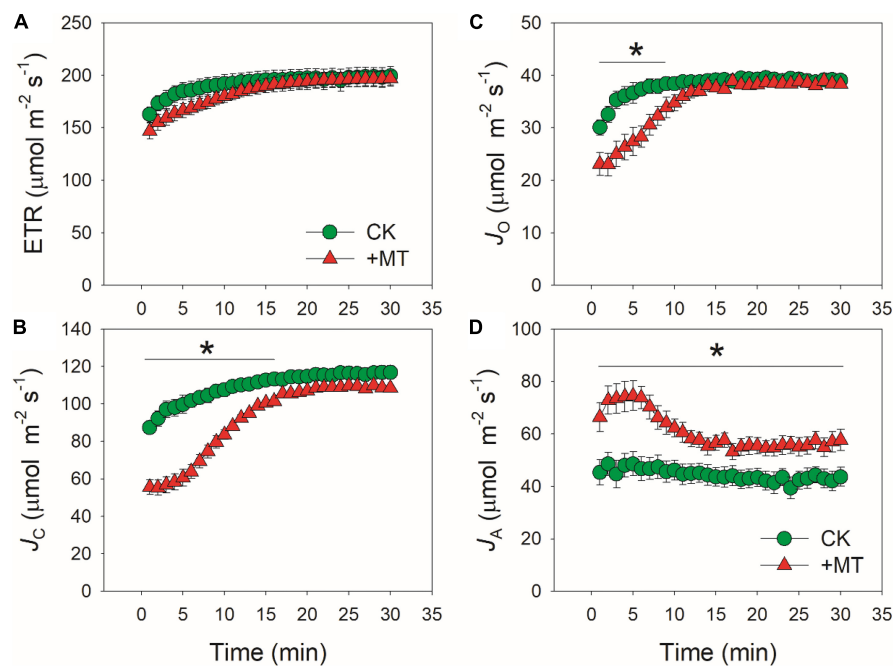


FIGURE 6

Effects of exogenous melatonin (MT, 100  $\mu\text{M}$ ) on the induction response of total electron transport rate (ETR) (A), electron flow for Rubisco carboxylation ( $J_C$ ) (B), electron flow for Rubisco oxygenation ( $J_O$ ) (C), and alternative electron sinks ( $J_A$ ) (D) after transition from 50 to 1500  $\mu\text{mol photons m}^{-2} \text{s}^{-1}$ . Values are means  $\pm$  SE ( $n = 5$ ). Asterisk indicates a significant difference between CK and MT-treated leaves.

Previous studies have reported that exogenous melatonin can affect the expression of antioxidant systems, such as SOD and APX (Kaya et al., 2019; Jahan et al., 2020; Siddiqui et al., 2020a,b). As we know, SOD and APX are two critical antioxidant enzymes participating in an important alternative electron sink, water-water cycle (Asada, 1999, 2000; Miyake, 2010). Furthermore, the inhibition of photosynthesis requires water-water cycle to dissipate excess light energy, which is essential for protecting photosynthetic apparatus against photoinhibition (Makino et al., 2002; Hirotsu et al., 2004, 2005). However, it is unclear whether exogenous melatonin can enhance the capacity of water-water cycle to favor photoprotection. We found that the MT-treated leaves displayed much higher alternative electron sinks when ETRs for Rubisco carboxylation and oxygenation were restricted during photosynthetic induction (Figure 6). This result strongly suggested the enhancement of water-water cycle in the MT-treated leaves, because most of alternative electron flow in higher plants was accounted for the electron flux to oxygen (Asada et al., 2000; Zivcak et al., 2013; Yang et al., 2020; Ferroni et al., 2021; Sun et al., 2021). Therefore, the upregulation of water-water cycle is an important reason for why exogenous MT can strengthen photoprotection when  $\text{CO}_2$  is restricted under environmental stresses.

Within the first seconds after light intensity abruptly increases, plants cannot build up an enough  $\Delta\text{pH}$  to fine-tune PSI redox state (Huang et al., 2019a,b). The resulting PSI

over-reduction induces PSI photoinhibition under fluctuating light (Suorsa et al., 2012; Yamamoto and Shikanai, 2019). Furthermore, a decreased  $g_s$  could aggravate the extent of PSI over-reduction under fluctuating light (Li T. Y. et al., 2021). Upon a sudden transitioning from low to high light, alternative electron sinks can rapidly consume the reducing power in PSI and thus prevents PSI over-reduction (Gerotto et al., 2016; Jokel et al., 2018; Storti et al., 2019, 2020). Recent studies have found that water-water cycle can protect PSI under fluctuating light more efficiently than cyclic electron flow (Huang et al., 2019b; Sun et al., 2020b; Yang et al., 2020). Consequently, PSI is tolerant to photoinhibition under fluctuating light in higher plants with high capacity of water-water cycle, such as in *Camellia* species (Huang et al., 2019b; Sun et al., 2020b), *Bryophyllum pinnatum* (Yang et al., 2019), *Dendrobium officinale* (Yang et al., 2020, 2021), *Vanilla planifolia* (Wang et al., 2022). Therefore, the enhancement of water-water cycle in the MT-treated leaves can facilitate PSI photoinhibition under fluctuating light. In addition, water-water cycle can dissipate excess excitation energy and helps the formation of  $\Delta\text{pH}$ , both of which are critical for photoprotection for PSII especially when  $\text{CO}_2$  assimilation is restricted (Miyake, 2010; Yi et al., 2014; Cai et al., 2017). Because water-water cycle generates ATP without reducing  $\text{NADP}^+$  and thus increases the ATP/NADPH production ratio (Miyake, 2010; Huang et al., 2016), the enhancement of water-water cycle in the MT-treated

leaves can regulate the energy balancing when CO<sub>2</sub> fixation is restricted. Taking together, up-regulation of water-water cycle in the MT-treated leaves has important physiological functions in photosynthetic regulation under environmental stresses.

## Conclusion

Although melatonin has many positive effects on plant tolerance under environmental stresses, we here for the first time documented that the spraying of moderate melatonin content (100  $\mu$ M) to healthy tobacco leaves strongly inhibited photosynthesis during photosynthetic induction. In particular, exogenous melatonin delayed the induction speed of  $g_s$  after transition from low to high light. Therefore,  $g_s$  is the primary target of the delay effect of exogenous melatonin on photosynthesis. Furthermore, we found that the capacity of water-water cycle was enhanced in the MT-treated leaves. When photosynthesis was restricted, water-water cycle facilitated photoprotection and photosynthetic regulation in the MT-treated leaves. Therefore, exogenous melatonin has large effects on gas exchange and photoprotection in plants grown under fluctuating light.

## Data availability statement

The raw data supporting the conclusions of this article will be made available by the authors, without undue reservation.

## Author contributions

Y-JY and WH designed the study. HS, X-QW, and Z-LZ performed the photosynthetic measurements. HS, Y-JY, and WH performed the data analysis. WH wrote the first draft of the manuscript, which was extensively edited by all authors.

## References

- Acevedo-Siaca, L. G., Coe, R., Wang, Y., Kromdijk, J., Quick, W. P., and Long, S. P. (2020). Variation in photosynthetic induction between rice accessions and its potential for improving productivity. *New Phytol.* 27, 1097–1108. doi: 10.1111/nph.16454
- Adachi, S., Tanaka, Y., Miyagi, A., Kashima, M., Tezuka, A., Toya, Y., et al. (2019). High-yielding rice Takanari has superior photosynthetic response to a commercial rice Koshihikari under fluctuating light. *J. Exp. Bot.* 70, 5287–5297. doi: 10.1093/jxb/erz304
- Ahammed, G. J., Wu, M., Wang, Y., Yan, Y., Mao, Q., Ren, J., et al. (2020). Melatonin alleviates iron stress by improving iron homeostasis, antioxidant defense and secondary metabolism in cucumber. *Sci. Hortic. (Amsterdam)* 265:109205. doi: 10.1016/j.scienta.2020.109205
- Ahammed, G. J., Xu, W., Liu, A., and Chen, S. (2018). COMT1 silencing aggravates heat stress-induced reduction in photosynthesis by decreasing chlorophyll content, photosystem II activity, and electron transport efficiency in tomato. *Front. Plant Sci.* 9:998. doi: 10.3389/fpls.2018.00998
- Alborese, A., Storti, M., and Morosinotto, T. (2019). Balancing protection and efficiency in the regulation of photosynthetic electron transport across plant evolution. *New Phytol.* 221, 105–109. doi: 10.1111/nph.15372
- Allahverdiyeva, Y., Suorsa, M., Tikkanen, M., and Aro, E. M. (2015). Photoprotection of photosystems in fluctuating light intensities. *J. Exp. Bot.* 66, 2427–2436. doi: 10.1093/jxb/eru463
- Arnao, M. B., and Hernández-Ruiz, J. (2015). Functions of melatonin in plants: a review. *J. Pineal Res.* 59, 133–150. doi: 10.1111/jpi.12253
- Arnao, M. B., and Hernández-Ruiz, J. (2019). Melatonin: a new plant hormone and/or a plant master regulator? *Trends Plant Sci.* 24, 38–48. doi: 10.1016/j.tplants.2018.10.010

## Funding

This work was supported by the National Natural Science Foundation of China (31971412 and 32171505), by Postdoctoral Research Funding Projects of Yunnan Province, and by Postdoctoral Directional Training Foundation of Yunnan Province.

## Conflict of interest

The authors declare that the research was conducted in the absence of any commercial or financial relationships that could be construed as a potential conflict of interest.

## Publisher's note

All claims expressed in this article are solely those of the authors and do not necessarily represent those of their affiliated organizations, or those of the publisher, the editors and the reviewers. Any product that may be evaluated in this article, or claim that may be made by its manufacturer, is not guaranteed or endorsed by the publisher.

## Supplementary material

The Supplementary Material for this article can be found online at: <https://www.frontiersin.org/articles/10.3389/fpls.2022.917784/full#supplementary-material>

### SUPPLEMENTARY FIGURE 1

Effects of exogenous melatonin (MT, 100  $\mu$ M) on the kinetics of transpiration rate after transition from 50 to 1,500  $\mu$ mol photons  $m^{-2} s^{-1}$ . Values are means  $\pm$  SE ( $n = 5$ ). Asterisk indicates a significant difference between CK and MT-treated leaves.

- Arnao, M., and Hernández-Ruiz, J. (2020). Is phyto-melatonin a new plant hormone? *Agronomy* 10:95. doi: 10.3390/agronomy10010095
- Asada, K. (1999). The water-water cycle in chloroplasts: scavenging of active oxygens and dissipation of excess photons. *Annu. Rev. Plant Physiol. Plant Mol. Biol.* 50, 601–639. doi: 10.1146/annurev.arplant.50.1.601
- Asada, K. (2000). The water-water cycle as alternative photon and electron sinks. *Philos. Trans. R. Soc. Lond. B. Biol. Sci.* 355, 1419–1431. doi: 10.1098/rstb.2000.0703
- Asada, K., Allen, J., Foyer, C. H., and Matthijs, H. C. P. (2000). The water-water cycle as alternative photon and electron sinks. *Philos. Trans. R. Soc. B Biol. Sci.* 355, 1419–1431.
- Bajwa, V. S., Shukla, M. R., Sherif, S. M., Murch, S. J., and Saxena, P. K. (2014). Role of melatonin in alleviating cold stress in *Arabidopsis thaliana*. *J. Pineal Res.* 56, 238–245. doi: 10.1111/jpi.12115
- Bhat, J. A., Faizan, M., Bhat, M. A., Huang, F., Yu, D., Ahmad, A., et al. (2022). Defense interplay of the zinc-oxide nanoparticles and melatonin in alleviating the arsenic stress in soybean (*Glycine max* L.). *Chemosphere* 288:132471. doi: 10.1016/j.chemosphere.2021.132471
- Bose, S. K., and Howlader, P. (2020). Melatonin plays multifunctional role in horticultural crops against environmental stresses: a review. *Environ. Exp. Bot.* 176:104063. doi: 10.1016/j.envexpbot.2020.104063
- Brestic, M., Zivcak, M., Kunderlikova, K., Sytar, O., Shao, H., Kalaji, H. M., et al. (2015). Low PSI content limits the photoprotection of PSI and PSII in early growth stages of chlorophyll b-deficient wheat mutant lines. *Photosynth. Res.* 125, 151–166. doi: 10.1007/s11120-015-0093-1
- Cai, Y.-F., Yang, Q.-Y., Li, S.-F., Wang, J.-H., and Huang, W. (2017). The water-water cycle is a major electron sink in *Camellia* species when CO<sub>2</sub> assimilation is restricted. *J. Photochem. Photobiol. B Biol.* 168, 59–66. doi: 10.1016/j.jphotobiol.2017.01.024
- Carriqui, M., Cabrera, H. M., Conesa, M., Coopman, R. E., Douthe, C., Gago, J., et al. (2015). Diffusional limitations explain the lower photosynthetic capacity of ferns as compared with angiosperms in a common garden study. *Plant Cell Environ.* 38, 448–460. doi: 10.1111/pce.12402
- Chen, Z., Cao, X., and Niu, J. (2021). Effects of melatonin on morphological characteristics, mineral nutrition, nitrogen metabolism, and energy status in alfalfa under high-nitrate stress. *Front. Plant Sci.* 12:694179. doi: 10.3389/fpls.2021.694179
- Dai, L., Li, J., Harmens, H., Zheng, X., and Zhang, C. (2020). Melatonin enhances drought resistance by regulating leaf stomatal behaviour, root growth and catalase activity in two contrasting rapeseed (*Brassica napus* L.) genotypes. *Plant Physiol. Biochem.* 149, 86–95. doi: 10.1016/j.plaphy.2020.01.039
- De Souza, A. P., Wang, Y., Orr, D. J., Carmo-Silva, E., and Long, S. P. (2020). Photosynthesis across African cassava germplasm is limited by Rubisco and mesophyll conductance at steady state, but by stomatal conductance in fluctuating light. *New Phytol.* 225, 2498–2512. doi: 10.1111/nph.16142
- Ding, W., Zhao, Y., Xu, J.-W., Zhao, P., Li, T., Ma, H., et al. (2018). Melatonin: a multifunctional molecule that triggers defense responses against high light and nitrogen starvation stress in *Haematococcus pluvialis*. *J. Agric. Food Chem.* 66, 7701–7711. doi: 10.1021/acs.jafc.8b02178
- Eyland, D., van Wesemael, J., Lawton, T., and Carpentier, S. (2021). The impact of slow stomatal kinetics on photosynthesis and water use efficiency under fluctuating light. *Plant Physiol.* 186, 998–1012. doi: 10.1093/PLPHYS/KIAB114
- Farouk, S., and Al-Amri, S. M. (2019). Exogenous melatonin-mediated modulation of arsenic tolerance with improved accretion of secondary metabolite production, activating antioxidant capacity and improved chloroplast ultrastructure in rosemary herb. *Ecotoxicol. Environ. Saf.* 180, 333–347. doi: 10.1016/j.ecoenv.2019.05.021
- Farquhar, G. D., von Caemmerer, S., and Berry, J. A. (1980). A biochemical model of photosynthetic CO<sub>2</sub> assimilation in leaves of C<sub>3</sub> species. *Planta* 149, 78–90. doi: 10.1007/BF00386231
- Ferroni, L., Brestič, M., Živčák, M., Cantelli, R., and Pancaldi, S. (2021). Increased photosynthesis from a deep-shade to high-light regime occurs by enhanced CO<sub>2</sub> diffusion into the leaf of *Selaginella martensii*. *Plant Physiol. Biochem.* 160, 143–154. doi: 10.1016/j.plaphy.2021.01.012
- Genty, B., Briantais, J.-M., and Baker, N. R. (1989). The relationship between the quantum yield of photosynthetic electron transport and quenching of chlorophyll fluorescence. *Biochim. Biophys. Acta Gen. Subj.* 990, 87–92. doi: 10.1016/S0304-4165(89)80016-9
- Gerotto, C., Alboresi, A., Meneghesso, A., Jokel, M., Suorsa, M., Aro, E.-M., et al. (2016). Flavodiiron proteins act as safety valve for electrons in *Physcomitrella patens*. *Proc. Natl. Acad. Sci. U.S.A.* 113, 12322–12327. doi: 10.1073/pnas.1606685113
- Giraldo Acosta, M., Cano, A., Hernández-Ruiz, J., and Arnao, M. B. (2022). Melatonin as a Possible natural safener in crops. *Plants* 11:890. doi: 10.3390/plants11070890
- Grassi, G., and Magnani, F. (2005). Stomatal, mesophyll conductance and biochemical limitations to photosynthesis as affected by drought and leaf ontogeny in ash and oak trees. *Plant Cell Environ.* 28, 834–849. doi: 10.1111/j.1365-3040.2005.01333.x
- Harley, P. C., Loreto, F., Di Marco, G., and Sharkey, T. D. (1992). Theoretical considerations when estimating the mesophyll conductance to CO<sub>2</sub> flux by analysis of the response of photosynthesis to CO<sub>2</sub>. *Plant Physiol.* 98, 1429–1436. doi: 10.1104/pp.98.4.1429
- Hermida-Carrera, C., Kapralov, M. V., and Galmés, J. (2016). Rubisco Catalytic properties and temperature response in crops. *Plant Physiol.* 171, 2549–2561. doi: 10.1104/pp.16.01846
- Hirotsu, N., Makino, A., Ushio, A., and Mae, T. (2004). Changes in the thermal dissipation and the electron flow in the water-water cycle in rice grown under conditions of physiologically low temperature. *Plant Cell Physiol.* 45, 635–644. doi: 10.1093/pcp/pch075
- Hirotsu, N., Makino, A., Yokota, S., and Mae, T. (2005). The photosynthetic properties of rice leaves treated with low temperature and high irradiance. *Plant Cell Physiol.* 46, 1377–1383. doi: 10.1093/pcp/pci149
- Hoque, M. N., Tahjib-Ul-Arif, M., Hannan, A., Sultana, N., Akhter, S., Hasanuzzaman, M., et al. (2021). Melatonin modulates plant tolerance to heavy metal stress: morphological responses to molecular mechanisms. *Int. J. Mol. Sci.* 22, 1–24. doi: 10.3390/ijms222111445
- Huang, W., Yang, Y.-J., and Zhang, S.-B. (2019a). Photoinhibition of photosystem I under fluctuating light is linked to the insufficient ΔpH upon a sudden transition from low to high light. *Environ. Exp. Bot.* 160, 112–119. doi: 10.1016/j.envexpbot.2019.01.012
- Huang, W., Yang, Y. J., and Zhang, S. B. (2019b). The role of water-water cycle in regulating the redox state of photosystem I under fluctuating light. *Biochim. Biophys. Acta Bioenerg.* 1860, 383–390. doi: 10.1016/j.bbabi.2019.03.007
- Huang, W., Yang, Y.-J., Hu, H., and Zhang, S.-B. (2016). Response of the water-water cycle to the change in photorespiration in tobacco. *J. Photochem. Photobiol. B Biol.* 157, 97–104. doi: 10.1016/j.jphotobiol.2016.02.006
- Huang, W., Zhang, S.-B., and Liu, T. (2018). Moderate photoinhibition of photosystem II significantly affects linear electron flow in the shade-demanding plant *Panax notoginseng*. *Front. Plant Sci.* 9:637. doi: 10.3389/fpls.2018.00637
- Imran, M., Shazad, R., Bilal, S., Imran, Q. M., Khan, M., Kang, S. M., et al. (2021). Exogenous Melatonin mediates the regulation of endogenous nitric oxide in *Glycine max* L. to reduce effects of drought stress. *Environ. Exp. Bot.* 188:104511. doi: 10.1016/j.envexpbot.2021.104511
- Jahan, M. S., Guo, S., Baloch, A. R., Sun, J., Shu, S., Wang, Y., et al. (2020). Melatonin alleviates nickel phytotoxicity by improving photosynthesis, secondary metabolism and oxidative stress tolerance in tomato seedlings. *Ecotoxicol. Environ. Saf.* 197:110593. doi: 10.1016/j.ecoenv.2020.110593
- Jahan, M. S., Shu, S., Wang, Y., Chen, Z., He, M., Tao, M., et al. (2019). Melatonin alleviates heat-induced damage of tomato seedlings by balancing redox homeostasis and modulating polyamine and nitric oxide biosynthesis. *BMC Plant Biol.* 19:414. doi: 10.1186/s12870-019-1992-7
- Jokel, M., Johnson, X., Peltier, G., Aro, E. M., and Allahverdiyeva, Y. (2018). Hunting the main player enabling *Chlamydomonas reinhardtii* growth under fluctuating light. *Plant J.* 94, 822–835. doi: 10.1111/tpj.13897
- Kaiser, E., Kromdijk, J., Harbinson, J., Heuvelink, E., and Marcelis, L. F. M. (2017). Photosynthetic induction and its diffusional, carboxylation and electron transport processes as affected by CO<sub>2</sub> partial pressure, temperature, air humidity and blue irradiance. *Ann. Bot.* 119, 191–205. doi: 10.1093/aob/mcw226
- Kaiser, E., Morales, A., Harbinson, J., Heuvelink, E., and Marcelis, L. F. M. (2020). High stomatal conductance in the tomato flacca mutant allows for faster photosynthetic induction. *Front. Plant Sci.* 11:1317. doi: 10.3389/fpls.2020.01317
- Kaya, C., Okant, M., Ugurlar, F., Alyemeni, M. N., Ashraf, M., and Ahmad, P. (2019). Melatonin-mediated nitric oxide improves tolerance to cadmium toxicity by reducing oxidative stress in wheat plants. *Chemosphere* 225, 627–638. doi: 10.1016/j.chemosphere.2019.03.026
- Kaya, C., Sarıoglu, A., Ashraf, M., Alyemeni, M. N., and Ahmad, P. (2022). The combined supplementation of melatonin and salicylic acid effectively detoxifies arsenic toxicity by modulating phytochelatin and nitrogen metabolism in pepper plants. *Environ. Pollut.* 297:118727. doi: 10.1016/j.envpol.2021.118727
- Kimura, H., Hashimoto-Sugimoto, M., Iba, K., Terashima, I., and Yamori, W. (2020). Improved stomatal opening enhances photosynthetic rate and biomass production in fluctuating light. *J. Exp. Bot.* 71, 2339–2350. doi: 10.1093/jxb/eraa090

- Kono, M., Noguchi, K., and Terashima, I. (2014). Roles of the cyclic electron flow around PSI (CEF-PSI) and O<sub>2</sub>-dependent alternative pathways in regulation of the photosynthetic electron flow in short-term fluctuating light in *Arabidopsis thaliana*. *Plant Cell Physiol.* 55, 990–1004. doi: 10.1093/pcp/pcu033
- Lee, H. Y., and Back, K. (2018). Melatonin induction and its role in high light stress tolerance in *Arabidopsis thaliana*. *J. Pineal Res.* 65:e12504. doi: 10.1111/jpi.12504
- Li, S., Guo, J., Wang, T., Gong, L., Liu, F., Brestic, M., et al. (2021). Melatonin reduces nanoplastic uptake, translocation, and toxicity in wheat. *J. Pineal Res.* 71:e12761. doi: 10.1111/jpi.12761
- Li, T. Y., Shi, Q., Sun, H., Yue, M., Zhang, S.-B., and Huang, W. (2021). diurnal response of photosystem i to fluctuating light is affected by stomatal conductance. *Cells* 10:3128. doi: 10.3390/cells10113128
- Li, X., Ahammed, G. J., Zhang, X.-N., Zhang, L., Yan, P., Zhang, L.-P., et al. (2021). Melatonin-mediated regulation of anthocyanin biosynthesis and antioxidant defense confer tolerance to arsenic stress in *Camellia sinensis* L. *J. Hazard. Mater.* 403:123922. doi: 10.1016/j.jhazmat.2020.123922
- Li, X., Brestic, M., Tan, D.-X., Zivcak, M., Zhu, X., Liu, S., et al. (2018). Melatonin alleviates low PS I-limited carbon assimilation under elevated CO<sub>2</sub> and enhances the cold tolerance of offspring in chlorophyll b -deficient mutant wheat. *J. Pineal Res.* 64:e12453. doi: 10.1111/jpi.12453
- Liang, C., Zheng, G., Li, W., Wang, Y., Hu, B., Wang, H., et al. (2015). Melatonin delays leaf senescence and enhances salt stress tolerance in rice. *J. Pineal Res.* 59, 91–101. doi: 10.1111/jpi.12243
- Lima-Melo, Y., Gollan, P. J., Tikkanen, M., Silveira, J. A. G., and Aro, E. M. (2019). Consequences of photosystem-I damage and repair on photosynthesis and carbon use in *Arabidopsis thaliana*. *Plant J.* 97, 1061–1072. doi: 10.1111/tjp.14177
- Liu, T., Barbour, M. M., Yu, D., Rao, S., and Song, X. (2022). Mesophyll conductance exerts a significant limitation on photosynthesis during light induction. *New Phytol.* 233, 360–372. doi: 10.1111/nph.17757
- Long, S. P., and Bernacchi, C. J. (2003). Gas exchange measurements, what can they tell us about the underlying limitations to photosynthesis? Procedures and sources of error. *J. Exp. Bot.* 54, 2393–2401. doi: 10.1093/jxb/erg262
- Makino, A., Miyake, C., and Yokota, A. (2002). Physiological functions of the water-water cycle (Mehler reaction) and the cyclic electron flow around PSI in rice leaves. *Plant Cell Physiol.* 43, 1017–1026. doi: 10.1093/pcp/pcf124
- Meng, S., Wang, X., Bian, Z., Li, Z., Yang, F., Wang, S., et al. (2021). Melatonin enhances nitrogen metabolism and haustorium development in hemiparasite *Santalum album* Linn. *Environ. Exp. Bot.* 186:104460. doi: 10.1016/j.envexpbot.2021.104460
- Miyake, C. (2010). Alternative electron flows (water-water cycle and cyclic electron flow around PSI) in photosynthesis: molecular mechanisms and physiological functions. *Plant Cell Physiol.* 51, 1951–1963. doi: 10.1093/pcp/pcq173
- Munekage, Y. N., Genty, B., and Peltier, G. (2008). Effect of PGR5 impairment on photosynthesis and growth in *Arabidopsis thaliana*. *Plant Cell Physiol.* 49, 1688–1698. doi: 10.1093/pcp/pcn140
- Munekage, Y., Hojo, M., Meurer, J., Endo, T., Tasaka, M., and Shikanai, T. (2002). PGR5 is involved in cyclic electron flow around photosystem I and is essential for photoprotection in *Arabidopsis*. *Cell* 110, 361–371. doi: 10.1016/S0092-8674(02)00867-X
- Murata, N., Takahashi, S., Nishiyama, Y., and Allakhverdiev, S. I. (2007). Photoinhibition of photosystem II under environmental stress. *Biochim. Biophys. Acta Bioenerg.* 1767, 414–421. doi: 10.1016/j.bbabi.2006.11.019
- Nishiyama, Y., Allakhverdiev, S. I., and Murata, N. (2005). Inhibition of the repair of photosystem II by oxidative stress in cyanobacteria. *Photosynth. Res.* 84, 1–7. doi: 10.1007/s11120-004-6434-0
- Nishiyama, Y., Yamamoto, H., Allakhverdiev, S. I., Inaba, M., Yokota, A., and Murata, N. (2001). Oxidative stress inhibits the repair of photodamage to the photosynthetic machinery. *EMBO J.* 20, 5587–5594. doi: 10.1093/emboj/20.20.5587
- Oguchi, R., Hikosaka, K., and Hirose, T. (2003). Does the photosynthetic light-acclimation need change in leaf anatomy? *Plant Cell Environ.* 26, 505–512. doi: 10.1046/j.1365-3040.2003.00981.x
- Park, S., Lee, D.-E., Jang, H., Byeon, Y., Kim, Y.-S., and Back, K. (2013). Melatonin-rich transgenic rice plants exhibit resistance to herbicide-induced oxidative stress. *J. Pineal Res.* 54, 258–263. doi: 10.1111/j.1600-079X.2012.01029.x
- Pearcy, R. W. (1990). Sunflecks and photosynthesis in plant canopies. *Annu. Rev. Plant Physiol. Plant Mol. Biol.* 41, 421–453. doi: 10.1146/annurev.pp.41.060190.002225
- Qi, C., Zhang, H., Liu, Y., Wang, X., Dong, D., Yuan, X., et al. (2020). CsSNAT positively regulates salt tolerance and growth of cucumber by promoting melatonin biosynthesis. *Environ. Exp. Bot.* 175:104036. doi: 10.1016/j.envexpbot.2020.104036
- Qiao, M.-Y., Zhang, Y.-J., Liu, L.-A., Shi, L., Ma, Q.-H., Chow, W. S., et al. (2020). Do rapid photosynthetic responses protect maize leaves against photoinhibition under fluctuating light? *Photosynth. Res.* 149, 57–68. doi: 10.1007/s11120-020-00780-5
- Qiao, Y., Yin, L., Wang, B., Ke, Q., Deng, X., and Wang, S. (2019). Melatonin promotes plant growth by increasing nitrogen uptake and assimilation under nitrogen deficient condition in winter wheat. *Plant Physiol. Biochem.* 139, 342–349. doi: 10.1016/j.plaphy.2019.03.037
- Sakoda, K., Yamori, W., Groszmann, M., and Evans, J. R. (2021). Stomatal, mesophyll conductance, and biochemical limitations to photosynthesis during induction. *Plant Physiol.* 185, 146–160. doi: 10.1093/plphys/kiaa011
- Sakoda, K., Yamori, W., Shimada, T., Sugano, S. S., Hara-Nishimura, I., and Tanaka, Y. (2020). Higher stomatal density improves photosynthetic induction and biomass production in *Arabidopsis* under fluctuating light. *Front. Plant Sci.* 11:1308. doi: 10.3389/fpls.2020.589603
- Sejima, T., Takagi, D., Fukayama, H., Makino, A., and Miyake, C. (2014). Repetitive short-pulse light mainly inactivates photosystem i in sunflower leaves. *Plant Cell Physiol.* 55, 1184–1193. doi: 10.1093/pcp/pcu061
- Seleiman, M. F., Ali, S., Refay, Y., Rizwan, M., Alhammad, B. A., and El-Hendawy, S. E. (2020). Chromium resistant microbes and melatonin reduced Cr uptake and toxicity, improved physio-biochemical traits and yield of wheat in contaminated soil. *Chemosphere* 250:126239. doi: 10.1016/j.chemosphere.2020.126239
- Sharma, A., and Zheng, B. (2019). Melatonin mediated regulation of drought stress: physiological and molecular aspects. *Plants* 8:190. doi: 10.3390/plants8070190
- Shikanai, T., and Yamamoto, H. (2017). Contribution of cyclic and pseudo-cyclic electron transport to the formation of proton motive force in chloroplasts. *Mol. Plant* 10, 20–29. doi: 10.1016/j.molp.2016.08.004
- Shimakawa, G., and Miyake, C. (2019). What quantity of photosystem I is optimum for safe photosynthesis? *Plant Physiol.* 179, 1479–1485. doi: 10.1104/pp.18.01493
- Siddiqui, M. H., Alamri, S., Alsubaie, Q. D., and Ali, H. M. (2020a). Melatonin and gibberellic acid promote growth and chlorophyll biosynthesis by regulating antioxidant and methylglyoxal detoxification system in tomato seedlings under salinity. *J. Plant Growth Regul.* 39, 1488–1502. doi: 10.1007/s00344-020-10122-3
- Siddiqui, M. H., Alamri, S., Nasir Khan, M., Corpas, F. J., Al-Amri, A. A., Alsubaie, Q. D., et al. (2020b). Melatonin and calcium function synergistically to promote the resilience through ROS metabolism under arsenic-induced stress. *J. Hazard. Mater.* 398:122882. doi: 10.1016/j.jhazmat.2020.12.2882
- Slattery, R. A., Walker, B. J., Weber, A. P. M., and Ort, D. R. (2018). The impacts of fluctuating light on crop performance. *Plant Physiol.* 176, 990–1003. doi: 10.1104/pp.17.01234
- Storti, M., Alboresi, A., Gerotto, C., Aro, E., Finazzi, G., and Morosinotto, T. (2019). Role of cyclic and pseudo-cyclic electron transport in response to dynamic light changes in *Physcomitrella patens*. *Plant. Cell Environ.* 42, 1590–1602. doi: 10.1111/pce.13493
- Storti, M., Segalla, A., Mellon, M., Alboresi, A., and Morosinotto, T. (2020). Regulation of electron transport is essential for photosystem I stability and plant growth. *New Phytol.* 228, 1316–1326. doi: 10.1111/nph.16643
- Sun, H., Shi, Q., Zhang, S.-B., and Huang, W. (2021). Coordination of cyclic electron flow and water–water Cycle facilitates photoprotection under fluctuating light and temperature stress in the epiphytic orchid *Dendrobium officinale*. *Plants* 10:606. doi: 10.3390/plants10030606
- Sun, H., Zhang, S.-B., Liu, T., and Huang, W. (2020b). Decreased photosystem II activity facilitates acclimation to fluctuating light in the understory plant *Paris polyphylla*. *Biochim. Biophys. Acta Bioenerg.* 1861:148135. doi: 10.1016/j.bbabi.2019.148135
- Sun, H., Yang, Y.-J., and Huang, W. (2020a). The water-water cycle is more effective in regulating redox state of photosystem I under fluctuating light than cyclic electron transport. *Biochim. Biophys. Acta Bioenerg.* 1861:148235. doi: 10.1016/j.bbabi.2020.148235
- Sun, H., Zhang, Y.-Q., Zhang, S., and Huang, W. (2022). Photosynthetic induction under fluctuating light is affected by leaf nitrogen content in tomato. *Front. Plant Sci.* 13:835571. doi: 10.3389/fpls.2022.835571
- Suorsa, M., Jarvi, S., Grieco, M., Nurmi, M., Pietrzykowska, M., Rantala, M., et al. (2012). PROTON GRADIENT REGULATION5 is essential for proper acclimation of *Arabidopsis* photosystem I to naturally and artificially fluctuating light conditions. *Plant Cell* 24, 2934–2948. doi: 10.1105/tpc.112.097162



- Takahashi, S., and Badger, M. R. (2011). Photoprotection in plants: a new light on photosystem II damage. *Trends Plant Sci.* 16, 53–60. doi: 10.1016/j.tplants.2010.10.001
- Takahashi, S., and Murata, N. (2005). Interruption of the Calvin cycle inhibits the repair of photosystem II from photodamage. *Biochim. Biophys. Acta Bioenerg.* 1708, 352–361. doi: 10.1016/j.bbabi.2005.04.003
- Takahashi, S., and Murata, N. (2006). Glycerate-3-phosphate, produced by CO<sub>2</sub> fixation in the Calvin cycle, is critical for the synthesis of the D1 protein of photosystem II. *Biochim. Biophys. Acta Bioenerg.* 1757, 198–205. doi: 10.1016/j.bbabi.2006.02.002
- Takahashi, S., and Murata, N. (2008). How do environmental stresses accelerate photoinhibition? *Trends Plant Sci.* 13, 178–182. doi: 10.1016/j.tplants.2008.01.005
- Takahashi, S., Milward, S. E., Fan, D.-Y., Chow, W. S., and Badger, M. R. (2009). How does cyclic electron flow alleviate photoinhibition in *Arabidopsis*? *Plant Physiol.* 149, 1560–1567. doi: 10.1104/pp.108.134122
- Tan, S.-L., Huang, J.-L., Zhang, F.-P., Zhang, S.-B., and Huang, W. (2021). Photosystem I photoinhibition induced by fluctuating light depends on background low light irradiance. *Environ. Exp. Bot.* 181:104298. doi: 10.1016/j.envexpbot.2020.104298
- Valentini, R., Epron, D., Angelis, P. D. E., Matteucci, G., and Dreyer, E. (1995). In situ estimation of net CO<sub>2</sub> assimilation, photosynthetic electron flow and photorespiration in Turkey oak (*Q. cerris* L.) leaves: diurnal cycles under different levels of water supply. *Plant Cell Environ.* 18, 631–640. doi: 10.1111/j.1365-3040.1995.tb00564.x
- Valladares, F., Allen, M. T., and Pearcy, R. W. (1997). Photosynthetic responses to dynamic light under field conditions in six tropical rainforest shrubs occurring along a light gradient. *Oecologia* 111, 505–514. doi: 10.1007/s004420050264
- von Caemmerer, S., and Evans, J. R. (2015). Temperature responses of mesophyll conductance differ greatly between species. *Plant Cell Environ.* 38, 629–637. doi: 10.1111/pce.12449
- Walker, B. J., Strand, D. D., Kramer, D. M., and Cousins, A. B. (2014). The response of cyclic electron flow around photosystem I to changes in photorespiration and nitrate assimilation. *Plant Physiol.* 165, 453–462. doi: 10.1104/pp.114.238238
- Wang, H., Wang, X.-Q., Zeng, Z.-L., Yu, H., and Huang, W. (2022). Photosynthesis under fluctuating light in the CAM plant *Vanilla planifolia*. *Plant Sci.* 317:111207. doi: 10.1016/j.plantsci.2022.111207
- Wang, Y., Reiter, R. J., and Chan, Z. (2018). Phytomelatonin: a universal abiotic stress regulator. *J. Exp. Bot.* 69, 963–974. doi: 10.1093/jxb/erx473
- Warren, C. R., and Dreyer, E. (2006). Temperature response of photosynthesis and internal conductance to CO<sub>2</sub>: results from two independent approaches. *J. Exp. Bot.* 57, 3057–3067. doi: 10.1093/jxb/erl067
- Xiong, D., Douthe, C., and Flexas, J. (2018). Differential coordination of stomatal conductance, mesophyll conductance, and leaf hydraulic conductance in response to changing light across species. *Plant Cell Environ.* 41, 436–450. doi: 10.1111/pce.13111
- Xiong, D., Liu, X., Liu, L., Douthe, C., Li, Y., Peng, S., et al. (2015). Rapid responses of mesophyll conductance to changes of CO<sub>2</sub> concentration, temperature and irradiance are affected by N supplements in rice. *Plant Cell Environ.* 38, 2541–2550. doi: 10.1111/pce.12558
- Yamamoto, H., and Shikanai, T. (2019). PGR5-dependent cyclic electron flow protects photosystem I under fluctuating light at donor and acceptor sides. *Plant Physiol.* 179, 588–600. doi: 10.1104/pp.18.01343
- Yamamoto, H., Takahashi, S., Badger, M. R., and Shikanai, T. (2016). Artificial remodelling of alternative electron flow by flavodiiron proteins in *Arabidopsis*. *Nat. Plants* 2:16012. doi: 10.1038/nplants.2016.12
- Yamori, W., Kusumi, K., Iba, K., and Terashima, I. (2020). Increased stomatal conductance induces rapid changes to photosynthetic rate in response to naturally fluctuating light conditions in rice. *Plant. Cell Environ.* 43, 1230–1240. doi: 10.1111/pce.13725
- Yang, Y.-J., Tan, S.-L., Huang, J.-L., Zhang, S.-B., and Huang, W. (2020). The water-water cycle facilitates photosynthetic regulation under fluctuating light in the epiphytic orchid *Dendrobium officinale*. *Environ. Exp. Bot.* 180:104238. doi: 10.1016/j.envexpbot.2020.104238
- Yang, Y.-J., Tan, S.-L., Sun, H., Huang, J.-L., Huang, W., and Zhang, S.-B. (2021). Photosystem I is tolerant to fluctuating light under moderate heat stress in two orchids *Dendrobium officinale* and *Bletilla striata*. *Plant Sci.* 303:110795. doi: 10.1016/j.plantsci.2020.110795
- Yang, Y.-J., Zhang, S.-B., and Huang, W. (2019). Photosynthetic regulation under fluctuating light in young and mature leaves of the CAM plant *Bryophyllum pinnatum*. *Biochim. Biophys. Acta Bioenerg.* 1860, 469–477. doi: 10.1016/j.bbabi.2019.04.006
- Yao, J., Ma, Z., Ma, Y., Zhu, Y., Lei, M., Hao, C., et al. (2021). Role of melatonin in UV-B signaling pathway and UV-B stress resistance in *Arabidopsis thaliana* <scp>. *Plant. Cell Environ.* 44, 114–129. doi: 10.1111/pce.13879
- Yi, X. P., Zhang, Y. L., Yao, H. S., Zhang, X. J., Luo, H. H., Gou, L., et al. (2014). Alternative electron sinks are crucial for conferring photoprotection in field-grown cotton under water deficit during flowering and boll setting stages. *Funct. Plant Biol.* 41, 737–747. doi: 10.1071/FP13269
- Zhang, H., Liu, L., Wang, Z., Feng, G., Gao, Q., and Li, X. (2021). Induction of low temperature tolerance in wheat by pre-soaking and parental treatment with melatonin. *Molecules* 26:1192. doi: 10.3390/molecules26041192
- Zhang, Y., Kaiser, E., Marcelis, L. F. M., Yang, Q., and Li, T. (2020). Salt stress and fluctuating light have separate effects on photosynthetic acclimation, but interactively affect biomass. *Plant. Cell Environ.* 43, 2192–2206. doi: 10.1111/pce.13810
- Zivcak, M., Brestic, M., Balatova, Z., Drevenakova, P., Olsovska, K., Kalaji, H. M., et al. (2013). Photosynthetic electron transport and specific photoprotective responses in wheat leaves under drought stress. *Photosynth. Res.* 117, 529–546. doi: 10.1007/s11120-013-9885-3
- Zivcak, M., Brestic, M., Kunderlikova, K., Sytar, O., and Allakhverdiev, S. I. (2015). Repetitive light pulse-induced photoinhibition of photosystem I severely affects CO<sub>2</sub> assimilation and photoprotection in wheat leaves. *Photosynth. Res.* 126, 449–463. doi: 10.1007/s11120-015-0121-1



## OPEN ACCESS

EDITED BY  
Vasilij Goltsev,  
Sofia University, Bulgaria

REVIEWED BY  
Abdallah Oukarroum,  
Mohammed VI Polytechnic University,  
Morocco  
Habib-ur-Rehman Athar,  
Bahauddin Zakariya University,  
Pakistan

\*CORRESPONDENCE  
Vera Cesar  
vcesarus@yahoo.com

SPECIALTY SECTION  
This article was submitted to  
Plant Abiotic Stress,  
a section of the journal  
Frontiers in Plant Science

RECEIVED 06 July 2022  
ACCEPTED 22 September 2022  
PUBLISHED 12 October 2022

CITATION  
Peršić V, Ament A,  
Antunović Dunić J,  
Drezner G and Cesar V (2022)  
PEG-induced physiological drought  
for screening winter wheat  
genotypes sensitivity – integrated  
biochemical and chlorophyll  
a fluorescence analysis.  
*Front. Plant Sci.* 13:987702.  
doi: 10.3389/fpls.2022.987702

COPYRIGHT  
© 2022 Peršić, Ament, Antunović Dunić,  
Drezner and Cesar. This is an open-  
access article distributed under the  
terms of the [Creative Commons  
Attribution License \(CC BY\)](#). The use,  
distribution or reproduction in other  
forums is permitted, provided the  
original author(s) and the copyright  
owner(s) are credited and that the  
original publication in this journal is  
cited, in accordance with accepted  
academic practice. No use,  
distribution or reproduction is  
permitted which does not comply with  
these terms.

# PEG-induced physiological drought for screening winter wheat genotypes sensitivity – integrated biochemical and chlorophyll a fluorescence analysis

Vesna Peršić<sup>1</sup>, Anita Ament<sup>1</sup>, Jasenka Antunović Dunić<sup>1</sup>,  
Georg Drezner<sup>2</sup> and Vera Cesar<sup>1,3\*</sup>

<sup>1</sup>Department of Biology, Josip Juraj Strossmayer University of Osijek, Osijek, Croatia, <sup>2</sup>Department of Small Cereal Crops, Agricultural Institute Osijek, Osijek, Croatia, <sup>3</sup>Faculty of Dental Medicine and Health, Josip Juraj Strossmayer University of Osijek, Osijek, Croatia

This study aimed to screen different winter wheat genotypes at the onset of metabolic changes induced by water deficit to comprehend possible adaptive features of photosynthetic apparatus function and structure to physiological drought. The drought treatment was the most influential variable affecting plant growth and relative water content, and genotype variability determined with what intensity varieties of winter wheat seedlings responded to water deficit. PEG-induced drought, as expected, changed phenomenological energy fluxes and the efficiency with which an electron is transferred to final PSI acceptors. Based on the effect size, fluorescence parameters were grouped to represent photochemical parameters, that is, the donor and acceptor side of PSII (PC1); the thermal phase of the photosynthetic process, or the electron flow around PSI, and the chain of electrons between PSII and PSI (PC2); and phenomenological energy fluxes per cross-section (PC3). Furthermore, four distinct clusters of genotypes were discerned based on their response to imposed physiological drought, and integrated analysis enabled an explanation of their reactions' specificity. The most reliable JIP-test parameters for detecting and comparing the drought impact among tested genotypes were the variable fluorescence at K, L, I step, and PI<sub>TOT</sub>. To conclude, developing and improving screening methods for identifying and evaluating functional relationships of relevant characteristics that are useful for acclimation, acclimatization, and adaptation to different types of drought stress can contribute to the progress in breeding research of winter wheat drought-tolerant lines.

## KEYWORDS

triticum aestivum, PEG-6000, photosynthesis, free proline, lipid peroxidation, HAC (hierarchical agglomerative clustering), PCA

# 1 Introduction

Plants' susceptibility to water deficit is genetically predetermined in molecular, biochemical, physiological, and phenological properties, while plant water status regulates the intensity of physiological processes (Boyer, 1996; Tuberosa, 2012; Lawlor, 2013; Ribeiro Reis et al., 2020). Partitioning of assimilates and reproductive success of plants is influenced mainly by water use and plant water status, making it the primary driver of yield under drought stress (Blum, 2009). Therefore, water deficit induces numerous biochemical and physiological responses affecting plant growth by modifying its anatomy and morphology (Reddy et al., 2004; Shao et al., 2008). These development limitations mainly happen due to photosynthesis-dependent reductions in carbon balance (Flexas et al., 2009). Therefore, crop cultivars improved to withstand water deficit possess distinct physiological adaptive traits directed mainly to support yield under drought. Although drought usually occurs at different intensities and crop growth stages, it is relatively less common during seedling development. Seedling survival becomes vital in seasonal rainfall lag and can be linked to yield performance under drought (Agbicodo et al., 2009; Blum, 2011b). The most apparent basis for seedling survival is an osmotic adjustment, allowing hydration retention in low water potential to sustain photosynthesis *via* turgor maintenance (Blum, 2005; Blum, 2011a; Blum, 2017).

Nevertheless, drought score at the seedling stage is considered an irrelevant indicator of grain yield because recovery and damage repair in young plants can still enable future gain in grain yield (Blum, 2005; Blum and Tuberosa, 2018); thus, the relevance of seedling research becomes less significant. However, the importance of seedling survival for genetic engineering is an opportune trait. After all, seedling survival is easier to assess and demonstrate since seedlings are not subjected to the complexities of development and reproduction, unlike fully developed plants (Blum, 2011a). Moreover, selection based on seedlings research gains importance regarding environmental conditions vital for seedlings establishment, like germination in the limited water supply. Today's changes in the frequency and occurrence of extreme weather conditions are also causing additional disturbances in plants' water absorption, despite sufficient soil water. Thus, physiological drought can be caused by high or low soil temperatures, increased salinization, reduced air humidity, and increased airflow intensity (Novák, 2009), emphasizing the importance of seedling research.

Photosynthesis is one of the plants' most essential and sensitive processes, which any minor stressful event can disrupt. Its efficiency is critical in determining genotypes' resistance to any stress. Inhibition of photosynthesis in water deficit conditions correlated well with reduced water potential and stomatal conductance (Flexas and Medrano, 2002; Flexas et al., 2004; Chaves et al., 2008; Flexas et al., 2016) and decreased

level of relative water content (Lawlor, 2002). Mild to moderate drought stress causes the stomata to close, promoting a reduction in net photosynthesis to avoid additional water loss. However, closed stomata reduce ribulose-1,5-bisphosphate carboxylase/oxygenase supply with CO<sub>2</sub>, favoring its oxygenase function (Chaves and Oliveira, 2004), thus correlating with the loss of ATP (Lawlor and Tezara, 2009). The inability to utilize light energy then creates an imbalance in the electron transport chain (Foyer et al., 2012), increases the production of reactive oxygen species (Miller et al., 2010), affects the ratio of photosynthetic pigments (Li and Kim, 2022), and leads to the disorganization of thylakoid membranes (Zhu et al., 2021), which are the first to respond to even the slightest disturbance in the functioning of the plant (Stirbet and Govindjee, 2011). It is well known that drought impacts the plant's photosynthetic apparatus (Goltsev et al., 2012; Jedmowski et al., 2013; Jedmowski et al., 2015; Kalaji et al., 2018; Bashir et al., 2021). Accordingly, drought causes changes in the redox state of PSI, impairs an electron transfer at both the acceptor and the donor side of PSII, affects the oxygen-evolving complex, and decreases energetic connectivity and electron transfer capacity (Zhou et al., 2019).

Compared to PSI, PSII has good resistance to drought, and permanent adverse effects on PSII are present only in extreme drought conditions (Lauriano et al., 2006; Desotgiu et al., 2012). Besides, photosynthesis has shown resilience and high stability of the quantum yield of primary photochemistry of PSII when exposed to various intensities of drought stress (Oukarroum et al., 2007; Oukarroum et al., 2009; Qi et al., 2021). Widely applied measurements of chlorophyll *a* fluorescence help detect these first non-visible changes in photosynthetic apparatus functioning and structure (Strasser et al., 2004b; Goltsev et al., 2009; Goltsev et al., 2016; Kalaji et al., 2016; Kalaji et al., 2018; Samborska et al., 2019). Apart from being a simple, *in vivo*, and susceptible method, the fluorescence measurement provides a large amount of information on the physiological state of plants, which is essential for investigating and explaining physiological changes in certain environmental conditions like nutrient deficiency (Živčák et al., 2014; Samborska et al., 2019; El-Mejjaoui et al., 2022; Lotfi et al., 2022), salt (Kalaji et al., 2011b; Dąbrowski et al., 2016; Dąbrowski et al., 2017; Khatri and Rathore, 2022), temperature (Yang et al., 2009; Kalaji et al., 2011a; Oukarroum et al., 2016; Mihaljević et al., 2020) or drought stress (Zivcak et al., 2008a; Oukarroum et al., 2009; Goltsev et al., 2012; Goltsev et al., 2016; Kalaji et al., 2016; Kalaji et al., 2018). Many papers show that the measurement of chlorophyll fluorescence can potentially be used as a method of screening sensitive and tolerant genotypes of a particular plant species (Oukarroum et al., 2007; Boureima et al., 2012; Guha et al., 2013; Jedmowski and Brüggemann, 2015; Banks, 2018; Chiango et al., 2021; Markulj Kulundžić et al., 2022).

The complex information obtained by fast chlorophyll fluorescence kinetics can be presented in several ways. A

typical fluorescence transient shows phases from the onset of illumination ( $F_{0(50\mu s)}$ ) to a maximal possible fraction of closed RCs ( $F_{M(P)}$ ) value, which is defined as the OJIP curve, and analyzed by JIP-test (for detailed literature review, cf. (Strasser and Strasser, 1995; Stirbet and Govindjee, 2011; Goltsev et al., 2016; Tsimilli-Michael, 2020). For various intensities of drought impact, among obtained parameters, photosynthetic efficiency indices (PIs) have proven to be very useful for screening plants and evaluating the overall effect of stress on photosynthetic performance, while individual expressions provided pieces of information on the impact on separate processes (Tsimilli-Michael and Strasser, 2013; Živčák et al., 2014; Kalaji et al., 2017; Tsimilli-Michael, 2020). Furthermore, double normalized differential chlorophyll *a* fluorescence data, especially in the form of L- ( $\Delta W_{OK}$ ) and K-bands ( $\Delta W_{OJ}$ ), were used to assess the plant's resistance to drought-induced stress (Oukarroum et al., 2007; Oukarroum et al., 2009; Brestic et al., 2012; Brestic and Zivcak, 2013; Guha et al., 2013; Kalaji et al., 2018; Zhou et al., 2019).

When developing drought-resistant genotypes, it is essential to understand the physiological processes concerning photosynthesis and transpiration when water is limited. Precisely because of the complex genetic control of drought tolerance, it is necessary to test the performance of all varieties at different stages and intensities of drought. A plant's response to a lack of water depends on the duration and severity of the water deficit and the time of occurrence. Numerous studies have shown the connection between seed germination, seedling establishment, and soil moisture (Bouaziz and Hicks, 1990; Farsiani and Ghobadi, 2009; Jabbari et al., 2013; Lamichhane et al., 2018). Unlike fully grown plants, seedlings are not subjected to long-term environmental influences. They can use all the potentials of plant primordia to turn distressed conditions into beneficial stress indicative of adaptation (Kranner et al., 2010). Although germination and the first stage of the seedling establishment are among the most vulnerable plant growth stages, they are also prerequisites for the success of crops since the physiological traits of early seedling growth can be transferred to later stages of their life cycle. Some studies have shown that drought during the first stages of growth can efficiently diminish drought stress in the following stages of plant development (Selote et al., 2004; Abid et al., 2018; Auler et al., 2021). Selecting cultivars based on their drought tolerance in the first stages of development, where the problem is water scarcity in the early season, can help improve crop yields (Ahmed et al., 2020; Lu et al., 2022; Ru et al., 2022). Thus, making the development of drought tolerant crops environmentally and economically important.

This research aimed to establish a reliable screening of 18 winter wheat genotypes for drought susceptibility by comparing the impact of PEG-induced physiological drought on morphological, biochemical, and physiological characteristics

of seedlings shoots and roots. Furthermore, the aim was to identify possible photosynthetic mechanisms which best explain the variability among genotypes and could serve to differentiate and describe the seedlings' response to imposed physiological drought conditions. Therefore, this study can further upgrade our understanding of water-stress physiology, contributing to the progress in breeding research of winter wheat drought-tolerant lines.

## 2 Materials and methods

### 2.1 Plant material and experimental conditions

Eighteen genotypes of winter wheat (*Triticum aestivum* L.) were obtained from Agricultural Institute Osijek, Croatia (L459-2012, Osk 54/15, Osk 78/14, Osk 108/04, Osk 251/02, Osk 70/14, Osk 52/13, Osk 106/03, Osk 114/08, Osk 120/06, Osk 84/15, Osk 102/03, Osk 51/15, Osk 111/08, Osk 4.40/7-82, Osk 44/11, Osk 381/06, L259-2009) to study the effect of drought at the seedling stage. All genotypes have good tolerance to low temperatures, lodging, and winter wheat diseases. A widely used polymer polyethylene glycol 6000 (PEG-6000, ACROS Organics<sup>TM</sup>) was used to simulate the impact of drought stress. PEG is chemically inert and non-toxic for plant cells and changes the water potential of solutions by inducing potential osmotic pressure. For each treatment and replicate, 50 healthy seeds were hand sorted, soaked in water for 5 h, and surface sterilized with 2.5% sodium hypochlorite to prevent mycosis. Washed seeds were inoculated aseptically on moist filter papers (GE Healthcare Whatman<sup>TM</sup> Grade 598) in Petri dishes and placed in the dark for 72h at 20°C for germination. Germinated seeds with emerged radicles and coleoptile were transferred on a half-strength Hoagland's nutrient solution (Hoagland and Arnon, 1950). Water potential ( $\psi$ , MPa) was adjusted with PEG-6000 for control ( $\psi = -0.033$  MPa) and drought-induced stress ( $\psi = -0.301$  MPa) conditions according to Michel and Kaufmann (Michel and Kaufmann, 1973). All experimental units were placed in a controlled climate chamber under a 16/8h light/dark photoperiod at 22°C, 70/75% relative humidity, and light intensity of 120  $\mu\text{mol m}^{-2} \text{s}^{-1}$  (CWL and TLD 36W, Philips) for 7 days enabling slow development of stress as the most desirable since it simulates natural conditions. A constant temperature was used for the growth conditions since PEG water potential can variate with temperature. The growth medium was replaced daily throughout the experiment. Wheat seedlings of different genotypes were grown in a completely randomized design with three replicates of each treatment, and the experiment was replicated twice. All subsequent measurements were made on the first fully developed leaf and roots of 10-day-old seedlings.



## 2.2 Initial screening for drought tolerance - PEG test

A slightly modified PEG test was used for initial drought sensitivity screening (Agarie et al., 1995; ElBasyoni et al., 2017). Ten small leaf cuttings, approximately 1 cm in length, of 10-day-old wheat seedlings were placed in 50 ml test tubes and washed with deionized water three times. The leaf cuttings were then submerged in 20 ml of PEG-6000 solution ( $\psi = -0.602$  MPa) for dehydration treatment (P) or deionized water as the control (C). The test tubes with samples were then placed in the dark for 24 h at room temperature, and conductivity ( $\mu\text{S cm}^{-1}$ ) was measured afterward using the Conductivity Meter (Mettler Toledo). Next, the leaf cuttings were washed rapidly three times with deionized water. Both the control and treatment samples were submerged in 20 ml of deionized water and placed in the dark for another 24 h at room temperature for rehydration. After the rehydration, conductivity was measured, and leaf tissue was killed by heating the samples for 20 min at 100°C. The final conductivity was measured after cooling to room temperature. Three replicates were analyzed for both the control and PEG treatment. Cell membrane stability of wheat seedlings was expressed as cell membrane integrity percentage (%) with higher rates indicating less damage using the equation:  $CMI (\%) = [(1 - \frac{P_{int}}{P_{tot}}) / (1 - \frac{C_{int}}{C_{tot}})] \times 100$ , where  $P_{int}$  and  $C_{int}$  are the sum of conductivity measurements of the PEG desiccation treatment and the control after dehydration and rehydration, and  $P_{tot}$  and  $C_{tot}$  are the final conductivity measurements after the tissue destruction by heating.

## 2.3 Determination of morphological, physiological, and biochemical indices

### 2.3.1 Growth measurements

Seedlings were harvested on the 10<sup>th</sup> day to determine the growth parameters. The straight ruler method was used to determine the height of seedlings. Each seedling's longest primary seminal root was measured (Image J). The dry weight of roots and shoots was measured after drying in an oven for 24 h at 80°C.

### 2.3.2 Relative water content

The relative water content of leaves (RWC) was determined in random leaves that were cut into approximately 1 cm long pieces, weighted fresh (FW, g), and placed to float on distilled water until fully rehydrated (approx. 4 h) in the dark, weighted to obtain turgid weight (TW, g) and then dried until a constant oven-dry weight (DW, g) is obtained (at 80°C for 24 h). The equation described by Turner et al. (Turner, 1986) was used to calculate the percentage of relative water content:  $RWC (\%) = (FW - DW) / (TW - DW) \times 100$ .

### 2.3.3 Electrolyte leakage

Electrolyte leakage (EL) was determined in random leaves cut to leaf segments (approx. 1 cm length) by placing them in closed vials containing 20 ml of deionized water for 24 h at room temperature in the dark. Relative EL of the samples was estimated according to the ratio of the initial conductivity ( $EC_1$ ,  $\mu\text{S cm}^{-1}$ ) to the absolute conductivity after heat disruption of cell membranes (100°C, 20 min,  $EC_2$ ,  $\mu\text{S cm}^{-1}$ ) with the equation:  $EL (\%) = (EC_1 / EC_2) \times 100$ .

### 2.3.4 Malondialdehyde and free proline content

For all genotypes and treatments, the lipid peroxidation and free proline content were determined in the leaves and roots of wheat seedlings. Lipid peroxidation was estimated by measuring the amount of malondialdehyde (MDA) produced by the thiobarbituric acid (TBA) reaction (Heath and Packer, 1968). Approximately 0.2 g of homogenized fresh tissue sample was extracted in 0.1% trichloroacetic acid (TCA). The mixture of extract and 0.5% thiobarbituric acid in 20% TCA was heated at 95°C for 30 min, then quickly cooled in an ice bath, and the absorbance was recorded at 532 (specific) and 600 (non-specific) nm (UV-VIS Spectrophotometer, Analytic Jena SPECORD 40). After subtracting the non-specific absorbance, the MDA content was calculated using its molar extinction coefficient ( $\epsilon_{532} = 155 \text{ mM}^{-1} \text{ cm}^{-1}$ ), and the results were expressed as nmol (MDA) g<sup>-1</sup> dry weight.

Free proline was analyzed by the ninhydrin-based colorimetric assay (Abrahám et al., 2010). Plant material (approximately 0.1 g of a homogenized fresh tissue sample) was extracted with 3% sulfosalicylic acid. The reaction mixture of proline extract, 3% sulfosalicylic acid, glacial acetic acid, and acidic ninhydrin was incubated at 95°C for 60 min. The reaction was terminated on ice. The red-colored chromophore was extracted with toluene, and the absorbance of the toluene fraction was measured at 520 nm. The free proline amount expressed as  $\mu\text{mol g}^{-1}$  of dry weight was calculated using a standard curve for L-proline.

### 2.3.5 Chlorophyll pigments

Carotenoids (Car), chlorophyll *a* (Chl *a*), and chlorophyll *b* (Chl *b*) of wheat seedlings were determined according to (Lichtenthaler and Buschmann, 2001). Pigments from fresh leaf samples (0.1 g) were extracted with pure acetone with several re-extractions, centrifuged each time at 18 000 × g and 4°C for 15 min. The absorbances of the extracts were recorded at 470, 644.8, and 661.6 nm and calculated using the following equations:

$$\text{Chl } a \text{ (mg/ml)} = 11.24 \times A_{661.6} - 2.04 \times A_{644.8}$$

$$\text{Chl } b \text{ (mg/ml)} = 20.13 \times A_{644.8} - 4.19 \times A_{661.6}$$

Car (mg/ml)

$$= (1000 \times A_{470} - 1.90 \times \text{Chl } a - 63.14 \times \text{Chl } b) / 214$$

## 2.4 Measurement of the chlorophyll *a* fluorescence transient (O-J-I-P)

The emission of the chlorophyll *a* fluorescence was measured on the first fully developed leaf of randomly chosen 20 plants for every genotype and treatment. The measurements were performed in leaves previously adapted to the dark for 30 min with a Handy PEA fluorometer (Hansatech, UK). The transient was induced with a red-light pulse of 3000  $\mu\text{mol m}^{-2} \text{s}^{-1}$  and analyzed using the JIP-test (Strasser and Strasser, 1995; Stirbet and Govindjee, 2011; Goltsev et al., 2016; Tsimilli-Michael, 2020). For a detailed evaluation of the OK, OJ, JI, and IP phases, a transient curve was normalized as a relative variable fluorescence at time *t*, as follows:  $F_t/F_0$ , where  $F_t$  is the fluorescence yield (Stirbet et al., 2014). The kinetic differences were calculated from the relative variable fluorescence by subtracting the transient of stressed and control plants. For detailed definitions and explanations of the JIP test parameters, see (Goltsev et al., 2016) and (Tsimilli-Michael, 2020).

## 2.5 Statistical analysis

The Shapiro-Wilks test was used to check if the data followed normality, and Levene's test was used to check the assumption of equal variances. Since the assumptions were not rejected, two-way ANOVA and Tukey HSD tests were used to determine significant genotype differences. To better observe the differences between the treatment and the control group and individual genotypes, the difference between the treatment's mean value and the control group's mean value was calculated. The calculation of the mean difference does not consider the standard deviation within the groups. Therefore, a quantitative measure of the strength of an effect (Hedges effect size) was calculated as the standardized mean difference between two groups ( $\bar{x}_1 - \bar{x}_2$ ) based on the pooled, weighted standard deviation ( $SD_{pooled}$ ) of the sampled population ( $N$ ) according to Hedges and Olkin (1985):

$$d = (\bar{x}_1 - \bar{x}_2) / SD_{pooled}$$

$$SD_{pooled} = \sqrt{((n_1 - 1)SD_1^2 + (n_2 - 1)SD_2^2) / (n_1 + n_2 - 2)}$$

Considering that this paper deals with data obtained in a laboratory experiment and small independent samples, an unbiased version of effect size was derived according to Ellis (2010):

$$\text{corrected (Hedges } d) \cong d[1 - (3 / (4(n_1 + n_2) - 9))]$$

Effect size assesses the degree to which the examined effect is present or the degree to which the null hypothesis is not valid, so it is not just binary data. In other words, if the null hypothesis is correct, the P-value indicates the probability that the observed difference exists. But also, P-values can indicate how incompatible the data are with a statistical model. A statistically insignificant result does not "prove" the null hypothesis. Neither statistically significant results "prove" any other hypothesis. Suppose we supplement the P-values obtained by testing the null hypothesis with the P-value from the test of a predetermined alternative (such as the minimum important effect size). In that case, we will get a better and more informative representation of the proven values (Nakagawa and Cuthill, 2007). The higher the effect size, the greater the increase of a parameter in the treatment compared to the control group. Negative effect size values indicate a decrease in a parameter compared to the control group. The large effect depends on the context and known sources of variability (Sawilowsky, 2009; Sawilowsky et al., 2011). All calculations using previously described equations: pooled SD, biased effect size, 95% confidence intervals, and statistical analyses from which these results were derived (p-value for the mean difference using 2-tailed T-test) were done in Excel (Microsoft Corporation, 2019). Effect size estimates with 95% confidence intervals were graphically presented by stock graphs (high-low-close) in combination with line plots of the mean difference.

Principal Component Analysis (PCA), a multivariate statistical technique, was used to reduce a large set of chlorophyll *a* fluorescence parameters to the most informative ones (Goltsev et al., 2012; Kalaji et al., 2017). PCA was also used to investigate the effect of genotype diversity on the structure of the variability in measured fluorescence parameters and their correlations with morphological and biochemical parameters with direct oblimin rotation. To classify the variability in response to mild drought stress among genotypes into groups, a hierarchical k-means clustering algorithm on main features was used to obtain optimal cluster solutions (Bussotti et al., 2020). PCA and HAC multivariate statistical analysis and graphical presentations of PCA and HAC were made with XLSTAT 2022.2.1.1304 (Addinsoft, 2022).

## 3 Results

### 3.1 Initial screening for drought tolerance – PEG test


For a preliminary screening of winter wheat varieties to drought susceptibility, seedlings of 18 wheat genotypes were

subjected to a PEG test as an efficient method to determine drought sensitivity. Cell membrane stability as the integrity percentage is shown in Table 1. Although desiccation treatment significantly increased electrolyte leakage in all genotypes (cell membrane integrity ranged from 41 to 69%) and differences (One-way ANOVA,  $F_{17,90} = 2.4$ ,  $p = 0.005$ ) among genotypes were found, the Tukey HSD test revealed that significant difference exists only between genotype with the lowest (Osk 106/03) and the highest cell membrane integrity (Osk 4.40/7-82, 114/08, 51/15, 108/04 and 381/06). Based on these results and to find phenotypic variability among genotypes, the potential osmotic pressure of PEG-6000 for the experimental treatment was reduced from moderate to mild drought stress (to -0.301 MPa).

### 3.2 Morphology and relative water content

Examining the influence of genotypic variability and drought treatment on plant growth, two-way ANOVA showed a significant effect of the tested factors: genotypes ( $p < 0.001$ ), PEG induced drought (-0.03 and -0.3 MPa;  $p < 0.001$ ) and their interactions ( $p < 0.001$ ) on the shoot and root growth, as well as their ratio, with treatment as the most influential variable that affects plant growth, and the interaction with genotype variability as the most significant variable that affected the root-to-shoot ratio (Table 2). Shoot height was significantly reduced by PEG-induced drought in all genotypes (Figure 1A, Tukey HSD,  $p < 0.05$ ), with a decrease ranging from 16% (Osk

TABLE 1 The initial screening and ranking of 18 different winter wheat genotypes based on cell membrane stability of wheat seedlings expressed as cell membrane integrity (CMI %) obtained by PEG test.



Genotype	CMI %	SE	CI (95%)		Tukey HSD
Osk 106/03	43.8	1.4	41	46.7	a
Osk 52/13	49.7	2.2	45.4	54	ab
Osk 78/14	51.6	0.5	50.6	52.7	ab
Osk 102/03	52.6	0.9	50.9	54.3	ab
Osk 70/14	52.9	0.9	51.1	54.6	ab
L459-2012	53.4	2.4	48.6	58.2	ab
Osk 44/11	54.4	1	52.4	56.5	ab
Osk 120/06	55.4	2.5	50.5	60.3	ab
Osk 251/02	55.6	2.8	50	61.3	ab
L259-2009	56.1	2.7	50.7	61.4	ab
Osk 84/15	56.4	2.3	51.9	61	ab
Osk 111/08	56.5	2	52.5	60.5	ab
Osk 54/15	56.9	1.4	54	59.8	ab
Osk 4.40/7-82	57.1	1.3	54.5	59.6	b
Osk 114/08	57.5	4	49.6	65.4	b
Osk 51/15	59.5	2.8	53.9	65	b
Osk 108/04	59.7	2.4	55	64.5	b
Osk 381/06	60.2	4.5	51.3	69.2	b

The results are the mean, standard error (SE), and 95 % confidence interval (CI). Means followed by a joint letter are not significantly different (the Tukey HSD-test at the 5% significance level). On the left side is an example of 10-days-old wheat seedlings (Osk 4.40/7-82) exposed to test conditions: control (CON,  $\psi = -0.033$  MPa) and physiological drought (PEG,  $\psi = -0.301$  MPa). Different hues of blue, yellow and red color scale were used for visualisation of CMI % data (min, average, max).

TABLE 2 Two-way ANOVA analysis of the effects of wheat cultivars and drought treatment on plant growth.

	df	Shoot height	Root length	Root/shoot ratio
F	35, 2101	223.72***	150.63***	55.41***
R <sup>2</sup>		0.78	0.72	0.48
Genotypes (G)	17	138.82***	94.03***	38.89***
Treatment (T)	1	4839.45***	2531.22***	12.89***
G×T	17	27.44***	53.18***	72.99***

\*\*\* ( $P < 0.001$ ).

Significant differences (F values) are marked with asterisks, and df are degrees of freedom.

102/03) to 53% (L459-2012) compared to the control plants. A statistically significant negative effect of drought on the root growth was observed in most of the tested genotypes except for L459-2012 and Osk 70/14 (Figure 1B), which in contrast to all the others, showed an increase in root length (by 11% and 9%).

The differences in shoot and root growth were reflected in their ratio. The Tukey difference test determined a non-significant difference between control and drought in the root-to-shoot ratio of eleven cultivars. However, the calculated standardized effect size (Hedges  $d$ ) revealed only three cultivars with a non-significant change in the ratio (Figure 1C). The most substantial increase in the root-to-shoot ratio under drought was found in the genotype L459-2012 (by 161%), although not the highest effect due to more considerable variation among the measured plants. At the same time, the most substantial decrease was found in Osk 120/06 (by 45%). Three groups of wheat response in the root-to-shoot ratio can be discerned, the ones with decreased ratio (120/06, 44/11, 381/06), the ones with very little to no change in the ratio (eleven cultivars, Figure 1C), and the ones with significantly increased

root-to-shoot ratio (70/14, 54/15, L459-2012, 78/14). In all varieties, at least a double increase in root dry matter was observed in conditions of PEG-induced drought (Supplementary Material Table 2). In addition to the increased accumulation of carbohydrates (since 50% of dry weight refers to carbohydrate content), an increase in osmolytes or secondary compounds like phenols and lignin is also possible (Ghanbari and Sayyari, 2018; Qayyum et al., 2021). Relative water content was also decreased (on average by 10%) in all genotypes when exposed to physiological drought, with no significant differences among genotypes referring to treatment as the most influential variable (Figure 1D, Supplementary Material Table 3).

### 3.3 Free proline and lipid peroxidation

A significant increase in PRO was induced by physiological drought in both roots and leaves of all genotypes (Figures 2A, B). The most considerable mean differences and the effect sizes in leaves were found for Osk 381/06 (Figure 2B). The two-way

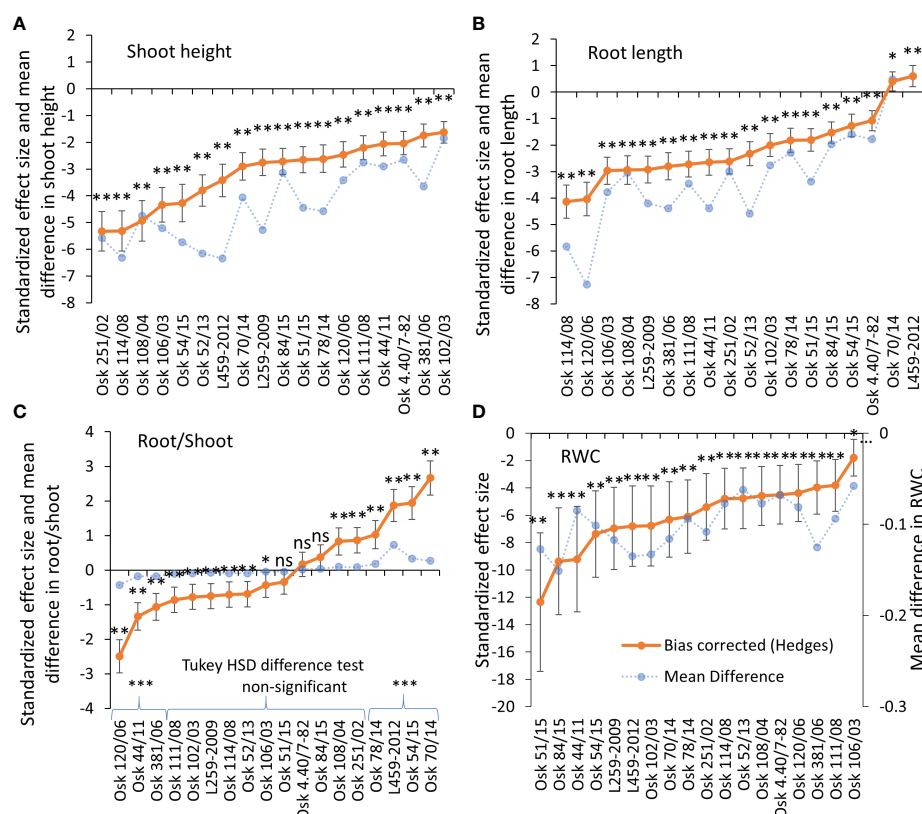


FIGURE 1

Hedges bias-corrected treatment effect size (with confidence interval) and the mean difference in shoot height (A), root length (B), root-to-shoot ratio (C), and relative water content (RWC) (D) between PEG-induced drought and control treatment in 18 genotypes of wheat seedlings. Significant effects of PEG-induced drought are marked with asterisks (\*  $p < 0.05$ , \*\*  $p < 0.01$ , \*\*\*  $p < 0.001$ ), and ns stands for non-significant ( $p > 0.05$ ). Based on the Tukey HSD difference test, significant differences were determined in root-to-shoot ratio for Osk 120/06, 44/11, and 381/06 (decreased root/shoot induced by drought) and for Osk 78/14, 54/15, 70/14, and L459-2012 (increased root/shoot ratio induced by drought).



ANOVA model explained more than 99% of the data with a significant treatment effect, genotype variability, and interaction in leaves and roots. Based on the Type III sum of squares, the most influential was genotype variability (Supplementary Material Table 3). As for the malondialdehyde content, MDA decreased in roots (except Osk 4.40/7-82) in almost all genotypes when exposed to PEG-induced physiological drought. At the same time, there was a significant increase in leaf MDA content (Figures 2C, D). Also, the two-way ANOVA showed that genotype variability is the most influential variable (Supplementary Material Table 3).

### 3.4 Pigment content

Physiological drought induced a significant Chl $a$  decrease in most samples. Three genotypes had no change in Chl $a$ , while in two genotypes, Chl $a$  content increased (Figure 3A). A similar trend was determined for Chl $b$  and Car content (Figures 3B, C). In those genotypes that responded to PEG-induced drought with an increase in pigment content (like L259-2009), it was evident that they had no problems adapting to osmotic stress by

maintaining high photosynthetic efficiency, which is an adaptive feature, thus enabling a better tolerance of physiological drought. At the same time, a decreasing Chl-to-Car ratio (Figure 3D) can imply some photosynthetic apparatus damage. In those genotypes with decreased pigment content, a lower degree of carotenoid loss also reflects adaptive strategy because of their role in antioxidative defense. Like for PRO and MDA, the Type III sum of squares in two-way ANOVA revealed that genotype variability was the most influential in determining the response of pigment content to physiological drought (Supplementary Material Table 3).

### 3.5 Chlorophyll $a$ fluorescence

#### 3.5.1 PCA and clustering

Up to now, the results showed that drought treatment was the most influential variable affecting plant growth and relative water content, while genotype variability determined with what intensity varieties of winter wheat seedlings responded to drought. In some cultivars, mild drought stress doesn't simply trigger acclimation to new conditions but results in various

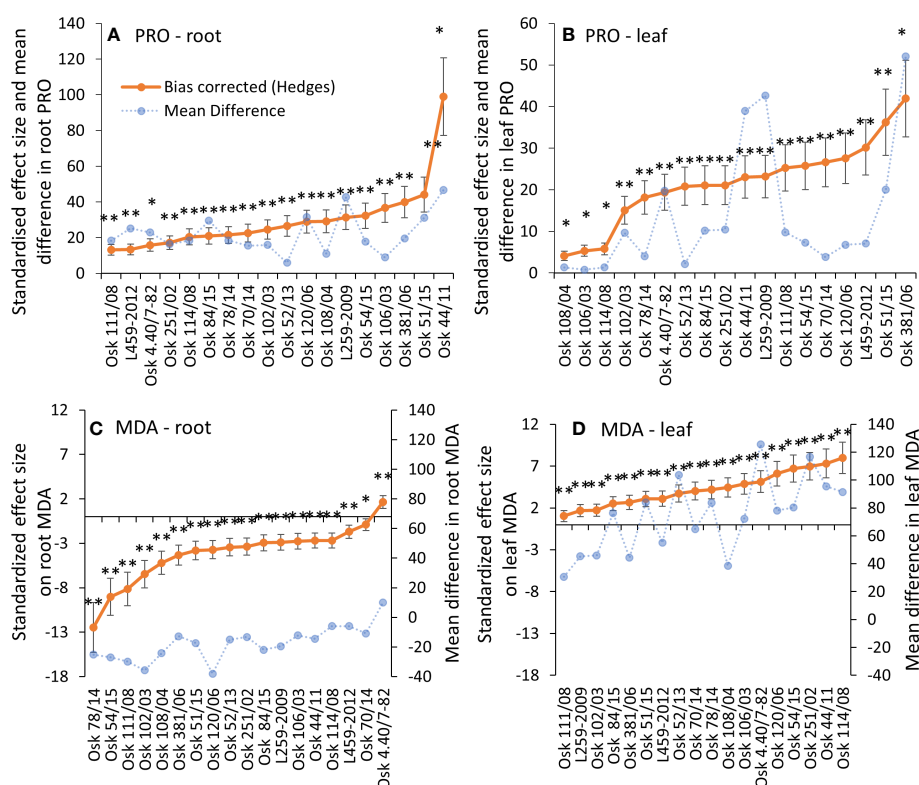


FIGURE 2

Hedges bias-corrected treatment effect size (with confidence interval) and the mean difference between PEG-induced drought and control treatments for proline and MDA contents in roots (A, C) and leaves (B, D) of 18 genotypes of winter wheat seedlings. Significant effects of PEG induced drought are marked with asterisks (\*  $p < 0.05$ , \*\*  $p < 0.01$ , \*\*\*  $p < 0.001$ ), and ns stands for non-significant ( $p > 0.05$ ).

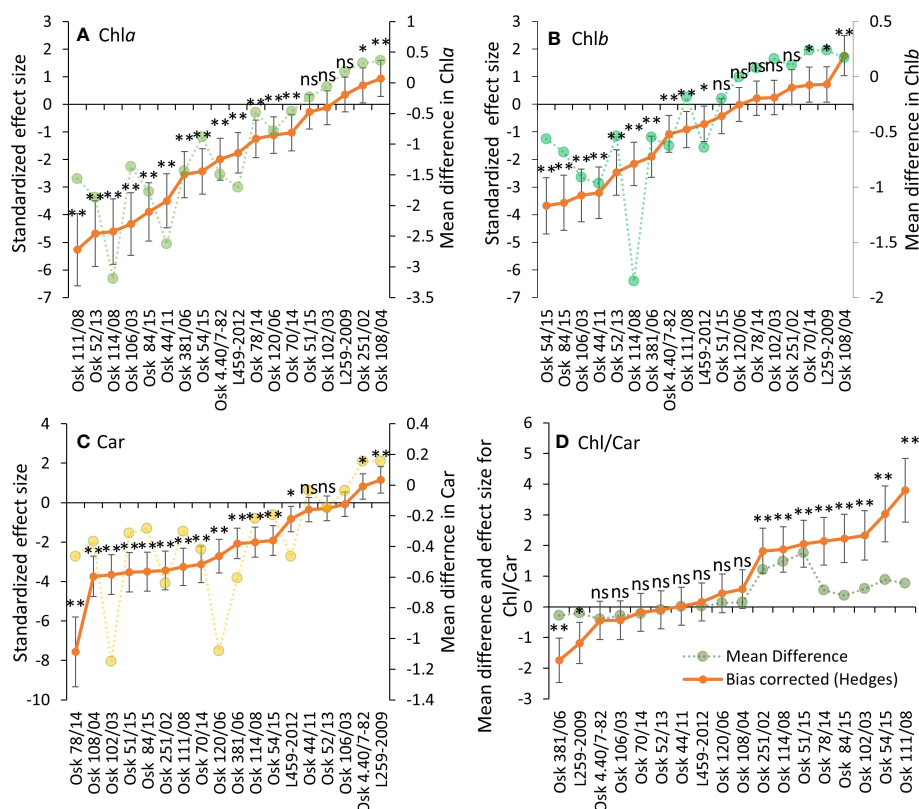


FIGURE 3

Hedges bias-corrected effect size (with confidence interval) and the mean difference between PEG-induced drought and control treatments for pigment content: Chla (A), Chlb (B), Car (C), and their ratio (D) in 18 genotypes of wheat seedlings. Significant effects of PEG induced drought are marked with asterisks (\*  $p < 0.01$ , \*\*  $p < 0.001$ ), and ns stands for non-significant ( $p > 0.05$ ).

degrees of damage. Therefore, chlorophyll *a* fluorescence measurements were used to obtain parameters regarded as indicators of photosynthetic efficiency that could be associated with the damage to the photosynthetic apparatus. A summary of correlations (Supplementary Material Tables 4–6) of all measured parameters considering all varieties and treatments (control and physiological drought) allows identification of potential structures in the matrix and quick detection of correlations of interest. Given the extensive range of data, separate and individual correlations were not explained. The results show that many data are in a complex interrelationship, so to provide a complete picture of linear connectivity, data were summarized in a smaller number of components by multivariate analyses.

Figure 4 shows the Principal component analysis of the combined chlorophyll *a* fluorescence and biochemical parameters obtained considering control and treatment together. The Kaiser-Meyer-Olkin measure of sampling adequacy was 0.66, and three principal components were distinguished, explaining the variance in 80.4% of the total data. However, complex variables contributing to correlation

among both dimensions made them challenging to interpret. After rotation, the first principal component (PC1) accounted for 31.2% of the variance, and the second (PC2) for 29.9%. Positive loadings that characterized the first component with 81.3% contribution were:  $ABS/CS_o$ ,  $DI_o/CS_o$ ,  $TR_o/CS_o$ ,  $ET_o/CS_o$ ,  $RE_o/CS_o$ ,  $ABS/CS_m$ ,  $DI_o/CS_m$ ,  $TR_o/CS_m$ ,  $ET_o/CS_m$ ,  $RE_o/CS_m$ ,  $RE_o/RC$ ,  $\delta R_o$ ,  $\delta R_o/1-\delta R_o$ , representing phenomenological energy fluxes per cross-section of PSII and the efficiency with which an electron is transferred to final PSI acceptors. Given the position of the control and PEG-treated samples along the PC1 axis, the PEG-induced drought has changed the phenomenological energy flows to some extent and affected the transport of electrons to the end receptors (Figure 4A).

The PC2 was characterized by positive loadings with 62.8% contribution, which were related to the efficiency of the water-splitting complex and the density of active reaction centers at the donor side of PSII ( $\phi P_o/1-\phi P_o$ ,  $\gamma RC/1-\gamma RC$ ), maximum quantum yield ( $\phi P_o$ ), the quantum yield of photoinduced electron transport at the acceptor side of PSII ( $\psi E_o$ ,  $\phi E_o$ ), the pool size of electron carriers ( $S_M$ ,  $N$ ) and the performance indices on absorption basis ( $PI_{ABS}$ ). Negative loadings contributed 24% and

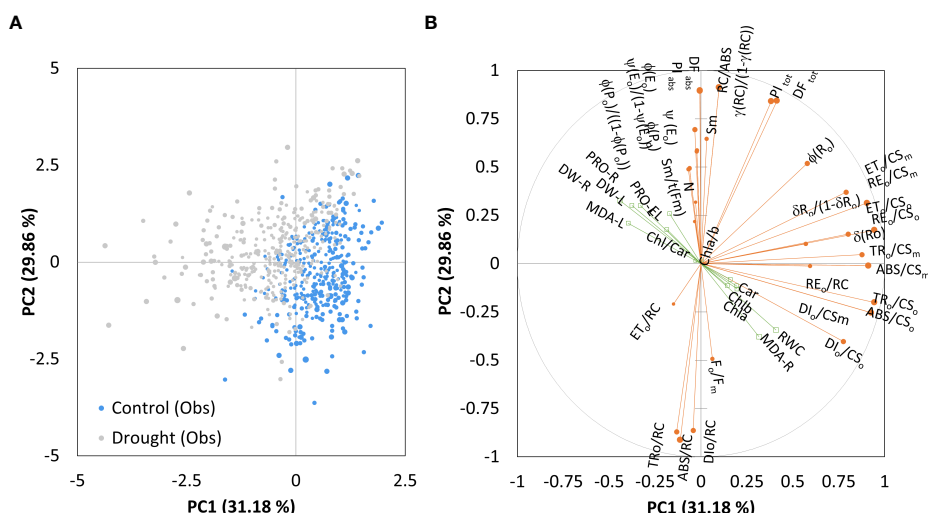


**FIGURE 4**  
Ordination of all observations **(A)** and correlation between variables on the first two main components **(B)** obtained by principal component analysis on measured parameters (chlorophyll *a* fluorescence as active variables and biochemical measurements as supplementary variables) for control and PEG-induced drought treatment of 18 winter wheat cultivars (*n* = 720).

included adsorbed photon flux by the antenna of PSII units, the part of trapped photon flow by PSII active units that leads to  $Q_A$  reduction, and the amount dissipated in the PSII antenna ( $ABS/RC$ ,  $TR_o/RC$ , and  $DI_o/RC$ ). When all samples were considered, biochemical measurements had a low contribution to all axes. RWC had the highest positive loading to PC1 (0.408), while negative loadings to PC1 were determined for root dry weight (-0.443) and leaf MDA (-0.397). All others were lower than that and contributed to the complexity, thus preventing differentiation between components.

To further evaluate and compare the magnitude of cultivar diversity among tested winter wheat seedlings in response to imposed physiological drought, principal component analysis was repeated on the results of the difference test between treatment and control samples. The main components (PC) scores explaining more than 80% variance in the data were then used as input variables for hierarchical cluster analysis (HAC) to classify wheat cultivars' entries based on their similarity and dissimilarity response. Figure 5 presents the chlorophyll *a* fluorescence parameters distribution on the first two principal components and locations of observed genotypes as centroids of tested data. Factor loadings after oblimin rotation differentiated three main components explaining 82.2% of the total variance in the data (Table 3). Significant positive loadings contributed to the first principal component with 83.4% contribution. They included parameters connected to the dissipation mechanisms (ABS/RC, DI<sub>0</sub>/RC, DI<sub>0</sub>/CS<sub>0</sub>), parameters related to the disconnection of the tripartite system (RC-core antenna-LHC) described by variable fluorescence at L-band (V<sub>L</sub>), inactivation of the oxygen-evolving system described by variable fluorescence at

K-band ( $V_K$ ), trapped photon flow and flow of electrons transferred from  $Q_A^-$  to PQ per active PSII ( $\Phi_{PQ}$ ), and simultaneously, negative loadings of the efficiency of the water-splitting complex and the density of active reaction centers at the donor side of PSII ( $\Phi_P/1-\Phi_P$ ,  $\gamma_{RC}/1-\gamma_{RC}$ ) as well as a maximum efficiency of PSII photochemistry ( $\Phi_P$ ) and performance index on absorption basis ( $PI_{ABS}$ ).

The second principal component (PC2) included positive loadings with a 93.0% contribution related to the pool size of electron carriers ( $S_m$ ,  $N$ ), reduction of end electron acceptors ( $\delta R_o$ ,  $\phi R_o$ ,  $RE_o/RC$ ,  $RE_o/CS_o$ ,  $RE_o/CS_m$ ,  $\delta R_o/1-\delta R_o$ ) that characterize IP-phase, as well as negative loadings related to variable fluorescence at I-step. All these parameters strongly correlated with PC2 and influenced the total performance on an absorption basis or the whole linear electron transport ( $PI_{TOT}$ ). Moderate correlations included the quantum yield of photoinduced electron transport at the acceptor side of PSII ( $\psi E_o$ ,  $\phi E_o$ ) and the ability to maintain an electron chain between two photosystems ( $\psi E_o/1-\psi E_o$ ) on the positive side of the PC2 axis. In contrast, variable fluorescence at J-step ( $V_j$ ) was on the opposing side.

And the third principal component (PC3) was related to the density of reaction centers (RC/CS) and the phenomenological energy fluxes per excited cross-section of PSII, the absorbed photon flux (ABS/CS<sub>o</sub>, ABS/CS<sub>m</sub>), maximum trapped photon flux (TR<sub>o</sub>/CS<sub>o</sub>, TR<sub>o</sub>/CS<sub>m</sub>), and the flux of electrons from Q<sub>A</sub><sup>-</sup> to PQ pool (ET<sub>o</sub>/CS<sub>o</sub>, ET<sub>o</sub>/CS<sub>m</sub>) per cross-section of PSII, all of which accounted for 88.1% contribution (Table 3).

Hierarchical k-means clustering on main components separated investigated genotypes into four distinctive groups

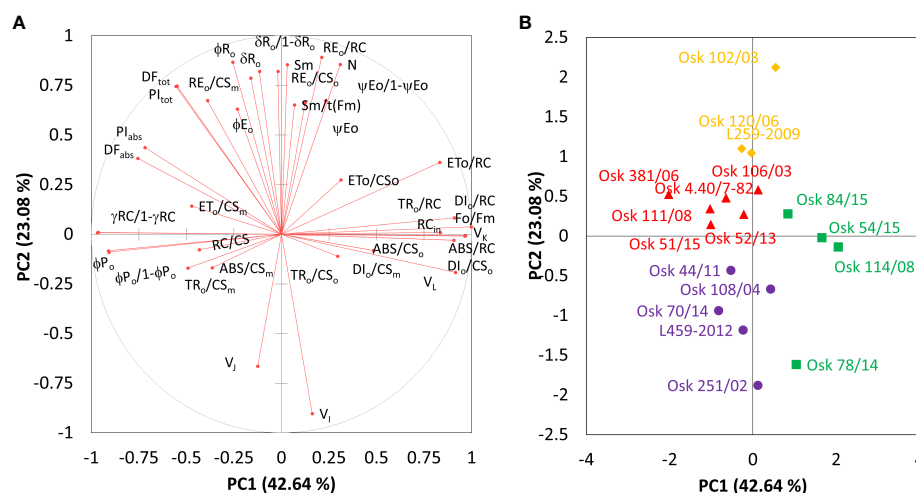


FIGURE 5

Principal component analysis of chlorophyll *a* fluorescence parameters derived as the mean difference between PEG-induced drought treatment and control samples for 18 winter wheat cultivars. Correlations between obtained parameters and the two principal components (A) and projections of genotypes (B) with only centroids that are displayed and sorted by hierarchical cluster analysis (● Cluster 1, ■ Cluster 2, ▲ Cluster 3, ◆ Cluster 4).

(Supplementary Material Figure 1) defined by their response to the physiological drought. The observation plot (Figure 5B) allowed exploring the correlations between PCs and investigated genotypes. The main advantage of this process was that each genotype was assigned to only one group reflecting the significance of the most important contributors to the total variance at each axis, thus enabling the selection of relevant parameters for classifying genotypes with similar traits. *Cluster 1* is represented by Osk 251/02, 108/04, 44/11, 70/14, and L459-2012; *Cluster 2* by Osk 54/15, 114/08, 84/15, and 78/14; *Cluster 3* by Osk 111/08, 51/15, 381/06, 4.40/7-82, 106/03, and 52/13; and *Cluster 4* by Osk 102/03, 120/06, and L259-2009. Clusters of winter wheat genotypes will be described with a few of the most frequently used damage indicators derived from chlorophyll *a* fluorescence measurements.

### 3.5.2 Stability of oxygen-evolving complex, energetic connectivity, and photosynthetic efficiency indices

A closer look into the earliest phases of the photosynthetic induction curve is presented in the form of differential curves of relative variable fluorescence O-J and O-K normalized induction curves (Figures 6 and 7). Positive inflections of K-band in genotypes of *Cluster 2* (Osk 54/15, 114/08, 84/15, and 78/14) suggested inhibition of electron flow from the acceptor side of PSII, indicating low OEC activity (Figure 6). These genotypes are in the group of drought-susceptible genotypes showing more significant damage to their OEC. Negative deviations of K-band in genotypes of *Cluster 3* indicated that they possess a potential to cope with stress due to their higher stability of OEC and

electron transport from PSII to PSI for driving energy synthesis. Genotypes with suppressed K-band (*Cluster 1* and *4*) indicated enhanced resistance of PSII to PEG-induced physiological drought since they can resist drought-induced imbalance in electron flow at the acceptor and donor sides of PSII.

Results shown in Figure 7 demonstrate that, in susceptible wheat genotypes, even mild drought stress caused a distinct decrease of the energetic connectivity with positive L-bands determined in genotypes of *Cluster 2*, based on the loss of OEC functionality or loss of stability in the tripartite system that controls the first stage of light-harvesting or the LHC-core antenna-RC complex. On the other hand, negative deviations of the L-band indicated an increase in cooperativity of excitation energy exchange between PSII units upon PEG treatment, thus resulting in more efficient consumption of the excitation energy and higher stability of the photosynthetic system (in lines of *Cluster 3*: Osk 111/08, 381/06, 51/15). In genotypes with the observed marginal change of L-band amplitude (*Cluster 1* and *4*), energy connectivity was maintained since the dissociation of LHCII from the PSII complex was prevented.

Since the calculated PIs values are relative, they alone cannot be used to characterize samples. What is significant are the changes that occur in  $PI_{ABS}$  and  $PI_{TOT}$  following any environmental disturbance or stress on the photosynthetic tissue. Figure 8 presents the estimates of the difference between control and treatment samples and shows variations in the response of genotype clusters to imposed physiological drought, which will be elaborated further in the discussion part.



TABLE 3 Correlations between variables and factors and variable contribution (%) after oblimin rotation.

	Correlations			Contribution (%)		
	PC1	PC2	PC3	PC1	PC2	PC3
F <sub>o</sub> /F <sub>m</sub>	<b>0.907</b>	-0.023	-0.176	5.266	0.068	0.182
V <sub>L</sub>	<b>0.936</b>	-0.302	-0.035	5.331	0.359	0.009
V <sub>K</sub>	<b>0.905</b>	-0.14	0.009	5.226	0.009	0.077
V <sub>J</sub>	-0.056	<b>-0.653</b>	0.187	0.099	4.307	0.394
V <sub>I</sub>	0.277	<b>-0.92</b>	-0.084	0.167	7.965	0.135
Sm	-0.061	<b>0.855</b>	-0.189	0.006	7.145	0.413
N	0.217	<b>0.822</b>	-0.199	0.606	7.153	0.37
S <sub>m</sub> /t(F <sub>m</sub> )	0.004	<b>0.648</b>	-0.21	0.03	4.15	0.536
ABS/RC	<b>0.965</b>	-0.123	-0.032	5.953	0	0.019
DI <sub>o</sub> /RC	<b>0.995</b>	-0.081	-0.106	6.335	0.014	0.019
TR <sub>o</sub> /RC	<b>0.905</b>	-0.14	0.009	5.226	0.009	0.077
ET <sub>o</sub> /RC	<b>0.792</b>	0.264	-0.117	4.407	1.283	0.037
RE <sub>o</sub> /RC	0.095	<b>0.863</b>	0.105	0.286	7.773	0.297
Φ(P <sub>o</sub> )	<b>-0.907</b>	0.023	0.176	5.266	0.068	0.182
Ψ(E <sub>o</sub> )	0.056	<b>0.653</b>	-0.187	0.099	4.307	0.394
Φ(E <sub>o</sub> )	-0.299	<b>0.661</b>	-0.116	0.342	3.891	0.203
δ(R <sub>o</sub> )	-0.268	<b>0.802</b>	0.162	0.167	6.048	0.431
Φ(R <sub>o</sub> )	-0.367	<b>0.895</b>	0.103	0.418	7.355	0.168
ABS/CS <sub>o</sub>	0.432	-0.16	<b>0.843</b>	1.487	0.064	11.457
DI <sub>o</sub> /CS <sub>o</sub>	<b>0.800</b>	-0.103	0.428	4.436	0.001	3.544
TR <sub>o</sub> /CS <sub>o</sub>	0.242	-0.169	<b>0.936</b>	0.556	0.119	13.62
ET <sub>o</sub> /CS <sub>o</sub>	0.222	0.216	<b>0.795</b>	0.623	0.732	10.145
RE <sub>o</sub> /CS <sub>o</sub>	-0.152	<b>0.811</b>	0.487	0.002	6.592	3.821
ABS/CS <sub>m</sub>	-0.405	-0.147	<b>0.903</b>	0.844	0.279	11.415
DI <sub>o</sub> /CS <sub>m</sub>	0.432	-0.16	<b>0.843</b>	1.487	0.064	11.457
TR <sub>o</sub> /CS <sub>m</sub>	<b>-0.527</b>	-0.13	<b>0.830</b>	1.544	0.283	9.37
ET <sub>o</sub> /CS <sub>m</sub>	<b>-0.541</b>	0.181	<b>0.763</b>	1.424	0.197	8.055
RE <sub>o</sub> /CS <sub>m</sub>	<b>-0.503</b>	<b>0.708</b>	0.492	0.963	4.433	3.472
RC/CS	-0.476	-0.045	<b>0.795</b>	1.188	0.06	8.709
PI <sub>ABS</sub>	<b>-0.770</b>	<b>0.523</b>	0.038	3.281	1.867	0
PI <sub>TOT</sub>	<b>-0.644</b>	<b>0.812</b>	0.089	1.922	5.461	0.07
DF <sub>ABS</sub>	<b>-0.798</b>	0.474	-0.011	3.64	1.429	0.045
DF <sub>TOT</sub>	<b>-0.651</b>	<b>0.809</b>	0.108	1.963	5.424	0.113
γRC/1-γRC	<b>-0.967</b>	0.124	0.037	5.968	0.001	0.014
ΦP <sub>o</sub> /1-ΦP <sub>o</sub>	<b>-0.904</b>	0.016	0.168	5.247	0.08	0.156
ΨE <sub>o</sub> /1-ΨE <sub>o</sub>	0.158	<b>0.648</b>	-0.127	0.342	4.43	0.135
δR <sub>o</sub> /1-δR <sub>o</sub>	-0.226	<b>0.83</b>	0.156	0.085	6.58	0.422

Bold red values represent strong correlations (> 0.7) and italic bold moderate correlations (> 0.5). A green (maximal) – yellow (minimal) color scale is applied to visualize variable contribution.

## 4 Discussion

Cell membrane stability appears to be a valuable preliminary method for screening wheat seedlings for drought susceptibility since the cell membrane is the primary site of damage under stress. The decrease in cell membrane integrity was evident in all genotypes, probably as a result of overproduction of H<sub>2</sub>O<sub>2</sub> (Naderi et al., 2020), which not only causes changes in the

composition of membrane proteins and lipids as evidenced by the content of MDA but also plays a signaling role and stimulates the synthesis of osmolytes and antioxidant enzymes that participate in the defense against oxidative stress (Singh et al., 2012). However, little phenotypic variability was noticeable in PEG-test since the differences were significant only between genotypes with the lowest and the highest cell membrane integrity. Therefore, moderate drought stress was reduced to

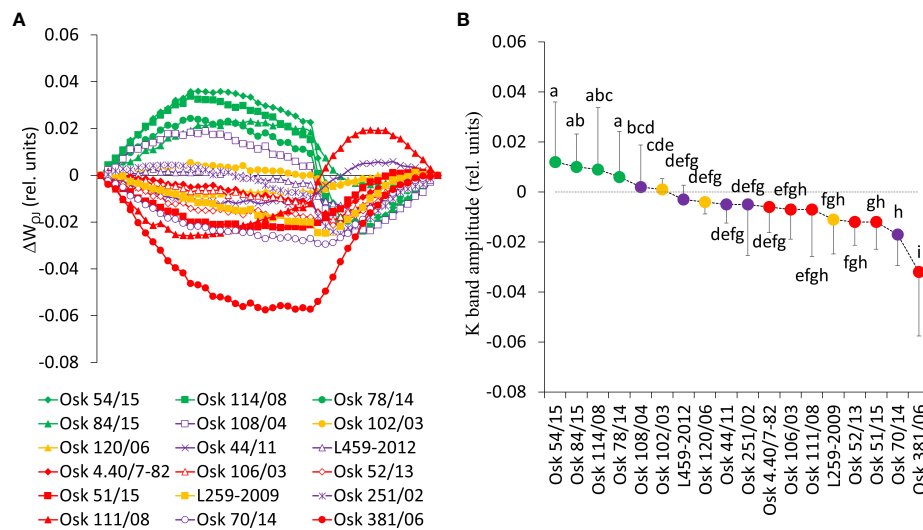


FIGURE 6

(A) Differential curves of relative variable fluorescence O-J normalized induction curves for eighteen wheat genotypes as  $W_{OJ} = (F_t - F_o) / (F_j - F_o)$ , each line averages 20 measurements. For the analysis of different kinetics and to reveal the band (K-band) that is typically hidden between steps O and J, the divergences between the relative variable fluorescence curves of the stress treatment (PEG induced water deficit,  $\Psi = -0.33$  MPa) and control (field conditions, water potential  $\Psi = -0.03$  MPa) were calculated as  $\Delta W_{OJ} = W_{Treatment} - W_{Control}$ . (B) Mean values of K-band divergences (dispersion refers to maximal values or amplitudes) and statistical differences among genotypes (one-way ANOVA  $F_{17,810} = 37.3$ ,  $p < 0.001$ , values followed by a common letter are not significantly different by the Tukey HSD-test at the 5% level of significance).

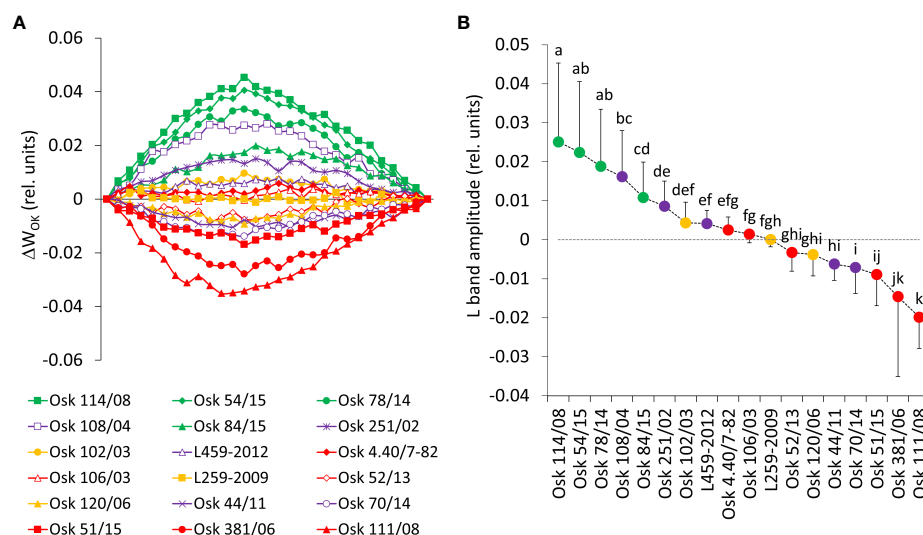


FIGURE 7

(A) Differential curves of relative variable fluorescence O-K normalized induction curves for 18 wheat genotypes as  $W_{OK} = (F_t - F_o) / (F_K - F_o)$ , each line averages 20 measurements. For the analysis of different kinetics and to reveal the band (L-band) that is typically hidden between steps O and K, the divergences between the relative variable fluorescence curves of the stress treatment (PEG induced water deficit,  $\Psi = -0.33$  MPa) and control (field conditions, water potential  $\Psi = -0.03$  MPa) were calculated as  $\Delta W_{OK} = W_{Treatment} - W_{Control}$ . (B) Mean values of L-band divergences (dispersion refers to maximal values or the amplitude) and statistical differences among genotypes (one-way ANOVA  $F_{17,522} = 87.7$ ,  $p < 0.0001$ , means followed by a common letter are not significantly different by the Tukey HSD-test at the 5% level of significance).

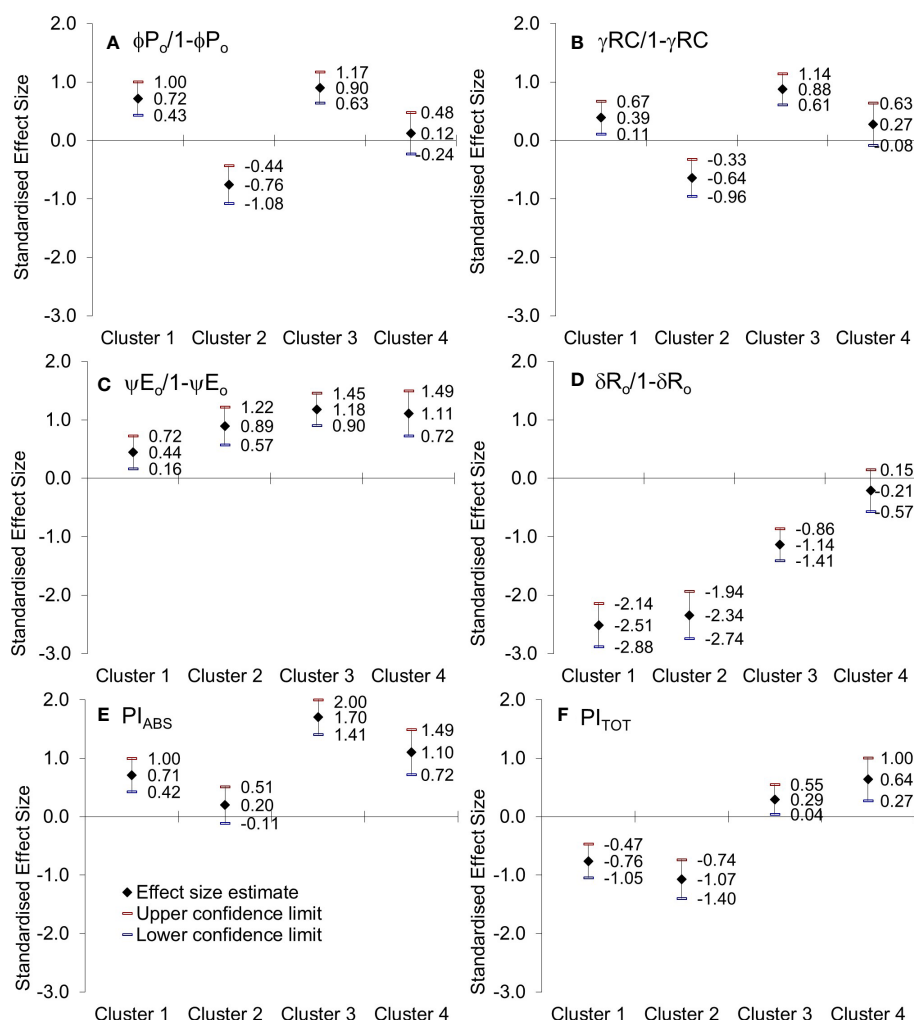


FIGURE 8

Hedges bias-corrected effect size (with confidence interval) of PEG-induced drought on (A) the efficiency of the water-splitting complex, (B) the density of active reaction centers at the donor side of PSII, (C) the ability to maintain an electron chain between two photosystems, and (D) reduction of end electron acceptors ( $\phi P_0/1-\phi P_0$ ,  $\gamma RC/1-\gamma RC$ ,  $\psi E_0/1-\psi E_0$ ,  $\delta R_0/1-\delta R_0$ ), (E) performance index on absorption basis ( $PI_{ABS}$ ) and (F) performance index (potential) for energy conservation from exciton to the reduction of PSI end acceptors ( $PI_{TOT}$ ) in four obtained Clusters of winter wheat genotypes.

mild, within physiological limits, because minor water deficit most likely results in lesser or greater acclimation to drought depending on plants' natural and inherent characteristics. Consequently, many changes occur in the structure and physiology of plants due to stress caused even by mild physiological drought. The results show that PEG-induced drought was the most influential variable that affected plant growth since shoot height was reduced in all genotypes and root length in most of them. In all genotypes, the whole plant underwent anatomical and morphological changes to prevent metabolic imbalance and maintain the content and transport of water. Since plants often show phenotypic plasticity to minimize the adverse effects of environmental stressors (Grenier et al.,

2016), genotypes that invest in the root system (like L459-2012 and Osk 70/14) are considered drought resistant (Liu et al., 2015). These differences in shoot and root growth were also reflected in their ratio. It is well known that as the plant ages, the root-to-shoot ratio decreases, showing priority to collecting light energy. However, in arid conditions, the increased root-to-shoot ratio indicates increased root growth that will provide plants with access to water (El Siddig et al., 2013). Therefore, a higher root-to-shoot ratio is essential when choosing drought-resistant varieties. Significant inter-genotypic differences were also observed in the dry matter accumulation among wheat varieties both in the root and in the shoot. Also, the translocation of a relatively higher percentage of dry weight

was observed towards the root system when exposed to PEG-induced drought (the most pronounced in genotypes Osk 70/14, Osk 381/06, and Osk 84/15). According to some authors (Carvalho et al., 2014), this indicates a better redistribution of accumulated carbon to the plant's root system and is an adaptive trait.

The evident water retention in all wheat genotypes resulted from effective water use, suggesting that all wheat seedlings' genotypes acclimated to imposed physiological drought to avoid dehydration (Sial et al., 2017). This was also visible in a common adaptive feature of leaf rolling in response to water deficit, reducing transpiration and water use. It is also possible that the osmotic adjustment contributed to maintaining a high relative water content (Silva et al., 2010) since it facilitates turgor maintenance by lowering the osmotic potential of the cell (Blum, 2017). However, osmotic adjustment can lead to anomalously low estimates of relative water content (Boyer et al., 2008). The activation of the metabolic pathways responsible for the synthesis of proline under conditions of mild stress suggested that all genotypes have possibilities for preventing adverse effects of imposed drought (Bandurska et al., 2017). Despite extensive research on proline accumulation under water deficit conditions, there are still conflicting opinions on the correlation between proline content and drought resistance. Some authors believe that increased proline content in plant tissues results from dehydration and is associated with sensitivity to drought (Schafleitner et al., 2007; Nazar et al., 2015; Blum, 2017; Mu et al., 2021). However, research on cereals such as barley and wheat shows that increased proline content is a feature of stress-tolerant varieties (Sultan et al., 2012; Ahmed et al., 2013). Nevertheless, the importance of proline accumulation for adaptation to drought is still uncertain. What is certain is that proline is a "compatible" solute that contributes to the osmotic adjustment of the cytoplasm (Blum, 2017). Decreased MDA levels in roots as opposed to increased MDA levels in leaves under mild drought stress can also be explained by the synthesis of osmolytes (Sultan et al., 2012) and indicate a higher antioxidant ability, which contributes to better drought resistance of wheat seedlings (Dhanda et al., 2004; Shao et al., 2005). However, one has to bear in mind that the primary sites of reactive oxygen accumulation are the plant leaves (Sahu and Kar, 2018; Liu et al., 2022), which also correlates well with higher carotenoid content in the same genotypes that reduce reactive oxygen species and inhibit lipid peroxidation (Shao et al., 2008; Jaleel et al., 2009). Overall, results show that biochemical and physiological responses to mild drought stress depend on the genetic predispositions of each variety, which has also been established in other plant species such as sesame (Fazeli et al., 2007), rice (Shobbar et al., 2010), cherries (Medeiros et al., 2012) and thyme (Bahreininejad, 2013).

Since photosynthesis is one of the plants' most essential and sensitive processes that any minor stressful event can disrupt, the best way to investigate changes in the functioning and the

structure of the photosynthetic apparatus under imposed drought conditions is by fast, non-destructive, and relatively simple chlorophyll *a* fluorescence technique (Strasser and Strasser, 1995; Strasser et al., 2004a; Tsimilli-Michael and Strasser, 2013; Dąbrowski et al., 2016; Goltsev et al., 2016; Kalaji et al., 2018). To find directions that best explain the variance in the data sets, a Principal Component Analysis reduced chlorophyll *a* fluorescence parameters to a group of most informative ones (Goltsev et al., 2012). Accordingly, control samples are characterized by suitable phenomenological energy fluxes per cross-section of PSII and the efficiency with which an electron is transferred to final PSI acceptors. At the same time, PEG-induced drought changed, to some extent, phenomenological energy fluxes, and the significant influence was on electron transport to end receptors. Similar responses were described in barley (Oukarroum et al., 2009), wheat (Brestic et al., 2012), rice (Wang et al., 2017), and *Tilia cordata* Mill (Kalaji et al., 2018).

The second direction that could explain variance in the results relates to the efficiency of the water-splitting complex and the density of active reaction centers at the donor side of PSII, the maximum quantum yield and the performance indices on an absorption basis, as well as absorbed photon flux, the part of trapped and the amount dissipated photon flow in the PSII antenna. However, considering the whole data set, this direction cannot be used to discern PEG-induced drought from the control samples due to high variability in winter wheat cultivars' response to imposed conditions. Therefore, PCA of the mean difference test data (by comparing the impact) and subsequent HAC analysis enabled trade-offs among chlorophyll *a* fluorescence parameters and revealed clustering of relevant parameters and genotypes based on their response to imposed physiological drought. Three groups of relevant fluorescence parameters were determined. The first, PC1, was characterized by photochemical parameters representing the donor and acceptor side of PSII. The second, PC2, is defined by the parameters of the thermal phase of the photosynthetic process and the acceptor side of PSI, representing the electron flow around PSI and the chain of electrons between PSII and PSI. While the third component, PC3, consisted of phenomenological energy fluxes per cross-section. This grouping of fluorescence parameters more accurately separated the investigated genotypes into four distinct clusters based on their response to imposed physiological drought conditions. It enabled an explanation of the specificity of their reaction.

## 4.1 Classification of winter wheat genotypes and their associated characteristics

Genotypes of *Cluster 1* were well correlated with PC2, characterized by an increase in variable fluorescence at the I-



step and a related decrease in the reduction of end electron acceptors that influenced the total performance ( $PI_{TOT}$ ), [Figure 8](#) and [Supplementary Material Figure 2](#). They were also characterized by no change in free proline, MDA levels, or relative water content. The suppressed K-band indicated enhanced resistance of PSII to PEG-induced physiological drought, meaning that they can resist drought-induced imbalance in electron flow at the acceptor and donor sides of PSII. Similarly, the observed marginal change of L-band amplitude indicated that energy connectivity was maintained since the dissociation of LHCII from the PSII complex was prevented. However, an attenuated L-band still can show a loss in energetic connectivity to some extent, which could be due to reaching the drought acclimation threshold or indicating the presence of drought avoidance mechanisms. Nevertheless, increased phenomenological parameters stimulated an increase in  $PI_{ABS}$ . Therefore, these genotypes were sensitive to PEG-induced drought but, most probably due to their excellent initial stability and tolerance of photosynthetic apparatus, were able to acclimate. Similar responses were determined in *Arabidopsis thaliana* plants adapted to different light intensities and temperature conditions ([Ballottari et al., 2007](#)) and in cold stress-tolerant zoysia grass cultivars ([Gururani et al., 2015](#)).

On the other hand, genotypes of *Cluster 2* were characterized by inactivation of reaction centers, disconnection of tripartite system LHC-core antenna-RC, inactivation of oxygen-evolving complex, and increase in dissipation, all leading to the decrease in the first reactions at PSII, that is, a reduction of maximum efficiency of PSII photochemistry, performance on absorption basis ( $PI_{ABS}$ ), as well as variable fluorescence at I-step. A similar decrease was determined in wheat exposed to slowly advancing drought stress in natural conditions ([Zivcak et al., 2008a](#); [Zivcak et al., 2008b](#)). Positive inflections of the K-band in these genotypes (Osk 54/15, 114/08, 84/15, and 78/14) suggested inhibition of electron flow from the acceptor side of PSII, indicating lower OEC activity that could lead to an incomplete water splitting process and result in ROS production undermining photosynthesis, i.e., distracting electron balance between OEC and tyrosine ([Guha et al., 2013](#); [Najafpour et al., 2013](#)). Similarly, positive L-bands demonstrated that even mild drought stress caused a distinct decrease in the energetic connectivity based on the loss of OEC functionality or stability in the tripartite system that controls the first stage of light-harvesting or the LHC-core antenna-RC complex ([Oukarroum et al., 2007](#); [Zhou et al., 2019](#)). Furthermore, these genotypes had increased free PRO in roots and leaves, although to a minor degree, and MDA level in leaves, all indicative of adjustment to some degree and activation of defense mechanisms. Since *Cluster 2* was characterized by a significant reduction in the RC/ABS parameter and correlated well with PC1 having moderate to low initial stability and, therefore, high sensitivity due to a considerable impact on photosynthetic apparatus results in their lower potential to cope with stress.

*Cluster 3* genotypes' responses were best described by PC1 and PC3. Their phenomenological energy fluxes per cross-section (ABS, TR, and ET per  $CS_o$  and  $CS_m$ ) were significantly decreased by PEG-induced drought. Reduced phenomenological parameters could indicate a negative influence of imposed drought at the early stages of its action. At the same time, the fraction of active reaction centers increased after stress. With its negative deviations, K-band indicated the better potential of these lines to cope with stress due to higher stability of OEC and electron transport from PSII to PSI for driving energy synthesis. Likewise, negative deviations of the L-band indicated an increase in cooperativity of excitation energy exchange between PSII units upon PEG treatment, thus resulting in more efficient consumption of the excitation energy and higher stability of the photosynthetic system ([Strasser et al., 2004a](#)). This boosted the first reactions in PSII (photon to exciton trapping events) and enhanced the ability to maintain the electron flow between PSII and PSI, thus increasing the driving forces of photosynthesis performance and  $PI_{ABS}$ . However, increased free PRO indicated osmotic adjustment, and the highest MDA level indicated possible oxidative damage. At the same time, carotenoids decreased, most probably because of involvement in the detoxification of reactive oxygen species. Therefore, genotypes of this cluster appeared to be sensitive to physiological drought due to the negative influence on PSI. Still, they successfully acclimated to some point by activation of defense mechanisms.

PEG-induced drought did not affect the energy flux associated with the electron transport from  $Q_A^-$  to final acceptors of PSI in genotypes Osk 120/06, 102/03, and L259-2009 that were grouped as *Cluster 4*. In addition, the response of these genotypes was best explained by their increased pool size of reduced PQ ( $N, S_m$ ),  $Q_A^-$  that is reduced more often, and by increased potential for the reduction of end electron acceptors. The accumulation of reducing equivalents favors cyclic electron transport around PSI, which supplies additional ATP to chloroplasts ([Huang et al., 2019](#); [Huang et al., 2021](#)). The acceleration of cyclic electron flow around PSI most probably accelerates repair of PSII activity, allowing these genotypes to perform better in mild stress. These genotypes were characterized by marginal change K- and L-band amplitude indicative of enhanced resistance to a drought-induced imbalance in electron flow at the acceptor and donor sides of PSII and maintained energy connectivity since the dissociation of LHCII from the PSII complex was prevented. Furthermore, these genotypes had the most increased PRO levels indicating an osmotic adjustment; RWC was no different from the control samples, and so were MDA levels in roots and leaves. All these adaptive features point out that these genotypes could resist physiological drought by showing a rapid acclimation of the photosynthetic system and osmotic adjustment, therefore, having a higher potential to cope with stress. As  $PI_{TOT}$  reflects the functionality of both photosystems and gives quantitative

information about the current status of the plant in stressful conditions (Zivcak et al., 2008b; Živčák et al., 2014; Samborska et al., 2019), an increase in *Cluster 4* implies outstanding functionality of PSI and PSII in mild drought stress conditions. This observed increase in electron transport in the early development of seedlings may be related to the activation of mechanisms responsible for drought tolerance (Kovačević et al., 2017). Similar findings that leave developing in drought conditions, especially under mild stress, increases its photosynthetic efficiency, most probably to compensate and use this to boost metabolism upon recovery are described in several papers (Xu et al., 2009; Avramova et al., 2015; Vincent et al., 2020). One more parameter indicative of drought stress is the IP phase which illustrates an imbalance between  $Q_A$  reduction and oxidation and the plastoquinone pool. Since the IP phase depends on the efficiency of the PSI acceptor's electron uptake and the number of available oxidized forms of NADP, the negative values of the IP phase (the data of which are not presented in this paper but can be correlated to  $V_I$ ) in genotypes of *Cluster 4* corresponded to a larger number of oxidized forms of NADP (NADP<sup>+</sup>) molecules per active center. This was reflected in the lower need for reductants on the PSI acceptor side (Ceppi et al., 2011; Pollastrini et al., 2014; Kula-Maximenko et al., 2021) and could be a compensatory mechanism for seedlings that have evolved in response to suboptimal environmental conditions.

Since every change in the OJIP curve is reflected in the index of photosynthetic efficiency ( $PI_{TOT}$ ) - an energy conversion from exciton to the reduction of the final electron acceptor in PSI (Zivcak et al., 2014; Kalaji et al., 2016; Kalaji et al., 2017; Tsimilli-Michael, 2020),  $PI_{TOT}$  showed to be the most sensitive parameter of the JIP-test in detecting and comparing the intensity of stress effect among tested genotypes. However, the explanation of the seedling's response inevitably included independent pieces of essential parameters embedded in PIs (as seen in Figure 8 and Supplementary Material Figure 2): the maximum quantum yield of primary photochemistry -  $\Phi P_o$  (using  $F_0$  and  $F_M$ ), the efficiency of electron transport further from  $Q_A^-$  -  $\Psi(E_o)$  (using  $V_j$ ), the efficiency with which the electron moves from the reduced electron acceptors to the final acceptors -  $\delta(R_o)$  (using  $V_j$  and  $V_I$ ) and the ratio of chlorophyll concentration of reaction centers and chlorophyll antennae - RC/ABS (using  $\Phi P_o$ ,  $V_j$  and the initial slope of the OJIP curve). However, can we honestly choose one or two chlorophyll fluorescence parameters to characterize drought tolerance of winter wheat genotypes? It does not seem like it. As stated in the review paper Tsimilli-Michael (2020), comparing the impact of imposed stress (i.e., physiological drought in this paper) on a whole set of parameters enables the identification of specific effects in the electron transport chain. Selecting those that better explain the individual plant's response gives a significant advantage in screening genotypes if the comparison of stress effect within physiological limits is in question. Multivariate analyses and data

mining of all parameters after stress enables the exploration of physiological processes. Nonetheless, these parameters only provide access to mechanisms. At the same time, biochemical and physiological measurements are needed for interpretation, which is proven in this paper.

The genetic contribution to drought adaptation is based on a combination of constituent and induced physiological and biochemical properties. Apprehending interactions of a complex collection of traits that enable acclimation to drought is much more complicated than understanding the functioning of an individual attribute. However, drought acclimation is often the result of a collective expression of many plant characteristics in the appropriate environment. Therefore, to better understand the relative importance of the different mechanisms, it is necessary to research a high number of varieties of the same species. Similarly, understanding the reactions of seedlings at all levels and to all factors affecting them has great value because the developmental stages in the same group generally show close similarities or several confusing differences, especially since the development of specialized adaptive traits has not yet begun. A critical step in conducting such research is developing and improving screening methods for identifying and evaluating functional relationships of relevant characteristics that are useful for acclimation, acclimatization, and adaptation to different types of drought stress and to be able to do it in all essential phenological stages of plant development. Therefore, the long-term vision of research and breeding programs should also include screening methods on seedlings to help identify, characterize, and select crucial phenotypic traits to find genetic markers for specific characteristics that can contribute to adaptation to, e.g., drought.

## 5 Conclusion

PEG-induced physiological drought enabled reliable screening of winter wheat genotypes in the first phase of seedling establishment. Chlorophyll *a* fluorescence appeared to be an effective method of differentiating sensitive and tolerant genotypes. Drought treatment was the most influential variable affecting plant growth and relative water content, while genotype variability determined with what intensity varieties of winter wheat seedlings responded to drought. As for chlorophyll *a* fluorescence parameters, PCA of all datasets showed that PEG-induced lack of water mainly influenced phenomenological energy fluxes and the efficiency with which an electron is transferred to final PSI acceptors. Fluorescence parameters that accurately described tested genotypes based on the effect size were grouped around three major components: photochemical parameters (PC1), representing the donor and acceptor side of PSII; thermal phase of the photosynthetic process and the acceptor side of PSI (PC2), representing the electron flow around PSI and the chain of electrons between PSII and PSI; and phenomenological energy fluxes per

cross-section (PC3). The most reliable parameters of the JIP-test in detecting and comparing the drought impact among tested genotypes were variable fluorescence at K, L, and I step and  $PI_{TOT}$ . Four distinct clusters of genotypes were discerned based on their response to imposed physiological drought, and the integrated analysis of biochemical and physiological parameters explained their reactions' specificity. Multivariate analyses and data mining of all parameters after stress enabled the exploration of physiological processes in all genotypes, thus complementing the knowledge needed to address fundamental issues, like plasticity, in young and fully developed plants and understand the physiological processes that lead to tolerance.

## Data availability statement

The original contributions presented in the study are included in the article/**Supplementary Material**. Further inquiries can be directed to the corresponding author.

## Author contributions

VP was responsible for conceptualization, methodology, research, formal analysis, supervision, writing of original draft, review & editing. AA and JD were accountable for the study, lab analysis, and data collection. GD and VC provided resources, funding acquisition, critical review & editing of the initial draft. All authors contributed to the article and approved the submitted version.

## References

- Abid, M., Hakeem, A., Shao, Y., Liu, Y., Zahoor, R., Fan, Y., et al. (2018). Seed osmopriming invokes stress memory against post-germinative drought stress in wheat (*Triticum aestivum* L.). *Environ. Exp. Bot.* 145, 12–20. doi: 10.1016/j.envexpbot.2017.10.002
- Abraham, E., Hourton-Cabassa, C., Erdei, L., and Szabados, L. (2010). Methods for determination of proline in plants. *Methods Mol. Biol.* 639, 317–331. doi: 10.1007/978-1-60761-702-0\_20
- Addinsoft (2022). *XLSTAT statistical and data analysis solution*. New York, US
- Agarie, S., Hanaoka, N., Kubota, F., Agata, W., and Kaufman, P. (1995). Measurement of cell membrane stability evaluated by electrolyte leakage as a drought and heat tolerance test in rice (*Oryza sativa* L.). *J. Faculty Agric. - Kyushu Univ. (Japan)* 40, 233–240. doi: 10.5109/24109
- Agbicodo, E. M., Fatokun, C. A., Muranaka, S., Visser, R. G. F., and Linden van der, C. G. (2009). Breeding drought tolerant cowpea: constraints, accomplishments, and future prospects. *Euphytica* 167, 353–370. doi: 10.1007/s10681-009-9893-8
- Ahmed, I. M., Dai, H., Zheng, W., Cao, F., Zhang, G., Sun, D., et al. (2013). Genotypic differences in physiological characteristics in the tolerance to drought and salinity combined stress between Tibetan wild and cultivated barley. *Plant Physiol. Biochem.* 63, 49–60. doi: 10.1016/j.plaphy.2012.11.004
- Ahmed, H. G. M.-D., Zeng, Y., Yang, X., Anwaar, H. A., Mansha, M. Z., Hanif, et al. (2020). Conferring drought-tolerant wheat genotypes through morpho-physiological and chlorophyll indices at seedling stage. *Saudi J. Biol. Sci.* 27, 2116–2123. doi: 10.1016/j.sjbs.2020.06.019
- Auler, P. A., Souza, G. M., da Silva Engela, M. R. G., do Amaral, M. N., Rossatto, T., da Silva, M. G. Z., et al. (2021). Stress memory of physiological, biochemical and metabolomic responses in two different rice genotypes under drought stress: The scale matters. *Plant Sci.* 311, 110994. doi: 10.1016/j.plantsci.2021.110994
- Avramova, V., Abdelgawad, H., Zhang, Z., Fotschki, B., Casadevall, R., Vergauwen, L., et al. (2015). Drought induces distinct growth response, protection, and recovery mechanisms in the maize leaf growth zone. *Plant Physiol.* 169, 1382–1396. doi: 10.1104/pp.15.00276
- Bahreinejad, B. (2013). Influence of water stress on morpho-physiological and phytochemical traits in thymus daenensis. *Int. J. Plant Prod.* 7 (1), 151–166. doi: 10.22069/IJPP.2012.927
- Ballottari, M., Dall'Osto, L., Morosinotto, T., and Bassi, R. (2007). Contrasting behavior of higher plant photosystem I and II antenna systems during acclimation. *J. Biol. Chem.* 282, 8947–8958. doi: 10.1074/jbc.M606417200
- Bandurska, H., Niedziela, J., Pietrowska-Borek, M., Nuc, K., Chadzinikolau, T., and Radzikowska, D. (2017). Regulation of proline biosynthesis and resistance to drought stress in two barley (*Hordeum vulgare* L.) genotypes of different origin. *Plant Physiol. Biochem.* 118, 427–437. doi: 10.1016/J.PLAPHY.2017.07.006
- Banks, J. M. (2018). Chlorophyll fluorescence as a tool to identify drought stress in acer genotypes. *Environ. Exp. Bot.* 155, 118–127. doi: 10.1016/j.envexpbot.2018.06.022
- Bashir, N., Athar, H.-U.-R., Kalaji, H. M., Wróbel, J., Mahmood, S., Zafar, Z. U., et al. (2021). Is photoprotection of PSII one of the key mechanisms for drought tolerance in maize? *Int. J. Mol. Sci. Article J. Mol. Sci.* 22, 13490. doi: 10.3390/ijms222413490
- Blum, A. (2005). Drought resistance, water-use efficiency, and yield potential—are they compatible, dissonant, or mutually exclusive? *Aust. J. Agric. Res. - Aust. J. AGR. Res.* 56 (11), 1159–1168. doi: 10.1071/AR05069

## Funding

This work was supported by the Department of Biology, Josip Juraj Strossmayer University of Osijek Research Block Grant Program.

## Conflict of interest

The authors declare that the research was conducted in the absence of any commercial or financial relationships that could be construed as a potential conflict of interest.

## Publisher's note

All claims expressed in this article are solely those of the authors and do not necessarily represent those of their affiliated organizations, or those of the publisher, the editors and the reviewers. Any product that may be evaluated in this article, or claim that may be made by its manufacturer, is not guaranteed or endorsed by the publisher.

## Supplementary material

The Supplementary Material for this article can be found online at: <https://www.frontiersin.org/articles/10.3389/fpls.2022.987702/full#supplementary-material>

- Blum, A. (2009). Effective use of water (EUW) and not water-use efficiency (WUE) is the target of crop yield improvement under drought stress. *Field Crops Res.* 112, 119–123. doi: 10.1016/j.fcr.2009.03.009
- Blum, A. (2011a). “Drought resistance and its improvement,” in *Plant breeding for water-limited environments*. Ed. A. Blum (New York, NY: Springer New York), 53–152. doi: 10.1007/978-1-4419-7491-4\_3
- Blum, A. (2011b). “Plant water relations, plant stress and plant production,” in *Plant breeding for water-limited environments*. Ed. A. Blum (New York, NY: Springer New York), 11–52. doi: 10.1007/978-1-4419-7491-4\_2
- Blum, A. (2017). Osmotic adjustment is a prime drought stress adaptive engine in support of plant production. *Plant, Cell & Environment*. 40 (1), 4–10. doi: 10.1111/pce.12800
- Blum, A., and Tuberosa, R. (2018). Dehydration survival of crop plants and its measurement. *J. Exp. Bot.* 69, 975–981. doi: 10.1093/jxb/erx445
- Bouaziz, A., and Hicks, D. R. (1990). Consumption of wheat seed reserves during germination and early growth as affected by soil water potential. *Plant Soil* 128, 161–165. doi: 10.1007/BF00011105
- Boureima, S., Oukarroum, A., Diouf, M., Cisse, N., and Van Damme, P. (2012). Screening for drought tolerance in mutant germplasm of sesame (*Sesamum indicum*) probing by chlorophyll a fluorescence. *Environ. Exp. Bot.* 81, 37–43. doi: 10.1016/j.envexpbot.2012.02.015
- Boyer, J. S. (1996). Advances in drought tolerance in plants. *Adv. Agron.* 56, 187–218. doi: 10.1016/S0065-2113(08)60182-0
- Boyer, J. S., James, R. A., Munns, R., Condon, T., and Passioura, J. B. (2008). Osmotic adjustment leads to anomalously low estimates of relative water content in wheat and barley. *Funct. Plant Biol.* 35, 1172. doi: 10.1071/FP08157
- Brestic, M., and Zivcak, M. (2013). “PSII fluorescence techniques for measurement of drought and high temperature stress signal in crop plants: Protocols and applications,” in *Molecular stress physiology of plants*. Eds. G. R. Rout and A. B. Das (India: Springer India), 87–131. doi: 10.1007/978-81-322-0807-5\_4
- Brestic, M., Zivcak, M., Kalaji, H. M., Carpentier, R., and Allakhverdiev, S. I. (2012). Photosystem II thermostability in situ: Environmentally induced acclimation and genotype-specific reactions in triticum aestivum L. *Plant Physiol. Biochem.* 57, 93–105. doi: 10.1016/j.plaphy.2012.05.012
- Bussotti, F., Gerosa, G., Digrado, A., and Pollastrini, M. (2020). Selection of chlorophyll fluorescence parameters as indicators of photosynthetic efficiency in large scale plant ecological studies. *Ecol. Indic.* 108, 105686. doi: 10.1016/j.ecolind.2019.105686
- Carvalho, P., Azam-Ali, S., and Foulkes, M. J. (2014). Quantifying relationships between rooting traits and water uptake under drought in Mediterranean barley and durum wheat. *J. Integr. Plant Biol.* 56, 455–469. doi: 10.1111/jipb.12109
- Ceppi, M., Oukarroum, A., Çiçek, N., Strasser, R., and Schansker, G. (2011). The IP amplitude of the fluorescence rise OJIP is sensitive to changes in the photosystem I content of leaves: A study on plants exposed to magnesium and sulfate deficiencies, drought stress and salt stress. *Physiol. Plant* 144, 277–288. doi: 10.1111/j.1399-3054.2011.01549.x
- Chaves, M., Flexas, J., and Pinheiro, C. (2008). Photosynthesis under drought and salt stress: Regulation mechanisms from whole plant to cell. *Ann. Bot.* 103, 551–560. doi: 10.1093/aob/mcn125
- Chaves, M. M., and Oliveira, M. M. (2004). Mechanisms underlying plant resilience to water deficits: prospects for water-saving agriculture. *J. Exp. Bot.* 55, 2365–2384. doi: 10.1093/jxb/erh269
- Chiango, H., Figueiredo, A., Sousa, L., Sinclair, T., and da Silva, J. M. (2021). Assessing drought tolerance of traditional maize genotypes of Mozambique using chlorophyll fluorescence parameters. *South Afr. J. Bot.* 138, 311–317. doi: 10.1016/j.sajb.2021.01.005
- Dąbrowski, P., Baczewska, A. H., Pawluśkiewicz, B., Paunov, M., Alexantrov, V., Goltsev, V., et al. (2016). Prompt chlorophyll a fluorescence as a rapid tool for diagnostic changes in PSII structure inhibited by salt stress in perennial ryegrass. *J. Photochem. Photobiol. B* 157, 22–31. doi: 10.1016/j.jphotobiol.2016.02.001
- Dąbrowski, P., Kalaji, M. H., Baczewska, A. H., Pawluśkiewicz, B., Mastalerczuk, G., Borawska-Jarmułowicz, B., et al. (2017). Delayed chlorophyll a fluorescence, MR 820, and gas exchange changes in perennial ryegrass under salt stress. *J. Lumin* 183, 322–333. doi: 10.1016/j.JLUMIN.2016.11.031
- Desotgiu, R., Pollastrini, M., Cascio, C., Gerosa, G., Marzuoli, R., and Bussotti, F. (2012). Chlorophyll a fluorescence analysis along a vertical gradient of the crown in a poplar (Oxford clone) subjected to ozone and water stress. *Tree Physiol.* 32, 976–986. doi: 10.1093/treephys/tps062
- Dhanda, S. S., Sethi, G. S., and Behl, R. K. (2004). Indices of drought tolerance in wheat genotypes at early stages of plant growth. *J. Agron. Crop Sci.* 190, 6–12. doi: 10.1111/j.1439-037X.2004.00592.x
- ElBasyoni, I., Saadalla, M., Baenziger, S., Bockelman, H., and Morsy, S. (2017). Cell membrane stability and association mapping for drought and heat tolerance in a worldwide wheat collection. *Sustainability (Switzerland)* 9, 1–16. doi: 10.3390/su9091606
- Ellis, P. D. (2010). *The essential guide to effect sizes : statistical power, meta-analysis, and the interpretation of research results* (Cambridge: Cambridge University Press).
- El-Mejjaoui, Y., Lahrir, M., Naciri, R., Zeroual, Y., Benjamin, B., Dumont, B., et al. (2022). How far can chlorophyll a fluorescence detect phosphorus status in wheat leaves (*Triticum durum* L.). *Environ. Exp. Bot.* 194, 104762. doi: 10.1016/J.ENVEXPBOT.2021.104762
- El Siddig, M. A., Baenziger, S., Dweikat, I., and El Hussein, A. A. (2013). Preliminary screening for water stress tolerance and genetic diversity in wheat (*Triticum aestivum* L.) cultivars from Sudan. *J. Genet. Eng. Biotechnol.* 11, 87–94. doi: 10.1016/j.jgeb.2013.08.004
- Farsiani, A., and Ghobadi, M. E. (2009). Effects of PEG and NaCl stress on two cultivars of corn (*Zea mays* L.) at germination and early seedling stages. *World Acad. Science Eng. Technology Int. J. Biological Biomolecular Agricultural Food Biotechnol. Eng.* 3, 442–445. doi: 10.5281/zenodo.1069947
- Fazeli, F., Ghorbanli, M., and Niknam, V. (2007). Effect of drought on biomass, protein content, lipid peroxidation and antioxidant enzymes in two sesame cultivars. *Biol. Plant* 51, 98–103. doi: 10.1007/s10535-007-0020-1
- Flexas, J., Barón, M., Bota, J., Ducruet, J.-M., Gallé, A., Galmés, J., et al. (2009). Photosynthesis limitations during water stress acclimation and recovery in the drought-adapted vitis hybrid Richter-110 (*V. berlandieri* × *V. rupestris*). *J. Exp. Bot.* 60, 2361–2377. doi: 10.1093/jxb/erp069
- Flexas, J., Bota, J., Loreto, F., Cornic, G., and Sharkey, T. D. (2004). Diffusive and metabolic limitations to photosynthesis under drought and salinity in C(3) plants. *Plant Biol. (Stuttg)* 6, 269–279. doi: 10.1055/s-2004-820867
- Flexas, J., Diaz-Espejo, A., Conesa, M. A., Coopman, R. E., Douthe, C., Gago, J., et al. (2016). Mesophyll conductance to CO<sub>2</sub> and rubisco as targets for improving intrinsic water use efficiency in C<sub>3</sub> plants. *Plant Cell Environ.* 39, 965–982. doi: 10.1111/pce.12622
- Flexas, J., and Medrano, H. (2002). Drought-inhibition of photosynthesis in C<sub>3</sub> plants: Stomatal and non-stomatal limitations revisited. *Ann. Bot.* 89, 183–189. doi: 10.1093/aob/mcf027
- Foyer, C. H., Neukermans, J., Queval, G., Noctor, G., and Harbinson, J. (2012). Photosynthetic control of electron transport and the regulation of gene expression. *J. Exp. Bot.* 63, 1637–1661. doi: 10.1093/jxb/ers013
- Ghanbari, F., and Sayyari, M. (2018). Controlled drought stress affects the chilling-hardening capacity of tomato seedlings as indicated by changes in phenol metabolisms, antioxidant enzymes activity, osmolytes concentration and abscisic acid accumulation. *Sci. Hortic.* 229, 167–174. doi: 10.1016/j.scienta.2017.10.009
- Goltsev, V. N., Kalaji, H. M., Paunov, M., Bába, W., Horacek, T., Mojski, J., et al. (2016). Variable chlorophyll fluorescence and its use for assessing physiological condition of plant photosynthetic apparatus. *Russian J. Plant Physiol.* 63, 881–907. doi: 10.1134/S1021443716050058
- Goltsev, V., Zaharieva, I., Chernev, P., Kouzmanova, M., Kalaji, H. M., Yordanov, I., et al. (2012). Drought-induced modifications of photosynthetic electron transport in intact leaves: Analysis and use of neural networks as a tool for a rapid non-invasive estimation. *Biochim. Biophys. Acta (BBA) - Bioenergetics* 1817, 1490–1498. doi: 10.1016/j.bbabi.2012.04.018
- Goltsev, V., Zaharieva, I., Chernev, P., and Strasser, R. (2009). Delayed chlorophyll fluorescence as a monitor for physiological state of photosynthetic apparatus. *Biotechnol. Equip.* 23, 452–457. doi: 10.1080/13102818.2009.10818461
- Grenier, S., Barre, P., and Litrico, I. (2016). Phenotypic plasticity and selection: Nonexclusive mechanisms of adaptation. *Scientifica (Cairo)* 2016, 1–9. doi: 10.1155/2016/7021701
- Guha, A., Sengupta, D., and Reddy, A. R. (2013). Polyphasic chlorophyll a fluorescence kinetics and leaf protein analyses to track dynamics of photosynthetic performance in mulberry during progressive drought. *J. Photochem. Photobiol. B* 119, 71–83. doi: 10.1016/j.jphotobiol.2012.12.006
- Gururani, M. A., Venkatesh, J., Ganesan, M., Strasser, R. J., Han, Y., Kim, J.-I., et al. (2015). *In vivo* assessment of cold tolerance through chlorophyll-a fluorescence in transgenic zoysiagrass expressing mutant phytochrome a. *Plos One* 10, e0127200. doi: 10.1371/journal.pone.0127200
- Heath, R. L., and Packer, L. (1968). Photoperoxidation in isolated chloroplasts: I. kinetics and stoichiometry of fatty acid peroxidation. *Arch. Biochem. Biophys.* 125, 189–198. doi: 10.1016/0003-9861(68)90654-1
- Hedges, L. V., and Olkin, I. (1985). Estimation of a Single Effect Size: Parametric and Nonparametric Methods. *Statistical Methods for Meta-Analysis*. 75–106. doi: 10.1016/B978-0-08-057065-5.50010-5
- Hoagland, D. R., and Arnon, D. I. (1950). Preparing the nutrient solution. *Water-Culture Method. Growing Plants without Soil* 347, 29–31. Available at: <https://archive.org/details/watercultureme3450hoag>



- Huang, W., Sun, H., Tan, S.-L., and Zhang, S.-B. (2021). The water-water cycle is not a major alternative sink in fluctuating light at chilling temperature. *Plant Sci.* 305, 110828. doi: 10.1016/j.plantsci.2021.110828
- Huang, W., Yang, Y. J., and Zhang, S. B. (2019). The role of water-water cycle in regulating the redox state of photosystem I under fluctuating light. *Biochim. Biophys. Acta (BBA) - Bioenergetics* 1860, 383–390. doi: 10.1016/j.BBABI.2019.03.007
- Jabbari, H., Akbari, G. A., Khosh Kholgh Sima, N. A., Shirani Rad, A. H., Alahdadi, I., Hamed, A., et al. (2013). Relationships between seedling establishment and soil moisture content for winter and spring rapeseed genotypes. *Ind. Crops Prod.* 49, 177–187. doi: 10.1016/j.indcrop.2013.04.036
- Jaleel, C. A., Manivannan, P., Wahid, A., Farooq, M., Al-Juburi, H. J., Somasundaram, R., et al. (2009). Drought stress in plants: A review on morphological characteristics and pigments composition. *Int. J. Agric. Biol.* 11, 100–105. doi: 10.1016/j.IGC-DYT/2009/11-1-100-105
- Jedrowski, C., Ashoub, A., and Brüggemann, W. (2013). Reactions of Egyptian landraces of *Hordeum vulgare* and *Sorghum bicolor* to drought stress, evaluated by the OJIP fluorescence transient analysis. *Acta Physiol. Plant* 35, 345–354. doi: 10.1007/s11738-012-1077-9
- Jedrowski, C., Ashoub, A., Momtaz, O., and Brüggemann, W. (2015). Impact of drought, heat, and their combination on chlorophyll fluorescence and yield of wild barley (*Hordeum spontaneum*). *J. Bot.* 2015, 1–9. doi: 10.1155/2015/120868
- Jedrowski, C., and Brüggemann, W. (2015). Imaging of fast chlorophyll fluorescence induction curve (OJIP) parameters, applied in a screening study with wild barley (*Hordeum spontaneum*) genotypes under heat stress. *J. Photochem. Photobiol. B* 151, 153–160. doi: 10.1016/j.JPHOTOB.2015.07.020
- Kalaji, H. M., Bosa, K., Kościelniak, J., and Hossain, Z. (2011a). Chlorophyll a fluorescence—a useful tool for the early detection of temperature stress in spring barley (*Hordeum vulgare* L.). *OMICS* 15, 925–934. doi: 10.1089/omi.2011.0070
- Kalaji, H. M., Govindjee Bosa, K., Kościelniak, J., and Zuk-Golaszewska, K. (2011b). Effects of salt stress on photosystem II efficiency and CO<sub>2</sub> assimilation of two Syrian barley landraces. *Environ. Exp. Bot.* 73, 64–72. doi: 10.1016/j.ENVEXPBOT.2010.10.009
- Kalaji, H. M., Jajoo, A., Oukarroum, A., Brestic, M., Zivcak, M., Samborska, I. A., et al. (2016). Chlorophyll a fluorescence as a tool to monitor physiological status of plants under abiotic stress conditions. *Acta Physiol. Plant* 38, 102. doi: 10.1007/s11738-016-2113-y
- Kalaji, H. M., Račková, L., Paganová, V., Swoczyna, T., Rusinowski, S., and Sitko, K. (2018). Can chlorophyll-a fluorescence parameters be used as bio-indicators to distinguish between drought and salinity stress in *tilia cordata* mill? *Environ. Exp. Bot.* 152, 149–157. doi: 10.1016/j.ENVEXPBOT.2017.11.001
- Kalaji, H. M., Schansker, G., Brestic, M., Bussotti, F., Calatayud, A., Ferroni, L., et al. (2017). Frequently asked questions about chlorophyll fluorescence, the sequel. *Photosynth Res.* 132, 13–66. doi: 10.1007/s11210-016-0318-y
- Khatri, K., and Rathore, M. S. (2022). Salt and osmotic stress-induced changes in physio-chemical responses, PSII photochemistry and chlorophyll a fluorescence in peanut. *Plant Stress* 3, 100063. doi: 10.1016/j.stress.2022.100063
- Kovačević, J., Mazur, M., Drezner, G., Lalić, A., Sudarić, A., Dvojković, K., et al. (2017). Photosynthetic efficiency parameters as indicators of agronomic traits of winter wheat cultivars in different soil water conditions. *Genetika* 49, 891–910. doi: 10.2298/GENSRI703891K
- Kranner, I., Minibayeva, F. V., Beckett, R. P., and Seal, C. E. (2010). What is stress? concepts, definitions and applications in seed science. *New Phytol.* 188, 655–673. doi: 10.1111/j.1469-8137.2010.03461.x
- Kula-Maximenko, M., Zieliński, K. J., and Ślesak, I. (2021). The role of selected wavelengths of light in the activity of photosystem II in *gloeobacter violaceus*. *Int. J. Mol. Sci. Article.* 22 (8), 4021. doi: 10.3390/ijms22084021
- Lamichhane, J. R., Debaeke, P., Steinberg, C., You, M. P., Barbetti, M. J., and Aubertot, J.-N. (2018). Abiotic and biotic factors affecting crop seed germination and seedling emergence: a conceptual framework. *Plant Soil* 432, 1–28. doi: 10.1007/s11104-018-3780-9
- Lauriano, J. A., Ramalho, J. C., Lidon, F. C., and Do Céu matos, M. (2006). Mechanisms of energy dissipation in peanut under water stress. *Photosynthetica* 44, 404–410. doi: 10.1007/s11099-006-0043-4
- Lawlor, D. (2002). Limitation to photosynthesis in water-stressed leaves: Stomata vs. metabolism and the role of ATP. *Ann. Bot.* 89, 871–885. doi: 10.1093/aob/mcf110
- Lawlor, D. W. (2013). Genetic engineering to improve plant performance under drought: physiological evaluation of achievements, limitations, and possibilities. *J. Exp. Bot.* 64, 83–108. doi: 10.1093/jxb/ers326
- Lawlor, D. W., and Tezara, W. (2009). Causes of decreased photosynthetic rate and metabolic capacity in water-deficient leaf cells: a critical evaluation of mechanisms and integration of processes. *Ann. Bot.* 103, 561–579. doi: 10.1093/aob/mcn244
- Lichtenthaler, H. K., and Buschmann, C. (2001). Chlorophylls and carotenoids: Measurement and characterization by UV-VIS spectroscopy. *Curr. Protoc. Food Analytical Chem.* 1, F4.3.1–F4.3.8. doi: 10.1002/0471142913.faf0403s01
- Li, M., and Kim, C. (2022). Chloroplast ROS and stress signaling. *Plant Commun.* 3, 100264. doi: 10.1016/j.XPLC.2021.100264
- Liu, L., Cao, X., Zhai, Z., Ma, S., Tian, Y., and Cheng, J. (2022). Direct evidence of drought stress memory in mulberry from a physiological perspective: Antioxidative, osmotic and phytohormonal regulations. *Plant Physiol. Biochem.* 186, 76–87. doi: 10.1016/j.plaphy.2022.07.001
- Liu, M., Li, M., Liu, K., and Sui, N. (2015). Effects of drought stress on seed germination and seedling growth of different maize varieties. *J. Agric. Sci.* 7, 231–240. doi: 10.5539/jas.v7n5p231
- Lotfi, R., Abbasi, A., Kalaji, H. M., Eskandari, I., Sedghieh, V., Khorsandi, H., et al. (2022). The role of potassium on drought resistance of winter wheat cultivars under cold dryland conditions: Probed by chlorophyll a fluorescence. *Plant Physiol. Biochem.* 182, 45–54. doi: 10.1016/j.plaphy.2022.04.010
- Lu, L., Liu, H., Wu, Y., and Yan, G. (2022). Wheat genotypes tolerant to heat at seedling stage tend to be also tolerant at adult stage: The possibility of early selection for heat tolerance breeding. *Crop J.* 10 (4), 1006–1013. doi: 10.1016/j.cj.2022.01.005
- Markulj Kulundžić, A., Josipović, A., Matoša Kočar, M., Viljevac Vuletić, M., Antunović Dunić, J., Varga, I., et al. (2022). Physiological insights on soybean response to drought. *Agric. Water Manag.* 268, 107620. doi: 10.1016/j.agwat.2022.107620
- Medeiros, D. B., da Silva, E. C., Santos, H. R. B., Pacheco, C. M., Musser, R., dos, S., et al. (2012). Physiological and biochemical responses to drought stress in Barbados cherry. *Braz. J. Plant Physiol.* 24, 181–192. doi: 10.1590/S1677-04202012000300005
- Michel, B. E., and Kaufmann, M. R. (1973). The osmotic potential of polyethylene glycol 6000. *Plant Physiol.* 51, 914–916. doi: 10.1104/pp.51.5.914
- Microsoft Corporation (2019). *Microsoft Excel*. Retrieved from <https://office.microsoft.com/excel>
- Mihaljević, I., Lepeduš, H., Šimić, D., Viljevac Vuletić, M., Tomaš, V., Vuković, D., et al. (2020). Photochemical efficiency of photosystem II in two apple cultivars affected by elevated temperature and excess light *in vivo*. *South Afr. J. Bot.* 130, 316–326. doi: 10.1016/J.SAJB.2020.01.017
- Miller, G., Suzuki, N., Ciftci-Yilmaz, S., and Mittler, R. (2010). Reactive oxygen species homeostasis and signalling during drought and salinity stresses. *Plant Cell Environ.* 33, 453–467. doi: 10.1111/j.1365-3040.2009.02041.x
- Mu, Q., Cai, H., Sun, S., Wen, S., Xu, J., Dong, M., et al. (2021). The physiological response of winter wheat under short-term drought conditions and the sensitivity of different indices to soil water changes. *Agric. Water Manag.* 243, 106475. doi: 10.1016/J.AGWAT.2020.106475
- Naderi, S., Fakheri, B.-A., Maali-Amiri, R., and Mahdinezhad, N. (2020). Tolerance responses in wheat landrace bolani are related to enhanced metabolic adjustments under drought stress. *Plant Physiol. Biochem.* 150, 244–253. doi: 10.1016/j.plaphy.2020.03.002
- Najafpour, M. M., Amouzadeh Tabrizi, M., Haghighi, B., and Govindjee, (2013). A 2-(2-hydroxyphenyl)-1H-benzimidazole-manganese oxide hybrid as a promising structural model for the tyrosine 161/histidine 190-manganese cluster in photosystem II. *Dalton. Trans.* 42, 879–884. doi: 10.1039/C2DT32236F
- Nakagawa, S., and Cuthill, I. C. (2007). Effect size, confidence interval and statistical significance: a practical guide for biologists. *Biol. Rev.* 82, 591–605. doi: 10.1111/j.1469-185X.2007.00027.x
- Nazar, R., Umar, S., Khan, N. A., and Sareer, O. (2015). Salicylic acid supplementation improves photosynthesis and growth in mustard through changes in proline accumulation and ethylene formation under drought stress. *South Afr. J. Bot.* 98, 84–94. doi: 10.1016/J.SAJB.2015.02.005
- Novák, V. (2009). Physiological Drought How to Quantify it? in: *BT - Bioclimatology and Natural Hazards*. Eds (K. Střelcová, C. Mátyás, A. Kleidon, M. Lapin, F. Matejka, M. Blaženec, et al. Netherlands: Springer 89–95. doi: 10.1007/978-1-4020-8876-6\_7
- Oukarroum, A., El Madidi, S., and Strasser, R. J. (2016). Differential heat sensitivity index in barley cultivars (*Hordeum vulgare* L.) monitored by chlorophyll a fluorescence OJIP. *Plant Physiol. Biochem.* 105, 102–108. doi: 10.1016/j.plaphy.2016.04.015
- Oukarroum, A., Madidi, S. E. L., Schansker, G., and Strasser, R. J. (2007). Probing the responses of barley cultivars (*Hordeum vulgare* L.) by chlorophyll a fluorescence OLKJIP under drought stress and re-watering. *Environ. Exp. Bot.* 60, 438–446. doi: 10.1016/j.envexpbot.2007.01.002
- Oukarroum, A., Schansker, G., and Strasser, R. J. (2009). Drought stress effects on photosystem I content and photosystem II thermotolerance analyzed using chl a fluorescence kinetics in barley varieties differing in their drought tolerance. *Physiol. Plant* 137, 188–199. doi: 10.1111/j.1399-3054.2009.01273.x

- Pollastrini, M., Desotgiu, R., Camin, F., Ziller, L., Gerosa, G., Marzuoli, R., et al. (2014). Severe drought events increase the sensitivity to ozone on poplar clones. *Environ. Exp. Bot.* 100, 94–104. doi: 10.1016/j.envexpbot.2013.12.016
- Qayyum, A., Al Ayoubi, S., Sher, A., Bibi, Y., Ahmad, S., Shen, Z., et al. (2021). Improvement in drought tolerance in bread wheat is related to an improvement in osmolyte production, antioxidant enzyme activities, and gaseous exchange. *Saudi J. Biol. Sci.* 28, 5238–5249. doi: 10.1016/j.sjbs.2021.05.040
- Qi, M., Liu, X., Li, Y., Song, H., Yin, Z., Zhang, F., et al. (2021). Photosynthetic resistance and resilience under drought, flooding and rewetting in maize plants. *Photosynth. Res.* 148, 1–15. doi: 10.1007/s11220-021-00825-3
- Reddy, A. R., Chaitanya, K. V., and Vivekanandan, M. (2004). Drought-induced responses of photosynthesis and antioxidant metabolism in higher plants. *J. Plant Physiol.* 161, 1189–1202. doi: 10.1016/j.jplph.2004.01.013
- Reis, R. R., Mertz-Henning, L. M., Marcolino-Gomes, J., Rodrigues, F. A., Rockenbach-Marín, S., Fuganti-Pagliarini, R., et al. (2020). Differential gene expression in response to water deficit in leaf and root tissues of soybean genotypes with contrasting tolerance profiles. *Genetics and Molecular Biology* 43 (2):1–17. doi: 10.1590/1678-4685-GMB-2018-0290
- Ru, C., Hu, X., Chen, D., Wang, W., and Song, T. (2022). Heat and drought priming induce tolerance to subsequent heat and drought stress by regulating leaf photosynthesis, root morphology, and antioxidant defense in maize seedlings. *Environ. Exp. Bot.* 202, 105010. doi: 10.1016/j.envexpbot.2022.105010
- Sahu, M., and Kar, R. K. (2018). Possible interaction of ROS, antioxidants and ABA to survive osmotic stress upon acclimation in vigna radiata l. wilczek seedlings. *Plant Physiol. Biochem.* 132, 415–423. doi: 10.1016/j.plaphy.2018.09.034
- Samborska, I. A., Kalaji, H. M., Sieczko, L., Borucki, W., Mazur, R., Kouzmanova, M., et al. (2019). Can just one-second measurement of chlorophyll a fluorescence be used to predict sulphur deficiency in radish (*Raphanus sativus* L. sativus) plants? *Curr. Plant Biol.* 19, 100096. doi: 10.1016/j.CPB.2018.12.002
- Sawilowsky, S. (2009). New effect size rules of thumb. *J. Modern. Appl. Stat. Methods* 8, 597–599. doi: 10.22237/jmasm/1257035100
- Sawilowsky, S., Sawilowsky, J., and Grissom, R. (2011). Effect Size. In: M. Lovric (eds) *International Encyclopedia of Statistical Science*. Berlin, Heidelberg: Springer. doi: 10.1007/978-3-642-04898-2\_226
- Schafleitner, R., Gaudin, A., Gutierrez Rosales, R., Alvarado, C., and Bonierbale, M. (2007). Proline accumulation and real time PCR expression analysis of genes encoding enzymes of proline metabolism in relation to drought tolerance in Andean potato. *Acta Physiol. Plant* 29, 19–26. doi: 10.1007/s11738-006-0003-4
- Selote, D. S., Bharti, S., and Khanna-Chopra, R. (2004). Drought acclimation reduces O<sub>2</sub><sup>-</sup> accumulation and lipid peroxidation in wheat seedlings. *Biochem. Biophys. Res. Commun.* 314, 724–729. doi: 10.1016/j.bbrc.2003.12.157
- Shao, H.-B., Chu, L.-Y., Jaleel, C. A., and Zhao, C.-X. (2008). Water-deficit stress-induced anatomical changes in higher plants. *C R Biol.* 331, 215–225. doi: 10.1016/j.crv.2008.01.002
- Shao, H. B., Liang, Z. S., Shao, M. A., and Wang, B. C. (2005). Changes of anti-oxidative enzymes and membrane peroxidation for soil water deficits among 10 wheat genotypes at seedling stage. *Colloids Surf. B Biointerfaces* 42, 107–113. doi: 10.1016/j.colsurfb.2005.01.011
- Shobbar, M. S., Niknam, V., Shobbar, Z. S., and Ebrahimzadeh, H. (2010). Effect of salt and drought stresses on some physiological traits of three rice genotypes differing in salt tolerance. *JUST* 36, 1–9. Available at: [https://jos.ut.ac.ir/article\\_21797\\_1e5c462b684376b71ac874180a698bf0.pdf](https://jos.ut.ac.ir/article_21797_1e5c462b684376b71ac874180a698bf0.pdf) (accessed 2nd May 2022).
- Sial, M. A., Mangrio, S. M., Bux, H., Channa, A. W., and Shaikh, M. (2017). Effect of water stress on some physiological traits of bread wheat genotypes. *Pakistan J. Agriculture Agric. Eng. Veterinary Sci.* 33, 1–11. Available at: <https://pjae.sau.edu.pk/index.php/ojs/article/view/77> (accessed 2nd May 2022).
- Silva, E. N., Ferreira-Silva, S. L., Viégas, R. A., and Silveira, J. A. G. (2010). The role of organic and inorganic solutes in the osmotic adjustment of drought-stressed jatroph curcas plants. *Environ. Exp. Bot.* 69, 279–285. doi: 10.1016/j.envexpbot.2010.05.001
- Singh, S., Gupta, A. K., and Kaur, N. (2012). Differential responses of antioxidative defence system to long-term field drought in wheat (*Triticum aestivum* L.) genotypes differing in drought tolerance. *J. Agron. Crop Sci.* 198, 185–195. doi: 10.1111/j.1439-037X.2011.00497.x
- Stirbet, A., and Govindjee, (2011). On the relation between the kautsky effect (chlorophyll a fluorescence induction) and photosystem II: Basics and applications of the OJIP fluorescence transient. *J. Photochem. Photobiol. B* 104, 236–257. doi: 10.1016/j.jphotobiol.2010.12.010
- Stirbet, A., Riznichenko, G., Rubin, A. B., and Govindjee, (2014). Modeling chlorophyll a fluorescence transient: Relation to photosynthesis. *Biochem. (Moscow)* 79, 291–323. doi: 10.1134/S0006297914040014
- Strasser, B. J., and Strasser, R. J. (1995). “Measuring fast fluorescence transients to address environmental questions: The JIP-test,” in *Photosynthesis: from light to biosphere*. Ed. P. Mathis (Dordrecht: Springer Netherlands), 4869–4872. doi: 10.1007/978-94-009-0173-5\_1142
- Strasser, R. J., Tsimilli-Michael, M., and Srivastava, A. (2004). Analysis of the Chlorophyll a Fluorescence Transient. In: G. C. PapageorgiouGovindjee (eds) *Chlorophyll a Fluorescence. Advances in Photosynthesis and Respiration*. 19. Dordrecht: Springer. doi: 10.1007/978-1-4020-3218-9\_12
- Strasser, R. J., Tsimilli-Michael, M., and Srivastava, A. (2004b). “Analysis of the chlorophyll a fluorescence transient BT - chlorophyll a fluorescence: A signature of photosynthesis,”. Eds. G. C. Papageorgiou and Govindjee, (Dordrecht: Springer Netherlands), 321–362. doi: 10.1007/978-1-4020-3218-9\_12
- Sultan, M. A. R. F., Hui, L., Yang, L. J., and Xian, Z. H. (2012). Assessment of drought tolerance of some triticum l. species through physiological indices. *Czech J. Genet. Plant Breed.* 48, 178–184. doi: 10.17221/21/2012-CJGPB
- Tsimilli-Michael, M. (2020). Special issue in honour of Prof. reto j. strasser - revisiting JIP-test: An educative review on concepts, assumptions, approximations, definitions and terminology. *Photosynthetica* 58, 275–292. doi: 10.32615/ps.2019.150
- Tsimilli-Michael, M., and Strasser, R. (2013). The energy flux theory 35 years later: Formulations applications. *Photosynth. Res.* 117 (1–3), 289–320. doi: 10.1007/s11220-013-9895-1
- Tuberosa, R. (2012). Phenotyping for drought tolerance of crops in the genomics era. *Front. Physiol.* 3. doi: 10.3389/fphys.2012.00347
- Turner, N. C. (1986). Crop water deficits: A decade of progress. *Adv. Agron.* 39, 1–51. doi: 10.1016/S0065-2113(08)60464-2
- Vincent, C., Rowland, D., Schaffer, B., Bassil, E., Racette, K., and Zurweller, B. (2020). Primed acclimation: A physiological process offers a strategy for more resilient and irrigation-efficient crop production. *Plant Sci.* 295, 110240. doi: 10.1016/j.plantsci.2019.110240
- Wang, Y., Xu, C., Wu, M., and Chen, G. (2017). Characterization of photosynthetic performance during reproductive stage in high-yield hybrid rice LYPJ exposed to drought stress probed by chlorophyll a fluorescence transient. *Plant Growth Regul.* 81, 489–499. doi: 10.1007/s10725-016-0226-3
- Xu, Z., Zhou, G., and Shimizu, H. (2009). Are plant growth and photosynthesis limited by pre-drought following rewetting in grass? *J. Exp. Bot.* 60, 3737–3749. doi: 10.1093/jxb/erp216
- Yang, J., Kong, Q., and Xiang, C. (2009). Effects of low night temperature on pigments, chl a fluorescence and energy allocation in two bitter melon (*Momordica charantia* L.) genotypes. *Acta Physiol. Plant* 31, 285–293. doi: 10.1007/s11738-008-0231-x
- Zhou, R., Kan, X., Chen, J., Hua, H., Li, Y., Ren, J., et al. (2019). Drought-induced changes in photosynthetic electron transport in maize probed by prompt fluorescence, delayed fluorescence, P700 and cyclic electron flow signals. *Environ. Exp. Bot.* 158, 51–62. doi: 10.1016/j.envexpbot.2018.11.005
- Zhu, J., Cai, D., Wang, J., Cao, J., Wen, Y., He, J., et al. (2021). Physiological and anatomical changes in two rapeseed (*Brassica napus* L.) genotypes under drought stress conditions. *Oil Crop Sci.* 6, 97–104. doi: 10.1016/j.OCSCL.2021.04.003
- Zivcak, M., Brestic, M., and Olsovska, K. (2008a). Assessment of physiological parameters useful in screening for tolerance to soil drought in winter wheat (*Triticum aestivum* L.) genotypes. *Cereal Res. Commun.* 36, 1943–1946. Available at: <https://www.jstor.org/stable/90003111>
- Zivcak, M., Brestic, M., Olsovska, K., and Slamka, P. (2008b). Performance index as a sensitive indicator of water stress in triticum aestivum L. *Plant Soil Environ.* 54, 133–139. doi: 10.17221/392-PSE
- Zivcak, M., Kalaji, H. M., Shao, H. B., Olsovska, K., and Brestic, M. (2014). Photosynthetic proton and electron transport in wheat leaves under prolonged moderate drought stress. *J. Photochem. Photobiol. B* 137, 107–115. doi: 10.1016/j.jphotobiol.2014.01.007
- Živčák, M., Olšovská, K., Slamka, P., Galambošová, J., Rataj, V., HB, S., et al. (2014). Application of chlorophyll fluorescence performance indices to assess the wheat photosynthetic functions influenced by nitrogen deficiency. *Plant Soil Environ.* 60, 210–215. doi: 10.17221/73/2014-PSE

## Glossary

ABS	absorbed photon flux
ABS/ RC	average absorbed photon flux per PSII reaction center
ABS/ CS	absorbed photon flux per excited cross-section of PSII (or also apparent antenna size)
Car	carotenoid
Chl	chlorophyll
CS	a cross-section of PSII
DI <sub>0</sub> / ABS	quantum yield of energy dissipation in PSII antenna
DI <sub>0</sub> / RC	The flux of energy dissipated per active RC
ET <sub>0</sub> / RC	electron transport flux from to PQ per active PSII
F <sub>0</sub>	initial fluorescence value
F <sub>300μs</sub>	fluorescence value at 300 μs
F <sub>m</sub>	maximal fluorescence intensity
F <sub>V</sub>	maximum variable fluorescence
OEC	oxygen-evolving complex
PCA	principal component analysis
PI <sub>ABS</sub>	Performance index (potential) for energy conservation from exciton to the reduction of intersystem electron acceptors
PI <sub>TOT</sub>	Performance index (potential) for energy conservation from exciton to the reduction of PSI end acceptors
Q <sub>A</sub> and Q <sub>B</sub>	primary and secondary quinone electron acceptor
PQ	the pool of free plastoquinone behind the PSII reaction center
PQH <sub>2</sub>	plastoquinol
PSI	photosystem I
PSII	photosystem II
RC	total number of PSII active reaction centers
RE <sub>0</sub> / RC	electron transport flux from to final PSI acceptors per active PSII
RE <sub>0</sub> / CS	electron transport flux from to final PSI acceptors per cross-section of PSII
S <sub>m</sub>	the normalized area between OJIP curve and the line
F <sub>m</sub>	which is a proxy of the number of electron carriers per electron transport chain
TR <sub>0</sub> / RC	maximum trapped exciton flux per active PSII
TR <sub>0</sub> / CS	maximum trapped exciton flux per cross-section
V <sub>I</sub>	relative variable fluorescence at 30 ms (I-step)
V <sub>J</sub>	relative variable fluorescence at 2 ms (J-step)
V <sub>K</sub>	relative variable fluorescence at 300 μs (K-step)
V <sub>L</sub>	variable fluorescence at L-band
V <sub>t</sub>	relative variable fluorescence at time t
ΔV <sub>IP</sub>	I-P normalized differential induction curves
ΔV <sub>OJ</sub>	O-J normalized differential induction curves
ΔV <sub>OK</sub>	O-K normalized differential induction curves

(Continued)

## Continued

ΔV <sub>OP</sub>	O-P normalized differential induction curves
δR <sub>0</sub>	efficiency with which an electron from Q <sub>B</sub> is transferred to final PSI acceptors
φE <sub>0</sub>	Quantum yield of electron transport from to PQ
φP <sub>0</sub>	maximum quantum yield of primary PSII photochemistry
φR <sub>0</sub>	quantum yield of electron transport from to the final PSI acceptors
ψE <sub>0</sub>	efficiency with which a PSII trapped electron is transferred from Q <sub>A</sub> to Q <sub>B</sub>
ψR <sub>0</sub>	efficiency with which a PSII trapped electron is transferred to final PSI acceptors



## OPEN ACCESS

## EDITED BY

Vasilij Goltsev,  
Sofia University, Bulgaria

## REVIEWED BY

Muhammad Ali,  
Zhejiang University, China  
Huihui Zhang,  
Northeast Forestry University, China

## \*CORRESPONDENCE

Jinxia Cui  
jinxiaacui77@163.com  
Huiying Liu  
liuhy\_bce@shzu.edu.cn

<sup>†</sup>These authors have contributed  
equally to this work

## SPECIALTY SECTION

This article was submitted to  
Plant Abiotic Stress,  
a section of the journal  
Frontiers in Plant Science

RECEIVED 28 August 2022

ACCEPTED 18 October 2022

PUBLISHED 03 November 2022

## CITATION

Wu P, Ma Y, Ahammed GJ, Hao B,  
Chen J, Wan W, Zhao Y, Cui H, Xu W,  
Cui J and Liu H (2022) Insights into  
melatonin-induced photosynthetic  
electron transport under low-  
temperature stress in cucumber.  
*Front. Plant Sci.* 13:1029854.  
doi: 10.3389/fpls.2022.1029854

## COPYRIGHT

© 2022 Wu, Ma, Ahammed, Hao, Chen,  
Wan, Zhao, Cui, Xu, Cui and Liu. This is  
an open-access article distributed under  
the terms of the [Creative Commons  
Attribution License \(CC BY\)](#). The use,  
distribution or reproduction in other  
forums is permitted, provided the  
original author(s) and the copyright  
owner(s) are credited and that the  
original publication in this journal is  
cited, in accordance with accepted  
academic practice. No use,  
distribution or reproduction is  
permitted which does not comply with  
these terms.

# Insights into melatonin-induced photosynthetic electron transport under low-temperature stress in cucumber

Pei Wu<sup>1,2†</sup>, Yadong Ma<sup>1,2†</sup>, Golam Jalal Ahammed<sup>3</sup>,  
Baoyu Hao<sup>1,2</sup>, Jingyi Chen<sup>1,2</sup>, Wenliang Wan<sup>1,2</sup>, Yanhui Zhao<sup>1,2</sup>,  
Huimei Cui<sup>1,2</sup>, Wei Xu<sup>1,2</sup>, Jinxia Cui<sup>1,2\*</sup> and Huiying Liu<sup>1,2\*</sup>

<sup>1</sup>Department of Horticulture, Agricultural College, Shihezi University, Shihezi, China, <sup>2</sup>The Key Laboratory of Special Fruits and Vegetables Cultivation Physiology and Germplasm Resources Utilization in Xinjiang Production and Construction Group, Shihezi University, Shihezi, China,

<sup>3</sup>College of Horticulture and Plant Protection, Henan University of Science and Technology, Luoyang, China

In this study, the differences in chlorophyll fluorescence transient (OJIP) and modulated 820 nm reflection (MR<sub>820</sub>) of cucumber leaves were probed to demonstrate an insight into the precise influence of melatonin (MT) on cucumber photosystems under low temperature stress. We pre-treated cucumber seedlings with different levels of MT (0, 25, 50, 100, 200, and 400  $\mu\text{mol} \cdot \text{L}^{-1}$ ) before imposing low temperature stress (10 °C/6 °C). The results indicated that moderate concentrations of MT had a positive effect on the growth of low temperature-stressed cucumber seedlings. Under low temperature stress conditions, 100  $\mu\text{mol} \cdot \text{L}^{-1}$  (MT 100) improved the performance of the active photosystem II (PSII) reaction centers (Plabs), the oxygen evolving complex activity (OEC centers) and electron transport between PSII and PSI, mainly by decreasing the L-band, K-band, and G-band, but showed differences with different duration of low temperature stress. In addition, these indicators related to quantum yield and energy flux of PSII regulated by MT indicated that MT (MT 100) effectively protected the electron transport and energy distribution in the photosystem. According to the results of  $W_{O-I} \geq 1$  and MR<sub>820</sub> signals, MT also affected PSI activity. MT 100 decreased the minimal value of MR/MR<sub>O</sub> and the oxidation rate of plastocyanin (PC) and PSI reaction center (P700) ( $V_{ox}$ ), while increased  $\Delta\text{MR}_{\text{slow}}/\text{MR}_O$  and deoxidation rates of PC<sup>+</sup> and P<sub>700</sub><sup>+</sup> ( $V_{red}$ ). The loss of the slow phase of MT 200 and MT 400-treated plants in the MR<sub>820</sub> kinetics was due to the complete prevention of electron movement from PSII to re-reduce the PC<sup>+</sup> and P<sub>700</sub><sup>+</sup>. These results suggest that appropriate MT concentration (100  $\mu\text{mol} \cdot \text{L}^{-1}$ ) can improve the photosynthetic performance of PS II and electron transport from primary quinone electron acceptor (Q<sub>A</sub>) to secondary quinone electron acceptor (Q<sub>B</sub>), promote the balance of energy distribution, strengthen the connectivity of PSI and PSII, improve the electron flow of PSII via Q<sub>A</sub> to PC<sup>+</sup> and P<sub>700</sub><sup>+</sup> from reaching PSI by regulating multiple sites of electron transport chain in photosynthesis, and increase the pool size and reduction rates of PSI in low



temperature-stressed cucumber plants, All these modifications by MT 100 treatment promoted the photosynthetic electron transfer smoothly, and further restored the cucumber plant growth under low temperature stress. Therefore, we conclude that spraying MT at an appropriate concentration is beneficial for protecting the photosynthetic electron transport chain, while spraying high concentrations of MT has a negative effect on regulating the low temperature tolerance in cucumber.

#### KEYWORDS

cucumber, low temperature, melatonin, OJIP,  $MR_{820}$  signal, JIP-test

## Introduction

Cucumber (*Cucumis sativus* L.), an important economic and nutritional crop, is cultivated in diverse climatic regions around the world, although it originated from tropical and subtropical areas. Due to high sensitivity to environmental factors, cucumber is often subjected to multiple environmental stresses, especially low temperature (0 °C to 15 °C) when grown in cool seasons (Chinnusamy et al., 2010; Theocharis et al., 2012). The adverse effects of low temperature on cucumber plant growth and development are mainly manifested through severe damage to photosynthetic components and efficiency (Ensminger et al., 2006; Ploschuk et al., 2014; Wu et al., 2020; Zhang et al., 2020; Lee et al., 2021). The deleterious effects on photosynthesis caused by low temperature are multifaceted, on the one hand, low temperature directly decreases the chlorophyll content and disrupts the chloroplast structure, resulting in the reduction of light energy capture that can be absorbed and utilized by plants (Liu et al., 2018); besides, low temperature indirectly reduces the carbon dioxide (CO<sub>2</sub>) fixation capacity by reducing the sensitivity of stomata to CO<sub>2</sub> (Xiong et al., 2015; Wu et al., 2020). Low temperature stress also exacerbates an imbalance between the energy absorption by photosystems and the metabolic sink of plants, and the imbalance activates the redox sensor within the photosynthetic electron transport chain, thereby regulating photophysical, photochemical and metabolic processes by photosynthetic electron transport in the chloroplast (Ensminger et al., 2006; Ruelland et al., 2009). Therefore, it is necessary to explore strategies to protect the photosystem damage and improve the photosynthesis of plants under low temperature stress. In recent years, studies on the application of exogenous plant growth regulators and/or signaling agents including nitric oxide (NO), brassinolide (BR), hydrogen sulfide (H<sub>2</sub>S), glutathione (GSH), calcium (Ca<sup>2+</sup>), and melatonin (MT) have provided a theoretical basis on protecting photosystems and improving the photosynthetic capacity of plants under abiotic stress (Cui et al., 2011; Zhou

et al., 2018; Corpas, 2019; Wu et al., 2020; Zhang et al., 2020; Feng et al., 2021).

Since its discovery in plants, MT has attracted more and more attention from plant scientists due to its involvement in plant growth, development, photosynthesis, rooting, seed germination, biotic, and abiotic stress responses (Arnao and Hernández-Ruiz, 2014; Reiter et al., 2015; Debnath et al., 2019; Khan et al., 2020; Sun et al., 2020; Li et al., 2021; Wang et al., 2022). The efficacy of MT in reactive oxygen species (ROS) scavenging and antioxidant defense responses are the two major mechanisms to cope with major abiotic stresses (Sun et al., 2020; Tiwari et al., 2020). Notably, MT is involved in regulating the functions of photosynthetic apparatus and photochemical reactions. For instance, MT treatment increases the maximal quantum yield of PSII (Fv/Fm), the actual photochemical efficiency of PSII (Y(II)), electron transport rate (ETR) and photochemical quenching (qP), while it decreases nonphotochemical quenching (NPQ) to increase the high-temperature tolerance of tomato plants (Jahan et al., 2021). Furthermore, exogenous MT can protect maize from drought stress by inhibiting excessive ROS accumulation, while promoting glutathione (GSH) metabolism, calcium (Ca<sup>2+</sup>) signals transduction, and jasmonic acid (JA) biosynthesis (Zhao et al., 2021). Notably, exogenous MT has also been reported to improve the photochemical processes of PSII, by directly increasing antioxidant enzyme activities, leading to altered metabolism in bermudagrass under cold stress (Fan et al., 2015). However, detailed and comprehensive information on the MT-induced alleviation of low temperature-inhibited photosynthetic energy allocation and electron transport in cucumber is still unavailable.

The energy captured by chloroplast is mostly used for photochemical reactions (Wang et al., 2020). After excitation, the reaction center chlorophylls P680 in PSII and P700 in PSI are photo-oxidized, allowing electron transport from H<sub>2</sub>O to NADP<sup>+</sup> along with electron transporters complexes (cytochrome *b<sub>6</sub>f* complex (cyt *b<sub>6</sub>f*) and quinone acceptors of

PSII ( $Q_A$ ,  $Q_B$ , plastocyanin (PC)), which are finally oxidized to produce the adenosine-triphosphate (ATP) and reduced coenzyme II (NADPH) (Shikanai, 2011; Krieger-Liszka and Shimakawa, 2022). In addition, a part of the energy that cannot be utilized for the photochemical reaction is dissipated by heat (internal conversion) and fluorescence, in which the energy used for fluorescence accounts for 3–5% of the total energy absorbed by chlorophyll (Strasser et al., 1995). Fortunately, as a sensitive, non-destructive, rather quickly, and reliable tool, chlorophyll *a* fluorescence provides convenience for investigating the ecophysiological indexes of plant stress (Strasser et al., 2004; Wang et al., 2020; Chen et al., 2021). The prompting fluorescence transient (OJIP) and modulated 820 nm reflection ( $MR_{820}$ ) signal are simultaneously measured by a new instrument (M-PEA) which are informative in evaluating the photochemical efficiency and the characteristics of the components related to photosynthetic electron transport (Strasser et al., 2010; Stirbet and Govindjee, 2011; Chen et al., 2016; Guo et al., 2020). OJIP transient analyses have revealed that abiotic stress including salt, cold, and high temperature could change the thylakoid component processes, light utilization efficiency, and excitation energy dissipation, and also reduce the stability of the photosynthetic system and the connectivity between PS1 and PSII in plants (Hu et al., 2018; Snider et al., 2018; Chen et al., 2021). The procedure for biophysical interpretation of fluorescence transient provides convenience for our research.

In this study, we hypothesized that MT could affect photosynthetic electron transport in low temperature-stressed cucumber plants to confer low temperature tolerance. Particularly, we aimed to get a better insight into the precise influence of MT on cucumber photosystems. Accordingly, cucumber seedlings pre-treated with different concentrations of MT were subject to low temperature stress and used to simultaneously measure the OJIP and  $MR_{820}$  signals. Based on the “theory of energy fluxes in biomembranes”, we investigated the effect of MT on the photochemical efficiency and the characteristics of the components related to photosynthetic electron transport using the JIP-test method. The results obtained provide valuable insight into the mechanism of MT-induced photosynthetic regulation which can be a reference for further understanding the regulatory pathway of MT-induced enhanced low temperature tolerance in cucumber plants.

## Materials and methods

### Plant materials and chemical treatment

The cucumber (*C. sativus* L.) cultivar ‘Jinyan No. 4’ was used for the current experiment. The seedlings were transplanted in pots (12-cm-diameter, with one seedling per pot) filled with the

specified substrate (peat: vermiculite, 2: 1, v/v) and raised in an incubator at a temperature of 25/18 °C (day/night), the light intensity of 300  $\mu\text{mol} \cdot \text{m}^{-2} \cdot \text{s}^{-1}$  (PPFD), and relative humidity of 75%–80%, and photoperiod of 14 h/10 h (day/night). The chemical treatments were conducted when the third true leaves were expanded. Twenty-four seedlings were divided into 6 groups and pre-treated with distilled water (LT) or different concentrations of melatonin (MT, purchased from Yuanye Company, China) such as 25  $\mu\text{mol} \cdot \text{L}^{-1}$  (MT 25), 50  $\mu\text{mol} \cdot \text{L}^{-1}$  (MT 50), 100  $\mu\text{mol} \cdot \text{L}^{-1}$  (MT 100), 200  $\mu\text{mol} \cdot \text{L}^{-1}$  (MT 200), and 400  $\mu\text{mol} \cdot \text{L}^{-1}$  (MT 400) and cultured at 25 °C, 0  $\mu\text{mol} \cdot \text{m}^{-2} \cdot \text{s}^{-1}$  (PPFD) and humidity of 75% for 4 h, and then 300  $\mu\text{mol} \cdot \text{m}^{-2} \cdot \text{s}^{-1}$  was restored. Twenty-four hours after the distilled water or chemical treatments, low temperature treatment (temperature of 10/6 °C (14 h-day/10 h-night cycle), light intensity of 100  $\mu\text{mol} \cdot \text{m}^{-2} \cdot \text{s}^{-1}$ , and relative humidity of 70%–75%) was initiated. And the prompting chlorophyll *a* fluorescence transient (OJIP) and modulated 820-nm reflection ( $MR_{820}$ ) signal were measured in the mature leaves (the second leaves from the bottom) of cucumber plants under low temperature stress at 24 h and 48 h.

### Phenotype of cucumber seedlings

We captured the pseudo color pictures of the maximal quantum yield of PSII (Fv/Fm) and the actual phenotype photos of cucumbers after low temperature stress for 72 h. And the Imaging-PAM-2500 (IMAG-MAX; Walz, Germany) was used to detect the value of Fv/Fm according to Zhang et al. (2020).

### Measurement of OJIP transient and $MR_{820}$ signal

The cucumber plants were initially dark adapted for two hours by putting them in a dark incubator along with attachments of special plastic clips to the leaves. And then the OJIP and  $MR_{820}$  signal were simultaneously detected using M-PEA (Hansatech, Norfolk, UK) according to Zhou et al. (2019). The OJIP transients were induced by a saturating light pulse of 3000  $\mu\text{mol} \cdot \text{m}^{-2} \cdot \text{s}^{-1}$  and recorded during a 5 s light pulse. Fluorescence values at 0.02 ms and 0.7 ms were considered to be the first reliable value of OJIP and  $MR_{820}$  signals, respectively. Then the JIP-test was used to analyze the OJIP and  $MR_{820}$  signals according to the method of Strasser et al. (2004). A series of data had been mentioned in the article including the performance of active reaction centers (RCs) (PIabs), potential activity of photosynthetic system (Fv/Fo), standardized variable fluorescence at J point ( $V_j$ ), the energy flux of per active RC ( $RE_O/RC$ ,  $TR_O/RC$ ,  $ABS/RC$ ,  $ET_O/RC$ , and  $DI_O/RC$ ), quantum yield ( $\Phi_{P_0}$ ,  $\Phi_{E_0}$ ,  $\Phi_{R_0}$ ), flux ratio ( $\Psi_{E_0}$ ,  $\delta_{R_0}$ ), normalized total

complementary area (Sm), and closing rate of PSII RCs (Mo). To further estimate the electron transport of the photosynthetic system, the O-P, O-K, O-J, and O-I periods were calculated by double normalization:  $V_t = (F_t - F_0)/(F_M - F_0)$ ,  $W_{O-K} = (F_t - F_0)/(F_K - F_0)$ ,  $W_{O-J} = (F_t - F_0)/(F_J - F_0)$ , and  $W_{O-I} = (F_t - F_0)/(F_I - F_0)$ . The fluorescence differences between MT treatments and LT were determined in the L-band, K-band, and G-band and calculated as:  $\Delta W_{O-K} = [W_{O-K(\text{treatment})} - W_{O-K(\text{control})}]$ ,  $\Delta W_{O-J} = [W_{O-J(\text{treatment})} - W_{O-J(\text{control})}]$ , and  $\Delta W_{O-I} = [W_{O-I(\text{treatment})} - W_{O-I(\text{control})}]$ , respectively (Strasser et al., 2004; Silva Dalberto et al., 2017).  $M_O$  was calculated as:  $M_O = 4 (F_{270\mu s} - F_0)/(F_M - F_0)$ ; OEC centers was calculated as: OEC centers =  $[1 - (V_K/V_J)]_{\text{treatment}}/[1 - (V_K/V_J)]_{\text{control}}$  (Guo et al., 2020).

Upon exclusion of the interference of other factors on the light reflection at 820 nm, the  $MR_{820}$  signals were represented by MR/MRo (Guo et al., 2020).  $MR_O$  represents the first reliable value of the MR/MRo (at 0.7 ms). Based on the MR/MRo curve, we analyzed the redox state of PSI electron carriers of cucumber seedlings: plastocyanin (PC) and PSI reaction center ( $P_{700}$ ) were oxidized by the initial light (corresponding to the decreased fraction of MR/MRo, which can be represented by  $\Delta MR_{\text{fast}}/MR_O$ ) and followed reduction (corresponding to the increased fraction of MR/MRo, which can be represented by  $\Delta MR_{\text{slow}}/MR_O$ ) (Schansker et al., 2003; Strasser et al., 2010). The redox rates of PC and  $P_{700}$  are denoted by  $V_{ox}$  and  $V_{red}$ , respectively. According to Guo et al. (2020), the following formulae were used for various calculations:  $\Delta MR_{\text{fast}}/MR_O = (MR_O - MR_{\text{min}})/MR_O$ ,  $\Delta MR_{\text{slow}}/MR_O = (MR_{\text{max}} - MR_{\text{min}})/MR_O$ ,  $V_{ox} = \Delta MR/\Delta t = (MR_{2\text{ ms}} - MR_{0.7\text{ ms}})/(1.3\text{ ms})$ , and the calculation formula of  $V_{red}$ .

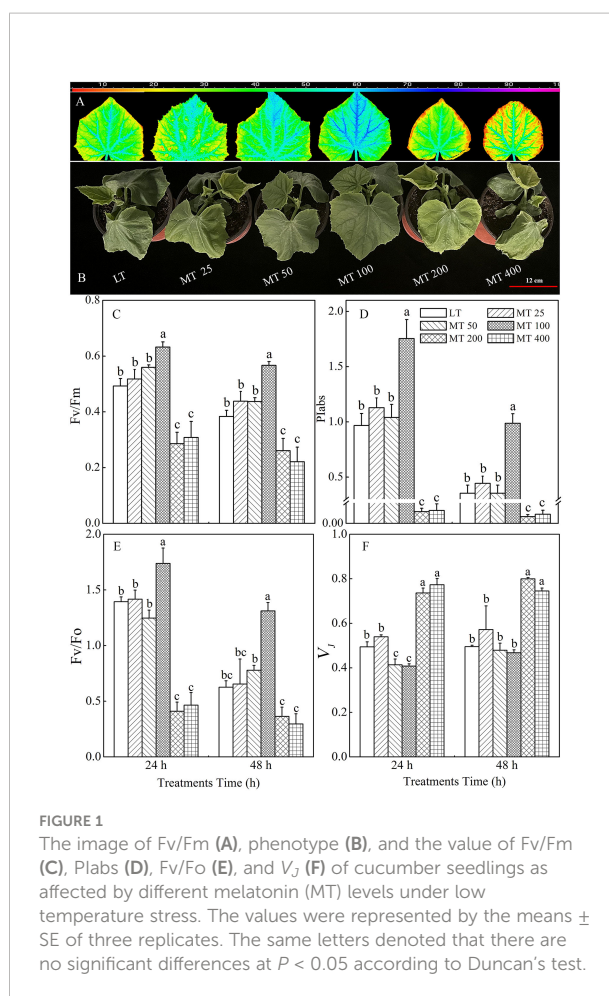
## Statistical analysis

Statistical analyses were performed using variance analysis (ANOVA). The values were presented by the means  $\pm$  SE of three replicates and the  $P < 0.05$  was considered to be significantly different.

## Results

### MT-induced changes in phenotypic and fluorescence parameters in response to low temperature

The phenotype of cucumber seedlings was significantly changed by different concentrations of MT under low temperature conditions (Figure 1). In comparison with the LT treatment, MT 50 and MT 100 treatments, especially the MT 100 treatment noticeably ameliorated the wilting phenotype and



visible cold injuries, while MT 200 and MT 400 aggravated cold-induced damage to cucumber seedlings (Figure 1).

The changes in Fv/Fm, PIabs, Fv/Fo, and  $V_j$  in cucumber plants treated with different MT concentrations under low temperature stress are shown in Figures 1A, C–F. The Fv/Fm was significantly increased with MT 100 treatment by 28.4% and 47.7% under low temperature stress for 24 h and 48 h, respectively, when compared with LT treatment (Figure 1C). The value of PIabs increased by 81.6% and 179.2% in 'MT 100'-treated plants under low temperature stress for 24 h and 48 h, respectively when compared with LT. However, MT 200 and MT 400 treatments significantly decreased the PIabs (Figure 1D). In addition, Consistent with the Fv/Fm quantitative values (Figure 1C), the pseudo color image of Fv/Fm in Figure 1A showed the same trend. Fv/Fo represents the potential activity of the photosynthetic system, and  $V_j$  reflects the closure degree of the active RCs of photosystem II (PSII). Under low temperature stress, MT significantly altered the value of Fv/Fo and  $V_j$  in the cucumber leaves (Figures 1E, F). The 'MT 100'-treated plants had higher, while MT 200 and MT 400 plants had lower Fv/Fo in

both 24 h and 48 h of low temperature stress than the LT-treated plants. In addition, MT 50 and MT 100 significantly decreased while the MT 200 and MT 400 treatments significantly increased the  $V_f$  when compared with LT treatment.

## Effects of different levels of MT on the OJIP transient of cucumber plants under low temperature stress

### Prompting fluorescence transient (OJIP) and the relative variable fluorescence ( $V_f$ )

OJIP transients of cucumber seedlings treated with different concentrations of MT under low temperature stress were presented in Figure 2. As shown in Figures 2A, B, the

traditional J, I, and P points (2 ms, 30 ms, and approximately 300 ms, respectively) were delayed to J point for 3 ms, I point for 80 ms, and P point did not reach the real maximum value under low temperature stress in our study. Clearly, treatments with different MT concentrations exhibited different influences on the OJIP transients. The OJIP transients of cucumber seedlings that were treated with LT, MT 25, MT 50, and MT 100, showed a typical shape, while MT 200 and MT 400 treatments significantly changed OJIP shape under low temperature stress. The highest point of the OJIP curve ( $F_p$ ) decreased progressively with the extension of stress time (Figures 2A, B). Compared with LT, MT treatments (MT 25, MT 50, MT 100, MT 200, and MT 400) significantly increased the  $F_o$  under cold stress for 24 h, while a significant decrease in  $F_o$  was observed after 48 h of stress. The MT 100-treated plants exhibited a higher

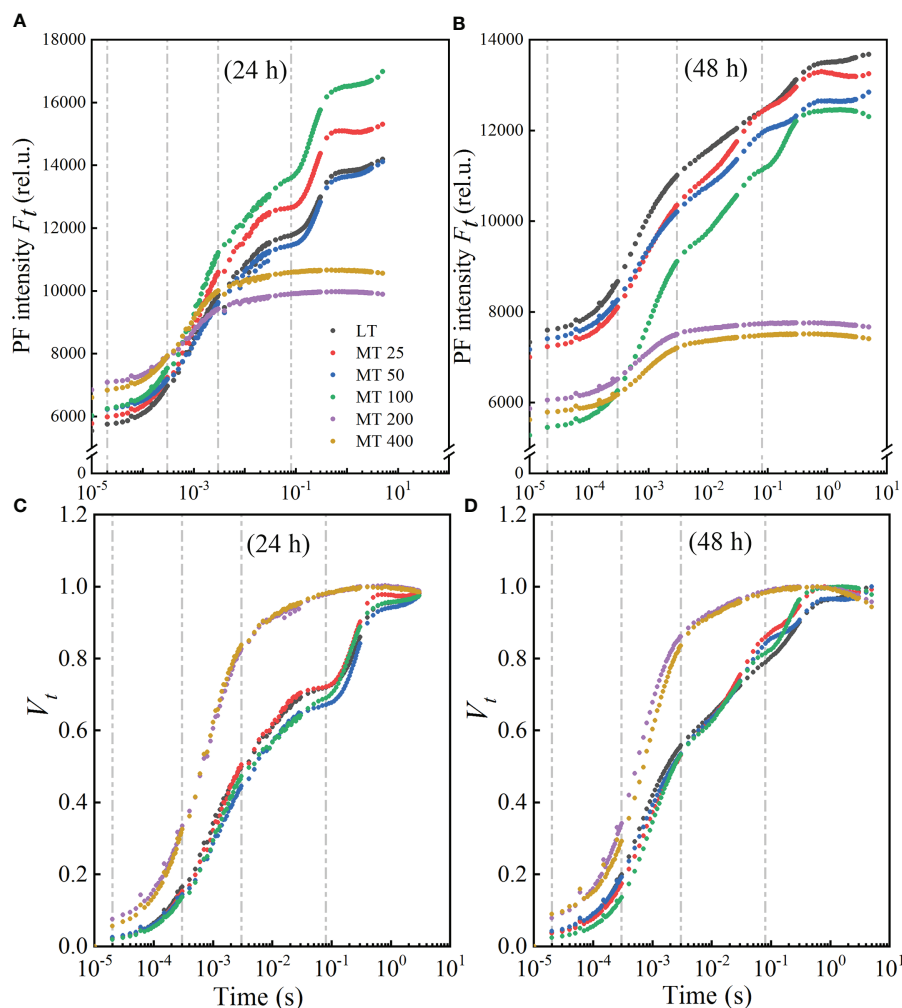


FIGURE 2

Effect of different melatonin (MT) concentrations on the induction of fluorescence transient (OJIP) of the cucumber seedlings under low temperature stress. The OJIP transients after low temperature stress for 24 h (A) and 48 h (B); Normalized transients of OJIP in cucumber seedlings after low temperature for 24 h (C) and 48 h (D). The  $V_t$  was calculated as  $V_t = [(F_t - F_o)/(F_M - F_o)]$ .



$F_p$  level in 24 h and a more normal characteristic curve in stress for 48 h than LT treatment. In addition, MT 100 significantly increased the  $F_p$  under stress for 24 h, while significantly decreased the  $F_o$  under stress for 48 h when compared with LT treatment. The K-step was increased by the five MT treatments under 24 h of low temperature stress, while decreased by these MT treatments under 48 h of low temperature stress (Figures 2A, B).

The double normalized OJIP curves from  $F_o$  to  $F_M$  were presented as  $V_t$  (Figures 2C, D), and to assess the characteristics of OJIP more clearly. Compared with the LT, the normalized OJIP curves of five MT concentrations-treated plants showed apparent and variable changes. The K-step and J-step decreased at MT 25, MT 50, and MT 100 treatments, while increased drastically at MT 200 and MT 400 treatments when compared with LT under low temperature conditions. In comparison with LT, different concentrations of MT (MT 25, MT 50, and MT 100) treatments led to a lower I-step under stress for 24 h, while a higher I-step under stress for 48 h. But the J-step and I-step were always the highest in MT 200 and MT 400 treatments under low temperature conditions (Figures 2C, D).

### The L-band of MT-pretreated cucumber plants under low temperature stress

The L-band was analyzed to evaluate the aggregation between different components of PSII or the connectivity of energy transfer between antenna pigment and PSII active RC (Strasser et al., 2004) in cucumber leaves. The OJIP curves of each treatment were normalized by O- and K-point to show L-band, as  $W_{O-K}$  kinetics (Figures 3A, B) and the difference kinetics  $\Delta W_{O-K}$  (Figures 3C, D) in the linear time variation from 0 to 300  $\mu$ s. It showed that there were no differences in L-band between MT 25, MT 100 and LT treatments at 24 h (Figure 3C) of low temperature stress, while MT 100 decreased L-band obviously at 48 h (Figure 3D) of low temperature stress. However, MT 200 and MT 400 always increased the low temperature-stressed L-band of cucumber seedlings when compared with LT treatment (Figures 3C, D). Under low temperature conditions, it is clear that MT 100 obviously changed the values of  $W_L$ ,  $\Delta W_L$  and  $F_L/F_J$  when compared with LT (Figures 3E, F). Specifically, there was no significant difference between LT- and MT-treated cucumber seedlings in  $W_L$  and  $\Delta W_L$ , while MT 100 significantly decreased the  $F_L/F_J$  at 48 h of low temperature stress. This suggests that MT-caused the change in L-band because of the increase of the J-step and the decrease in the L-step at stress for 24 h, while only the increase of the J-step at stress for 48 h.

### The K-band of MT-pretreated cucumber plants under low temperature stress

The OJIP curves were normalized by O and J points to show the K-band and were presented by  $W_{O-J}$  (Figures 4A, B) and  $\Delta W_{O-J}$  (Figures 4C, D). The  $\Delta W_{O-J}$  showed that the five MT

treatments induced the occurrence of the K-band. Compared with LT, MT 25, MT 50, and MT 100 treatments significantly decreased, while MT 200 and MT 400 treatments increased the K-band under low temperature stress (Figures 4C, D). In addition, compared with LT, only MT 100 treatment decreased the value of  $W_K$  and  $F_K/F_J$  of cucumber plants under low temperature stress. The OEC center was increased by MT 100 treatment at a certain degree (Figures 4E, F), which is highly consistent with the trend of  $\Delta W_{O-J}$  under low temperature stress. These results corroborated that MT 100 treatment can effectively protected the part of the active OEC centers.

### The G-band of MT-pretreated cucumber plants under low temperature stress

At the low temperature stress conditions, the normalizations and corresponding subtractions (difference kinetics) of OJIP curves from O to I point (80 ms) were presented in Figures 5C–F, as well as  $W_{O-I} \geq 1$  plotted in the linear 80–1000 ms to show the IP phase (Figures 5A, B).  $\Delta W_{O-I}$  represented the effects of different MT concentrations on the G-band. The results showed that the G-band of MT 25, MT 50, and MT 100 treatment was lower than LT, while MT 200 and MT 400 had higher G-band than LT treatment in low temperature-stressed cucumber plants (Figures 5E, F). The maximum amplitude of the  $W_{O-I} \geq 1$  curve is negatively correlated with the pool size of the terminal electron receptor on the PSI receptor side; specifically, the small amplitude corresponds to the strong inhibition effect on the pool size (Guo et al., 2020). Compared with LT, the amplitude of  $W_{O-I}$  curves was significantly increased to various degrees by MT 25, MT 50, and MT 100 treatments, while significantly decreased by MT 200 and MT 400 treatments after low temperature stress for 24 h (Figure 5A). While only MT 100 treatment increased the amplitude, and the other treatments decreased the amplitude of  $W_{O-I} \geq 1$  when compared with LT after low temperature stress for 48 h (Figure 5B).

### Effect of different MT concentrations on the JIP- test parameters of PSII

#### Specific fluxes per active RC

It is interesting to find out if MT influences the specific fluxes per active RC. The energy absorbed and dissipated by active RC (ABS/RC and DIO/RC), and excitation energy flux captured by each active RC (TRo/RC) were significantly decreased by MT 100, while increased by MT 200 and MT 400 treatments relative to LT treatment (Figures 6A, B, D). In comparison with LT, an increase of energy flux transferred by each active RC (ETo/RC) and electron transport from  $Q_A^-$  to the PSI electron acceptors by each RC (REo/RC) was observed in MT 100 treated plants (Figures 6C, E).

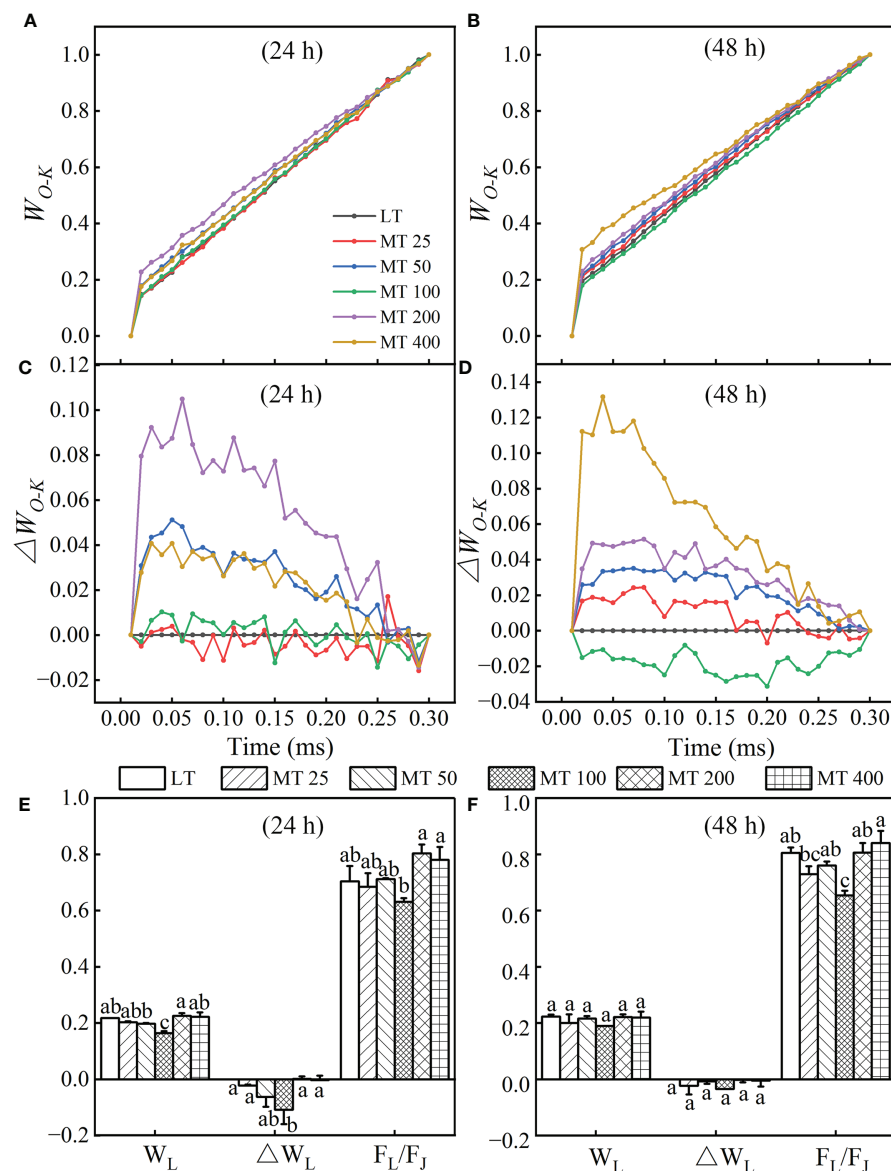


FIGURE 3

Effect of different melatonin (MT) concentrations on the L-band of low temperature-stressed cucumber plants. The OJIP kinetics normalized by O and K points, and calculated as:  $W_{O-K} = (F_t - F_O)/(F_K - F_O)$ . The difference kinetics  $\Delta W_{O-K}$  was calculated as  $\Delta W_{O-K} = W_{O-K}(\text{treatment}) - W_{O-K}(\text{control})$ . (A, C) and (B, D) represent low temperature stress for 24 h and 48 h, respectively. The  $W_L$ ,  $\Delta W_L$  and  $F_L/F_J$  values of MT-pretreated cucumber plants at the low temperature stress for 24 h (E) and 48 h (F). The values were represented by the means  $\pm$  SE. The same letters denoted that there are no significant differences at  $P < 0.05$  according to Duncan's test.

The energy pipeline models were developed to visualize and understand the symptoms of low temperature-stressed cucumber through analyzing the light absorption, trapping, electron transport, and dissipation of per excited cross section ( $CS_O = F_O$ ) (Figure 7). Results showed that MT 100 significantly improved the number of active RCs and light trapping. In addition, almost all energy fluxes were increased by MT 100 and decreased by MT 200 and MT 400. These results of the

energy pipeline models were highly consistent with the values in Figure 6.

### $M_O$ , $S_m$ , and quantum yields or efficiencies/probabilities

The relative value of the  $M_O$  and other chlorophyll fluorescence parameters are shown in Figure 8. Under low

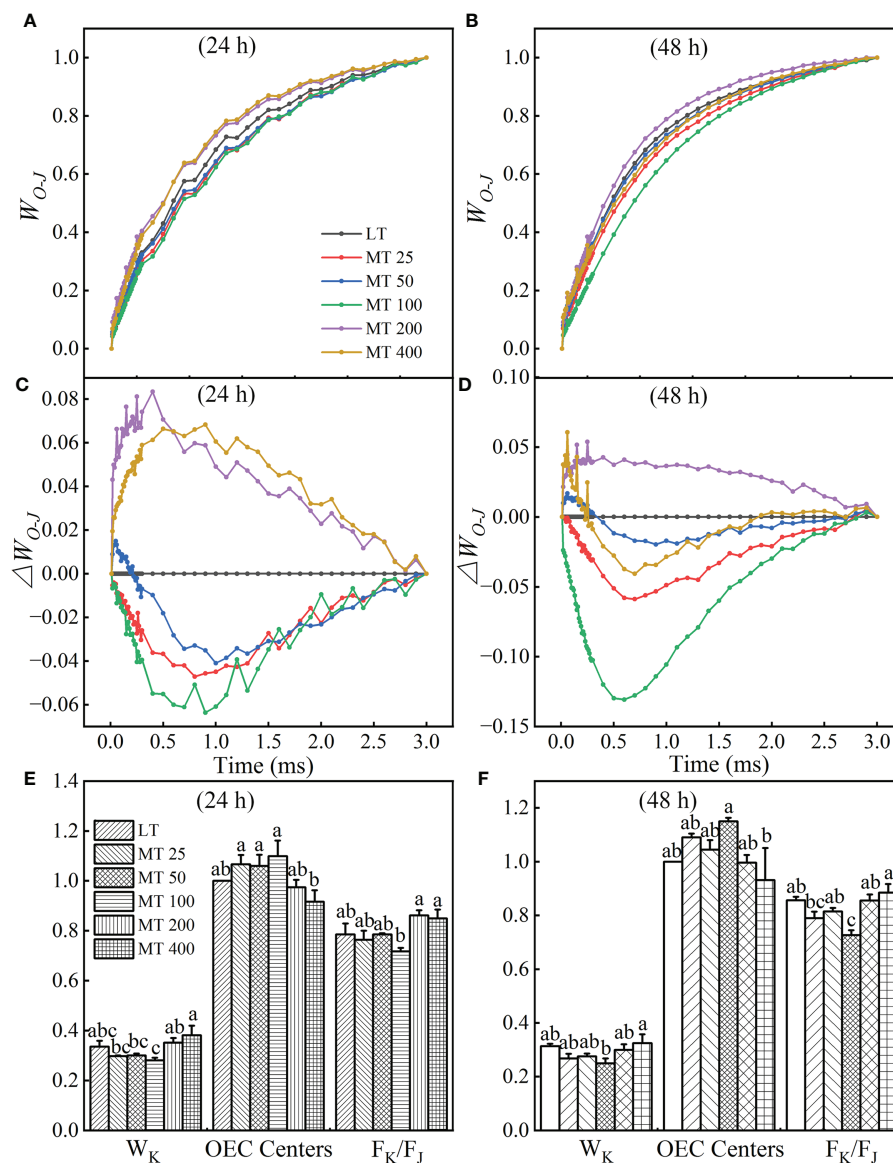


FIGURE 4

Effect of different concentrations of melatonin (MT) on the K-band of cucumber plants under low temperature stress. The OJIP curves were normalized by O and J points as  $W_{O-J} = (F_t - F_O)/(F_J - F_O)$ , and the difference kinetics  $\Delta W_{O-J} = W_{O-J}(\text{treatment}) - W_{O-J}(\text{control})$ . (A, C) and (B, D) represent low temperature stress for 24 h and 48 h, respectively. Effect of different levels of MT on the values of  $W_K$ , OEC centers and  $F_K/F_J$  at 24 h (E) and 48 h (F) of low temperature stress. The values were represented by the means  $\pm$  SE. The same letters denoted that there is no significant difference at  $P < 0.05$  according to Duncan's test. Data are presented as the means of three biological replicates.

temperature conditions, different levels of MT had different effects on JIP parameter, and specific changes in different treatments were observed. For instance, the values of  $\Phi_{RO}$ ,  $\Phi_{EO}$ ,  $\Phi_{PO}$ ,  $\Psi_{EO}$ ,  $\delta_{RO}$ , and Sm in MT 100-treated leaves were markedly higher than in LT-treated plants, while the Mo was obviously lower than in LT-treated plants. However, the MT 200 and MT 400 treatments showed the opposite effect to MT 100 when compared with LT (Figures 8A, B).

## The modulated 820 nm reflection ( $MR_{820}$ ) signals and the parameters of low temperature-stressed cucumber plants pretreated with different levels of MT

The  $MR_{820}$  signals normalized by  $MR_O$  ( $MR_{0.7ms}$ ) ( $MR/MR_O$ ) were used to further analyze the effect of MT on the PSI

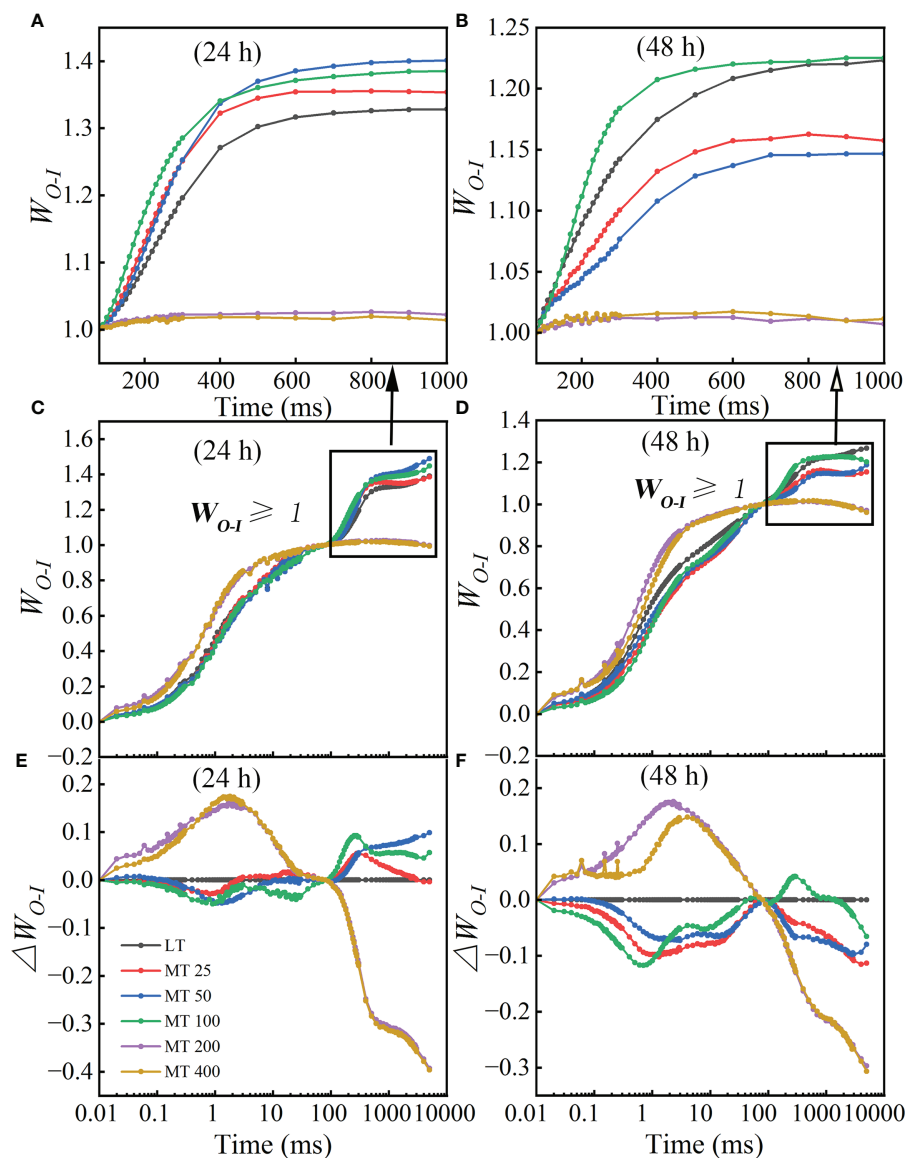


FIGURE 5

Different concentrations of melatonin (MT) induced the change in G-band shape in cucumber plants under low temperature stress. (A, B) The  $W_{O-I}$  curves from 80 ms to 1000 ms after 24 h and 48 h of low temperature-stressed cucumber seedlings. (C, D) The OJIP curves were normalized by O and I points as  $W_{O-I} = (F_t - F_0)/(F_I - F_0)$ . (E, F) The difference kinetics calculated as  $D_{W_{O-I}} = W_{O-I}(\text{treatment}) - W_{O-I}(\text{control})$  in a logarithmic time scale. Data are presented as the means of three biological replicates.

activity of low temperature-stressed cucumber seedlings (Figures 9A, B). The rapid descent phase (oxidation of PC and P700) was induced by the two red-light pulses of M-PEA, indicating that the slow rise phase (re-reduction of  $PC^+$  and  $P_{700}^+$ ) would be later induced in electrons transport from PSII. Under low temperature stress, different MT treatments led to the deformation of  $MR_{820}$  signals in cucumber seedlings, which showed changes in the lowest point of the rapid decline stage and in the highest point of the slow rise stage (Figures 9A, B). Compared with LT, different MT treatments significantly

decreased the lowest point of the oxidation phase of cucumber seedlings. In addition, the time reaching the lowest point of the oxidation phase was also advanced by the MT 50 and MT 100 treatments, while delayed by the MT 200 and MT 400 treatments when compared with LT treatment. The highest point of the re-reduction phase was also changed by different MT treatments. Compared with LT, MT 50 and MT 100 treatments significantly increased, while MT 200 and MT 400 treatments significantly decreased the highest point of the re-reduction phase after low temperature stress for 24 h, and MT 100 significantly increased,



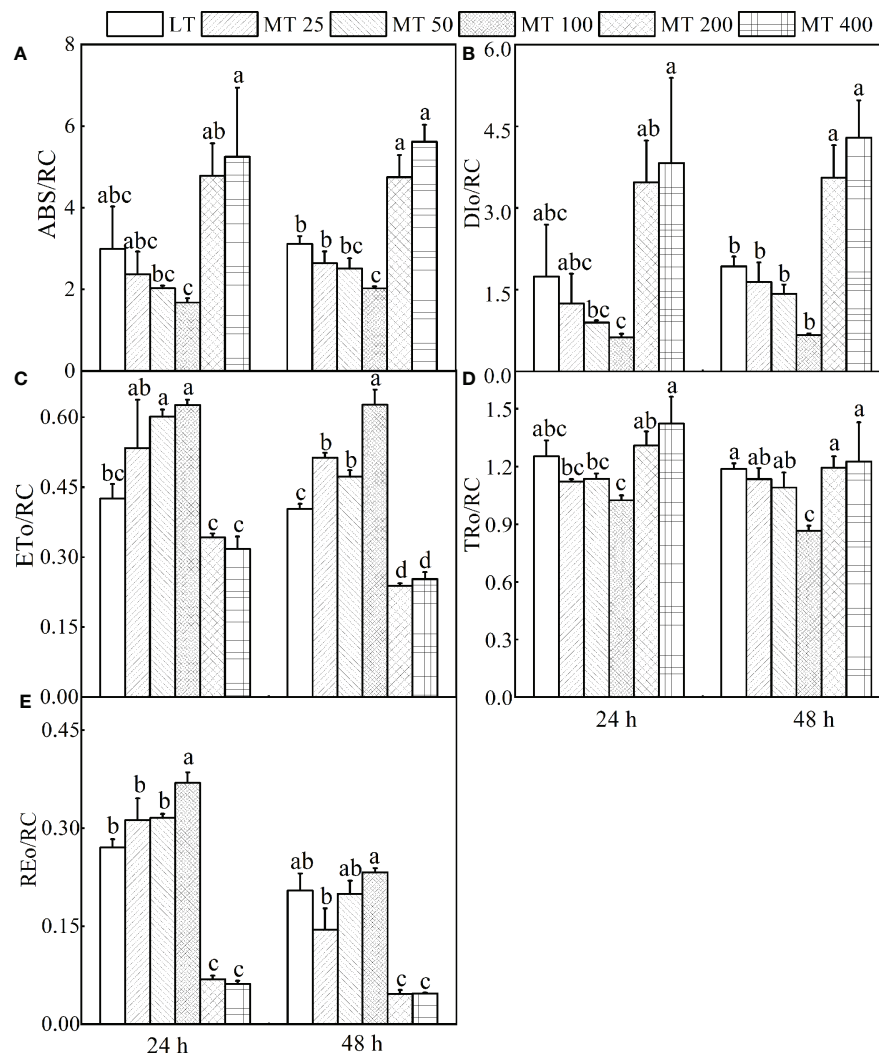


FIGURE 6

Parameters derived from OJIP transients of cucumber plants treated with different concentrations of melatonin (MT) under low temperature stress. (A) The energy absorbed by each active reaction center (RC). (B) The energy dissipated by each active RC. (C) The energy flux transferred by each active RC. (D) Excitation energy flux captured by each active RC. (E) The electron transport from QA<sup>-</sup> to the PSI electron acceptors by each RC. The values were represented by the means  $\pm$  SE. The same letters denoted that there is no significant difference at  $P < 0.05$  according to Duncan's test.

while the other treatments significantly decreased the highest point of re-reduction phase under low temperature stress for 48 h (Figures 9A, B). These results indicated that the appropriate concentration of MT (MT 50 and MT 100) can enhance the redox capacity of PSI.

Based on the MR<sub>820</sub> transient, several parameters derived from MR<sub>820</sub> signals including  $\Delta\text{MR}_{\text{fast}}/\text{MR}_0$ ,  $\Delta\text{MR}_{\text{slow}}/\text{MR}_0$ , PC and P700 oxidation rate ( $V_{\text{ox}}$ ) as well as the re-reduction rate of PC<sup>+</sup> and P700<sup>+</sup> ( $V_{\text{red}}$ ) were proposed in Figures 9C–F. The fast and slow phases can be quantified, respectively as  $\Delta\text{MR}_{\text{fast}}/\text{MR}_0$  and  $\Delta\text{MR}_{\text{slow}}/\text{MR}_0$ . Compared with LT, different concentrations of MT treatments increased distinctly the

values of  $\Delta\text{MR}_{\text{fast}}/\text{MR}_0$  at different levels (Figure 9C). On the other hand, MT 100 treatments led to a significant rise, while MT 200 and MT 400 treatments led to a significant decrease of  $\Delta\text{MR}_{\text{slow}}/\text{MR}_0$  and there was no obvious difference between LT and MT 25 or LT and MT 50 treatments (Figure 9D).  $V_{\text{ox}}$  and  $V_{\text{red}}$  were used to represent the oxidation of PC and P700 and reduction of PC<sup>+</sup> and P700<sup>+</sup>, respectively. It is clear that MT 100 decreased  $V_{\text{ox}}$  by 51.7% and 22.82% relative to LT after 24 h and 48 h of low temperature stress, respectively. There were no obvious changes in  $V_{\text{ox}}$  after MT 25 and MT 50 treatment when compared with LT (Figure 9E). With MT 100 treatment, the value of  $V_{\text{red}}$  was increased by 457.43% and 125.75% relative to

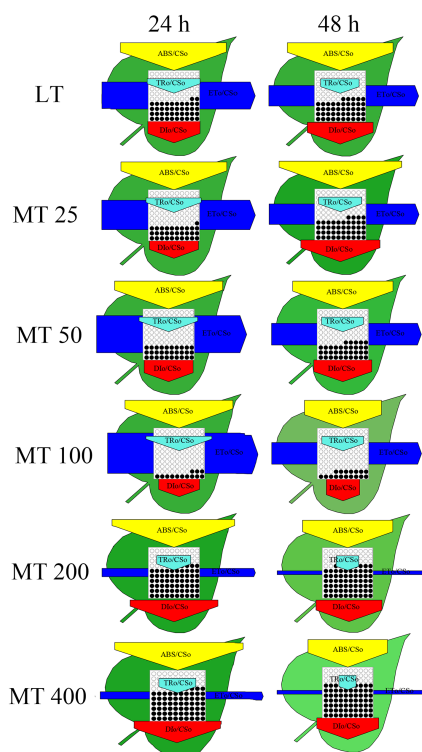


**FIGURE 7**  
The energy flux models (leaf models) of low temperature-stressed cucumber plants pre-treated with different concentrations of melatonin (MT).

LT for 24 h and 48 h, respectively. There was no obvious difference between LT, MT 25, and MT 50 treatment. Meanwhile, the value of  $V_{red}$  in MT 200- and MT 400- treated leaves declined close to zero (Figure 9F).

## Discussion

Photosynthesis in plants starts from the light-harvesting systems. The part of the energy used for photochemical reaction drives the electron transport along with the thylakoid membrane of chloroplasts, and eventually produces ATP and NADPH as the energy of the Calvin-Benson cycle and photorespiratory cycle (Heber et al., 1978; Heber and Walker, 1992). The prompt fluorescence (OJIP) and modulated 820-nm reflection ( $MR_{820}$ ) can reflect all the changes in photochemical reactions because of the close connection with the photochemical reaction and heat dissipation (Zhu et al., 2005; Murchie and Lawson, 2013). Using the OJIP and  $MR_{820}$  signals, researchers have revealed the cultivar differences under chilling or heat stress, and the adverse effects of abiotic stresses including temperature, salinity, and drought, as well as the beneficial effect

of exogenous signal molecules on photosynthesis, growth and development of plants (Kan et al., 2017; Zushi and Matsuzoe, 2017; Ahammed et al., 2018; Hu et al., 2018; Snider et al., 2018; Zhou et al., 2019; Chen et al., 2021). As a common environmental factor, low temperature stress seriously affects crop productivity by influencing plant growth and development (Ding et al., 2019). In this study, we applied MT in cucumber plants to study the changes in the photosynthetic electron transport chain and energy distribution by using OJIP and  $MR_{820}$  signals and attempted to explain how MT improved the adaptability of cucumber plants to low temperature stress.

As an antistress agent, MT has been reported against a number of abiotic stressors including low temperature (Arnao and Hernandez-Ruiz, 2015). Consistent with this, we found that MT 100 had a positive effect on plant phenotype, while the high concentration of MT (more than  $200 \mu\text{mol} \cdot \text{L}^{-1}$ ) aggravated the damage of low temperature stress to cucumber seedlings (Figures 1A, B). A previous study showed that MT regulated low temperature tolerance of cucumbers by activating the antioxidant enzymes and inducing the key genes related to PSI, PSII and carbon assimilation (Zhang et al., 2021). The Mo represents the rate of closing PSII RCs (Guo et al., 2020). In our study, we also found that appropriate concentrations of MT could improve the activity of PSII of cucumber plants ( $F_v/F_m$ ,  $F_v/F_o$ ,  $PI_{abs}$ ) mainly by increasing the Mo under low temperature stress (Figures 1, 8). The energy absorbed by plants drives electrons forward along the electron transport chain (Heber et al., 1978). The J-step ( $V_j$ ) increase indicates that the D1 protein is damaged and the electron transport from the primary quinone acceptor ( $Q_A$ ) to the secondary receptor quinone ( $Q_B$ ) is blocked, resulting in a large accumulation of  $Q_A^-$  in RCs of PSII (Oukarroum et al., 2004; Guo et al., 2020). Our results demonstrated that the  $V_j$  was significantly decreased by MT 50 and MT 100, suggesting that appropriate concentrations of MT (MT 50 and MT 100) could effectively protect D1 protein and promote electron transport.

We further analyzed OJIP and  $MR_{820}$  transients using the JIP-test method to investigate the mechanism of MT-induced changes in the electron transport chain of cucumber plants under low temperature stress. Generally, the OJIP transient shows polyphasic steps including O ( $F_o$ , at 20  $\mu\text{s}$  with M-PEA, all RCs open), J ( $\sim 2$  ms), I ( $\sim 30$  ms) and P ( $F_m$ , maximal fluorescence yield) (Strasser et al., 1995; Strasser et al., 2004). However, other steps such as K- and L-step between O and J, G- and H-steps between I and P also appear in certain conditions (Strasser et al., 2004; Chen et al., 2016; Xia et al., 2019). Similarly, a study reported by Stirbet and Govindjee (2012) showed that the J- and I-step did not always appear at 2 ms and 30 ms, which might move to another position with different stress conditions. Compared with the traditional positions of J, I and P points, the positions of these three points lagged slightly (J point for 3 ms, I point for 80 ms, and P point did not reach the maximum value in

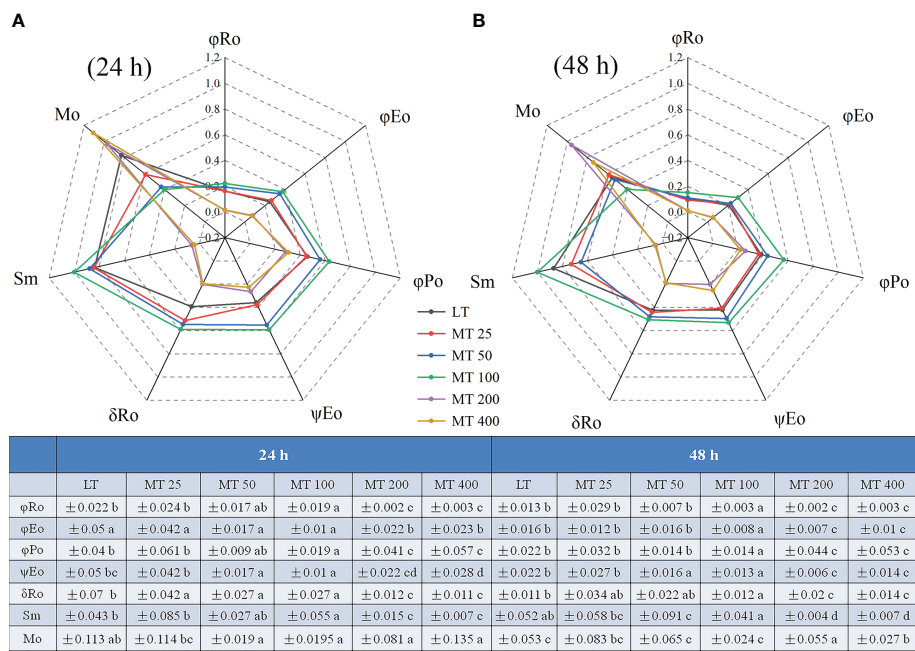


FIGURE 8 Radar plot of the JIP parameters of cucumber leaves under low temperature stress for 24 h (A) and 48 h (B). The values were represented by the means  $\pm$  SE. The same letters denoted that there is no significant difference at  $P < 0.05$  according to Duncan's test.

our study) in our study (Figure 2). Furthermore, the structure and order of light-harvesting-complexes can be reflected by  $F_O$  to a certain extent (Guo et al., 2020). Our study found that OJIP transient is sensitive to MT under low temperature stress. The OJIP transient was steep in MT 25- and MT 100-treated leaves than that in the LT, because of the increases from J-step to P-step at 24 h of low temperature stress (Figure 2A). The  $F_O$  was increased by MT at 24 h of low temperature stress, while decreased by MT at 48 h of low temperature stress (Figures 2A, B). The characteristics of the OJIP curve were most obvious in the MT 100 treatment, because the MT 100 treatment significantly reduced the O-step at 48 h of low temperature (Figure 2B). These findings indicated that MT mainly regulates the RCs of PSII under 24 h of low temperature stress, and with the extension of stress (48 h), MT can enhance the cucumber tolerance to low temperature by regulating energy capture efficiency of PSII, of which  $100 \mu\text{mol} \cdot \text{L}^{-1}$  MT (MT 100) had the best remission effect. The OJIP curve of MT 200- and MT 400-treated plants showed an increase after J-step, resulting in the disappearance of the IP phase (Figure 2). These results are highly consistent with Figure 1F. Combined with the previous research that reported the state of light absorption, chloroplast damage, and the activity response centers of PSII that can be partly reflected by the  $F_O$ ,  $F_M$  and  $V_J$  (Strasser et al., 2010), we concluded that MT 100 could

regulate the energy absorption by regulating the internal structure of light-harvesting-complexes and protect PSII donor end deterioration caused by low temperature, thereby promoting the capacity of the PSII donor end to provide electrons due to an increase in the opened RCs of PSII.

From the L-band and K-band, we can understand the group of the PSII subunits or energetic connectivity between the antenna and RCs of PSII and the situation of OEC centers at the PSII donor side (Strasser et al., 2004; Kalaji et al., 2018). Studies showed that the K-band usually occurred in plants that suffer from chilling, heat or drought stress (Strasser et al., 2004; Chen et al., 2016; Silva Dalberto et al., 2017; Dimitrova et al., 2020; Zeng et al., 2022). This phenomenon might be indirectly caused by the block of PSII electron flow beyond  $Q_A$ , resulting in a large accumulation of reactive oxygen species (ROS) in PSII (Rutherford and Krieger-Liszskay, 2001; Guo et al., 2020). In addition, the G-band represented the size of the PSI terminal electron acceptor pool. Furthermore, the maximal amplitude of the  $W_{O-I} \geq 1$  curve is negatively correlated with the pool size of the terminal electron receptor on the PSI receptor side (Guo et al., 2020). Here, MT 100 induced a decrease in L-band, K-band, as well as G-band and an increase in OEC centers,  $Sm$ , and the maximal amplitude of the  $W_{O-I} \geq 1$  curve (the IP phase), (Figures 3, 4, 5A, B, and 8). These results corroborated that MT 100 increased the low temperature tolerance of cucumber by

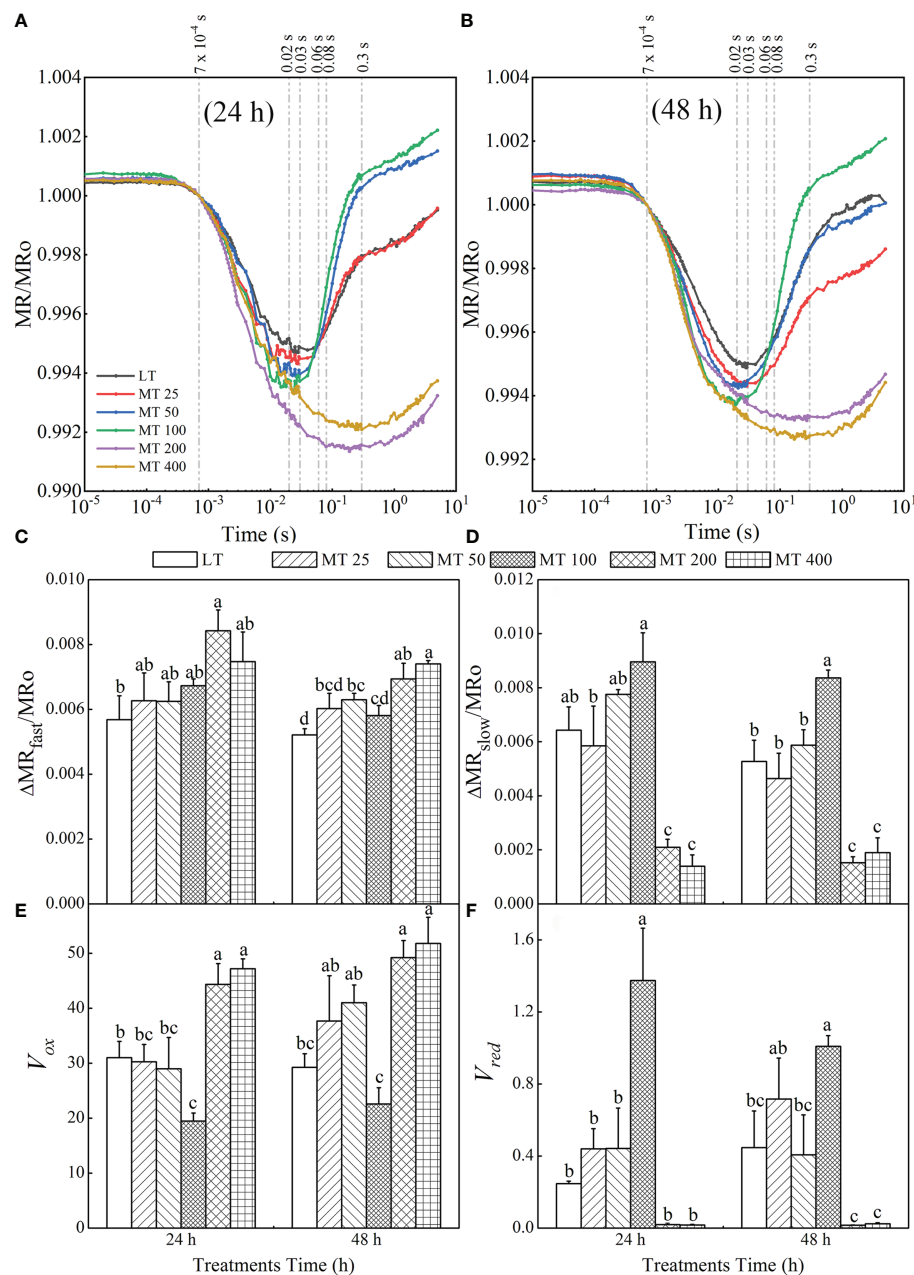


FIGURE 9

Effect of melatonin (MT) on the MR<sub>820</sub> signal after low temperature stress for 24 h (A) and 48 h (B). The time point  $7 \times 10^{-4}$  s represents the first reliable value of the MR/MR<sub>0</sub> (MR<sub>0</sub>) of each treatment; the time point 0.02 s represents the MR<sub>min</sub> of MT 50 and MT 100 treatments, the time point 0.03 s represents the MR<sub>min</sub> of LT and MT 25 treatments, the time point 0.06 s represents the end of  $V_{red}$  in LT and MT 25 treatments, the time point 0.08 s represents the end of  $V_{red}$  in MT 50 and MT 100 treatments, the time point 0.3 s represents the end of  $V_{red}$  in MT 200 and MT 400 treatments, and the time point 0.6 s represents the end of  $V_{red}$  in MT 200 and MT 400 treatments. The fast phase (C) was calculated as  $\Delta MR_{fast}/MR_0 = (MR_0 - MR_{min})/MR_0$ . The slow phase (D) was calculated as  $\Delta MR_{slow}/MR_0 = (MR_0 - MR_{max})/MR_0$ . The oxidation rate of plastocyanin (PC) and PSI reaction center (P<sub>700</sub>) (E) was achieved:  $V_{ox} = \Delta MR/\Delta t = (MR_{2ms} - MR_{0.7ms})/(1.3ms)$ . The reduction rate of PC<sup>+</sup> and P<sub>700</sub><sup>+</sup> (F) was calculated as  $V_{red} = \Delta MR/\Delta t$ . The  $V_{red}$  of LT and MT 25 treatments were calculated by  $V_{red} = (MR_{80ms} - MR_{30ms})/(50ms)$ ; The  $V_{red}$  of MT 50 and MT 100 treatments were calculated by  $V_{red} = (MR_{60ms} - MR_{20ms})/(40ms)$ ; and The  $V_{red}$  of MT 200 and MT 400 treatments were calculated by  $V_{red} = (MR_{600ms} - MR_{300ms})/(300ms)$ . In this experiment, the MR of each treatment did not reach the maximum value, so the last value of MR was taken as MR<sub>max</sub>. The values were represented by the means  $\pm$  SE. The same letters denoted that there is no significant difference at  $P < 0.05$  according to Duncan's test.



enhancing the connectivity between PSII antenna pigment and PSII reaction center, protecting the fraction of the OEC activity, increasing the electron transfer rate, and repairing the electron acceptor pool at the receptor side of PSI terminal, thereby promoting PSII electron flow beyond  $Q_A$ .

JIP-test has been demonstrated to reveal the stepwise flow of energy through PSII (Strasser et al., 2004; Guo and Tan, 2015; Tsimilli-Michael, 2020). According to the energy absorption, capture and transfer, it is clear that MT changed the multiple sites of the electron transport chain of low temperature-stressed cucumber plants. Previous research has shown that iron deficiency and saline-alkali stress induced the increase of ABS/RC, which indicates that part of PSII RCs is inactivated (Kalaji et al., 2014). Our study showed the ABS/RC, TRo/RC, and DIO/RC were significantly lower in MT 100-treated plants than in LT treatment. However, the light energy was used mainly for transfer ( $ET_o/RC$ ,  $RE_o/RC$ ) and beyond, and less for capture ( $TR_o/RC$ ) and dissipation ( $DI_o/RC$ ), which explains the high efficiency parameters related to quantum yields ( $\Phi_{P_{680}}$ ,  $\Phi_{E_o}$ ,  $\Phi_{R_o}$ ) (Figure 8). This is consistent with the conclusion presented by Shomali et al. (2021), who suggested that MT protected the photosynthetic apparatus and further improved the photosynthetic performance (Shomali et al., 2021). In other words, MT 100 can enhance the low temperature tolerance of cucumber seedlings by activating part of PSII reaction centers, reducing energy absorption and capture, enhancing energy

transfer in the PSII and improving light energy utilization. Coincidentally, the leaf energy flux models (Figure 7) also confirm these results. Electron transport (ET) is more sensitive to low temperature than excitation energy capture (TR). MT 100 induced the higher values of  $ET_o/TR$  and  $\Psi_{E_o}$  (Figures 6, 8) possibly because energy was activated at ET by MT under low temperature conditions, which might be the main reason for the increase of  $\Phi_{R_o}$ . Furthermore,  $\delta_{R_o}$  was different between LT and MT treatments (Figure 8), which meant that RE was affected by MT under low temperature stress. MT 100 significantly reduced ABS/RC and DIO/RC, while increased  $ET_o/RC$  and  $RE_o/RC$  (Figures 6, 7). This may be because the photosystem electron transfer chain of cucumber leaves is partly recovered by MT 100 under low temperature conditions. These suggested that MT protected the photosynthetic machinery, increased the utilization of captured energy for the photochemical reaction, greatly reduced the excitation pressure on the RC and allowed smoother energy flow.

Our results also revealed that MT had a vital impact on PSI. The  $MR_{820}$  signal can reflect the electron transport and the redox state of PC and P700 in PSI (Gao et al., 2014; Hamdani et al., 2015; Guo et al., 2020). Accumulation of  $PC^+$  and  $P_{700}^+$  results in a fast decrease in  $MR/MR_o$  (fast phase), which can be expressed as  $\Delta MR_{fast}/MR_o$ . The minimal  $MR/MR_o$  is a relatively stable state, where the oxidation rate is equal to the reduction rates of PC and P700. Subsequently, electrons coming from  $P_{680}$  arrive at

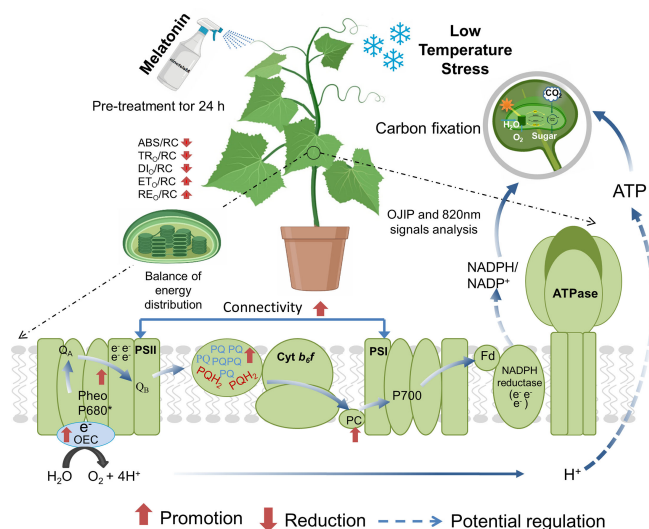


FIGURE 10

A hypothetical model showing melatonin (MT)-induced regulation of photosynthesis and photosystem performance under low temperature stress in cucumber. MT could improve light reactions and electron transport from PSII via  $Q_A$  to  $PC^+$  and  $P_{700}^+$  in the photosystem by strengthening the connectivity between PSI and PSII. MT also improved the OEC activity, resulting in an increase in the photochemical decomposition of water and more  $H^+$  drives ATP synthesis via ATP synthase. In addition, MT increased the PSI activity, deoxidation rates of  $PC^+$  and  $P_{700}^+$  and decreased the oxidation rate of PC and P700 and further increased the electron transport.  $Q_A$ , primary quinone electron acceptor; PSII, photosystem II; PSI, photosystem I; OEC, oxygen evolving complex; PC, plastocyanin; P700, PSI reaction center.

$P_{700}^+$  and  $PC^+$ , where they are oxidized, that is,  $P_{700}^+$  and  $PC^+$  are re-reduced, causing an increased stage in  $MR/MR_O$  (slow phase), which can be represented by  $\Delta MR_{slow}/MR_O$  (Strasser et al., 2010). The minimal of  $MR/MR_O$  was decreased by MT (Figures 9A, B), whereas the  $\Delta MR_{fast}/MR_O$  was gradually increased by MT at low temperature conditions (Figure 9C). In addition, the time reaching to the lowest point of the oxidation phase was obviously advanced by the MT 50 and MT 100 treatments, while delayed by the MT 200 and MT 400 treatments when compared with LT treatment. These indicated the faster oxidation rates of  $P_{700}$  and  $PC$ , and the photochemical activity of PSI was enhanced by MT under low temperature stress. Obviously, the MT had an essential effect on the slow phase of the  $MR_{820}$  signals (Figure 9D). The slow rising phase of MT 100-treated samples significantly increased, while almost disappeared in MT 200- and MT 400-treated plants in the  $MR_{820}$  signal (Figures 9A, B). Our results were highly consistent with Zhang et al. (2021). These results suggested that the MT 100 could improve entirely PSII electron flow via  $Q_A$  to  $PC^+$  and  $P_{700}^+$ . The  $V_{ox}$  and  $V_{red}$  were used to further quantify the redox rate of  $PC$  and  $P_{700}$ . The traditional  $V_{ox}$  and  $V_{red}$  were calculated in two particular time ranges, 0.7–3 ms (fast phase) and 7–300 ms (slow phase), respectively (Gao et al., 2014). However, the  $MR/MR_O$  signal vs. linear time scale of these two particular time ranges is not a straight line. So, the new time ranges from 0.7 to 2 ms ( $V_{ox}$ ) were proposed for the calculation of  $V_{ox}$  in our study (Figure 9E). In addition, for the  $V_{red}$ , the appearance of the lowest point of  $MR/MR_O$  kinetics is different for each treatment under low temperature stress. So analysis at the new particular time was carried out and the calculation formulas were presented in Figure 9. In this study, the  $V_{ox}$  was limited by MT 100, while  $V_{red}$  was improved by MT 100 under low temperature stress. This may be because MT 100 connects or increases the core complexes and electron transporters of PSI, thereby allowing more electrons to flow to PSI to reduce  $P_{700}^+$  and  $PC^+$  under low temperature stress (Zhou et al., 2019). The reduced oxidation rate of  $PC$  and  $P_{700}$  and the increased reduction rate of  $PC^+$  and  $P_{700}^+$  by MT 100 make the electron transfer in the photosynthetic mechanism smoother, and then improve the photosynthesis of cucumber seedlings at low temperature conditions. The reduction activity of PSI can result from the capacity of pumping electrons to the intersystem electron transport chain by PSII (Kan et al., 2017), the connection state between PSII and PSI, and the improvement of the PSI acceptor side (Dąbrowski et al., 2021). Based on these studies and our analysis of the OJIP,  $MR_{820}$  signal, and related JIP-test parameters, we conclude that MT could regulate the multiple sites of the photosynthetic electron transport chain and increase the PSII activity and electron transfer capacity under low temperature stress.

## Conclusions

Low temperature stress damaged the effectiveness of photosynthesis, which was manifested by severely inhibited photosystem performance and impaired plant phenotype. Foliar application of MT before low temperature stress can induce the efficiency of PSII (Fv/Fm and Fv/Fo), the performance of the photosystem II donor/acceptor side (Plabs,  $W_K$  and  $V_j$ ), the activity of PSI ( $W_{OI} \geq 1$ ), redox rate of PSI ( $V_{ox}$  and  $V_{red}$ ), the balance of the energy distribution (ABS/RC,  $TR_O/RC$ ,  $DI_O/RC$ ,  $ET_O/RC$  and  $RE_O/RC$ ), and the quantum yields ( $\Phi_{Po}$ ,  $\Phi_{Eo}$ ,  $\Phi_{Ro}$ ,  $\Psi_{Eo}$  and  $\delta_{Ro}$ ) of cucumber leaves, thus repairing the photosynthetic electron transport chain under low temperature stress. We conclude that an appropriate concentration of MT ( $100 \mu\text{mol} \cdot \text{L}^{-1}$ ) is beneficial for the improvement of the connectivity between PSI and PSII and the performance of electron transfer and energy distribution in cucumber leaves, which result from the MT-induced regulation of multiple sites of the photosynthetic electron transport chain, and potential synthesis of more energy (ATP and NADPH) under low temperature stress (Figure 10). However, high concentrations of MT ( $\geq 200 \mu\text{mol} \cdot \text{L}^{-1}$ ) showed completely negative effects on low temperature tolerance in cucumber plants.

## Data availability statement

The original contributions presented in the study are included in the article/Supplementary Material. Further inquiries can be directed to the corresponding authors.

## Author contributions

This work was carried out in collaboration between all the authors. PW, JXC, and HL conceived designed the experiments. PW, YM, BH, JYC, WW, and YZ performed the experiments, analyzed the data, prepared figures and/or tables. PW and YM wrote the original draft. JXC, GA, HL, HC, and WX reviewed and edited the manuscript. All authors reviewed drafts of the paper, and approved the final manuscript.

## Funding

We are grateful to the National Natural Science Foundation of China, China (No. 31560571) for providing financial support to our research.

## Conflict of interest

The authors declare that the research was conducted in the absence of any commercial or financial relationships that could be construed as a potential conflict of interest.

## Publisher's note

All claims expressed in this article are solely those of the authors and do not necessarily represent those of their affiliated

organizations, or those of the publisher, the editors and the reviewers. Any product that may be evaluated in this article, or claim that may be made by its manufacturer, is not guaranteed or endorsed by the publisher.

## Supplementary material

The Supplementary Material for this article can be found online at: <https://www.frontiersin.org/articles/10.3389/fpls.2022.1029854/full#supplementary-material>

## References

- Ahammed, G. J., Xu, W., Liu, A., and Chen, S. (2018). *COMT1* silencing aggravates heat stress-induced reduction in photosynthesis by decreasing chlorophyll content, photosystem II activity, and electron transport efficiency in tomato. *Front. Plant Sci.* 9. doi: 10.3389/fpls.2018.00998
- Arnao, M. B., and Hernández-Ruiz, J. (2014). Melatonin: plant growth regulator and/or biostimulator during stress? *Trends Plant Sci.* 19, 789–797. doi: 10.1016/j.tplants.2014.07.006
- Arnao, M. B., and Hernandez-Ruiz, J. (2015). Functions of melatonin in plants: a review. *J. Pineal Res.* 59, 133–150. doi: 10.1111/jpi.12253
- Chen, S., Yang, J., Zhang, M., Strasser, R. J., and Qiang, S. (2016). Classification and characteristics of heat tolerance in *Ageratina adenophora* populations using fast chlorophyll *a* fluorescence rise O-J-I-P. *Environ. Exp. Bot.* 122, 126–140. doi: 10.1016/j.envexpbot.2015.09.011
- Chen, X., Zhou, Y., Cong, Y., Zhu, P., Xing, J., Cui, J., et al. (2021). Ascorbic acid-induced photosynthetic adaptability of processing tomatoes to salt stress probed by fast OJIP fluorescence rise. *Front. Plant Sci.* 12. doi: 10.3389/fpls.2021.594400
- Chinnusamy, V., Zhu, J. K., and Sunkar, R. (2010). Gene regulation during cold stress acclimation in plants. *Methods Mol. Biol.* 639, 39–55. doi: 10.1007/978-1-60761-702-0\_3
- Corpas, F. J. (2019). Hydrogen sulfide: a new warrior against abiotic stress. *Trends Plant Sci.* 24, 983–988. doi: 10.1016/j.tplants.2019.08.003
- Cui, J., Zhou, Y., Ding, J., Xia, X., Shi, K., Chen, S., et al. (2011). Role of nitric oxide in hydrogen peroxide-dependent induction of abiotic stress tolerance by brassinosteroids in cucumber. *Plant Cell Environ.* 34, 347–358. doi: 10.1111/j.1365-3040.2010.02248.x
- Dąbrowski, P., Baczewska-Dąbrowska, A. H., Bussotti, F., Pollastrini, M., Piekut, K., Kowalik, W., et al. (2021). Photosynthetic efficiency of microcystis ssp. under salt stress. *Environ. Exp. Bot.* 186, 104459. doi: 10.1016/j.envexpbot.2021.104459
- Debnath, B., Islam, W., Li, M., Sun, Y., Lu, X., Mitra, S., et al. (2019). Melatonin mediates enhancement of stress tolerance in plants. *Int. J. Mol. Sci.* 20, 1040. doi: 10.3390/ijms20051040
- Dimitrova, S., Paunov, M., Pavlova, B., Dankov, K., Kouzmanova, M., Velikova, V., et al. (2020). Photosynthetic efficiency of two *Platanus orientalis* l. ecotypes exposed to moderately high temperature –JIP–test analysis. *Photosynthetica* 58, 657–670. doi: 10.32615/ps.2020.012
- Ding, Y., Shi, Y., and Yang, S. (2019). Advances and challenges in uncovering cold tolerance regulatory mechanisms in plants. *New Phytol.* 222, 1690–1704. doi: 10.1111/nph.15696
- Ensminger, I., Busch, F., and Huner, N. P. A. (2006). Photostasis and cold acclimation: sensing low temperature through photosynthesis. *Physiol. Plant* 126, 28–44. doi: 10.1111/j.1399-3054.2006.00627.x
- Fan, J., Hu, Z., Xie, Y., Chan, Z., Chen, K., Amombo, E., et al. (2015). Alleviation of cold damage to photosystem II and metabolisms by melatonin in bermudagrass. *Front. Plant Sci.* 6. doi: 10.3389/fpls.2015.00925
- Feng, Y., Fu, X., Han, L., Xu, C., Liu, C., Bi, H., et al. (2021). Nitric oxide functions as a downstream signal for melatonin-induced cold tolerance in cucumber seedlings. *Front. Plant Sci.* 12. doi: 10.3389/fpls.2021.686545
- Gao, J., Li, P., Ma, F., and Goltsev, V. (2014). Photosynthetic performance during leaf expansion in *Malus micromalus* probed by chlorophyll *a* fluorescence and modulated 820nm reflection. *J. Photochem. Photobiol. B-Biol.* 137, 144–150. doi: 10.1016/j.jphotobiol.2013.12.005
- Guo, Y., Lu, Y., Goltsev, V., Strasser, R. J., Kalaji, H. M., Wang, H., et al. (2020). Comparative effect of tenuazonic acid, diuron, bentazone, dibromothymoquinone and methyl viologen on the kinetics of chl *a* fluorescence rise OJIP and the MR820 signal. *Plant Physiol. Biochem.* 156, 39–48. doi: 10.1016/j.plaphy.2020.08.044
- Guo, Y., and Tan, J. (2015). Recent advances in the application of chlorophyll *a* fluorescence from photosystem II. *Photochem. Photobiol.* 91, 1–14. doi: 10.1111/php.12362
- Hamdani, S., Qu, M., Xin, C. P., Li, M., Chu, C., Govindjee, et al. (2015). Variations between the photosynthetic properties of elite and landrace Chinese rice cultivars revealed by simultaneous measurements of 820 nm transmission signal and chlorophyll *a* fluorescence induction. *J. Plant Physiol.* 177, 128–138. doi: 10.1016/j.jplph.2014.12.019
- Heber, U., Egneus, H., Hanck, U., Jensen, M., and K6ster, S. (1978). Regulation of photosynthetic electron transport and photophosphorylation in intact chloroplasts and leaves of *Spinacia oleracea* l. *Planta* 143, 41–19. doi: 10.1007/BF00389050
- Heber, U., and Walker, D. (1992). Concerning a dual function of coupled cyclic electron transport in leaves. *Plant Physiol.* 100, 1621–1626. doi: 10.1104/pp.100.4.1621
- Hu, W., Snider, J. L., Chastain, D. R., Slaton, W., and Tishchenko, V. (2018). Sub-Optimal emergence temperature alters thermotolerance of thylakoid component processes in cotton seedlings. *Environ. Exp. Bot.* 155, 360–367. doi: 10.1016/j.envexpbot.2018.07.020
- Jahan, M. S., Guo, S., Sun, J., Shu, S., Wang, Y., El-Yazied, A. A., et al. (2021). Melatonin-mediated photosynthetic performance of tomato seedlings under high-temperature stress. *Plant Physiol. Biochem.* 167, 309–320. doi: 10.1016/j.plaphy.2021.08.002
- Kalaji, H. M., Bába, W., Gediga, K., Goltsev, V., Samborska, I. A., Cetner, M. D., et al. (2018). Chlorophyll fluorescence as a tool for nutrient status identification in rapeseed plants. *Photosynth. Res.* 136, 329–343. doi: 10.1007/s11120-017-0467-7
- Kalaji, H. M., Oukarroum, A., Alexandrov, V., Kouzmanova, M., Brestic, M., Zivcak, M., et al. (2014). Identification of nutrient deficiency in maize and tomato plants by in vivo chlorophyll *a* fluorescence measurements. *Plant Physiol. Biochem.* 81, 16–25. doi: 10.1016/j.plaphy.2014.03.029
- Kan, X., Ren, J., Chen, T., Cui, M., Li, C., Zhou, R., et al. (2017). Effects of salinity on photosynthesis in maize probed by prompt fluorescence, delayed fluorescence and P700 signals. *Environ. Exp. Bot.* 140, 56–64. doi: 10.1016/j.envexpbot.2017.05.019
- Khan, T. A., Fariduddin, Q., Nazir, F., and Saleem, M. (2020). Melatonin in business with abiotic stresses in plants. *Physiol. Mol. Biol. Plants* 26, 1931–1944. doi: 10.1007/s12298-020-00878-z
- Krieger-Liszkay, A., and Shimakawa, G. (2022). Regulation of the generation of reactive oxygen species during photosynthetic electron transport. *Biochem. Soc Trans.* 50, 1025–1034. doi: 10.1042/BST20211246
- Lee, H. J., Lee, J. H., Wi, S., Jang, Y., An, S., Choi, C. K., et al. (2021). Exogenously applied glutamic acid confers improved yield through increased photosynthesis efficiency and antioxidant defense system under chilling stress condition in *Solanum lycopersicum* l. cv. dotaerang dia. *Sci. Hortic.* 277, 109817. doi: 10.1016/j.scienta.2020.109817
- Li, H., Guo, Y., Lan, Z., Xu, K., Chang, J., Ahammed, G. J., et al. (2021). Methyl jasmonate mediates melatonin-induced cold tolerance of grafted watermelon plants. *Hortic. Res.* 8, 57. doi: 10.1038/s41438-021-00496-0

- Liu, X., Zhou, Y., Xiao, J., and Bao, F. (2018). Effects of chilling on the structure, function and development of chloroplasts. *Front. Plant Sci.* 9. doi: 10.3389/fpls.2018.01715
- Murchie, E. H., and Lawson, T. (2013). Chlorophyll fluorescence analysis: a guide to good practice and understanding some new applications. *J. Exp. Bot.* 64, 3983–3998. doi: 10.1093/jxb/ert208
- Oukarroum, A., Strasser, R. J., and Staden, J. V. (2004). Phenotyping of dark and light adapted barley plants by the fast chlorophyll *a* fluorescence rise OJIP. *S. Afr. J. Bot.* 70, 277–283. doi: 10.1016/S0254-6299(15)30246-5
- Ploschuk, E. L., Bado, L. A., Salinas, M., Wassner, D. F., Windauer, L. B., and Insausti, P. (2014). Photosynthesis and fluorescence responses of *Jatropha curcas* to chilling and freezing stress during early vegetative stages. *Environ. Exp. Bot.* 102, 18–26. doi: 10.1016/j.envexpbot.2014.02.005
- Reiter, R., Tan, D. X., Zhou, Z., Cruz, M., Fuentes-Broto, L., and Galano, A. (2015). Phytomelatonin: assisting plants to survive and thrive. *Molecules* 20, 7396–7437. doi: 10.3390/molecules20047396
- Ruelland, E., Vaultier, M. N., Zachowski, A., and Hurry, V. (2009). Cold signalling and cold acclimation in plants. *Adv. Bot. Res.* 49, 35–150. doi: 10.1016/S0065-2296(08)00602-2
- Rutherford, A. W., and Krieger-Liszka, A. (2001). Herbicide-induced oxidative stress in photosystem II. *Trends Biochem. Sci.* 26, 648–653. doi: 10.1016/S0968-0004(01)01953-3
- Schansker, G., Srivastava, A., Govindjee, and Strasser, R. J. (2003). Characterization of the 820-nm transmission signal paralleling the chlorophyll *a* fluorescence rise (OJIP) in pea leaves. *Funct. Plant Biol.* 30, 785–796. doi: 10.1071/fp03032
- Shikanai, T. (2011). Regulation of photosynthetic electron transport. *Biochim. Biophys. Acta* 1807, 375–383. doi: 10.1016/j.bbabi.2010.11.010
- Shomali, A., Aliniaieifard, S., Didaran, F., Lotfi, M., Mohammadian, M., Seif, M., et al. (2021). Synergistic effects of melatonin and gamma-aminobutyric acid on protection of photosynthesis system in response to multiple abiotic stressors. *Cells* 10, 1631. doi: 10.3390/cells10071631
- Silva Dalberto, D., Garbin Martinazzo, E., and Antonio Bacarin, M. (2017). Chlorophyll *a* fluorescence reveals adaptation strategies in drought stress in *Ricinus communis*. *Braz. J. Bot.* 40, 861–870. doi: 10.1007/s40415-017-0412-1
- Snider, J. L., Thangthong, N., Pilon, C., Virk, G., and Tishchenko, V. (2018). OJIP-fluorescence parameters as rapid indicators of cotton (*Gossypium hirsutum* L.) seedling vigor under contrasting growth temperature regimes. *Plant Physiol. Biochem.* 132, 249–257. doi: 10.1016/j.plaphy.2018.09.015
- Stirbet, A., and Govindjee, (2011). On the relation between the kautsky effect (chlorophyll *a* fluorescence induction) and photosystem II: Basics and applications of the OJIP fluorescence transient. *J. Photochem. Photobiol. B-Biol.* 104, 236–257. doi: 10.1016/j.jphotobiol.2010.12.010
- Stirbet, A., and Govindjee, (2012). Chlorophyll *a* fluorescence induction: a personal perspective of the thermal phase, the J-I-P rise. *Photosynth. Res.* 113, 15–61. doi: 10.1007/s11120-012-9754-5
- Strasser, R. J., Srivastava, A., and Govindjee, (1995). Polyphasic chlorophyll *a* fluorescence transient in plants and cyanobacteria. *Photochem. Photobiol.* 61, 32–42. doi: 10.1111/j.1751-1097.1995.tb09240.x
- Strasser, R. J., Tsimilli-Michael, M., Qiang, S., and Goltsev, V. (2010). Simultaneous *in vivo* recording of prompt and delayed fluorescence and 820-nm reflection changes during drying and after rehydration of the resurrection plant *Haberlea rhodopensis*. *Biochim. Biophys. Acta* 1797, 1313–1326. doi: 10.1016/j.bbabi.2010.03.008
- Strasser, R. J., Tsimilli-Michael, M., and Srivastava, A. (2004). *Analysis of the chlorophyll *a* fluorescence transient* (Dordrecht: Springer), 321–362. doi: 10.1007/978-1-4020-3218-9\_12
- Sun, C., Liu, L., Wang, L., Li, B., Jin, C., and Lin, X. (2020). Melatonin: A master regulator of plant development and stress responses. *J. Integr. Plant Biol.* 63, 126–145. doi: 10.1111/jipb.12993
- Theocharis, A., Clément, C., and Barka, E. A. (2012). Physiological and molecular changes in plants grown at low temperatures. *Planta* 235, 1091–1105. doi: 10.1007/s00425-012-1641-y
- Tiwari, R. K., Lal, M. K., Naga, K. C., Kumar, R., Chourasia, K. N., Shivaramu, et al. (2020). Emerging roles of melatonin in mitigating abiotic and biotic stresses of horticultural crops. *Sci. Hortic.* 272, 109592. doi: 10.1016/j.scienta.2020.109592
- Tsimilli-Michael, M. (2020). Revisiting JIP-test: An educative review on concepts, assumptions, approximations, definitions and terminology. *Photosynthetica* 58, 275–292. doi: 10.32615/ps.2019.150
- Wang, K., Xing, Q., Ahammed, G. J., and Zhou, J. (2022). Functions and prospects of melatonin in plant growth, yield and quality. *J. Exp. Bot.* 2022, erac233. doi: 10.1093/jxb/erac233
- Wang, F., Yan, J., Ahammed, G. J., Wang, X., Bu, X., Xiang, H., et al. (2020). PGR5/PGRL1 and NDH mediate far-red light-induced photoprotection in response to chilling stress in tomato. *Front. Plant Sci.* 11. doi: 10.3389/fpls.2020.00669
- Wu, P., Xiao, C., Cui, J., Hao, B., Zhang, W., Yang, Z., et al. (2020). Nitric oxide and its interaction with hydrogen peroxide enhance plant tolerance to low temperatures by improving the efficiency of the calvin cycle and the ascorbate-glutathione cycle in cucumber seedlings. *J. Plant Growth Regul.* 40, 2390–2408. doi: 10.1007/s00344-020-10242-w
- Xia, Q., Tan, J., Cheng, S., Jiang, Y., and Guo, Y. (2019). Sensing plant physiology and environmental stress by automatically tracking *F<sub>j</sub>* and *F<sub>i</sub>* features in PSII chlorophyll fluorescence induction. *Photochem. Photobiol.* 95, 1495–1503. doi: 10.1111/php.13141
- Xiong, D., Liu, X., Liu, L., Douthe, C., Li, Y., Peng, S., et al. (2015). Rapid responses of mesophyll conductance to changes of CO<sub>2</sub> concentration, temperature and irradiance are affected by n supplements in rice. *Plant Cell Environ.* 38, 2541–2550. doi: 10.1111/pce.12558
- Zeng, J. J., Hu, W. H., Hu, X. H., Tao, H. M., Zhong, L., and Liu, L. L. (2022). Upregulation of the mitochondrial alternative oxidase pathway improves PSII function and photosynthetic electron transport in tomato seedlings under chilling stress. *Photosynthetica* 60, 271–279. doi: 10.32615/ps.2022.019
- Zhang, X., Feng, Y., Jing, T., Liu, X., Ai, X., and Bi, H. (2021). Melatonin promotes the chilling tolerance of cucumber seedlings by regulating antioxidant system and relieving photoinhibition. *Front. Plant Sci.* 12. doi: 10.3389/fpls.2021.789617
- Zhang, Z., Wu, P., Zhang, W., Yang, Z., Liu, H., Ahammed, G. J., et al. (2020). Calcium is involved in exogenous NO-induced enhancement of photosynthesis in cucumber (*Cucumis sativus* L.) seedlings under low temperature. *Sci. Hortic.* 261, 108953. doi: 10.1016/j.scienta.2019.108953
- Zhao, C., Yang, M., Wu, X., Wang, Y., and Zhang, R. (2021). Physiological and transcriptomic analyses of the effects of exogenous melatonin on drought tolerance in maize (*Zea mays* L.). *Plant Physiol. Biochem.* 168, 128–142. doi: 10.1016/j.plaphy.2021.09.044
- Zhou, Y., Diao, M., Cui, J. X., Chen, X. J., Wen, Z. L., Zhang, J. W., et al. (2018). Exogenous GSH protects tomatoes against salt stress by modulating photosystem II efficiency, absorbed light allocation and H<sub>2</sub>O<sub>2</sub>-scavenging system in chloroplasts. *J. Integr. Agric.* 17, 2257–2272. doi: 10.1016/S2095-3119(18)62068-4
- Zhou, R., Kan, X., Chen, J., Hua, H., Li, Y., Ren, J., et al. (2019). Drought-induced changes in photosynthetic electron transport in maize probed by prompt fluorescence, delayed fluorescence, P700 and cyclic electron flow signals. *Environ. Exp. Bot.* 158, 51–62. doi: 10.1016/j.envexpbot.2018.11.005
- Zhu, X. G., Govindjee, Baker, N. R., deSturler, E., Ort, D. R., and Long, S. P. (2005). Chlorophyll *a* fluorescence induction kinetics in leaves predicted from a model describing each discrete step of excitation energy and electron transfer associated with photosystem II. *Planta* 223, 114–133. doi: 10.1007/s00425-005-0064-4
- Zushi, K., and Matsuzoe, N. (2017). Using of chlorophyll *a* fluorescence OJIP transients for sensing salt stress in the leaves and fruits of tomato. *Sci. Hortic.* 219, 216–221. doi: 10.1016/j.scienta.2017.03.016





## OPEN ACCESS

## EDITED BY

Hazem M. Kalaji,  
Warsaw University of Life Sciences –  
SGGW, Poland

## REVIEWED BY

Habib-ur-Rehman Athar,  
Bahauddin Zakariya University,  
Pakistan  
Mohamed Ait El Mokhtar,  
Université Hassan II Mohammedia,  
Morocco  
Ounoki Roumaissa,  
Eötvös Loránd University, Hungary

## \*CORRESPONDENCE

Aicha Loudari  
Aicha.loudari@um6p.ma

## SPECIALTY SECTION

This article was submitted to  
Plant Abiotic Stress,  
a section of the journal  
Frontiers in Plant Science

RECEIVED 07 September 2022

ACCEPTED 25 October 2022

PUBLISHED 10 November 2022

## CITATION

Loudari A, Mayane A, Zeroual Y,  
Colinet G and Oukarroum A (2022)  
Photosynthetic performance and  
nutrient uptake under salt stress:  
Differential responses of wheat  
plants to contrasting phosphorus  
forms and rates.  
*Front. Plant Sci.* 13:1038672.  
doi: 10.3389/fpls.2022.1038672

## COPYRIGHT

© 2022 Loudari, Mayane, Zeroual,  
Colinet and Oukarroum. This is an  
open-access article distributed under  
the terms of the [Creative Commons  
Attribution License \(CC BY\)](#). The use,  
distribution or reproduction in other  
forums is permitted, provided the  
original author(s) and the copyright  
owner(s) are credited and that the  
original publication in this journal is  
cited, in accordance with accepted  
academic practice. No use,  
distribution or reproduction is  
permitted which does not comply with  
these terms.

# Photosynthetic performance and nutrient uptake under salt stress: Differential responses of wheat plants to contrasting phosphorus forms and rates

Aicha Loudari<sup>1,2\*</sup>, Asmae Mayane<sup>1</sup>, Youssef Zeroual<sup>1</sup>,  
Gilles Colinet<sup>2</sup> and Abdallah Oukarroum<sup>1,3</sup>

<sup>1</sup>Plant Stress Physiology Laboratory–AgroBioSciences, Mohammed VI Polytechnic University (UM6P), Benguerir, Morocco, <sup>2</sup>Terra Research Center, Gembloux Agro Bio Tech Faculty, Liege University (ULIEGE), Gembloux, Belgium, <sup>3</sup>High Throughput Multidisciplinary Research Laboratory, Mohammed VI Polytechnic University (UM6P), Benguerir, Morocco

Salt stress impacts phosphorus (P) bioavailability, mobility, and its uptake by plants. Since P is involved in many key processes in plants, salinity and P deficiency could significantly cause serious damage to photosynthesis, the most essential physiological process for the growth and development of all green plants. Different approaches have been proposed and adopted to minimize the harmful effects of their combined effect. Optimising phosphorus nutrition seems to bring positive results to improve photosynthetic efficiency and nutrient uptake. The present work posed the question if soluble fertilizers allow wheat plants to counter the adverse effect of salt stress. A pot experiment was performed using a Moroccan cultivar of durum wheat: Karim. This study focused on different growth and physiological responses of wheat plants grown under the combined effect of salinity and P-availability. Two Orthophosphates (Ortho-A & Ortho-B) and one polyphosphate (Poly-B) were applied at different P levels (0, 30 and 45 ppm). Plant growth was analysed on some physiological parameters (stomatal conductance (SC), chlorophyll content index (CCI), chlorophyll a fluorescence, shoot and root biomass, and mineral uptake). Fertilized wheat plants showed a significant increase in photosynthetic performance and nutrient uptake. Compared to salt-stressed and unfertilized plants (C+), CCI increased by 93%, 81% and 71% at 30 ppm of P in plants fertilized by Poly-B, Ortho-B and Ortho-A, respectively. The highest significant SC was obtained at 45 ppm using Ortho-B fertilizer with an increase of 232% followed by 217% and 157% for both Poly-B and Ortho-A, respectively. The Photosynthetic performance index (PI<sub>tot</sub>) was also increased by 128.5%, 90.2% and 38.8% for Ortho-B, Ortho-A and Poly B, respectively. In addition, Poly-B showed a significant enhancement in roots and shoots biomass (49.4% and 156.8%, respectively) compared to C+. Fertilized and salt-stressed plants absorbed more phosphorus. The P content significantly increased mainly at 45 ppm of P. Positive correlations were found between phosphorus uptake, biomass, and

photosynthetic yield. The increased photochemical activity could be due to a significant enhancement in light energy absorbed by the enhanced Chl antenna. The positive effect of adequate P fertilization under salt stress was therefore evident in durum wheat plants.

#### KEYWORDS

durum wheat, polyphosphate, phosphorus, photosynthetic performance, salinity, nutrient uptake

## 1 Introduction

It is well known that soil salinity causes an imbalance in mineral uptake and plant nutrition (Shabala and Munns, 2017; Behdad et al., 2021) and the initial action of salinity is revealed by a decrease in water absorption capacity in the rooting zone (Zhao et al., 2020). This nutritional disorder induces changes in the plant at morphological, physiological, and metabolic levels (Kumari et al., 2022). The response of plants to an excess of sodium ions ( $\text{Na}^+$ ), the most important salinity-causing substance, is complex and involves a cascade of mechanisms to reduce the adverse effects of  $\text{Na}^+$  (Chavarria et al., 2020). Furthermore, tolerance to high salinity may be expected to vary with plant species and different growth stages of plants (Xue et al., 2009). There is evidence that high salt stress provokes a multitude of negative plant responses such as induction of osmotic stress generating reactive oxygen species (ROS) (Kumar et al., 2017; Hasanuzzaman et al., 2021), reduction in photosynthesis (Chaves et al., 2011; Oukarroum et al., 2015; Rahimi et al., 2021), degradation of photosynthetic pigments (Muhammad et al., 2021), and reduction in stomatal conductance (Lotfi et al., 2020). However, salinity adaptive in plants is activated by a series of defence mechanisms at all plant levels as well as at anatomical levels (Chavarria et al., 2020). In the current context of intensive agriculture and the increasing effects of salinity which appear in several regions in the world

(Pulido-Bosch et al., 2018), Different approaches have been proposed and adopted to minimize the adverse effects of salt stress on plant development and productivity. Among the strategies reported is the use of arbuscular mycorrhizal fungi (AMF) (Elhindi et al., 2017; Li et al., 2020), inoculation with plant-growth-promoting rhizobacteria (PGPR) (Ilangumaran and Smith, 2017; Tirry et al., 2021), nutritional supplementation of silicon (Altuntas et al., 2018; Muhammad et al., 2022), the addition of organic soil amendment (Yang et al., 2020; Kumari et al., 2022; Xiao et al., 2022) and exogenous application of hormones (Kaya et al., 2013). Regarding phosphorus (P) being the most important nutrient after nitrogen (N) for plant growth and development, salt stress has been reported to impact its bioavailability and mobility in the plant-soil continuum, and therefore root uptake (Demiral, 2017; Khan et al., 2018; Bouras et al., 2021; Bouras et al., 2022). The P deficiency impacts all vital processes: respiration, photosynthesis and plant growth and development (Carstensen et al., 2018). Leaves become smaller, thinner, and change colour into blue-green due to carbohydrate accumulation and the delay in protein synthesis (Meng et al., 2021). Similarly, the  $\text{O}_2$  absorption speed is decreased, and the enzyme activity involved in respiration is altered (Meng et al., 2021). P deficiency and salinity significantly alter the photosynthesis machinery and the mesophyll metabolism in different ways (Chaves et al., 2011; Kalaji et al., 2018) but their effects on photosynthetic metabolic processes and the ultrastructure of organelles are additional and important (Meng et al., 2021). The salinity effect is directly attributed to the limitation in gas diffusion due to the stomatal closure (Zribi et al., 2011; Asrar et al., 2017) and to the high accumulation of  $\text{Na}^+$  and  $\text{Cl}^-$  in the chloroplasts which damages the membrane of thylakoids (Ashraf and Harris, 2013), while P deficiency disturbs ultimately the  $\text{CO}_2$  assimilation since P is implicated in the transport of fixed carbon from chloroplasts to the cytosol with its triose-phosphate form (Rychter et al., 2018). Hence, any alteration of the photosynthesis mechanism caused either by P deficiency or by salinity may reduce the overall photosynthetic capacity of the plant (Kalaji et al., 2016; 2018). This reduction causes a decline in crop yield which affects food security around the world (Muhammad et al., 2021).

**Abbreviations:** CCI, Chlorophyll content index; CEC, Cation exchange capacity; Chl, Chlorophyll; Corg, Organic carbon; DTPA, Diethylene triamine penta acetic acid; DW, Dry weight; e-, electron; EC, Electrical conductivity; FW, Fresh weight; IAA, Indole-3-acetic acid; NT, Total Nitrogen; OEC, Oxygen-evolving complex; OM, Organic matter; PGPR, Plant-growth-promoting rhizobacteria; PIABS, Photosynthetic performance index; PI<sub>tot</sub>, Photosynthetic performance; PSB, Phosphate solubilizing bacteria; PSI, Photosystem I; PSII, Photosystem II; Pt, Total Phosphorus; RC, Reaction centres; RDW, Root dry weight; ROS, Reactive oxygen species; RuBP, Ribulose-1,5-bisphosphate; SC, Stomatal conductance; SDW, Shoot dry weight; SPS, Sucrose phosphate synthase; TWC, Tissue water content; WAS, Week after sowing; WUE, water use efficiency;  $\phi\text{Po}$ , Quantum yield of electron transport.

A better understanding of the photosynthetic processes could therefore help to assess the potential of key photosynthetic components under the combined effect of salinity and P deficiency to balance the photosynthetic light reactions with downstream metabolism and a higher crop yield. Optimising phosphorus nutrition seems to bring positive results (Khan et al., 2018; Mohamed et al., 2021; Bouras et al., 2021; 2022). However, the P use efficiency in salt-stressed plants differs depending on the severity of stress in the rhizosphere (Zhao et al., 2020). Several investigations have been conducted to understand the effects of salt stress and phosphorus interaction in different plant species, degree of salinity severity, and growing conditions (Abbas et al., 2018). Most results agreed that salinity reduces P accumulation in plant tissues (Khan et al., 2018; Belouchrani et al., 2020).

However, phosphorus uptake by plants, in the form of phosphate ions, depends on soil physicochemical parameters (Pereira et al., 2020), the application method and its frequency (Rady et al., 2018; Chtouki et al., 2022), the root exudation and architecture (Khouchi et al., 2022a), and the rhizosphere microbial activity (Wahid et al., 2020). In this regard, different studies have proven the effectiveness of phosphate solubilizing bacteria (PSB) in improving crop yield due to improved P levels in the soil (Khouchi et al., 2022b). Kohler et al. (2009) found that *Pseudomonas mendocina* enhanced the salt tolerance of lettuce plants resulting in a reduction of catalase activity with an increase in shoot dry weight and proline concentration in leaves. Furthermore, in a recent study, Belouchrani et al. (2020) showed that phosphorus supplies improved sorghum tolerance to soil salinity which is observed by an increase in morphological parameters, nitrogen and phosphorus uptake, and proline accumulation. In a growing hydroponic condition, it has been observed in salt-stressed tomato plant that increasing the phosphorus amounts in the solution improve root length and root surface area (Loudari et al., 2020). Also, in barley plants, increasing plant phosphorus in nutrient solution enhances salt tolerance by reducing sodium and increasing potassium (K) concentrations in the shoot (Chen et al., 2007). In pepper and cucumber plants grown under salinity, the supply of  $\text{KH}_2\text{PO}_4$  mitigated the harmful effects of salinity on fruit yield and plant biomass and restored the K and P in leaves and roots (Kaya et al., 2013). Shibli et al. (2001) concluded that P plays a pivotal role in understanding the physiological response to salt stress in different plant species. At the microculture level of African violet (*Saintpaulia ionantha*), P supply restored nutrient uptake (Shibli et al., 2001). This positive effect was also tested by the foliar application of P in wheat plants (Khan et al., 2013) and common bean plants (Rady et al., 2018) grown under salinity, revealed by the increase in the total performances of plants. Hence, while the interaction between P and salt stress positively affects plant growth and yield, there is an urgent need to concentrate also on the reasonable application of more efficient P sources in order to cope with the limited P

availability and improve plant productivity mainly in salt-affected soil. Polyphosphates (PolyP) have been applied in agriculture and are renowned for releasing available P to plants in agricultural soil slowly and continuously (Kulakovskaya et al., 2012). These characteristics make PolyP a sustainable source of P to satisfy plant requirements and prevent phosphorus losses in soils over time (Khouchi et al., 2022a). Furthermore, it has also been found that PolyP fertilizers differ from orthophosphates (OrthoP) by their capacity to chelate certain micronutrients such as manganese, iron, and zinc (Wang et al., 2019; Gao et al., 2020). Compared to OrthoP, the plant responses to PolyP application under saline conditions are not commonly studied. In our study, we posed the question if soluble P-fertilizers allow wheat plants to counter the adverse effect of salt stress. Hence, we hypothesize that using contrasting forms of P-fertilizers at various P doses could have a positive effect on durum wheat growth under moderate salt stress. Three soluble fertilizers were used: Two Orthophosphates and one polyphosphate were applied at different P levels. Afterwards, wheat plant growth, physiological parameters (chlorophyll content index, stomatal conductance, chlorophyll a fluorescence), and mineral uptake were assessed.

## 2 Material and methods

### 2.1 Plant material, fertilisation, and experimental design

The experiment was installed in open field conditions at the Experimental Farm of Mohammed VI Polytechnic University (UM6P), Benguerir, Morocco. During the growth season, the temperatures in Benguerir ranged from 0°C (minimum) and 45°C (maximum), with an average of 19°C. The mean light intensity per day was around PAR 280  $\mu\text{mol m}^{-2} \text{s}^{-1}$ . The cumulative rainfall during December, October, May, March, and January was 99 mm. A representative soil sample from a 20 cm layer of agricultural land (Rass El Ain- Morocco) was collected and analysed before the experiment to refine the treatments (pH, Electrical Conductivity (EC), texture, assimilable Phosphorus (P), Total Nitrogen (NT), Organic matter (OM),  $\text{Na}_2\text{O}$ , Potassium (K),  $\text{CaCO}_3$ , micronutrients.). For every analysis, we have undertaken three repetitions. EC was determined with Conductivity-meter in  $\text{dS m}^{-1}$ . The pH of the soil was determined in deionized water. Phosphorus in percentage was revealed by OLSEN Method, Organic matter (OM) in,  $\text{OM} \% = \text{Organic Carbon (Corg)} \% \times 1.72$ . Cation exchange capacity (CEC) was determined by the percolation method with ammonium acetate 1 N. The results of soil analysis are reported in Table 1. The soil has the same properties as most soils of the R'hamna region- Morocco but was mainly moderately deficient in assimilable P ( $\text{P}_2\text{O}_5 = 30.33 \text{ ppm}$ ). The soil was air-dried and sieved (8 mm). Each pot was preliminarily

TABLE 1 Physicochemical properties of the experimental soil.

**Soil parameters**

Soil Texture	Clay (%)	15
	Slit (%)	26
	Sand (%)	58
EC ext1/5 (dS/m)		1,587
pH <sub>water</sub>		7,893
P <sub>2</sub> O <sub>5</sub> (ppm)		30,33
K <sub>2</sub> O (ppm)		228,3
N-NO <sub>3</sub> (mg/Kg)		54,017
N-NH <sub>4</sub> (mg/Kg)		7,893
MO (%)		3,11
C <sub>org</sub> (%)		1,806
CaCo <sub>3</sub> total (%)		2,490
C.E.C (meq/100g)		12
Na <sub>2</sub> O (ppm)		1546,66
MgO (ppm)		624
CaO (ppm)		6472
Cu (ppm)		0,71
Mn (ppm)		11,04
Fe (ppm)		6,26
Zn (ppm)		0,62

filled with a thin layer of gravel (1 cm). The deficit nutrients were added according to the method suggested by COMIFER (French Committee for the Study and Development of Reasoned Fertilization). Basal amendment consists of three different doses of phosphorus (0, 30 and 45) for each NPK soluble fertilizer (Ortho-A, Poly-B and Ortho-B). The OrthoP fertilizers used in the experiment are phosphoric acid-based fertilizers with potassium (Ortho-A) or Nitrogen (Ortho-B) containing 52% and 62% of P<sub>2</sub>O<sub>5</sub>, respectively, with 100% OrthoP for each one. Poly-B fertilizer is a linear PolyP with a short chain which contains 47% P<sub>2</sub>O<sub>5</sub> with 100% PolyP in form of tripolyphosphates. According to wheat requirements and to the amount of nitrogen and potassium in the selected soil and fertilizers, NH<sub>4</sub>NO<sub>3</sub> (33.5% N) and potassium sulphate (51% K<sub>2</sub>O) were applied to equalize N and K amounts for all treatments. The quantities were adjusted also for controls. A control combination consists of negative control (C-): unfertilized plants without salt application, and positive control (C+): salt-stressed and unfertilized plants.

A Moroccan variety of durum wheat (*Triticum durum*) was used. Karim cultivar is one of the most cultivated varieties in Morocco, known for its adaptation zone (bour and irrigated lands), its precocity, medium straw production, and tolerance to rust and *Septoria*. Ten dry, healthy, and uniform size seeds were sown into polythene pots (24 cm in diameter and 35 cm in length) containing 10 kg of dried soil per pot, and only six seedlings (same size and appearance) were kept after plant emergence. The experiment was conducted in a completely

randomized design with ten replicates per treatment. During the experiment, the plants were watered with tap water when soil moisture content had fallen to 60% of its initial value. Initial electrical conductivity of soil was EC= 1,587 dS/m (Table 1).

The salinity treatment was applied by adding saline water (with definite EC) after seedlings establishment, which is usually two weeks after sowing (WAS). The salinity level was gradually increased in order to achieve moderate saline conditions (EC= 3.003 dS/m). Moisture and EC were measured before and after each irrigation using the HH2 WET sensor (Delta-T devices). During the wheat growth, the measurements were taken every two (WAS), starting from 6 WAS. The samples of plants and rhizosphere soils were taken at 12 WAS, which corresponds to Z68 – Z71 of Zadok's scale (the heading stage).

## 2.2 Chlorophyll content index

Chlorophyll Content Index (CCI) was estimated by using a non-destructive portable chlorophyll meter (CL-O1, Hansatech instruments). This parameter was measured from the middle part of the fully mature and expanded functional leaves after 1 min kept in dark. CCI was measured in all treated plants at 6, 8, 10 and 12 weeks after sowing. At each treatment, the CCI was measured at least on 12 independent leaves.

## 2.3 Stomatal conductance

Stomatal conductance (SC) was measured by a leaf porometer (SC-1 Leaf porometer Decagon Devices, Inc.) in the morning and was measured from the middle part of the fully mature and expanded functional leaves in all treated plants at 6, 8, 10 and 12 weeks after sowing. At least 5 independent measurements were taken.

## 2.4 Chlorophyll a fluorescence and total photosynthetic performance

Chlorophyll *a* fluorescence of wheat leaves held in dark for 15 minutes was measured by using a handheld fluorometer (Handy PEA+, Hansatech instruments). For each treatment, at least 15 measurements were made from the middle part of the fully mature and expanded functional leaves, and each measurement consisted of 1s single and strong light pulse (3000 μmol s<sup>-1</sup> m<sup>-2</sup>), this light is provided by an array of six light-emitting diodes (peak 650 nm). The OJIP fluorescence curve is a typical curve of chlorophyll fluorescence with the three transition phases (OJ, JI and IP). The O–J phase indicates a photochemical phase, and the J–I–P phase indicates a thermal phase (Stirbet, 2012). This OJIP transient reflects diverse reduction processes of the electron transport chain (Strasser et al., 2004; Stirbet, 2012). The photochemical phase O–J is



reported to be deeply light-dependent (Schansker et al., 2006) and informs connectivity between PSII reaction centres. The thermal phase, J to P rise, indicates a reduction of the rest of the electron transport chain (Kalaji et al., 2017).

The fluorescence parameter  $PI_{total}$  was calculated from the fluorescence transient measured during the 1<sup>st</sup> second of illumination.  $PI_{total}$  (1) is estimated to be a product of the  $PI_{ABS}$  (photosynthetic performance index) (2) and the probability that an electron ( $e^-$ ) can move from the reduced intersystem electron acceptors to the PSI end-electron-acceptors (3) (Tsimilli-Michael and Strasser, 2008):

$$PI_{total} = PI_{ABS} \cdot \delta_{Ro} / (1 - \delta_{Ro}) \quad (1)$$

$$PI_{ABS} = [RC/ABS] \times [\phi_{Po}/(1 - \phi_{Po})] \times [\psi_o/(1 - \psi_o)] \quad (2)$$

With:

ABS/RC: Specific absorption flux per reaction centre (RC)

$\phi_{Po}$ : Quantum yield of electron transport (at  $t = 0$ ),  $\phi_{Po} = (1 - F_0/F_M)$

$\phi_o$ : Probability (at  $t = 0$ ) that a trapped exciton moves an electron into the electron transport chain beyond  $Q_A^-$ ,  $\psi_o = 1 - V_J$

$\delta_{Ro}$  indicates the efficiency with which an electron can move from the reduced intersystem electron acceptors to the PSI end electron acceptors, and can be expressed as:

$$\delta_{Ro} = (1 - V_I) / (1 - V_J) \quad (3)$$

$V_t$  (4) is described as the relative variable Chl *a* fluorescence at time *t*. It corresponds to:

$$V_t = (F_t - F_0) / (F_M - F_0) \quad (4)$$

This equation can be identified as a measure of the fraction of the primary quinone electron acceptor of PSII in its reduced state [ $Q_A^- / Q_{A\ (total)}$ ].  $\Delta V_t$  (5) could indicate additional information and bands that might be hidden in the kinetic curves of Chl *a* fluorescence OJIP (Chen et al., 2016). It was calculated as the difference between  $V_t$  values obtained by plants at the different P doses (0, 30 and 45 ppm P minus the respective values of unfertilized plants without salt stress (negative control):

$$\Delta V_t = V_t(P) - V_t(P - P_{negative\ control}) \quad (5)$$

## 2.5 Biomass

Plants were separated into shoots and roots, washed and dried at 75°C in an oven until the root and shoot dry weights stabilized.

Root and shoot Tissue Water Content (TWC) was calculated using the following formula (6):

$$TWC = (FW - DW) / DW \quad (6)$$

With:

FW: Fresh weight, DW: Dry weight

## 2.6 Nutrient analysis

Elemental concentrations of P, K, and Na were analyzed on a dry-weight basis using Inductively Coupled Plasma Optical Emission Spectrometry (Agilent 5110 ICP-OES, USA).

## 2.7 Statistical analysis

Statistical analysis was performed using one-way ANOVA (for  $P < 0.05$ ) and SPSS data processing software (SPSS 20.0), considering three independent replicates per treatment. Based on the ANOVA results, and for a 95% confutation level, a GT2 of the Hochberg test for the comparison of means was performed, to reveal the significant differences between treatments. Pearson's Correlation coefficients *r* were calculated to determine the association between dry weight yield of shoot and root and their mineral content.

## 3 Results

### 3.1 Chlorophyll content index

Chlorophyll Content Index (CCI) measured in salt-stressed and unfertilized plants (C+) showed a reduction compared to measured CCI in unfertilized plants without salinity stress (C-) (Figure 1A). For instance, growth at 12 weeks after sowing, CCI reduced by 22.6% in C+ compared to C- plants. However, fertilized plants showed an increase in CCI compared to control plants (C+ and C-). After 12 weeks of growth and with a dose of 30 ppm of P, CCI increased by 93%, 81%, and 71% in plants fertilized by Poly-B, Ortho-B and Ortho-A, respectively compared to C+ (Figure 1A). The different doses of P in the different fertilizers did not show a significant effect on CCI. The difference between fertilizer forms was significant mainly for Poly-B which increased by 17.42% at 30 ppm of P compared to Ortho-A and Ortho-B at 45 ppm of P.

### 3.2 Stomatal conductance

Stomatal conductance (SC) decreased in salt-stressed and unfertilized plants (C+) compared to unfertilized plants without salinity stress (C-) except at the beginning of growth, 6 weeks after sowing (Figure 1B). This decrease was significant in plants

grown 12 weeks after sowing. However, fertilized plants showed a significant increase in SC compared to C- and C+ plants except for plants grown 6 weeks after sowing. Furthermore, P dose in different soluble fertilizers showed a significant effect on SC while the fertilizers forms did not affect this physiological parameter. Indeed, compared to C+, Poly-B and Ortho-A showed similar results in SC with an increase of 157% and 217% at 30 and 45 ppm of P, respectively. The highest significant value of SC was obtained with Ortho-B fertilizer at 45 ppm with an increase of 232% and 56% compared to C+ and C- plants, respectively.

### 3.3 Chlorophyll a fluorescence and photosynthetic performance index

Figure 2A shows no visual difference in the effect of salinity on the fluorescence curve; however, a difference in fluorescence yield in the J-I-P phase was observed. The subtraction of the different curves from the curve measured in the negative control (C-) plants ( $\Delta Vt$ ) showed the presence of two bands (Figure 2B), the first in the J-I phase and the second during the I-P phase. In salt-stressed and unfertilized plants (C+), measurements showed

only a single positive band in the J-I phase and another band was also observed in the O-J phase with a peak of around 300  $\mu s$ . The fully mature leaves of fertilized wheat plants showed a significant increase in the photosynthetic performance index  $PI_{tot}$ , compared to negative (C-) and positive control (C+) plants (Figure 3). Furthermore, the P dose and fertilizers forms showed a significant effect on  $PI_{tot}$ .

Compared to C+, the  $PI_{tot}$  was increased by 128.5%, 90.2% and 38.8% for Ortho-B, Ortho-A and Poly B, respectively. For the same fertilizer, the dose did not affect the  $PI_{tot}$ .

### 3.4 Biomass and tissue water content

Figure 4A shows an increase in the dry weight (DW) of the shoot in fertilized plants compared to unfertilized plants exposed to salinity (C+) or not (C-). The source of fertilizers has a significant effect but depends on the dose of P. The increase in shoot DW was significant mainly with Poly-B fertilizer (156.8%) for both doses followed by Ortho-A (125.6%) and Ortho-B (114.2%) at 45 and 30 ppm of P, respectively in comparison with C+ plants. However, the dry weight of the roots depends both on the dose and the form of the soluble fertilizers.

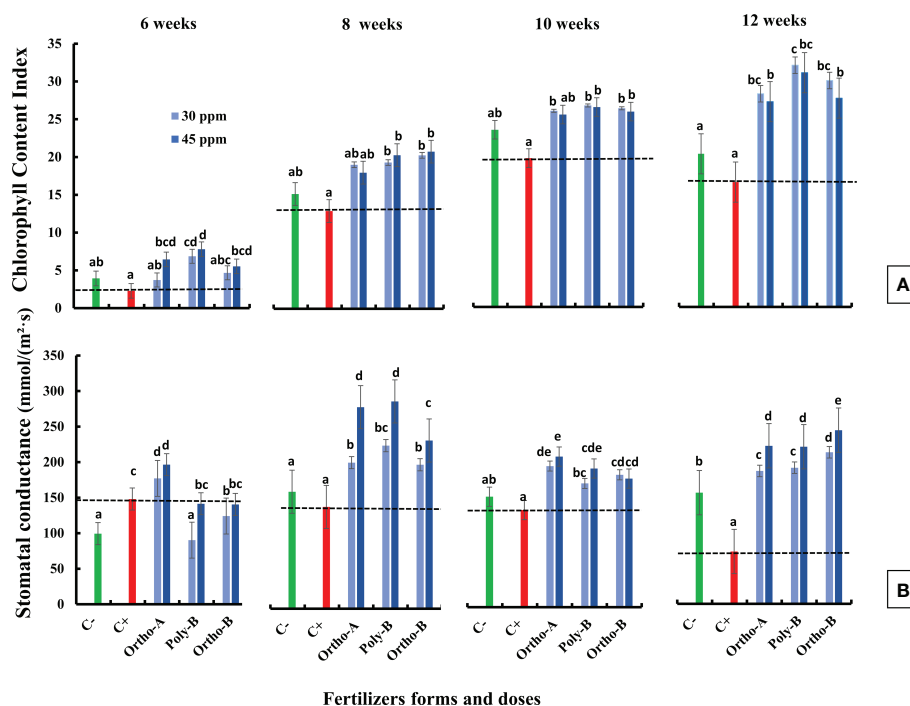


FIGURE 1

The combined effect of P-fertilizer forms (Ortho-A, Poly-B and Ortho-B) and doses (0, 30 and 45 ppm) on Chlorophyll content index (CCI) (A) and Stomatal conductance (SC) (B) of wheat plants grown under salt stress conditions, measured at 6, 8, 10 and 12 WAS. C-: unfertilized plants without salt application, C+ salt-stressed and unfertilized plants. Statistical analysis was performed using one-way ANOVA and SPSS data processing software. GT2 of the Hochberg test was used for the comparison of means. Treatments having the same letters are not significantly different at the 5% level.

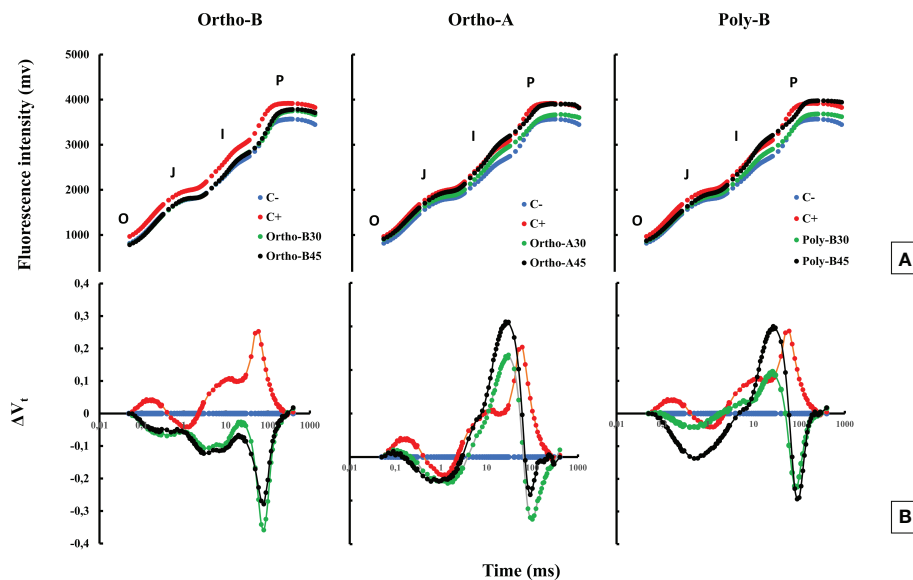


FIGURE 2

The combined effect of P-fertilizer forms (Ortho-A, Poly-B and Ortho-B) and doses (0, 30 and 45 ppm) on OJIP curves (A) and  $\Delta V_t$  fluorescence parameter (B) of wheat plants grown under salt stress conditions at 12 WAS. C-: unfertilized plants without salt application, C+ salt-stressed and unfertilized plants.

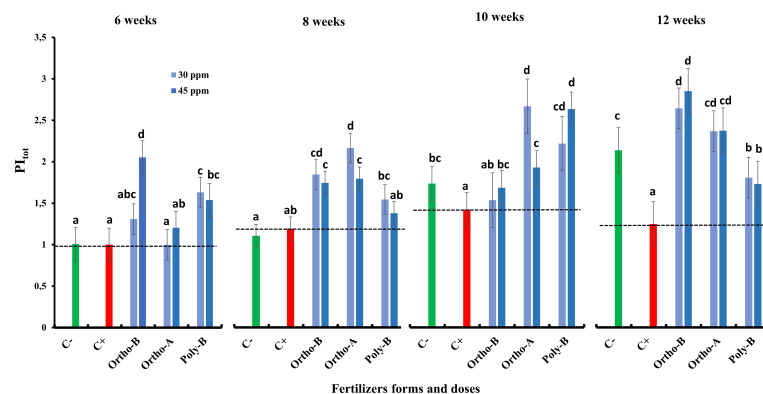


FIGURE 3

The combined effect of P-fertilizer forms (Ortho-A, Poly-B and Ortho-B) and doses (0, 30 and 45 ppm) on Photosynthetic Performance Index ( $PI_{tot}$ ) of wheat plants grown under salt stress conditions, measured at 6, 8, 10 and 12 WAS. C-: unfertilized plants without salt application, C+ salt-stressed and unfertilized plants. Statistical analysis was performed using one-way ANOVA and SPSS data processing software. GT2 of the Hochberg test was used for the comparison of means. Treatments having the same letters are not significantly different at the 5% level.

Furthermore, Poly-B fertilizer showed the best performance at 30 ppm of P with an increase of 49.4% and 98.9% in root DW compared to C+ and C- respectively, while other P-treatments did not show a significant difference with the C+. In addition, Root Tissue Water Content (TWC) (Figure 4B) significantly decreased in unfertilized plants under saline conditions (C+) or not (C-) compared to salt-stressed and fertilized plants. The root TWC increased by 33.7% compared to C+ for Ortho-B and Poly B with a similar response for both doses, followed by Ortho-A

(23.5% and 16.73% for 45 and 30 ppm of P, respectively). However, our results showed that the shoot TWC in unfertilized plants has not been reduced under salinity, whereas it has been significantly decreased for other P-treatments. This response was not strongly influenced by forms or doses of P-fertilizers (Figure 4B). After 12 weeks after sowing, the ratio of the DW of roots to the DW of shoots decreased in the salt-stressed and fertilized plants compared to unfertilized plants (C+ and C-)(Figure 4C). At 45 ppm of P,

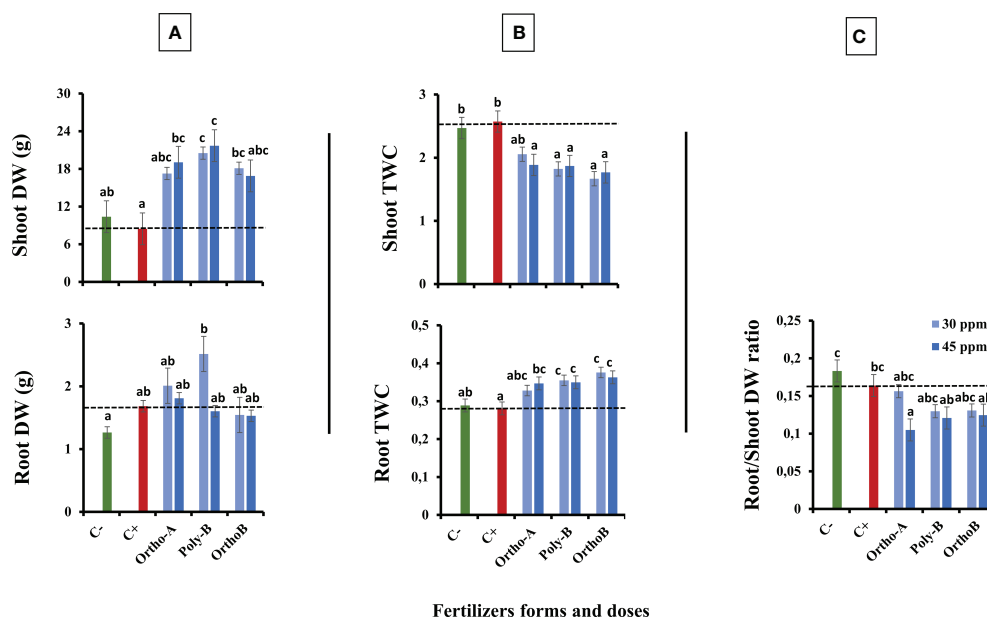


FIGURE 4

The combined effect of P-fertilizer forms (Ortho-A, Poly-B and Ortho-B) and doses (0, 30 and 45 ppm) on Shoot and Root dry weight (DW) (A), Shoot and Root Tissue water content (TWC) (B) and Root/Shoot DW ratio (C) of wheat plants grown under salt stress conditions, measured at 12 WAS. C-: unfertilized plants without salt application, C+ salt-stressed and unfertilized plants. Statistical analysis was performed using one-way ANOVA and SPSS data processing software. GT2 of the Hochberg test was used for the comparison of means. Treatments having the same letters are not significantly different at the 5% level.

Ortho-A showed a significant decrease in this ratio (-56%) compared to 30 ppm of P and C+ while the Ortho-B and Poly-B treatments did not show significant differences between each other.

### 3.5 Mineral analysis

#### 3.5.1 Root and shoot mineral content

Figures 5, 6 show an increase in the total P (Pt) content in the root and shoot of fertilized plants compared to unfertilized plants exposed to salinity (C+) or not (C-). The form of fertilizers has a significant effect but depends on the P dose. At 45 ppm of P, P fertilizers showed similar results with an increase of 104% in Pt root content of salt-stressed plants in comparison with C+ (Figure 5). However, Ortho-B did not show any difference with the C+ at 30 ppm of P. The same tendency was observed for Pt shoot content, where the dose 45 ppm of P showed a significant rise in shoot-Pt for all P fertilizers compared to the 30 ppm dose (Figure 6). Compared to unfertilized plants (C- and C+), OrthoP fertilizers (Ortho-A and Ortho-B) showed similar results for both doses with an increase of 62% and 115% at 30 and 45 ppm of P, respectively. The Pt shoot content was significantly improved using Poly-B fertilizer compared to C+ and C- and showed the highest significant Pt accumulation in shoots estimated by 84% and 131% at 30 and 45 ppm of P,

respectively (Figure 6). The response was, therefore, dose/form dependent. However, the K shoot content decreased significantly for all fertilized plants compared to unfertilized ones (-20%) (Figure 6). Accordingly, there is no significant difference between P-treatments and controls (C+ and C-) in the amount of K in root except for Ortho-B and Poly-B at 30 ppm of P which showed the lowest value of K accumulation (Figure 5). As unexpected results, the Na root content increased in the root and shoot of fertilized plants compared to unfertilized ones under salinity (C+). The effect was more relevant using Ortho-A at 30 ppm of P with an increase of 28% and 42% in Na content in shoots and roots, respectively (Figures 5, 6).

#### 3.5.2 Correlation matrix

Pearson's correlation coefficients among plant dry weight (shoot and root dry weight) and different nutrients in the shoot and root of wheat salt-stressed plants cultivated with different forms and doses of soluble P-fertilizers were shown in Table 2. At 12 WAS, there was no significant correlation between shoot and root DW, but a positive significant correlation was observed between shoot-Pt content ( $P \leq 0.01$ ) and Shoot DW ( $r = 0.770^{**}$ ), root-Na ( $r = 0.587^{**}$ ) and root-Pt content ( $r = 0.742^{**}$ ). However, there was a negative significant correlation between shoot-K content ( $P \leq 0.01$ ) and Shoot DW ( $r = -0.637^{**}$ ), root-Na ( $r = -0.686^{**}$ ), Pt-shoot ( $r = -0.653^{**}$ ) and Pt-root content ( $r = -0.514^{*}$ ) ( $P \leq 0.05$ ). The latter shows a positive



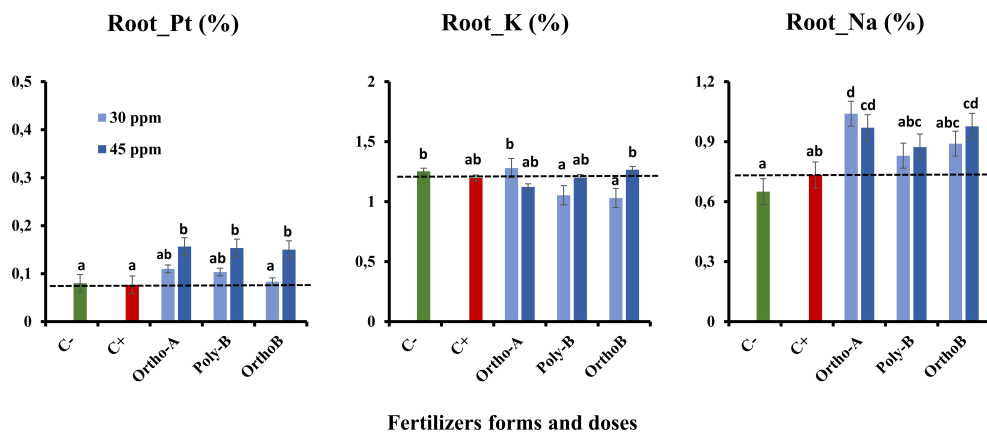


FIGURE 5

The combined effect of P-fertilizer forms (Ortho-A, Poly-B and Ortho-B) and doses (0, 30 and 45 ppm) on total phosphorus (Pt), Potassium (K) and Sodium (Na) in roots of wheat plants grown under salt stress conditions, measured at 12 WAS. C-: unfertilized plants without salt application, C+ salt-stressed and unfertilized plants. Statistical analysis was performed using one-way ANOVA and SPSS data processing software. GT2 of the Hochberg test was used for the comparison of means. Treatments having the same letters are not significantly different at the 5% level.

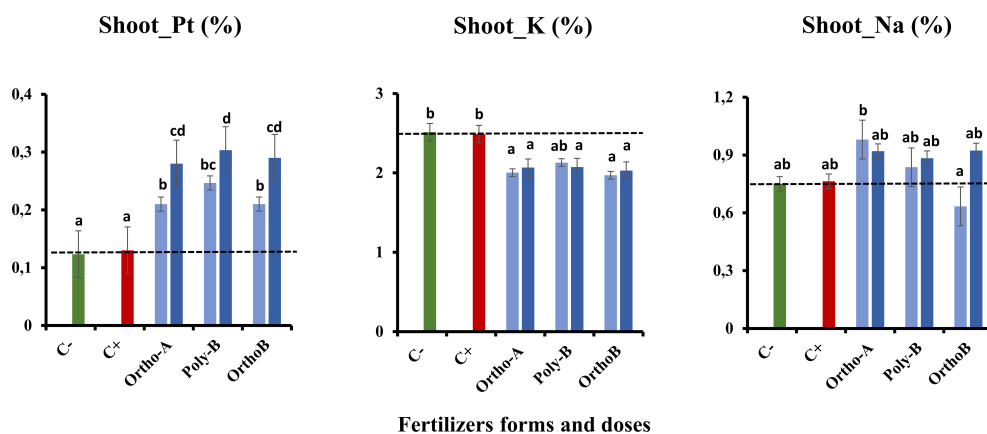


FIGURE 6

The combined effect of P-fertilizer forms (Ortho-A, Poly-B and Ortho-B) and doses (0, 30 and 45 ppm) on total phosphorus (Pt), Potassium (K) and Sodium (Na) in shoots of Wheat plants grown under salt stress conditions, measured at 12 WAS. C-: unfertilized plants without salt application, C+ salt-stressed and unfertilized plants. Statistical analysis was performed using one-way ANOVA and SPSS data processing software. GT2 of the Hochberg test was used for the comparison of means. Treatments having the same letters are not significantly different at the 5% level.

significant association ( $P \leq 0.05$ ) with the shoot DW ( $r = 0.491^*$ ), Na-shoot ( $r = 0.486^*$ ). The Pt-root content was also significantly correlated ( $P \leq 0.01$ ) to shoot-Pt content ( $r = 0.742^{**}$ ) and Na-root content ( $r = 0.554^{**}$ ).

## 4 Discussion

Salt stress limits wheat growth and development by inducing a series of physiological dysfunctions in different organs such as

leaves, shoots, and roots. However, soluble fertilizer forms and P doses enhanced plant responses and countered the negative effect of this stress.

### 4.1 Salt-stressed and unfertilized wheat plants' responses

The reduction of chlorophyll content in salt-stressed leaves of wheat observed in our study was reported in many studies focused

TABLE 2 Pearson's correlation coefficients among plant dry weight (shoot and root dry weight) and measured nutrients in the shoot and root of wheat plants grown with different forms and doses of soluble P-fertilizers under salinity at 12 WAS (n = 24).

#### Pearson's correlation coefficients

Trait	Shoot_Pt	Shoot_K	Shoot_Na	SDW	Root_Pt	Root_K	Root_Na	RDW
Shoot_Pt	1,00	-0,653**	0,32	0,770**	0,742**	-0,11	0,587**	0,21
Shoot_K		1,00	-0,10	-0,637**	-0,514*	0,10	-0,686**	-0,21
Shoot_Na			1,00	-0,10	0,486*	0,12	0,35	0,23
SDW				1,00	0,491*	-0,19	0,39	0,23
Root_Pt					1,00	0,27	0,554**	-0,05
Root_K						1,00	0,26	-0,38
Root_Na							1,00	0,12
RDW								1,00

\*\* and \*: significant at 0.01 and 0.05 levels, respectively; Pt, total phosphorus; K, potassium; Na, sodium; SDW, shoot dry weight, RDW, Root dry weight, WAS, Week after sowing.

on the effect of salinity on plants (Ashraf and Harris, 2013; Sharma et al., 2020). A significant decrease in CCI was observed at 6, 8, 10 and 12 WAS, which reached -23%. In C+ plants compared to C- (Figure 1A). This reduction has been associated with an increase in chlorophyllase activity which is an enzyme degrading the chlorophyll (Shoukat et al., 2019) and with the instability of pigment-protein complexes (Renger et al. 2011). Also, photoinhibition and reactive oxygen species (ROS) formation during salt stress could cause a decrease in chlorophyll content (Hasanuzzaman et al., 2021; Muhammad et al., 2021). Additionally, the decline of stomatal conductance was significantly observed in unfertilized and salt-stressed wheat plants (C+) compared to C-. The difference was significant at 12 WAS with a reduction of -113% in C+ compared to C- plants (Figure 1B). This is consistent with previous observations on the effect of salt stress on plants (Lotfi et al., 2020; Behdad et al., 2021). As was reported, salt stress provokes osmotic stress in the root, and then the limited water absorption affects the aperture of stomata to preserve water in plant tissues and decrease water loss *via* transpiration (Zribi et al., 2021). In such situations, plants usually adopt defensive strategies by the increase of water use efficiency (WUE), control of the net CO<sub>2</sub> and the rate of transpiration in leaves (Muhammad et al., 2021). However, under severe salt stress conditions, the mesophyll cell dehydration allows the use of available CO<sub>2</sub>, which significantly inhibits photosynthesis metabolic processes, leading to a decrease in water use efficiency and hydraulic conductivity of root (Din et al., 2011). Indeed, stomatal conductance plays an essential role in water balance regulation and stomatal closure has also a direct effect on plant growth by reducing cell expansion and plant development causing a decrease in biomass and plant productivity (Nemeskéri et al., 2019). Fahad et al. (2015) reported that the major effects of moderate salt stress on growth could be attributed to a major investment of energy in defence mechanisms rather than in biomass production. Accordingly, root and shoot dry weights (DW) decrease toward salt stress (Fig 4. A) which has also been reported in previous studies (Yan and

Marschner, 2012; Muhammad et al., 2021). This reduction was more relevant in shoot DW than root DW in comparison with C- and fertilized plants. Eker et al. (2006) reported that root DW was less affected by salinity than shoot DW for two varieties of hybrid maize. These findings indicate that shoot growth could be a more useful parameter than root growth for assessing the salinity tolerance of plants. We assume that the decrease in dry biomass was resulting in the reduction of chlorophyll content and stomata closure (Nemeskéri et al., 2019). This positive association between photosynthetic capacity and biomass production has been confirmed under salinity for maize plants (Hessini et al., 2019), quinoa (Manaa et al., 2019) and pepper (Altuntas et al., 2018). In the last decades, the root/shoot ratio was adopted for assessing plant growth and was considered a sensitive growth parameter and indicator in plant stress physiology (Rahimi et al., 2021). To minimize the negative effect of salt stress, the plant developed phenotypic plasticity (Rewald et al., 2012). Contrary to what has been reported in previous studies, that the root/shoot ratio increased in stress conditions (Khorshid et al., 2018; Rahimi et al., 2021), in our investigation, this ratio decreased for all P treatments. This reduction was more relevant at 45 ppm of P for Ortho-A followed by Poly-B and Ortho-B which were similar for both doses of P. Thus, biomass was more allocated in shoots than in roots. Contradictory reports exist regarding the influence of salinity and P deficiency on the root/shoot biomass ratio. Low P availability has been shown to increase the allocation of dry matter to roots while suppressing shoot growth, resulting in increased root/shoot ratios (Kim and Li, 2016). This ratio has been reported to be affected (increase or decrease) in different plants like tomato and petunia (Kim et al., 2008), common bean (Lynch and Brown, 2006) or unaffected (Broschat and Klock-Moore, 2000). Biomass allocation to root or shoot depends on the salt degree, time and duration of exposure, plant species, and developmental stage (Shabala and Munns, 2017).

The salt-stress effects on photosynthesis range from the limitation of CO<sub>2</sub> diffusion into the chloroplast, through limiting stomatal opening, which is regulated by hormones

produced in shoot and root, and on the CO<sub>2</sub> mesophyll transport, up to major modifications in the photochemistry of leaves and C metabolism, or they may induce oxidative stress. This appears as a secondary effect (Chaves et al., 2011), which can seriously alter the photosynthetic machinery of leaves (Sharma et al., 2020; Muhammad et al., 2021). Moreover, Dekker and Boekema (2005) reported that the key functional chloroplast protein complexes, implicated in harvesting light energy (PSI, PSII, ATP-synthase and Cytb6f), are affected in salt-stressed plants. The changes in the oxygen-evolving complex (OEC) and proteins of the PSII reaction centre are recognized to enable PSII to deal with saline environments (Duarte et al., 2013; Oukarroum et al., 2015). Furthermore, it has been previously demonstrated that OJIP transient shape changes under different abiotic stresses including salt stress (Sarkar and Ray, 2016). This change differs depending on the severity and duration of stress. In our study, the thermal phase J-I-P seems to be affected by salinity (Figure 2A). The difference between fertilized and C- plants was determined in salt-stressed wheat and showed a positive band with a pic at 300 us (Figure 2B). The appearance of this band named K-band reflects a restriction on the donor side of PSII (Strasser et al., 2004; Oukarroum et al., 2007). This K-band can be seen in the fluorescence rise of, e.g., plants under heat and drought stress (Brestic et al., 2012). We found that the salinity stress induced a reduction in the photosynthetic performance index PI<sub>tot</sub> (Figure 3). The estimated performance index reflects the photosynthetic performance up to the reduction of PSI end e- acceptors. The highest significant difference between C+ and C- plants (-71%) was observed at 12 WAS which suggests an additive effect of salinity and P deficiency over time. This decrease in PI<sub>tot</sub> indicates that the plant vitality was inhibited to a certain degree under our salinity and P deficiency conditions.

Among the negative consequences of salt stress on plants is ROS formation. It has been well reported that ROS can damage cellular components and disturb many physiological mechanisms (Kumar et al., 2017; Hasanuzzaman et al., 2021). Moreover, ROS acts also as signal transduction in cells to reduce this effect in stressed plants (Kumar et al., 2017).

## 4.2 Salt-stressed and fertilized wheat plants' responses

Major effects of moderate salt stress on growth could be attributed to a major investment of energy on defence mechanisms rather than on biomass production (Fahad et al., 2015) or due to the reduced water uptake which leads to a reduction in toxic ion assimilation (Shabala and Munns, 2017; Zhao et al., 2020). Furthermore, when P nutrition was sufficient, growth reductions and visual symptoms of salt toxicity were minimized and were more accentuated by P deficiency (Mohamed et al., 2021; Zribi et al., 2021). Supply soluble

fertilizers enhance wheat growth and improve salt tolerance as observed in all studied parameters. This positive role has been previously observed in other plant species exposed to salt stress and supplied by different P doses (Khan et al., 2013; Bargaz et al., 2016; Rady et al., 2018; Bouras et al., 2021; Mohamed et al., 2021; Zribi et al., 2021; Bouras et al., 2022). We assume that adding P to plants grown under salt stress could mitigate the negative effects caused on different plant organ development. Indeed, it has been shown that phosphorus is an important factor in the growth of shoots and roots, and low phosphorus uptake under salinity may reduce biomass development (Demiral, 2017; Khan et al., 2018). In the present work, shoot and root dry weights significantly declined in unfertilized plants grown under salinity (C+) compared to fertilized ones (Figure 4A). These findings are in line with previous reports (Parvez et al., 2020; Zribi et al., 2021). This reduction might be a plant survival strategy associated with carbon (C) assimilation failure (Shoukat et al., 2019) or with the major investment of energy on defence mechanisms rather than in biomass production (Fahad et al., 2015). In addition, our findings showed that the source of fertilizers has a significant effect but depends also on the dose of P. Poly-B fertilizer significantly increased shoot DW (156.8%) at both doses followed by Ortho-A (125.6%) and Ortho-B (114.2%) at 45 and 30 ppm of P, respectively (Fig 4. A). Furthermore, compared to OrthoP fertilizers, Poly-B showed the best performance at 30 ppm for root DW with an increase of 49.4% and 98.9% compared to C+ and C-, respectively. Therefore, an optimal P-supply stimulated vegetative growth and the creation of strong root systems which is primordial to the efficient absorption of soil nutrients (Sharma et al., 2020). In addition, the effect could be related to the improved P availability in the soil solution due to the slow and continuous release property of polyphosphate. However, a high dose of P-soluble fertilizers (60 ppm) had detrimental effects on salt-stressed wheat (data not shown). In this regard, a harmful reverse effect of high phosphorus dose was also reported in other crops such as common bean (Bargaz et al., 2016), Barley (Zribi et al., 2011) Soybean (Phang et al., 2009) and Maize (Tang et al., 2019). The partitioning of biomass could be regarded as a process for growth optimisation. Balanced growth of both roots and shoots might be a strategy to improve plant productivity in salty soil, which leads to optimal allocation (Hermans et al., 2006) and enhances both P-uptake and water acquisition (Fujita et al., 2004; Meng et al., 2021). In our study, the K content was similar in the roots of fertilized and unfertilized salt-stressed plants (C+) (Figure 5), but we noticed a reduction (-20%) in the concentration of potassium in the aerial part in salt-stressed and fertilized plants (C+) (Figure 6). The difference between P fertilizers was not significant since we equalized the amount of K for all treatments. Remarkably, it was found that salinity caused sodium injury, which impacts potassium uptake by root cells (Conde et al., 2011; Rahimi et al., 2021). Accordingly, the Na concentration significantly

increased in the root and shoot of fertilized plants compared to C+ which was unexpected. The effect was more relevant using Ortho-A at 30 ppm of P with an increase of 28% and 42% in Na accumulation in shoots and roots, respectively (Figures 5, 6). Indeed, it is worth noting that potassium and sodium might exist in competition and induce K+ deficiency in the rhizosphere, and depolarization of the plasma membrane also stimulates the K+ outward rectifying channels to mediate the efflux of K+ and the influx of Na+ (Behdad et al., 2021). Additionally, it was reported that many enzymes (including photosynthetic ones) were severely inhibited by sodium at a concentration above 100 mM (about 10 dS/m) (Shabala and Munns, 2017). Furthermore, the enzymes which need potassium as a cofactor are especially sensitive to the high concentration of sodium (Chaves et al., 2011; García-Ortiz et al., 2012). Our findings were consistent with previous works in the literature (Chen et al., 2007; Rodríguez-Martín et al., 2018). However, it is interesting to mention that the reduction in both phosphorus and potassium concentration under high salinity is accompanied by a significant increase in sodium content in root and shoot (Demiral, 2017; Loudari et al., 2020).

Accordingly, Singh et al. (2016) found that P-fertilization supported the formation of a well-developed root system of lentil plants which optimizes their ability to absorb other minerals from the soil such as N, K+, and Ca2+. Consequently, their amounts increased after the phosphorus application (Singh et al., 2016; Loudari et al., 2020). Besides, it has been reported that phosphorus and potassium are implicated in salt stress mitigation in most crops (Bargaz et al., 2016; Chakraborty et al., 2021). Kaya et al., 2013 reported that phosphorus and potassium, and indole-3-acetic acid (IAA) were efficient in enhancing the maize plant's fitness when subjected to salt stress. Indeed, Rubio et al. (2005) observed in the leaf and root cells of *Zostera marina* L, a Na-dependent high-affinity phosphate transporter in their plasma membrane. In addition, Zribi et al. (2021) reported that phosphorus availability disturbed Na transportation to shoots which were in line with our results related to Poly-B response to Na accumulation in shoots and roots compared to OrthoP. Accordingly, P fertilizers exhibit similar responses in the total P (Pt) content in the root and shoot of fertilized plants mainly at 45 ppm of P. The increase reached 104% in Root-Pt content in comparison with C+ (Figure 5). The same tendency was observed for shoot-Pt content where OrthoP fertilizers showed similar results for both doses (62% and 115% at 30 and 45 ppm of P, respectively) (Figure 6). The response was dose-dependent. Moreover, Poly-B fertilizer showed the highest Pt concentration in shoots estimated at 84% and 131% at 30 and 45 ppm of P, respectively (Figure 6). Indeed, the rise in P-content in fertilized wheat plants under salinity (Figures 5, 6) could be attributed to a synergistic effect of Na, which is implicated in P acquisition and/or transportation to the aerial part of plants (Grattan and Grieve, 1992). However, high

external phosphorus enhanced sodium acquisition and reduced the soybean tolerance to salinity (Phang et al., 2009). This is consistent with our results at 12 WAS, the sodium in shoots of salt-stressed and fertilized plants was significantly higher than in plants grown under salinity and phosphorus deficiency (C+) (Figures 5, 6). Besides, a special partitioning of sodium ions between shoot and root was observed (Keisham et al., 2018). Our findings agree with this statement since we found that Na+ accumulation was important in roots of salt-stressed and fertilized plants compared to shoots (Figures 5, 6). For instance, Na content in plants fertilized by Ortho-A increased by 28% in shoots at 30 ppm of P while it reached +42% in roots compared to C+ plants. It has also been shown that the decrease in growth under salinity might be attributed to a nutritional imbalance and excessive sodium acquisition (Isayenkov and Maathuis, 2019). Furthermore, it has been reported that photosynthetic and respiratory electron transport were inactivated by sodium accumulation (Stirbet, 2012), which was revealed in our results by a reduction in  $PI_{tot}$  (Figure 3) and I-P phase (loss of PSI reaction centres) in salt-stressed and unfertilized plants (C+) (Figures 2A, B). In the present work, the diminution in J-I-P fluorescence yield (Figure 2A) was more significant for salt-stressed and unfertilized plants (C+) in comparison with fertilized ones. These results suggest a restriction of both donor and acceptor-side of PSI (reduced J-I-P yield), which indicates that P in wheat leaves stimulated the intersystem electron transport regulation between PSII and PSI (El-Mejjaoui et al., 2022). This could reveal a cellular adaptation to alleviate the harmful effect of salt stress and ensure photosynthetic electron transport equilibrium (Kalaji et al., 2016; Loudari et al., 2020; Muhammad et al., 2021). The P doses and fertilizers forms showed a significant effect on  $PI_{tot}$ . Compared to C+, the  $PI_{tot}$  increased by 128.5%, 90.2% and 38.8% for Ortho-B, Ortho-A and Poly-B, respectively for both doses. Here, the dose did not affect the  $PI_{tot}$  but the P supply as OrthoP showed positive responses compared to Poly-B. Indeed, the mild salt tolerance of plants could be partially attributed to their faculty to maintain photosynthetic ability (Sharma et al., 2020) since P is implicated in the transport of fixed carbon from chloroplasts to the cytosol with its triose-phosphate form (Rychter et al., 2018), together with a lower sodium concentration and a higher cytosolic potassium/sodium ratio (Rahimi et al., 2021). Under moderate stress, a small decrease in stomatal conductance could provide protective effects against salinity, through limited water loss and improved plant water-use efficiency (Wilkinson and Davies, 2002). These phenomena restrict CO<sub>2</sub> influx and water vapour efflux mainly for C3 plants. Besides, Koyro (2006) reported that the stomatal closure could be considered an adaptive mechanism to mitigate salt stress, rather than its negative consequence. In our study, the P dose of soluble P fertilizers showed a significant effect on stomatal conductance (SC) while the fertilizers forms did not affect this physiological parameter. Indeed, compared to C+, Poly-B and



Ortho-A showed similar results in SC with an increase of 157% and 217% at 30 and 45 ppm of P, respectively. The highest significant value of SC was obtained with Ortho-B fertilizer at 45 ppm with an increase of 232% and 56% compared to C+ and C- plants, respectively. The increased SC in salt-stressed plants grown under sufficient P supply leads to an improvement in plant salt tolerance (Behdad et al., 2021). In the present work, Root Tissue Water Content (TWC) (Figure 4B) significantly decreased in salt-stressed and unfertilized plants (C-) mainly at 12 WAS compared to fertilized plants under saline conditions. The root TWC increased by 33.7% for Ortho-B and Poly B with a similar response for both doses compared to C+ followed by Ortho-A which showed a response dose-dependent (23.5% and 16.73% at 45 and 30 ppm of P, respectively). These findings support the previous work of Li et al. (2009), who revealed that P shortage altered root hydraulic conductance and lowered plant water potential by reducing the water channel proteins activity: the aquaporins. Additionally, our results showed that the shoot water content in salt-stressed and unfertilized plants (C+) has not been reduced under salinity, but this parameter has been significantly decreased for other P-treatments. This response was not strongly influenced by forms or doses of P-fertilizers (Figure 4B). Our results are in accord with those of Zribi et al. (2021) on *Aeluropus littoralis* plants. In addition, Asrar et al. (2017) reported that stomata closure can lead to low photosynthetic rates, but our data showed that although the salt-stressed and unfertilized wheat plants (C+) presented a higher TWC of shoots compared to salt-stressed and fertilized plants (+36%) (Figure 4B), the performance index ( $PI_{total}$ ) increases significantly for all rates and forms of P in comparison with C+ plants at 6, 8, 10 and 12 WAS (Figure 3). Thus, the disturbed water potential under salt stress could not be the cause of the reduced photosynthetic performance. Instead, many studies proposed that diffusional constraints are the main reason for photosynthesis inhibition (Pérez-López et al., 2012; Chen et al., 2015). The downregulation of the photosynthetic metabolism leads to leaf biochemistry variations in response to a reduction in net CO<sub>2</sub> assimilation under prolonged stresses (Chaves et al., 2011). Prolonged exposure to salt stress or/and P deficiency disturbs biochemical processes (e.g., the activity of Rubisco and Ribulose-1,5-bisphosphate (RuBP) and triose phosphates regeneration) which control gas exchange (Meng et al., 2021). Additionally, several studies showed that P deficiency disturbs ultimately CO<sub>2</sub> assimilation (Rychter et al., 2018; El-Mejjaouy et al., 2022). Besides, it has been reported that in response to the decrease in CO<sub>2</sub> concentration in leaf intercellular airspaces, the activity of other enzymes (Sucrose phosphate synthase (SPS) or nitrate reductase) was reduced (Muhammad et al., 2021). Indeed, under those conditions limiting the fixation of CO<sub>2</sub>, the rate of reduction of energy production is greater than the rate of its use by the Calvin cycle. This might create competition for the use of the energy absorbed during stress, resulting in a reduction in the quantum yield of

PSII (Wieneke et al., 2022). Previous studies have shown that adequate phosphate nutrition is crucial for the efficient compartmentation of ions by contributing to the effective partitioning of carbon and the use of photo-assimilates in salt-stressed wheat (Khan et al., 2013; Abbas et al., 2018). Chlorophyll content reduction was observed in salt-stressed and unfertilized plants (C+) (Figure 1A). This reduction could be caused either by the limitation in the biosynthesis of chlorophyll or the degradation of existing chlorophyll (Ashraf and Harris, 2013; Carstensen et al., 2018), induces structural variations in the light-harvesting complex, disturbs light fixation ability and reduces photosynthetic efficiency (Duarte et al., 2013; Meng et al., 2021), while a higher chlorophyll content in fertilized plants promotes photosynthetic activity, intensive growth and higher biomass yield (Mohamed et al., 2021). This statement confirms our findings in plants treated with soluble fertilizers under saline conditions where the CCI increased by 93%, 81% and 71% in plants fertilized by Poly-B, Ortho-B and Ortho-A, respectively, compared to C+ (Figure 1A). The P doses did not show a significant effect on CCI while the difference between fertilizer forms was significant mainly for Poly-B which increased by 17.42% at 30 ppm of P compared to Ortho-A and Ortho-B at 45 ppm of P.

## 5 Conclusion

This study focused on different growth and physiological responses of wheat grown under the combined effect of salt stress and phosphorus availability using different rates and forms of soluble P-fertilizers. Furthermore, our work shows the relative contribution of stomatal, photochemical, and biochemical factors in restricting plant growth and the photosynthetic performance of durum wheat under salt stress. The results obtained have demonstrated that phosphorus fertilization significantly improved photochemical activity, which was due to enhanced light energy absorbed by enhanced Chl antenna to improve CO<sub>2</sub> assimilation rate and increased all other growth parameters of the salt-stressed wheat plants. Compared to OrthoP Poly-B fertilizer showed the best performance. Poly-B enriched soil with high quantities of available P which positively impacts the P uptake by plants grown under salinity. The slow and continuous release of available P in the soil and the property of chelating micronutrients make PolyP a promising alternative to reduce the frequency of P application for effective management of P fertilization under salt stress with a higher yield.

## Data availability statement

The original contributions presented in the study are included in the article/supplementary materials. Further inquiries can be directed to the corresponding author.

## Author contributions

AL and AO conceptualized and designed the experiment and lab studies. AL and AM performed the studies. AL, AO, and GC analysed the samples and data. AL, YZ, and AO, wrote the paper. All authors contributed to the article and approved the submitted version.

## Acknowledgments

OCP Group and Prayon, the SoilPhorLife project sponsors, are greatly acknowledged for funding this study. The authors also thank Mrs. Sabah Fathallah and Mr. Aziz Soulaïmani for their help and support in sample chemical analysis. The UM6P language laboratory team is acknowledged for proofreading the article.

## References

- Abbas, G., Chen, Y., Khan, F. Y., Feng, Y., Palta, J. A., and Siddique, K. H. (2018). Salinity and low phosphorus differentially affect shoot and root traits in two wheat cultivars with contrasting tolerance to salt. *Agronomy* 8 (8), 155. doi: 10.3390/agronomy8080155
- Altuntas, O., Dasgan, H. Y., and Akhoundnejad, Y. (2018). Silicon-induced salinity tolerance improves photosynthesis, leaf water status, membrane stability, and growth in pepper (*Capsicum annuum* L.). *HortScience* 53 (12), 1820–1826. doi: 10.21273/HORTSCI13411-18
- Ashraf, M. H. P. J. C., and Harris, P. J. (2013). Photosynthesis under stressful environments: an overview. *Photosynthetica* 51 (2), 163–190. doi: 10.1007/s11099-013-0021-6
- Asrar, H., Hussain, T., Hadi, S. M. S., Gul, B., Nielsen, B. L., and Khan, M. A. (2017). Salinity induced changes in light harvesting and carbon assimilating complexes of *desmostachya bipinnata* (L.) staph. *Environ. Exp. Bot.* 135, 86–95. doi: 10.1016/j.envexpbot.2016.12.008
- Bargaz, A., Nassar, R. M. A., Rady, M. M., Gaballah, M. S., Thompson, S. M., Brestic, M., et al. (2016). Improved salinity tolerance by phosphorus fertilizer in two phaseolus vulgaris recombinant inbred lines contrasting in their p-efficiency. *J. Agron. Crop Sci.* 202 (6), 497–507. doi: 10.1111/jac.12181
- Behdad, A., Mohsenzadeh, S., and Azizi, M. (2021). Growth, leaf gas exchange and physiological parameters of two glycyrrhiza glabra L. populations subjected to salt stress condition. *Rhizosphere* 17, 100319. doi: 10.1016/j.rhisph.2021.100319
- Belouchrani, A. S., Latati, M., Ounane, S. M., Drouiche, N., and Lounici, H. (2020). Study of the interaction salinity: Phosphorus fertilization on sorghum. *J. Plant Growth Regul.* 39 (3), 1205–1210. doi: 10.1007/s00344-019-10057-4
- Bouras, H., Bouaziz, A., Bouazzama, B., Hirich, A., and Choukr-Allah, R. (2021). How phosphorus fertilization alleviates the effect of salinity on sugar beet (*Beta vulgaris* L.) productivity and quality. *Agronomy* 11 (8), 1491. doi: 10.3390/agronomy11081491
- Bouras, H., Choukr-Allah, R., Amouaouch, Y., Bouaziz, A., Devkota, K. P., El Mouttaqi, A., et al. (2022). How does quinoa (*Chenopodium quinoa* willd.) respond to phosphorus fertilization and irrigation water salinity? *Plants* 11 (2), 216. doi: 10.3390/plants11020216
- Brestic, M., Zivcak, M., Kalaji, H. M., Carpentier, R., and Allakhverdiev, S. I. (2012). Photosystem II thermostability in situ: environmentally induced acclimation and genotype-specific reactions in triticum aestivum L. *Plant Physiol. Biochem.* 57, 93–105. doi: 10.1016/j.plaphy.2012.05.012
- Broschat, T. K., and Klock-Moore, K. A. (2000). Root and shoot growth responses to phosphate fertilization in container-grown plants. *HortTechnology* 10 (4), 765–767. doi: 10.21273/HORTTECH.10.4.765
- Carstensen, A., Herdean, A., Schmidt, S. B., Sharma, A., Spetea, C., Pribil, M., et al. (2018). The impacts of phosphorus deficiency on the photosynthetic electron transport chain. *Plant Physiol.* 177 (1), 271–284. doi: 10.1104/pp.17.01624
- Chakraborty, D., Prasad, R., Bhatta, A., and Torbert, H. A. (2021). Understanding the environmental impact of phosphorus in acidic soils receiving repeated poultry litter applications. *Sci. Total Environ.* 779, 146267. doi: 10.1016/j.scitotenv.2021.146267
- Chavarria, M. R., Wherley, B., Jessup, R., and Chandra, A. (2020). Leaf anatomical responses and chemical composition of warm-season turfgrasses to increasing salinity. *Curr. Plant Biol.* 22, 100147. doi: 10.1016/j.cpb.2020.100147
- Chaves, M. M., Costa, J. M., and Saibo, N. J. M. (2011). Recent advances in photosynthesis under drought and salinity. *Adv. botanical Res.* 57, 49–104. doi: 10.1016/B978-0-12-387692-8.00003-5
- Chen, L., Mao, F., Kirumba, G. C., Jiang, C., Manefield, M., and He, Y. (2015). Changes in metabolites, antioxidant system, and gene expression in microcystis aeruginosa under sodium chloride stress. *Ecotoxicology Environ. Saf.* 122, 126–135. doi: 10.1016/j.ecoenv.2015.07.011
- Chen, S., Yang, J., Zhang, M., Strasser, R. J., and Qiang, S. (2016). Classification and characteristics of heat tolerance in ageratina adenophora populations using fast chlorophyll a fluorescence rise OJIP. *Environ. Exp. Bot.* 122, 126–140. doi: 10.1016/j.envexpbot.2015.09.011
- Chen, Z., Zhou, M., Newman, I. A., Mendham, N. J., Zhang, G., and Shabala, S. (2007). Potassium and sodium relations in salinised barley tissues as a basis of differential salt tolerance. *Funct. Plant Biol.* 34 (2), 150–162. doi: 10.1071/FP06237
- Chtouki, M., Naciri, R., Garré, S., Nguyen, F., Zeroual, Y., and Oukarroum, A. (2022). Phosphorus fertilizer form and application frequency affect soil p availability, chickpea yield, and p use efficiency under drip fertigation. *J. Plant Nutr. Soil Sci.* 185, 603–611. doi: 10.1002/jpln.202100439
- Conde, A., Chaves, M. M., and Gerós, H. (2011). Membrane transport, sensing and signaling in plant adaptation to environmental stress. *Plant Cell Physiol.* 52 (9), 1583–1602. doi: 10.1093/pcp/pcr107
- Dekker, J. P., and Boekema, E. J. (2005). Supramolecular organization of thylakoid membrane proteins in green plants. *Biochim. Biophys. Acta (BBA)-Bioenergetics* 1706 (1–2), 12–39. doi: 10.1016/j.bbabo.2004.09.009
- Demiral, M. A. (2017). Effect of salt stress on the concentration of nitrogen and phosphorus in root and leaf of strawberry plant. *Eurasian J. Soil Sci.* 6 (4), 357–364. doi: 10.18393/ejss.319198
- Din, M. R., Ullah, F., Akmal, M., Shah, S., Ullah, N., Shafi, M., et al. (2011). Effects of cadmium and salinity on growth and photosynthesis parameters. *Pak J. Bot.* 43, 333–340.
- Duarte, B., Santos, D., Marques, J. C., and Caşador, I. (2013). Ecophysiological adaptations of two halophytes to salt stress: photosynthesis, PS II photochemistry and anti-oxidant feedback-implications for resilience in climate change. *Plant Physiol. Biochem.* 67, 178–188. doi: 10.1016/j.plaphy.2013.03.004
- Eker, S., Cömertpay, G., Konuşkan, Ö., Ülger, A. C., Öztürk, L., and Çakmak, İ. (2006). Effect of salinity stress on dry matter production and ion accumulation in hybrid maize varieties. *Turkish J. Agric. forestry* 30 (5), 365–373.

- Elhindi, K. M., El-Din, A. S., and Elgorban, A. M. (2017). The impact of arbuscular mycorrhizal fungi in mitigating salt-induced adverse effects in sweet basil (*Ocimum basilicum* L.). *Saudi J. Biol. Sci.* 24 (1), 170–179. doi: 10.1016/j.sjbs.2016.02.010
- El-Mejjaoui, Y., Lahrir, M., Naciri, R., Zeroual, Y., Mercatoris, B., Dumont, B., et al. (2022). How far can chlorophyll a fluorescence detect phosphorus status in wheat leaves (*Triticum durum* L.). *Environ. Exp. Bot.* 194, 104762. doi: 10.1016/j.envexpbot.2021.104762
- Fahad, S., Hussain, S., Matloob, A., Khan, F. A., Khaliq, A., Saud, S., et al. (2015). Phytohormones and plant responses to salinity stress: a review. *Plant Growth Regul.* 75 (2), 391–404. doi: 10.1007/s10725-014-0013-y
- Fujita, K., Kai, Y., Takayanagi, M., El-Shemy, H., and Adu-Gyamfi, J. J. (2004). Genotypic variability of pigeonpea in distribution of photosynthetic carbon at low phosphorus level. *Plant Science* 166(3), 641–649. doi: 10.1016/j.plantsci.2003.10.032
- Gao, Y., Wang, X., Shah, J. A., and Chu, G. (2020). Polyphosphate fertilizers increased maize (*Zea mays* L.) p, fe, zn, and Mn uptake by decreasing p fixation and mobilizing microelements in calcareous soil. *J. Soils Sediments* 20, 1–11. doi: 10.1007/s11368-019-02375-7
- García-Ortiz, L., Recio-Rodríguez, J. I., Rodríguez-Sánchez, E., Patino-Alonso, M. C., Agudo-Conde, C., Rodríguez-Martin, C., et al. (2012). Sodium and potassium intake present a J-shaped relationship with arterial stiffness and carotid intima-media thickness. *Atherosclerosis* 225 (2), 497–503. doi: 10.1016/j.atherosclerosis.2012.09.038
- Grattan, S. R., and Grieve, C. M. (1992). Mineral element acquisition and growth response of plants grown in saline environments. *Agriculture Ecosyst. Environ.* 38 (4), 275–300. doi: 10.1016/0167-8809(92)90151-Z
- Hasanuzzaman, M., Raihan, M. R. H., Masud, A. A. C., Rahman, K., Nowroz, F., Rahman, M., et al. (2021). Regulation of reactive oxygen species and antioxidant defence in plants under salinity. *Int. J. Mol. Sci.* 22 (17), 9326. doi: 10.3390/ijms22179326
- Hermans, C., Hammond, J. P., White, P. J., and Verbruggen, N. (2006). How do plants respond to nutrient shortage by biomass allocation? *Trends Plant Sci.* 11 (12), 610–617. doi: 10.1016/j.tplants.2006.10.007
- Hessini, K., Issaoui, K., Ferchichi, S., Saif, T., Abdelly, C., Siddique, K. H., et al. (2019). Interactive effects of salinity and nitrogen forms on plant growth, photosynthesis and osmotic adjustment in maize. *Plant Physiol. Biochem.* 139, 171–178. doi: 10.1016/j.plaphy.2019.03.005
- Ilangumaran, G., and Smith, D. L. (2017). Plant growth promoting rhizobacteria in amelioration of salinity stress: a systems biology perspective. *Front. Plant Sci.* 8, 1768. doi: 10.3389/fpls.2017.01768
- Isayenkov, S. V., and Maathuis, F. J. (2019). Plant salinity stress: many unanswered questions remain. *Front. Plant Sci.* 10, 80. doi: 10.3389/fpls.2019.00080
- Kalaji, H. M., Jajoo, A., Oukarroum, A., Brestic, M., Zivcak, M., Samborska, I. A., et al. (2016). Chlorophyll a fluorescence as a tool to monitor physiological status of plants under abiotic stress conditions. *Acta physiologiae plantarum* 38 (4), 1–11. doi: 10.1007/s11738-016-2113-y
- Kalaji, H. M., Račková, L., Paganová, V., Swoczyna, T., Rusinowski, S., and Sitko, K. (2018). Can chlorophyll-a fluorescence parameters be used as bio-indicators to distinguish between drought and salinity stress in *tilia cordata* mill? *Environ. Exp. Bot.* 152, 149–157. doi: 10.1016/j.envexpbot.2017.11.001
- Kalaji, H. M., Schansker, G., Brestic, M., Bussotti, F., Calatayud, A., Ferroni, L., et al. (2017). Frequently asked questions about chlorophyll fluorescence, the sequel. *Photosynthesis Res.* 132 (1), 13–66. doi: 10.1007/s11120-016-0318-y
- Kaya, C., Ashraf, M., Dikilitas, M., and Tuna, A. L. (2013). Alleviation of salt stress-induced adverse effects on maize plants by exogenous application of indoleacetic acid (IAA) and inorganic nutrients-a field trial. *Aust. J. Crop Sci.* 7 (2), 249–254. doi: 10.3316/informit.260789621744643
- Keisham, M., Mukherjee, S., and Bhatla, S. C. (2018). Mechanisms of sodium transport in plants—progresses and challenges. *Int. J. Mol. Sci.* 19 (3), 647. doi: 10.3390/ijms19030647
- Khan, A., Ahmad, I., Shah, A., Ahmad, F., Ghani, A., Nawaz, M., et al. (2013). Amelioration of salinity stress in wheat (*Triticum aestivum* L.) by foliar application of phosphorus. *Phyton (Buenos Aires)* 82 (2), 281–287.
- Khan, M. Z., Islam, M. A., Azom, M. G., and Amin, M. S. (2018). Short-term influence of salinity on uptake of phosphorus by *ipomoea aquatica*. *Int. J. Plant Soil Sci.* 25 (2), 1–9. doi: 10.9734/IJPS/2018/44822
- Khorshid, A. M., Moghadam, F. A., Bernousi, I., Khayamim, S., and Rajabi, A. (2018). Comparison of some physiological responses to salinity and normal conditions in sugar beet. *Indian J. Agric. Res.* 52 (4), 362–367. doi: 10.18805/IJAReA-320
- Khourchi, S., Elhassoufi, W., Loum, M., Ibnyasser, A., Haddine, M., Ghani, R., et al. (2022b). Phosphate solubilizing bacteria can significantly contribute to enhance p availability from polyphosphates and their use efficiency in wheat. *Microbiological Res.* 262, 127094. doi: 10.1016/j.micres.2022.127094
- Khourchi, S., Oukarroum, A., Tika, A., Delaplace, P., and Bargaz, A. (2022a). Polyphosphate application influences morpho-physiological root traits involved in p acquisition and durum wheat growth performance. *BMC Plant Biol.* 22 (1), 1–15. doi: 10.1186/s12870-022-03683-w
- Kim, H. J., and Li, X. (2016). Effects of phosphorus on shoot and root growth, partitioning, and phosphorus utilization efficiency in *lantana*. *HortScience* 51 (8), 1001–1009. doi: 10.21273/HORTSCI.51.8.1001
- Kim, H. J., Lynch, J. P., and Brown, K. M. (2008). Ethylene insensitivity impedes a subset of responses to phosphorus deficiency in tomato and petunia. *Plant Cell Environ.* 31 (12), 1744–1755. doi: 10.1111/j.1365-3040.2008.01886.x
- Koyro, H. W. (2006). Effect of salinity on growth, photosynthesis, water relations and solute composition of the potential cash crop halophyte *plantago coronopus* (L.). *Environ. Exp. Bot.* 56 (2), 136–146. doi: 10.1016/j.envexpbot.2005.02.001
- Kohler, J., Hernández, J. A., Caravaca, F., and Roldán, A. (2009). Induction of antioxidant enzymes is involved in the greater effectiveness of a PGPR versus AM fungi with respect to increasing the tolerance of lettuce to severe salt stress. *Environmental and Experimental Botany*, 65(2-3), 245–252. doi: 10.1016/j.envexpbot.2008.09.008
- Kulakovskaya, T. V., Vagabov, V. M., and Kulaev, I. S. (2012). Inorganic polyphosphate in industry, agriculture and medicine: Modern state and outlook. *Process Biochem.* 47, 1–10. doi: 10.1016/j.procbio.2011.10.028
- Kumari, R., Bhatnagar, S., Mehla, N., and Vashistha, A. (2022). Potential of organic amendments (AM fungi, PGPR, vermicompost and seaweeds) in combating salt stress—a review. *Plant Stress* 6, 100111. doi: 10.1016/j.stress.2022.100111
- Kumar, V., Khare, T., Sharma, M., and Wani, S. H. (2017). “ROS-induced signaling and gene expression in crops under salinity stress,” in *Reactive oxygen species and antioxidant systems in plants: role and regulation under abiotic stress* (Singapore: Springer), 159–184.
- Li, Z., Wu, N., Meng, S., Wu, F., and Liu, T. (2020). Arbuscular mycorrhizal fungi (AMF) enhance the tolerance of *euonymus maackii* rupr. at a moderate level of salinity. *PLoS One* 15 (4), e0231497. doi: 10.1371/journal.pone.0231497
- Li, M., Wu, Y. J., Yu, Z. L., Sheng, G. P., and Yu, H. Q. (2009). Enhanced nitrogen and phosphorus removal from eutrophic lake water by *ipomoea aquatica* with low-energy ion implantation. *Water Res.* 43 (5), 1247–1256. doi: 10.1016/j.watres.2008.12.013
- Lotfi, R., Ghassemi-Golezani, K., and Pessarakli, M. (2020). Salicylic acid regulates photosynthetic electron transfer and stomatal conductance of mung bean (*Vigna radiata* L.) under salinity stress. *Biocatalysis Agric. Biotechnol.* 26, 101635. doi: 10.1016/j.bcab.2020.101635
- Loudari, A., Benadis, C., Naciri, R., Soulaïmani, A., Zeroual, Y., Gharous, M. E., et al. (2020). Salt stress affects mineral nutrition in shoots and roots and chlorophyll a fluorescence of tomato plants grown in hydroponic culture. *J. Plant Interact.* 15 (1), 398–405. doi: 10.1080/17429145.2020.1841842
- Lynch, J. P., and Brown, K. M. (2006). “Whole plant adaptations to low phosphorus availability,” in *Plant-environment interactions*, 3rd edn. Ed. B. Huang (New York: Taylor and Francis).
- Manaa, A., Goussi, R., Derbali, W., Cantamessa, S., Abdelly, C., and Barbato, R. (2019). Salinity tolerance of quinoa (*Chenopodium quinoa* willd.) as assessed by chloroplast ultrastructure and photosynthetic performance. *Environ. Exp. Bot.* 162, 103–114. doi: 10.1016/j.envexpbot.2019.02.012
- Meng, X., Chen, W. W., Wang, Y. Y., Huang, Z. R., Ye, X., Chen, L. S., et al. (2021). Effects of phosphorus deficiency on the absorption of mineral nutrients, photosynthetic system performance and antioxidant metabolism in *citrus grandis*. *PLoS One* 16 (2), e0246944. doi: 10.1371/journal.pone.0246944
- Mohamed, H. I., El-Sayed, A. A., Rady, M. M., Caruso, G., Sekara, A., and Abdelhamid, M. T. (2021). Coupling effects of phosphorus fertilization source and rate on growth and ion accumulation of common bean under salinity stress. *PeerJ* 9, e11463. doi: 10.7717/peerj.11463
- Muhammad, H. M. D., Abbas, A., and Ahmad, R. (2022). Fascinating role of silicon nanoparticles to mitigate adverse effects of salinity in fruit trees: a mechanistic approach. *Silicon* 14, 1–8. doi: 10.1007/s12633-021-01604-4
- Muhammad, I., Shalmani, A., Ali, M., Yang, Q. H., Ahmad, H., and Li, F. B. (2021). Mechanisms regulating the dynamics of photosynthesis under abiotic stresses. *Front. Plant Sci.* 11, 615942. doi: 10.3389/fpls.2020.615942
- Nemeskéri, E., Neményi, A., Böcs, A., Pék, Z., and Helyes, L. (2019). Physiological factors and their relationship with the productivity of processing tomato under different water supplies. *Water* 11 (3), 586. doi: 10.3390/agronomy9080447
- Oukarroum, A., Bussotti, F., Goltsev, V., and Kalaji, H. M. (2015). Correlation between reactive oxygen species production and photochemistry of photosystems I and II in *lemna gibba* L. plants under salt stress. *Environ. Exp. Bot.* 109, 80–88. doi: 10.1016/j.envexpbot.2014.08.005
- Oukarroum, A., El Madidi, S., Schansker, G., and Strasser, R. J. (2007). Probing the responses of barley cultivars (*Hordeum vulgare* L.) by chlorophyll a fluorescence



OLKJIP under drought stress and re-watering. *Environ. Exp. Bot.* 60 (3), 438–446. doi: 10.1016/j.envexpbot.2007.01.002

Parvez, S., Abbas, G., Shahid, M., Amjad, M., Hussain, M., Asad, S. A., et al. (2020). Effect of salinity on physiological, biochemical and photostabilizing attributes of two genotypes of quinoa (*Chenopodium quinoa* Willd.) exposed to arsenic stress. *Ecotoxicology and environmental safety* 187, 109814. doi: 10.1016/j.ecoenv.2019.109814

Pereira da Silva, G., Prado, R. D. M., Wadt, P. G. S., Moda, L. R., and Caione, G. (2020). Accuracy of nutritional diagnostics for phosphorus considering five standards by the method of diagnosing nutritional composition in sugarcane. *J. Plant Nutr.* 43 (10), 1485–1497. doi: 10.1080/01904167.2020.1730902

Pérez-López, U., Robredo, A., Lacuesta, M., Mena-Petite, A., and Munoz-Rueda, A. (2012). Elevated CO<sub>2</sub> reduces stomatal and metabolic limitations on photosynthesis caused by salinity in hordeum vulgare. *Photosynthesis Res.* 111 (3), 269–283. doi: 10.1007/s11120-012-9721-1

Phang, T. H., Shao, G., Liao, H., Yan, X., and Lam, H. M. (2009). High external phosphate (Pi) increases sodium ion uptake and reduces salt tolerance of 'Pitolerant' soybean. *Physiologia Plantarum* 135 (4), 412–425. doi: 10.1111/j.1399-3054.2008.01200.x

Pulido-Bosch, A., Rigol-Sanchez, J. P., Vallejos, A., Andreu, J. M., Ceron, J. C., Molina-Sanchez, L., et al. (2018). Impacts of agricultural irrigation on groundwater salinity. *Environ. Earth Sci.* 77 (5), 1–14. doi: 10.1007/s12665-018-7386-6

Rady, M. M., El-Shewy, A. A., Seif El-Yazal, M. A., and Abdelaal, K. E. (2018). Response of salt-stressed common bean plant performances to foliar application of phosphorus (MAP). *Int. Lett. Natural Sci.* 72, 7–20. doi: 10.18052/www.scipress.com/ILNS.72.7

Rahimi, E., Nazari, F., Javadi, T., Samadi, S., and da Silva, J. A. T. (2021). Potassium-enriched clinoptilolite zeolite mitigates the adverse impacts of salinity stress in perennial ryegrass (*Lolium perenne* L.) by increasing silicon absorption and improving the K/Na ratio. *J. Environ. Manage.* 285, 112142. doi: 10.1016/j.jenvman.2021.112142

Renger, G., Pieper, J., Theiss, C., Trostmann, I., Paulsen, H., Renger, T., et al. (2011). Water soluble chlorophyll binding protein of higher plants: a most suitable model system for basic analyses of pigment–protein and pigment–protein interactions in chlorophyll protein complexes. *Journal of plant physiology* 168 (12), 1462–1472. doi: 10.1016/j.jplph.2010.12.005

Rewald, B., Raveh, E., Gendler, T., Ephraim, J. E., and Rachmilevitch, S. (2012). Phenotypic plasticity and water flux rates of citrus root orders under salinity. *J. Exp. Bot.* 63 (7), 2717–2727. doi: 10.1093/jxb/err457

Rodríguez-Martín, J. A., Gutiérrez, C., Torrijos, M., and Nanos, N. (2018). Wood and bark of *Pinus halepensis* as archives of heavy metal pollution in the Mediterranean Region. *Environmental Pollution* 239, 438–447. doi: 10.1016/j.envpol.2018.04.036

Rubio, L., Linares-Rueda, A., García-Sánchez, M. J., and Fernández, J. A. (2005). Physiological evidence for a sodium-dependent high-affinity phosphate and nitrate transport at the plasma membrane of leaf and root cells of *zostera marina* L. *J. Exp. Bot.* 56 (412), 613–622. doi: 10.1093/jxb/eri053

Rychter, A. M., Rao, I. M., and Cardoso, J. A. (2018). "Role of phosphorus in photosynthetic carbon assimilation and partitioning," in *Handbook of photosynthesis* (CRC Press, Boca Raton), 603–625. doi: 10.1201/9781315372136

Sarkar, R. K., and Ray, A. (2016). Submergence-tolerant rice withstands complete submergence even in saline water: Probing through chlorophyll a fluorescence induction OJIP transients. *Photosynthetica* 54 (2), 275–287. doi: 10.1007/s11099-016-0082-4

Schansker, G., Tóth, S. Z., and Strasser, R. J. (2006). Dark recovery of the chl a fluorescence transient (OJIP) after light adaptation: the qT-component of non-photochemical quenching is related to an activated photosystem I acceptor side. *Biochim. Biophys. Acta (BBA)-Bioenergetics* 1757 (7), 787–797. doi: 10.1016/j.bbabi.2006.04.019

Shabala, S., and Munns, R. (2017). "Salinity stress: physiological constraints and adaptive mechanisms," in *Plant stress physiology* (Wallingford UK: Cabi), 24–63.

Sharma, A., Kumar, V., Shahzad, B., Ramakrishnan, M., Singh Sidhu, G. P., Bali, A. S., et al. (2020). Photosynthetic response of plants under different abiotic stresses: a review. *J. Plant Growth Regul.* 39, 509–531. doi: 10.1007/s00344-019-10018-x

Shibli, R. A., Sawwan, J., Swaidat, I., and Tahat, M. (2001). Increased phosphorus mitigates the adverse effects of salinity in tissue culture. *Commun. Soil Sci. Plant Anal.* 32 (3–4), 429–440. doi: 10.1081/CSS-100103019

Shoukat, E., Abideen, Z., Ahmed, M. Z., Gulzar, S., and Nielsen, B. L. (2019). Changes in growth and photosynthesis linked with intensity and duration of salinity in phragmites karka. *Environ. Exp. Bot.* 162, 504–514. doi: 10.1016/j.envexpbot.2019.03.024

Singh, N., Singh, G., and Khanna, V. (2016). Growth of lentil (*Lens culinaris* medikus) as influenced by phosphorus, rhizobium and plant growth promoting rhizobacteria. *Indian J. Agric. Res.* 50 (6), 567–572. doi: 10.18805/ijare.v0i0F.4573

Stirbet, A. (2012). Chlorophyll a fluorescence induction: a personal perspective of the thermal phase, the J–I–P rise. *Photosynthesis Res.* 113 (1), 15–61. doi: 10.1007/s11120-012-9754-5

Strasser, R. J., Tsimilli-Michael, M., and Srivastava, A. (2004). "Analysis of the chlorophyll a fluorescence transient," in *Chlorophyll a fluorescence* (Dordrecht: Springer), 321–362.

Tang, H., Niu, L., Wei, J., Chen, X., and Chen, Y. (2019). Phosphorus limitation improved salt tolerance in maize through tissue mass density increase, osmolytes accumulation, and na<sup>+</sup> uptake inhibition. *Front. Plant Sci.* 10, 856. doi: 10.3389/fpls.2019.00856

Tirry, N., Kouchou, A., Laghmari, G., Lemjereb, M., Hnadi, H., Amrani, K., et al. (2021). Improved salinity tolerance of medicago sativa and soil enzyme activities by PGPR. *Biocatalysis Agric. Biotechnol.* 31, 101914. doi: 10.1016/j.bcab.2021.101914

Tsimilli-Michael, M., and Strasser, R. J. (2008). "In vivo assessment of stress impact on plant's vitality: applications in detecting and evaluating the beneficial role of mycorrhization on host plants," in *Mycorrhiza* (Berlin, Heidelberg: Springer), 679–703.

Wahid, F., Fahad, S., Danish, S., Adnan, M., Yue, Z., Saud, S., et al. (2020). Sustainable management with mycorrhizae and phosphate solubilizing bacteria for enhanced phosphorus uptake in calcareous soils. *Agriculture* 10 (8), 334. doi: 10.3390/agriculture10080334

Wang, X., Gao, Y., Hu, B., and Chu, G. (2019). Comparison of the hydrolysis characteristics of three polyphosphates and their effects on soil p and micronutrient availability. *Soil Use Manag.* 35, 664–674. doi: 10.1111/sum.12526

Wieneke, S., Balzarolo, M., Asard, H., Abd Elgawad, H., Peñuelas, J., Rascher, U., et al. (2022). Fluorescence ratio and photochemical reflectance index as a proxy for photosynthetic quantum efficiency of photosystem II along a phosphorus gradient. *Agric. For. Meteorology* 322, 109019. doi: 10.1016/j.agrformet.2022.109019

Wilkinson, S., and Davies, W. J. (2002). ABA-based chemical signalling: the co-ordination of responses to stress in plants. *Plant Cell Environ.* 25 (2), 195–210. doi: 10.1046/j.0016-8025.2001.00824.x

Xiao, L., Yuan, G., Feng, L., Shah, G. M., and Wei, J. (2022). Biochar to reduce fertilizer use and soil salinity for crop production in the yellow river delta. *J. Soil Sci. Plant Nutr.* 22, 1–12. doi: 10.1007/s42729-021-00747-y

Xue, D., Huang, Y., Zhang, X., Wei, K., Westcott, S., Li, C., et al. (2009). Identification of QTLs associated with salinity tolerance at late growth stage in barley. *Euphytica* 169 (2), 187–196. doi: 10.1007/s10681-009-9919-2

Yang, A., Akhtar, S. S., Li, L., Fu, Q., Li, Q., Naem, M. A., et al. (2020). Biochar mitigates combined effects of drought and salinity stress in quinoa. *Agronomy* 10 (6), 912. doi: 10.3390/agronomy10060912

Yan, N., and Marschner, P. (2012). Response of microbial activity and biomass to increasing salinity depends on the final salinity, not the original salinity. *Soil Biol. Biochem.* 53, 50–55. doi: 10.1016/j.soilbio.2012.04.028

Zhao, C., Zhang, H., Song, C., Zhu, J. K., and Shabala, S. (2020). Mechanisms of plant responses and adaptation to soil salinity. *Innovation* 1 (1), 100017. doi: 10.1016/j.xinn.2020.100017

Zribi, O., Abdelli, C., and Debez, A. (2011). Interactive effects of salinity and phosphorus availability on growth, water relations, nutritional status and photosynthetic activity of barley (*Hordeum vulgare* L.). *Plant Biology*, 13(6), 872–880. doi: 10.1111/j.1438-8677.2011.00450.x

Zribi, O., Mbarki, S., Metoui, O., Trabelsi, N., Zribi, F., Ksouri, R., et al. (2021). Salinity and phosphorus availability differentially affect plant growth, leaf morphology, water relations, solutes accumulation and antioxidant capacity in *aeuropus littoralis*. *Plant Biosystems-An Int. J. Dealing all Aspects Plant Biol.* 155 (4), 935–943. doi: 10.1080/11263504.2020.1810808





## OPEN ACCESS

EDITED BY  
Pavel Kerchev,  
Mendel University in Brno, Czechia

REVIEWED BY  
Wei Huang,  
Kunming Institute of Botany (CAS),  
China  
Abdallah Oukarroum,  
Mohammed VI Polytechnic University,  
Morocco

\*CORRESPONDENCE  
Tatiana Swoczyna  
tatiana\_swoczyna@sggw.edu.pl  
Hazem M. Kalaji  
hazem@kalaji.pl

SPECIALTY SECTION  
This article was submitted to  
Plant Abiotic Stress,  
a section of the journal  
Frontiers in Plant Science

RECEIVED 19 September 2022  
ACCEPTED 14 November 2022  
PUBLISHED 14 December 2022

CITATION  
Swoczyna T, Kalaji HM, Bussotti F,  
Mojski J and Pollastrini M (2022)  
Environmental stress - what can we  
learn from chlorophyll a fluorescence  
analysis in woody plants? A review.  
*Front. Plant Sci.* 13:1048582.  
doi: 10.3389/fpls.2022.1048582

COPYRIGHT  
© 2022 Swoczyna, Kalaji, Bussotti,  
Mojski and Pollastrini. This is an open-  
access article distributed under the  
terms of the [Creative Commons  
Attribution License \(CC BY\)](#). The use,  
distribution or reproduction in other  
forums is permitted, provided the  
original author(s) and the copyright  
owner(s) are credited and that the  
original publication in this journal is  
cited, in accordance with accepted  
academic practice. No use,  
distribution or reproduction is  
permitted which does not comply with  
these terms.

# Environmental stress - what can we learn from chlorophyll a fluorescence analysis in woody plants? A review

Tatiana Swoczyna<sup>1\*</sup>, Hazem M. Kalaji<sup>2\*</sup>, Filippo Bussotti<sup>3</sup>,  
Jacek Mojski<sup>4,5</sup> and Martina Pollastrini<sup>3</sup>

<sup>1</sup>Department of Environment Protection and Dendrology, Institute of Horticultural Sciences, Warsaw University of Life Sciences SGGW, Warsaw, Poland, <sup>2</sup>Department of Plant Physiology, Institute of Biology, Warsaw University of Life Sciences SGGW, Warsaw, Poland, <sup>3</sup>Department of Agriculture, Food, Environment and Forestry, University of Florence, Florence, Italy, <sup>4</sup>Twój Świat Jacek Mojski, Łukow, Poland, <sup>5</sup>Fundacja Zielona Infrastruktura, Łukow, Poland

Chlorophyll a fluorescence (ChF) signal analysis has become a widely used and rapid, non-invasive technique to study the photosynthetic process under stress conditions. It monitors plant responses to various environmental factors affecting plants under experimental and field conditions. Thus, it enables extensive research in ecology and benefits forestry, agriculture, horticulture, and arboriculture. Woody plants, especially trees, as organisms with a considerable life span, have a different life strategy than herbaceous plants and show more complex responses to stress. The range of changes in photosynthetic efficiency of trees depends on their age, ontogeny, species-specific characteristics, and acclimation ability. This review compiles the results of the most commonly used ChF techniques at the foliar scale. We describe the results of experimental studies to identify stress factors that affect photosynthetic efficiency and analyse the experience of assessing tree vigour in natural and human-modified environments. We discuss both the circumstances under which ChF can be successfully used to assess woody plant health and the ChF parameters that can be useful in field research. Finally, we summarise the advantages and limitations of the ChF method in research on trees, shrubs, and woody vines.

## KEYWORDS

forests, JIP-test, PAM fluorescence, shrubs, trees, urban trees

## Introduction

Long-lived woody plants, i.e., trees and shrubs, build up their structure over the years and adapt it to environmental and climatic conditions; moreover, temporal variations in the length and intensity of periods of cold, heat, drought, etc., provide some flexibility in responding to environmental stressors (Kozłowski et al., 2012). From leaf emergence,

woody plants tend to extend leaf life to the end of the season (deciduous species) or beyond (evergreen species), whereas, in herbaceous plants, leaf life is usually shortened due to shading of primary leaves and investment in newly emerging leaves (Diemer et al., 1992; Kikuzawa, 1995; Kikuzawa and Ackerly, 1999). In the early stages, seedlings and young trees (saplings) differ from mature specimens in terms of leaf structure and photosynthetic activity (Bond, 2000; Niinemets, 2002; Mediavilla et al., 2014). Because of their longevity, woody plants have a greater potential to recover from damage (Haukioja and Koricheva, 2000). The continuous (annual) growth of trees is under the control of growth regulators and biochemical and physical balances that tend to keep various processes and structures in equilibrium (Kozłowski et al., 2012).

In the face of environmental stress, woody plants have evolved various mechanisms to protect themselves from damage and adverse conditions (Bussotti and Pollastrini, 2021). These mechanisms operate on a plant-wide level. The results of experiments conducted under controlled conditions provide the basis for interpreting plant responses observed in the environment. Usually, a stressor is applied at a high intensity so that the stress response becomes evident and clear conclusions can be drawn (Kalaji et al., 2018). Most of these experiments are conducted on seedlings or small saplings, i.e., in the early stages of life. However, the complexity of factors affecting woody plants and the variability in the intensity of these factors during their life (extreme summers or winters, human-induced changes in the soil environment, etc.) can sometimes make it difficult to explain the background of the responses of the trees/shrubs studied (Swoczyna and Latocha, 2020). The complexity of environmental conditions may affect the magnitude and duration of the response to stress, e.g., limited access to nitrogen in the soil may increase the effect of drought stress, triggering a change in growth strategy and physiology (Ögren, 1988). Indeed, one type of response identified as a stress response, e.g., defoliation, may not be mirrored by another, e.g., reduced photosynthetic efficiency of the remaining leaves or shoots (Desotgiu et al., 2012b; Suchocka et al., 2021).

In recent decades, the diversity of chlorophyll *a* fluorescence (ChF) research has increased considerably, and for the last decade there has been a tremendous development in this discipline (Baba et al., 2019). During this time, methods and protocols have been developed and tested, as well as instruments whose design and operating principles have been refined (Strasser et al., 2004; Stirbet and Govindjee, 2011; Tsimilli-Michael, 2020). This optical method, in contrast to, for example, time-consuming infrared gas exchange measurements or chemical analyses of collected samples, enables numerous non-destructive and non-invasive experiments on plants in which their photosynthetic properties are recorded in response to environmental conditions (Kalaji et al., 2014b). The available instruments are portable and can be used in field conditions, allowing the study of plants both in plantations and in natural or urban environments (Christen et al., 2007; Fini et al., 2009; Ugolini et al., 2012; Pollastrini et al., 2016b). In addition, the ChF method

examines the efficiency of the photosynthetic apparatus, i.e., the current state or conformation of photosystems and their compounds, rather than the process of photosynthesis itself, which is why it is possible to perform measurements on detached leaves (Percival and Fraser, 2002). Advances in the development of easy-to-use equipment have expanded the application of the ChF technique in numerous research studies in agriculture, horticulture, arboriculture, forestry, and environmental studies, as well as in practical applications in commerce. The different techniques for measuring ChF provide specific parameters whose importance overlaps to some extent. Some review articles have already provided an overview of the application of ChF measurements in stress detection using different techniques: pulse amplitude modulated ChF (Baker and Rosenqvist, 2004; Murchie and Lawson, 2013), chlorophyll fluorescence imaging techniques (Baker and Rosenqvist, 2004; Baker, 2008; Gorbe and Calatayud, 2012), chlorophyll fluorescence induction curve analysis (OJIP analysis) based mainly on crop research (Kalaji et al., 2016) or forest research (Pollastrini et al., 2016b; Bussotti et al., 2020).

The measured ChF signal is mainly from PSII and is the re-emitted excess energy that was neither involved in photochemical processes nor dissipated as heat. Photochemistry, heat dissipation, and fluorescence are competing processes, so fluorescence measurements can be used to evaluate the balance between photochemistry and non-photochemical dissipation of absorbed light (Maxwell, 2000). Chlorophyll fluorescence measurements made directly on leaf samples provide numerous parametric data that allow deeper analysis of physiological processes associated with the light phase of photosynthesis. Fluorimeters with different operating principles are used for this purpose (Baker and Rosenqvist, 2004; Kalaji et al., 2014b; Banks, 2017; Padhi et al., 2021). Signals of chlorophyll fluorescence can be detected from samples previously adapted to darkness (when all photochemical reactions have been quenched) as well as from samples in ambient light. Separate protocols had to be developed for these two approaches. Adaptation of a leaf sample to darkness allows suppression of all light-dependent processes. For rapid exposure to actinic saturating light, two of the most commonly used values,  $F_0$  and  $F_M$ , are determined and used to calculate the maximum efficiency of the photosystem II,  $F_V/F_M$ . The latter ratio has long been attractive for determining differences in photosynthetic performance between plants (Ögren, 1990; Percival, 2002).

Pulse amplitude modulated fluorimeters use actinic light (blue or red), which stimulates photosynthesis, and additional emitted measurement light, which is used to study the state of the photosynthetic system (Baker and Rosenqvist, 2004; Kalaji et al., 2014b). The measuring light is applied with constant pulse amplitude. The on and off switching of the actinic light is synchronised to be in the middle of the dark periods between the measurement light pulses and is used to evaluate the maximum fluorescence yield. Any non-modulated fluorescence signal (e.g., from daylight) is completely suppressed by the amplifier system in the PAM fluorimeter (Schreiber, 2004). PAM method allows

evaluation of the so-called “photochemical quenching”,  $q_P$ , which is related to photochemical energy utilisation by charge separation at the reaction centres of PSII. “Non-photochemical quenching”, a non-radiative dissipation of energy into heat, can be expressed in two ways,  $q_N$  (Schreiber, 2004) or NPQ (Bilger and Björkman, 1990). The operating efficiency of PSII photochemistry is determined by calculating  $\Delta F/F_M'$ , also called  $\Phi_{PSII}$  (Genty and Briantais, 1989; Murchie and Lawson, 2013). The possibility of measuring the incident photosynthetically active photon flux density (PPFD) with some PAM fluorimeters allows the calculation of another parameter, the estimated electron transport rate (ETR) (Flexas et al., 1999). The theoretical basis, assumptions regarding the parameters of PAM, and their calculations have been described in detail in the works of Genty and Briantais, 1989; Bilger and Björkman (1990); Maxwell (2000); Schreiber (2004); Baker (2008), and Murchie and Lawson (2013) (Table 1).

The fast (or prompt) fluorescence analysis is based on the initial fluorescence signal after at least 20 minutes of dark adaptation of a leaf sample followed by a saturating pulse of actinic light (Strasser et al., 2004; Kalaji et al., 2014b). A fluorescence rise plotted on a logarithmic scale shows the so-called steps (L-, K-, J-, I-step) reflecting different phenomena occurring in and around PSII. This visualisation is often called the OJIP transient or the OJIP curve. The first part of the transient curve (O-I) expresses the photochemical events until the primary electron acceptor  $Q_A$  is reduced (Strasser et al., 2004; Bussotti et al., 2011a). The J-P section of OJIP transient (thermal phase) is related to electron transfer to end electron acceptors (Bussotti et al., 2011a). Prompt fluorescence analysis allows the

assessment of the probability that a trapped exciton moves an electron into the electron transport chain beyond  $Q_A$  ( $ET_0/TR_0 = \Psi_{E_0}$ ) and the probability that the moved electron reaches PSI acceptors ( $RE_0/ET_0 = \delta_{R_0}$ ) (Strasser et al., 2004; Strasser et al., 2010). Additionally, specific energy fluxes expressed per active reaction centre (RC) and so-called ‘phenomenological energy fluxes per cross-section’ (CS) can be calculated, as absorption (ABS), trapping ( $TR_0$ ), thermal dissipation ( $DI_0$ ), electron transport rate beyond RC of photosystem II ( $ET_0$ ) and electron movement until end electron acceptors at the acceptor side of PSI ( $RE_0$ ). The parameter RC/CS reflects the total amount of active reaction centres per cross-section (Strasser et al., 2004). The analysis of OJIP parameters may be widened by analysis of additional steps on the OJIP curve, L-step, reflecting a decrease of energetic connectivity between PSII antennae, and K-step, which coincides with a limitation in the donor side of PSII (Strasser et al., 2004; Oukarroum et al., 2007). In many papers combined efficiency of electron transport up to end electron acceptors of PSI,  $\delta_{R_0}$ , and the efficiency of a movement of an electron into the electron transport chain beyond  $Q_A$ ,  $\Psi_{E_0}$ , appeared to be a good indicator of the stress response of plants (Bussotti et al., 2020). This combined parameter, denoted as  $\Psi_{RE_0}$  or  $\Delta V_{IP}$ , shows the total efficiency of electron transport from PSII to PSI. Finally, two integrative parameters, so-called performance indices, were proposed by Strasser et al., 2004; Strasser et al., 2010, i.e. Performance Index on absorption basis ( $PI_{ABS}$ ) and total Performance Index ( $PI_{total}$ ). The calculations of all these parameters have been described in the papers noted above (Table 2).

TABLE 1 Description of general and commonly used PAM chlorophyll fluorescence parameters.

Fluorescence parameters	Description	References
General parameters		
$F_0$	initial fluorescence obtained in a dark adapted sample	Schreiber, 2004; Strasser et al., 2004
$F_M$	maximum fluorescence after illumination of a dark adapted sample	Schreiber, 2004; Strasser et al., 2004
$F_v/F_M = (F_M - F_0)/F_M$	maximum quantum yield of PSII photochemistry	Schreiber, 2004; Strasser et al., 2004
Modulate fluorescence parameters		
$F_0'$	minimal fluorescence yield measured shortly after darkening of an illuminated sample	Schreiber, 2004
$F_M'$	maximum fluorescence after illumination of a light adapted sample	Schreiber, 2004
$F_S = F_t$	steady-state value of fluorescence yield	Maxwell, 2000
$q_P = (F_M' - F_S)/(F_M' - F_0')$	photochemical quenching related to photochemical energy utilisation by charge separation at the reaction centres of PSII	Schreiber, 2004
$q_N = 1 - (F_M' - F_0')/(F_M - F_0)$	non-photochemical quenching related to a rate of non radiative energy dissipation into heat	Schreiber, 2004
$NPQ = (F_M - F_M')/F_M'$	non-photochemical quenching	Bilger and Björkman, 1990
$\Phi_{PSII} = \Delta F/F_M' = (F_M' - F_S)/F_M'$	operational efficiency of PSII photochemistry	Genty and Briantais, 1989
$ETR = \Phi_{PSII} \times PPFD \times 0.5$	electron transport rate	Flexas et al., 1999

TABLE 2 Description of commonly used prompt fluorescence (JIP-test) parameters.

Fluorescence parameters	Description	References
$F_0 = ABS/CS_0$	initial fluorescence obtained in a dark adapted sample	Strasser et al., 2004
$F_L = F_{150}$	fluorescence at 150 $\mu$ s after illumination of a dark adapted sample	Oukarroum et al., 2007
$F_K = F_{300}$	fluorescence at 300 $\mu$ s after illumination of a dark adapted sample	Strasser et al., 2004
$F_J = F_{2ms}$	fluorescence at 2 ms after illumination of a dark adapted sample	Strasser et al., 2004
$F_I = F_{30ms}$	fluorescence at 30 ms after illumination of a dark adapted sample	Strasser et al., 2004
$F_M = F_P$	maximum fluorescence after illumination of a dark adapted sample	Strasser et al., 2004
$V_L = (F_{150} - F_0)/(F_M - F_0)$	relative variable fluorescence at 150 $\mu$ s after illumination of a dark adapted sample	Oukarroum et al., 2007
$V_K = (F_{300} - F_0)/(F_M - F_0)$	relative variable fluorescence at 300 $\mu$ s after illumination of a dark adapted sample	Strasser et al., 2004
$V_J = (F_{2ms} - F_0)/(F_M - F_0)$	relative variable fluorescence at 2 ms after illumination of a dark adapted sample	Strasser et al., 2004; Strasser et al., 2010
$V_I = (F_{30ms} - F_0)/(F_M - F_0)$	relative variable fluorescence at 30 ms after illumination of a dark adapted sample	Strasser et al., 2004; Strasser et al., 2010
$V_K/V_J$	efficiency of electron flow from OEC to PSII reaction centres	Strasser et al., 2004; Strasser et al., 2010
$M_0 = 4 (F_{300} - F_0)/(F_M - F_0)$	approximated initial slope of the fluorescence transient, expressing the rate of RCs' closure	Strasser et al., 2004
$\phi_{P_0} = TR_0/ABS = F_V/F_M = (F_M - F_0)/F_M$	maximum quantum yield of PSII photochemistry	Strasser et al., 2004
$\psi_o = ET_0/TR_0 = (F_M - F_{2ms})/(F_M - F_0) = 1 - V_J$	probability that a trapped exciton moves an electron into the electron transport chain beyond $Q_A$	Strasser et al., 2004; Strasser et al., 2010
$\delta_{Ro} = RE_0/ET_0 = (F_M - F_{30ms})/(F_M - F_{2ms})$	probability that an electron from the intersystem electron carriers is transferred to reduce end electron acceptors at the PSI acceptor side	Strasser et al., 2010
$\psi_{RE_0} = \Delta V_{IP} = \psi_{E_0} \times \delta_{Ro}$	total efficiency of electron transport from PSII to PSI	Strasser et al., 2010; Bussotti et al., 2020
$RC/ABS = \gamma_{RC}/(1 - \gamma_{RC}) = \phi_{P_0}(V_J/M_0)$	$Q_A$ reducing RCs per PSII antenna chlorophyll	Strasser et al., 2004
$RC/CS_0 = \phi_{P_0}(V_J/M_0) (ABS/CS_0)$	density of active RCs ( $Q_A$ reducing RCs) per cross section at point 0	Strasser et al., 2004
$PI_{ABS} = RC/ABS \times \phi_{P_0}/(1 - \phi_{P_0}) \times \psi_{E_0}/(1 - \psi_{E_0})$	performance index (potential) for energy conservation from photons absorbed by PSII to the reduction of intersystem electron acceptors	Strasser et al., 2004
$PI_{total} = RC/ABS \times \phi_{P_0}/(1 - \phi_{P_0}) \times \psi_{E_0}/(1 - \psi_{E_0}) \times \delta_{Ro}/(1 - \delta_{Ro})$	performance index (potential) for energy conservation from photons absorbed by PSII to the reduction of PSI end electron acceptors	Strasser et al., 2010

In this paper, we review the research conducted to date on woody plants using ChF methods to monitor their response to different types of environmental stress. We have compiled the results of two of the most commonly used techniques performed at the foliar scale: PAM and prompt fluorescence, in particular, the JIP-test. The first part of the article describes experimental studies to identify stress factors affecting photosynthetic efficiency. Then, the role of photosynthetic efficiency screening in assessing tree vigour in natural and human-altered environments is analysed. Finally, we summarise the advantages and limitations of the ChF method in research on trees, shrubs, and woody vines.

## Chlorophyll *a* fluorescence measurements in laboratory and field experiments

ChF measurements, conducted to evaluate the effects of stress on the efficiency of the photosynthetic apparatus, are used to establish optimal conditions for crop production in the context of producing plant biomass, increasing yields, improving vigour, or selecting genotypes with greater resistance. Such

research is widespread in annual crops such as wheat, rice, maize, and vegetables (Brestic and Zivcak, 2013; Kalaji et al., 2014a). However, there are also numerous papers describing experiments on woody plants (Table 3). The latter focused on crop production, the improvement of plant material for horticulture and urban greening, and applied studies in forest ecology.

## Drought

Drought stress is the most commonly discussed problem in experiments using chlorophyll *a* fluorescence. Since water is the source of electrons used in the light-dependent photosynthetic process, the unimpeded availability of water may be critical for the successful conversion of light energy. Under moderate drought, the downregulation of the photosynthesis is mainly restricted by a decrease in stomatal conductance rather than the water-splitting reaction. Nevertheless, under severe drought the PSII efficiency may also be affected. Indeed, some experiments performed on detached leaves showed a correlation between the degree of dehydration and changes in the maximum quantum



TABLE 3 Chlorophyll a fluorescence measurements in stress detection in woody plants: species examined in the cited literature.

Stress factor	Reference	Examined species
Drought	Ögren, 1990; Percival and Fraser, 2002; Percival et al., 2006; Bacelar et al., 2007; Christen et al., 2007; Fini et al., 2009; Bussotti et al., 2010; Faraloni et al., 2011; Wang et al., 2012; Guha et al., 2013; Lee et al., 2016; Falqueto et al., 2017; Banks, 2018; Kalaji et al., 2018; Guadagno et al., 2021; Mihaljević et al., 2021; Fini et al., 2022	<i>Olea europaea</i> ; <i>Acer platanoides</i> , <i>Acer pseudoplatanus</i> , <i>Acer campestre</i> ; <i>Quercus petraea</i> ; <i>Vitis vinifera</i> ; <i>Olea europaea</i> ; <i>Hevea brasiliensis</i> ; <i>Tilia platyphyllos</i> , <i>Acer platanoides</i> ; <i>Celtis australis</i> , <i>Fraxinus ornus</i> ; <i>Pinus ponderosa</i> , <i>Populus tremuloides</i> ; <i>Morus indica</i> , <i>Tilia cordata</i> ; <i>Populus x sibirica</i> ; <i>Prunus avium</i> ; <i>Salix</i> sp.; 9 <i>Fraxinus</i> species/cultivars; 30 woody species; <i>Vitis amurensis</i>
Light	Björkman and Powles, 1984; Brodribb and Hill, 1997; Hamerlynck, 2001; Gonçalves et al., 2001; Lichtenthaler et al., 2004; Dias and Marengo, 2007; Cascio et al., 2010; Desotgiu et al., 2012a; Song and Li, 2016	<i>Nerium oleander</i> ; Podocarpaceae family; <i>Fagus sylvatica</i> ; <i>Minuartia guianensis</i> ; <i>Ailanthus altissima</i> ; <i>Platanus hybrida</i> ; <i>Euonymus fortunei</i> ; <i>Bombacopsis macrocalyx</i> , <i>Eugenia cumini</i> , <i>Iryanthera macrophylla</i> , <i>Senna reticulata</i>
UV-B radiation	Bavcon et al., 1996; Albert et al., 2005; Trošć Sedej and Rupar, 2013; Grifoni et al., 2016	<i>Salix arctica</i> ; <i>Picea abies</i> ; <i>Arbutus unedo</i> , <i>Vitis vinifera</i> ; <i>Fagus sylvatica</i> , <i>Picea abies</i>
Heat	Percival, 2005; Duan et al., 2015; Esperon-Rodriguez et al., 2021	<i>Quercus ilex</i> , <i>Q. robur</i> , <i>Q. rubra</i> ; <i>Malus domestica</i> ; <i>Elaeocarpus reticulatus</i> , <i>Lophostemon confertus</i> , <i>Lagerstroemia indica</i> , <i>Liriodendron tulipifera</i>
Chilling, freezing	García-Plazaola et al., 1999; Jiang et al., 1999; Hakam et al., 2000; Percival and Fraser, 2001; Bussotti, 2004; Martínez-Ferri et al., 2004; Oliveira and Peñuelas, 2005; de Oliveira et al., 2009; Pflug and Brüggemann, 2012; Vitale et al., 2012; Míguez et al., 2017; Swoczyna et al., 2020	<i>Quercus ilex</i> ; <i>Coffea arabica</i> ; <i>Quercus ilex</i> ; <i>Rosa rugosa</i> , <i>Rosa hybrida</i> ; <i>Vitis labruscana</i> ; <i>Juniperus phoenicea</i> , <i>Pinus halepensis</i> , <i>Q. ilex</i> , <i>Q. coccifera</i> ; different subalpine species; <i>Cistus albidus</i> , <i>Quercus ilex</i> ; 6 <i>Crataegus</i> species/cultivars; <i>Quercus ilex</i> ; shrubs and herbaceous perennials, 23 species/cultivars; <i>Phillyrea angustifolia</i>
Chlorophyll deficiency	Torres Netto et al. (2005); Percival et al., 2008; de Oliveira et al., 2009; Chen and Cheng, 2010; Swoczyna et al., 2010b; Castro et al., 2011	<i>Carica papaya</i> ; <i>Malus domestica</i> ; <i>Coffea arabica</i> ; <i>Acer pseudoplatanus</i> , <i>Fagus sylvatica</i> , <i>Quercus robur</i> ; <i>Acer campestre</i> , <i>Quercus rubra</i> , <i>Gleditsia triacanthos</i> , <i>Pyrus calleryana</i> , <i>Platanus x hispanica</i> 'Acerifolia', <i>Ginkgo biloba</i> , <i>Tilia cordata</i> , <i>Tilia x europaea</i>
Nitrogen deficiency	DaMatta et al., 2002; Percival et al., 2008; Nikiforou and Manetas, 2011; De Castro et al., 2014; Swoczyna et al., 2019	<i>Coffea canephora</i> ; <i>Carica papaya</i> ; <i>Pistacia lentiscus</i> ; <i>Acer pseudoplatanus</i> , <i>Fagus sylvatica</i> , <i>Quercus robur</i> ; <i>Actinidia arguta</i>
Phosphorus deficiency	Bosa et al., 2014	<i>Pyrus communis</i>
Salinity	Percival and Fraser, 2001; Percival et al., 2003; Percival, 2005; Naumann et al., 2008; Kalaji et al., 2018; Bashir et al., 2021	<i>Moringa oleifera</i> ; <i>Tilia cordata</i> ; <i>Myrica cerifera</i> ; <i>Acer pseudoplatanus</i> , <i>Fagus sylvatica</i> , <i>Quercus robur</i> ; 30 <i>Acer</i> species/cultivars; <i>Quercus ilex</i> , <i>Q. robur</i> , <i>Q. rubra</i>
Ozone	Gerosa et al., 2003; Gravano et al., 2004; Bussotti et al., 2005; Bussotti et al., 2007a; Bussotti et al., 2007b; Gielen et al., 2007; Cascio et al., 2010; Desotgiu et al., 2012b; Gottardini et al., 2014; Pollastrini et al., 2014a	<i>Acer pseudoplatanus</i> , <i>Ailanthus altissima</i> , <i>Fagus sylvatica</i> , <i>Fraxinus excelsior</i> , <i>Viburnum lantana</i> ; <i>Fagus sylvatica</i> , <i>Quercus robur</i> , <i>Populus nigra</i> ; <i>Populus maximowiczii</i> x <i>P. xberolinensis</i> (Oxford clone); <i>Viburnum lantana</i> ; <i>Populus maximowiczii</i> x <i>P. xberolinensis</i> (Oxford clone); <i>Viburnum lantana</i> , <i>Fraxinus excelsior</i> , <i>Populus nigra</i> , <i>Prunus avium</i> , <i>Quercus robur</i>
Gaseous air pollutants	Pukacki, 2000; Odaş-Albrigtsen et al., 2000; Alessio et al., 2002; Naidoo and Chirkoot, 2004; Matsushima et al., 2009; Fusaro et al., 2021; Wang et al., 2019	<i>Pinus pinea</i> , <i>Quercus ilex</i> ; <i>Hibiscus</i> sp.; <i>Avicennia marina</i> ; <i>Betula pubescens</i> , <i>Pinus sylvestris</i> and 5 shrub species; <i>Morus alba</i>
Heavy metals	Kitao et al., 1998; Pereira et al., 2000; Dezhban et al., 2015; Zhang et al., 2020; Hachani et al., 2021; Reyes et al., 2022	<i>Robinia pseudoacacia</i> ; <i>Pinus halepensis</i> ; <i>Betula ermanii</i> , <i>Alnus hirsuta</i> ; 4 <i>Citrus</i> species/cultivars; <i>Quercus ilex</i> , <i>Nerium oleander</i> , <i>Pittosporum tobira</i> ; <i>Citrus grandis</i> , <i>Citrus sinensis</i>
Pests and pathogens	Percival and Fraser, 2002; Aldea et al., 2006; Christen et al., 2007; Percival, 2008; Cséfalvay et al., 2009; Muniz et al., 2014; Ugolini et al., 2014; Percival and Banks, 2015; Keča et al., 2018; Nowakowska et al., 2020	24 tree species; <i>Vitis vinifera</i> ; <i>Fraxinus excelsior</i> ; <i>Anacardium occidentale</i> ; <i>Betula pendula</i> ; <i>Aesculus hippocastanum</i> , <i>Quercus robur</i> , <i>Rosa rugosa</i> ; <i>Malus cv.</i> , <i>Castanea sativa</i>
Agrotechnical treatment	Bosa et al., 2014; Cirillo et al., 2021	<i>Pyrus communis</i> ; <i>Olea europaea</i>
Urban paved surfaces	Philip and Azlin, 2005; Wang and Wang, 2010; Rahman et al., 2013	<i>Lagerstromia speciosa</i> ; <i>Pyrus calleryana</i> ; <i>Firmiana simplex</i>
Agrotechnical treatment	Bosa et al., 2014; Cirillo et al., 2021	<i>Pyrus communis</i> ; <i>Olea europaea</i>

efficiency of PSII (Faraloni et al., 2011), whereas others did not (Ögren, 1990). These discrepancies may be due to different characteristics of taxa (species or varieties) and different biochemical mechanisms that ensure the balanced function of physiological processes. In the experiment described by Percival

and Fraser (2002), nine of 30 ornamental taxa showed no significant changes in  $F_v/F_m$  after 24-h dehydration.

From a practical point of view, information on whole-plant response is more useful in horticulture, plant breeding, evaluating suitability for urban environments, etc., because

experiments conducted on whole plants reveal a plant's overall strategy for coping with water deficiency. Indeed, the maximum quantum efficiency of PSII decreased during experimental drought stress in potted ornamental shrubs (Percival and Fraser (2002)), nine *Fraxinus* genotypes (Percival et al., 2006), six cultivars of *Olea europaea* L. (Faraloni et al., 2011), two cultivars of *Vitis amurensis* Rupr. (Wang et al., 2012), two clones of *Hevea brasiliensis* L. (Falqueto et al., 2017), *Tilia cordata* Mill. (Kalaji et al., 2018), two cultivars of *Prunus avium* L. (Mihaljević et al., 2021), 8-year-old *Olea europaea* trees in a commercial orchard (Bacelar et al., 2007) and two-year-old *Populus ×sibirica* seedlings planted in a reforestation area (Lee et al., 2016).

It should be noted, however, that in the laboratory, greenhouse and field experiments, the plants were generally treated with drought stress to the maximum water deficit in ambient light. Bukhov and Carpentier (2004) summarised several experiments and found that the maximum quantum efficiency was not strictly related to the water status of the plant and that moderate stress may not alter this parameter (Wang et al., 2012). Under low light,  $F_V/F_M$  remained stable despite the reduced water potential of leaves, resulting in a decrease in stomatal conductance and  $CO_2$  assimilation rate in wheat (Lu and Zhang, 1998). These results suggest that drought stress exacerbates rather than triggers photoinhibition when there is an imbalance between light and water availability for photosynthetic performance (Bacelar et al., 2007). Moreover, the magnitude of changes in  $F_V/F_M$  depends on the species or cultivar (Percival and Fraser, 2002; Wang et al., 2012). For example, the maximum quantum efficiency of PSII may not respond to drought in tolerant tree species (Fini et al., 2009; Swoczynna et al., 2010a; Fini et al., 2022).

In numerous experiments, the first symptom of drought stress is increased heat release of excess energy. In a 28-day experiment on *Tilia cordata*, Kalaji et al. (2018) found an increased dissipation rate after two weeks, which continued to rise in the following weeks. These results were also confirmed by Wang et al. (2012) and Lee et al. (2016). Similarly, drought treatment increased dissipation rates in different *Fraxinus* genotypes, but the effects were not the same across species and cultivars (Percival et al., 2006); these ChF parameters, including  $F_V/F_M$ , allowed the authors to rank 9 *Fraxinus* species and cultivars based on their drought resistance. The increase in  $F_0$  in response to drought was also found in *Vitis vinifera* L. (Christen et al., 2007) and *Hevea brasiliensis* (Falqueto et al., 2017). Fini et al. (2009) found significantly higher  $F_0$  in non-irrigated young *Tilia platyphyllos* L. and *Acer platanoides* L. trees during a dry July. Although the authors did not statistically compare the results between the lower and higher rainfall months, it clearly showed that  $F_0$  was significantly lower in *Tilia* species during a dry July (regardless of irrigation) than in June or August, when rainfall was more favourable. On the other hand, this finding can also be considered a synergistic effect of insufficient water availability and photoinhibition due to heat

and high light conditions in July, the warmest month in northern Italy (Climate-data.org).

In addition to maximum quantum efficiency and dissipation parameters, there are other parameters that help detect drought stress, although  $F_V/F_M$  does not clearly indicate the effects of stress (Bussotti et al., 2010). Faraloni et al. (2011) used the PAM instrument and found that ETR changed on the 14<sup>th</sup> day of drought treatment and in the following days. The electron transport parameters downstream of PSII,  $ET_0/RC$ , derived from OJIP analysis significantly decreased after two weeks, while  $\Psi_{E_0}$  and  $\Phi_{E_0}$  decreased after three weeks of drought treatment in *Tilia cordata* (Kalaji et al., 2018). Guha et al. (2013) attributed the decrease in  $ET_0/RC$  and  $ET_0/CS_m$  to the maintenance of an intrinsic balance between electron transfer reactions and reductive carbon metabolism without severe damage to PSII in drought-resistant, five-month-old potted seedlings of *Morus indica* L. cultivar. On the other hand, Wang et al. (2012) found an increase in  $ET_0/RC$  in drought-stressed *Vitis amurensis* and interpreted this as an acclimation response. Similarly, Lee et al. (2016) found unchanged  $ET_0/RC$  and  $ET_0/CS_0$  in *Populus ×sibirica* as a result of a compensatory mechanism.

Drought experiments revealed enhanced  $ABS/RC$  and  $TR_0/RC$  (Wang et al., 2012; Falqueto et al., 2017; Mihaljević et al., 2021). This should be interpreted as the inactivation of PSII reaction centres, shown as reduced  $RC/CS_0$  by Lee et al. (2016) or  $RC/CS_m$  (Guha et al., 2013). However, in Christen et al. (2007) experiment  $ABS/CS_0$  and  $TR_0/CS_0$ ,  $ABS/RC$  and  $TR_0/RC$  values were significantly higher in drought-stressed *Vitis* plants, although  $RC/CS_0$  ratio was not significantly altered in relation to non-stressed plants.

Drought stress may also be detected by the appearance of L- and K-bands on OJIP transient, suggesting disturbances in energetic connectivity between PSII units and in the oxygen-evolving complex on the donor side of PSII, respectively. Falqueto et al. (2017) found positive L- and K-bands in one-year-old *Hevea brasiliensis* seedlings. However, they occurred only 36 days after drought treatment. Young *Tilia cordata* specimens showed the appearance of L- and K-bands on the 27<sup>th</sup> day of drought treatment (Kalaji et al., 2018). Guha et al. (2013) found changes in L- and K-step on days 8 and 10 of drought in *Morus* saplings, while dissipation parameters increased since the 2<sup>nd</sup> day of the experiment. On the other hand, Banks (2018) noticed the appearance of the K-band, but L-band was not evident. A clear K-step as a response to drought was noticed in one-year-old *Vitis amurensis* seedlings by Wang et al. (2012), but only in a drought-sensitive cultivar. Mihaljević et al. (2021) found the drought-induced appearance of L- and K-bands in *Prunus avium*, with a slight shift in the drought-tolerant cultivar and a strong response in the drought-sensitive one.

All the presented results indicate that water deficiency affects both the donor and acceptor sides of PSII, as well as the pool of

reaction centres (Guadagno et al., 2021). In consequence, the performance indices  $PI_{ABS}$  and  $PI_{total}$ , as integrative parameters, serve as good indicators of water deficit, as was shown by Guha et al. (2013); Falqueto et al. (2017) and Mihaljević et al. (2021).  $PI_{ABS}$  significantly decreased in drought-affected *Tilia cordata* on the 21st day of the experiment (Kalaji et al., 2018). Banks (2018) ascertained that  $PI_{ABS}$  responded to both drought and desiccation earlier than  $F_v/F_m$ .

## Light and UV-B radiation

Although light is the source of energy for plants, it is known that both too little and too much light can be a source of stress. Both leaves and chloroplasts are structurally adapted to the given light conditions (Lichtenthaler et al., 2004). For example, light-exposed and light-stressed leaves of trees have lower amounts of chlorophyll and smaller antennae. Lichtenthaler et al., 2004 found a higher maximum quantum efficiency in sun leaves than in shade leaves of *Fagus sylvatica* L., but this was not supported by Cascio et al. (2010) and Desotgiu et al. (2012a). The latter showed that trapping capacity was lower in light-exposed leaves of *Fagus sylvatica* seedlings than in shaded foliage, while electron transport efficiency to end-acceptors was higher beyond PSI. These properties allow balancing the energy flow between both photosystems and avoiding the formation of reactive oxygen species in case of electron excess. Changes in light conditions alter the performance of the photosynthetic apparatus. Under full sunlight at midday, the maximum quantum efficiency of PSII ( $F_v/F_m$ ) decreases sharply (Dias and Marenco, 2007; Desotgiu et al., 2012a). The opposite trend was observed for the dissipation rate expressed by  $F_0$  (Dias and Marenco, 2007). Indeed, the ChF response in plants reflects their ecophysiological characteristics. In shade-grown and shade-tolerant plants, smaller values of PPFD may saturate non-photochemical quenching (qN), whereas, in species with high light requirements, a saturation of qN may not occur even at high maximum daily irradiances (Brodribb and Hill, 1997). A shade-tolerant mahogany (*Swietenia macrophylla* King) showed higher  $F_0$  values, especially in sun-exposed leaves, but lower  $F_m$  and  $F_v$  when exposed to strong light, in contrast to the sun-tolerant tonka bean (*Dipteryx odorata* (Aubl.) Willd.), which had similar  $F_0$  values in both sun-exposed and shaded seedlings (Gonçalves et al., 2001). These results indicate that ecophysiological traits are an important factor to consider when interpreting fluorescence results. Light stress may not affect PSII alone. Björkman and Powles (1984) found that daylight combined with water stress resulted in increased photoinhibition in *Nerium oleander* L., whereas shaded leaves showed no changes in the primary photochemistry of PSII.

UV-B radiation regulates various processes in plants, but it may also have a negative impact on photosynthetic efficiency. In fact, Bavcon et al. (1996) found that UV-B radiation combined

with low temperatures affected  $F_v/F_m$  and net photosynthetic activity in *Picea abies* (L.) Karst. UVB may determine the breakdown of OEC and enhancement of the K-band (Grifoni et al., 2016). As stated by Day et al. (1992), the resistance to UV-B radiation is higher in coniferous trees than in deciduous species. The seasonal changes in susceptibility to UV-B radiation were noted by Albert et al. (2005) in *Salix arctica* Pall. In late season limitation of the natural dose of UV-B was not visible, while in July, natural radiation resulted in diminished maximum quantum efficiency of PSII ( $F_v/F_m$ ), the estimated number of reaction centres ( $RC/CS_m$ ), rate of electron transport beyond PSII ( $ET_0/TR_0$ ,  $ET/CS_m$ ) and, in consequence,  $PI_{ABS}$ , compared to specimens with limited access to UV-B. Likewise, Trošt Sedej and Rupar (2013) found a seasonal influence of enhanced UV-B radiation on  $F_v/F_m$  in seedlings of *Fagus sylvatica* and *Picea abies*.

## Extreme temperatures

Heat stress initially increases heat dissipation, as reflected by an increase in  $F_0$ , and decreases the maximum quantum efficiency of PSII (Percival, 2005; Duan et al., 2015). OJIP analysis by Duan et al. (2015) demonstrated the complexity of the effects of heat stress by showing perturbations in OEC, reaction centre pool, and electron transport to the end of electron acceptors PSI. However, young leaves studied at the beginning of the growing season are more susceptible to heat stress. There are also differences between genotypes, e.g., leaves of *Quercus ilex* L. (an evergreen species) are more resistant to heat, while those of *Q. robur* L. and *Q. rubra* L. (deciduous) are more susceptible (Percival, 2005). The susceptibility of PSII to heat stress, expressed by an elevated  $F_0$  value, was used by Esperon-Rodriguez et al. (2021) to determine critical temperatures for studying heat tolerance in urban trees.

Both cold and frost stress adversely affect physiological processes in plants. Chilling decreases the quantum efficiency of PSII (Hakam et al., 2000; de Oliveira et al., 2009), but the effect depends on the species characteristics (Oliveira and Peñuelas, 2005). Percival and Fraser, (2001) studied the effects of freezing and salt in six *Crataegus* genotypes. As a result of freezing stress, decreases in  $F_v/F_m$  and  $PI_p$  were associated with increases in heat release ( $F_0$ ). Chlorophyll *a* fluorescence was also used to evaluate the woody tissue viability of Concord grapevine (*Vitis labruscana* Bailey) after controlled frost stress (Jiang et al., 1999). The ratio  $F_v/F_m$  correlated well with freezing temperatures and leaf tissue damage. Evergreen Mediterranean plants exposed to winter stress often show reduced maximum quantum efficiency and quantum yield of PSII electron transport ( $\Phi_{PSII}$ ) (Vitale et al., 2012). In contrast, Swoczyna et al. (2020) found that neither  $F_v/F_m$  nor  $PI_{ABS}$ , but parameters related to PSII reaction centres, showed significant correlations with winter survival of woody plants and perennials cultivated in a vertical garden on

the wall of an urban building. However, according to Pflug and Brüggemann (2012), dissipation and absorption rates were negatively correlated with minimum temperatures in evergreen *Quercus ilex*, whereas the correlation of  $F_V/F_M$  and  $ET_0/TR_0$  with  $T_{min}$  was positive. This suggests that frost not only slows down the processes but also affects the structures of the photosynthetic apparatus. The sensitivity of PSII to winter stress in *Quercus ilex* was confirmed by Bussotti (2004) in forest stands when morning photoinhibition was observed as a reduced number of active reaction centres ( $RC/CS_0$ ),  $F_V/F_M$  and performance index  $PI_{ABS}$ . Photoinhibition caused by low temperatures and concomitant high solar radiation is more pronounced in broadleaf evergreen species (angiosperms) than in conifers or semi-deciduous species in Mediterranean habitats (García-Plazaola et al., 1999; Martínez-Ferri et al., 2004). However, in response to winter stress, woody plants show a more conservative strategy than herbaceous species to survive the damaging period (Míguez et al., 2017), involving different phenomorphological adaptations and protective biochemical mechanisms.

## Chlorophyll content

Numerous studies in plants have shown that photosynthetic efficiency is usually associated with adequate levels of photosynthetic pigments (de Oliveira et al., 2009; Swoczyna et al., 2010b). Torres Netto et al (2005) found that a reduction in chlorophyll content in leaves resulted in a decreased fluorescence emission, as reflected by a change in the values of some parameters:  $F_M$  and  $F_V/F_M$ , with only chlorophyll-rich leaves showing optimal values for  $F_V/F_M$ . Similar observations were made by Percival et al. (2008); regardless of the species studied, relative chlorophyll content of SPAD-502 below 25 resulted in a decrease in  $F_V/F_M$ . Chen and Cheng (2010) studied 7-year-old apple trees in an orchard with foliar chlorosis. Compared to normal leaves, chlorotic leaves exhibited increased deactivation of oxygen-evolving complexes (OEC), minimal fluorescence ( $F_0$ ), dissipated energy, and relative variable fluorescence at L, K, J, and I bands. Simultaneously, maximum fluorescence ( $F_M$ ) and quantum yields, i.e. maximum quantum yield for primary photochemistry ( $F_V/F_M = TR_0/ABS$ ), quantum yield for electron transport ( $ET_0/ABS$ ) and quantum yield for the reduction of end acceptors of photosystem I (PSI) ( $\Phi_{R_0}$  and  $RE_0/ABS$ ) were decreased. Likewise, the maximum amplitude of the IP phase, the density of active reaction centres of PSII ( $RC/CS_0$ ) and performance indices ( $PI_{total}$ ,  $PI_{ABS}$ ) were diminished. This means that photoinhibition occurred at both the donor (i.e., the OEC) and the acceptor sides of PSII in chlorotic leaves. However, the acceptor side was damaged more severely than the donor side, which possibly was the consequence of the over-reduction of PSII due to the slowdown of the Calvin cycle. Castro et al. (2011) showed a clear positive relationship between

the results of optically determined chlorophyll content and  $RC/CS_0$ , while in the case of  $ABS/RC$  and  $TR_0/RC$ , the relationship was negative.

## Nutrient availability

The insufficiently available element whose deficiency is most frequently detected by the ChF method is nitrogen (N). An important constituent of amino acids, nitrogen plays an essential role in protein synthesis and in numerous biochemical processes in the form of enzymes, including light and dark reactions in chloroplasts (Lawlor, 2002). Nitrogen is also a component of chlorophyll, so N deficiency is clearly indicated by decreases in chlorophyll content (De Castro et al., 2014) and negatively affects net  $CO_2$  assimilation rates (DaMatta et al., 2002; De Castro et al., 2014). DaMatta et al. (2002) studied the effect of abundant and limited nitrogen fertilisation on *Coffea canephora* Pierre plants. N limitation resulted in a slight decrease in  $F_V/F_M$ , a more significant decrease in photochemical quenching and operational quantum efficiency ( $qP$  and  $\Phi_{PSII}$ , respectively), and an increase in non-photochemical quenching (NPQ) in well-watered plants. However, there was no significant difference in NPQ and other parameters due to N availability in water-deficient plants. Percival et al. (2008) showed that low N content in leaves, which is strongly linked to chlorophyll content, leads to a decrease in  $F_V/F_M$ . An optimum of  $F_V/F_M$  was found at leaf N contents of at least 1%, 1.5%, and 2% in *Acer pseudoplatanus*, *Fagus sylvatica*, and *Quercus robur*, respectively (Percival et al., 2008).

Nutritional factors were assessed by Nikiforou and Manetas (2011) on *Pistacia lentiscus* L. in field conditions. These authors concluded that nitrogen deficiency affected the parameters related to the I-P phase. This relationship was visible independently of the season, while parameters related to the PSII activity (i.e. quantum yields for photon trapping and electron flow along PSII and the efficiency of a trapped exciton to move an electron from the first plastoquinone electron acceptor of PSII to intermediate carriers) were limited by low nitrogen only during the winter period.

On the other hand, in a field study by Swoczyna et al. (2019) on *Actinidia arguta* (Sieb. & Zucc.) Planch. ex Miq. grown on a commercial plantation, the results suggested lower dependence of the performance of end electron acceptors around PSI upon N content while the effect of the 'climate-conditions  $\times$  N-treatment' combination on the PSII performance was higher. During the more favourable season the differences in N-treatment were well pronounced in  $V_K/V_J$ ,  $RC/ABS$ ,  $F_V/F_M$ ,  $\Psi_{E_0}$ ,  $PI_{ABS}$ , and  $PI_{total}$ . The most sensitive parameter to N nutrition was the density of active RCs per cross-section ( $RC/CS_0$ ) as it allowed the distinction effects of N-treatment independently of the season. The similar patterns of both  $RC/CS_0$  and  $RC/ABS$  differences suggested these parameters to be good indicators for N deficiency.



The strong dependence of photosynthetic efficiency on N availability is not shared in the case of other nutrients. According to Bosa et al. (2014), potassium fertilisation did not show significant effects on the light energy conversion process in pear trees grown in an experimental orchard.

## Salt stress

Salt stress affects plants in a similar manner to drought stress, causing osmotic limitations in water uptake, tissue desiccation, and hyperionic and hyperosmotic stress in cells. If salinity persists, additional stress leads to toxic effects on photosynthesis and other important metabolic processes (Chaves et al., 2009). The response of photosynthetic efficiency to salt stress has been studied at both the leaf and whole plant levels.

Percival and Fraser, 2001 used ChF to examine foliar salt tolerance in detached leaves in 6 *Crataegus* genotypes. Initial fluorescence  $F_0$  increased in three taxa in response to increasing salinity, while  $F_V/F_M$  and  $PI_P$  decreased in 5 genotypes. The authors explained the  $PI_P$  parameter in the next publication (Percival et al., 2003) as a calculation of  $RC/ABS \times \Phi_{P_0}/(1 - \Phi_{P_0}) \times \Psi_o/(1 - \Psi_o)$ , thus it may be identified as  $PI_{ABS}$ . The combined freezing  $\times$  salt stress had a serious negative effect in all six genotypes. Differences in  $PI_P$  response to salt between detached leaves of 30 *Acer* genotypes facilitated the ranking of *Acer* genotypes according to their salt tolerance (Percival et al., 2003). In that examination  $F_0$  and  $F_V/F_M$  did not give such clear results.

On the other hand, young potted and field-grown *Quercus* trees revealed clear changes of  $F_V/F_M$  and  $F_0$  as a response to sodium chloride solution applied as a spray to the foliage (Percival, 2005). Salt stress-induced gradual decline in maximum quantum efficiency ( $F_V/F_M$ ) and the increase in  $F_0$ , the most pronounced reaction to stress treatment in young trees, occurred in the 3–4th week after treatment. The time necessary to recover from salt damage was the 12<sup>th</sup> (*Q. ilex*, *Q. rubra*) or 14<sup>th</sup> week (*Q. robur*). These findings demonstrate that, at the level of the whole plant, the response to salt stress is delayed due to (1) slow and gradual accumulation of salt and (2) mobilisation of metabolic processes towards defence and/or acclimation to stress (Chaves et al., 2009). The tendency to maintain the high maximum quantum efficiency of PSII during stress conditions was found in numerous research. Naumann et al. (2008) noticed that  $F_V/F_M$  was diminished significantly in salt-flooded potted seedlings of *Myrica cerifera* L. (a shrub species sensitive to salt stress) only after noticeable damage to leaves. However, other PAM parameters were better indicators: stress was effectively detected through the decrease of  $\Delta F/F_M'$  and increase of  $\Phi_{NPQ}$  prior to visible signs. Thus, the calculation of parameters other than  $F_V/F_M$  gives more information and allows the detection of stress at an earlier stage of its occurrence. In the experiment by

Bashir et al. (2021) on 4-week-old seedlings of *Moringa oleifera* Lam. two levels of NaCl stress showed alterations in ChF in comparison to control. In light-adapted samples, parameters of PAM fluorometry  $Y(II)$  decreased while NPQ increased. Quantum yield of non-photochemical fluorescence quenching by non-dissipation energy,  $Y(NO)$ , increased by 25% and 80% at a lower and higher level of salt stress, respectively, indicating that in highly stressed seedlings, both photochemical energy conversion and protective regulatory mechanisms were inefficient in protection against photodamage. Additionally, analysed OJIP parameters,  $PI_{ABS}$ ,  $\Phi_{P_0}$  ( $=F_V/F_M$ ) and  $\Psi_{E_0}$ , decreased in stressed plants, while  $ABS/RC$  had already increased with the lower stress level. In the experiment of Kalaji et al. (2018) on *Tilia cordata* potted saplings, salt stress significantly reduced maximum fluorescence,  $F_M$ , on the 14<sup>th</sup> day of the experiment, causing a decrease of  $F_V/F_M$  ( $=\Phi_{P_0}$ ) in the next days. On the 21<sup>st</sup> day of the experiment  $\Phi_{D_0}$  and  $ET_0/RC$  were changed significantly. Finally (on the 28<sup>th</sup> day), most of both donor ( $DI_0/RC$ ,  $\Phi_{D_0}$  and K-step) and acceptor PSII side parameters ( $ET_0/RC$ ,  $\Phi_{E_0}$ ,  $\Psi_o$ ) were significantly changed. In general, in that experiment, the results of salt stress were similar to drought stress. However, the principal component analysis revealed a separate arrangement of the salt and drought stress cases. The cases of drought stress were more or less directly along PC1 and its determinants, whereas the plotting of salt stress appeared more disorderly, with the pattern changing with increasing salt pressure. This suggests that salt stress more strongly affects the various structures and/or physiological processes around PSII.

## Ozone, air pollution, soil contamination

The effects of the tropospheric ozone ( $O_3$ ) as a pollutant on chlorophyll fluorescence traits were one of the main questions raised in experimental and field studies, as reviewed by Bussotti et al. (2007b); Bussotti et al. (2011a). As a general result,  $F_V/F_M$  was demonstrated to be quite insensitive, at least in the first phases of ozone treatment, whereas the most sensitive parameters were those related to the I-P phase and the concentration of reaction centres per cross-section ( $RC/CS_0$ ). NPQ was the main parameter connected with ozone impacts in modulated fluorescence. Experimental studies were carried out on young trees (seedling and potted plants) in open-top chambers facilities, both with enriched and ambient ozone pollution levels, to screen the relative sensitivity of different species such as *Viburnum lantana* L., *Fraxinus excelsior* L., *Populus nigra* L., *Prunus avium* and *Quercus robur* (Gravano et al., 2004). In these experiments, it was probed that the intensity of the responses was related to leaf structure, with higher sensitivity in species with high SLA and in sunny exposed leaves (Gerosa et al., 2003; Bussotti et al., 2007a; Cascio et al., 2010). The sensitive poplar clone *Populus maximowiczii* Henry  $\times$  *P. xberolinensis* Dippel (Oxford clone)

was adopted as a model plant to study the mechanisms of ozone damage with the application of chlorophyll fluorescence techniques (Desotgiu et al., 2012b; Pollastrini et al., 2014a). In field studies, the main subject was the responses connected to visible foliar symptoms. Bussotti et al. (2005) found that species-specific behaviours were connected to the de-excitation mechanisms. Such mechanisms were related to the irreversible damage of PSII in *Ailanthus altissima* (Mill.) Swingle and a more effective quenching capacity (as a process of compensative photosynthesis) in *Fraxinus excelsior* and *Acer pseudoplatanus*. In the experimental field site of Kranzberger (Germany), where tall *Fagus sylvatica* trees were subjected to artificial ozone treatment, Gielen et al. (2007) found only a limited decrease in the quantum yield efficiency. Gottardini et al. (2014) observed the pattern of ChlF on *Viburnum lantana* shrubs with different levels of ozone symptoms. Symptomatic plants showed significantly lower values of the maximal fluorescence ( $F_M$ ), the maximum quantum yield of primary photochemistry ( $F_V/F_M$ ), J phase and Performance Index Total ( $PI_{TOT} = PI_{total}$ ), according to the most used abbreviation showed in the Table 2 and significantly higher values of minimal fluorescence ( $F_0$ ) throughout the growing season, respect to non-symptomatic plants.

Other gaseous air pollutants may have different effects on photosynthetic efficiency. Sulphur dioxide ( $SO_2$ ) had negative effects on the maximum quantum efficiency of PSII due to its toxic effect on leaf tissue (Pukacki, 2000; Matsushima et al., 2009). On the other hand, low atmospheric  $NO_2$  pollution may serve as an additional N source for plants and consequently increase photosynthetic efficiency (Wang et al., 2019). Unfortunately, studies on the effects of gaseous pollutants on photosynthetic efficiency investigated with ChF are sparse.

In several studies, ChF was used to assess the impact of heavy metal contamination on PSII performance. Kitao et al. (1998) examined Mn toxicity in two-year-old potted seedlings of four deciduous broad-leaved tree species differing in successional traits using PAM fluorescence. The authors confirmed differences between early-successional species (*Betula ermanii* Cham. and *Alnus hirsuta* Turcz.) having a higher tolerance to excessive accumulations of Mn in leaves than two other mid- and late-successional species. The toxicity of aluminium salts decreased maximum quantum efficiency in citrus genotypes (Pereira et al., 2000; Zhang et al., 2020). The efficiency of electron transport beyond PSII reaction centres was diminished in *Citrus grandis* L. only, while *Citrus sinensis* L. did not respond to Al treatment (Zhang et al., 2020). Likewise, Dezhban et al. (2015) ascertained the negative impact of cadmium and Pb chloride on  $F_V/F_M$  and increased  $F_0$  values in one-year-old *Robinia pseudoacacia* L. seedlings. On the other hand, the ChF method allowed to confirm the beneficial effect of ectomycorrhizal fungi on recovery from contamination stress (Pb, Zn and Cd) in *Pinus halepensis* Mill. (Hachani et al., 2021). The research on soil pollution influence was conducted mostly on crop plants. However, it would be interesting to gain more

knowledge on the impact of heavy metal contamination on trees with regard to the accumulation of contaminants.

## Pests and pathogens

Arthropod herbivory and pathogen infections alter plant physiological processes in different ways depending on which parts of the plant are damaged. Damage to vascular tissue and leaf vein reduces water supply to photosynthesizing cells and alters nutrient and osmotic transport, cell content feeding reduces photosynthesis, and defoliation damage can disrupt the water balance in remaining tissues, and release of biocidal compounds against attackers can alter photosynthetic and homeostatic mechanisms, while some pathogens and pests can also produce toxins that directly or indirectly affect photosynthetic metabolism or produce compounds that act as plant growth regulators (Nabity et al., 2009; Rolfe and Scholes, 2010). Welter (1989, cited by Nabity et al., 2009) found that over 50% of all plant-insect interactions resulted in a loss of photosynthetic capacity. On the other hand, in some cases, local injury contributes to increased  $CO_2$  assimilation in remaining tissues or organs (Nabity et al., 2009).

Because the ChF method is non-invasive, it allows, in combination with other methods, e.g., gas exchange, thermal imaging, UV imaging, the tracking of plant-pathogen interactions throughout the life cycle of a pathogen and indirect effects of pathogens and herbivorous arthropods on the photosynthesis of a host plant (Aldea et al., 2006). The contribution of chlorophyll fluorescence imaging techniques to understanding metabolic changes in plants due to biotic hazards has been discussed in reviews by Nabity et al. (2009), arthropod herbivory, and Rolfe and Scholes (2010), pathogen infections, as well as in the recent work by Pérez-Bueno et al. (2019). Biotic injury on leaves is generally scattered across the leaf surface, and likewise vascular constraints, leads to specifically localised changes in leaf chemistry, which is why the fluorescence imaging technique is often used to map changes in infected leaves or plants in laboratory research. This technique allows the identification of sites for pathogen or herbivore activity but also enables the analysis of conventional parameters:  $F_0$ ,  $F_M$ ,  $F_V/F_M$ ,  $\Phi_{PSII}$ ,  $q_N$ ,  $q_P$ , NPQ (Pérez-Bueno et al., 2019). Cséfalvay et al. (2009) used a kinetic imaging fluorometer to detect the effect of artificial inoculation with *Plasmopara viticola* (Berk. & M.A. Curtis) Berl. & De Toni (the causal agent of downy mildew) on *Vitis vinifera* leaves. The distribution of changed  $F_V/F_M$  and  $\Phi_{PSII}$  across the leaf lamina was associated with the presence of the developing mycelium three days before the occurrence of visible symptoms and five days before the release of spores. The reduction of maximum quantum efficiency of PSII (reflecting the injury of PSII complexes) was restricted to the leaf area that later yielded sporulation, while the area with significantly lower  $\Phi_{PSII}$  (often correlated with the yield of  $CO_2$  fixation) was larger.

Three types of interactions between host and pathogen are possible: biotrophic, deriving nutrients from living cells and maintaining their viability, necrotrophic, destroying host cells and digesting its tissues, and hemi-biotrophic, initially feeding on nutrients from living cells and then feeding as necrotrophs (Scholes and Rolfe, 2009). In many studies on biotrophs and hemi-biotrophs changed photosynthetic efficiency was detected in asymptomatic tissues as an announcement of the disease development, with  $\Phi_{PSII}$ ,  $q_P$  and NPQ being more sensitive pre-symptomatic signals of infection than  $F_V/F_M$ . The timing of changes in the above-mentioned parameters in necrotrophs was more variable, and NPQ appeared to be more valuable for pre-symptomatic signalling (Pérez-Bueno et al., 2019). Host leaves may not show any changes in photosynthetic efficiency except in infected sites and surrounding areas, destruction of vascular tissues in woody plants may reduce water availability for leaf cells, as well as nutrients and assimilates supplied to all plant tissues. Muniz et al. (2014) investigated the early symptoms of *Lasiodiplodia theobromae* (Pat.) Griffon & Maubl. (an endophyte colonising stem tissues) in two-month-old *Anacardium occidentale* L. seedlings inoculated with pathogen mycelium. The infection significantly changed the maximum and operational quantum efficiency of PSII ( $F_V/F_M$  and  $\Phi_{PSII}$ ), both photochemical and non-photochemical quenching ( $q_P$  and NPQ), prior to visible symptoms, which may be attributed to the limitations of water supply.

The fast-fluorescence method provides several sensitive parameters which may be useful in the early detection of infection. Early research was done by Percival and Fraser (2002), who studied changes in PSII performance in woody species (ornamental rose, oak and horse chestnut) infected by powdery mildew agents (*Sphaerotheca pannosa* (Wallr.) Lev. var. *rosae* Wor., *Phyllactinia* sp., *Uncinula necator* (Schwein.) Burrill), biotrophic fungi. Photosynthetic  $CO_2$  fixation tended to be reduced prior to the visible signs of infection, while changes in  $F_0$  and  $F_V/F_M$  were visible when the mycelium had covered more than 25% of the leaf blade. However, the performance index calculated on the basis of the OJIP curve showed a decrease when the first symptoms of infection were visible (less than 10% of the leaf blade covered with the mycelium). Pathogens developing in the vascular system also influenced photosynthetic efficiency in asymptomatic leaves in 16-year-old *Vitis vinifera* L. plants grown in a vineyard (Christen et al., 2007) before confirming the symptoms of white rot and necrosis on the basis of wood decay. An early stage of the esca disease was signalled by a significant increase in dissipation, expressed by  $DI_0/RC$ ,  $DI_0/CS_0$  and  $\Phi_{D_0}$ , and a decrease in  $\Phi_{P_0}$ ,  $\Psi_{E_0}$ , and  $PI_{ABS}$ . Infection diminished a pool of active reaction centres ( $RC/CS_0$ ) and electron transport rates ( $ET_0/RC$  and  $ET_0/CS_0$ ) in infected plants but not significantly. Likewise, increased dissipation  $DI_0/CS_0$  and decreased  $\Phi_{P_0}$ ,  $\Psi_{E_0}$ ,  $PI_{ABS}$  and  $PI_{total}$  were shown by Keča et al. (2018) in the research on *Fraxinus excelsior* L. seedlings inoculated with *Hymenoscyphus fraxineus* Baral et al.

and *Phytophthora* spp. Nowakowska et al. (2020) investigated the interactions between two hazardous pathogens *Phytophthora cactorum* (Lebert & Cohn) J. Schröt., *Armillaria gallica* Marxm. & Romagn. and *Betula pendula* Roth. seedlings, the authors noticed that the pathogen infection increased thermal dissipation of energy absorbed by PSII (via shifted  $DI_0/RC$  and  $DI_0/CS_0$ ) but also downregulated electron transport beyond primary acceptors (as is shown by a decrease of  $\Psi_{E_0}=ET_0/TR_0$ ) and diminished the number of active reaction centres.

In some papers, ChF is used to evaluate the effect of chemical control in infected plants. Percival (2008) assessed the effectiveness of paclobutrasol as a fungicide against *Venturia inaequalis* (Cooke) G. Wint., and *Guignardia aesculi* (Peck) VB Stewart on *Malus* cv. Crown Gold and *Aesculus hippocastanum* L., respectively. The application of paclobutrasol had a positive effect on the visually evaluated leaf health status and the photosynthetic efficiency expressed by performance index (PI) values calculated from chlorophyll *a* fluorescence measurements. Percival and Banks (2015) applied the ChF technique to investigate the effect of preventative and curative treatment with potassium or silicon phosphite on the health condition of *Aesculus hippocastanum* saplings inoculated with *Pseudomonas syringae* pv. *aesculi*. That experiment gave the perception that preventative treatment had a greater protecting effect than the application three weeks after the inoculation.

## Rootstock effect and agrotechnical treatments

Finally, the ChF method is a sensitive and rapid tool for screening the effects of evolving agrotechnical practices. The type of rootstock affected the photosynthetic efficiency of grafted pear trees. The higher  $F_V/F_M$  and  $PI_{ABS}$  values indicated that the rootstock type provided better photosynthetic productivity of the grafted cultivar, which was confirmed by higher chlorophyll content and net photosynthetic rate (Bosa et al., 2016). Cirillo et al. (2021) studied the effect of biostimulants, kaolin (administered as Manisol by Manica S.p.a, Rovereto, Italy) and di-1-p-mentene (administered as Vapor Gard® by Biogard®, Bergamo, Italy), on two-year-old potted olive seedlings during a hot summer.  $F_V/F_M$  proved to be a sufficient parameter for evaluating the usefulness of these anti-transpiration products.

## Chlorophyll *a* fluorescence measurements in the natural environment and urban landscape

With the development of portable fluorimeters, ChF technology has opened new opportunities for *in situ* research (Figure 1). Extensive experience in experimental research has



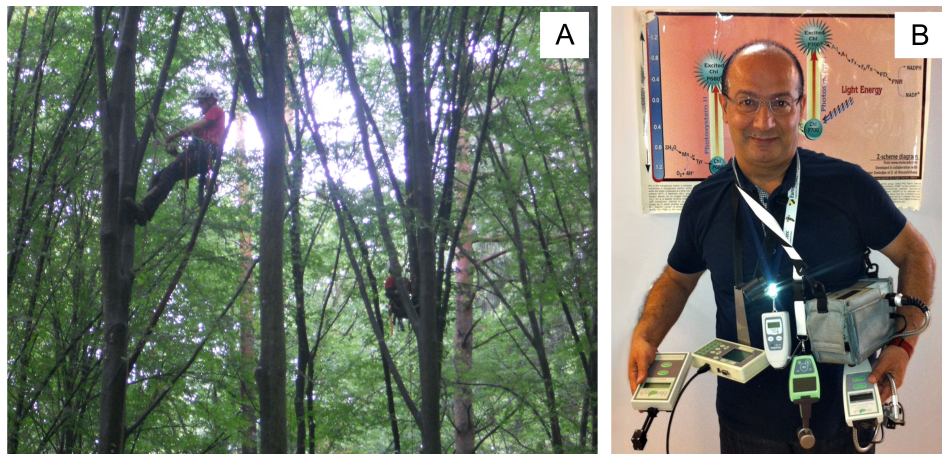


FIGURE 1

The sampling for chlorophyll fluorescence measurement at the Białowieża forest (2013) for the FunDiv EUROPE project, photo: F. Bussotti (A). The various available portable fluorometers to be used in forestry and other scientific disciplines, photo: H.M. Kalaji (B).

provided the basis for investigations and interpretation of results at experimental sites where environmental conditions were not well defined and where multiple stress effects are expected. Such studies are important because they provide the opportunity to learn how plants actually function in a natural environment. They also allow monitoring of the condition of plants in a man-made environment, such as a city, where human attention is not usually focused on plant well-being. The results of these studies are particularly important for trees, on which carbon sequestration, habitat maintenance, local climate regulation and, in cities, human well-being depend.

## Assessing a tree

Sampling and measuring chlorophyll fluorescence parameters on the leaves of mature trees in forests or urban parks poses several problems. Leaves can be difficult to reach, and measurements at canopy height are not readily possible unless trees are scaffolded; therefore, it is preferable to work on detached leaves.

Sampling techniques for leaves from tall trees include the use of loppers, tree climbers, and shooting, depending on tree height, crown structure, and local operational constraints (Bussotti and Pollastrini, 2015b). The number of leaves to be sampled depends on the variability of the assessed parameters between and within trees (Gottardini et al., 2014). Leaves should be randomly sampled within the crown (to represent the entire tree) or concentrated in a particular stratum, e.g., from the top only (to reduce the source of variability). Significant differences between sun and shade leaves (top and bottom of the canopy, respectively) were observed in forest trees for the parameters  $F_V/F_M$

and I-P phase (Pollastrini et al., 2017), combining lower values of  $F_V/F_M$  with higher values of IP phase in sun leaves.

Chlorophyll fluorescence parameters show a typical diurnal pattern (Zhang and Gao, 2000). The high intensity of solar radiation leads to photoinhibition of the photosynthetic apparatus with depression of  $F_V/F_M$  at midday (Epron et al., 1992; Kalaji et al., 2017). Under the same light conditions, there may be an increase in electron transport beyond photosystem I (PSI) (Pollastrini et al., 2017). Therefore, leaves should be sampled and measured at similar times of day, or dynamic and chronic photoinhibition should be eliminated (or at least reduced) by long dark adaptation (at least 4–5 h) so that leaves collected at different times of day are comparable (Pollastrini et al., 2016a).

Percival and Fraser (2002) have shown that there is no difference between the results of intact and detached leaves when they are protected from dehydration stress. Therefore, users often collect leaves from plants and perform measurements under laboratory conditions (Bussotti and Pollastrini, 2015b) or even in the field but in a shaded area (Swoczyna et al., 2019). The possibility of taking samples for later measurements facilitates the task when samples from tall trees are difficult to obtain.

Variability in chlorophyll fluorescence parameters is an important consideration when planning a field survey. In a pan-European survey, Pollastrini et al. (2016a),  $F_V/F_M$  proved to be very stable within a tree (coefficient of variation, CV = 1.42 within the crown, in 16 sampled leaves) and between trees (coefficient of variation, CV = 1.46 in 6 sampled trees), whereas composite indices (i.e., performance indices in the JIP test) show large variability ( $PI_{ABS}$ : CV = 29.81 with six trees sampled). In general, ratios and normalised parameters (fluxes



and yields) are less variable than the original ChF signals, such as  $F_0$  and  $F_M$ . This is an important aspect of the comparability of results from different fluorimeters (Bussotti et al., 2011b). ChF parameters correlate with each other and can be grouped into clusters in terms of the information they provide. Bussotti et al. (2020) suggest that in large-scale surveys, overall photochemical efficiency can be represented by two independent parameters,  $F_V/F_M$  and I-P phase, which is representative of photosystem II (PSII) and PSI efficiency, respectively.

The ChF signal is determined by the age of a leaf and its phenological stage. Young and senescent leaves have different ChF properties than mature, fully developed leaves due to incomplete assembly of the photosynthetic machinery and degradation of chlorophyll and photosystems (Jiang et al., 2006a; Jiang et al., 2006b; Lepeduš et al., 2010; Holland et al., 2014; Duan et al., 2015; Sitko et al., 2019). Lepeduš et al. (2010) observed that changes in  $F_V/F_M$  in ageing leaves were less pronounced than changes in PSII capacity for  $O_2$  evolution determined using a gas-phase oxygen electrode system. Holland et al. (2014) found that the appearance of the K-band indicated disturbances in the oxygen-evolving complex but at the later stage of ageing. It has also been noted that during the growing season, the strength of the ChF signal may decrease (Swoczyna et al., 2020; Suchocka et al., 2021), reflected in decreased  $F_0$  and  $F_M$  in the late season, and is not caused by leaf physiology, but rather by morphological changes, i.e., thickening of the cuticle, etc. In evergreen conifers and deciduous trees, differences between the different age classes are to be expected.

## Assessing a forest

Chlorophyll fluorescence analysis is widely used in forest research (Epron et al., 1992; Aldea et al., 2006; dos Santos and Ferreira, 2020) but rarely directly on tall trees in forest ecosystems and for operational purposes (Ball et al., 1995), although it provides important insights into photosynthesis and plant physiology (Mohammed et al., 1995). Forests are complex ecosystems with a stratified structure of woody and herbaceous plant species that include mature trees, shrubs, herbs, regeneration, and epiphytes, each with a different size and life span.

Among the publications dealing with the analysis of active chlorophyll fluorescence of forest trees, important scientific findings come from the studies conducted within the FP7 project “FunDivEUROPE - The functional significance of forest tree diversity in Europe” (Baeten et al., 2013). In this project, the ChF characteristics of trees in six European forests, from the Mediterranean to the boreal, were assessed. The data presented by Pollastrini et al. (2016a) show that different tree species growing in the same site have specific chlorophyll fluorescence signatures (with differences between conifers and deciduous trees and between early- and late-growing species),

while ChF characteristics change in the same species growing in different sites. Moreover, photosynthetic performance assessed by ChF was higher in central European forests than in southern (Mediterranean) and northern (Boreal) borders. In mixed stands, the main factor that changed ChF parameters was inter-tree competition: dominant trees were more affected by photoinhibition of leaves in the upper part of the canopy, with a reduction of  $F_V/F_M$ , than leaves in the lower part of the canopy (Bussotti and Pollastrini, 2015a).

The ChF analysis on forest trees was applied to investigate the health condition of forests (Odasz-Albrigtsen et al., 2000). Special attention was paid to the relationships between defoliation and ChF parameters. Partial defoliation allows the penetration of light into the crown, then allowing better exploitation of sunlight energy, but, at the same time, induces photoinhibition processes of the PSII (Gottardini et al., 2016; Gottardini et al., 2020). A rise in the electron transport rate beyond the PSI compensates for the reduction of  $F_V/F_M$  with species-specific patterns, as shown by Pollastrini et al. (2014b); Pollastrini et al., 2016c; Pollastrini et al., 2017). *Castanea sativa* Mill. trees defoliated by the insect *Dryocosmus kuriphilus* (Asian chestnut gall wasp) demonstrated the reduction of the IP phase in the infected leaves (Ugolini et al., 2014). Based also on these results, ChF analysis has been proposed as a tool to integrate the current activities concerning the assessment of the conditions of forests in the monitoring networks (Bussotti and Pollastrini, 2017) within the ICP Forests programme (<http://icp-forests.net>).

## Assessing urban forests and trees

Both ChF techniques, PAM and prompt ChF, have been used for stress detection in urban environments and human-altered habitats, such as degraded areas. Such sites are characterised by variable edaphic and microclimatic conditions and are usually quite different from natural habitats. ChF analysis makes it possible to detect stress in urban trees before visible signs appear (Swoczyna et al., 2010b; Ugolini et al., 2012; Reyes et al., 2022) or to indicate which specimens are particularly affected by road stress (Hermans et al., 2003). In this way, ChF can be a tool for identifying specimens that need more intensive care. ChF also provides arguments for better design of public spaces that provide suitable growing conditions for trees. Highly compacted soils (Philip and Azlin, 2005), artificially created pits for tree plantings (Rahman et al., 2013), and impermeable soil surfaces (Wang and Wang, 2010) negatively affect photosynthetic efficiency. Urban trees and other plants are expected to improve environmental conditions for human well-being, assimilate  $CO_2$ , and provide shade and aesthetic values. Air and soil pollution and dust deposition on leaves reduces photosynthetic efficiency (Alessio et al., 2002; Naidoo and Chirkoot, 2004; Popek et al., 2018; Fusaro et al., 2021; Reyes et al., 2022). Other environmental factors, e.g.,

shading or excessive light in open areas such as plazas and parking lots, can also be assessed using the ChF method (Hamerlynck, 2001; Song and Li, 2016), keeping in mind that different types of stress can have a synergistic or additive effect on photosynthetic efficiency (Fusaro et al., 2021). Finally, the ChF technique allows the selection of species tolerant to urban environments (Swoczyna et al., 2010b; Swoczyna et al., 2015; Reyes et al., 2022). Assessment of photosynthetic efficiency helps explain the successful adaptation of selected alien species that can easily adapt to unfavourable conditions; this knowledge is particularly important in the case of invasive alien species (Mlinarić et al., 2021).

In numerous papers, only  $F_0$ ,  $F_M$ , and  $F_V/F_M$  were used as indicators of stress. This sometimes resulted in weak or no changes in ChF in stressed trees, in contrast to, for example, stomatal conductance (Martinez-Trinidad et al., 2010; Benson et al., 2019). Analysis of parameters describing the donor side and electron transport on the acceptor side of PSII, in particular OJIP analysis, provides more sensitive indicators of environmental stress in the case of moderate changes (Bussotti et al., 2010; Ugolini et al., 2012). It should also be considered that, as a living organism in a given habitat, a tree tends to maintain an adequate state of photosynthetic structures to provide sufficient nutrition to all parts of the organism. Thus, damage in one part of a tree can lead to the upregulation of photosynthetic output in another part through what is known as compensatory photosynthesis (Martinez-Trinidad et al., 2010; Suchocka et al., 2021).

## Conclusions: Advantages and limitations

The most important advantage of using chlorophyll fluorescence is that it provides a tool for objective evaluation of the photosynthetic efficiency of trees. The collection of a large amount of comparable data in forest tree communities is, therefore, crucial for the early diagnosis of changes in plant vigour, as it allows many samples to be examined *in situ* over a short time. Among ChF techniques, the JIP assay is a powerful tool for *in vivo* analysis of plant stress (Strasser et al., 2000; 2004) that has been widely used in plant physiology and ecology research for many decades and has been applied in forest ecology research (Gottardini et al., 2014; Pollastrini et al., 2016a; Pollastrini et al., 2016b; Pollastrini et al., 2016c; Pollastrini et al., 2017).

Chlorophyll fluorescence has been successfully used in applied research to evaluate the effects of stressors on tree seedlings and small plants and to screen genotypes adapted to specific environmental conditions (Kuhlgert et al., 2016; Çiçek et al., 2020; Dimitrova et al., 2020). ChF analysis has been used by Bantis et al. (2020); Bantis et al. (2021); Bashir et al., (2021)

and Pollastrini et al. (2020) to select tree species for reforestation under climate change conditions by analysing the results of a system of community gardens across Europe. ChF is also applied in nurseries to determine young tree vigour and potential seedling performance (Perks et al., 2001; L'Hirondelle et al., 2007), stand quality (Binder et al., 1996), and winter hardiness (Fisker et al., 1995). The main limitation is the time required for dark adaptation of the leaves, but when working with detached leaves, this problem can be overcome.

Due to technical and operational constraints, active fluorescence techniques (i.e., the use of artificially generated actinic light) are not widely applied in tall tree research, whereas there is increasing interest in the application of passive (sun-induced) fluorescence through remote sensing techniques (from satellite to UAV, Rossini et al., 2006; Yang et al., 2017; Mohammed et al., 2019). Remote sensing surveys evaluate the optical properties of foliage to assess parameters such as leaf area index, chlorophyll content, and photosynthetic efficiency (Serbin et al., 2012). In the Sentinel 3/FLEX programme, passive chlorophyll fluorescence (ChlF) emitted by vegetation is assessed to evaluate the state of vegetation across Europe (Mohammed et al., 2019). Photosystem functionality is considered an indicator of photosynthetic efficiency (Baker and Oxborough, 2004). In remote sensing studies, ChlF parameters are associated with the net primary production of both terrestrial and aquatic ecosystems (Norton et al., 2019). However, we believe that active fluorescence can play an important role in answering specific tree-level questions (passive fluorescence provides surface-level data) and validating remote observations.

## Author contributions

Review of the literature: TS, FB, MP; manuscript revision: FB, MP, HK; final preparation: TS, HK, JM. Percentage contribution of the Authors to the manuscript preparation is as follows: TS = 70%, MP = 20%, FB = 5%, JM = 3% and HK = 2%. All authors contributed to the article and approved the submitted version.

## Acknowledgments

The Authors would like to thank Ms. Charlotte Aldred for her kind English proofreading.

## Conflict of interest

The authors declare that the paper was written in the absence of any commercial or financial relationships that could be construed as a potential conflict of interest.

## Publisher's note

All claims expressed in this article are solely those of the authors and do not necessarily represent those of their affiliated

organizations, or those of the publisher, the editors and the reviewers. Any product that may be evaluated in this article, or claim that may be made by its manufacturer, is not guaranteed or endorsed by the publisher.

## References

- Albert, K. R., Mikkelsen, T. N., and Ro-Poulsen, H. (2005). Effects of ambient versus reduced UV-B radiation on high arctic *Salix arctica* assessed by measurements and calculations of chlorophyll *a* fluorescence parameters from fluorescence transients. *Physiol. Plant* 124, 208–226. doi: 10.1111/j.1399-3054.2005.00502.x
- Aldea, M., Hamilton, J. G., Resti, J. P., Zangerl, A. R., Berenbaum, M. R., Frank, T. D., et al. (2006). Comparison of photosynthetic damage from arthropod herbivory and pathogen infection in understory hardwood saplings. *Oecologia* 149, 221–232. doi: 10.1007/s00442-006-0444-x
- Alessio, M., Anselmi, S., Conforto, L., Improta, S., Manes, F., and Manfra, L. (2002). Radiocarbon as a biomarker of urban pollution in leaves of evergreen species sampled in Rome and in rural areas (Lazio – central Italy). *Atmos. Environ.* 36, 5405–5416. doi: 10.1016/S1352-2310(02)00409-0
- Climate-data. Available at: <https://en.climate-data.org/europe/italy/lombardy/como-1097/> (Accessed May 20, 2022).
- Bąba, W., Kompała-Bąba, A., Zabochnicka-Świątek, M., Luźniak, J., Hanczaruk, R., Adamski, A., et al. (2019). Discovering trends in photosynthesis using modern analytical tools: More than 100 reasons to use chlorophyll fluorescence. *Photosynthetica* 57, 668–679. doi: 10.32615/ps.2019.069
- Bacelar, E. A., Santos, D. L., Moutinho-Pereira, J. M., Lopes, J. I., Gonçalves, B. C., Ferreira, T. C., et al. (2007). Physiological behaviour, oxidative damage and antioxidative protection of olive trees grown under different irrigation regimes. *Plant Soil* 292, 1–12. doi: 10.1007/s11104-006-9088-1
- Baeten, L., Verheyen, K., Wirth, C., Bruelheide, H., Bussotti, F., Finér, L., et al. (2013). A novel comparative research platform designed to determine the functional significance of tree species diversity in European forests. *Perspect. Plant Ecol. Evol. Syst.* 15, 281–291. doi: 10.1016/j.ppees.2013.07.002
- Baker, N. R. (2008). Chlorophyll fluorescence: A probe of photosynthesis *in vivo*. *Annu. Rev. Plant Biol.* 59, 89–113. doi: 10.1146/annurev.arplant.59.032607.092759
- Baker, N. R., and Oxborough, K. (2004). "Chlorophyll fluorescence as a probe of photosynthetic productivity," in *Chlorophyll a fluorescence: A signature of photosynthesis*. Eds. G. C. Papageorgiou and Govindjee, (Dordrecht, The Netherlands: Springer), 65–82. doi: 10.1007/978-1-4020-3218-9\_3
- Baker, N. R., and Rosenqvist, E. (2004). Applications of chlorophyll fluorescence can improve crop production strategies: an examination of future possibilities. *J. Exp. Bot.* 55, 1607–1621. doi: 10.1093/jxb/erh196
- Ball, M. C., Butterworth, J. A., Roden, J. S., Christian, R., Egerton, J. J. G., Wydrzynski, T. J., et al. (1995). Applications of chlorophyll fluorescence to forest ecology. *Funct. Plant Biol.* 22, 311–319. doi: 10.1071/PP9950311
- Banks, J. M. (2017). Continuous excitation chlorophyll fluorescence parameters: A review for practitioners. *Tree Physiol.* 37, 1128–1136. doi: 10.1093/treephys/tpx059
- Banks, J. M. (2018). Chlorophyll fluorescence as a tool to identify drought stress in *Acer* genotypes. *Environ. Exp. Bot.* 155, 118–127. doi: 10.1016/j.envexpbot.2018.06.022
- Bantis, F., Fruchtenicht, E., Graap, J., Ströll, S., Reininger, N., Schäfer, L., et al. (2020). The JIP-test as a tool for forestry in times of climate change. *Photosynthetica* 58, 224–236. doi: 10.32615/ps.2019.173
- Bantis, F., Graap, J., Fruchtenicht, E., Bussotti, F., Radoglou, K., and Brüggemann, W. (2021). Field performances of Mediterranean oaks in replicate common gardens for future reforestation under climate change in central and southern Europe: First results from a four-year study. *Forests* 12, 678. doi: 10.3390/f12060678
- Bashir, S., Amir, M., Bashir, F., Javed, M., Hussain, A., Fatima, S., et al. (2021). Structural and functional stability of photosystem-II in *Moringa oleifera* under salt stress. *Aust. J. Crop Sci.* 15, 676–682. doi: 10.21475/ajcs.21.15.05.p2996
- Bavcon, J., Gaberščik, A., and Batič, F. (1996). Influence of UV-B radiation on photosynthetic activity and chlorophyll fluorescence kinetics in Norway spruce [*Picea abies* (L.) karst.] seedlings. *Trees* 10, 172–176. doi: 10.1007/BF02340768
- Benson, A. R., Morgenroth, J., and Koeser, A. K. (2019). The effects of root pruning on growth and physiology of two *Acer* species in New Zealand. *Urban For. Urban Gree.* 38, 64–73. doi: 10.1016/j.ufug.2018.11.006
- Bilger, W., and Björkman, O. (1990). Role of the xanthophyll cycle in photoprotection elucidated by measurements of light-induced absorbance changes, fluorescence and photosynthesis in leaves of *Hedera canariensis*. *Photosyn. Res.* 25, 173–185. doi: 10.1007/BF00033159
- Binder, W. D., Fielder, P., Mohammed, G. H., and L'Hirondelle, S. J. (1996). Applications of chlorophyll fluorescence for stock quality assessment with different types of fluorimeters. *New For.* 13, 63–89. doi: 10.1023/A:1006513720073
- Björkman, O., and Powles, S. B. (1984). Inhibition of photosynthetic reactions under water stress: Interaction with light level. *Planta* 161, 490–504. doi: 10.1007/BF00407081
- Bond, B. J. (2000). Age-related changes in photosynthesis of woody plants. *Trends Plant Sci.* 5, 349–353. doi: 10.1016/S1360-1385(00)01691-5
- Bosa, K., Jadczyk-Tobiasz, E., and Kalaji, M. H. (2016). Photosynthetic productivity of pear trees grown on different rootstocks. *Ann. di Bot.* 6, 69–75. doi: 10.4462/annbotm-13172
- Bosa, K., Jadczyk-Tobiasz, E., Kalaji, M. H., Majewska, M., and Allakhverdiev, S. I. (2014). Evaluating the effect of rootstocks and potassium level on photosynthetic productivity and yield of pear trees. *Russ. J. Plant Physiol.* 61, 231–237. doi: 10.1134/S1021443714020022
- Brestic, M., and Zivcak, M. (2013). "PSII fluorescence techniques for measurement of drought and high temperatures stress signal in crop plants: Protocols and applications", in *Mol. Stress Physiol. Plants*, eds. Rout, G., and Das, A. (Springer, India), 87–131. doi: 10.1007/978-81-322-0807-5\_4
- Brodribb, T., and Hill, R. S. (1997). Light response characteristics of a morphologically diverse group of southern hemisphere conifers as measured by chlorophyll fluorescence. *Oecologia* 110, 10–17. doi: 10.1007/s004420050127
- Bukhov, N. G., and Carpentier, R. (2004). "Effects of water stress on the photosynthetic efficiency of plants," in *Chlorophyll a fluorescence: A signature of photosynthesis*. Eds. G. C. Papageorgiou and Govindjee, (Dordrecht, The Netherlands: Springer), 623–635.
- Bussotti, F. (2004). Assessment of stress conditions in *Quercus ilex* L. leaves by O-J-I-P chlorophyll *a* fluorescence analysis. *Plant Biosyst.* 138, 101–109. doi: 10.1080/11263500412331283708
- Bussotti, F., Agati, G., Desotgiu, R., Matteini, P., and Tani, C. (2005). Ozone foliar symptoms in woody plant species assessed with ultrastructural and fluorescence analysis. *N. Phytol.* 166, 941–955. doi: 10.1111/j.1469-8137.2005.01385.x
- Bussotti, F., Desotgiu, R., Cascio, C., Pollastrini, M., Gravano, E., Gerosa, G., et al. (2011a). Ozone stress in woody plants assessed with chlorophyll *a* fluorescence: a critical reassessment of existing data. *Environ. Exp. Bot.* 73, 19–30. doi: 10.1016/j.envexpbot.2010.10.022
- Bussotti, F., Desotgiu, R., Cascio, C., Strasser, R. J., Gerosa, G., and Marzuoli, R. (2007a). Photosynthesis responses to ozone in young trees of three species with different sensitivities, in a 2-year open-top chamber experiment (Curno, Italy). *Physiol. Plant* 130, 122–135. doi: 10.1111/j.1399-3054.2007.00894.x
- Bussotti, F., Desotgiu, R., Pollastrini, M., and Cascio, C. (2010). The JIP test: A tool to screen the capacity of plant adaptation to climate change. *Scand. J. For. Res.* 25 (Suppl 8), 43–50. doi: 10.1080/02827581.2010.485777
- Bussotti, F., Gerosa, G., Digrao, A., and Pollastrini, M. (2020). Selection of chlorophyll fluorescence parameters as indicators of photosynthetic efficiency in large scale plant ecological studies. *Ecol. Indic.* 108, 105686. doi: 10.1016/j.ecolind.2019.105686
- Bussotti, F., and Pollastrini, M. (2015a). Do tree-species richness, stand structure and ecological factors affect the photosynthetic efficiency in European forests? *Web Ecol.* 15, 39–41. doi: 10.5194/we-15-39-2015
- Bussotti, F., and Pollastrini, M. (2015b). Evaluation of leaf features in forest trees: Methods, techniques, obtainable information and limits. *Ecol. Indic.* 52, 219–230. doi: 10.1016/j.ecolind.2014.12.010
- Bussotti, F., and Pollastrini, M. (2017). Traditional and novel indicators of climate change impacts on European forest trees. *Forests* 8, 137. doi: 10.3390/f8040137

- Bussotti, F., and Pollastrini, M. (2021). Revisiting the concept of stress in forest trees at the time of global change and issues for stress monitoring. *Plant Stress* 2, 100013. doi: 10.1016/j.stress.2021.100013
- Bussotti, F., Pollastrini, M., Cascio, C., Desotgiu, R., Gerosa, G., Marzuoli, R., et al. (2011b). Conclusive remarks. Reliability and comparability of chlorophyll fluorescence data from several field teams. *Environ. Exp. Bot.* 73, 116–119. doi: 10.1016/j.envexpbot.2010.10.023
- Bussotti, F., Strasser, R. J., and Schaub, M. (2007b). Photosynthetic behavior of woody species under high ozone exposure probed with the JIP-test: A review. *Environ. pollut.* 147, 430–437. doi: 10.1016/j.envpol.2006.08.036
- Cascio, C., Schaub, M., Novak, K., Desotgiu, R., Bussotti, F., and Strasser, R. J. (2010). Foliar responses to ozone of *Fagus sylvatica* l. seedlings grown in shaded and in full sunlight conditions. *Environ. Exp. Bot.* 68, 188–197. doi: 10.1016/j.envexpbot.2009.10.003
- Castro, F. A., Camprotrini, E., Torres Netto, A., and Viana, L. H. (2011). Relationship between photochemical efficiency (JIP-test parameters) and portable chlorophyll meter readings in papaya plants. *Braz. J. Plant Physiol.* 23, 295–304. doi: 10.1590/S1677-04202011000400007
- Chaves, M. M., Flexas, J., and Pinheiro, C. (2009). Photosynthesis under drought and salt stress: Regulation mechanisms from whole plant to cell. *Ann. Bot.* 103, 551–560. doi: 10.1093/aob/mcn125
- Chen, L. S., and Cheng, L. (2010). The acceptor side of photosystem II is damaged more severely than the donor side of photosystem II in 'Honeycrisp' apple leaves with zonal chlorosis. *Acta Physiol. Plant* 32, 253–261. doi: 10.1007/s11738-009-0402-4
- Christen, D., Schönmann, S., Jermini, M., Strasser, R. J., and Défago, G. (2007). Characterization and early detection of grapevine (*Vitis vinifera*) stress responses to esca disease by *in situ* chlorophyll fluorescence and comparison with drought stress. *Environ. Exp. Bot.* 60, 504–514. doi: 10.1016/j.envexpbot.2007.02.003
- Çiçek, N., Kalaji, H. M., and Ekmekçi, Y. (2020). Probing the photosynthetic efficiency of some European and Anatolian scots pine populations under UV-b radiation using polyphasic chlorophyll a fluorescence transient. *Photosynthetica* 58, 468–478. doi: 10.32615/ps.2019.151
- Cirillo, A., Conti, S., Graziani, G., El-Nakhel, C., Roupheal, Y., Ritieni, A., et al. (2021). Mitigation of high-temperature damage by application of kaolin and pinolene on young olive trees (*Olea europaea* L.): A preliminary experiment to assess biometric, eco-physiological and nutraceutical parameters. *Agronomy* 11: 1884. doi: 10.3390/agronomy11091884
- Cséfaly, L., Di Gasparo, G., Matouš, K., Bellin, D., Ruperti, B., and Olejníčková, J. (2009). Pre-symptomatic detection of *Plasmopara viticola* infection in grapevine leaves using chlorophyll fluorescence imaging. *Eur. J. Plant Pathol.* 125, 291–302. doi: 10.1007/s10658-009-9482-7
- DaMatta, F. M., Loos, R. A., Silva, E. A., and Loureiro, M. E. (2002). Limitations to photosynthesis in *Coffea canephora* as a result of nitrogen and water availability. *J. Plant Physiol.* 159, 975–981. doi: 10.1078/0176-1617-00807
- Day, T. A., Vogelmann, T. C., and DeLucia, E. H. (1992). Are some plant life forms more effective than others in screening out ultraviolet-b radiation? *Oecologia* 92, 513–519. doi: 10.1007/BF00317843
- De Castro, F. A., Camprotrini, E., Netto, A. T., de Assis-Gomes, M. M., Ferraz, T. M., and Glenn, D. M. (2014). Portable chlorophyll meter (PCM-502) values are related to total chlorophyll concentration and photosynthetic capacity in papaya (*Carica papaya* L.). *Theor. Exp. Plant Physiol.* 26, 201–210. doi: 10.1007/s40626-014-0018-y
- de Oliveira, J. G., Alves, P. L. D. C. A., and Vitória, A. P. (2009). Alterations in chlorophyll a fluorescence, pigment concentrations and lipid peroxidation to chilling temperature in coffee seedlings. *Environ. Exp. Bot.* 67, 71–76. doi: 10.1016/j.envexpbot.2009
- Desotgiu, R., Cascio, C., Pollastrini, M., Gerosa, G., Marzuoli, R., and Bussotti, F. (2012a). Short and long term photosynthetic adjustments in sun and shade leaves of *Fagus sylvatica* L., investigated by fluorescence transient (FT) analysis. *Plant Biosyst.* 146, 206–216. doi: 10.1080/11263504.2012.705350
- Desotgiu, R., Pollastrini, M., Cascio, C., Gerosa, G., Marzuoli, R., and Bussotti, F. (2012b). Chlorophyll a fluorescence analysis along a vertical gradient of the crown in a poplar (Oxford clone) subjected to ozone and water stress. *Tree Physiol.* 32, 976–986. doi: 10.1093/treephys/tps062
- Dezhban, A., Shirvany, A., Attarod, P., Delshad, M., Matiniazadeh, M., and Khoshnevis, M. (2015). Cadmium and lead effects on chlorophyll fluorescence, chlorophyll pigments and proline of *Robinia pseudoacacia*. *J. For. Res.* 26, 323–329. doi: 10.1007/s11676-015-0045-9
- Dias, D. P., and Marenco, R. A. (2007). Fluorescence characteristics and photoinhibition in saplings of manwood on clear days and under overcast conditions. *Sci. Agric.* 64, 595–600. doi: 10.1590/S0103-90162007000600006
- Diemer, M., Körner, C., and Prock, S. (1992). Leaf life spans in wild perennial herbaceous plants: A survey and attempts at a functional interpretation. *Oecologia* 89, 10–16. doi: 10.1007/BF00319009
- Dimitrova, S., Paunov, M., Pavlova, B., Dankov, K., Kouzmanova, M., Velikova, V., et al. (2020). Photosynthetic efficiency of two *Platanus orientalis* L. ecotypes exposed to moderately high temperature–JIP-test analysis. *Photosynthetica* 58, 657–670. doi: 10.32615/ps.2020.012
- dos Santos, V. A. H. F., and Ferreira, J. M. J. (2020). Are photosynthetic leaf traits related to the first-year growth of tropical tree seedlings? A light-induced plasticity test in a secondary forest enrichment planting. *For. Ecol. Manage.* 460, 117900. doi: 10.1016/j.foreco.2020.117900
- Duan, Y., Zhang, M., Gao, J., Li, P., Goltsev, V., and Ma, F. (2015). Thermotolerance of apple tree leaves probed by chlorophyll a fluorescence and modulated 820 nm reflection during seasonal shift. *J. Photochem. Photobiol. B: Biol.* 152, 347–356. doi: 10.1016/j.photobiol.2015.08.010
- Epron, D., Dreyer, E., and Bréda, N. (1992). Photosynthesis of oak trees [*Quercus petraea* (Matt.) Liebl.] during drought under field conditions: Diurnal course of net CO<sub>2</sub> assimilation and photochemical efficiency of photosystem II. *Plant Cell Environ.* 15, 809–820. doi: 10.1111/j.1365-3040.1992.tb02148.x
- Esperon-Rodriguez, M., Power, S. A., Tjoelker, M. G., and Marchin, R. M. (2021). And rymer, p Contrasting heat tolerance of urban trees to extreme temperatures during heatwaves. *D Urban For. Urban Gree.* 66, 127387. doi: 10.1016/j.ufug.2021.127387
- Falqueto, A. R., da Silva Júnior, R. A., Gomes, M. T. G., Martins, J. P. R., and Silva, D. M. (2017). And partelli, f Effects of drought stress on chlorophyll a fluorescence in two rubber tree clones. *L. Sci. Hortic.* 224, 238–243. doi: 10.1016/j.scienta.2017.06.019
- Faraloni, C., Cutino, I., Petrucci, R., Leva, A. R., Lazzeri, S., and Torzillo, G. (2011). Chlorophyll fluorescence technique as a rapid tool for *in vitro* screening of olive cultivars (*Olea europaea* L.) tolerant to drought stress. *Environ. Exp. Bot.* 73, 49–56. doi: 10.1016/j.envexpbot.2010.10.011
- Finì, A., Ferrini, F., Frangi, P., Amoroso, G., and Piatti, R. (2009). Withholding irrigation during the establishment phase affected growth and physiology of Norway maple (*Acer platanoides*) and linden (*Tilia* spp.). *Arboric. Urban For.* 35, 241–251. doi: 10.48044/jauf.2009.038
- Finì, A., Frangi, P., Comin, S., Vigevani, I., Rettori, A. A., Brunetti, C., et al. (2022). Effects of pavements on established urban trees: Growth, physiology, ecosystem services and disservices. *Landsc Urban Plan.* 226, 104501. doi: 10.1016/j.landurbplan.2022.104501
- Fisker, S. E., Rose, R., and Haase, D. L. (1995). Chlorophyll fluorescence as a measure of cold hardiness and freezing stress in 1 + 1 Douglas-fir seedlings. *For. Sci.* 41, 564–575. doi: 10.1093/forestscience/41.3.564
- Flexas, J., Escalona, J. M., and Medrano, H. (1999). Water stress induces different levels of photosynthesis and electron transport rate regulation in grapevines. *Plant Cell Environ.* 22, 39–48. doi: 10.1046/j.1365-3040.1999.00371.x
- Fusaro, L., Salvatori, E., Winkler, A., Frezzini, M. A., De Santis, E., Sagnotti, L., et al. (2021). Urban trees for biomonitoring atmospheric particulate matter: An integrated approach combining plant functional traits, magnetic and chemical properties. *Ecol. Indic.* 126, 107707. doi: 10.1016/j.ecolind.2021.107707
- García-Plazaola, J. I., Artetxe, U., and Duñabedia, M. K. (1999). And becerril, J Role of photoprotective systems of holm-oak (*Quercus ilex*) in the adaptation to winter conditions. *M. J. Plant Physiol.* 155, 625–630. doi: 10.1016/S0176-1617(99)80064-9
- Genty, B., and Briantais, J. M. (1989). And baker, n The relationship between the quantum yield of photosynthetic electron transport and quenching of chlorophyll fluorescence. *R. Biochim. Biophys. Acta* 990, 87–92. doi: 10.1016/S0304-4165(89)80016-9
- Gerosa, G., Marzuoli, R., Bussotti, F., Pancrazi, M., and Ballarin-Denti, A. (2003). Ozone sensitivity of *Fagus sylvatica* and *Fraxinus excelsior* young trees in relation to leaf structure and foliar ozone uptake. *Environ. pollut.* 125, 91–98. doi: 10.1016/S0269-7491(03)00094-0
- Gielen, B., Löw, M., Deckmyn, G., Metzger, U., Franck, F., Heerd, C., et al. (2007). Chronic ozone exposure affects leaf senescence of adult beech trees: A chlorophyll fluorescence approach. *J. Exp. Bot.* 58, 785–795. doi: 10.1093/jxb/erl222
- Gonçalves, J. F. D. C., Marenco, R. A., and Vieira, G. (2001). Concentration of photosynthetic pigments and chlorophyll fluorescence of mahogany and tonka bean under two light environments. *Rev. Bras. Fisiol. Veg.* 13, 149–157. doi: 10.1590/S0103-31312001000200004
- Goebel, E., and Calatayud, A. (2012). Applications of chlorophyll fluorescence imaging technique in horticultural research: A review. *Sci. Hortic.* 138, 24–35. doi: 10.1016/j.scienta.2012.02.002
- Gottardini, E., Cristofolini, F., Cristofori, A., Camin, F., Calderisi, M., and Ferretti, M. (2016). Consistent response of crown transparency shoot growth and leaf traits on Norway spruce (*Picea abies* (L.) h. karst.) trees along an elevation gradient in northern Italy. *Ecol. Indic.* 60, 1041–1044. doi: 10.1016/j.ecolind.2015.09.006
- Gottardini, E., Cristofolini, F., Cristofori, A., Pollastrini, M., Camin, F., and Ferretti, M. (2020). A multi-proxy approach reveals common and species-specific



features associated with tree defoliation in broadleaved species. *For. Ecol. Manage.* 467, 118151. doi: 10.1016/j.foreco.2020.118151

Gottardini, E., Cristofori, A., Cristofolini, F., Nali, C., Pellegrini, E., Bussotti, F., et al. (2014). Chlorophyll-related indicators are linked to visible ozone symptoms: Evidence from a field study on native *Viburnum lantana* L. plants in northern Italy. *Ecol. Indic.* 39, 65–74. doi: 10.1016/j.ecolind.2013.11.021

Gravano, E., Bussotti, F., Strasser, R. J., Schaub, M., Novak, K., Skelly, J., et al. (2004). Ozone symptoms in leaves of woody plants in open-top chambers: Ultrastructural and physiological characteristics. *Physiol. Plant* 121, 620–633. doi: 10.1111/j.1399-3054.2004.00363.x

Grifoni, D., Agati, G., Bussotti, F., Michelozzi, M., Pollastrini, M., and Zipoli, G. (2016). Different responses of *Arbutus unedo* and *Vitis vinifera* leaves to UV filtration and subsequent exposure to solar radiation. *Environ. Exp. Bot.* 128, 1–10. doi: 10.1016/j.envexpbot.2016.03.012

Guadagno, C. R., Beverly, D. P., and Ewers, B. E. (2021). The love-hate relationship between chlorophyll *a* and water in PSII affects fluorescence products. *Photosynthetica* 59, 409–421. doi: 10.32615/ps.2021.023

Guha, A., Sengupta, D., and Reddy, A. R. (2013). Polyphasic chlorophyll *a* fluorescence kinetics and leaf protein analyses to track dynamics of photosynthetic performance in mulberry during progressive drought. *J. Photochem. Photobiol. B: Biol.* 119, 71–83. doi: 10.1016/j.jphotobiol.2012.12.006

Hachani, C., Lamhamed, M. S., Zine El Abidine, A., Abassi, M., Khasa, D. P., and Béjaoui, Z. (2021). Water relations, gas exchange, chlorophyll fluorescence and electrolyte leakage of ectomycorrhizal *Pinus halepensis* seedlings in response to multi-heavy metal stresses (Pb, Zn, Cd). *Microorganisms* 10, 57. doi: 10.3390/microorganisms10010057

Hakam, N., DeEll, J. R., Khanzadeh, S., and Richer, C. (2000). Assessing chilling tolerance in roses using chlorophyll fluorescence. *HortScience* 35, 184–186. doi: 10.21273/HORTSCI.35.2.184

Hamerlynck, E. P. (2001). Chlorophyll fluorescence and photosynthetic gas exchange responses to irradiance of tree of heaven (*Ailanthus altissima*) in contrasting urban environments. *Photosynthetica* 39, 79–86. doi: 10.1023/A:1012448019931

Haukioja, E., and Koricheva, J. (2000). Tolerance to herbivory in woody vs. herbaceous plants. *Evol. Ecol.* 14, 551–562. doi: 10.1023/A:1011091606022

Hermans, C., Smeyers, M., Rodriguez, R. M., Eyletters, M., and Strasser, R. J. (2003). And delhay, J Quality assessment of urban trees: a comparative study of physiological characterisation, airborne imaging and on site fluorescence monitoring by the OJIP-test. *P. J. Plant Physiol.* 160, 81–90. doi: 10.1078/0176-1617-00917

Holland, V., Koller, S., and Bräggemann, W. (2014). Insight into the photosynthetic apparatus in evergreen and deciduous European oaks during autumn senescence using OJIP fluorescence transient analysis. *Plant Biol.* 16, 801–808. doi: 10.1111/plb.12105

Jiang, H., Howell, G. S., and Flore, J. A. (1999). Efficacy of chlorophyll fluorescence as a viability test for freeze-stressed woody grape tissues. *Can. J. Plant Sci.* 79, 401–409. doi: 10.4141/P98-088

Jiang, C. D., Jiang, G. M., Wang, X., Li, L. H., Biswas, D. K., and Li, Y. G. (2006a). Increased photosynthetic activities and thermostability of photosystem II with leaf development of elm seedlings (*Ulmus pumila*) probed by the fast fluorescence rise OJIP. *Environ. Exp. Bot.* 58, 261–268. doi: 10.1016/j.envexpbot.2005.09.007

Jiang, C. D., Shi, L., Gao, H. Y., Schansker, G., Tóth, S. Z., and Strasser, R. J. (2006b). Development of photosystems 2 and 1 during leaf growth in grapevine seedlings probed by chlorophyll *a* fluorescence transient and 820 nm transmission *in vivo*. *Photosynthetica* 44, 454–463. doi: 10.1007/s11099-006-0050-5

Kalaji, H. M., Jajoo, A., Oukarroum, A., Brestic, M., Zivcak, M., Samborska, I. A., et al. (2016). Chlorophyll *a* fluorescence as a tool to monitor physiological status of plants under abiotic stress conditions. *Acta Physiol. Plant* 38, 1–11. doi: 10.1007/s11738-016-2113-y

Kalaji, H. M., Oukarroum, A., Alexandrov, V., Kouzmanova, M., Brestic, M., Zivcak, M., et al. (2014a). Identification of nutrient deficiency in maize and tomato plants by *in vivo* chlorophyll *a* fluorescence measurements. *Plant Physiol. Biochem.* 81, 16–25. doi: 10.1016/j.plaphy.2014.03.029

Kalaji, H. M., Račková, L., Paganová, V., Swoczyna, T., Rusinowski, S., and Sitko, K. (2018). Can chlorophyll-*a* fluorescence parameters be used as bio-indicators to distinguish between drought and salinity stress in *Tilia cordata* mill? *Environ. Exp. Bot.* 152, 149–157. doi: 10.1016/j.envexpbot.2017.11.001

Kalaji, H. M., Schansker, G., Brestic, M., Bussotti, F., Calatayud, A., Ferroni, L., et al. (2017). Frequently asked questions about chlorophyll fluorescence, the sequel. *Photosynth. Res.* 132, 13–66. doi: 10.1007/s11120-016-0318-y

Kalaji, H. M., Schansker, G., Ladle, R. J., Goltsev, V., Bosa, K., Allakhverdiev, S. I., et al. (2014b). Frequently asked questions about *in vivo* chlorophyll fluorescence: Practical issues. *Photosynth. Res.* 122, 121–158. doi: 10.1007/s11120-014-0024-6

Keča, N., Tkaczyk, M., Żółciak Stocki, A.M., Kalaji, H. M., Nowakowska, J. A., and Oszako, T. (2018). Survival of European ash seedlings treated with phosphite

after infection with the *Hymenoscyphus fraxineus* and *Phytophthora* species. *Forests* 9, 442. doi: 10.3390/f9080442

Kikuzawa, K. (1995). Leaf phenology as an optimal strategy for carbon gain in plants. *Can. J. Bot.* 73, 158–163. doi: 10.1139/b95-019

Kikuzawa, K., and Ackerly, D. (1999). Significance of leaf longevity in plants. *Plant Species Biol.* 14, 39–45. doi: 10.1046/j.1442-1984.1999.00005.x

Kitao, M., Lei, T. T., and Koike, T. (1998). Application of chlorophyll fluorescence to evaluate Mn tolerance of deciduous broad-leaved tree seedlings native to northern Japan. *Tree Physiol.* 18, 135–140. doi: 10.1093/treephys/18.2.135

Kozłowski, T. T., Kramer, P. J., and Pallardy, S. G. (2012). *The physiological ecology of woody plants* (San Diego, CA: Academic press.), 657 pp.

Kuhlgert, S., Austic, G., Zegarac, R., Osei-Bonsu, I., Hoh, D., Chilvers, M. I., et al. (2016). MultispeQ beta: A tool for large-scale plant phenotyping connected to the open PhotosynQ network. *R. Soc. Open Sci.* 3, 160592. doi: 10.1098/rsos.160592

Lawlor, D. W. (2002). Carbon and nitrogen assimilation in relation to yield: Mechanisms are the key to understanding production systems. *J. Exp. Bot.* 53, 773–787. doi: 10.1093/jexbot/53.370.773

Lee, T. Y., Woo, S. Y., Kwak, M. J., Inkyun, K., Lee, K. E., Jang, J. H., et al. (2016). Photosynthesis and chlorophyll fluorescence responses of populus sibirica to water deficit in a desertification area in Mongolia. *Photosynthetica* 54, 317–320. doi: 10.1007/s11099-015-0180-8

Lepeduš, H., Jurković, V., Štolfa, I., Čurković-Perica, M., Fulgosi, H., and Cesar, V. (2010). Changes in photosystem II photochemistry in senescing maple leaves. *Croat. Chem. Acta* 83, 379–386.

L'Hirondelle, S., Simpson, D. G., and Binder, W. D. (2007). Chlorophyll fluorescence, root growth potential, and stomatal conductance as estimates of field performance potential in conifer seedlings. *New For.* 34, 235–251. doi: 10.1007/s11056-007-9051-x

Lichtenthaler, H. K., Babani, F., and Govindjee, (2004). “Light adaptation and senescence of the photosynthetic apparatus. changes in pigment composition, chlorophyll fluorescence parameters and photosynthetic activity,” in *Chlorophyll *a* fluorescence: A signature of photosynthesis*. Ed. G. C. Papageorgiou (Dordrecht, The Netherlands: Springer), 713–736. doi: 10.1007/978-1-4020-3218-9\_28

Lu, C., and Zhang, J. (1998). Effects of water stress on photosynthesis, chlorophyll fluorescence and photoinhibition in wheat plants. *Funt. Plant Biol.* 25, 883–892. doi: 10.1071/PP98129

Martinez-Ferri, E., Manrique, E., Valladares, F., and Balaguer, L. (2004). Winter photoinhibition in the field involves different processes in four co-occurring Mediterranean tree species. *Tree Physiol.* 24, 981–990. doi: 10.1016/j.jufug.2010.02.003

Martinez-Trinidad, T., Watson, W. T., Arnold, M. A., Lombardini, L., and Appel, D. N. (2010). Comparing various techniques to measure tree vitality of live oaks. *Urban For. Urban Gree.* 9, 199–203. doi: 10.1016/j.ufug.2010.02.003

Matsushima, U., Kardjilov, N., Hilger, A., Manke, I., Shono, H., and Herppich, W. B. (2009). Visualization of water usage and photosynthetic activity of street trees exposed to 2 ppm of SO<sub>2</sub> – a combined evaluation by cold neutron and chlorophyll fluorescence imaging. *Nucl. Instrum. Methods Phys. Res. A* 60, 185–187. doi: 10.1016/j.nima.2009.01.150

Maxwell, K. (2000). And Johnson, G Chlorophyll fluorescence – a practical guide. *N. J. Exp. Bot.* 51, 659–668. doi: 10.1093/jexbot/51.345.659

Mediavilla, S., Herranz, M., González-Zurdo, P., and Escudero, A. (2014). Ontogenetic transition in leaf traits: A new cost associated with the increase in leaf longevity. *J. Plant Ecol.* 7, 567–575. doi: 10.1093/jpe/rtt059

Míguez, F., Fernández-Marín, B., Becerril, J. M., and García-Plazaola, J. I. (2017). Diversity of winter photoinhibitory responses: A case study in co-occurring lichens, mosses, herbs and woody plants from subalpine environments. *Physiol. Plant* 160, 282–296. doi: 10.1111/ppl.12551

Mihaljević, I., Viljevac Vuletić, M., Tomaš, V., Horvat, D., Zdunić, Z., and Vuković, D. (2021). PSII photochemistry responses to drought stress in autochthonous and modern sweet cherry cultivars. *Photosynthetica* 59, 517–528. doi: 10.32615/ps.2021.045

Mlinarić, S., Pfeiffer, T., Krstin, L., Špoljarić Maronić, D., Ožura, M., Stević, F., et al. (2021). Adaptation of *Amorpha fruticosa* to different habitats is enabled by photosynthetic apparatus plasticity. *Photosynthetica* 59, 137–147. doi: 10.32615/ps.2021.008

Mohammed, G. H., Binder, W. D., and Gillies, S. L. (1995). Chlorophyll fluorescence: A review of its practical forestry applications and instrumentation. *Scand. J. For. Res.* 10, 383–410. doi: 10.1080/02827589509382904

Mohammed, G. H., Colombo, R., Middleton, E. M., Rascher, U., van der Tol, C., Nedbal, L., et al. (2019). Remote sensing of solar-induced chlorophyll fluorescence (SIF) in vegetation: 50 years of progress. *Remote Sens. Environ.* 231, 111177. doi: 10.1016/j.rse.2019.04.030

Muniz, C. R., Freire, F. C. O., Viana, F. M. P., Cardoso, J. E., Sousa, C. A. F., Guedes, M. I. F., et al. (2014). Monitoring cashew seedlings during interactions

with the fungus *Lasiodiplodia theobromae* using chlorophyll fluorescence imaging. *Photosynthetica* 52, 529–537. doi: 10.1007/s11099-014-0061-6

Murchie, E. H., and Lawson, T. (2013). Chlorophyll fluorescence analysis: A guide to good practice and understanding some new applications. *J. Exp. Bot.* 64, 3983–3998. doi: 10.1093/jxb/ert208

Nabity, P. D., Zavala, J. A., and DeLucia, E. H. (2009). Indirect suppression of photosynthesis on individual leaves by arthropod herbivory. *Ann. Bot.* 103, 655–663. doi: 10.1093/aob/mcn127

Naidoo, G., and Chirkoot, D. (2004). The effects of coal dust on photosynthetic performance of the mangrove, *Avicennia marina* in richards bay, south Africa. *Environ. pollut.* 127, 359–366. doi: 10.1016/j.envpol.2003.08.018

Naumann, J. C., Young, D. R., and Anderson, J. E. (2008). Leaf chlorophyll fluorescence, reflectance, and physiological response to freshwater and saltwater flooding in the evergreen shrub, *Myrica cerifera*. *Environ. Exp. Bot.* 63, 402–409. doi: 10.1016/j.envexpbot.2007.12.008

Niinimets, Ü. (2002). Stomatal conductance alone does not explain the decline in foliar photosynthetic rates with increasing tree age and size in *Picea abies* and *Pinus sylvestris*. *Tree Physiol.* 22, 515–535. doi: 10.1093/treephys/22.8.515

Nikiforou, C., and Manetas, Y. (2011). Inherent nitrogen deficiency in *Pistacia lentiscus* preferentially affects photosystem I: A seasonal field study. *Funct. Plant Biol.* 38, 848–855. doi: 10.1071/FP11040

Norton, A. J., Rayner, P. J., Koffi, E. N., Scholze, M., Silver, J. D., and Wang, Y. P. (2019). Estimating global gross primary productivity using chlorophyll fluorescence and a data assimilation system with the BETHY-SCOPE model. *Biogeosciences* 16, 3069–3093. doi: 10.5194/bg-16-3069-2019

Nowakowska, J. A., Stocki, M., Stocka, N., Ślusarski, S., Tkaczyk, M., Caetano, J. M., et al. (2020). Interactions between *Phytophthora cactorum*, *Armillaria gallica* and *Betula pendula* roth. seedlings subjected to defoliation. *Forests* 11: 1107. doi: 10.3390/f11101107

Odasz-Albrigtsen, A. M., Tømmervik, H., and Murphy, P. (2000). Decreased photosynthetic efficiency in plant species exposed to multiple airborne pollutants along the Russian-Norwegian border. *Can. J. Bot.* 78, 1021–1033. doi: 10.1139/b00-075

Ögren, E. (1988). Suboptimal nitrogen status sensitizes the photosynthetic apparatus in willow leaves to long term but not short term water stress. *Photosynth. Res.* 18, 263–275. doi: 10.1007/BF00034831

Ögren, E. (1990). Evaluation of chlorophyll fluorescence as a probe for drought stress in willow leaves. *Plant Physiol.* 93, 1280–1285. doi: 10.1104/pp.93.4.1280

Oliveira, G., and Peñuelas, J. (2005). Effects of winter cold stress on photosynthesis and photochemical efficiency of PSII of the Mediterranean *Cistus albidus* L. and *Quercus ilex* L. *Plant Ecol.* 175, 179–191. doi: 10.1007/s11258-005-4876-x

Oukarroum, A., El Madidi, S., Schanser, G., and Strasser, R. J. (2007). Probing the responses of barley cultivars (*Hordeum vulgare* L.) by chlorophyll a fluorescence OLKJIP under drought stress and re-watering. *Environ. Exp. Bot.* 60, 438–446. doi: 10.1016/j.envexpbot.2007.01.002

Padhi, B., Chauhan, G., Kandoi, D., Stirbet, A., Tripathy, B. C., and Govindjee, G. (2021). A comparison of chlorophyll fluorescence transient measurements, using handy PEA and FluorPen fluorimeters. *Photosynthetica* 59, 399–408. doi: 10.32615/ps.2021.026

Percival, G. C. (2002) and sheriffs cIdentification of drought-tolerance woody perennials using chlorophyll fluorescence *N. J. Arboresc.* 28, 215–223. doi: 10.48044/jauf.2002.032

Percival, G. C. (2005). The use of chlorophyll fluorescence to identify chemical and environmental stress in leaf tissue of three oak (*Quercus*) species. *J. Arboresc.* 31, 215–227. doi: 10.48044/jauf.2005.028

Percival, G. C. (2008). Paclobutrazol soil drenches provide partial reductions in symptoms of apple scab of ornamental trees and *Guignardia* leaf blotch of horse chestnut. *J. Environ. Hortic.* 26, 87–92. doi: 10.24266/0738-2898-26.2.87

Percival, G. C., and Banks, J. M. (2015). Phosphite-induced suppression of *Pseudomonas* bleeding canker (*Pseudomonas syringae* pv. *aesculi*) of horse chestnut (*Aesculus hippocastanum* L.). *Arboresc. J.* 37, 7–20. doi: 10.48044/jauf.2008.012

Percival, G. C., and Fraser, G. A. (2001). Measurement of the salinity and freezing tolerance of *Crataegus* genotypes using chlorophyll fluorescence. *J. Arboresc.* 27, 233–245. doi: 10.48044/jauf.2001.025

Percival, G. C., and Fraser, G. A. (2002). The influence of powdery mildew infection on photosynthesis, chlorophyll fluorescence, leaf chlorophyll and carotenoid content of three woody plant species. *Arboresc. J.* 26, 333–346. doi: 10.1080/03071375.2002.9747348

Percival, G. C., Fraser, G. A., and Oxenham, G. (2003). Foliar salt tolerance of *Acer* genotypes using chlorophyll fluorescence. *Arboresc. Urban For.* 29, 61–65. doi: 10.48044/jauf.2003.008

Percival, G. C., Keary, I. P., and AL-Habsi, S. (2006). An assessment of the drought tolerance of *Fraxinus* genotypes for urban landscape plantings. *Urban For. Urban Gree.* 5, 17–27. doi: 10.1016/j.ufug.2006.03.002

Percival, G. C., Keary, I. P., and Noviss, K. (2008). The potential of a chlorophyll content SPAD meter to quantify nutrient stress in foliar tissue of sycamore (*Acer pseudoplatanus*), English oak (*Quercus robur*), and European beech (*Fagus sylvatica*). *Arboresc. Urban For.* 34, 89–100. doi: 10.48044/jauf.2008.012

Pereira, W. E., de Siqueira, D. L., Martínez, C. A., and Puiatti, M. (2000). Gas exchange and chlorophyll fluorescence in four citrus rootstocks under aluminium stress. *J. Plant Physiol.* 157, 513–520. doi: 10.1016/S0176-1617(00)80106-6

Pérez-Bueno, M. L., Pineda, M., and Barón, M. (2019). Phenotyping plant responses to biotic stress by chlorophyll fluorescence imaging. *Front. Plant Sci.* 10: 1135. doi: 10.3389/fpls.2019.01135

Perks, M. P., Monaghan, S., O'Reilly, C., Osborne, B. A., and Mitchell, D. T. (2001). Chlorophyll fluorescence characteristics, performance and survival of freshly lifted and cold stored Douglas fir seedlings. *Ann. For. Sci.* 58, 225–235. doi: 10.1051/forest:2001122

Pflug, E., and Brüggemann, W. (2012). Frost-acclimation of photosynthesis in overwintering Mediterranean holm oak, grown in central Europe. *Int. J. Plant Biol.* 3, e1. doi: 10.4081/pb.2012.el

Philip, E., and Azlin, Y. N. (2005). Measurement of soil compaction tolerance of *Lagostromia speciosa* (L.) pers. using chlorophyll fluorescence. *Urban For. Urban Gree.* 3, 203–208. doi: 10.1016/j.ufug.2005.04.003

Pollastrini, M., Desotgiu, R., Camin, F., Ziller, L., Gerosa, G., Marzuoli, R., et al. (2014a). Severe drought events increase the sensitivity to ozone on poplar clone. *Environ. Exp. Bot.* 100, 94–104. doi: 10.1016/j.envexpbot.2013.12.016

Pollastrini, M., Feducci, M., Bonal, D., Fotelli, M., Gessler, A., Gossiorci, C., et al. (2016c). Physiological significance of forest tree defoliation: Results from a survey in a mixed forest in Tuscany (central Italy). *For. Ecol. Manage.* 361, 170–178. doi: 10.1016/j.foreco.2015.11.018

Pollastrini, M., García Nogales, A., Benavides, R., Bonal, D., Finér, L., Fotelli, M., et al. (2017). Tree diversity affects chlorophyll a fluorescence and other leaf traits of tree species in a boreal forest. *Tree Physiol.* 37, 199–208. doi: 10.1093/treephys/tpw132

Pollastrini, M., Holland, V., Brüggemann, W., Bruelheide, H., Dănilă, I. C., Jaroszewicz, B., et al. (2016a). Taxonomic and ecological relevance of the chlorophyll a fluorescence signature of tree species in mixed European forests. *N. Phytol.* 212, 51–65. doi: 10.1111/nph.14026

Pollastrini, M., Holland, V., Brüggemann, W., and Bussotti, F. (2016b). Chlorophyll a fluorescence analysis in forests. *Ann. di Bot.* 6, 23–37. doi: 10.4462/annbotm-13257

Pollastrini, M., Holland, V., Brüggemann, W., Koricheva, J., Jussila, I., Scherer-Lorenzen, M., et al. (2014b). Interactions and competition processes among tree species in young experimental mixed forests, assessed with chlorophyll fluorescence and leaf morphology. *Plant Biol.* 16, 323–331. doi: 10.1111/plb.12068

Pollastrini, M., Salvatori, E., Fusaro, L., Manes, F., Marzuoli, R., Gerosa, G., et al. (2020). Selection of tree species for forests under climate change: is PSI functioning a better predictor for net photosynthesis and growth than PSII? *Tree Physiol.* 44, 1561–1571. doi: 10.1093/treephys/tpaa084

Popek, R., Przybysz, A., Gawrońska, H., Klamkowski, K., and Gawroński, S. W. (2018). Impact of particulate matter accumulation on the photosynthetic apparatus of roadside woody plants growing in the urban conditions. *Ecotoxicol. Environ. Saf.* 163, 56–62. doi: 10.1016/j.ecoenv.2018.07.051

Pukacki, P. M. (2000). Effects of sulphur, fluoride and heavy metal pollution on the chlorophyll fluorescence of Scots pine (*Pinus sylvestris* L.) needles. *Dendrobiology* 45, 83–88.

Rahman, M. A., Stringer, P., and Ennos, A. R. (2013). Effect of pit design and soil composition on performance of *Pyrus calleryana* street trees in the establishment period. *Arboresc. Urban For* 39, 256–266. doi: 10.48044/jauf.2013.033

Reyes, T. H., Scartazza, A., Bretzel, F., Di Baccio, D., Guglielminetti, L., Pini, R., et al. (2022). Urban conditions affect soil characteristics and physiological performance of three evergreen woody species. *Plant Physiol. Biochem.* 171, 169–181. doi: 10.1016/j.plaphy.2021.12.030

Rolfe, S. A., and Scholes, J. D. (2010). Chlorophyll fluorescence imaging of plant-pathogen interactions. *Protoplasma* 247, 163–175. doi: 10.1007/s00709-010-0203-z

Rossini, M., Panigada, C., Meroni, M., and Colombo, R. (2006). Assessment of oak forest condition based on leaf biochemical variables and chlorophyll fluorescence. *Tree Physiol.* 26, 1487–1496. doi: 10.1093/treephys/26.11.1487

Scholes, J. D., and Rolfe, S. A. (2009). Chlorophyll fluorescence imaging as tool for understanding the impact of fungal diseases on plant performance: A phenomics perspective. *Funct. Plant Biol.* 36, 880–892. doi: 10.1071/FP09145

Schreiber, U. (2004). “Pulse-amplitude-modulation (PAM) fluorometry and saturation pulse method: an overview,” in *Chlorophyll a fluorescence: A signature of photosynthesis*. Eds. G. C. Papageorgiou and Govindjee, (Dordrecht, The Netherlands: Springer), 279–319. doi: 10.1007/978-1-4020-3218-9\_11

Serbin, S. P., Dillaway, D. N., Kruger, E. L., and Townsend, P. A. (2012). Leaf optical properties reflect variation in photosynthetic metabolism and its sensitivity to temperature. *J. Exp. Bot.* 63, 489–502. doi: 10.1093/jxb/err294

- Sitko, K., Rusinowski, S., Pogrzeba, M., Daszkowska-Golec, A., Gieron, Z., Kalaji, H. M., et al. (2019). Development and aging of photosynthetic apparatus of *Vitis vinifera* L. during growing season. *Photosynthetica* 57, 1–8. doi: 10.32615/ps.2019.107
- Song, X., and Li, H. (2016). Effects of building shade on photosynthesis and chlorophyll fluorescence of *Euonymus fortunei*. *Acta Ecol. Sin.* 36, 350–355. doi: 10.1016/j.chnaes.2016.05.008
- Stirbet, A., and Govindjee, (2011). On the relation between the kautsky effect (chlorophyll a fluorescence induction) and photosystem II: Basics and applications of the OJIP fluorescence transient. *J. Photochem. Photobiol. B: Biol.* 104, 236–257. doi: 10.1016/j.jphotobiol.2010.12.010
- Strasser, R. J., Srivastava, A., and Tsimilli-Michael, M. (2000). “The fluorescence transient as a tool to characterize and screen photosynthetic samples,” in *Probing photosynthesis: Mechanisms, regulation and adaptation*. Eds. M. Yunus, U. Pathre and P. Mohanty (London: Taylor and Francis), 445–483.
- Strasser, R. J., Tsimilli-Michael, M., Qiang, S., and Goltsev, V. (2010). Simultaneous *in vivo* recording of prompt and delayed fluorescence and 820-nm reflection changes during drying and after rehydration of the resurrection plant *Habelea rhodopensis*. *Biochim. Biophys. Acta* 1797, 1313–1326. doi: 10.1016/j.bbabio.2010.03.008
- Strasser, R. J., Tsimilli-Michael, M., and Srivastava, A. (2004). “Analysis of the chlorophyll a fluorescence transient,” in *Chlorophyll a fluorescence: A signature of photosynthesis*. Eds. G. C. Papageorgiou and Govindjee, (Dordrecht, The Netherlands: Springer), 321–362. doi: 10.1007/978-1-4020-3218-9\_12
- Suchocka, M., Swoczyzna, T., Kosno-Jończy, J., and Kalaji, H. M. (2021). Impact of heavy pruning on development and photosynthesis of *Tilia cordata* mill. trees. *PLoS One* 16, e0256465. doi: 10.1371/journal.pone.0256465
- Swoczyzna, T., Kalaji, H. M., Pietkiewicz, S., and Borowski, J. (2015). Ability of various tree species to acclimation in urban environments probed with the JIP-test. *Urban For. Urban Gree.* 14, 544–553. doi: 10.1016/j.ufug.2015.05.005
- Swoczyzna, T., Kalaji, H. M., Pietkiewicz, S., Borowski, J., and Zará-Januszkiewicz, E. (2010a). Monitoring young urban trees tolerance to roadside conditions by application of chlorophyll fluorescence. *Zesz. Probl. Postepow Nauk Roln.* 545, 303–309.
- Swoczyzna, T., Kalaji, H. M., Pietkiewicz, S., Borowski, J., and Zará-Januszkiewicz, E. (2010b). Photosynthetic apparatus efficiency of eight tree taxa as an indicator of their tolerance to urban environments. *Dendrobiology* 63, 65–75.
- Swoczyzna, T., Łata, B., Stasiak, A., Stefaniak, J., and Latocha, P. (2019). JIP-test in assessing sensitivity to nitrogen deficiency in two cultivars of *Actinidia arguta* (Siebold et zucc.) planch. ex miq. *Photosynthetica* 57, 646–658. doi: 10.32615/ps.2019.057
- Swoczyzna, T., and Latocha, P. (2020). Monitoring seasonal damage of photosynthetic apparatus in mature street trees exposed to road-side salinity caused by heavy traffic. *Photosynthetica* 58, 573–584. doi: 10.32615/ps.2020.006
- Swoczyzna, T., Mojski, J., Baczewska-Dąbrowska, A. H., Kalaji, H. M., and Elsheery, N. I. (2020). Can we predict winter survival in plants using chlorophyll a fluorescence? *Photosynthetica* 58, 433–442. doi: 10.32615/ps.2019.181
- Torres Netto, A., Camprotrini, E., de Oliveira, J. G., and Bressan-Smith, R. E. (2005). Photosynthetic pigments, nitrogen, chlorophyll a fluorescence and SPAD-502 readings in coffee leaves. *Sci. Hortic.* 104, 199–209. doi: 10.1016/j.scienta.2004.08.013
- Trošt Sedej, T., and Rupar, D. (2013). Deciduous and evergreen tree responses to enhanced UV-b treatment during three years. *Acta Biol. Slov.* 56, 2.
- Tsimilli-Michael, M. (2020). Revisiting JIP-test: An educative review on concepts, assumptions, approximations, definitions and terminology. *Photosynthetica* 58, 275–292. doi: 10.32615/ps.2019.150
- Ugolini, F., Bussotti, F., Lanini, G. M., Raschi, A., Tani, C., and Tognetti, R. (2012). Leaf gas exchanges and photosystem efficiency of the holm oak in urban green areas of Florence, Italy. *Urban For. Urban Gree.* 11, 313–319. doi: 10.1016/j.ufug.2012.02.006
- Ugolini, F., Massetti, L., Pedrazzoli, F., Tognetti, R., Vecchione, A., Zulini, L., et al. (2014). Ecophysiological responses and vulnerability to other pathologies in European chestnut coppices, heavily infested by the Asian chestnut gall wasp. *For. Ecol. Manage.* 314, 38–49. doi: 10.1016/j.foreco.2013.11.031
- Vitale, L., Arena, C., and De Santo, A. V. (2012). Seasonal changes in photosynthetic activity and photochemical efficiency of the Mediterranean shrub *Phillyrea angustifolia* L. *Plant Biosyst.* 146, 443–450. doi: 10.1080/11263504.2011.651507
- Wang, Z. X., Chen, L., Ai, J., Qin, H. Y., Liu, Y. X., Xu, P. L., et al. (2012). Photosynthesis and activity of photosystem II in response to drought stress in amur grape (*Vitis amurensis* Rupr.). *Photosynthetica* 50, 189–196. doi: 10.1007/s11099-012-0023-9
- Wang, Y., Jin, W., Che, Y., Huang, D., Wang, J., Zhao, M., et al. (2019). Atmospheric nitrogen dioxide improves photosynthesis in mulberry leaves via effective utilization of excess absorbed light energy. *Forests* 10, 312. doi: 10.3390/f10040312
- Wang, X., and Wang, Z. (2010). Influence of crust-covered paving on photosynthesis and chlorophyll fluorescence parameters of a city landscape plant, *Firmiana simplex*. *Front. Agric. China* 4, 91–95. doi: 10.1007/s11703-009-0084-0
- Weather-and-climate.com. Available at: <https://weather-and-climate.com/average-monthly-min-max-Temperature,eu-upper-normandy-fr,France>.
- Yang, H., Yang, X., Zhang, Y., Heskell, M. A., Lu, X., Munger, J. W., et al. (2017). Chlorophyll fluorescence tracks seasonal variations of photosynthesis from leaf to canopy in a temperate forest. *Glob. Change Biol.* 23, 2874–2886. doi: 10.1111/gcb.13590
- Zhang, S., and Gao, R. (2000). Diurnal changes of gas exchange, chlorophyll fluorescence, and stomatal aperture of hybrid poplar clones subjected to midday light stress. *Photosynthetica* 37, 559–571. doi: 10.1023/A:1007119524389
- Zhang, H., Li, X. Y., Chen, L. S., and Huang, Z. R. (2020). The photosynthetic performance of two *Citrus* species under long-term aluminium treatment. *Photosynthetica* 58, 228–235. doi: 10.32615/ps.2019.145

# Frontiers in Plant Science

Cultivates the science of plant biology and its applications

The most cited plant science journal, which advances our understanding of plant biology for sustainable food security, functional ecosystems and human health.

## Discover the latest Research Topics

[See more →](#)

### Frontiers

Avenue du Tribunal-Fédéral 34  
1005 Lausanne, Switzerland  
[frontiersin.org](https://frontiersin.org)

### Contact us

+41 (0)21 510 17 00  
[frontiersin.org/about/contact](https://frontiersin.org/about/contact)

